Mathematical modelling and optimisation of a water to water heat pump

David Cameron Hetherington

Doctor of Philosophy

The University of Aston in Birmingham

September 1988

Acknowledgements

It is only fair to give due credit to the many people who have helped me to complete this work. Credit for helping me to understand thermodynamics must go to Bobby Berman, fellow of University College, Oxford, and thanks to the timely advice of John Wilks, fellow of Pembroke college, Oxford, I stopped wasting my time pursuing a much less useful line of research.

At Aston University, the conventional token recognition of the assistence given by the workshop staff would be quite inadequate. The importance of the help and co-operation given by Howard Arrowsmith and Dick Blunt cannot be overstated.

I would also like to thank Ewart Neal, Paul Cooper, Mike Wrenn and Roy Summers for their many useful discussions and encouragement.

Particular thanks are due to George Pearce who has been very halpful as my supervisor.

Finally, I am anxious to express my appreciation of the hospitality shown to me by Mr. Sam Windley, of GEC small motors, Newcastle under Lyme, during a very interesting visit there.

The University of Aston in Birmingham

Mathematical modelling and optimisation of a water to water heat pump

The purpose of the work described here has been to seek methods of narrowing the present gap between currently realised heat pump performance and the theoretical limit.

The single most important pre-requisite to this objective is the identification and quantitative assessment of the various non-idealities and degradative phenomena responsible for the present shortfall.

The use of availability analysis has been introduced as a diagnostic tool, and applied to a few very simple, highly idealised Rankine cycle optimisation problems. From this work, it has been demonstrated that the scope for improvement through optimisation is small in comparison with the extensive potential for improvement by reducing the compressor's losses.

A fully instrumented heat pump was assembled and extensively tested. This furnished performance data, and led to an improved understanding of the system's behaviour. From a very simple analysis of the resulting compressor performance data, confirmation of the compressor's low efficiency was obtained. In addition, in order to obtain experimental data concerning specific details of the heat pump's operation, several novel experiments were performed.

The experimental work was concluded with a set of tests which attempted to obtain definitive performance data for a small set of discrete operating conditions. These tests included an investigation of the effect of two compressor modifications.

The resulting performance data was analysed by a sophisticated calculation which used the measurements to quantify each degradative phenomenon occurring in the compressor, and so indicate where the greatest potential for improvement lies.

Finally, in the light of everything that was learnt, specific technical suggestions have been made, to reduce the losses associated with both the refrigerant circuit and the compressor.

Keywords:
Heat pump, Compressor, Thermodynamics, Equations of state, Modelling

David Cameron Hetherington PhD

1988

List of Contents

Chapter 1. An informal overview of heatpumps 12

1.1 Introduction 12
1.2 Other methods of obtaining heatpump operation 17
1.3 Heat pump sources 22
1.4 Drying . 30
1.5 Conclusion 30

Chapter 2. Thermodynamics and simple cycle analysis 32

2.1 Performance calculation 32
2.2 Derivation of functions of state from equations of state 33
2.3 Cycle analysis 44
2.4 Calculated cycle performance & losses 57
2.5 Performance calculations for optimised configuration 69
2.6 Heating water 73
2.7 Cycle calculations for immersed condenser 81
2.8 Non azeotropic mixed working fluids 91
2.9 Turbocharging - a way to recover the throttling loss 98
2.10 Summing up, further implications, and conclusion. 99

Chapter 3.
Construction and instrumentation of an experimental heat pump 100

3.1 The compressor 100
3.2 The condenser 102
3.3 The expansion valve 104
3.4 The evaporator 104
3.5 The assembled heat pump and its instrumentation 104
3.6 The wattmeter 107
3.7 Mains voltage and current consumption monitor 111
3.8 The flowmeters 113
3.9 The pressure transducers 120
3.10 The thermocouples 125

Chapter 4. The experimental investigation 135

4.1 Introduction 135
4.2 First attempt to determine the performance map 135
4.3 Further pursuit of the power step 137
4.4 More direct measurement of mechanical losses 137
4.5 Compressor temperature variation 138
4.6 Preliminary analysis 142
4.7 Compressor's losses 144
4.8 Further experiments 146
4.9 More novel tests 146
4.10 First attempt at modelling 148

Chapter 5. The experiments of 1985 149

5.1 Introduction 149
5.2 First attempted performance map determination 149
5.3 TXV limited operation 151
5.4 Anomalous orifice flow 159
5.5 Bistability of the power consumption 163
5.6 Differences between the new and the original compressors 184
Tables of results relevant to chapter 5 187

Chapter 6. Experiments on the lubrication system 201

6.1 Introduction 201
6.2 Description of the lubrication system 203
6.3 Excluding oil from the motor 204
6.4 Improved oil delivery 206
6.5 A novel oil delivery system 207
6.6 Customised centrifugal pump 212
6.7 Trials with the customised oil pump 213
6.8 Direct suction gas cooling of the stator 217
6.9 The free running tests 218

Chapter 7. Heat pump tests of 1986 221

7.1 Oil temperature test 221
7.2 Dis-assembly and re-assembly of the new compressor 230
7.3 Siting of the liquid reservoir 236
7.4 Tests on the expansion valve setting 244
7.5 The effect of by-passing the suction system 259
7.6 Improvised piston leakage mesurement 262
7.7 Conclusions and further implications 268
Tables of results relevant to section 7.5 270

Chapter 8. The final set of experiments

8.1 Purpose of final tests 286
8.2 The experiments 291

Chapter 9. A mathematical model to interpret the results 293

9.1 Introduction 293
9.2 Flow rate calculation 296
9.3 Compressor capacity calculation 299
9.4 Modelling the discharge system 302
9.5 Leakage past the piston 310
9.6 Suction stroke algorithm 314
9.7 Discharge stroke algorithm 321
Listing of the system definition program 327
Listing of the interpretive model 330

Chapter 10. Results of the interpretive model

10.1 Introduction. Explanation of the model's output 346
10.2 Results of the interpretive model, & tests of consistency 353
10.3 Using the compressor's heat loss as a diagnostic 360
10.4 Further effects of minimising the oil distribution 363

Tables of results from the interpretive model 370

Chapter 11.
Further work, including suggestions to improve performance 409

11.1 Introduction 409
11.2 Use of standard components 409
11.3 Less conservative modifications 413
11.4 Other suggestions for further work 416

Appendix 1 Converting Downing's imperial co-efficients to S.I. 418

Appendix 2 Incompleteness of the subcooled liquid specification 426

Appendix 3 Attempts to model the valve dynamics. 428

Appendix 4 Empirical fits to Danfoss' motor data. 432

Appendix 5 The viscosity of Alkylbenzene. 435

References 437

List of figures

Figures of chapter 1

1.1a Rankine cycle heat pump circuit. 16

1.1b Rankine heat pump cycle on P-h plane. 16

1.1c Rankine engine cycle on P-h plane. 16

1.2 Joule, Carnot & Stirling cycles. 18

1.3a Schematic reversed engine energy flows. 21

1.3b Schematic heat actuated heat pump heat flows. 21

1.4 Air source heat pump circuit 24

1.5 Mismatch problem of air-source heat pump. 25

1.6 Directly coupled ground source heat pump. 28

1.7 Ground source, using secondary refrigerant. 29

Figures of chapter 2

2.1 Differences between the Carnot cycle and Rankine cycles. 45

2.2 Diagram for derivation of Availability equation. 47

2.3 Rankine cycle with & without suction gas superheating. 50

2.4 Critical condensate temperatures for suction gas superheating 50

2.5 T - s diagram for discussion of throttling availability loss. 55

2.6 Throttling loss dependence on subcooling. 60

2.7 Temperature - enthalpy diagram to illustrate limiting behaviour of counterflow condenser. 74

2.8 Raoult's law compared with Hildebrand model. 93

2.9 Condensing isobars for a non-azeotropic refrigerant mixture. 96

Chapter 3 figures

3.1	Photograph of back of rig.	101
3.2	Sight glass accumulator design	103
3.3	Themostatic expansion valve (TXV) in section	105
3.4	Experimental rig. Water & R12 systems.	106
3.5	Wattmeter calibration. Power v frequency.	110
3.6	Wattmeter calibration. Power v bits.	110
3.7	Circuit diagram for I & V monitor.	112
3.8	Current monitor calibration.	112
3.9a	Schematic diagram of Pelton wheel flowmeter	114
3.9b	Pelton wheel flowmeter output signal	114
3.10a	R12 flowmeter calibration. Total pulses v flowrate.	117
3.10b	Flowmeter LM23646. Total pulses v flowrate.	117
3.10c	Flowmeter LM23344. Total pulses v flowrate.	117
3.11a	Condenser flow rate v bits 21/2/85	118
3.11b	Condenser flow rate v bits 21/5/85	118
3.11c	Condenser flow rate v bits 5/10/86	118
3.12a	Evaporator flow rate v bits 21/2/85	119
3.12b	Evaporator flow rate v bits 21/5/85	119
3.12c	Evaporator flow rate v bits 5/10/86	119
3.13	Photograph of pressure transducer coupling & thermowell assembly	121
3.14	Pressure transducer bit output v pressure.	123
3.15	Thermocouple ADC, PCI1002, schematic diagram to illustrate principle of operation.	126
3.16	Differential thermocouple equivalent circuit using an ice-point reference.	128

Figures of chapter 5

5.1a	Capacity v evaporator water entry temperature. Discharge pressure regulator set to 3. Evaporator water flow rate as parameter.	152
5.1b	C.O.P. corresponding to 5.1a	152

5.2a	Capacity v evaporator water entry temperature. Evaporator water flow rate of 90cc/s. Discharge pressure regulator setting as parameter.	153
5.2b	C.O.P. corresponding to 5.2a	153
5.3a	First & last time resolved R12 flow rate records from run of 25/5/85	155
5.3b	First & last time resolved R12 flow rate records from run of 27/5/85	155
5.4	Further symptoms of TXV saturation	157
5.5	Search for spontaneous flow transitions in orifice flow	160
5.6a	Discharge & suction pressure histories of 11/5/85.	168
5.6b	Power & oil temperature histories of 11/5/85.	168
5.6c	Discharge temperature & discharge - sump temperature difference on 11/5/85	169
5.7a	Discharge & suction pressure histories of first time-resolved record of 11/5/85	170
5.7b	Power & oil temperature histories of first time-resolved record of 11/5/85	170
5.7c	Discharge temperature & discharge - sump temperature difference of first time-resolve record of 11/5/85	171
5.7d	Metered R12 flow rate & suction temperature from first time-resolved record of 11/5/85	171
5.8a	Discharge & suction pressure histories of 25/5/85	172
5.8b	Power & oil temperature histories of 25/5/85	172
5.8c	Discharge temperature & discharge - sump temperature difference on 25/5/85	173
5.9a	Discharge & suction pressure histories of 7/6/85	174
5.9b	Power & oil temperature histories of 7/6/85	174
5.9c	Discharge temperature & discharge - sump temperature difference on 7/6/85	175
5.10a	Discharge & suction pressure histories of 14/7/85	176
5.10b	Power & oil temperature histories of 14/7/85	176
5.10c	Discharge temperature & discharge - sump temperature difference on 14/7/85	177
5.11a	Discharge & suction pressure histories of 17/10/85	178
5.11b	Power & oil temperature histories of 17/10/85	178

5.11c Discharge temperature & discharge - sump temperature difference on 17/10/85 179

5.12a Discharge & suction pressure histories of 18/10/85 180

5.12b Power & oil temperature histories of 18/10/85 180

5.12c R12 & oil temperatures on 18/10/85, the 're-heat' trial 181

5.13a Discharge & suction pressure histories of 21/10/85 182

5.13b Time resolved power & current consumption histories, 21/10/85 182

5.13c Discharge temperature & discharge - sump temperature difference on 21/10/85 183

5.14 Photograph of the original compressor removed from its can 185

5.15 Photograph of new compressor after total dis-assembly 186

Figures of chapter 6

6.1 Sectional view of the rotating assembly, indicating the journal bearings & top thrust bearing. 202

6.2 4 Power consumption records;- 205
Oil drain holes covered.
Sump baffle used for enhanced oil delivery.
As above, but with oil drain holes restored.
Return to status quo.

6.3 Like figure 6.1, showing impeller modification. 209

6.4 6 Power consumption records;- 211
First use of 4.5mm feeder, crankshaft bores closed at the top.
Repeat of above
Repeat, but with crankshaft bores open at the top.
5.1mm feeder.
6mm feeder
6mm feeder. Rotor supply ducts blocked.

6.5 Like 6.1 only for perspex impeller 214

6.6 4 Power consumption records with perspex impeller 216
Perspex impeller alone, top bores open
4.5mm feeder attached.
Perspex impeller alone, top bores closed
Perspex impeller, top bores closed, and plate heat exchangers clamped to stator, for direct suction gas cooling of the stator.

Figures of chapter 7

Figures connected with oil temperature test of 15/2/86

7.1a Oil temperature record 222

7.1b Power consumption record 222

7.1c	Current consumption record	222
7.2a	Compressor power v oil temperature	223
7.2b	Useful work v oil temperature	223
7.2c	Compressor losses v oil temperature	223
7.3	R12 mass flow efficiency v oil temperature	226
7.4	Subcooled R12 approach to condenser water entry temperature with increasing sump oil temperature.	226
7.5	Correlation of Tbdc & Tdis with sump oil temperature	228
7.6	R12 flow rate plotted against oil T	228

Figures involved with new compressor re-assembly

7.7a & b	Axial section of rotor/crankshaft assembly before & after re-build	231
7.8a & b	Transverse section of above	232

Further heat pump runs

7.9a	Power, suction pressure & sump oil temperature histories for run of 18/4/86 (High discharge pressure)	234
7.9b	Expanded time scale, blow up of fig 7.9a, first 30 minutes.	234
7.10a	Subcooling record with insufficient R12, 20/4/86	239
7.10b	Subcooling record with sufficient R12, 21/4/86	239
7.10c	Subcooling record. Accumulator at condenser's end, 22/4/86	239
7.11a	Tdis & Tsump histories for TXV test of 26/7/85.	248
7.11b	Suction pressure history for TXV test of 26/7/85.	248
7.11c	Compressor power history for TXV test of 26/7/85.	248
7.12a	Tdis & Tsump histories for TXV test of 23/4/86.	249
7.12b	Suction pressure history for TXV test of 23/4/86.	249
7.12c	Compressor power history for TXV test of 23/4/86	249
7.13a	Tdis & Tsump histories for TXV test of 27/4/86.	256
7.13b	Suction pressure history for TXV test of 27/4/86.	256
7.13c	Compressor power history for TXV test of 27/4/86	256
7.14a	Mass flow efficiency v Psuc for the suction by-pass test of 18 & 19/5/86.	261
7.14b	Compressor power consumption v Psuc for the suction	261

by-pass test of 18 & 19/5/86.

7.14c Compressor losses v Psuc for the suction by-pass test of 18 & 19/5/85 - search for loss associated with suction system. 261

7.15a Mass flow efficiency v Psuc for the rotor duct test of 18 & 20/5/86. 263

7.15b Compressor power consumption v Psuc for the rotor duct test of 18 & 20/5/86. 263

7.15c Compressor losses v Psuc. Tests of 18 & 20/5/85 - search for the loss associated with the oil spray from the rotor. 263

7.16 Accumulator liquid level v time for improvised piston leakage measurement. 266

<u>Figures of chapter 9</u>

9.1 Condenser temperature distribution 297

9.2 Discharge system heat loss model 303

9.3 Deriving the equation for leakage past the piston 311

9.4 Section through the compressor showing gas flows 315

9.5 Equivalent suction system for the suction stroke calculation 316

9.6 Discharge stroke model. Illustrating proportionality of flow rate to overpressure for gas flow out of the discharge plenum. 323

<u>Figures of chapter 10</u>

10.1 Discharge thermocouple error v R12 flow rate 349

10.2 Indicator diagram breakdown 349

10.3 Compressor capacity v reference density ratio for all tests 355

10.4 Like 10.3, but only for tests at 150psi discharge pressure 355

10.5 Like 10.4, but for 220 psi dscharge pressure 358

10.6 Effect on capacity of eliminating non-essential oil sprays, plotted for the remaining tests 358

10.7 Compressor heat loss plot. 361

A.1 Temperature dependence of Alkylbenzene viscosity 436

Chapter 1. An informal overview of heatpumps

1.1 Introduction

A heat pump is a heat producing machine which is best employed wherever a need exists for large quantities of heat at a temperature only slightly above ambient, as in domestic heating, for instance. An electrically driven heat pump produces significantly more heat than electricity consumed. Consequently, the potential exists for heat pump technology to furnish a very attractive alternative to current conventional means of producing heat.

Apart from the difference in emphasis of application, a heat pump is essentially the same in principle as a refrigerator. A refrigerator extracts low temperature heat from its contents and rejects it at a temperature above ambient to its surroundings. There is, however, no net gain, as the heat extracted is just heat which has leaked in from the surroundings.

The purpose of a heat pump is to refrigerate some part of the external environment and to use the extracted heat. The ratio of heat delivered to electricity consumed defines the "Co-efficient of performance" - C.O.P. for short. C.O.Ps. typically fall in the range of 2 to 4, the exact value depending on the details of the machine, and the operating condition.

It is generally well known that the spontaneous or 'natural' direction of heat flow is from hotter to colder, not the other way around. This point is implicit in Clausius' statement of the second law of thermodynamics (1);-

> It is impossible to devise an engine which, working in a cycle, shall produce no effect other than the transfer of heat from a colder to a hotter body.

In addition to the transfer of heat from a colder to a hotter body, a heat pump requires a supply of power, usually electricity. Thus it can be seen that there is no violation of the second law. Nonetheless, its accomplishment, in reversing the natural direction of heat flow, can justifiably be considered quite remarkable. The key to understanding how it works is to first understand how heat can be extracted from a low temperature source.

Of the several physical principles upon which heat pump operation has been based, the 'vapour compression cycle' probably offers the greatest potential for widespread use of heat pumps. It is based on the principle that for liquid-vapour equilibrium, the equilibrium temperature is a monotonic function of the hydrostatic pressure. For instance, a volatile liquid can be made to boil at a temperature well below ambient by enclosing it in a vessel connected to a vacuum pump (2). Having obtained a boiling point below ambient, in this way, the latent heat of evaporation is supplied by heat flow from the surroundings into the vessel, so sustaining boiling as long as the vapour is continuously evacuated to keep the pressure sufficiently low. This was first demonstrated as far back as 1748 by William Cullen (3).

The crucial feature to note is that the latent heat of evaporation has been extracted from the surroundings. Any material used in this way is called a 'refrigerant'.

Figure 1.1a is a schematic diagram of a heat pump, which shows how the principle explained above can be incorporated into a closed circuit. The evaporator is continuously evacuated, not by a vacuum pump, but by the suction side of a compressor. The resulting vapour is compressed to a higher pressure by the compressor and discharged to the condenser, where it is condensed, giving up the latent heat of condensation at the condensing temperature. During compression, the vapour temperature rises. However, this is not the feature principally responsible for the functioning of the heat pump. Because of the high pressure in the condenser, the condensing temperature is correspondingly raised. Thus the latent heat, originally extracted from a low temperature source, can be made available at the desired high temperature, by raising the vapour to the appropriate high pressure.

Finally, the rate of return of condensate to the evaporator is controlled by the throttle valve to match the pumping rate of the compressor.

Cycle Analysis

Figure 1.1b shows a plot on the pressure enthalpy diagram of the locus of all state points traversed by the working fluid in the course of one circuit. The standard theoretical cycle shown here has saturated liquid at point 2 and saturated vapour at point 4. The throttling 2-3 is assumed to be isenthalpic, and the compression 4-1 is assumed to be isentropic. Furthermore, the processes 1-2 & 3-4 are treated as isobaric.

While any real cycle deviates from this specification on all these counts, the theoretical cycle furnishes a convenient standard referance. For instance, it allows one to calculate the theoretical C.O.P. for different refrigerants, and so assist in deciding which refrigerant to use.

Refrigerant Choice

A wide choice of refrigerants suitable for heatpump duty is now available. In order to obtain a compact and efficient compressor, it is advantageous to have a high product of latent heat & suction gas density. Of the 4 refrigerants considered by Sumner, (4) dichlorodifluoromethane, CCl_2F_2, also known as R12, is the best on this count. While R502 and R22 (not considereo by Sumner) have a more favourable product of latent heat and density, their use in a heat pump introduces other penalties. For the purpose of illustration, consider the operation of the system with an evaporating temperature of 0C and a condensing temperature of 50C, as summarised in table 1.1 below.

Comparison of capacity and C.O.P. for three refrigerants

	R12	R502	R22
Evaporating pressure, Bar	3.1	5.7	5.0
Condensing pressure, Bar	12.2	21.0	19.4
Discharge temperature, C	56	60	78
Work of Compression KJ/Kg	25	27	35
Heat produced KJ/Kg	127	113	177
C.O.P.	5.1	4.2	5.1
Suction Volume/output, L/KJ	0.35	0.26	0.26

Table 1.1

As can be seen, the suction gas volume per unit output is more favourable for R22 and R502 than for R12. However, in the case of R502 this is alloyed by the poorer theoretical C.O.P. and the higher discharge gas pressure. A compressor designed to cope with a high discharge pressure such as this has to have correspondingly more substantial bearings, with an additional further penalty on mechanical losses, so eroding the initial promise held out by the favourable suction density. While R22 affords the same theoretical C.O.P. as R12, like R502 it necessitates a high discharge pressure. Additionally, the temperature rise on compression is appreciably greater (5). While the discharge temperature of 78C is acceptable, for real cycles the suction gas is appreciably superheated before entry into the cylinder, which results in a corresponding increase in superheat of the discharge gas. For these reasons, R12 is commonly regarded as the best compromise available for heat pump duty, while R22 is used for refrigerators and freezers, as these normally involve a lower condensing temperature than that required of a heat pump.

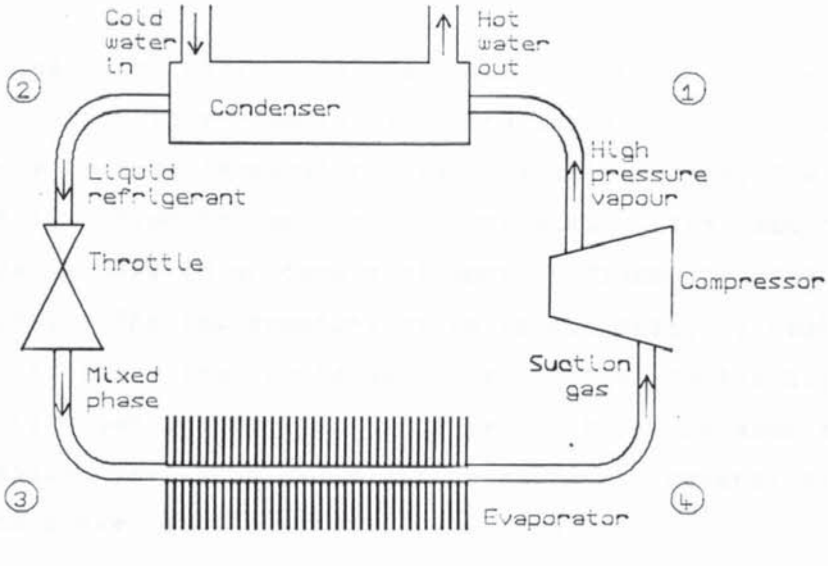

Figure 1.1a. Rankine cycle heat pump circuit

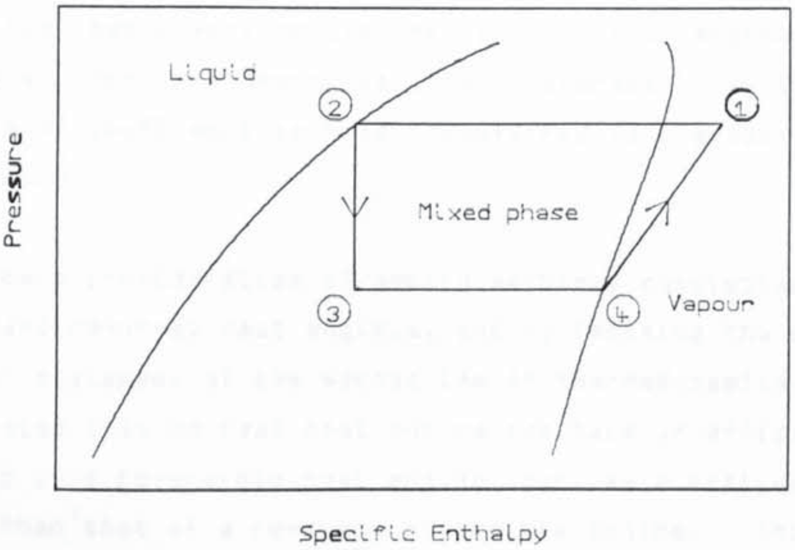

Figure 1.1b. Rankine heat pump cycle on P - h plane

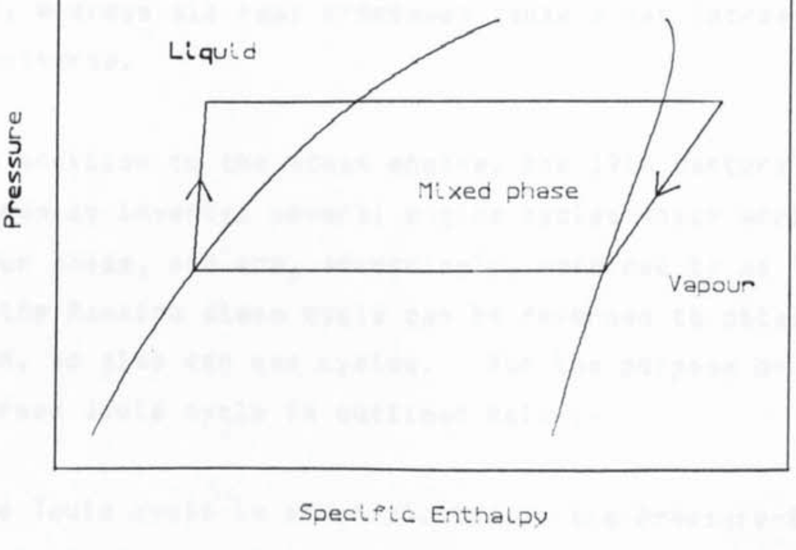

Figure 1.1c. Rankine engine cycle on P - h plane

1.2 Other Methods of Obtaining Heatpump Operation

During the 19th century, interest was primarily focused on engines, the most obvious example being the steam engine. In a steam engine a source of high temperature heat, usually burning fuel, is used to boil water at a high temperature and pressure. The resulting high pressure steam is used to produce shaftwork by de-compressing it in a suitable engine. The low pressure steam is condensed by heat transfer to ambient. Finally, the liquid water is returned to the boiler by a pump. This is known as the Rankine cycle. It can be seen that the vapour compression heat pump cycle approximates the reverse of the Rankine engine cycle, as illustrated by figure 1.1c.

It should be mentioned that in thermodynamics the word 'reversible' has a very special meaning. If an engine is described as reversible, then this means that, when reversed to work as a heatpump, the ratio of shaft work to heat transferred is the same as in operation as an engine.

From a consideration of hybrid machines consisting of coupled heat engines and reversed heat engines, and by imposing the constraint of Clausius' statement of the second law of thermodynamics, it has been demonstrated that no real heat engine can have an efficiency greater than that of a reversible heat engine, nor, as a heatpump, have a C.O.P. greater than that of a reversed reversible engine. This ultimately leads to the establishment of entropy as a function of state, and the demonstration that reversible processes conserve the entropy of the universe, whereas all real processes cause a net increase in the entropy of the universe.

In addition to the steam engine, the 19th century pioneers of thermodynamics invented several engine cycles which worked entirely in the vapour phase, and are, accordingly, referred to as 'gas cycles'. Just as the Rankine steam cycle can be reversed to obtain heatpump operation, so also can gas cycles. For the purpose of illustration, the reversed Joule cycle is outlined below;-

The Joule cycle is shown plotted in the Pressure-Entropy plane in figure 1.2a. Isentropic compression is followed by cooling to the same

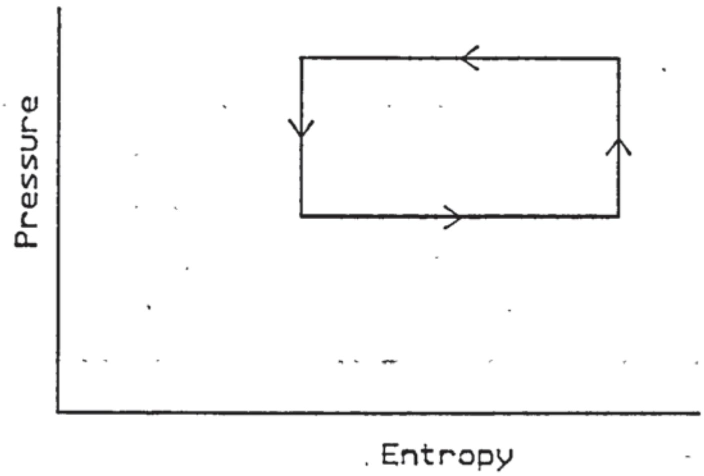

Figure 1.2a. Reversed Joule cycle in P - s plane

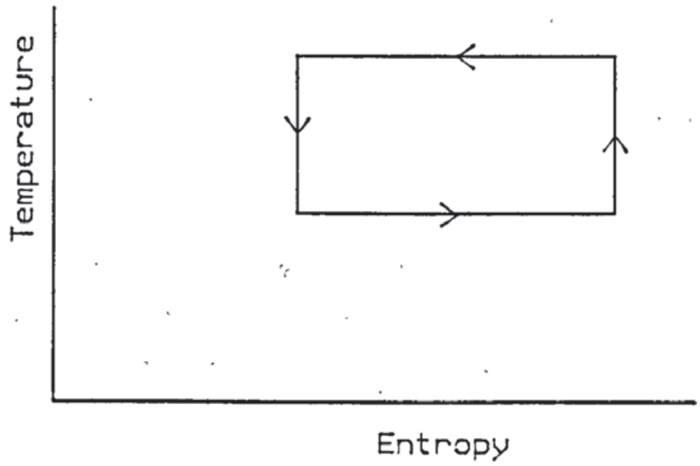

Figure 1.2b. Reversed Carnot cycle in T - s plane

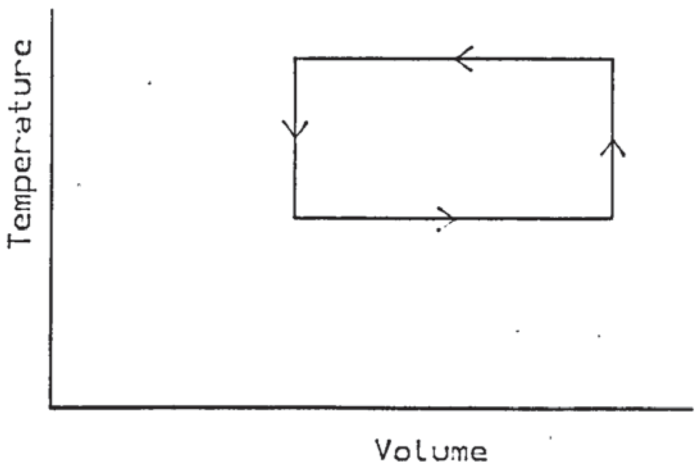

Figure 1.2c. Reversed Stirling cycle in T - v plane

temperature as at the start of the compression stroke. The cooled high pressure gas is then de-compressed through an isentropic expander, from which shaft-work is taken. This brings the gas to a still lower temperature. It is then returned to the starting temperature by heat flow from an ambient source. For an ideal gas, the heat removed during cooling is equal in magnitude to the work done during the compression stroke, thus returning the gas to its initial enthalpy. However, the key point is that in its cooled state, the gas still has the potential to do work by virtue of its high pressure, and it is this work, subsequently made available on re-expansion, that allows a C.O.P. greater than 1.

For a gas cycle working on air it is not necessary to keep the working fluid in a closed cycle. For instance, if the Joule cycle is to be used for cooling, then the re-expanded cold air can be discharged directly into the cooled space, so eliminating the need for a second heat-exchanger (6). W. Thomson first outlined this principle in his pioneering paper of 1852 (7).

There are several other gas cycles. Those of Stirling and Carnot come immediately to mind. Whereas, in the Joule cycle, both heat transfers take place isobarically at a varying temperature, in the Carnot cycle both heat transfers take place isothermally, at a varying pressure. Like the Carnot cycle, the Stirling cycle uses isothermal compression and expansion to transfer heat, but instead of isentropic compression and expansion, it uses constant density heating and cooling to change the pressure. These cycles are shown on figures 1.2b & 1.2c.

<u>Heat Actuated Cycles</u>

If an internal combustion engine working at an efficiency of 30% drives a heat pump with a C.O.P. of 4, then 120% of the heat of combustion of the fuel is made available. Additionally, the waste heat from the engine can be recovered directly at the load temperature. Even if this heat recovery is only 60% efficient, the total useful heat obtained is still 162% of the heat of combustion. This figure of 1.62 is known as the 'Primary Energy ratio', or P.E.R. (8, 9, 10). By comparison, the P.E.R. of an electrically driven heatpump is only 0.3 x C.O.P., because electricity generation and transmission is only about 30% efficient. This is one reason for interest in heat pumps which can be driven by high temperature heat instead of electricity.

As mentioned earlier, the Stirling cycle engine can be reversed to function as a Stirling cycle heat pump. The Stirling engine is an *external* combustion engine. It depends for its operation only on an external source of heat, so that its working fluid can be hermetically sealed in. This has led to recent interest in the possibility of constructing a heat actuated heat pump by using a Stirling engine to drive a reversed Stirling engine. The attraction of this system is that if the engine and heatpump use the same working fluid, then a completely hermetic machine can be constructed, without the problems of shaft seals encountered when using an internal combustion engine to drive a compressor (11).

Similarly, there has been some interest in a Rankine - Rankine heat actuated heat pump, using a Rankine cycle engine to drive a vapour compression heatpump. Again, the use of the same working fluid, a refrigerant, permits an economy and elegance of design (12, & 6 pp 23-27).

Apart from these mechanical engineering subterfuges to obtain a heat-actuated heatpump, there are two heatpump designs in common use which achieve this through the cunning exploitation of two-component thermodynamics. The Electrolux cycle might justifiably be described as a completely passive system. It consists of heat exchangers, piping and 3 working fluids, ammonia, water and hydrogen. The entire system is isobaric, and there is not a single moving part. The absorption cycle is similar in principle, but easier to understand. It usually uses water and ammonia. It works at two pressures, which necessitates the use of a liquid pump, but it is otherwise passive (6, 13)

Thermodynamic limiting performance

Reliance on C.O.P. as a figure of merit can produce misleading conclusions. A more rigorous approach is introduced in the following chapter, but as an illustration of the point, it is helpful to compare the upper limits to C.O.P. for a reversed engine, and for a heat actuated heat pump.

Figure 1.3a is a schematic diagram of a reversed heat engine working between two fixed temperatures, T_1 & T_2. Figure 1.3b similarly shows a heat actuated heat pump, working between the same two temperatures and driven by heat at a fixed higher temperature, T_3. By writing down the equations for the conservation of energy and entropy, one can deduce the upper limit to the C.O.P. of each machine.

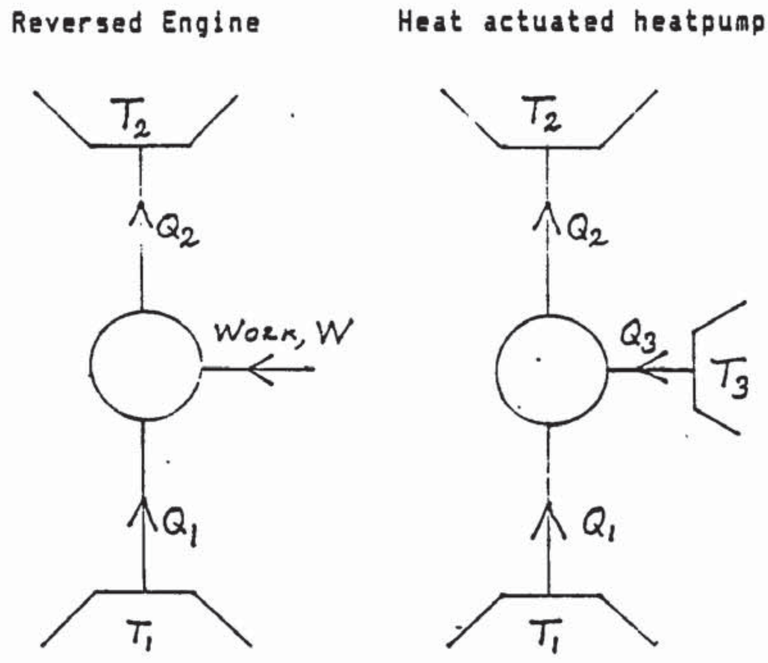

Figure 3a

Figure 3b

Energy conservation	$Q_2 = W + Q_1$	$Q_2 = Q_1 + Q_3$	1.1
Entropy conservation	$\frac{Q_2}{T_2} = \frac{Q_1}{T_1}$	$\frac{Q_2}{T_2} = \frac{Q_1}{T_1} + \frac{Q_3}{T_3}$	1.2
C.O.P.	$\frac{Q_2}{W} = \frac{T_2}{T_2 - T_1}$	$\frac{Q_2}{Q_3} = \frac{T_2}{T_2 - T_1}(1-T_1/T_3)$	1.3

It can be seen that for a heat actuated heat pump, the upper limit to C.O.P. is lower than that for a mechanically driven heatpump by the factor $(1 - T_1/T_3)$.

About 3/4 of the heat of combustion of natural gas is recovered if the combustion products are cooled to 500C. Taking T_1 as 270K, T_3 as 770K, and T_2 as 320K gives an overall upper limit to the C.O.P. of (320/50)(500/770) = 4.16. The P.E.R. is then (3/4)x4.16 = 3.12. For the electrically driven heat pump, the upper limit to the C.O.P. is

(320/50) = 6.4. Guided by C.O.P. alone, one might thus conclude that the electrically driven heat pump has more potential than a heat actuated heat pump. However, such a conclusion is fatally flawed, because it takes no account of the low efficiency with which fuel is used to produce electricity. Taking account of this brings the P.E.R. down to about 2.

In internal combustion engines, the heat of combustion of the fuel is utilised at a high temperature. i.e. T_3 is high, which accounts for the favourable P.E.R. obtainable by using an engine to drive the heatpump. However, for the Stirling - Stirling and Rankine - Rankine systems mentioned earlier, T_3 is limited by considerations of chemical stability of the working fluid and of the lubricant. For the absorption and Electrolux cycles, also, technical constraints preclude the use of a high value of T_3. For instance, limiting T_3 to 450K reduces the upper limit of C.O.P. from 4.16 to 2.56 in the above example.

It should be added that the criticism of electrically driven heat pumps on the basis of P.E.R. overlooks the fact that electricity can be generated from sources that are either unsuitable or inaccessible for domestic use, e.g. nuclear power and hydro-electric power. Furthermore, if one aspires to the ideal of universal use of renewable energy sources, then the criticism in terms of P.E.R. becomes totally invalid.

1.3 Heat pump Sources

As indicated above, the electrical power needed to drive the compressor is a fraction of the heat delivered at the condenser. In view of this, it might seem surprising that heat pumps are not yet popular in Britain. There are several reasons for this. The experience of Sumner (4) suggests that in addition to the technical difficulties, which are not insurmountable, there have also been impediments of a broadly political nature, which are. Before discussing the technical difficulties, it is necessary to mention the choice of ambient sources available, as each proposed source has its own peculiar set of associated advantages and penalties. With the exception of fire, Sumner has identified as potential ambient sources the remaining three elements of ancient Greek philosophy, namely air, earth & water. The general feature common to these three potential sources is an inverse relationship between accessibility and suitability as an ambient source for a heat pump. (6, ch.5)

Air

Air is universally available. An air source heat pump can be assembled in a factory as an integral unit, so minimising the work required for its installation. The evaporator is similar in appearance and design to a car's radiator. Heat is extracted from air which must be blown through it by a fan, figure 1.4. There are 3 major drawbacks which result from the use of an air-source evaporator.

As outdoor air temperature falls, the pressure in the evaporator must be brought still lower by the compressor, in order to maintain the boiling point below the air temperature. This results in a fall in vapour density. Current standard compressor designs have an approximately constant swept volume rate. Consequently, the effect of a fall in suction gas density is to lower the mass flow rate of refrigerant, and correspondingly lower the power output at the condenser. On the other hand, the power requirement to maintain indoor air temperature rises with falling outdoor temperature, figure 1.5.

The second major difficulty is that of defrosting. In typical Winter weather, the air temperature is rarely high enough for the evaporating temperature to exceed OC. At the same time, the air temperature is rarely low enough to make the water vapour fraction negligible. Consequently, water vapour from the air freezes onto the evaporator. The frost that accumulates on the evaporator has a high thermal resistance, because of the air trapped in it. Its accumulation thus makes the evaporator increasingly ineffective. Whereas one would only expect to need to defrost a refrigerator every few weeks, because air has to be continuously blown through the air evaporator of a heatpump, it can require defrosting as often as once every hour, during continuous operation.

Several control strategies have been used by McMullan & Morgan (14) to periodically defrost the evaporator, and to automatically switch

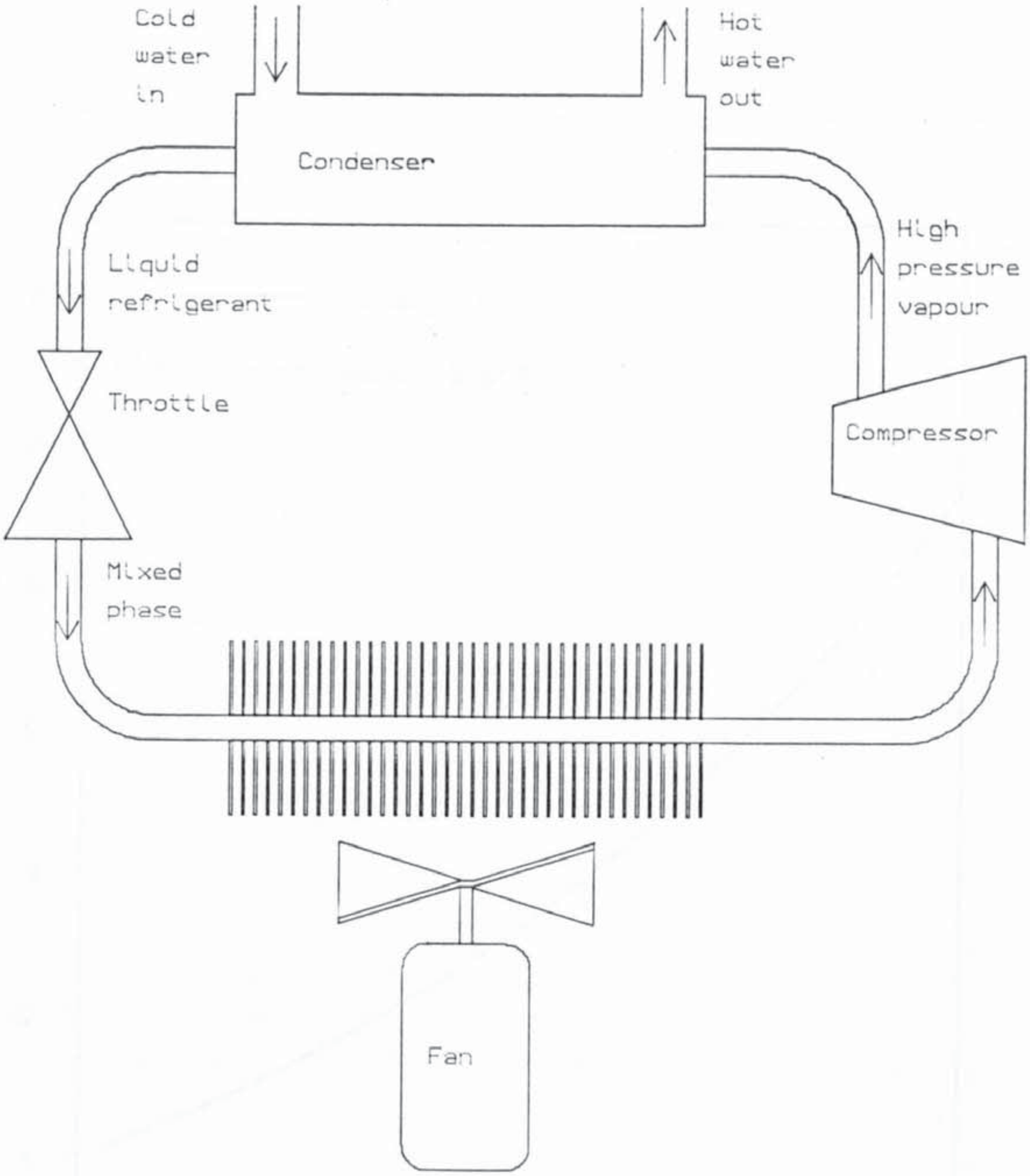

Figure 1.4: Air source heat pump

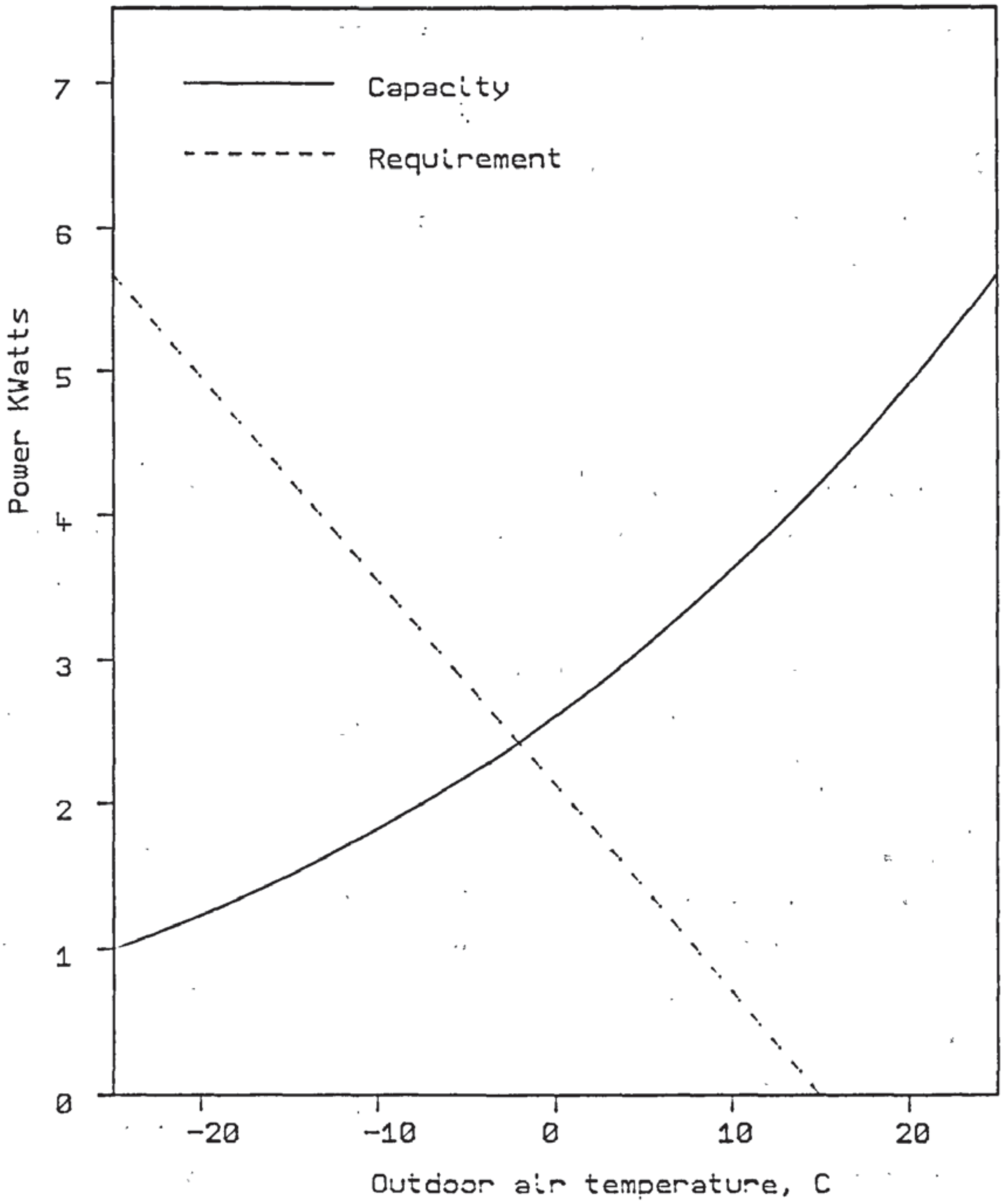

Figure 1.5. Mismatch problem of air-source heat pump

in electric resistance heating at very low ambient temperature, when the heat pump output cannot match the demand.

To summarise, then, there are three designed-in parasitic losses, eroding the initially promising performance of the basic heat pump.

i) The need to drive a fan continuously.

ii) The need to defrost the evaporator periodically.

iii) The use of electric resistance heaters during periods of very cold weather.

Five years earlier, in his book, (4) Sumner considered these points and criticised these 'crude expedients' as being 'a gross misuse of energy' (pp61-63). Instead, a very strong case was proposed in favour of a ground source.

Earth

If the ground outside a building is used as the heat source for the evaporator, then the three principal penalties incurred by using an air-source can be avoided.

The basis of the ground source heatpump is a long length, typically 100-300m, of pipe buried in a suitable piece of ground, usually the back garden. A variety of different pipe configurations has been considered at Brookhaven National Laboratory, where an impressive research effort has been directed at the potential of ground coupled heat pumps. (15, 16, 17) This pipe can be used as the evaporator, liquid admitted directly into it from the throttle valve, with the compressor inlet connected directly at the other end, figure 6. While this configuration is ideal, from the thermodynamic viewpoint, in that it minimises the difference between the evaporating temperature and the ground temperature, it carries with it a potential hazard of a technical nature. Specifically, in such a long length of pipe, there could be a considerable accumulation of oil, which escapes from the compressor with the discharge gas. This incurs 3 penalties.

i) The compressor may run short of oil.

ii) The evaporating pressure is depressed due to admixture of oil in the liquid phase (Raoult's law).

iii) The suction pressure may be further, significantly reduced due to aggravation of the flow pressure drop by the oil in the ground coil.

These problems have been avoided in the past by circulating brine or antifreeze solution through the ground coil. This liquid is known as a 'secondary refrigerant'. This serves as an intermediate heat transfer medium from the ground to the refrigerant in the evaporator. The evaporator cools the secondary refrigerant to a temperature sufficiently below the ground temperature to ensure heat flow into it during its subsequent circuit through the ground coil, figure 1.7. It is this heat which ultimately furnishes the latent heat of evaporation of the refrigerant.

The very favorable specific heat per unit volume of the secondary refrigerant permits a more compact evaporator design, and results in a less serius pumping power penalty than in the case of the air evaporator. However, it should be pointed out that since the evaporating temperature cannot exceed the lowest secondary refrigerant temperature, this strategy incurs the penalty of reducing the evaporating temperature and pressure with a concomitant loss in capacity & C.O.P.

In normal operation, the water in the soil adjacent to the ground coil freezes. Unlike the air evaporator, however, the resulting degradation of heat transfer is tolerable, and the sizing of the ground coil is based on the supposition that this occurs. i.e. there is no defrosting problem. However, care must be taken when planning a ground coil layout to avoid proximity to water pipes, drains, gas pipes, electrical cables etc.

By using a ground source heat pump, one achieves considerable immunity from short periods of very low air temperature. For the purpose of illustration, suppose one's ground coil draws heat from 100m^3 of soil, e.g. 5m x 10m x 2m depth. Assuming a heat capacity per unit volume similar to that of water, the total heat capacity comes to 400MJ/K, or roughly 5KWdays/K. In the course of an ambient temperature depression by, for example, 10K for 2 days, one might realistically expect only a 2 or 3 Kelvin fall in the source temperature, and so avoid

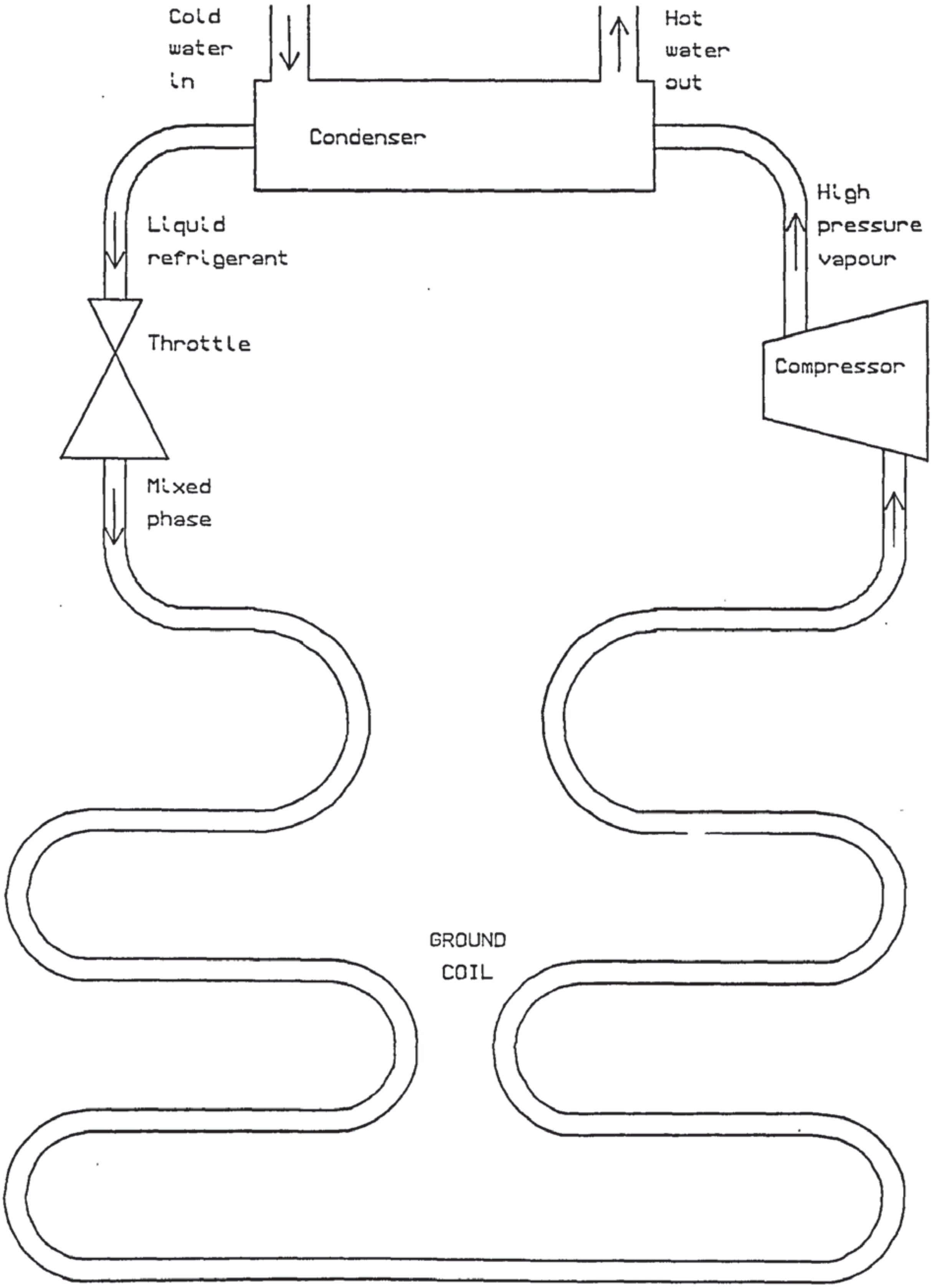

Figure 1.6. Directly coupled ground source

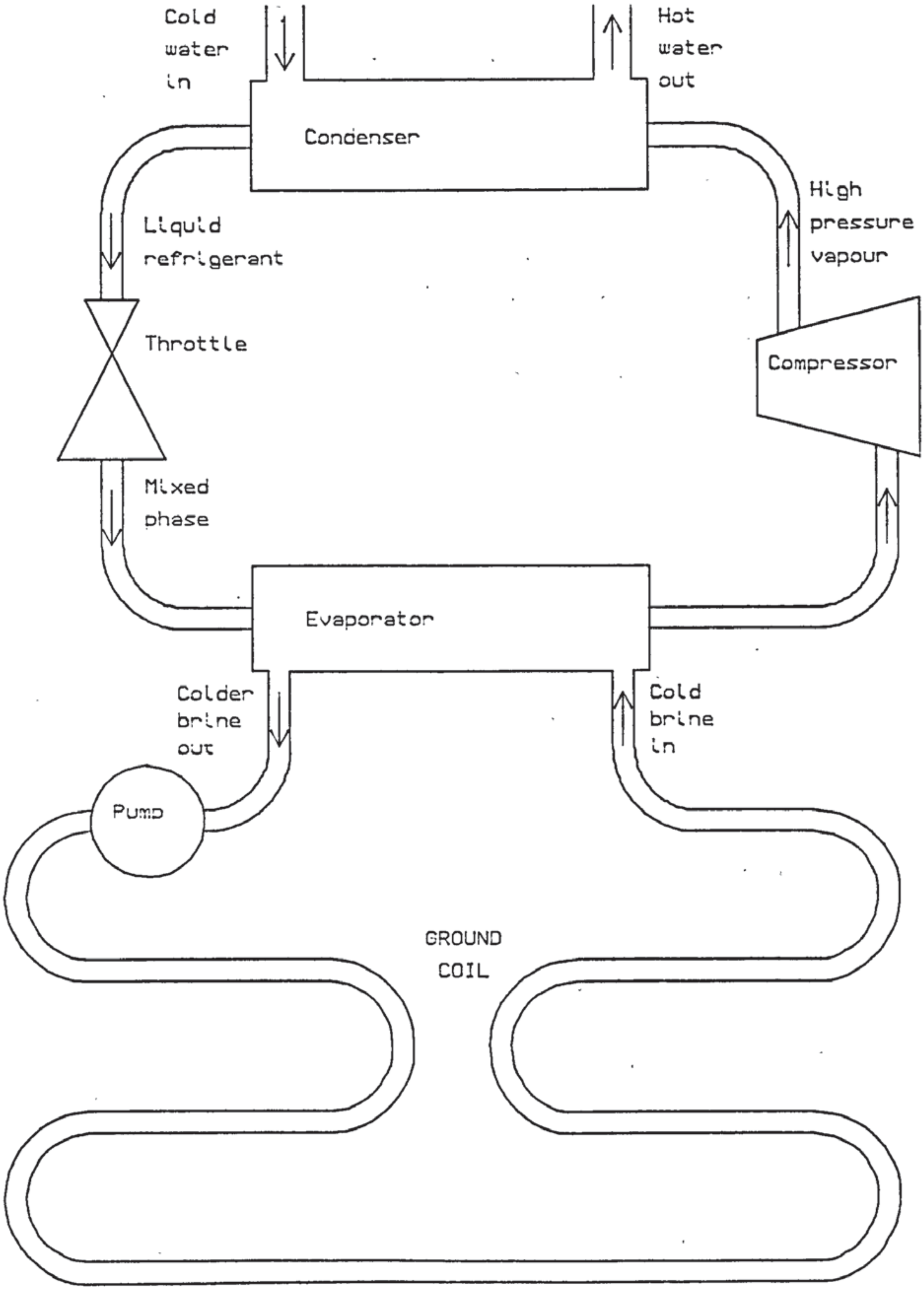

Figure 1.7. Ground source, using secondary refrigerant

the need to incorporate backup electric resistance heating into the system. The above estimate is actually very conservative, as it ignores the latent heat of formation of ice. At 320MJ/m^3, or 4KWdays/m^3, it can be seen that the total potentially accessible heat is an order of magnitude greater than that indicated by a consideration of sensible heat alone.

It is worth pointing out that while the heat capacity of a ground source is impressive, it normally falls short of sufficient for a complete heating season. Most of the heat obtained derives originally from the combined effects of solar gain and transfer from the air above. For this reason, it can be thought of as an air source, which enjoys the advantages of a very large thermal reservoir, and immunity from the need to defrost.

Water

The high heat capacity per unit volume and favourable temperature of liquid water makes this an ideal source for a heatpump, if a sufficient quantity is available. While heat recovery from waste water from sinks and baths can make a useful contribution, this can yield only a fraction of the normal winter heating requirement. Where sufficient surface water is available, whether a stream or a pool, favourable heatpump operating conditions have been obtained. Additionally, by direct immersion of the evaporator, the 2 penalties associated with a secondary refrigerant circuit, pumping power and evaporating temperature depression, can be eliminated. (4, p45)

The feasibility of using deep ground water has also been demonstrated, but there are additional technical difficulties. The principle advantage of ground water over surface water is its near constant year-round temperature.

1.4 Drying

Unlike any other method of producing heat, the heat pump enjoys the unique ability to reduce the concentration of water vapour in air, and utilise the latent heat so recovered, which makes it emminently suitable for drying. A domestic drying unit was proposed in 1975 (18), but the greatest potential for saving lies with industry (19). So far, greatest interest has been shown in wood seasoning.

A drying unit uses air heat exchangers for both the evaporator and the condenser. Air is cooled by blowing it through the evaporator. This condenses out a proportion of the water vapour in it. The air then passes through the condenser to heat it. There is an overall temperature lift due to the latent heat recovered at the evaporator, and due to the power consumption of the compressor. The warm, dry air then circulates through the timber, to emerge at a lower temperature and near 100% humidity. This is recirculated through the evaporator, and so the air circuit goes on.. (6, ch 7)

Of all industrially used primary energy, 25% is used for drying. This high cost of drying is mainly due to the continuing profligate practice of disposing of the water so removed as a vapour, instead of recovering the latent heat. This situation is not helped by current legislation which deems as an "industrial effluent" the water produced by latent heat recovery.

1.5 Conclusion

Since the first outline of the potential of heat pump technology to save fuel used for heating, all the multitudinous proposed system designs have been beset by a combination of technical difficulties and thermodynamic penalties which have eroded the spectacular performance possible in theory to a comparatively marginal gain over more conventional means of heating. Gas fired heating systems, in particular, have low running costs, with which heat pumps cannot yet compete. (3, p.3) The key to making heat pump technology attractive to its potential customers is to narrow the gulf between the performance currently achieved in practice and the theoretical limit. This is the reason why ongoing research is necessary.

2.1 Performance Calculation

The analysis of a Rankine cycle heat pump is based on the evaluation of the state of the working fluid at points 1,2 & 4 of figure 1.1b. The specific enthalpy lift 1 - 4 is furnished by the electricity supplied to the compressor. The specific enthalpy change 1 - 2 indicates the amount of heat supplied at the condenser by unit mass of refrigerant. Thus the C.O.P. is given as;-

$$\text{C.O.P.} = (h_1 - h_2)/(h_1 - h_4) \qquad 2.1$$

The capacity is given by;-

$$\text{Condenser power output} = \dot{m}_r (h_1 - h_2) \qquad 2.2$$

Where the refrigerant mass flowrate is given by;-

$$\dot{m}_r = \eta_{vol} \dot{V}/v_4 \qquad 2.3$$

Where $\dot{V}$ is the product of the compressor's swept volume and frequency. This last equation follows from the definition of η_{vol}, the volumetric efficiency;-

$$\eta_{vol} = \frac{\text{suction gas volume displacement rate}}{\text{Compressor's swept volume rate}} \qquad 2.4$$

Since η_{vol} is normally close to 1, and insensitive to changes in operating conditions, one can see that the system's capacity is dictated primarily by the suction gas specific volume, v_4.

The calculations outlined above used to be executed by the tedious and laborious method of looking up tables of thermodynamic data, and manually interpolating between the available data points to obtain the relevant functions of state for the operating conditions of interest. However, if it is required to perform a comparison of several design options for a range of operating conditions, then the anticipated large number of such calculations justifies automation of the procedure by writing a computer programme based on the equations of state.

2.2 Derivation of Functions of State from Equations of State

The specification of the state of the working fluid at any point in the cycle is not complete unless the values of temperature, pressure, specific entropy, specific volume, and specific enthalpy are known. (Of the four energy functions, any one is sufficient to complete the specification. It is convenient to use the enthalpy, as this implicitly includes flow work.)

In order to solve the Rankine cycle, it is necessary to be able to obtain this complete specification given values of 2 of these functions of state. For instance, the discharge pressure, P_1, suction pressure, P_4, and suction temperature, T_4, may be known. Given P_4 & T_4, it is possible to find v_4, s_4, & h_4 from the equations of state. If the compression is isentropic, then $s_1 = s_4$. Now the discharge state can be solved, given that P_1 & s_1 are known. It will be shown later that the need also arises to solve for s, v & T given known values of P & h.

For the superheated vapour, two equations are necessary & sufficient for the calculation of all functions of state. The following explanation was inspired by Haywood's paper of 1969 (20). The first equation is usually presented as an algebraic equation for the pressure as an explicit function of the independent variables T & v.

$$P = P(T,v) \qquad 2.5$$

The second equation is an expression for the isochoric specific heat in the ideal gas limit as an explicit function of T alone;-

$$c_{v\to\infty} = c_v(T) \qquad 2.6$$

At this stage, for the purpose of showing how the functions of state can be derived, it is not appropriate to introduce explicit algebraic equations, as this would risk obscuring with detail the underlying thermodynamic principles.

From equations 2.5 & 2.6 an explicit algebraic expression for entropy can be derived as a function of T & v. This follows from the two identities;-

$$\frac{\partial s}{\partial v}_T = \frac{\partial P}{\partial T}_v \qquad 2.7$$

$$\frac{\partial s}{\partial T}_v = \frac{1}{T} c_v \qquad 2.8$$

Equation 2.7 is just a Maxwell relation. The equations of state are chosen deliberately to ensure that equations 2.7 & 2.8 are analytically integrable to yield an explicit algebraic expression for s as a function of v & T.

Having chosen to work with T & v as independent variables, the most straightforward route to the energy functions is to use the specific Helmholtz free energy, f, which satisfies the two identities;-

$$\frac{\partial f}{\partial T}_v = -s(T,v) \qquad 2.9$$

$$\frac{\partial f}{\partial v}_T = -P(T,v) \qquad 2.10$$

Once again then, an explicit algebraic expression in T & v can be found by straightforward integration. The specific enthalpy then follows from $h = f + Ts + Pv$.

Equations and Functions of State of Vapour

A wide variety of functionally different equations of state have been fitted for different refrigerant vapours. Fortunately, the properties of more than a dozen refrigerants have been fitted to the Martin-Hou equation of state (21,22) and the different sets of co-efficients have been collected in Downing's paper of 1974 (23). Thus, by basing the thermodynamic algorithms on the Martin-Hou equation, cycle analyses can be performed for different refrigerants simply by loading the appropriate set of co-efficients.

Unfortunately, Downing's co-efficients are all in imperial units. It is preferable to work entirely in S.I. units, as this eliminates the need to include conversion factors in a programme. As explained in Appendix 1, a short programme has been written which converts Downing's co-efficients to S.I. units and stores them on a floppy disc file. In the following derivations a close adherence to the symbolism of Downing's paper has been maintained.

Derivation of s(T,v)

The Martin-Hou equation is;-

$$P(T,v) = \frac{RT}{v - b} + \sum_{j=2}^{5} \frac{A_j + B_jT + C_j\exp(-KT/T_c)}{(v - b)^j} \qquad 2.11$$

It has been found helpful to define three functions of volume $Y_1(v)$, $Y_2(v)$ & $Y_3(v)$ by the following equations;-

$$Y_1(v) = \sum_{j=2}^{5} \frac{A_j}{(v - b)^j} \qquad 2.12$$

$$Y_2(v) = \frac{R}{(v - b)} + \sum_{j=2}^{5} \frac{B_j}{(v - b)^j} \qquad 2.13$$

$$Y_3(v) = \sum_{j=2}^{5} \frac{C_j}{(v - b)^j} \qquad 2.14$$

Expressed in terms of these functions, the Martin-Hou equation becomes;-

$$P(T,v) = Y_1(v) + Y_2(v)T + Y_3(v)\exp(-KT/T_c) \qquad 2.15$$

For the isochoric specific heat in the ideal gas limit, a simple polynomial is used;-

$$c_v(T,v\to\infty) = a + bT + cT^2 + dT^3 + g/T^2 \qquad 2.16$$

The differential equations for entropy, 2.7 & 2.8, then become;-

$$\frac{\partial s}{\partial v}_T = Y_2(v) - (K/T_c)\exp(-KT/T_c)Y_3(v) \qquad 2.17$$

$$\frac{\partial s}{\partial T}_v = a/T + b + cT + dT^2 + g/T^3 \qquad 2.18$$

Upon integrating equations 2.17 & 2.18, the solution for s(T,v) can be written as;-

$$s = a\ln T + bT + \frac{cT^2}{2} + \frac{dT^3}{3} - \frac{g}{2T^2} + Z_2 - (\frac{K}{T_c})\exp(-\frac{KT}{T_c})Z_3 + s_o \qquad 2.19$$

where $Z_i(v)$ is the indefinite integral w.r.t. v of $Y_i(v)$ i.e;-

$$Z_1(v) = -\sum_{j=2}^{5} \frac{A_j}{(j-1)(v-b)^{(j-1)}} \qquad 2.20$$

$$Z_2(v) = R\ln(v-b) - \sum_{j=2}^{5} \frac{B_j}{(j-1)(v-b)^{(j-1)}} \qquad 2.21$$

$$Z_3(v) = -\sum_{j=2}^{5} \frac{C_j}{(j-1)(v-b)^{(j-1)}} \qquad 2.22$$

Derivation of f(T,v) & h(T,v)

The differential equations for the specific Helmholtz free energy, f(T,v), can now be obtained by substituting equations 2.15 & 2.19 into identities 2.9 & 2.10;-

$$\frac{\partial f}{\partial v}_T = - Y_1(v) - Y_2(v)T - Y_3(v)\exp(-KT/T_c) \qquad 2.23$$

$$\frac{\partial f}{\partial T}_v = - a\ln T - bT - \frac{cT^2}{2} - \frac{dT^3}{3} + \frac{g}{2T^2} - Z_2 + (\frac{K}{T_c})\exp(-\frac{KT}{T_c})Z_3 - s_o \qquad 2.24$$

Upon integrating these two differential equations, the result is;-

$$f=-a(T\ln T-T)- \frac{bT^2}{2}- \frac{cT^3}{6}- \frac{dT^4}{12}- \frac{g}{2T} -TZ_2-\exp(- \frac{KT}{T_c})Z_3-Ts_o-Z_1+f_o \qquad 2.25$$

An algebraic expression for the specific enthalpy, h, can now be written down by adding Ts + Pv to f. A considerable simplification results thanks to cancellation of several terms in Ts with identical terms in f. The result is;-

$$h = aT + \frac{bT^2}{2} + \frac{cT^3}{3} + \frac{dT^4}{4} - \frac{q}{T} - (1+\frac{KT}{T_c})\exp(-\frac{KT}{T_c})Z_3 - Z_1 + f_o + Pv \qquad 2.26$$

The programme which converts Downing's co-efficients to S.I. units ends by calculating the integration constants s_o & f_o. The convention is adopted that at 0C, the liquid's enthalpy is 200 KJ/Kg and its entropy is 1 KJ/(KgK).

Differential coefficients

As indicated earlier, it is not usually T & v that are known. It may be P & T, or P & s, for instance. For this reason, it is necessary to use algorithms based on the Newton-Raphson method to solve the appropriate equation(s) for v, T, or both. This requires that equations be included for the evaluation of the three differential co-efficients $(\partial P/\partial T)_v$, $(\partial P/\partial v)_T$, $(\partial s/\partial T)_v$ which can be found by differentiation of equations 2.15 & 2.19;-

$$\frac{\partial P}{\partial T_v} = Y_2(v) - (K/T_c)\exp(-KT/T_c)Y_3(v) \qquad 2.27$$

$$\frac{\partial P}{\partial v_T} = X_1(v) + X_2(v)T + X_3(v)\exp(-KT/T_c) \qquad 2.28$$

where $X_i(v)$ is the derivative w.r.t. v of $Y_i(v)$. i.e.

$$X_1(v) = -\sum_{j=2}^{5} \frac{(j+1)A_j}{(v-b)^{(j+1)}} \qquad 2.29$$

$$X_2(v) = \frac{-R}{(v-b)^2} - \sum_{j=2}^{5} \frac{(j+1)B_j}{(v-b)^{(j+1)}} \qquad 2.30$$

$$X_3(v) = -\sum_{j=2}^{5} \frac{(j+1)C_j}{(v-b)^{(j+1)}} \qquad 2.31$$

And lastly;-

$$\frac{\partial s}{\partial T}_v = a/T + b + cT + dT^2 + g/T^3 + (K/T_c)^2 \exp(-KT/T_c) Z_3 \qquad 2.32$$

Newton Raphson method

For the purpose of illustration, consider the problem of finding the state of the gas after an isentropic change of pressure. i.e. the problem of finding v & T given that s & P are known.

Let s,v,P,T pertain to the true state point of interest.
Let v_t, T_t = trial values of specific volume and temperature.
Let δv, δT = required corrections to v_t & T_t. i.e $v = v_t + \delta v$ & $T = T_t + \delta T$

By considering a first order Taylor expansion, one can write;-

$$P(T,v) = P(T_t,v_t) + \frac{\partial P}{\partial T}_v (T-T_t) + \frac{\partial P}{\partial v}_T (v-v_t) \qquad 2.33$$

$$s(T,v) = s(T_t,v_t) + \frac{\partial s}{\partial T}_v (T-T_t) + \frac{\partial s}{\partial v}_T (v-v_t) \qquad 2.34$$

These two approximations furnish two linear algebraic equations for the two corrections required to the trial values of volume and temperature. Rewriting as a matrix equation;-

$$\begin{bmatrix} \frac{\partial P}{\partial T}_v & \frac{\partial P}{\partial v}_T \\ \frac{\partial s}{\partial T}_v & \frac{\partial s}{\partial v}_T \end{bmatrix} \begin{bmatrix} \delta T \\ \delta v \end{bmatrix} = \begin{bmatrix} P(T,v)-P(T_t,v_t) \\ s(T,v)-s(T_t,v_t) \end{bmatrix} \qquad 2.35$$

From the well known inversion of a 2x2 matrix, and using the identity 2.7, this becomes;-

$$\begin{bmatrix} \delta T \\ \delta v \end{bmatrix} = \frac{1}{\frac{\partial P}{\partial T}_v^2 - \frac{\partial P}{\partial v}_T \frac{\partial s}{\partial T}_v} \begin{bmatrix} \frac{\partial P}{\partial T}_v & -\frac{\partial P}{\partial v}_T \\ -\frac{\partial s}{\partial T}_v & \frac{\partial P}{\partial T}_v \end{bmatrix} \begin{bmatrix} P(T,v)-P(T_t,v_t) \\ s(T,v)-s(T_t,v_t) \end{bmatrix} \qquad 2.36$$

Then $v_{improved} = v_t + \delta v$ & $T_{improved} = T_t + \delta T$

By using the improved values of T & v as a new trial solution at which to recalculate $s(T_t, v_t)$, $P(T_t, v_t)$, and the differential co-efficients, the exact solution can be approached to any desired accuracy.

The above illustration is an example of the two dimensional Newton-Raphson method. While the one dimensional form of this method is well known, its application to higher dimensions is less generally appreciated.

Equations & Functions of State for Liquid

In order to solve the Rankine cycle, it is necessary to deduce the complete specification of the working fluid at the end of the condenser, vertex 2 on the cycle diagram, figure 1.1. For this purpose, two further equations are essential. These are the vapour pressure equation, $P_{sat}(T)$, and the saturated liquid density as a function of temperature, $\rho_{sat}(T)$.

If the temperature is specified, then the saturated vapour's pressure, entropy, specific volume and enthalpy all follow from the appropriate equations. By first calculating the saturated liquid density from $\rho_{sat}(T)$, s_{liq} & h_{liq} can be found from the Clausius Clapeyron equation;-

$$(s_{vap} - s_{liq}) = (v_{vap} - v_{liq})\frac{dP}{dT}_{sat} \qquad 2.37$$

Since the entropy change of condensation occurs isothermally, the latent heat, Δh_{lat}, is given simply as;-

$$\Delta h_{lat} = T(s_{vap} - s_{liq}) \qquad 2.38$$

In this way, for any condensing or evaporating temperature, a complete specification of the saturated liquid state can be deduced.

The Equations

For the saturated liquid density, the equation is;-

$$\rho = A_L + B_L(1 - X)^{1/3} + C_L(1 - X)^{2/3} + D_L(1 - X)$$

$$+ E_L(1 - X)^{4/3} + F_L(1 - X)^{1/2} + G_L(1 - X)^2 \qquad 2.39$$

where $X = T/T_c$, the reduced temperature.

For the saturated vapour pressure, the equation is;-

$$Ln(P) = A + B/T + CLn(T) + DT + E((F-T)/T)Ln(F - T) \qquad 2.40$$

Then, the Clausius Clapeyron equation becomes;-

$$\Delta s = (v_{vap}-v_{liq})P[-B/T^2 + C/T + D T - (E/T)[1+(F/T)\ln(F-T)]] \qquad 2.41$$

Subcooled Liquid

Given that it is possible to deduce all the functions of state of saturated liquid over a temperature range from the triple point to the critical point, it comes as a surprise to realise that a unique derivation of the state of subcooled liquid remains elusive. This is demonstrated in Appendix 2, where it is shown that the subcooled liquid specification is best obtained by adding appropriate pressure corrections to the functions of state of the saturated liquid at the same temperature.

Thermodynamics Procedure Library

On the following three pages the procedures are listed in which the foregoing has been put into practice.

Loading equation of state co-efficients, and manipulating P(T,v)

```
 9000 DEF PROCloadCo_effs(R$)
 9500 A$="C."+R$
 9510 D%=OPENIN(A$)
 9520 INPUT£D%,A1,B1,C1,D1,E1,F1,G1:  REM Saturated liquid density
 9530 INPUT£D%,A,B,C,D,E,F         :  REM Saturated vapour pressure
 9540 INPUT£D%,a,b,c,d,f           :  REM Isochoric specific heat
 9550 INPUT£D%,R,bv                :  REM Vapour P(T,v) co-efficients
 9560 INPUT£D%,A2,B2,C2,A3,B3,C3,A4,B4,C4,A5,B5,C5
 9570 INPUT£D%,K,Tc,so,fo,Pc,vc
 9580 CLOSE£D%
 9590 K=K/Tc
 9600
 9610 xA5=A5*5:xA4=A4*4:xA3=A3*3:xA2=A2*2:  REM co-efficients for dP/dv
 9620 xB5=B5*5:xB4=B4*4:xB3=B3*3:xB2=B2*2
 9630 xC5=C5*5:xC4=C4*4:xC3=C3*3:xC2=C2*2
 9650
 9660 zA5=A5/4:zA4=A4/3:zA3=A3/2:  REM co-efficients for integral(Pdv)
 9670 zB5=B5/4:zB4=B4/3:zB3=B3/2
 9680 zC5=C5/4:zC4=C4/3:zC3=C3/2
 9700 ENDPROC
10000  REM     THERMODYNAMICS OF VAPOUR
10001  REM     ~~~~~~~~~~~~~~~~~~~~~~~~
10002
10010  REM  Volume dependent terms in dP/dv
10020  REM  ~~~~~~~~~~~~~~~~~~~~~~~~~~~~~~~~
10025 DEF PROCXs(v)
10027 Ro=1/(v-bv):R2=Ro*Ro:R3=R2*Ro
10030 X1=-R3*(Ro*(Ro*(Ro*xA5+xA4)+xA3)+xA2)
10040 X2=-R2*(Ro*(Ro*(Ro*(Ro*xB5+xB4)+xB3)+xB2)+R)
10050 X3=-R3*(Ro*(Ro*(Ro*xC5+xC4)+xC3)+xC2)
10060 ENDPROC
10090
10100  REM  Volume dependent terms in P(v,T)
10110  REM  ~~~~~~~~~~~~~~~~~~~~~~~~~~~~~~~~~
10115 DEF PROCYs(v)
10117 Ro=1/(v-bv):R2=Ro*Ro
10120 Y1=R2*(Ro*(Ro*(Ro*A5+A4)+A3)+A2)
10130 Y2=Ro*(Ro*(Ro*(Ro*(Ro*B5+B4)+B3)+B2)+R)
10140 Y3=R2*(Ro*(Ro*(Ro*C5+C4)+C3)+C2)
10160 ENDPROC
10190
10200  REM  Volume dependent terms in Integral(Pdv)
10210  REM  ~~~~~~~~~~~~~~~~~~~~~~~~~~~~~~~~~~~~~~~~
10215 DEF PROCZs(v)
10217 Ro=1/(v-bv)
10220 Z1=-Ro*(Ro*(Ro*(Ro*zA5+zA4)+zA3)+A2)
10230 Z2=-Ro*(Ro*(Ro*(Ro*zB5+zB4)+zB3)+B2)-R*LN(Ro)
10240 Z3=-Ro*(Ro*(Ro*(Ro*zC5+zC4)+zC3)+C2)
10260 ENDPROC
```

Functions of state and differential co-efficients

```
10500  REM  Functions of state P(T,v), h(T,v), s(T,v)
10510  REM  ~~~~~~~~~~~~~~~~~~~~~~~~~~~~~~~~~~~~~~~~~
10520  REM  Ensure that Xs, Ys & are evaluated at correct v
10530  REM  Ensure that eKT=EXP(-KT) is evaluated at correct T.
10540
10550 DEF FNP(T)=Y1+T*Y2+Y3*eKT
10560 DEF FNs(T)=a*LN(T)+b*T+c*T^2/2+d*T^3/3-f/(2*T^2)+Z2-K*Z3*eKT+so
10565 DEF FNu(T)=a*T+b*T^2/2+c*T^3/3+d*T^4/4-f/T-Z1-(1+K*T)*eKT*Z3+fo
10570 DEF FNh(T)=a*T+b*T^2/2+c*T^3/3+d*T^4/4-f/T-Z1-(1+K*T)*eKT*Z3+
v*(Y1+T*Y2+Y3*eKT)+fo
10600
10700  REM  Differential co-efficients dP/dT, dP/dV, ds/dT
10710  REM  ~~~~~~~~~~~~~~~~~~~~~~~~~~~~~~~~~~~~~~~~~~~~~~
10720
10730 DEF FNPT(T)=Y2-K*eKT*Y3
10740 DEF FNPv(T)=X1+T*X2+eKT*X3
10750 DEF FNsT(T)=a/T+b+c*T+d*T^2+f/T^3+eKT*Z3*K^2
10755 DEF FNcP(T)=T*(FNsT(T)-(FNPT(T))^2/FNPv(T))
10760
10800  REM  Speed of sound
10805  REM  ~~~~~~~~~~~~~~
10900 DEF FNuson(T,v)=v*SQR((FNPT(T))^2/FNsT(T)-FNPv(T))
10960
10990  REM  End of thermodynamics of vapour
10995  REM  ~~~~~~~~~~~~~~~~~~~~~~~~~~~~~~~
10997
11000  REM  THERMODYNAMICS OF LIQUID
11010  REM  ~~~~~~~~~~~~~~~~~~~~~~~~
11020
11030  REM  Liquid Density
11032  REM  ~~~~~~~~~~~~~~
11034
11040 DEF PROCliquid_rho(T)
11050 X1=1-T/Tc
11060
Lro=A1+B1*X1^(1/3)+C1*X1^(2/3)+D1*X1+E1*X1^(4/3)+F1*SQR(X1)+G1*X1^2
11065 ENDPROC
11100
11120  REM Saturated vapour pressure
11121  REM ~~~~~~~~~~~~~~~~~~~~~~~~~
11122
11130 DEF FNPs(T)=EXP(A+B/T+C*LN(T)+D*T+E*(F/T-1)*LN(F-T))
11150
11200  REM  Clausius-Clapeyron Equation
11210  REM  ~~~~~~~~~~~~~~~~~~~~~~~~~~~
11220
11230 DEF PROCC_Cequn(T)
11240 PROCliquid_rho(T):Lv=1/Lro
11250 P=FNPs(T)
11260 PROCv(P,T)
11265 dPdT=P*(-B/T^2+C/T+D-(E/T)*(1+(F/T)*LN(F-T)))
11270 DsCon=(v-Lv)*dPdT
11290 PROCZs(v)
11300 Vs=FNs(T):Vh=FNh(T)                  :REM  Vapour s & h
11310 Ls=Vs-DsCon:Lh=Vh-T*DsCon            :REM  Liquid s & h
11390 ENDPROC
```

Newton Raphson algorithms for inverting equations of state

```
12000  REM   Solution for v given P & T
12010  REM   ~~~~~~~~~~~~~~~~~~~~~~~~~~
12015 DEF PROCv(P,T)
12020 eKT=EXP(-K*T):v=R*T/P
12030 PROCXs(v):PROCYs(v)
12040 dv=0.8*(P-FNP(T))/FNPv(T)
12050 v=v+dv
12060 IF ABS(dv/v)>.00001 THEN 12030
12070 ENDPROC
12080
12100  REM   Solution for T given s & v
12105  REM   ~~~~~~~~~~~~~~~~~~~~~~~~~~
12110 DEF PROCTsoln(s,v,Tt): T=Tt: PROCYs(v): PROCZs(v):
slope=1/FNsT(T)
12130
12140 REPEAT:eKT=EXP(-K*T):dT=(s-FNs(T))*slope:T=T+dT:UNTIL
ABS(dT)<.001
12180 ENDPROC
12200
12210  REM   Solution for v & T given s & P
12220  REM   ~~~~~~~~~~~~~~~~~~~~~~~~~~~~~~
12230 DEF PROCsPsoln(s,P,vt,Tt)
12240 PROCXs(vt):PROCYs(vt):PROCZs(vt):eKT=EXP(-K*Tt)
12250 Pv=FNPv(Tt):sT=FNsT(Tt):PT=FNPT(Tt):Pt=FNP(Tt):st=FNs(Tt)
12260 Det=PT^2-Pv*sT
12270 dT= (PT*(P-Pt)-Pv*(s-st))/Det
12280 dv=(-sT*(P-Pt)+PT*(s-st))/Det
12290 vt=vt+dv:Tt=Tt+dT
12300 IF ABS(dv/vt)<.00001 AND ABS(dT/Tt)<.00001 THEN 12340
12310 GOTO 12240
12340 v=vt:T=Tt
12350 ENDPROC
12360
12400  REM   Solution for v & T given h & P
12410  REM   ~~~~~~~~~~~~~~~~~~~~~~~~~~~~~~
12430 DEF PROChPsoln(h,P,vt,Tt)
12435 v=vt:T=Tt
12440 PROCXs(v):PROCYs(v):PROCZs(v):eKT=EXP(-K*T)
12450 Pv=FNPv(T):sT=FNsT(T):PT=FNPT(T):Pt=FNP(T):ht=FNh(T)
12460 dhdT=T*sT+v*PT
12470 dhdv=T*PT+v*Pv
12480 Det=T*(PT^2-Pv*sT)
12490 dT= (dhdv*(P-Pt)-Pv*(h-ht))/Det
12500 dv=(-dhdT*(P-Pt)-PT*(h-ht))/Det
12510 v=v+dv:T=T+dT
12520 IF ABS(dv/v)<.00001 AND ABS(dT/T)<.00001 THEN 12550
12530 GOTO 12440
12550 ENDPROC
```

2.3 Cycle Analysis

Having developed equations for the functions of state, and established data-files of all the co-efficients for the refrigerants of interest, it is possible to write a programme to calculate capacity and C.O.P. as outlined in section 2.1. It is now appropriate to discuss the utility of calculating the C.O.P.

For any energy conversion process it is possible to calculate the theoretical minimum primary energy requirement for a given duty. If that duty requires the extraction of heat at ambient temperature, and the delivery of heat at a higher, constant temperature, then it is the Carnot cycle which requires the minimum primary energy, and so offers the highest C.O.P. With its isothermal evaporation, isentropic compression, and isothermal condensation, the standard Rankine cycle is thermodynamically similar to the Carnot cycle. There are just two points of difference. The isenthalpic throttling of the condensed refrigerant increases its entropy, whereas the Carnot cycle has an isentropic de-compression, in which useful work is recovered. Secondly, the discharge gas temperature exceeds the condensing temperature, which results in a net creation of entropy if this superheat is degraded down to the condensing temperature. By contrast, the Carnot cycle has a totally isothermal delivery of heat.

By calculating the Rankine cycle C.O.P. and comparing with the Carnot C.O.P. for the same source and delivery temperatures, one obtains a diagnostic measure of the significance of these two losses *combined*. From knowledge of the C.O.P. alone there is no way of ascertaining the individual significance of each. The picture becomes still more confused if liquid subcooling occurs. This can result in the Carnot C.O.P. being exceeded. This is not a violation of the second law of thermodynamics. Rather, it is a consequence of persisting with the Carnot C.O.P. for a cycle whose resemblance to that of Carnot has receded to the point of uselessness. This is illustrated by figure 2.1, which shows temperature - entropy (Ts) diagrams for the Carnot cycle, the Rankine cycle, the Rankine cycle with subcooling, and the Rankine cycle with subcooling & superheating.

For these reasons, calculation of the effective primary energy

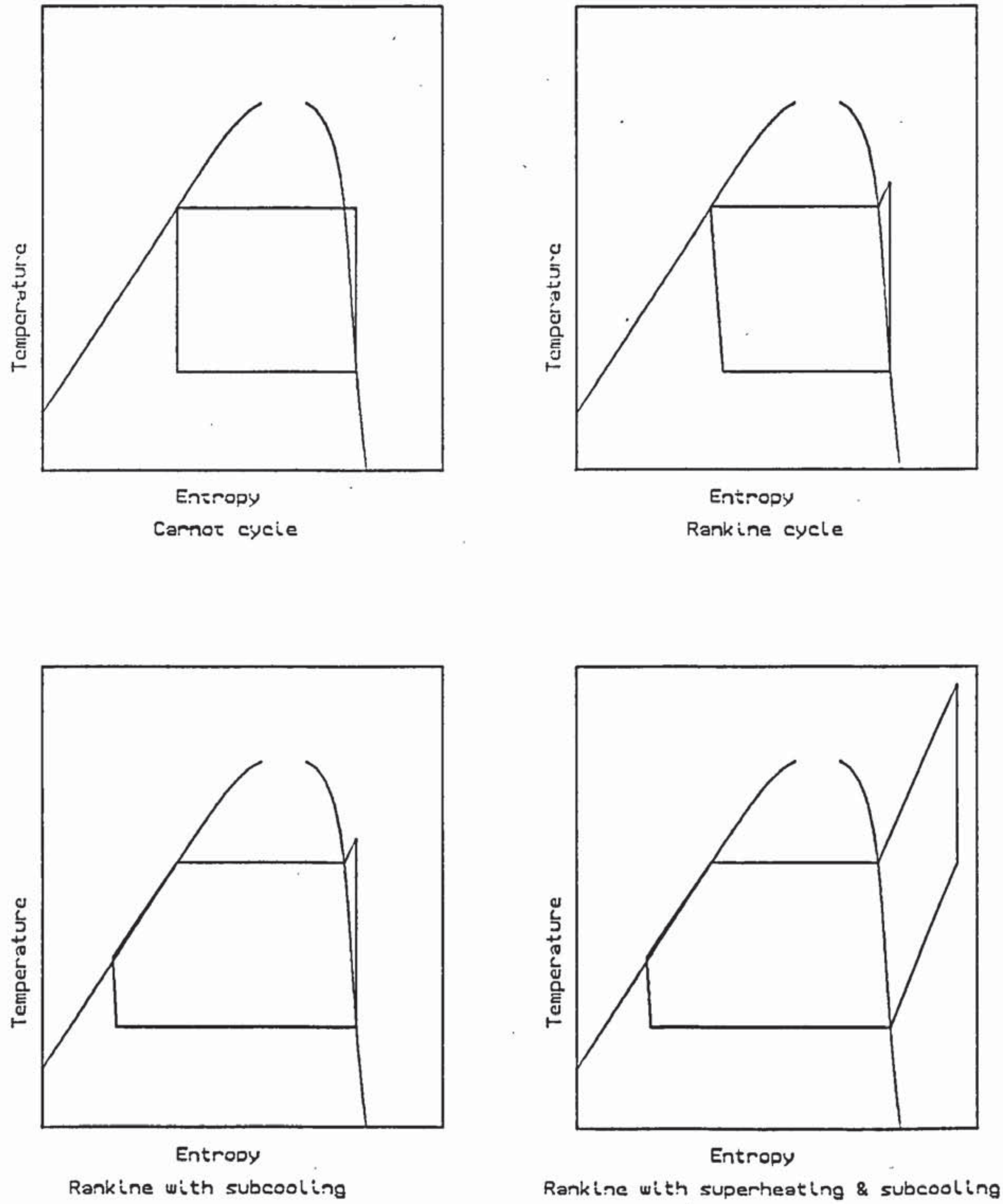

Figure 2.1. Differences between the Carnot cycle and Rankine cycles

loss at each component is more useful than calculation of the overall C.O.P. This is known variously as "exergy" analysis or "availability" analysis.

The availability of a system can be defined as the upper theoretical limit to the work that can be extracted from it. From this definition one can derive equations for the availability of any system, whether it be water behind a dam, a fuel/air mixture, a clock spring, a magnetic field, liquid air, or .... anything.

This definition has a very important corollary, which follows from the impossibility of a perpetual motion machine: - The theoretical minimum expenditure of work required to prepare a system, starting from its equilibrium state, is given by its final availability. Thus, by calculating the availability increment of the load upon delivering heat to it, the minimum necessary expenditure of work can be deduced. In this way, for any given heating duty, the theoretical limiting C.O.P. can be found unambiguously as the ratio of the load's enthalpy increment to its availability increment. Only in one special case, that of constant source and delivery temperatures, is this correctly given by the Carnot C.O.P.

Although availability analysis has only recently received widespread recognition (24, 25, 26), it was established over a century ago by Gibbs (27). It is thus irritating that some contemporary authors create the impression of its being a new concept, and fail to give due credit to its Victorian founders.

Availability increment of a load

Consider a finite reservoir at a temperature, T, not equal to ambient temperature, T_o. If the entropy of this reservoir is raised isobarically by an amount ΔS by supplying heat to it using a perfectly reversible heat pump, then the amount of heat extracted from ambient must be $T_o\Delta S$. Since the reservoir's enthalpy must increase with this increment in entropy, it follows from the first law that the amount of work, W, performed by the heatpump must be $\Delta H - T_o\Delta S$, where ΔH is the increase in enthalpy of the load. Thus it follows that one can write

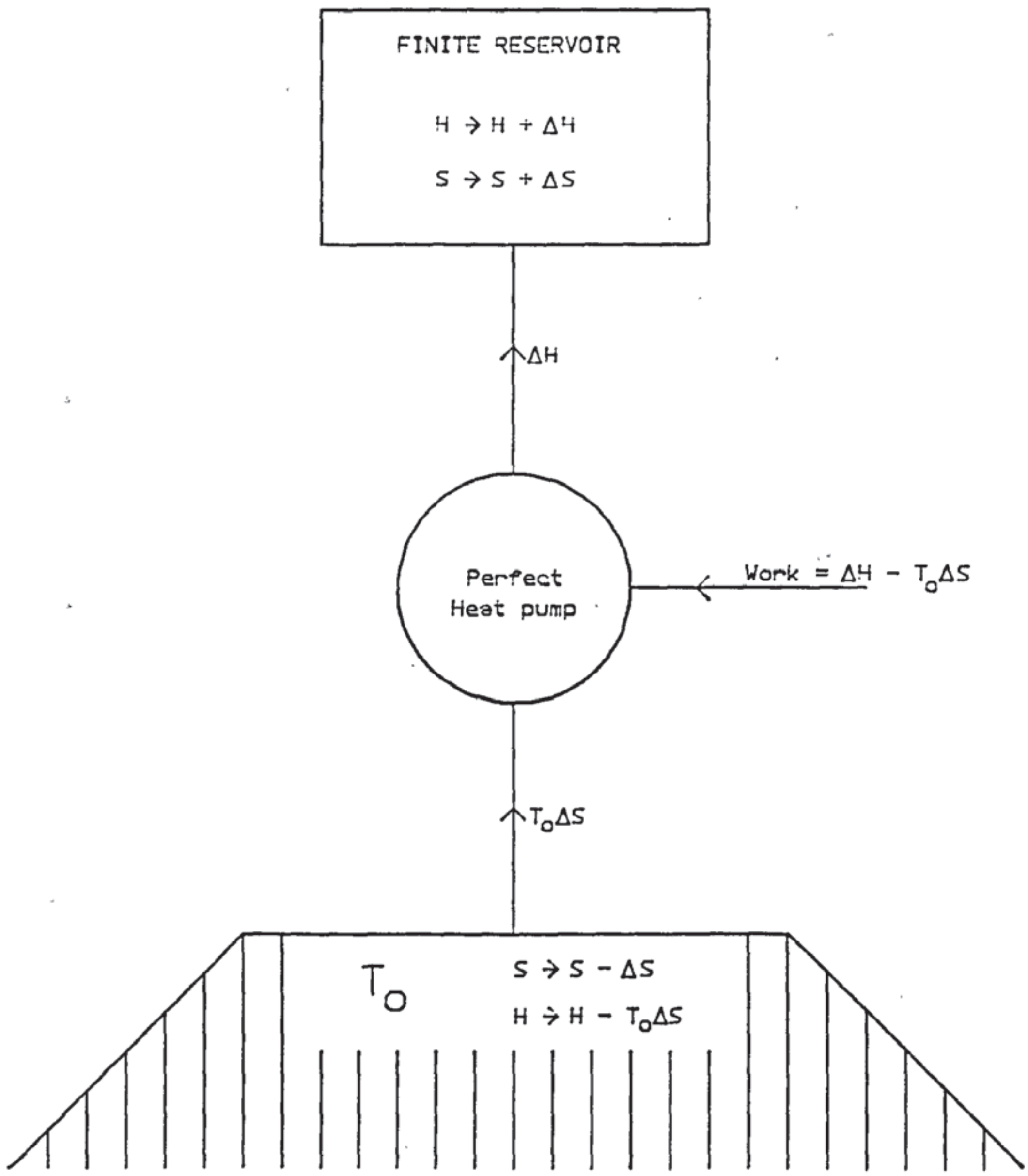

Figure 2.2 Availability increment of a finite reservoir

$$\Delta A = \Delta H - T_o \Delta S \qquad 2.42$$

where ΔA is the increase in availability of the reservoir which results from increments ΔH & ΔS in its enthalpy & entropy. Figure 2.2 illustrates this derivation using the conventional symbolism of thermodynamics texts. Note that no explicit reference to the reservoir's temperature is necessary, although there is an implicit dependence through the relationship between ΔH & ΔS. In particular, this expression for the reservoir's availability increment remains valid even if its temperature is variable.

If T, the reservoir's temperature, exceeds T_o, then $\Delta H > T_o \Delta S$, and this corresponds to the familiar heat pumping situation in which work has to be done to raise heat to a higher temperature. However, if $T < T_o$, then $\Delta H < T_o \Delta S$, and so the load's availability increment is negative. i.e. there is a loss in the availability of a reservoir upon heating it, if it is initially at a temperature below ambient.

This illustrates two important points. Any reservoir whose temperature is below ambient has a positive availability - It requires work to prepare it, and work could, in principle, be extracted from it. Secondly, the expression $\Delta A = \Delta H - T_o \Delta S$ is universally valid, unqualified by the reservoir temperature, provided that a consistent sign convention is used for ΔA, ΔH & ΔS.

Availability Losses

For a Rankine cycle heatpump, there are just three processes responsible for availability degradation. These are;-

i) Throttling at the refrigerant flow regulating valve.

ii) Heat transfer at the heat exchangers.

iii) Degradation of primary energy to heat by the compressor.

Compressor Cooling

It has been found that the compressor used in the experimental heatpump is not very efficient. Idling tests, to be discussed later, have shown that the motor power requirement exceeds 100 Watts even when zero compression work is ensured by removal of the cylinder head. This is mainly due to the electrical losses of the motor, and partly due to mechanical losses at the bearing surfaces. Although it is difficult to obtain sufficiently detailed specifications from compressor manufacturers, there is reason to believe that there is no appropriately sized compressor currently available which is significantly more efficient. Consequently, in normal operation, a significant amount of waste heat has to be disposed of. This raises the question of whether it is possible to limit this unavoidable loss by making use of the waste heat.

Three fates are possible for the waste heat. It can be transferred to the suction gas, transferred to the load, or dissipated to ambient.

Transfer to the suction gas has been generally adopted as the standard practice for compressor cooling. For this reason, induction systems are commonly designed to enhance heat transfer from the compressor to the suction gas. This practice has even led one manufacturer (28) to claim that this method of heat 'recovery' enhances the overall efficiency of the heat pump. Armed with this argument, the next logical step would be to claim that there is no point in trying to reduce the compressor's losses, since all such losses are ultimately recovered. This argument is rooted in a simple-minded first law way of thinking. Its fallacy can be demonstrated by a second law treatment. A simpler, more mechanistic counter-argument starts by noting that additional superheating results in a lower gas density in the suction plenum, with a consequent reduction in the mass flow rate. This point has been demonstrated by showing that a 6% improvement in refrigerating capacity can be obtained by reducing the heat transfer to the suction gas (29, 30, 31). However, the problem is less obvious in the case of a heat pump, since the flow-rate penalty that results from extra suction gas heating is offset by the increased discharge gas enthalpy. This is illustrated in figure 2.3, which shows, superposed, the cycle diagrams

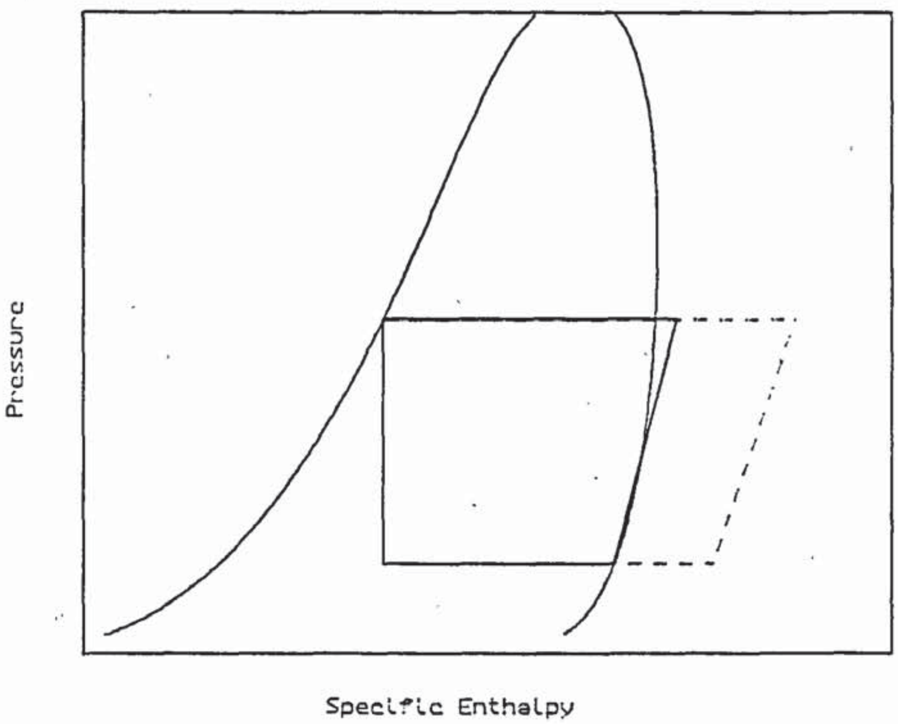

Figure 2.3. Effect of suction gas pre-heat on cycle diagram

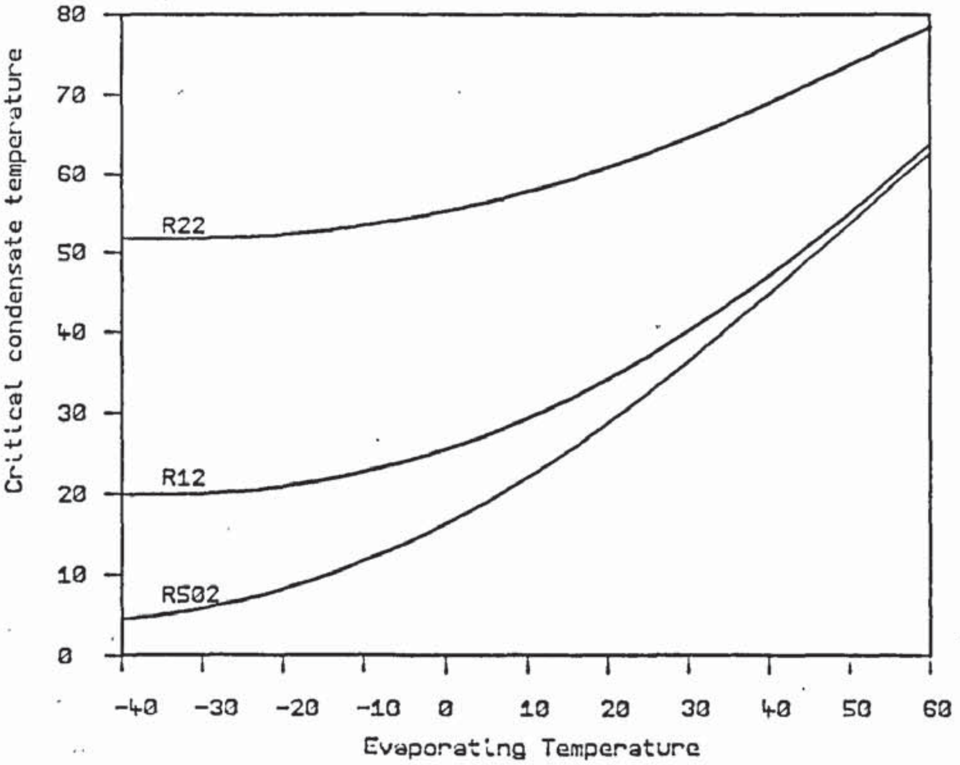

Figure 2.4. Condensate temperature for pre-heat / no pre-heat decision

with and without suction gas superheating.

It will be shown that the unsurpassable ideal would be to transfer the waste heat to the load at the peak load temperature. There is no fundamental reason to preclude this strategy. However, it would require a completely different compressor design, including thermal isolation of the suction gas.

If some heat is needed at a low temperature, then it is still possible to transfer the waste heat to the load. However, it will be shown that this strategy also is not without penalty.

Finally, dissipation of the waste heat to ambient is always possible. In the case of a heat pump, this is most effectively achieved by using the waste heat to boil liquid refrigerant from the evaporator. This is equivalent to rejection to ambient, as it reduces the amount of heat extracted by the evaporator. This is potentially advantageous as it reduces the depression of the evaporating temperature below ambient.

If effective heat transfer from the compressor to the load is not possible, and if there is no requirement for heat at a temperature exceeding the condensing temperature, then a simple criterion can be derived by which to decide whether it is better to superheat the suction gas, or dissipate the waste heat to ambient.

A simple criterion to decide whether or not to superheat

The condenser output, Q, can be expressed as;-

$$Q = \dot{m}_r (h_{suc} - h_2) + W_{comp} \qquad 2.43$$

W_{comp}, the compressor's power requirement, is very insensitive to suction gas superheating for fixed suction and discharge pressures. This will be illustrated numerically in the calculations presented in the following section. In equation 2.43, the dependence of the output on suction gas density enters implicitly through the mass flow rate. Equation 2.3 can be substituted to express this dependence explicitly;-

$$Q = \eta_{vol}(\dot{V}/v_{suc})(h_{suc} - h_2) + W_{comp} \qquad 2.44$$

By differentiating equation 2.44 wrt h_{suc} at constant suction pressure, one can ascertain whether superheating improves or degrades the capacity. The result is;-

$$\frac{dQ}{dh} = \eta_{vol}\dot{V}(h_2 - (h_{suc} - \alpha v_{suc}))/(\alpha v_{suc}^2) \qquad 2.45$$

$$\text{where } \alpha = (\partial h/\partial v)_P = T((\partial s/\partial T)_v(\partial T/\partial v)_P + (\partial P/\partial T)_v) \qquad 2.46$$

Since $(h_{suc} - \alpha v_{suc}) = (h_{sat} - \alpha v_{sat})$ to first order, one can see that this bracket is a function of the evaporating temperature alone.

If $h_2 < (h_{sat} - \alpha v_{sat})$, then the derivative, equation 2.45, is negative, showing that the capacity would be degraded by increased suction gas heating. Consequently, in this case, the best option is to dissipate the waste heat to ambient, in order to maximise the suction gas density and flow rate.

Conversely, if $h_2 > (h_{sat} - \alpha v_{sat})$, then the derivative, equation 2.45, is positive, showing that the capacity can be enhanced by using the waste heat to superheat the suction gas. This is due to the increased discharge gas enthalpy more than offsetting the reduced refrigerant flow rate.

Since the condensate enthalpy, h_2, is insensitive to the pressure, h_2 is essentially a function of the condensate temperature alone. Thus, for any given evaporating temperature, a critical condensate temperature can be deduced, above which it is better to superheat the suction gas, and below which it is better to dissipate the waste heat to ambient.

Figure 2.4 shows this critical condensate temperature plotted against evaporating temperature for R12, R22 & R502. This plot was obtained by solving equation 2.47, below, for T_2.

$$h_{liq}(T_2) = h_{vap} - \frac{\partial h}{\partial v_p} v_{vap} \qquad 2.47$$

In equation 2.47, the quantities on the RHS were evaluated for saturated vapour at all evaporating temperatures in steps of 1K. Then, at each evaporating temperature, the critical value of T_2 was found from this equation.

While the above analysis is useful, in furnishing a simple criterion by which to choose between waste heat rejection to ambient, or transfer to the suction gas, it must be pointed out that this is based solely on the first law, concerned only with maximising the total amount of heat output, irrespective of the temperature at which this heat is made available. This is the reason for the qualifications which preceeded this discussion. A second law treatment, based on availability analysis, is explained next, and in the sections which follow, calculational examples are presented demonstrating that under some circumstances, the first-law optimisation explained above would lead to the diametrically wrong decision regarding whether or not to superheat the suction gas.

Availability loss due to compressor cooling

Whether the compressor's waste heat is transferred to the suction gas, dissipated to ambient, or transferred to the load, there is an associated enthalpy and entropy increment of the cooling medium. Thus, the availability increment of the coolant is given by $\Delta A = \Delta H - T_o \Delta S$ where $\Delta H = W_{loss}$, the total mechanical and electrical loss by the compressor. Since the availability increment of the coolant is potentially useful, the overall availability loss is then given by $W_{loss} - \Delta A$. Substituting the expression $\Delta A = W_{loss} - T_o \Delta S$, for the coolant's availability increment, yields the result;-

$$\text{Availability loss} = T_o \Delta S \qquad 2.48$$

where ΔS is the increase in entropy of the coolant. For a given amount of heat rejected, the entropy created is inversely related to the temperature at which it is rejected. This is why rejection to the load at its peak temperature is unsurpassable. Conversely, if the waste heat is rejected to ambient, then $T_o\Delta S = W_{loss}$, and so the availability loss reduces to W_{loss}.

Availability loss due to heat transfer in the heat exchangers

Consider two fluids traversing a heat exchanger. Fluid 1 enters hot, and exits cold. Fluid 2 enters cold, and exits hot. The change in availability of fluid 1 is given by $\Delta A_1 = \Delta H_1 + T_o\Delta S_1$, while the change in availability of fluid 2 is given by $\Delta A_2 = \Delta H_2 + T_o\Delta S_2$, where ΔA_1, ΔH_1, ΔS_1 are all negative, and ΔA_2, ΔH_2, ΔS_2 are all positive. The overall change in availability is just the sum of these two availability increments;-

$$\Delta A = \Delta A_1 + \Delta A_2 = \Delta H_1 + \Delta H_2 - T_o(\Delta S_1 + \Delta S_2) \qquad 2.49$$

If heat loss from the heat exchanger can be ignored, then $\Delta H_1 + \Delta H_2 = 0$. The total change in availability then reduces to;-

$$\Delta A = -T_o(\Delta S_1 + \Delta S_2) \qquad 2.50$$

Since the second law requires that the net change in entropy of the universe cannot be negative, it follows that there is a loss in availability, which is given by;-

$$\text{Availability loss} = T_o\Delta S_{universe} \qquad 2.51$$

Availability loss due to throttling

It is a completely general result that the availability loss for any process is given by $T_o\Delta S$, where ΔS is the total entropy created. This availability loss is known as the "Irreversibility" (32), and is denoted by "I". Upon first considering the availability loss at the throttle, the lost work seemed to be given by $T_e\Delta S$. i.e. the evaporating temperature entered instead of ambient temperature. This paradox is resolved in the following explanation.

Conventionally, the high pressure condensate at the end of the condenser is isenthalpically throttled down to the evaporating pressure,

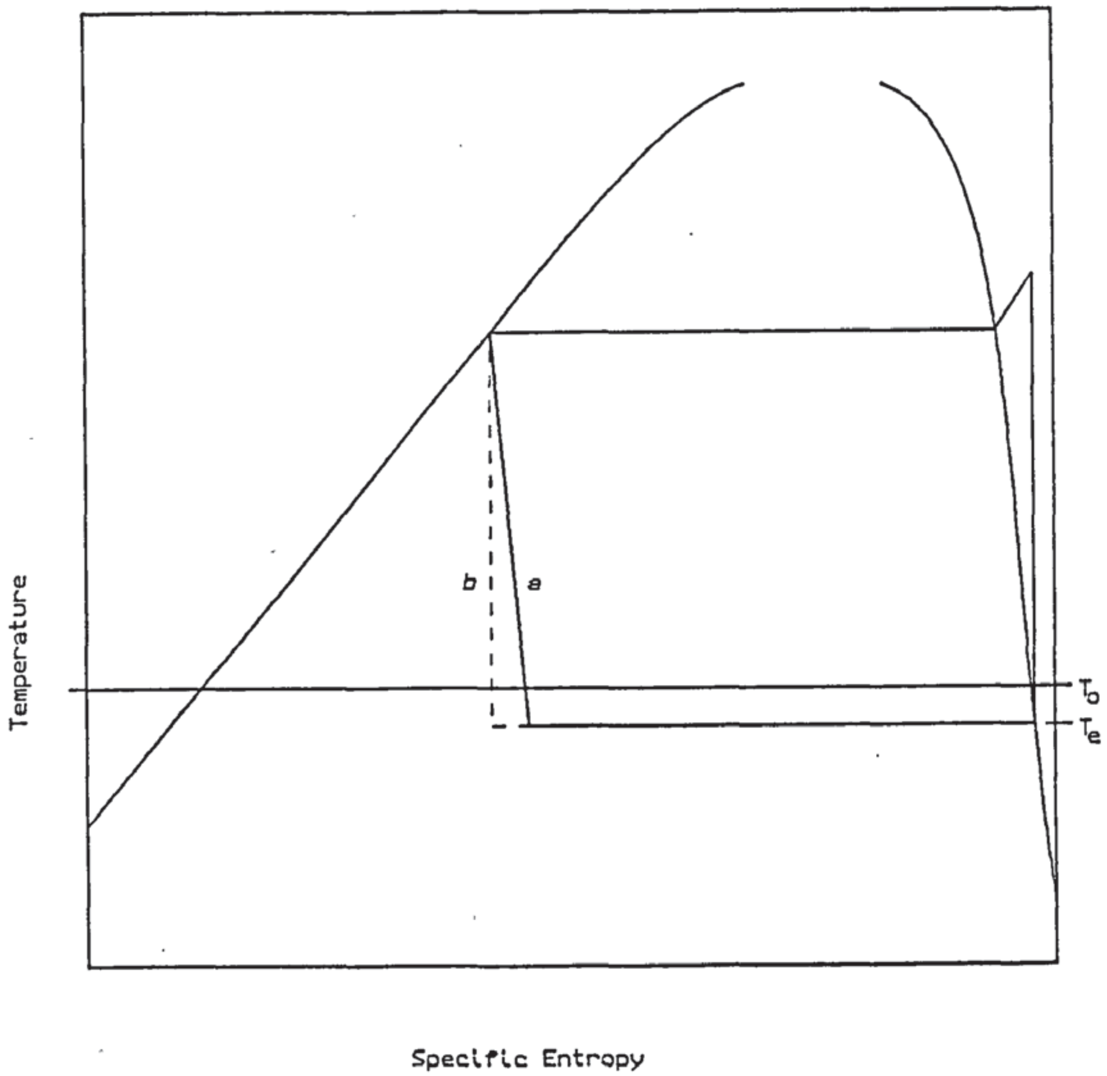

Figure 2.5. Resolution of the throttling irreversibility paradox

with a concomitant increase in its entropy, ΔS. In order to see why the availability loss is given by $T_o\Delta S$, consider the Ts digram, figure 2.5, which shows two paths by which the refrigerant may be brought to the evaporating pressure at the condensate enthalpy. Path *a* is just the isenthalpic expansion of common acquaintance. Path *b* shows an isentropic expansion during which useful work is recovered, followed by heat transfer from ambient. One can see that the useful work recovered by the isentropic expander is given by $T_e\Delta S$. However, this is followed by an entropy creating transfer of heat, equal in magnitude to $T_e\Delta S$, from T_o to T_e. The entropy created by this process is given by $T_e\Delta S(1/T_e - 1/T_o)$, and so the associated availability loss is seen to be $T_oT_e\Delta S(1/T_e - 1/T_o) = \Delta S(T_o - T_e)$. For path *b*, then, useful work of $T_e\Delta S$ is recovered, followed by an availability loss of $\Delta S(T_o - T_e)$. Thus, for path a the total availability loss must be given by the sum of these two terms, which reduces to $T_o\Delta S$.

This is a further example illustrating the validity of the expression

$$I = T_o\Delta S_{universe} \qquad 2.52$$

There is at least one example in the literature of confusion on the part of the author over exactly what temperature to use for T_o (33).

In the cycle analyses presented in the following sections, the availability breakdown has been laid out in such a way as to illustrate what might be termed the "Law of accountability of availability". If all the availability losses are added up, and this figure added to the availability lift of the load, then this sum reproduces the total electrical consumption. This is the whole point of availability analysis. It accounts for every non-ideality, and puts the losses into a quantitative perspective. But it only works if the calculations adhere to the theory. In particular, if the same value for ambient temperature is not used consistently throughout, internal consistency is lost, and the calculated results become equivocal.

2.4 Calculated cycle performance & losses

Standard cycle

Before embarking on detailed availability analyses of the Rankine cycle for different heating duties, it is instructive to consider simple cycle analyses with a minimum of complicating features.

Consider first the standard Rankine cycle, for which the compression is isentropic, starting with saturated vapour, while the decompression is isenthalpic, starting with saturated liquid. Table 2.1 presents the results for this cycle for the three refrigerants R12, R22 & R502, for evaporating & condensing temperatures of 0C & 50C respectively. In the following calculations, a suction gas displacement rate of 400cc/s has been assumed, which is typical of Danfoss' SC10H. Rather than perform calculations specifically for the use of a hypothetical ideal compressor, the same model for the compressor's inefficiency has been consistently used throughout. When it has been desired to investigate the Rankine cycle performance for an ideally efficient compressor, as in table 2.1, then rejection of the waste heat to ambient is used, in order that the cycle thermodynamics remain unperturbed by the waste heat. Reference to "COP, mechanical work only" then furnishes the cycle C.O.P. for use of a perfect compressor.

As explained at the end of section 2.3, the availability breakdown has been laid out to show how the sum of all the losses, added to the useful availability gain, reproduces the electrical power consumption. In order that the effect of the compressor's inefficiency may be distinguished from the Rankine cycle's losses, two figures for availability efficiency are provided. The "Overall availability efficiency" is the ratio of the "Load Availability lift" to the total power input, while the "Cycle's availability efficiency" is given by the ratio;

$$\frac{\text{(Load Availability lift - Compressor coolant availability increment)}}{\text{Work of compression}}$$

Since the purpose of this figure of merit is to separate out the influence of the compressor's inefficiency, the only way to do this consistently is to subtract the availability gain furnished by the compressor's waste heat, as indicated above. In the case of waste heat rejection to ambient, the coolant's availability gain is zero, and this expression reduces to the conceptually acceptable ratio of availability gain over work of compression.

Where a load is specified, such as heating water from cold, the availability lift of the load is calculated using equation 2.42. However, in the case of a pure cycle analysis, with no load specified, an upper limit to the load's availability lift is estimated by assuming that the latent heat of condensation, and the desuperheating enthalpy drop are both used at the condensing temperature. If some subcooling is specified, it is also assumed that the subcooling enthalpy drop is transferred without creating entropy. i.e., in the absence of a specified load, the "Load availability increment" is simply the availability of the discharge gas, offset by the desuperheating loss.

Upon considering either the "COP, mechanical work only", or the "Cycle's Availability efficiency", table 2.1 shows that use of R502 results in a 10% poorer cycle efficiency than use of either R12 or R22.

Reference to the availability loss analysis illuminates two points. The desuperheating loss is consistently at least an order of magnitude less than the throttling loss, even for R22, which is notorious for its high discharge gas temperature, and secondly, for both R12 & R22 the ratio of throttle loss to work of compression is less than 1/5, but for R502 it is over 1/4. This is the reason why the Rankine C.O.P. is 10% lower for R502 than for either R12 or R22.

For a real cycle, the temperature of the vapour in the cylinder immediately before compression is normally significantly higher than the evaporating temperature. It is also common for the condensate temperature immediately before the expansion valve to be lower than the condensing temperature. In the following cycle analyses, the effect of liquid subcooling is first considered in isolation. This is followed by a consideration of the effect of suction gas superheating. Transfer of waste heat to the suction gas, and use of an intercooler are both considered. It is because the intercooler also subcools the liquid that it has been considered best to discuss subcooling first.

Effect of subcooling

Table 2.2 presents the same comparison as in table 2.1, but this time the liquid has been subcooled down to the evaporating temperature. Several important features result;-

i) The C.O.P. exceeds the Carnot C.O.P.

ii) The throttling loss is very much reduced.

iii) The C.O.P. obtained with R502 is no worse than that obtained with either R12 or R22.

This last point is a consequence of the reduced throttling loss, since it has already been shown that the poorer C.O.P. of R502 for the standard cycle is entirely due to the high throttling loss.

There are two reasons for the C.O.P. exceeding the Carnot C.O.P.;-

1) A totally reversible machine which delivers some heat at a temperature below the condensing temperature will inevitably have a C.O.P. greater than that of Carnot.

2) The effect of subcooling is to reduce the availability loss at the throttle, which permits the Rankine C.O.P. to approach the theoretical limit more closely.

Figure 2.6 shows the throttling loss plotted against condensate temperature for R12, working between 0C & 50C, as before. The results of calculations presented in table 2.3 were used to plot this. For practical purposes, there is no scope for further reduction once the liquid has been subcooled to the evaporating temperature. This is because the specific availability loss is essentially just given by the product of liquid specific volume and pressure drop, if the throttling occurs entirely in the liquid phase. The large reduction in the throttling loss obtained by subcooling may be thought of as a consequence of the liquid's specific volume being very much lower than the vapour's.

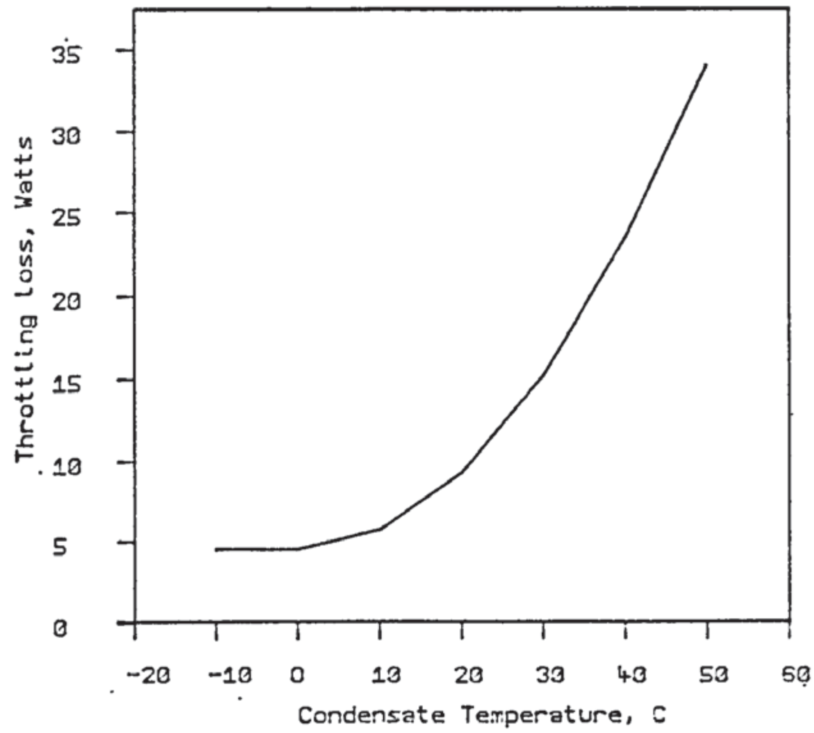

Figure 2.6. Effect of subcooling on throttling loss

Effect of superheating

In all these calculations, a simple linear model for the motor's electrical power consumption is used to account for its inefficiency;-

Power requirement = 100Watts + 1.1(Isentropic compression power) 2.53

This is an approximate fit, based on performance figures supplied by Danfoss (34).

Table 2.1 showed that the overall COP and efficiency were better for R502 than for R12, in spite of the intrinsic disadvantage of R502's throttling loss. This is a consequence of the large constant term, 100 Watts, in this motor loss model. Consequently, this model favours R502 over R12 because of the higher capacity which results from using it.

In section 2.3 a criterion was derived by which to assess whether there is a net penalty or gain upon transferring waste heat to the suction gas. This criterion, plotted in figure 2.4, was based on the first law alone. The purpose of the following calculations is to test the criterion, firstly in a situation where it is expected to work, and later, in a situation not satisfying the qualification that there should be no need for heat at a temperature exceeding the condensing temperature.

In table 2.4, two cycle analyses are presented in which excess superheating is compared with waste heat rejection to ambient. The refrigerant is R12, condensing at 50C, subcooled to 0C, and evaporating at 0C. It can be seen that rejecting the waste heat to the suction gas results in the poorer C.O.P. and capacity. This is in accord with expectation, because figure 2.4 shows that in order for extra suction gas heating to enhance the output, the condensate temperature would have to exceed 26C.

It is instructive to see what interpretation results from the availability analysis. Consider the Compressor cooling loss. For rejection of the waste heat to ambient this is identically equal to the compressor's "Excess" power requirement, as explained in section 2.3. Alternatively, by transferring this waste heat to the suction gas, there is an increase in the availability of the suction gas due to its increased temperature. By inspecting the figures, one sees that this amounts to a 6 Watt recovery of availability, out of a 118 Watt loss - not an impressive gain! Unimpressive as this recovery is, further condemnation is found by observing that it is totally negated by a 7 Watt increment in the desuperheating loss, which has resulted from the substantially increased discharge gas temperature.

The bottom line is that there is no change in the overall availability efficiency. This result is not inconsistent with the C.O.P.'s being made poorer by superheating the suction gas. By superheating the suction gas, a higher fraction of the heat output is available at the condensing temperature, rather than from subcooling, and thus, for a given availability efficiency, one would expect a lower C.O.P.

The discussion above was concerned with the case of deep subcooling, for which it had been anticipated that it is better to avoid superheating the suction gas. The calculations summarised in table 2.5

address the complementary situation of having no subcooling. In the first two columns, rejection of the compressor's waste heat to ambient is again compared with transfer to the suction gas. It can be seen that, in contrast to the case of subcooled condensate, the higher C.O.P. and capacity is obtained by superheating the suction gas. Again, this is in accord with the expectation from figure 2.4, since the condensate temperature exceeds the threshold value of 26C. Note that the compressor power requirement is almost unaffected by superheating the suction gas, which justifies the simplification used in deriving equation 2.45.

For given suction conditions and discharge pressure, the desuperheating loss and compressor loss cannot be affected by the extent of liquid subcooling. It might thus seem suspicious that, depending on the extent of liquid subcooling, it is possible to reverse the result of comparing waste heat transfer to ambient with transfer to the suction gas. Perusal of the availability analysis shows that the answer lies with the throttling loss. Both comparisons (tables 2.4 & 2.5) have shown that the throttling loss is reduced by superheating the suction gas. This is due solely to the reduced refrigerant flow rate, since, for a given condensate state and evaporating pressure, the specific availability loss on throttling is not dependent on suction gas heating. In the case of deep subcooling, the specific throttling loss is so small that reducing the flow rate has a negligible effect on the cycle's total loss. However, throttling saturated liquid incurs a much larger specific throttling loss. Consequently, the flow rate reduction caused by suction gas superheating results in a significant reduction in the throttling loss. This accounts for the dependence on subcooling of comparing superheated suction gas with saturated suction gas.

If the scope exists to improve the capacity by further superheating, then, in addition to cooling the compressor with the suction gas, use of an intercooler is justified. The result of considering the use of an intercooler is presented as the third column of table 2.5. It has been assumed that the intercooler is an ideal counter-current heat exchanger capable of bringing the suction gas temperature up to the condensate temperature. It can be seen that this has produced a further improvement in C.O.P., capacity and overall availability efficiency. This time, the throttling loss is additionally reduced by the deeper subcooling which results from the use of the intercooler. However, in addition to the increased desuperheating loss offsetting this gain, there is also an inevitable loss at the intercooler due to the specific heat mis-match of liquid & vapour.

While this numerical example has illustrated the validity of the foregoing thermodynamic discussion, it has also illuminated a practical penalty of attempting to improve thermodynamic performance by suction gas superheating. The high discharge temperature of 142C is undesirable, and introduces the likelihood of deleterious chemical changes of the refrigerant and lubricating oil.

Comparison of R12 R22 & R502 for a standard Rankine cycle

Refrigerant	R12	R22	R502
Waste heat rejected to;-	Ambient	Ambient	Ambient
Intercooler used ?	No	No	No
Evaporating Temperature	0.000	0.000	0.000
Condensing Temperature	50.000	50.000	50.000
Condensate Temperature	50.000	50.000	50.000
Functions of state at cycle vertices			
Discharge Temperature	56.644	72.197	57.129
Pressure	12.188	19.418	21.013
Enthalpy	375.892	439.668	369.773
Cond. end Enthalpy	248.881	263.261	261.313
Entropy	1.162	1.208	1.201
Evap. sat. liq. Entropy	1.000	1.000	1.000
Evap. sat. liq. Enthalpy	200.000	200.000	200.000
Saturated vapour Entropy	1.555	1.752	1.537
Enthalpy	351.481	405.363	346.629
Pressure	3.084	4.974	5.731
specific volume	55.417	47.151	30.838
Suction Entropy	1.555	1.752	1.537
Enthalpy	351.481	405.363	346.629
specific volume	55.417	47.151	30.838
temperature	0.000	0.000	0.000
Cycle Performance			
Refrigerant flow rate g/s	7.218	8.483	12.971
Condenser output power	916.770	1496.542	1406.813
Work of compression Watts	176.199	291.023	300.190
Excess requirement Watts	117.620	129.102	130.019
Carnot COP.	6.463	6.463	6.463
COP., mechanical work only	5.203	5.142	4.686
COP. overall	3.120	3.562	3.270
Availability Analysis, Watts			
Desuperheating loss	0.338	5.031	0.900
Throttling loss	34.012	54.437	81.618
Compressor cooling loss	117.620	129.102	130.019
Load Availability lift	141.849	231.555	217.672
Total power input	293.819	420.126	430.209
Cycle's Availability efficiency	0.805	0.796	0.725
Overall Availability efficiency	0.483	0.551	0.506

Table 2.1

Comparison of R12 R22 & R502 for cycle with deep subcooling

	R12	R22	R502
Refrigerant	R12	R22	R502
Waste heat rejected to;-	Ambient	Ambient	Ambient
Intercooler used ?	No	No	No
Evaporating Temperature	0.000	0.000	0.000
Condensing Temperature	50.000	50.000	50.000
Condensate Temperature	0.000	0.000	0.000
Functions of state at cycle vertices			
Discharge Temperature	56.644	72.197	57.129
Pressure	12.188	19.418	21.013
Enthalpy	375.892	439.668	369.773
Cond. end Enthalpy	200.000	199.841	199.690
Entropy	0.998	0.996	0.995
Evap. sat. liq. Entropy	1.000	1.000	1.000
Evap. sat. liq. Enthalpy	200.000	200.000	200.000
Saturated vapour Entropy	1.555	1.752	1.537
Enthalpy	351.481	405.363	346.629
Pressure	3.084	4.974	5.731
specific volume	55.417	47.151	30.838
Suction Entropy	1.555	1.752	1.537
Enthalpy	351.481	405.363	346.629
specific volume	55.417	47.151	30.838
temperature	0.000	0.000	0.000
Cycle Performance			
Refrigerant flow rate g/s	7.218	8.483	12.971
Condenser output power	1269.597	2034.559	2206.111
Work of compression Watts	176.199	291.023	300.190
Excess requirement Watts	117.620	129.102	130.019
Carnot COP.	6.463	6.463	6.463
COP, mechanical work only	7.205	6.991	7.349
COP. overall	4.321	4.843	5.128
Availability Analysis, Watts			
Desuperheating loss	0.338	5.031	0.900
Throttling loss	4.460	8.976	14.043
Compressor cooling loss	117.620	129.102	130.019
Load Availability lift	171.401	277.017	285.247
Total power input	293.819	420.126	430.209
Cycle's Availability efficiency	0.973	0.952	0.950
Overall Availability efficiency	0.583	0.659	0.663

Table 2.2

Dependence of throttling loss on subcooling

Refrigerant	R12	R12	R12	R12	R12
Waste heat rejected to;-	Ambient	Ambient	Ambient	Ambient	Ambient
Intercooler used ?	No	No	No	No	No
Evaporating Temperature	0.000	0.000	0.000	0.000	0.000
Condensing Temperature	50.000	50.000	50.000	50.000	50.000
Condensate Temperature	40.000	30.000	20.000	10.000	-10.000
Functions of state at cycle vertices					
Discharge Temperature	56.644	56.644	56.644	56.644	56.644
Pressure	12.188	12.188	12.188	12.188	12.188
Enthalpy	375.892	375.892	375.892	375.892	375.892
Cond. end Enthalpy	238.424	228.410	218.718	209.267	190.874
Entropy	1.129	1.096	1.064	1.031	0.964
Evap. sat. liq. Entropy	1.000	1.000	1.000	1.000	1.000
Evap. sat. liq. Enthalpy	200.000	200.000	200.000	200.000	200.000
Saturated vapour Entropy	1.555	1.555	1.555	1.555	1.555
Enthalpy	351.481	351.481	351.481	351.481	351.481
Pressure	3.084	3.084	3.084	3.084	3.084
specific volume	55.417	55.417	55.417	55.417	55.417
Suction Entropy	1.555	1.555	1.555	1.555	1.555
Enthalpy	351.481	351.481	351.481	351.481	351.481
specific volume	55.417	55.417	55.417	55.417	55.417
temperature	0.000	0.000	0.000	0.000	0.000
Cycle Performance					
Refrigerant flow rate g/s	7.218	7.218	7.218	7.218	7.218
Condenser output power	992.245	1064.530	1134.486	1202.703	1335.466
Work of compression Watts	176.199	176.199	176.199	176.199	176.199
Excess requirement Watts	117.620	117.620	117.620	117.620	117.620
Carnot COP.	6.463	6.463	6.463	6.463	6.463
COP, mechanical work only	5.631	6.042	6.439	6.826	7.579
COP. overall	3.377	3.623	3.861	4.093	4.545
Availability Analysis, Watts					
Desuperheating loss	0.338	0.338	0.338	0.338	0.338
Throttling loss	23.333	15.120	9.250	5.687	4.412
Compressor cooling loss	117.620	117.620	117.620	117.620	117.620
Load Availability lift	152.528	160.740	166.611	170.174	171.448
Total power input	293.819	293.819	293.819	293.819	293.819
Cycle's Avail'y efficiency	0.866	0.912	0.946	0.966	0.973
Overall Avail'y efficiency	0.519	0.547	0.567	0.579	0.584

Table 2.3

Suction superheating v rejection to ambient, with subcooling

Refrigerant	R12	R12
Waste heat rejected to;-	Ambient	Suction
Intercooler used ?	No	No
Evaporating Temperature	0.000	0.000
Condensing Temperature	50.000	50.000
Condensate Temperature	0.000	0.000
Functions of state at cycle vertices		
Discharge Temperature	56.644	85.039
Pressure	12.188	12.188
Enthalpy	375.892	398.138
Cond. end Enthalpy	200.000	200.000
Entropy	0.998	0.998
Evap. sat. liq. Entropy	1.000	1.000
Evap. sat. liq. Enthalpy	200.000	200.000
Saturated vapour Entropy	1.555	1.555
Enthalpy	351.481	351.481
Pressure	3.084	3.084
specific volume	55.417	55.417
Suction Entropy	1.555	1.619
Enthalpy	351.481	370.077
specific volume	55.417	63.162
temperature	0.000	28.679
Cycle Performance		
Refrigerant flow rate g/s	7.218	6.333
Condenser output power	1269.597	1254.799
Work of compression Watts	176.199	177.709
Excess requirement Watts	117.620	117.771
Carnot COP.	6.463	6.463
COP, mechanical work only	7.205	7.061
COP. overall	4.321	4.247
Availability Analysis, Watts		
Desuperheating loss	0.338	7.400
Throttling loss	4.460	3.913
Compressor cooling loss	117.620	111.985
Load Availability lift	171.401	172.182
Total power input	293.819	295.480
Cycle's Availability efficiency	0.973	0.936
Overall Availability efficiency	0.583	0.583

Table 2.4

Rejection to ambient v suction superheating, without subcooling

Refrigerant	R12	R12	R12
Waste heat rejected to;-	Ambient	Suction	Suction
Intercooler used ?	No	No	Yes
Evaporating Temperature	0.000	0.000	0.000
Condensing Temperature	50.000	50.000	50.000
Condensate Temperature	50.000	50.000	50.000
Functions of state at cycle vertices			
Discharge Temperature	56.644	85.039	142.447
Pressure	12.188	12.188	12.188
Enthalpy	375.892	398.138	441.142
Cond. end Enthalpy	248.881	248.881	248.881
Entropy	1.162	1.162	1.162
Intercooler exit enthalpy			216.329
Intercooler exit entropy			1.056
Intercooler exit temp.			17.493
Evap. sat. liq. Entropy	1.000	1.000	1.000
Evap. sat. liq. Enthalpy	200.000	200.000	200.000
Saturated vapour Entropy	1.555	1.555	1.555
Enthalpy	351.481	351.481	351.481
Pressure	3.084	3.084	3.084
specific volume	55.417	55.417	55.417
Suction Entropy	1.555	1.619	1.731
Enthalpy	351.481	370.077	406.711
specific volume	55.417	63.162	76.944
temperature	0.000	28.679	84.001
Cycle Performance			
Refrigerant flow rate g/s	7.218	6.333	5.199
Condenser output power	916.770	945.238	999.490
Work of compression Watts	176.199	177.709	178.993
Excess requirement Watts	117.620	117.771	117.899
Carnot COP.	6.463	6.463	6.463
COP, mechanical work only	5.203	5.319	5.584
COP. overall	3.120	3.199	3.367
Availability Analysis, Watts			
Desuperheating loss	0.338	7.400	36.874
Intercooler loss	0.000	0.000	4.771
Throttling loss	34.012	29.841	5.862
Compressor cooling loss	117.620	111.985	94.734
Load Availability lift	141.849	146.254	154.650
Total power input	293.819	295.480	296.892
Cycle's Availability efficiency	0.805	0.790	0.735
Overall Availability efficiency	0.483	0.495	0.521

Table 2.5

2.5 Performance calculations for optimised configuration

Finally, in table 2.6, refrigerants R12, R22 & R502 are compared for the best possible combination of operating conditions. Since transfer of the motor's waste heat to the load is unsurpassable, a hypothetical load, water at 50C, has been introduced. The total power output to the load is then the sum of the "Condenser output power" and the compressor's excess power requirement. The "COP mechanical work only" is the ratio of the condenser output to the work of compression and thus, correctly, does not include the waste heat transfer to the load. The "COP. overall" is the ratio of the total power output over the compressor's total power consumption. The two availability efficiencies, similarly, take consistent account of the waste heat transfer to the load.

Having no scope to transfer heat at any lower temperature, subcooling is precluded. For R502 and R12, figure 2.4 shows that at this condensate temperature, it is advantageous to superheat the suction gas. This is the reason for including an intercooler. On the other hand, figure 2.4 shows that the performance with R22 would be degraded by superheating the suction gas, which is the reason for not using an intercooler with R22.

The advantage of intercooling

In common with rejection to ambient, rejection of the waste heat to the load also leaves the cycle thermodynamics unperturbed. Thus, for R12 & R502, the improvement introduced by the intercooler alone can be assessed by comparing the results on table 2.6 with those of table 2.1. From table 2.1, for the R12 cycle, the combined losses of desuperheating and throttling amount to 34.35 Watts. Upon comparing with table 2.6, one sees that the throttling loss is reduced from 34 Watts to 6.6 Watts. However, the combined losses of desuperheating, throttling and intercooling total 28.8 Watts. The net gain is thus only 7 Watts. This has resulted in a 4% improvement in C.O.P. from 5.2 to 5.4. For R502, the corresponding net reduction in availability loss is from 82.52 Watts to 66.01 Watts, with a corresponding C.O.P. improvement by 8%, from 4.7 to 5.1. In this way, one can see that while the intercooler can produce an impressive reduction in the throttling loss, the resultant additional heat transfer penalties significantly erode this gain.

The advantage of waste heat transfer to the load

By comparing the "Compressor cooling loss" with the "Excess requirement" it can be seen that transfer of waste heat directly to the load consistently reduces this loss by about 20 Watts, without incurring an additional desuperheating penalty. This is a significant improvement over transfer to the suction gas, for which the compressor cooling loss was reduced by just 6 Watts, only to be negated by the increased desuperheating loss (tables 2.4 & 2.5).

This improvement can be more definitively examined by comparing the overall C.O.P. for the R22 calculations on tables 2.1 & 2.6. The sole difference between these calculations is transfer of the waste heat to the load, instead of to ambient. As mentioned above, the compressor's losses of 129 Watts, in this case, are offset by a 20 Watt gain in the availability of the load. This has resulted in an improvement in overall C.O.P. by 8.6%, from 3.56 to 3.87.

While this 20 Watt offset of the compressor's losses is undeniably helpful, as a fraction of this loss, it is unimpressive. This is no accident. The following paragraph explains why the availability gain through heat recovery will always be disappointing.

A fallacy exposed

The Carnot C.O.P. for this duty is 6.463. This means that upon transferring 100 Joules of heat to the load, the availability increment of the load is only 15.5 Joules. This is the reason why, upon comparing the "Excess" power requirement with the Compressor cooling loss, the amelioration produced by this transfer of heat to the load amounts only to a rather disappointing 20 Watts out of a loss of around 130 Watts. This is the fundamental truth, exposing the fallacy of the suggestion that compressor losses can be significantly mitigated by recovering the waste heat (28). In any application where it is worth using a heat pump - i.e. a high Carnot C.O.P. - it is inevitable that the availability gained by heat recovery is a correspondingly small fraction of the original loss, the reciprocal of the Carnot C.O.P., to be exact. The inescapable conclusion then follows that waste heat recovery can never make more than a marginal impression on the overall availability efficiency.

This in turn leads to the conclusion that no dramatic improvement in performance will be possible until a more efficient compressor becomes available. The thermodynamic fine-tuning which has been discussed in this section can produce only marginal gains.

Comparison of R12, R22 & R502 for optimal heat rejection

Refrigerant	R12	R22	R502
Waste heat rejected to;-	Water out	Water out	Water out
Intercooler used ?	Yes	No	Yes
Condenser entry Temperature	50.000	50.000	50.000
Condenser exit Temperature	50.000	50.000	50.000
Evaporating Temperature	0.000	0.000	0.000
Condensing Temperature	50.000	50.000	50.000
Condensate Temperature	50.000	50.000	50.000
Functions of state at cycle vertices			
Discharge Temperature	106.882	72.197	104.223
Pressure	12.188	19.418	21.013
Enthalpy	414.621	439.668	413.862
Cond. end Enthalpy	248.881	263.261	261.313
Entropy	1.162	1.208	1.201
Intercooler exit enthalpy	216.329		224.126
Intercooler exit entropy	1.056		1.081
Intercooler exit temp.	17.493		21.053
Evap. sat. liq. Entropy	1.000	1.000	1.000
Evap. sat. liq. Enthalpy	200.000	200.000	200.000
Saturated vapour Entropy	1.555	1.752	1.537
Enthalpy	351.481	405.363	346.629
Pressure	3.084	4.974	5.731
specific volume	55.417	47.151	30.838
Suction Entropy	1.664	1.752	1.662
Enthalpy	384.032	405.363	383.815
specific volume	68.599	47.151	39.040
temperature	50.000	0.000	50.000
Cycle Performance			
Refrigerant flow rate g/s	5.831	8.483	10.246
Condenser output power	966.429	1496.542	1563.017
Work of compression Watts	178.363	291.023	307.860
Excess requirement Watts	117.836	129.102	130.786
Carnot COP.	6.463	6.463	6.463
COP, mechanical work only	5.418	5.142	5.077
COP. overall	3.661	3.869	3.861
Availability Analysis, Watts			
Desuperheating loss	16.902	5.031	32.762
Condensing loss	0.000	0.000	0.000
Subcooling loss	0.000	0.000	0.000
Intercooler loss	5.351	0.000	12.783
Throttling loss	6.575	54.437	20.461
Compressor cooling loss	99.604	109.127	110.550
Load Availability lift	167.767	251.531	262.090
Total power input	296.199	420.126	438.646
Cycle's Availability efficiency	0.838	0.796	0.786
Overall Availability efficiency	0.566	0.599	0.597

Table 2.6

2.6 Heating water

Consider this problem. A tank of cold water has to be heated to 50C using a heatpump. It is desired to use as little primary energy as possible. Before considering the use of a real Rankine cycle heatpump, it is helpful to calculate the thermodynamic limiting C.O.P. by computing the ratio ΔH/ΔA for the process.

$$C.O.P._{lim} = (\Delta H/\Delta A) = \frac{T_f - T_i}{T_f - T_i - T_o \ln(T_f/T_i)} \qquad 2.54$$

where T_f = final temperature, T_i = initial temperature, & T_o = ambient temperature. If Ti = To = 0C, and Tf = 50C, then this comes to 12.241, which is almost double the Carnot C.O.P. of 6.463 for operation between fixed reservoir temperatures of 0C & 50C.

As discussed by Carrington (35,36,37) there are two distinct methods of achieving the necessary heating duty. It is possible to heat the cold water in a single pass through a counter-current condenser. This makes it possible to maintain a low condensate temperature throughout the heating duty, so minimising the throttling loss. However, this results in an inevitable availability loss due to heat transfer. This is indicated on figure 2.7 which shows, superposed, the temperature-enthalpy diagrams of those masses of refrigerant & water which flow in equal times through an ideal condenser. An ideal condenser achieves the minimum possible temperature difference for heat transfer by allowing the subcooled liquid refrigerant to reach the water entry temperature while simultaneously allowing the water to reach the condensing temperature at the condensing/desuperheating boundary. Although impossible in practice, discussion in terms of an ideal heat exchanger allows the inevitable losses due to the specific heat mis-match of the two fluids to be clearly differentiated from the losses which are due to the finite heat transfer capability of a real condenser.

The alternative to use of a counter-current condenser is to immerse the condenser in the water tank. In the theoretical limit for an ideally large heat exchanger, and for ideally mixed water, the water temperature is uniform and equal to the condensing temperature

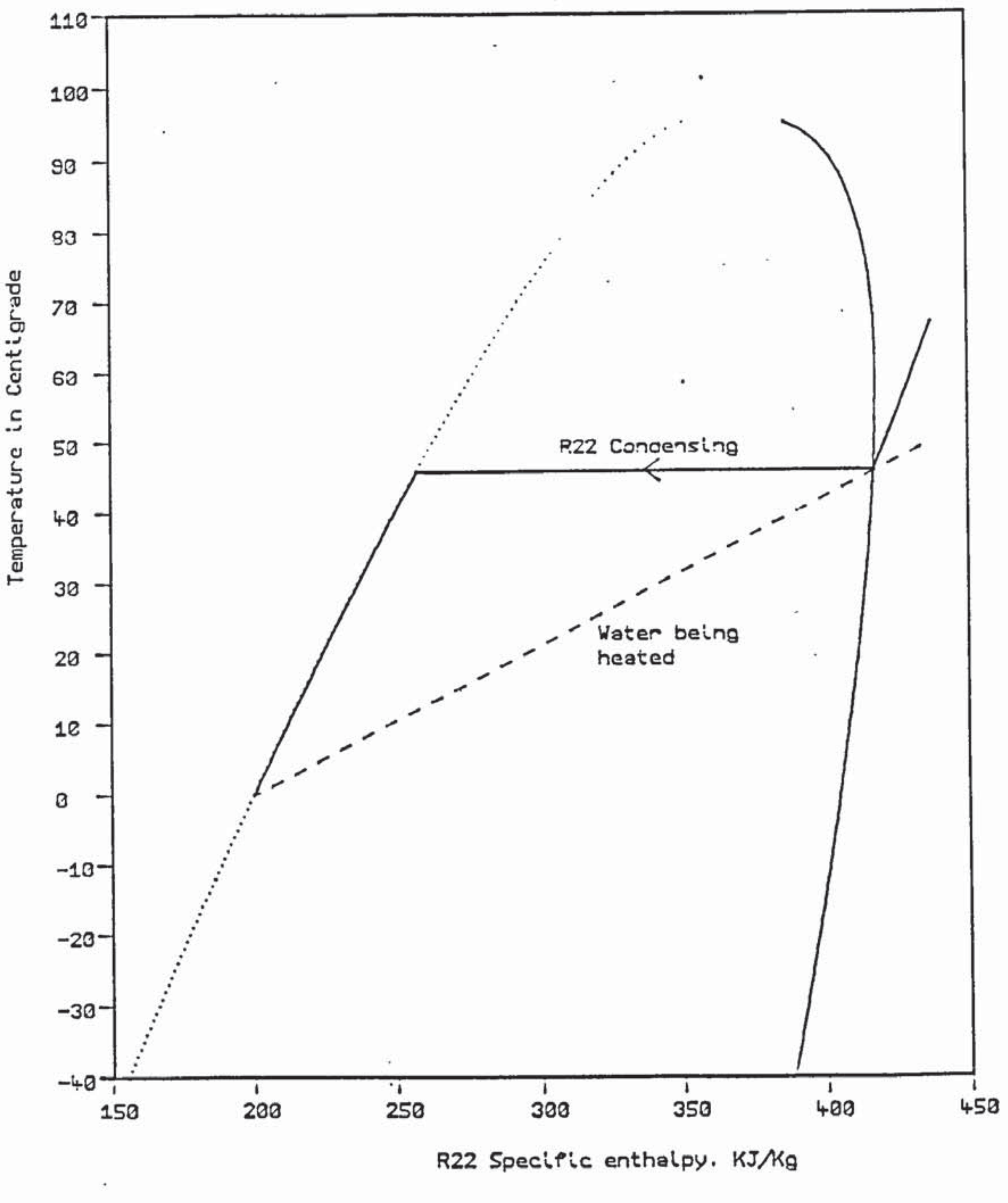

Figure 2.7. Condenser's limiting performance for counterflow heating

Water & refrigerant temperatures from table 2.7, R22 calculation throughout the heating duty. Thus the discharge pressure is initially low and rises with the rising water temperature. For this strategy, the degradation of latent heat by transfer to a lower temperature is no longer inevitable. However, unlike the single-pass method, there is no scope to reduce the throttling loss by subcooling the liquid, nor is there any scope to reduce the desuperheating loss.

Cycle calculations for single pass water heating

Figure 2.7 shows that for an ideal condenser, the water exit temperature can exceed the condensing temperature. In the following cycle analyses, the minimum necessary condensing temperature has been found, given that the water starts at 0C and is raised to 50C.

Table 2.8 presents a comparison of refrigerants R12, R22 & R502 assuming rejection to ambient of the compressor's waste heat. The system performance for a perfect, loss-free compressor can be observed by considering the figures for "COP, mechanical work only". In table 2.7, below, the essential minimum availability loss comparison is presented. The columns headed "Throttle loss" & "Condenser loss" indicate the availability losses due to throttling and due to heat transfer as percentages of the work of compression. η_A is the availability efficiency for the cycle, defined as the ratio of the load's availability increment to the work of compression.

C.O.Ps for heating water from 0C to 50C — Losses

Cycle	Ref't	C.O.P.	η_A%	Throttle	Condenser
Carnot		6.463	52.8	0.0	47.2
Rankine, heating water to 50C from 0C.	R12	7.372	60.22	2.60	37.18
	R22	7.473	61.05	3.33	35.62
	R502	7.580	61.92	4.85	33.23
Absolute limit		12.241	100.0	0.0	0.0

Table 2.7

The point of this analysis is to show that, even for an ideally large condenser, the specific heat mismatch between the water and the condensing refrigerant makes a heat transfer loss inevitable. An incoming water temperature of 0C has been used in order to evaluate the significance of this effect in the worst case. Rather gratifyingly, the Carnot cycle shows the greatest penalty, its heat transfer loss being 25% to 50% more serious than for the Rankine cycle. This is mainly due to the advantage won by the Rankine cycle's subcooling of the liquid down to the water entry temperature.

Dependence on compressor cooling method

Table 2.9 presents the results of solving the cycle for R12 for the four compressor cooling methods - rejection to ambient, transfer to the cold water incomer, transfer to the suction gas, and transfer to the exiting hot water.

Use of the cold water incomer produces a negligible improvement in the compressor cooling loss, compared with rejection to ambient, because the waste heat is still, essentially, transferred to a sink at ambient temperature. Furthermore, a slight increase in the throttling loss results, because the pre-heat of the water makes it impossible to subcool the liquid as far. Nonetheless, there is a significant improvement in the overall C.O.P. The availability analysis shows that this is due to a reduction in the heat transfer loss of condensing & subcooling. Those few degrees by which the water is preheated introduces a negligible availability increment of the load, but by reducing the temperature difference for subsequent heat transfer, a significant reduction in the total cycle loss is obtained.

In section 2.3 a criterion was deduced by which to choose between rejection of waste heat to ambient, or transfer to the suction gas. It was pointed out that this criterion was limited in its applicability by the qualification;- "If there is no requirement for heat at a temperature exceeding the condensing temperature...."

If, in table 2.9, the result for heat transfer to the suction gas is compared with that for rejection to ambient, then it can be seen that transfer to the suction gas results in the more favourable overall C.O.P. However, unquestioning application of the criterion deduced in section 2.3 would have erroneously predicted a more favourable performance by rejecting the waste heat to ambient. The point is that for the current calculation, it has been possible to exploit the superheat to significantly reduce the condensing temperature necessary for the required result. This, in turn, has resulted in a 15 Watt reduction in the work of compression. This illustrates the practical relevance of second-law thinking. It is of more than academic interest. Real savings can be made.

Transfer of waste heat to the water exit results in the greatest improvement in the compressor cooling loss, because this is the highest temperature available for rejection of its waste heat. As anticipated, this has resulted in the best C.O.P. Compared with waste heat transfer to the water incomer, two advantages are won;- The output power is slightly higher, because there is no loss in the ability to subcool the liquid, and the work of compression is 12 Watts lower, thanks to the lower necessary discharge pressure.

In table 2.10, refrigerants R12, R22 & R502 are compared for single pass water heating, with waste heat transfer to the hot water. A little caution is required before declaring R502 the clear winner. By virtue of the model used for the motor's power requirement, with its large constant term, the higher capacity that results from using R502 means that the motor is being operated more efficiently. However, if one refers back to table 2.7, it can again be seen that R502 is the best of the three. This is significant, because in table 2.6, which dealt instead with the problem of obtaining heat uniformly at the condensing temperature, R502 was not the best. This demonstrates that there is no absolutely best refrigerant, but for a well specified heating duty, it is possible to work out which refrigerant is best.

A study by the U.S. air force of its own residential heat pumps (5) came to the conclusion that R502 was better than R22. Their main interest was in reliability, and the lower discharge temperature of R502 was identified as the feature which accounted for the observed improvement. However, there are two reasons for the discharge temperature of R22 being excessive. The first reason is that R22 vapour has a low heat capacity. The second reason is that compressors are designed to transfer waste heat to the suction gas. Thus, one can see that use of a different compressor, which was either intrinsically more efficient, or designed for waste heat transfer to the load, would have altered the result of this comparison.

Comparison of R12, R22 & R502 for heating cold water

Refrigerant	R12	R22	R502
Waste heat rejected to;-	Ambient	Ambient	Ambient
Intercooler used ?	No	No	No
Water initial Temperature	0.000	0.000	0.000
Required final Temperature	50.000	50.000	50.000
Evaporating Temperature	0.000	0.000	0.000
Condensing Temperature	48.482	45.850	47.891
Condensate Temperature	0.000	0.000	0.000
Functions of state at cycle vertices			
Discharge Temperature	54.981	66.511	54.708
Pressure	11.766	17.635	20.058
Enthalpy	375.254	437.112	368.961
Cond. end Enthalpy	200.001	199.868	199.714
Entropy	0.998	0.996	0.995
Evap. sat. liq. Entropy	1.000	1.000	1.000
Evap. sat. liq. Enthalpy	200.000	200.000	200.000
Saturated vapour Entropy	1.555	1.752	1.537
Enthalpy	351.481	405.363	346.629
Pressure	3.084	4.974	5.731
specific volume	55.417	47.151	30.838
Suction Entropy	1.555	1.752	1.537
Enthalpy	351.481	405.363	346.629
specific volume	55.417	47.151	30.838
temperature	0.000	0.000	0.000
Cycle Performance			
Refrigerant flow rate g/s	7.218	8.483	12.971
Condenser output power	1264.985	2012.648	2195.271
Work of compression Watts	171.598	269.339	289.656
Excess requirement Watts	117.160	126.934	128.966
Carnot COP.	6.634	6.957	6.704
COP, mechanical work only	7.372	7.473	7.579
COP. overall	4.381	5.079	5.244
Availability Analysis, Watts			
Desuperheating loss	0.247	3.441	0.559
Condensing loss	44.130	66.023	57.891
Subcooling loss	19.615	27.524	38.644
Throttling loss	4.264	7.929	13.221
Compressor cooling loss	117.160	126.934	128.966
Load Availability lift	103.342	164.422	179.341
Total power input	288.758	396.273	418.622
Cycle's Availability efficiency	0.602	0.610	0.619
Overall Availability efficiency	0.358	0.415	0.428

Table 2.8

Comparison of different compresor cooling methods

Refrigerant	R12	R12	R12	R12
Waste heat rejected to;-	Ambient	Water in	Suction	Water out
Intercooler used ?	No	No	No	No
Water initial Temperature	0.000	0.000	0.000	0.000
Condenser entry Temperatur	0.000	4.329	0.000	0.000
Condenser exit Temperature	50.000	50.000	50.000	45.765
Required final Temperature	50.000	50.000	50.000	50.000
Evaporating Temperature	0.000	0.000	0.000	0.000
Condensing Temperature	48.482	48.578	43.285	44.475
Condensate Temperature	0.000	4.329	0.000	0.000
Functions of state at cycle vertices				
Discharge Temperature	54.981	55.087	77.273	50.587
Pressure	11.766	11.793	10.402	10.704
Enthalpy	375.254	375.295	394.363	373.542
Cond. end Enthalpy	200.001	203.994	200.005	200.004
Entropy	0.998	1.012	0.998	0.998
Evap. sat. liq. Entropy	1.000	1.000	1.000	1.000
Evap. sat. liq. Enthalpy	200.000	200.000	200.000	200.000
Saturated vapour Entropy	1.555	1.555	1.555	1.555
Enthalpy	351.481	351.481	351.481	351.481
Pressure	3.084	3.084	3.084	3.084
specific volume	55.417	55.417	55.417	55.417
Suction Entropy	1.555	1.555	1.618	1.555
Enthalpy	351.481	351.481	369.700	351.481
specific volume	55.417	55.417	63.011	55.417
temperature	0.000	0.000	28.099	0.000
Cycle Performance				
Refrigerant flow rate g/s	7.218	7.218	6.348	7.218
Condenser output power	1264.985	1236.459	1233.805	1252.605
Work of compression Watts	171.598	171.892	156.565	159.241
Excess requirement Watts	117.160	117.189	115.656	115.924
Carnot COP.	6.634	6.623	7.311	7.142
COP, mechanical work only	7.372	7.193	7.880	7.866
COP. overall	4.381	4.683	4.532	4.973
Availability Analysis, Watts				
Desuperheating loss	0.247	0.253	5.593	0.228
Condensing loss	44.130	40.951	38.213	43.674
Subcooling loss	19.615	16.507	14.351	17.061
Throttling loss	4.264	4.516	3.187	3.766
Compressor cooling loss	117.160	116.270	110.083	98.635
Load Availability lift	103.342	110.585	100.795	111.801
Total power input	288.758	289.081	272.221	275.165
Cycle's Avail'y efficiency	0.602	0.638	0.608	0.594
Overall Avail'y efficiency	0.358	0.383	0.370	0.406

Table 2.9

Comparison of R12, R22 & R502 for water heating

Refrigerant	R12	R22	R502
Waste heat rejected to;-	Water out	Water out	Water out
Intercooler used ?	No	No	No
Water initial Temperature	0.000	0.000	0.000
Condenser entry Temperatur	0.000	0.000	0.000
Condenser exit Temperature	45.765	47.044	47.236
Required final Temperature	50.000	50.000	50.000
Evaporating Temperature	0.000	0.000	0.000
Condensing Temperature	44.475	43.359	45.386
Condensate Temperature	0.000	0.000	0.000
Functions of state at cycle vertices			
Discharge Temperature	50.587	63.080	51.845
Pressure	10.704	16.625	18.968
Enthalpy	373.542	435.554	367.980
Cond. end Enthalpy	200.004	199.882	199.740
Entropy	0.998	0.996	0.996
Evap. sat. liq. Entropy	1.000	1.000	1.000
Evap. sat. liq. Enthalpy	200.000	200.000	200.000
Saturated vapour Entropy	1.555	1.752	1.537
Enthalpy	351.481	405.363	346.629
Pressure	3.084	4.974	5.731
specific volume	55.417	47.151	30.838
Suction Entropy	1.555	1.752	1.537
Enthalpy	351.481	405.363	346.629
specific volume	55.417	47.151	30.838
temperature	0.000	0.000	0.000
Cycle Performance			
Refrigerant flow rate g/s	7.218	8.483	12.971
Condenser output power	1252.605	1999.307	2182.205
Work of compression Watts	159.241	256.119	276.930
Excess requirement Watts	115.924	125.612	127.693
Carnot COP.	7.142	7.300	7.018
COP, mechanical work only	7.866	7.806	7.880
COP. overall	4.973	5.567	5.709
Availability Analysis, Watts			
Desuperheating loss	0.228	3.201	0.515
Condensing loss	43.674	65.827	58.962
Subcooling loss	17.061	25.117	35.768
Throttling loss	3.766	7.328	12.273
Compressor cooling loss	98.635	106.665	108.400
Load Availability lift	111.801	173.594	188.705
Total power input	275.165	381.731	404.623
Cycle's Availability efficiency	0.594	0.604	0.612
Overall Availability efficiency	0.406	0.455	0.466

Table 2.10

2.7 Cycle calculations for immersed condenser

For the immersed condenser, analysis of the performance requires that the work of compression and the availability losses be integrated over the course of the heating duty. Having discussed use of an intercooler, and different compressor cooling options, it would be perverse to reconsider all these variations. For the purpose of computational convenience and conceptual simplicity, the following calculations consider the problem of heating a 100 Litre water tank.

For each refrigerant, two calculations are necessary. In the first calculation, in order to obtain a unique comparison of the refrigerants, uncomplicated by the compressor inefficiency model, rejection of the motor's waste heat to ambient is supposed. The absolute upper limit to C.O.P. and availability efficiency can then be found using the calculated mechanical work of compression.

In the second calculation, rejection of the motor's waste heat to the water tank is supposed, in order to find the practical upper limit to the performance.

In both calculations it has been supposed that an intercooler is available, and that an intelligent control system brings it into operation only when the appropriate condensate temperature has been reached, using equation 2.46, the criterion deduced in section 2.3.

Tables 2.11 - 2.13 present the results of the first calculation for R12, R22 & R502. The limiting C.O.Ps, for use of a hypothetical ideal compressor, are seen to be 10.798, 10.534, & 10.306, respectively. The corresponding availability efficiencies can be found by dividing by 12.241. For example, the highest C.O.P, obtained with R12, corresponds to an availability efficiency of 88%.

In order to answer the question "How significant is the improvement obtained by using an intelligent intercooler control ?", the calculation for R502, presented in table 2.13, has been repeated in table 2.14, but without any use of an intercooler. The resulting C.O.P. of 9.966 is 3.4% poorer. Reference to the "Mechanical work" in tables 2.13 & 2.14 shows that using the intercooler reduces it by 69

KJoules, which corresponds exactly to the reduction in the total of the desuperheating, throttling, & intercooler losses, as can be seen by inspection of the figures. This is another illustration of the "Law of accountability of availability" introduced in section 2.3.

Tables 2.15 to 2.17 present the results of the second calculation, for rejection of waste heat to the load. The figures for the overall C.O.P. are collated in table 2.18 below, which includes a comparison with the results of the counter flow, single pass calculation, table 2.10.

	Overall C.O.P.		
Waste heat rejected to;-	Ambient	Load	Load
	Immersed condenser		single pass
R12	5.011	5.561	4.973
R22	6.031	6.478	5.567
R502	6.057	6.490	5.709

Table 2.18

In this example, the immersed condenser gives a better C.O.P. than single-pass heating. For the immersed condenser, transfer of the latent heat of condensation across a temperature difference is not inevitable, unlike single pass counterflow heating, figure 2.7. Against this, the subcooling which is possible in single-pass heating gives a reduction in the throttling loss. For the immersed condenser, this feature appears to be precluded by the absence of subcooling. However, for the immersed condenser there is a reduction in the throttling loss thanks to the initially low condensate pressure. Thus, in spite of one's initial impression, the immersed heat exchanger gives a throttling loss reduction similar in magnitude to the case of single pass counterflow heating. This leaves a net advantage thanks to the reduced heat transfer loss.

It is worth noting that for R12 in a loss free compressor the C.O.P. is increased from 7.9 for single pass heating to 10.8 for the immersed condenser - an improvement of 36%. The overall C.O.P, on the other hand, shows only an 11% improvement. This is symptomatic of an important general point. If the compressor is inefficient, then the value of optimisation is degraded, because the dominant feature is the compressor's availability degradation rate. Note that in every table of calculated results, the largest entry in the list of losses has always been the compressor cooling loss. One is thus led to recognise that there is greater scope for improvement by addressing the compressor's losses than by seeking to optimise the rest of the system.

Limiting C.O.P. Perfect compressor. Immersed condenser. Intercooler

Heating a 100 L water tank from 0C to 50C using R12 evaporating at 0C

Waste heat rejected to;-		Ambient	Ambient	Ambient	Ambient
Intercooler used ?		No	No	Yes	Yes
Condensing Temperature		0.500	24.500	26.500	49.500
Functions of state at cycle vertices					
Discharge	Temperature	0.603	28.450	57.313	105.833
	Pressure	3.135	6.425	6.783	12.048
	Enthalpy	351.761	364.343	384.337	413.966
Cond. end	Enthalpy	200.462	223.163	225.109	248.354
	Entropy	1.002	1.080	1.087	1.160
Intercooler exit enthalpy				207.929	216.131
Intercooler exit entropy				1.028	1.055
Intercooler exit temp.				8.528	17.282
Saturated vapour	Entropy	1.555	1.555	1.555	1.555
	Enthalpy	351.481	351.481	351.481	351.481
	Pressure	3.084	3.084	3.084	3.084
	specific volume	55.417	55.417	55.417	55.417
Suction	Entropy	1.555	1.555	1.615	1.663
	Enthalpy	351.481	351.481	368.660	383.703
	specific volume	55.417	55.417	62.594	68.474
	temperature	0.000	0.000	26.500	49.500
Cycle Performance					
Refrigerant flow rate g/s		7.218	7.218	6.390	5.842
Condenser output power		1092.084	1019.039	1017.531	967.455
Work of compression Watts		2.025	92.838	100.182	176.788
Excess requirement Watts		100.203	109.284	110.018	117.679
Carnot COP.		547.300	12.149	11.308	6.518
COP, mechanical work only		539.208	10.977	10.157	5.472
COP. overall		10.683	5.042	4.841	3.285
Availability Analysis, Watts					
Desuperheating loss		0.001	0.125	6.159	16.650
Intercooler loss		0.000	0.000	1.598	5.249
Throttling loss		0.029	8.834	2.436	6.464
Compressor cooling loss		100.203	109.284	110.018	117.679
Load Availability lift		1.995	83.879	89.989	148.426
Total power input		102.228	202.121	210.200	294.467
Availability efficiency		0.020	0.415	0.428	0.504

Result of integration. All energies in KJoules. Heating time = 5h 41m

Availability lift	1709.451	Load enthalpy lift	20925.000
Desuperheat loss	114.511		
Intercooler Loss	33.217		
Throttle loss	80.606		
Cooling loss	2237.942	Excess consumption	2237.942
Total energy input	4175.769	Mechanical work	1937.827
C.O.P. for process	5.011	C.O.P. work only	10.798

Availability efficiency: 0.409 overall.   Rankine cycle only = 0.882

Table 2.11

Limiting C.O.P. Perfect compressor. Immersed condenser

Heating a 100 L water tank from 0C to 50C using R22 evaporating at 0C

Waste heat rejected to;-	Ambient	Ambient	Ambient	Ambient
Intercooler used ?	No	No	No	No
Condensing Temperature	0.500	19.500	34.500	49.500

Functions of state at cycle vertices

Discharge Temperature	0.776	29.309	50.752	71.514
Pressure	5.056	8.970	13.374	19.197
Enthalpy	405.745	419.673	429.862	439.363
Cond. end Enthalpy	200.586	223.464	242.461	262.566
Entropy	1.002	1.082	1.144	1.206
Saturated vapour Entropy	1.752	1.752	1.752	1.752
Enthalpy	405.363	405.363	405.363	405.363
Pressure	4.974	4.974	4.974	4.974
specific volume	47.151	47.151	47.151	47.151
Suction Entropy	1.752	1.752	1.752	1.752
Enthalpy	405.363	405.363	405.363	405.363
specific volume	47.151	47.151	47.151	47.151
temperature	0.000	0.000	0.000	0.000

Cycle Performance

Refrigerant flow rate g/s	8.483	8.483	8.483	8.483
Condenser output power	1740.456	1664.525	1589.807	1499.845
Work of compression Watts	3.240	121.393	207.835	288.433
Excess requirement Watts	100.324	112.139	120.784	128.843
Carnot COP.	547.300	15.008	8.917	6.518
COP, mechanical work only	537.186	13.712	7.649	5.200
COP. overall	16.806	7.128	4.838	3.594

Availability Analysis, Watts

Desuperheating loss	0.001	1.022	2.729	4.949
Throttling loss	0.058	9.460	26.825	53.383
Compressor cooling loss	100.324	112.139	120.784	128.843
Load Availability lift	3.180	110.911	178.282	230.102
Total power input	103.564	233.533	328.619	417.276
Availability efficiency	0.031	0.475	0.543	0.551

Result of integration. All energies in KJoules. Heating time = 3h 34m

Availability lift	1709.451	Load enthalpy lift	20925.000
Desuperheat loss	24.985		
Intercooler Loss	0.000		
Throttle loss	251.938		
Cooling loss	1482.985	Excess consumption	1482.985
Total energy input	3469.378	Mechanical work	1986.393
C.O.P. for process	6.031	C.O.P. work only	10.534

Availability efficiency: 0.493 overall.   Rankine cycle only = 0.861

Table 2.12

Limiting C.O.P. Perfect compressor. Immersed condenser

Heating a 100 L water tank from 0C to 50C using R502 evaporating at 0C

Waste heat rejected to;-	Ambient	Ambient	Ambient	Ambient
Intercooler used ?	No	Yes	Yes	Yes
Condensing Temperature	0.500	19.500	34.500	49.500

Functions of state at cycle vertices

Discharge Temperature	0.589	41.638	72.718	103.214
Pressure	5.821	10.062	14.723	20.784
Enthalpy	346.904	372.239	392.472	413.164
Cond. end Enthalpy	200.567	222.802	241.272	260.647
Entropy	1.002	1.079	1.140	1.199
Intercooler exit enthalpy		208.373	215.703	223.837
Intercooler exit entropy		1.029	1.054	1.080
Intercooler exit temp.		7.367	13.746	20.802
Saturated vapour Entropy	1.537	1.537	1.537	1.537
Enthalpy	346.629	346.629	346.629	346.629
Pressure	5.731	5.731	5.731	5.731
specific volume	30.838	30.838	30.838	30.838
Suction Entropy	1.537	1.588	1.625	1.661
Enthalpy	346.629	361.058	372.198	383.438
specific volume	30.838	34.191	36.621	38.963
temperature	0.000	19.500	34.500	49.500

cycle Performance

Refrigerant flow rate g/s	12.971	11.699	10.923	10.266
Condenser output power	1898.116	1748.267	1651.489	1565.770
Work of compression Watts	3.564	130.804	221.445	305.168
Excess requirement Watts	100.356	113.080	122.144	130.517
Carnot COP.	547.300	15.008	8.917	6.518
COP, mechanical work only	532.576	13.366	7.458	5.131
COP. overall	18.265	7.168	4.807	3.594

Availability Analysis, Watts

Desuperheating loss	0.001	7.069	18.424	32.271
Intercooler loss	0.000	2.162	6.389	12.546
Throttling loss	0.095	5.080	11.428	20.126
Compressor cooling loss	100.356	113.080	122.144	130.517
Load Availability lift	3.468	116.493	185.204	240.226
Total power input	103.920	243.885	343.589	435.685
Availability efficiency	0.033	0.478	0.539	0.551

Result of integration. All energies in KJoules. Heating time = 3h 24m

Availability lift	1709.451	Load enthalpy lift	20925.000
Desuperheat loss	154.407		
Intercooler Loss	54.903		
Throttle loss	111.625		
Cooling loss	1424.348	Excess consumption	1424.348
Total energy input	3454.794	Mechanical work	2030.446
C.O.P. for process	6.057	C.O.P. work only	10.306

Availability efficiency: 0.495 overall. Rankine cycle only = 0.842

Table 2.13

R502 with no intercooler, to see what penalty results

Heating a 100 L water tank from 0C to 50C using R502 evaporating at 0C

Waste heat rejected to;-	Ambient	Ambient	Ambient	Ambient
Intercooler used ?	No	No	No	No
Condensing Temperature	0.500	19.500	34.500	49.500
Functions of state at cycle vertices				
Discharge Temperature	0.589	22.515	39.492	56.554
Pressure	5.821	10.062	14.723	20.784
Enthalpy	346.904	356.672	363.491	369.581
Cond. end Enthalpy	200.567	222.802	241.272	260.647
Entropy	1.002	1.079	1.140	1.199
Saturated vapour Entropy	1.537	1.537	1.537	1.537
Enthalpy	346.629	346.629	346.629	346.629
Pressure	5.731	5.731	5.731	5.731
specific volume	30.838	30.838	30.838	30.838
Suction Entropy	1.537	1.537	1.537	1.537
Enthalpy	346.629	346.629	346.629	346.629
specific volume	30.838	30.838	30.838	30.838
temperature	0.000	0.000	0.000	0.000
Cycle Performance				
Refrigerant flow rate g/s	12.971	12.971	12.971	12.971
Condenser output power	1898.116	1736.404	1585.282	1412.973
Work of compression Watts	3.564	130.266	218.715	297.708
Excess requirement Watts	100.356	113.027	121.872	129.771
Carnot COP.	547.300	15.008	8.917	6.518
COP, mechanical work only	532.576	13.330	7.248	4.746
COP. overall	18.265	7.137	4.655	3.305
Availability Analysis, Watts				
Desuperheating loss	0.001	0.156	0.425	0.879
Throttling loss	0.095	14.409	40.516	80.055
Compressor cooling loss	100.356	113.027	121.872	129.771
Load Availability lift	3.468	115.701	177.774	216.774
Total power input	103.920	243.292	340.587	427.479
Availability efficiency	0.033	0.476	0.522	0.507

Result of integration. All energies in KJoules. Heating time = 3h 30m

Availability lift	1709.451	Load enthalpy lift	20925.000
Desuperheat loss	4.118		
Intercooler Loss	0.000		
Throttle loss	386.023		
Cooling loss	1469.488	Excess consumption	1469.488
Total energy input	3569.098	Mechanical work	2099.611
C.O.P. for process	5.863	C.O.P. work only	9.966

Availability efficiency: 0.479 overall. Rankine cycle only = 0.814

Table 2.14

Immersed condenser integration. Heat rejection optimised (cf table 2.11)

Heating a 100 L water tank from 0C to 50C using R12 evaporating at 0C

Waste heat rejected to;-	Water	Water	Water	Water
Intercooler used ?	No	No	Yes	Yes
Condensing Temperature	0.500	24.500	26.500	49.500
Functions of state at cycle vertices				
Discharge Temperature	0.603	28.450	57.313	105.833
Pressure	3.135	6.425	6.783	12.048
Enthalpy	351.761	364.343	384.337	413.966
Cond. end Enthalpy	200.462	223.163	225.109	248.354
Entropy	1.002	1.080	1.087	1.160
Intercooler exit enthalpy			207.929	216.131
Intercooler exit entropy			1.028	1.055
Intercooler exit temp.			8.528	17.282
Saturated vapour Entropy	1.555	1.555	1.555	1.555
Enthalpy	351.481	351.481	351.481	351.481
Pressure	3.084	3.084	3.084	3.084
specific volume	55.417	55.417	55.417	55.417
Suction Entropy	1.555	1.555	1.615	1.663
Enthalpy	351.481	351.481	368.660	383.703
specific volume	55.417	55.417	62.594	68.474
temperature	0.000	0.000	26.500	49.500
Cycle Performance				
Refrigerant flow rate g/s	7.218	7.218	6.390	5.842
Condenser output power	1092.084	1019.039	1017.531	967.455
Work of compression Watts	2.025	92.838	100.182	176.788
Excess requirement Watts	100.203	109.284	110.018	117.679
Carnot COP.	547.300	12.149	11.308	6.518
COP, mechanical work only	539.208	10.977	10.157	5.472
COP. overall	11.663	5.582	5.364	3.685
Availability Analysis, Watts				
Desuperheating loss	0.001	0.125	6.159	16.650
Intercooler loss	0.000	0.000	1.598	5.249
Throttling loss	0.029	8.834	2.436	6.464
Compressor cooling loss	100.019	100.288	100.289	99.625
Load Availability lift	2.178	92.874	99.719	166.480
Total power input	102.228	202.121	210.200	294.467
Availability efficiency	0.021	0.459	0.474	0.565

Result of integration. All energies in KJoules. Heating time = 5h 8m

Availability lift	1709.451	Load enthalpy lift	20925.000
Desuperheat loss	102.605		
Intercooler Loss	29.756		
Throttle loss	72.597		
Cooling loss	1848.686	Excess consumption	2020.504
Total energy input	3763.133	Mechanical work	1742.629
C.O.P. for process	5.561	C.O.P. work only	10.848

Availability efficiency: 0.454 overall. Rankine cycle only = 0.882

Table 2.15

Immersed condenser integration. Heat rejection optimised. cf table 2.12

Heating a 100 L water tank from 0C to 50C using R22 evaporating at 0C

Waste heat rejected to;-	Water	Water	Water	Water
Intercooler used ?	No	No	No	No
Condensing Temperature	0.500	19.500	34.500	49.500
Functions of state at cycle vertices				
Discharge Temperature	0.776	29.309	50.732	71.514
Pressure	5.056	8.970	13.374	19.197
Enthalpy	405.745	419.673	429.862	439.363
Cond. end Enthalpy	200.586	223.464	242.461	262.566
Entropy	1.002	1.082	1.144	1.206
Saturated vapour Entropy	1.752	1.752	1.752	1.752
Enthalpy	405.363	405.363	405.363	405.363
Pressure	4.974	4.974	4.974	4.974
specific volume	47.151	47.151	47.151	47.151
Suction Entropy	1.752	1.752	1.752	1.752
Enthalpy	405.363	405.363	405.363	405.363
specific volume	47.151	47.151	47.151	47.151
temperature	0.000	0.000	0.000	0.000
Cycle Performance				
Refrigerant flow rate g/s	8.483	8.483	8.483	8.483
Condenser output power	1740.456	1664.525	1589.807	1499.845
Work of compression Watts	3.240	121.393	207.835	288.433
Excess requirement Watts	100.324	112.139	120.784	128.843
Carnot COP.	547.300	15.008	8.917	6.518
COP, mechanical work only	537.186	13.712	7.649	5.200
COP. overall	17.774	7.608	5.205	3.903
Availability Analysis, Watts				
Desuperheating loss	0.001	1.022	2.729	4.949
Throttling loss	0.058	9.460	26.825	53.383
Compressor cooling loss	100.141	104.667	107.239	109.077
Load Availability lift	3.363	118.384	191.826	249.869
Total power input	103.564	233.533	328.619	417.276
Availability efficiency	0.032	0.507	0.584	0.599

Result of integration. All energies in KJoules. Heating time = 3h 20m

Availability lift	1709.451	Load enthalpy lift	20925.000
Desuperheat loss	23.184		
Intercooler Loss	0.000		
Throttle loss	233.720		
Cooling loss	1263.952	Excess consumption	1383.678
Total energy input	3230.325	Mechanical work	1846.647
C.O.P. for process	6.478	C.O.P. work only	10.582

Availability efficiency: 0.529 overall. Rankine cycle only = 0.861

Table 2.16

Immersed condenser integration. Optimal heat rejection. cf table 2.13

Heating 100 L water tank from 0C to 50C using R502 evaporating at 0C

Waste heat rejected to;-	Water	Water	Water	Water
Intercooler used ?	No	Yes	Yes	Yes
Condensing Temperature	0.500	19.500	34.500	49.500
Functions of state at cycle vertices				
Discharge Temperature	0.589	41.638	72.718	103.214
Pressure	5.821	10.062	14.723	20.784
Enthalpy	346.904	372.239	392.472	413.164
Cond. end Enthalpy	200.567	222.802	241.272	260.647
Entropy	1.002	1.079	1.140	1.199
Intercooler exit enthalpy		208.373	215.703	223.837
Intercooler exit entropy		1.029	1.054	1.080
Intercooler exit temp.		7.367	13.746	20.802
Saturated vapour Entropy	1.537	1.537	1.537	1.537
Enthalpy	346.629	346.629	346.629	346.629
Pressure	5.731	5.731	5.731	5.731
specific volume	30.838	30.838	30.838	30.838
Suction Entropy	1.537	1.588	1.625	1.661
Enthalpy	346.629	361.058	372.198	383.438
specific volume	30.838	34.191	36.621	38.963
temperature	0.000	19.500	34.500	49.500
Cycle Performance				
Refrigerant flow rate g/s	12.971	11.699	10.923	10.266
Condenser output power	1898.116	1748.267	1651.489	1565.770
Work of compression Watts	3.564	130.804	221.445	305.168
Excess requirement Watts	100.356	113.080	122.144	130.517
Carnot COP.	547.300	15.008	8.917	6.518
COP, mechanical work only	532.576	13.366	7.458	5.131
COP. overall	19.231	7.632	5.162	3.893
Availability Analysis, Watts				
Desuperheating loss	0.001	7.069	18.424	32.271
Intercooler loss	0.000	2.162	6.389	12.546
Throttling loss	0.095	5.080	11.428	20.126
Compressor cooling loss	100.173	105.546	108.447	110.493
Load Availability lift	3.652	124.028	198.901	260.249
Total power input	103.920	243.885	343.589	435.685
Availability efficiency	0.035	0.509	0.579	0.597

Result of integration. All energies in KJoules. Heating time = 3h 11m

Availability lift	1709.451	Load enthalpy lift	20925.000
Desuperheat loss	143.505		
Intercooler Loss	51.008		
Throttle loss	103.962		
Cooling loss	1216.015	Excess consumption	1332.187
Total energy input	3223.997	Mechanical work	1891.810
C.O.P. for process	6.490	C.O.P. work only	10.357

Availability efficiency: 0.530 overall. Rankine cycle only = 0.842

Table 2.17

2.8 Non Azeotropic mixed working fluids

As explained in section 2.6, if a counter fluid is to be heated through a non-negligible temperature rise by the condenser, then the constancy of the condensing temperature results in a serious second law loss. In table 2.8, for instance, this exceeded 1/3 of the work of compression, and in the last column of table 2.9, the heat transfer loss of 61 Watts compares unfavourably with the 159 Watt work of compression.

It is possible to engineer a working fluid for which the condensing temperature falls as the liquid fraction increases. Any non azeotropic mixture has this property.

Two-component thermodynamics

There is just one fundamental principle which determines the pressure and composition of the vapour phase in equilibrium with a liquid phase of specified composition and temperature. For each component, the partial molar Gibb's function of the vapour equals that of the liquid.

In general, if two liquids or two real gases are mixed isothermally and isobarically, there is a total volume change and a total enthalpy change. In such a case, pressure, temperature and composition (PTx) data are either measured directly, or calculated on the basis of experimentally measured enthalpy and volume changes of mixing.

In some cases, the enthalpy and volume changes are negligible. If, furthermore, the partial molar entropy change of component i is given by the equation;-

$$\Delta s_i = R\ln(x_i) \qquad 2.55$$

where x_i is the mole fraction of component i, then the mixture is known as a "Hildebrand regular solution" (38)

It is not obvious that this expression for the change in partial molar entropy is universally valid. It has the mathematical significance of being the simplest analytic function which satisfies the Gibb's Duhem equation. The Gibb's Duhem equation is explained in texts on physical chemistry, e.g. (39). Equation 2.55 also has the physical significance of exactness for a mixture of perfect gases. However, in general, it is not necessarily exact.

Using the Hildebrand regular solution concept, it is possible to retain real gas equations of state when calculating the composition and pressure of vapour in equilibrium with a specified liquid mixture, as shown in (40).

Figure 2.8 shows the result of calculating the vapour pressure of an oil/R12 mixture, as a function of oil mole fraction, assuming that this is a Hildebrand regular solution. This was a particularly simple calculation, as it was assumed that no oil was present in the vapour. The partial molar Gibb's function of the vapour was then found from pure freon vapour thermodynamics. The partial molar Gibb's function of the liquid was found from the known Gibb's function of the pure liquid, and equation 2.55 for the entropy of mixing. The vapour pressure was then found by iterating trial values for pressure, until the vapour's Gibb's function equalled that of the liquid.

In fact, for a mixture of R12 and Alkylbenzene, the oil of interest, there is a slight positive enthalpy of mixing. This results in the actual vapour pressure exceeding the Hildebrand vapour pressure. Figure 2.9 shows the experimentally determined vapour pressure curve (41,42). This linear relationship illustrates "Raoult's" law.

The point is, that in the absence of information about enthalpy and volume changes of mixing, the additional refinement of the Hildebrand analysis over use of Raoult's law cannot be justified, in view of the potentially large uncertainty introduced by these unknowns.

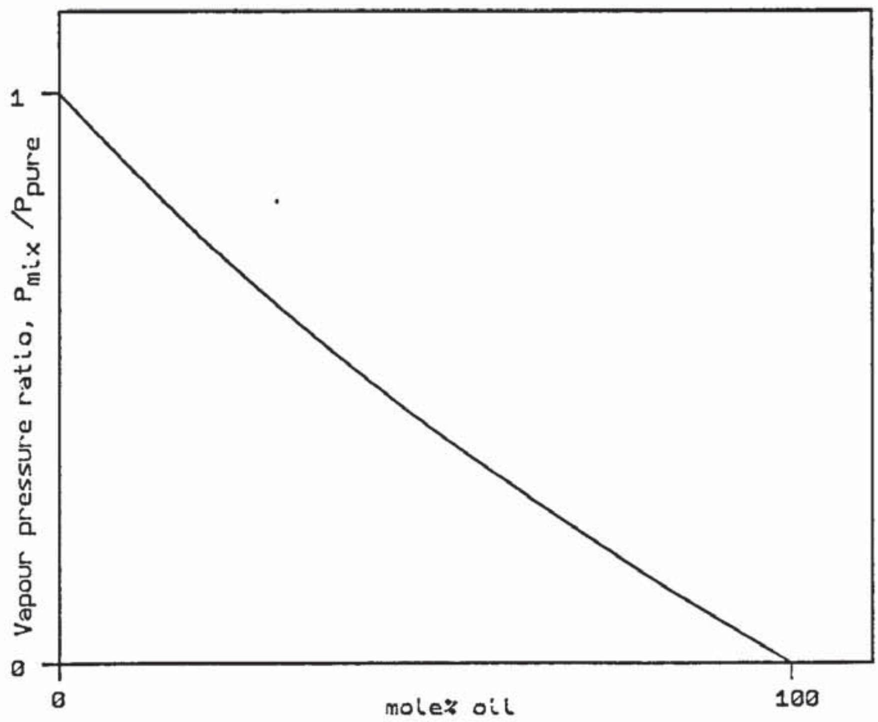

Figure 2.8a. Vapour pressure of a Hildebrand regular solution of R12 in oil

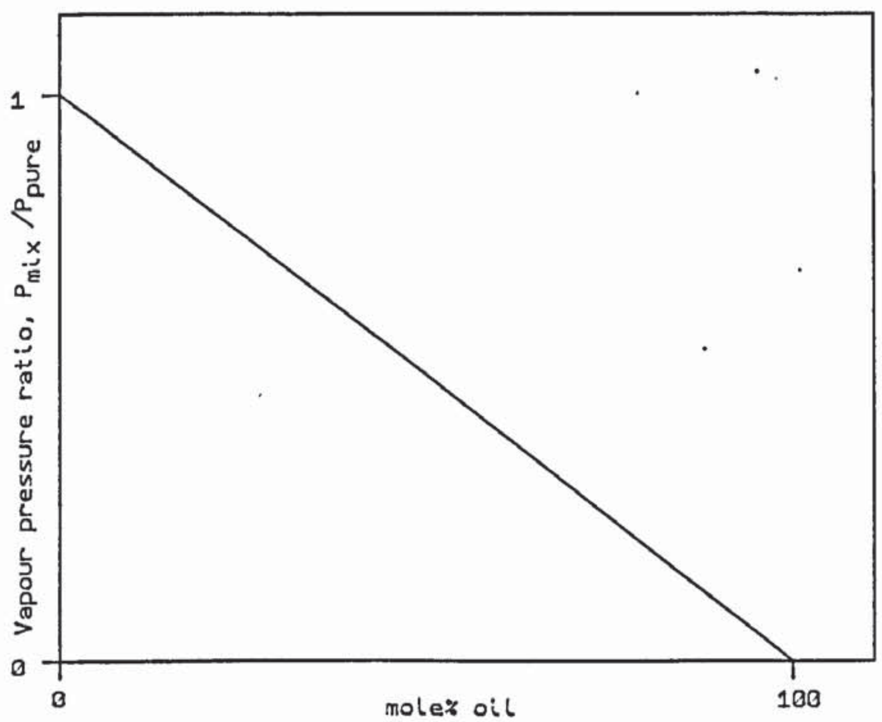

Figure 2.8b. Vapour pressure of an oil/R12 mixture satisfying Raoult's law

Determination of dew point and bubble point from Raoult's law

Consider a gas mixture of 30 mole% R11 and 70 mole% R12 at a pressure of 6 Bar. Using Raoult's law, it has been calculated that this mixture begins to condense at 54C, and is not fully condensed until the temperature falls to 33C. Because the calculation uses a complicated iterative algorithm, the underlying principles are more easily explained by starting with the answer, and showing why it is consistent.

In table 2.19, below, the vapour pressures of R12 & R11 are listed for the temperature range of 30C to 60C.

Temperature	vapour pressure R12	vapour pressure R11
30	7.446	1.254
33	8.051	1.386
35	8.474	1.479
40	9.603	1.735
45	10.839	2.023
50	12.188	2.346
54	13.354	2.633
55	13.658	2.708
60	15.254	3.111

Table 2.19

Consider first the calculation of the bubble point of the liquid mixture. Using Raoult's law, it is necessary to find the temperature for which 0.3x(R11 vapour pressure) + 0.7x(R12 vapour pressure) = 6 Bar. By inspection of the figures above, a little mental arithmetic shows that at 30C the vapour pressure of this liquid mixture would be 5.6 Bar, and at 35C it would be 6.4 Bar. At 33C the required answer is found.

The calculation of the dew point is less straightforward, because the composition of the first condensate is not known. It is the vapour composition which is known. For this pressure of 6 bar, the partial pressures are 4.2 Bar for R12, and 1.8 Bar for R11. Suppose 50C is used as a trial solution. Taking the ratios of these partial pressures to the vapour pressures, one would deduce an initial condensate composition of 34% R12, and 77% R11. This adds up to more than 100%, because 50C is not the right answer. By iterating the temperature until the liquid composition is correctly normalised, the dew point can be found. One can verify that 54C is correct.

Temperature - enthalpy diagrams for binary mixtures, using Raoult's law

Figure 2.9 shows the temperature - enthalpy diagram for the binary mixture discussed above. 14 isobars are plotted for pressures of 1 Bar to 16 Bar. Table 2.20, below, lists the dew point and bubble point of this composition for the isobars of figure 2.9. Note that there is consistently over 20C difference between the start and end of condensation. Figure 2.9 shows that for this composition, there is an approximately linear relationship between temperature and enthalpy. If the need existed to heat water, for instance, by 20C, then the availability loss due to transfer of the latent heat could be made very much smaller than for the conventional Rankine cycle.

Dew & bubble points for 70-30 mole % R12/R11 mixture

Pressure, bar	Dew Point	Bubble point
0.5	-16.5	-38.4
1.0	-0.6	-22.5
2.0	17.8	-3.9
3.0	30.0	8.5
4.0	39.4	18.1
5.0	47.2	25.9
6.0	53.9	32.7
7.0	59.8	38.6
8.0	65.2	44.0
9.0	70.0	48.9
10.0	74.5	53.4
12.0	82.5	61.5
14.0	89.6	68.6
16.0	96.0	75.0

Table 2.20

Figure 2.9 also betrays the penalty of using a binary fluid in a heat pump. Suppose an ambient source is available at a temperature of 0C. Reference to table 2.20 shows that in order to maintain complete evaporation of the mixture, the evaporating pressure would be 1 Bar, and the initial evaporating temperature would be -20C, roughly. For a constant temperature source, then, the advantage of a reduced condenser loss is negated by a seriously increased heat transfer loss at the

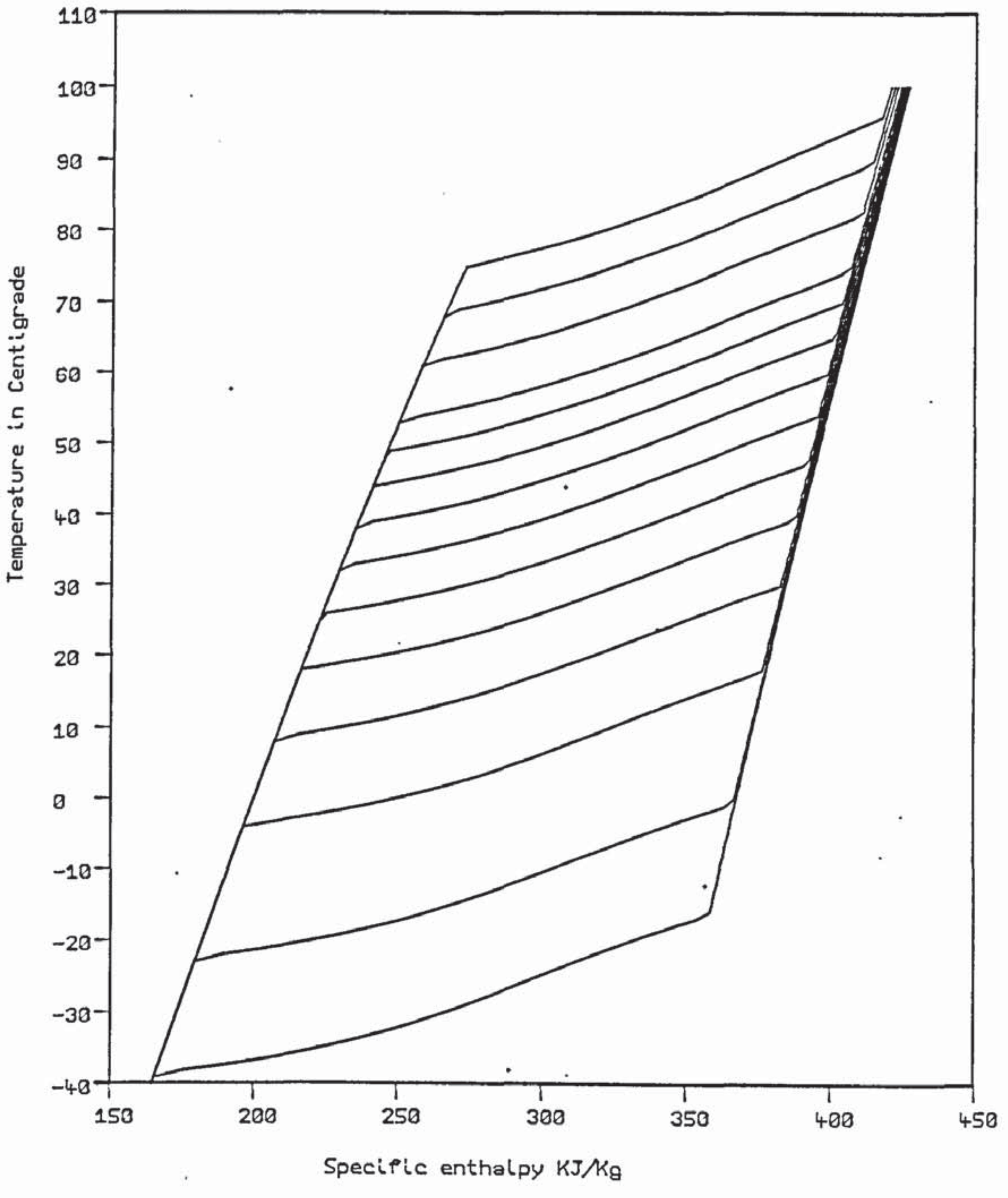

Figure 2.9. Condensing isobars for mixture of 70 mole% R12 & 30 mole% R11

evaporator.

Calculations have been reported (43) which claim that for a 30% mass fraction of R11 in a mixture of R12 & R11, a 23% improvement in C.O.P. was possible. While precise details of the source and load specifications were not provided, it was stated that the system under consideration was required to lower the temperature of the source fluid in a single-pass counter-current evaporator.

It is only in this case that no additional heat transfer penalty at the evaporator is introduced. For domestic applications in which the evaporator draws from an ambient source there seems to be no scope for other than a marginal gain, if any.

2.9 Turbocharging - a proposal for recovering the throttling loss

After the compressor, the next most significant loss of availability is due to the use of a throttle, instead of a work-recovering expander. A common objection to the suggestion that shaft work be recovered by the expansion device is the impossibility of matching the flow through the expander to the pumping rate of the compressor, unless each can operate independently of the other. For instance, use of a turbine mounted on the compressor's crank shaft would result in this matching problem.

There is a way of using a work recovering expander without losing the independence of the compressor from the expander. Instead of using a throttle, the condensed liquid is supplied to a turbine, which drives a centrifugal compressor working on the suction gas. The purpose of this turbine driven centrifugal compressor is to partially compress the suction gas before delivery to the main compressor. In this way, it is possible to recover the availability of the high pressure liquid by using it to increase the availability of the suction gas. This is analogous to use of an intercooler, which exchanges enthalpy. However, whereas an intercooler can yield only a marginal gain, due to the inevitable extra heat transfer losses introduced by its use, there is no inevitable entropy creation introduced by suction gas pre-compression.

It has to be stressed that this is not meant as an opinion about the relative technical limitations or merits of heat exchangers and turbines. Even in the thermodynamic limit, intercooling introduces inevitable availability losses due to the specific heat mis-match between the liquid and the suction gas, and due to the increased discharge gas temperature. Conversely, the thermodynamic limit of the proposed availability exchange, using a turbine and a pre-compressor, incurs no availability degradation at all.

With this more complicated expansion device, control of the liquid flow rate to match the compressor's pumping rate becomes a more difficult problem. Since the availability loss of throttling is mainly due to the large specific volume of the flash gas, one might propose throttling the liquid to an intermediate pressure, and then using the turbine to complete the decompression. Control of the liquid flow rate would then have to be based on controlling the orifice area for the initial throttling. It is also worth noting that two-phase de-compression is outwith the general experience of turbine development. However, it should be stressed that the pursuit of this technology is not yet justified by the efficiency of currently available compressors.

2.10 Summing up, further implications, and Conclusion

The utility of Availability analysis for both diagnosis and optimisation has been illustrated by considering a few special cases. This has included the development of optimisation criteria for the disposal of the compressor's waste heat, use of an intercooler, and the mode of operation of the condenser.

For the standard Rankine cycle, it has been found that the desuperheating availability loss is very small in comparison with the other losses. This has a bearing on the question of whether there can be any advantage in wet compression, which has recently been proposed for a rotary sliding vane compressor (44). The distinguishing feature of wet compression is elimination of the desuperheating loss. The upper limit to any improvement in efficiency can thus be assessed by inspection of the figures for the availability breakdown. For instance, R22's desuperheating loss on table 2.1 is 2% of the work of compression. Elimination of this loss would thus give a 2% reduced power requirement for the same output. If wet compression is to entail a significant increase in complication, then one can see that it would not be worthwhile. The power of availability analysis, illustrated here, is that it permits definite quantitative conclusions to be drawn without the need to model the details of any proposed hardware. Indeed, in this example, a conclusion about the value of the modification can be drawn even before a design has been considered.

It has been observed that, using a realistic model of the compressor's power consumption, the most serious loss is due to the compressor's poor efficiency. This major handicap has the effect of diminishing the advantages which are theoretically possible through optimisation.

Chapter 3. Construction and instrumentation of an experimental heat pump

In order to obtain detailed information about the functioning of a heat pump, a small water to water heat pump was constructed and extensively instrumented. Figure 3.1 shows the back view of the rig. The compressor and condenser sit on the middle shelf, with the evaporator on the lower shelf. The principal components had all been used previously in a rig built and tested by Mr. Othman (45). The following descriptions deal first with the heat pump, and latterly with the instrumentation. It is worth pointing out that in addition to the formal calibration tests reported here, because of the instrumentation's critical nature, informal checks of internal consistency were made very frequently.

3.1 The compressor

A Danfoss SC10H was used (46). The SC10H is a small hermetic compressor intended for use with R12. The specifications are listed below.

Gas displacement

Bore	32 mm.
Stroke	12.7 mm.
Swept volume	10.2 cc.
TDC dead space	0.5 cc.

Discharge system

Plenum	29 cc.
Internal pipe	5mm I.D. 6.35mm O.D. 50cm length.
Valve	Self-acting reed, augmented by a backing spring.

Suction system

Intake stub	6 mm I.D.
Outer plenum	70 cc
Inner plenum	55 cc
Interplenum bores	5 mm I.D. 2 off.
Valve	Self-acting reed.

turbine to complete the decompression. Control of the liquid flow rate would then have to be based on controlling the orifice area for the initial throttling. It is also worth noting that two-phase de-compression is outwith the general experience of turbine development. However, it should be stressed that the pursuit of this technology is not yet justified by the efficiency of currently available compressors.

2.10 Summing up, further implications, and Conclusion

The utility of Availability analysis for both diagnosis and optimisation has been illustrated by considering a few special cases. This has included the development of optimisation criteria for the disposal of the compressor's waste heat, use of an intercooler, and the mode of operation of the condenser.

For the standard Rankine cycle, it has been found that the desuperheating availability loss is very small in comparison with the other losses. This has a bearing on the question of whether there can be any advantage in wet compression, which has recently been proposed for a rotary sliding vane compressor (44). The distinguishing feature of wet compression is elimination of the desuperheating loss. The upper limit to any improvement in efficiency can thus be assessed by inspection of the figures for the availability breakdown. For instance, R22's desuperheating loss on table 2.1 is 2% of the work of compression. Elimination of this loss would thus give a 2% reduced power requirement for the same output. If wet compression is to entail a significant increase in complication, then one can see that it would not be worthwhile. The power of availability analysis, illustrated here, is that it permits definite quantitative conclusions to be drawn without the need to model the details of any proposed hardware. Indeed, in this example, a conclusion about the value of the modification can be drawn even before a design has been considered.

It has been observed that, using a realistic model of the compressor's power consumption, the most serious loss is due to the compressor's poor efficiency. This major handicap has the effect of diminishing the advantages which are theoretically possible through optimisation.

Chapter 3. Construction and instrumentation of an experimental heat pump

In order to obtain detailed information about the functioning of a heat pump, a small water to water heat pump was constructed and extensively instrumented. Figure 3.1 shows the back view of the rig. The compressor and condenser sit on the middle shelf, with the evaporator on the lower shelf. The principal components had all been used previously in a rig built and tested by Mr. Othman (45). The following descriptions deal first with the heat pump, and latterly with the instrumentation. It is worth pointing out that in addition to the formal calibration tests reported here, because of the instrumentation's critical nature, informal checks of internal consistency were made very frequently.

3.1 The compressor

A Danfoss SC10H was used (46). The SC10H is a small hermetic compressor intended for use with R12. The specifications are listed below.

Gas displacement

Bore	32 mm.
Stroke	12.7 mm.
Swept volume	10.2 cc.
TDC dead space	0.5 cc.

Discharge system

Plenum	29 cc.
Internal pipe	5mm I.D. 6.35mm O.D. 50cm length.
Valve	Self-acting reed, augmented by a backing spring.

Suction system

Intake stub	6 mm I.D.
Outer plenum	70 cc
Inner plenum	55 cc
Interplenum bores	5 mm I.D. 2 off.
Valve	Self-acting reed.

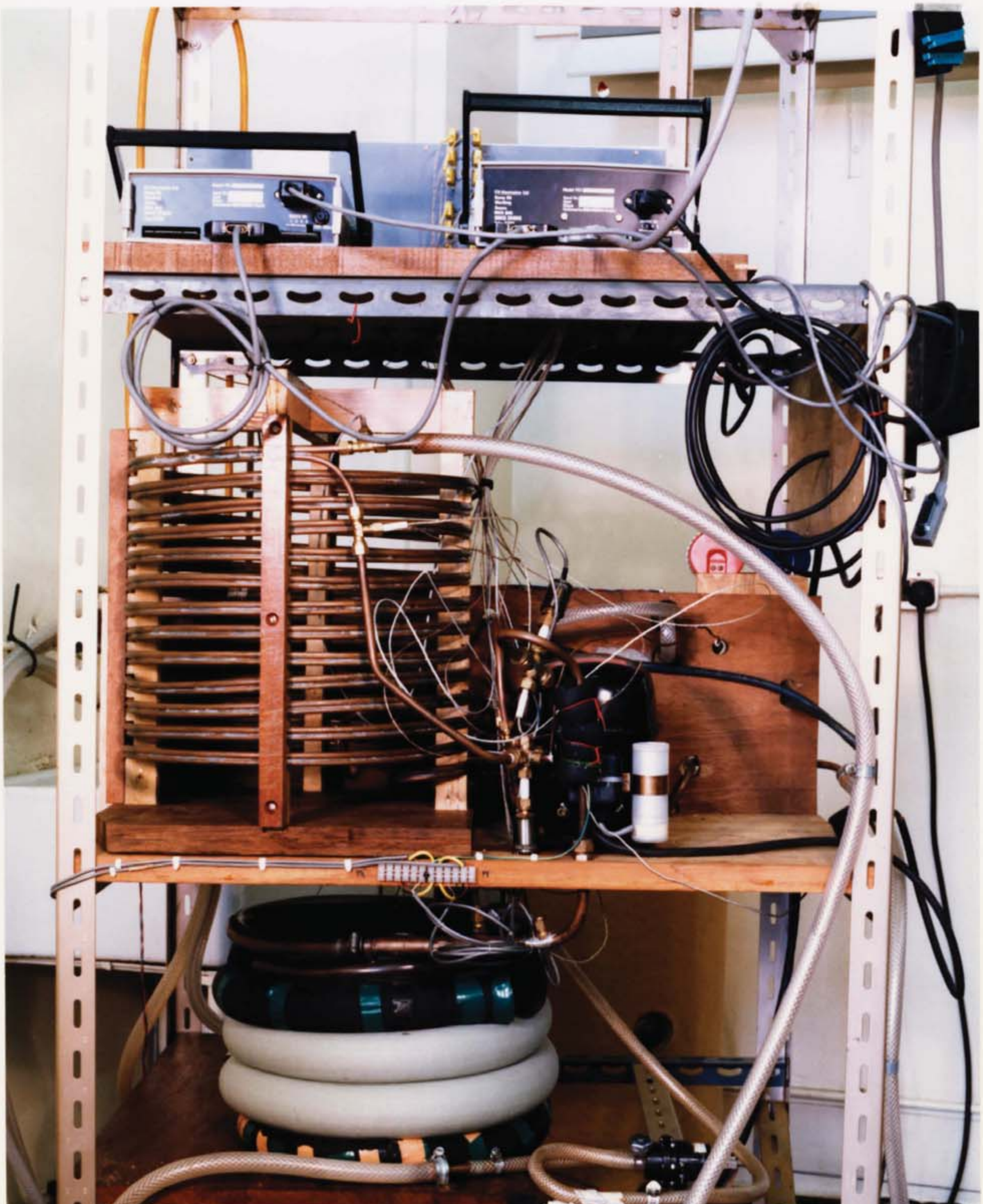

Figure 3.1. Rear view of rig, showing the compressor, the condenser and (below) the evaporator.

The motor

The compressor uses a nominal 250 Watt synchronous induction motor with a skew squirrel cage aluminium conductor cast through the rotor. Start-up uses a small start winding at 90^{o} to the main winding. The start winding is supplied through a capacitor, connected by a relay actuated by the high current transient of starting.

The lubricant

Danfoss originally specified 650 cc of 'Zerol 150' which was the brand name for Alkylbenzene manufactured by Du-Pont. Danfoss later advised (47) that they had changed their recommended fill to 500 cc. Du-Pont transferred manufacture of Zerol 150 to a different maker around 1984 (48), as a result of which it appears that the specification of Zerol 150 has changed.

3.2 The condenser

This consists of an 8 mm water pipe soldered against a 6 mm pipe carrying refrigerant. It is 15 m long and is normally used in the counter-current configuration. This heat exchanger can be seen on figure 3.1 as the helical copper winding beside the compressor. It was later lagged.

In order to accomodate the variations in the required R12 charge with varying operating conditions, a liquid accumulator is included near the end of the condenser. A special accumulator was designed and constructed to include a sight glass, so that the liquid level in the accumulator would be observable, figure 3.2.

It has been stated (49) that the liquid accumulator is best situated upstream from the expansion valve, rather than at the condenser's end. By including a set of 6 valves in the construction, it was made possible to situate the accumulator either at the condenser's end, or 2 m upstream from the condenser's end, merely by choosing one of two settings of these valves. This facilitated an experimental investigation of the choice of accumulator position.

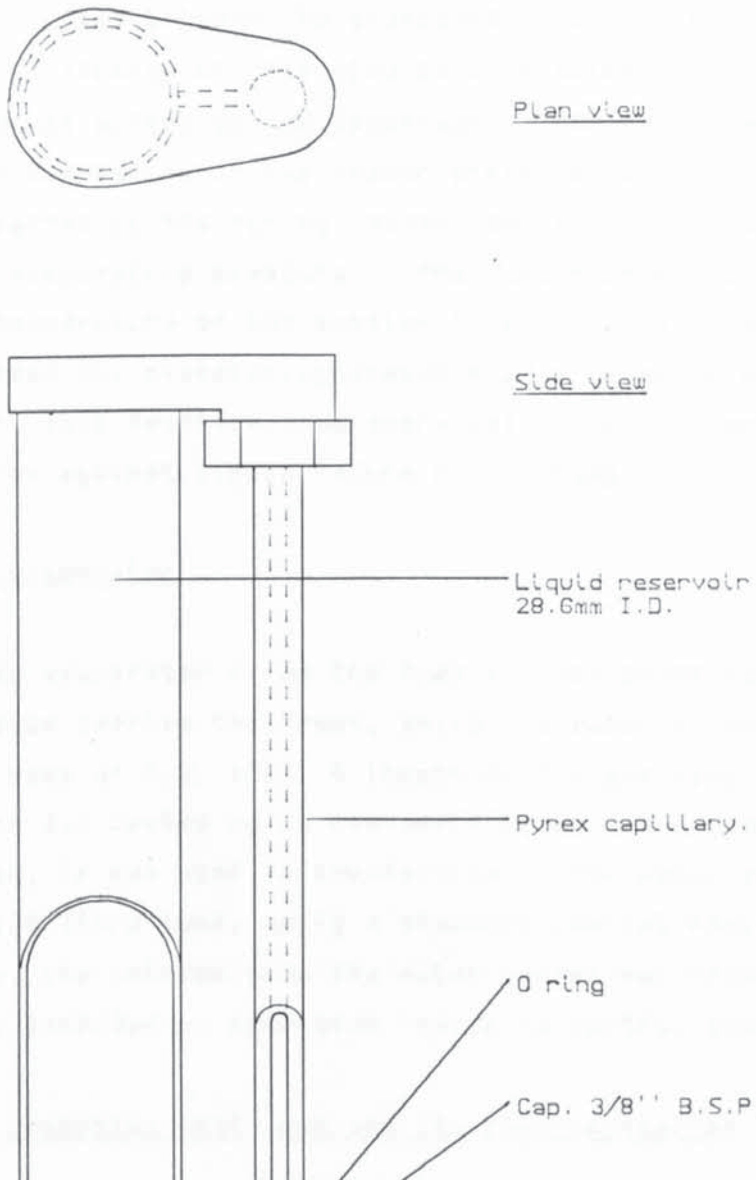

Figure 3.2. Liquid reservoir design with sight glass.

3.3 The expansion valve

Danfoss make a range of thermostatic expansion valves, and supply technical information to assist one's choice (50). A "TF2" was used. This is a simple valve with an internal pressure equaliser, and without a maximum opening pressure. Figure 3.3 shows the principle of operation. The actual orifice through which the liquid flows is annular, formed between the truncated conical plug and its seat. The opening or closing of this plug is controlled by the balance of the three forces acting on the diaphragm. The valve is opened if there is sufficient pressure in the vapour pressure bulb to overcome the combined force exerted by the spring, whose compression is set by the adjustor, and the evaporating pressure. The vapour pressure in the bulb depends on the temperature of the suction line. Since this vapour pressure must exceed the evaporating pressure by a fixed value set by the adjustor, this feedback loop guarantess some suction gas superheat, and so ensures against liquid return to the sump.

3.4 The evaporator

The evaporator is of the tube in tube geometry. The inner 1/2" copper pipe carries the freon, while the water flows in the outer plastic hose of I.D. 1". A length of 5 m was used, and it can be seen on figure 3.1 coiled up on the shelf below the condenser. Like the condenser, it was used in counterflow. The water side was supplied from a 100 litre tank, using a standard central heating pump. Normally, the outflow from the water jacket was returned to the tank. The tank included an immersion heater to control the water temperature.

3.5 The assembled heat pump and its instrumentation

Figure 3.4 is a circuit diagram of the heat pump. In order to obtain comprehensive diagnostic data many measurements are necessary. Pressure transducers were mounted at the four principle vertices of the freon circuit, situated on the compressor's suction and discharge stubs, and on either side of the expansion valve. There are likewise four essential water temperature measurements, at the beginning and end of each heat exchanger. The corresponding four R12 temperature measurements are thus also essential.

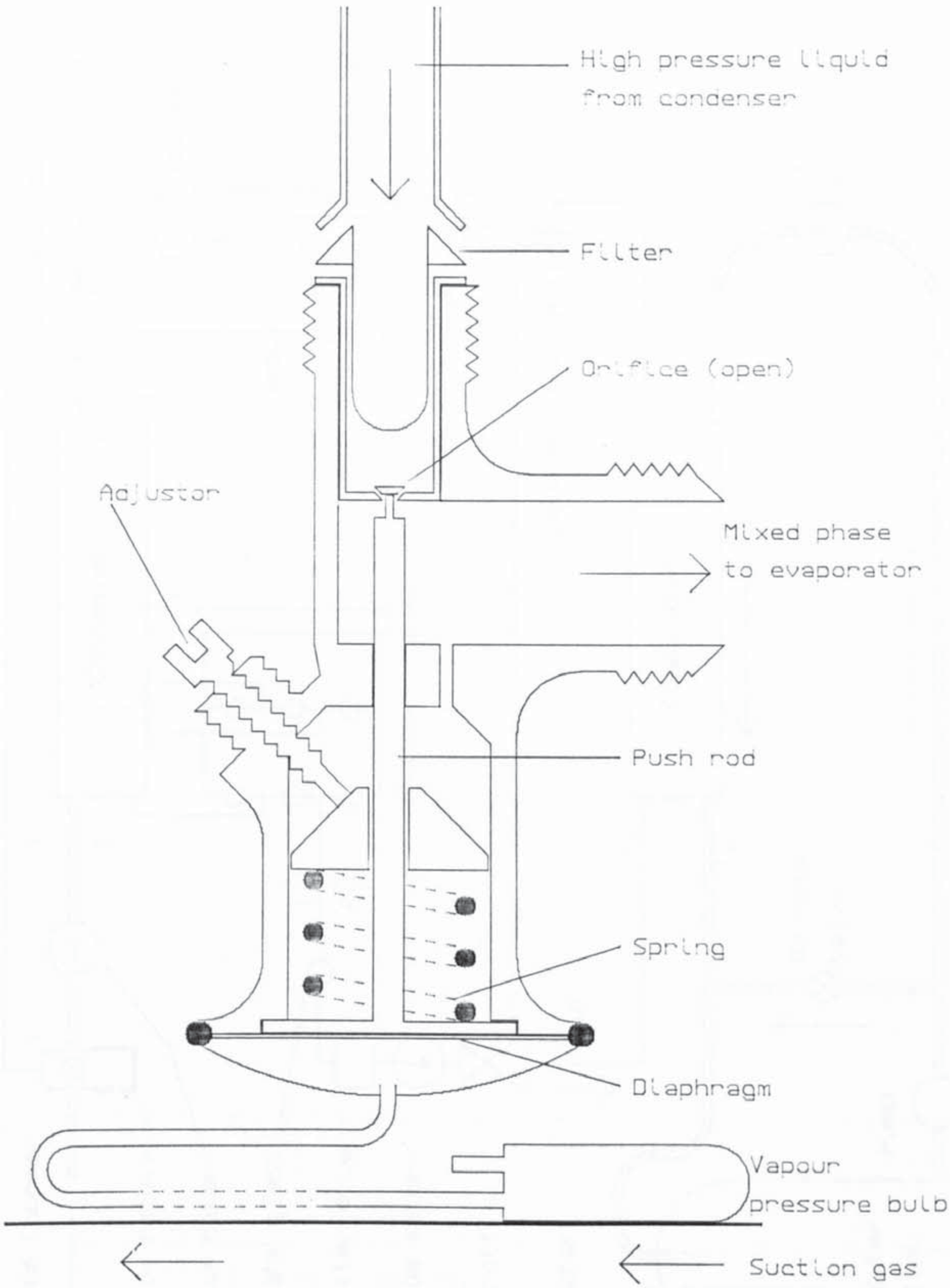

Figure 3.3. Thermostatic expansion valve, in section

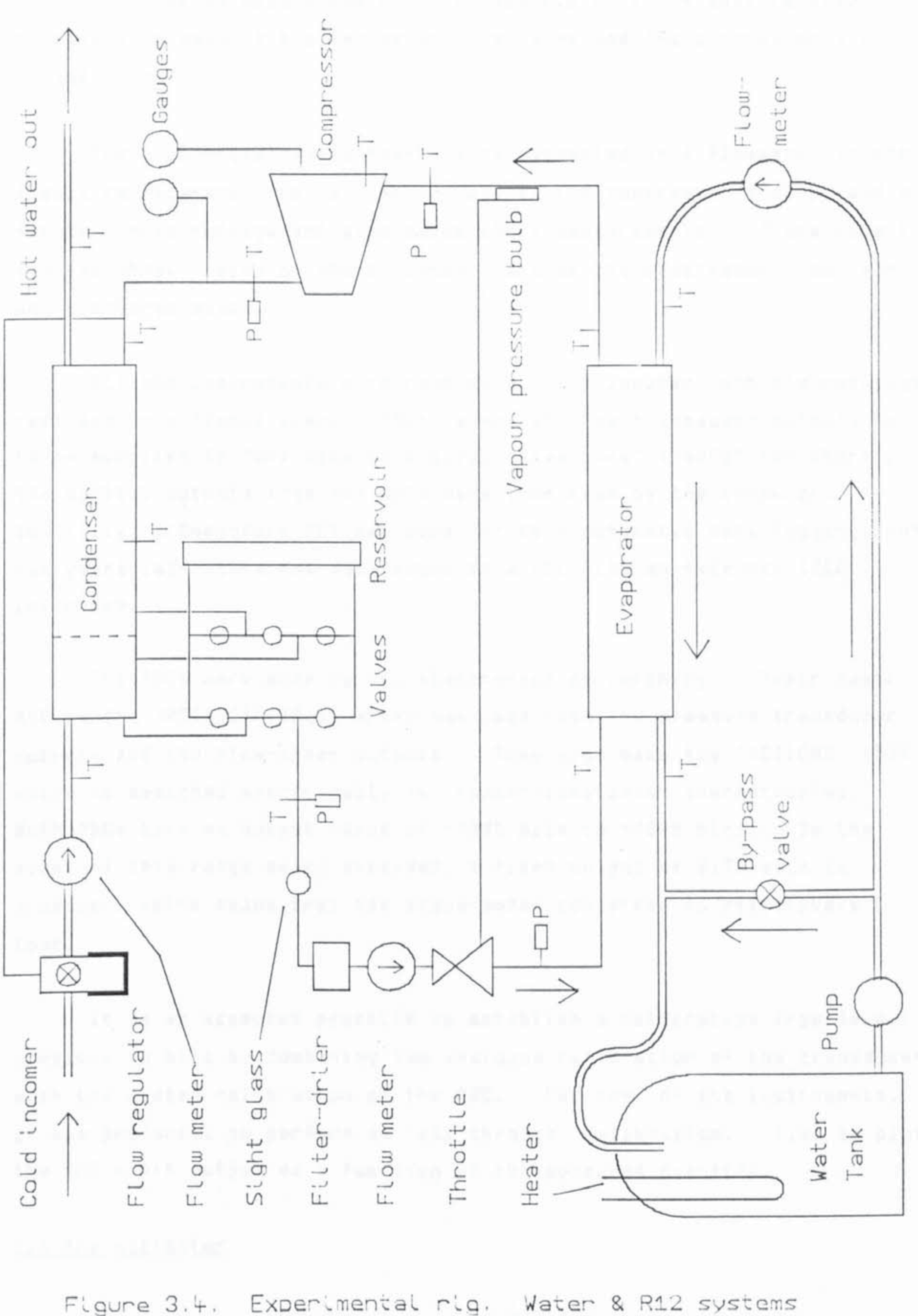

Figure 3.4. Experimental rig. Water & R12 systems

In order to obtain the capacity and C.O.P. it is additionally necessary to measure the two water flow rates and the compressor's power consumption.

These essential measurements were augmented by a flowmeter in the liquid refrigerant line, a thermocouple in the compressor's sump, and a further three refrigerant side temperature measurements. These were in the two-phase region of the condenser, and at the compressor's suction and discharge stubs.

All the instruments were read by a microcomputer, and the readings recorded on a floppy disc. This is why all the transducer outputs had to be supplied to "analogue to digital converters" ("ADCs" for short). The digital outputs from the ADCs were then read by the computer. Initially, a Commodore PET was used for this automatic data logging, but two years later this was superseded by a BBC with an external IEEE interface.

The ADCs were made by CIL electronics of Worthing. Their basic ADC is the 'PCI1001' (51), which was used with the pressure transducer outputs and the flow-meter outputs. They also make the 'PCI1002' (52) which is designed specifically for copper-constantan thermocouples. Both ADCs have an output range of -4095 bits to +4095 bits. In the event of this range being exceeded, a fixed output of 8196 bits is produced, which means that the measurement concerned is effectively lost.

It is an accepted practice to establish a calibration from (e.g.) pressure to bits by combining the analogue calibration of the transducer with the quoted calibration of the ADC. For most of the instruments, it was preferred to perform an 'all-through' calibration. i.e. to plot the ADC's bit output as a function of the measured quantity.

3.6 The wattmeter

As described in (45), a standard C.E.G.B. KwH meter had been modified to give a power measurement. The passage of the gradations at the edge of its aluminium disc is detected by an opto-electronic device comprising an infra red L.E.D. which shines down onto the surface, and a photo transistor oriented to detect the reflection. After amplification, the signal is fed to a frequency-to-voltage ("f-v") converter and thence to the ADC.

The only shortcoming of this arrangement was that the C.E.G.B. wattmeter was oversized. It was rated for 40 Amps, corresponding to 10 KWatts for unit power factor. The compressor's consumption is typically 2 Amps and 300 Watts. For this reason, the current coil in the Wattmeter was rewound, increasing the number of turns by a factor of 8. This brought the typical frequency input to the f-v converter up from about 4 Hz to over 30 Hz.

Since the compressor presents an inductive load, it was important to ensure phase shift independance of the wattmeter's calibration. There are a couple of adjustor's on the wattmeter, one of which allows a phase shift dependance to be adjusted out. Because of the difficulty of obtaining a pure inductance, this adjustment was carried out using two 2uFd capacitors in parallel.

For the calibration of wattmeter frequency against power, a range of loads was used from 40 Watts to a 1 Kwatt heater. The power was measured independently using an ammeter and a voltmeter, with no reactive load in the circuit. At each resistance used, the 4 uFd capacitor was switched into parallel with the load to check that the wattmeter's speed remained constant. The resulting figures for output frequency against power are summarised below;-

Power, Watts	Frequency, Hertz
0	0
39.5	5.25
60.0	7.9
96.0	12.6
156.6	20.4
188.5	24.55
246.0	32.15
305.4	39.9
336.8	44.0
394.2	51.45

Table 3.1

These points are plotted on figure 3.5. They are matched by the calibration equation

$$\text{Power (Watts)} = 7.66 \times \text{frequency (Hertz)} \qquad 3.1$$

Having obtained a calibration of the wattmeter which was unaffected by capacitive loading, the calibration was checked with inductive loads. In order to make an independent measurement of the power, a two beam oscilloscope was used to inspect the current and voltage waveforms. Additionally, the resistances of the various inductances were measured in order to obtain corroborative checks of the power measurement using I^2R.

These measurements lacked the precision of the calibration using capacitive loading, because the current waveform was so badly distorted by the inductors. However, there was no evidence of a change of calibration due to inductive loading.

By calibrating the combination of f-v converter and ADC, a relationship between input frequency and output bits was deduced. Upon combining this with the above wattmeter calibration, the net result was obtained;-

$$\text{Power} = 0.15974 \times (\text{Bits} + 27) \qquad 3.2$$

This calibration was occasionally checked by running the data acquisition programme and ascertaining that it reported the correct power when a known load was plugged in.

In October 1986 a more thorough re-calibration was performed in preparation for the final set of experiments. Table 3.2 lists the result.

Power, Watts	Output bits
0	-27
101	585
265	1551
425	2510

Table 3.2

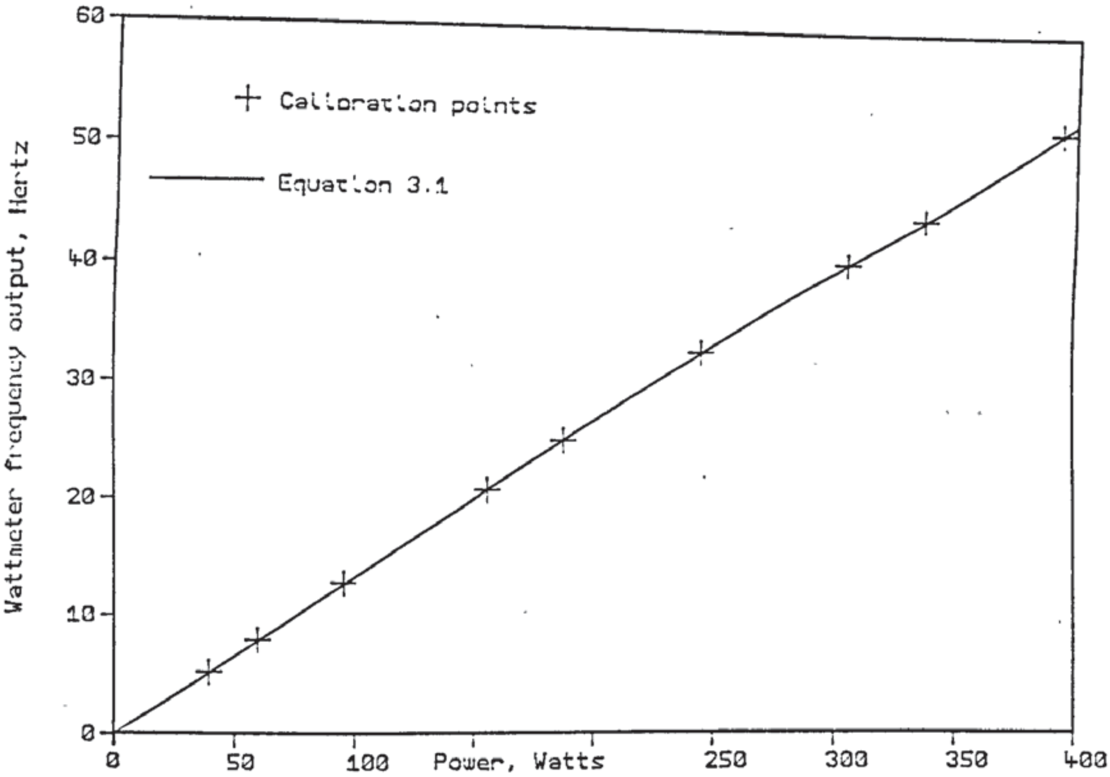

Figure 3.5 Wattmeter calibration

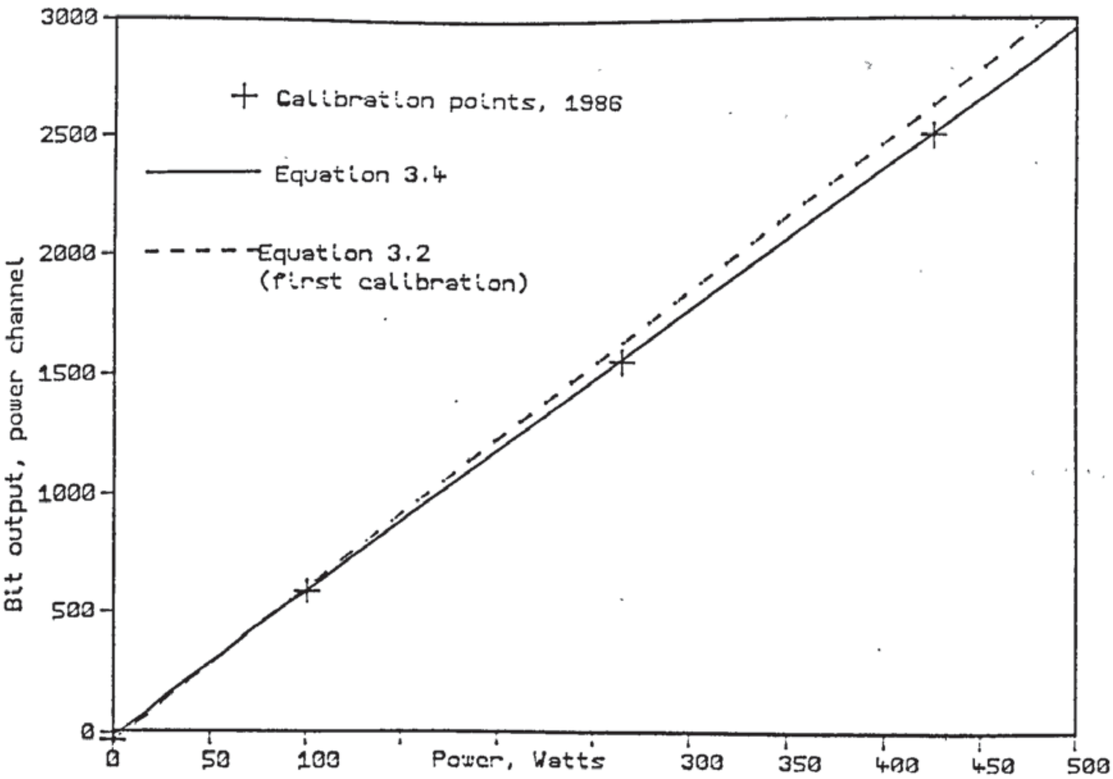

Figure 3.6 Wattmeter calibration. First & last compared

The calibration equation

$$\text{Power} = 4 \text{ Watts} + 0.1683 \times \text{bits} \qquad 3.3$$

fits these points. However, a check on the zero point immediately before starting the first run precipitated the adjustment to;

$$\text{Power} = 0.1683 \times (\text{bits} + 9) \qquad 3.4$$

This new calibration shows that at a given power, the bit output is 5% lower than originally. Figure 3.6 compares this later calibration with the original.

3.7 Mains voltage and current consumption monitor

For reasons explained in chapter 4, it was found desirable to augment the instrumentation with a facility for including a record of mains voltage and compressor current consumption. For the sake of completeness, the details of the instrument are shown on the circuit diagram figure 3.7.

This instrument produced two analogue outputs, approximately proportional to mains voltage, and to the compressor's current consumption. These were supplied to channels 1 & 2 of the thermocouple ADC, which are straightforward analogue inputs, designed for signals of up to 1 Volt. The current meter was calibrated by noting the bit output for a range of different loads, while measuring the current consumption with an ammeter.

Figure 3.8 shows the resulting calibration plot. Because the compressor's consumption is always around 2 amps, the calibration equation was chosen as the tangent to this curve at 2 amps. This gives;

$$\text{Current, mA} = 246 + 1.256 \times \text{bits} \qquad 3.5$$

The results are summarised in table 3.3 below, which compares this current calibration with the measured current.

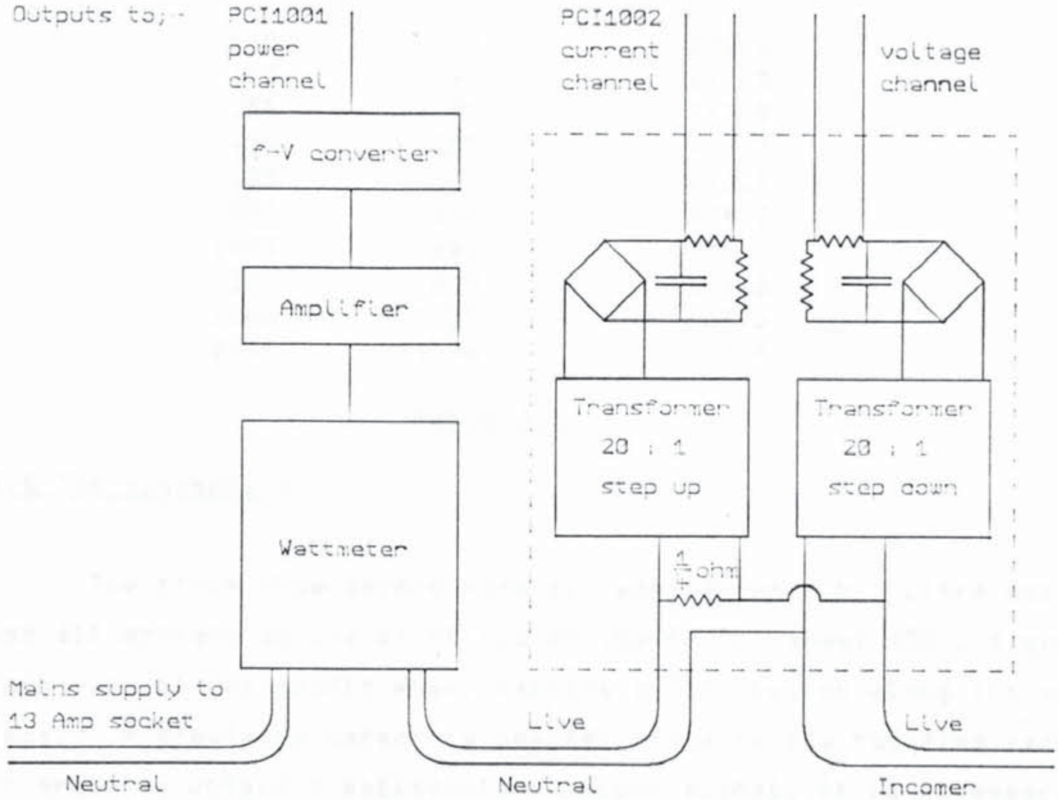

Figure 3.7. Current & voltage monitor, and Wattmeter schematic

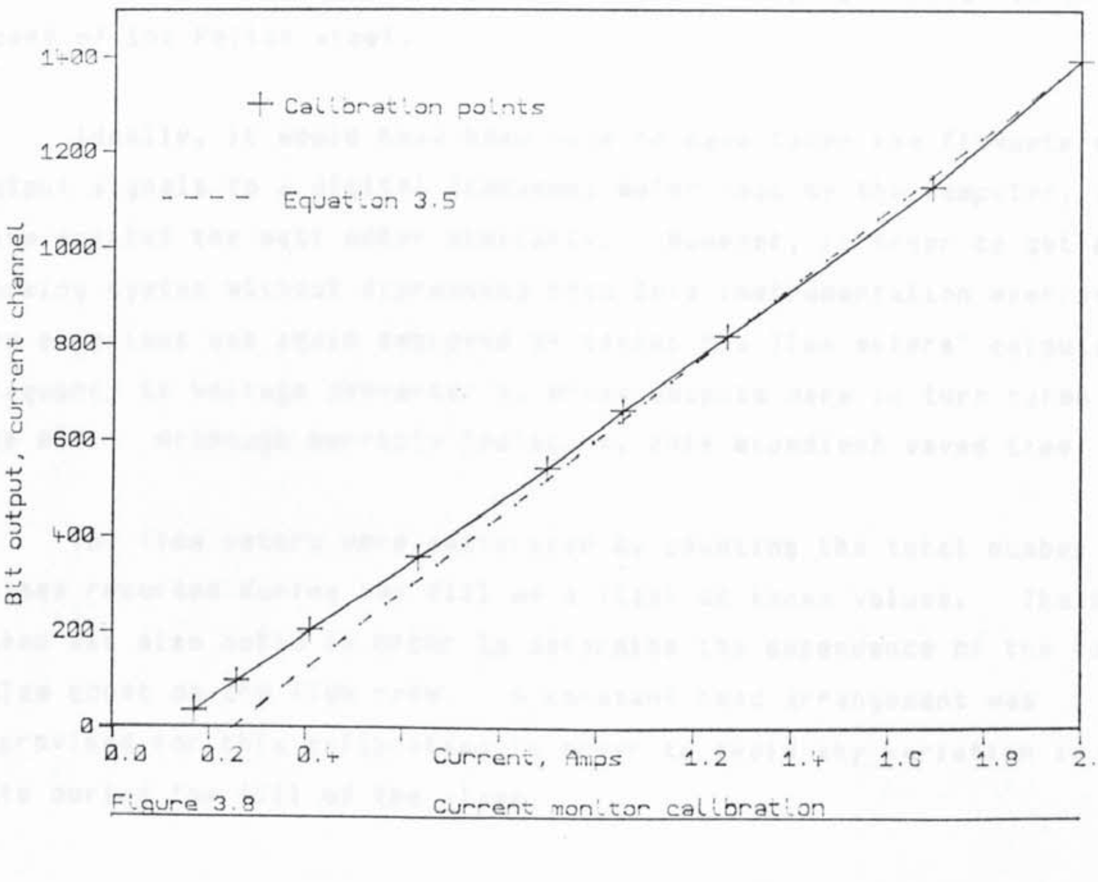

Figure 3.8 Current monitor calibration

Current mA	Bits	Calibration mA
0	5	252.3
170	41	297.5
258	97	367.8
410	201	498.5
635	356	693.1
897	540	924.2
1053	660	1075.0
1270	815	1269.6
1693	1127	1661.5
2000	1396	1999.4

Table 3.3

3.8 The flowmeters

The three flow meters were all manufactured by "Litre meter" Ltd. and all operate on the principle of the Pelton wheel (53), figure 3.9. Each vane of the paddle wheel carries a ferrite rod along its outer edge. A proximity sensor is mounted close to the rotating vane tips. In order to obtain a satisfactory output signal, it is necessary to connect an external 10 Kohm pull-up resistor between the 12 volt rail and the output terminal. The electronics package responds to the proximity sensor by pulling the output rail down close to 0 volts. A square wave is thus produced whose frequency is proportional to the speed of the Pelton wheel.

Ideally, it would have been nice to have taken the flowmeters' output signals to a digital frequency meter read by the computer, and to have treated the watt meter similarly. However, in order to get a working system without digressing into this instrumentation exercise, the expedient was again employed of taking the flow meters' outputs to frequency to voltage convertor's, whose outputs were in turn taken to the ADC. Although horribly inelegant, this expedient saved time.

The flow meters were calibrated by counting the total number of pulses recorded during the fill of a flask of known volume. The time taken was also noted in order to determine the dependence of the total pulse count on the flow rate. A constant head arrangement was improvised for this calibration in order to avoid any variation in flow rate during the fill of the flask.

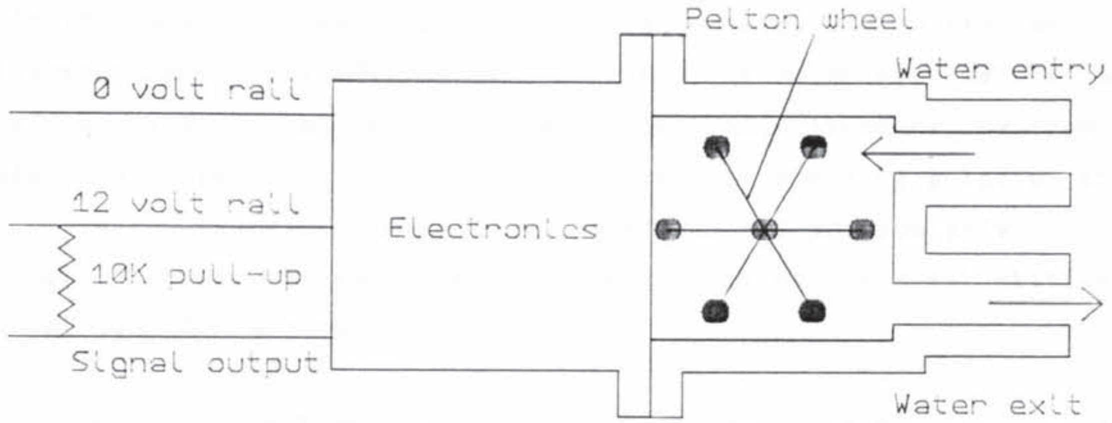

Figure 3.9a. Pelton wheel flow meter assembly

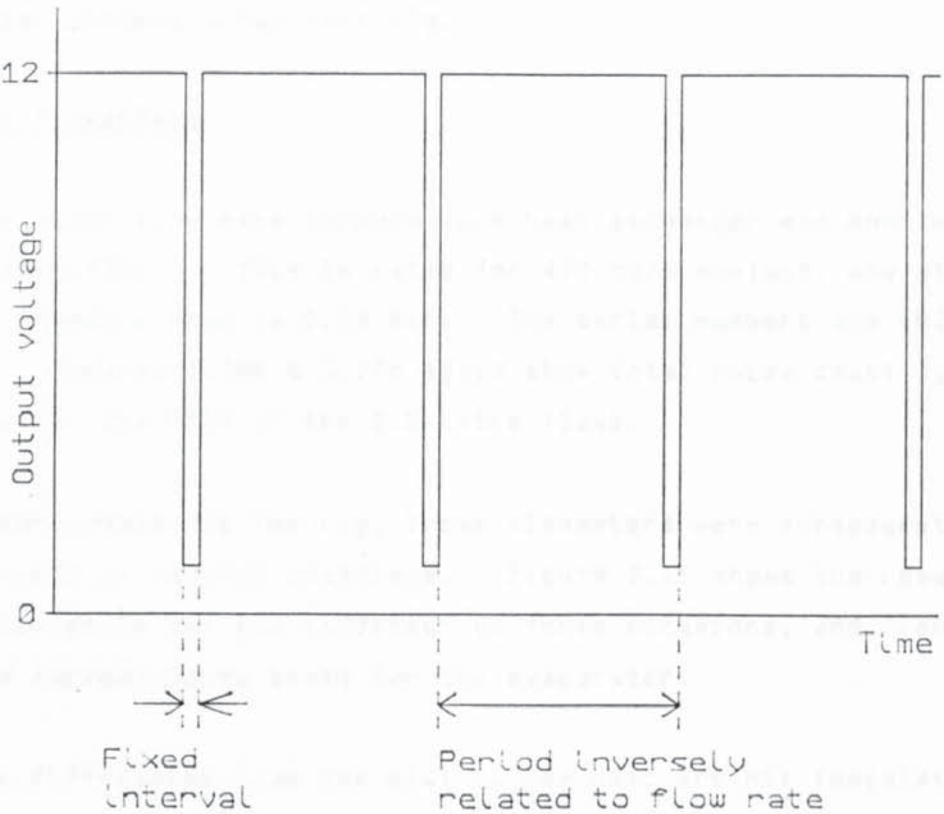

Figure 3.9b. Output signal voltage history

The refrigerant flowmeter

A Litre-meter 'LM45SS' was intended for use in the subcooled refrigerant line. This is rated for a peak flow rate of 100 cc/s. At the more typical flow rate of 5 cc/s the pressure drop is 0.003 Bar. With the benefit of hindsight, it is now realised that a smaller flowmeter would have been better. Unlike the water flow meters, which could be recalibrated in-situ, the initial calibration of the freon flow meter had to suffice, which was the reason for spending a lot of time on it. In the event, the freon flow meter was not particularly successful, and eventually failed totally, the Pelton wheel stationary for all but the highest flow rates.

It was found that the calibration was reproducible provided that the flow rate was not too low. However, at low flow rates the total pulse count showed a spread of 4%. Figure 3.10a shows the total pulse count recorded for the fill of a 5.5 litre flask at several different flow rates. Note that at flow rates below about 4 cc/s, the calibration becomes irreproducible.

The water flowmeters

The water flow rate through each heat exchanger was monitored by a Litre Meter LM220. This is rated for 470 cc/s maximum, and at 100 cc/s the pressure drop is 0.04 Bar. The serial numbers are LM23344 & LM23646. Figures 3.10b & 3.10c again show total pulse count against flow rate for the fill of the 5.5 Litre flask.

After assembling the rig, these flowmeters were subsequently re-calibrated on several occasions. Figure 3.11 shows the resulting calibration plots for the condenser on three occasions, and figure 3.12 shows the corresponding plots for the evaporator.

The differences from one plot to the next are not immediately apparent by inspection. The equations that fit these points are summarised below, in order to assist the reader's assessment of the significance of long-term calibration drift.

Condenser calibration

Calibration of 21/2/85: Flowrate = 0.01213 x (Bits + 2.6) 3.6

Calibration of 21/5/85: Flowrate = 0.0123 x (Bits + 2.0) 3.7

Calibration of 4/2/86: Flowrate = 0.0127 x (Bits - 16)

Calibration of 10/10/86: Flowrate = 0.01308 x (Bits + 4.0) 3.8

Evaporator calibration

$$\text{Flowrate} = (\text{Bits} + a)[B - C\times 10^{-7}(\text{Bits} + a)]$$

where:-

On 21/2/85 a = 24, B = 0.02575, C = 4.967 3.9

On 21/5/85 a = 23, B = 0.02585, C = 5.421 3.10

Calibration of 10/10/86: Flowrate = 0.0254 x Bits 3.11

In October 1986 the evaporator was used in parallel flow instead of counterflow, so that the flow direction of equation 3.11 is reversed, relative to the previous occasions.

Equation 3.10 refers to a water temperature of 13C. For a water temperature of 38C a better fit was obtained with B = 0.02525 & C = 4.204. In the calibration programme, these two co-efficients were accordingly made linear functions of the water temperature. However, subsequent experience with these flow meters suggested that this refinement was not appropriate.

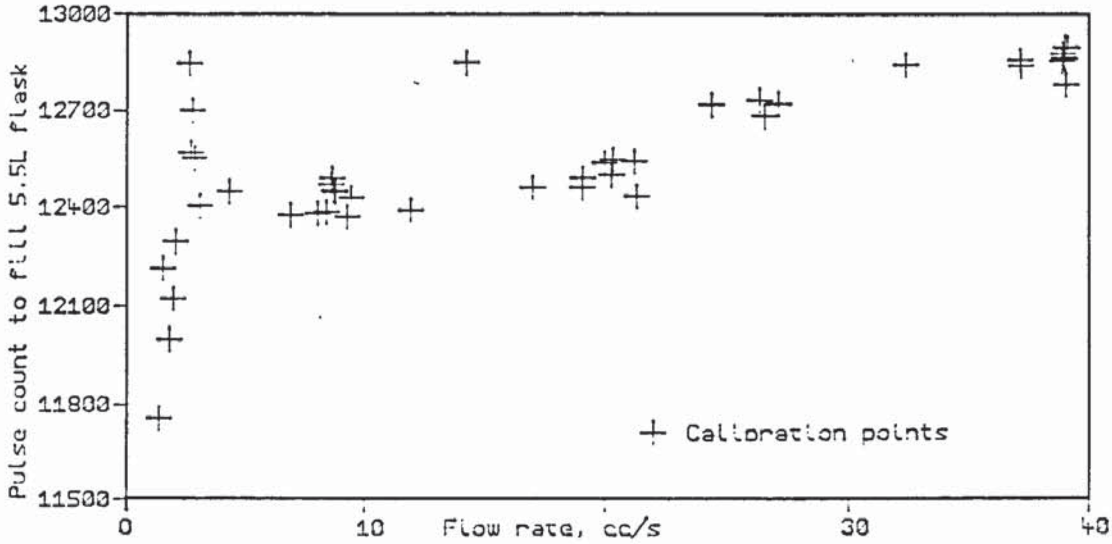

Figure 3.10a R12 flow meter calibration. Pulse count v flow rate

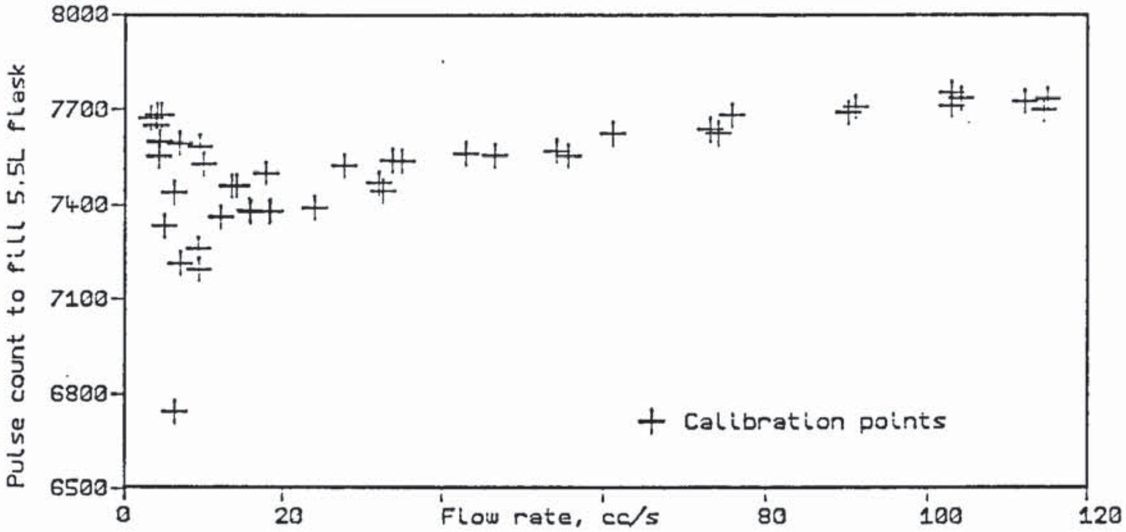

Figure 3.10b LM23646 calibration. Pulse count v flow rate

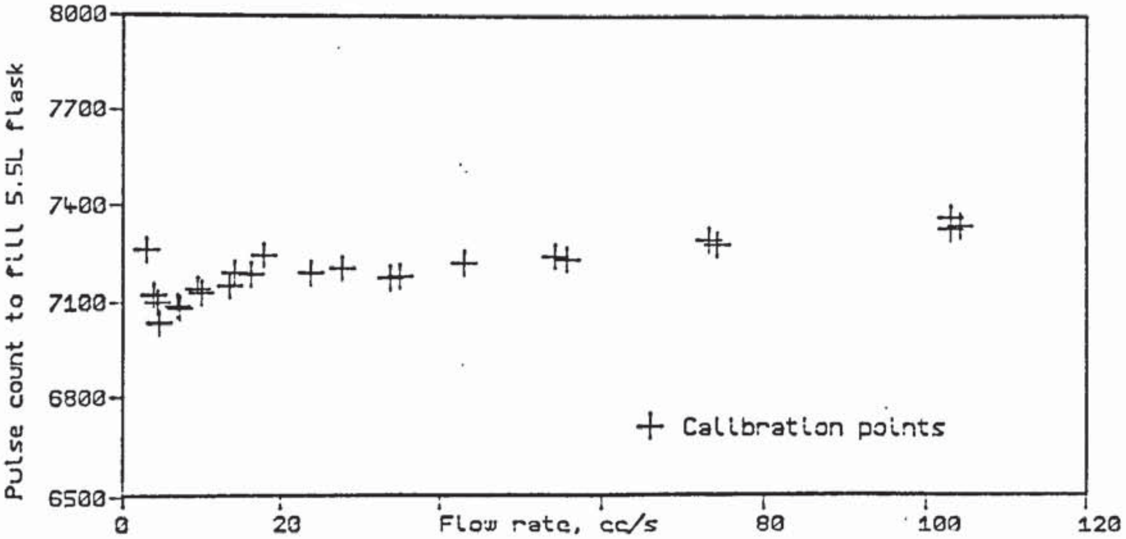

Figure 3.10c LM23344 calibration. Pulse count v flow rate

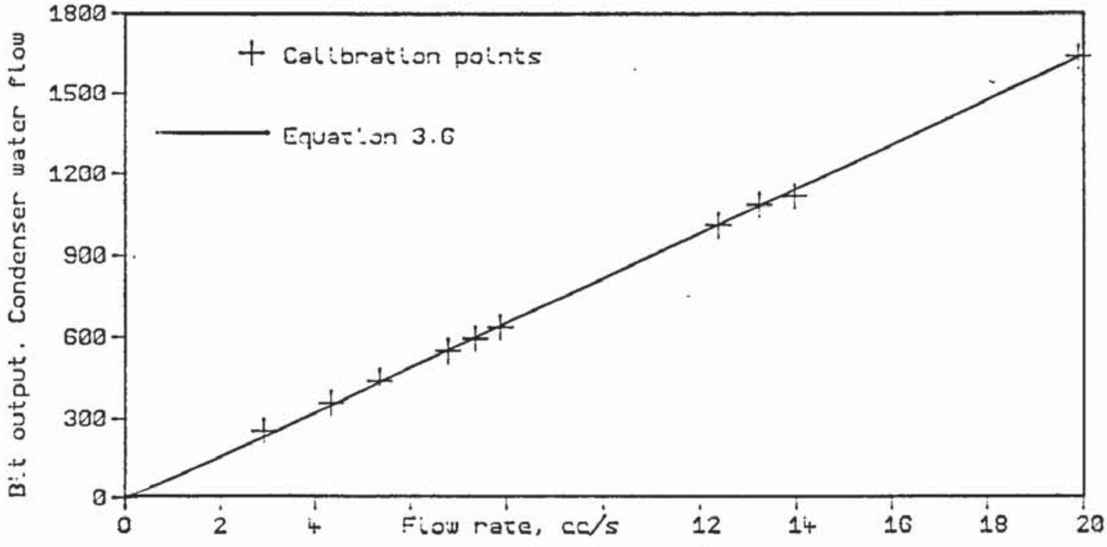

Figure 3.11a Condenser water flow meter calibration, 21/2/85

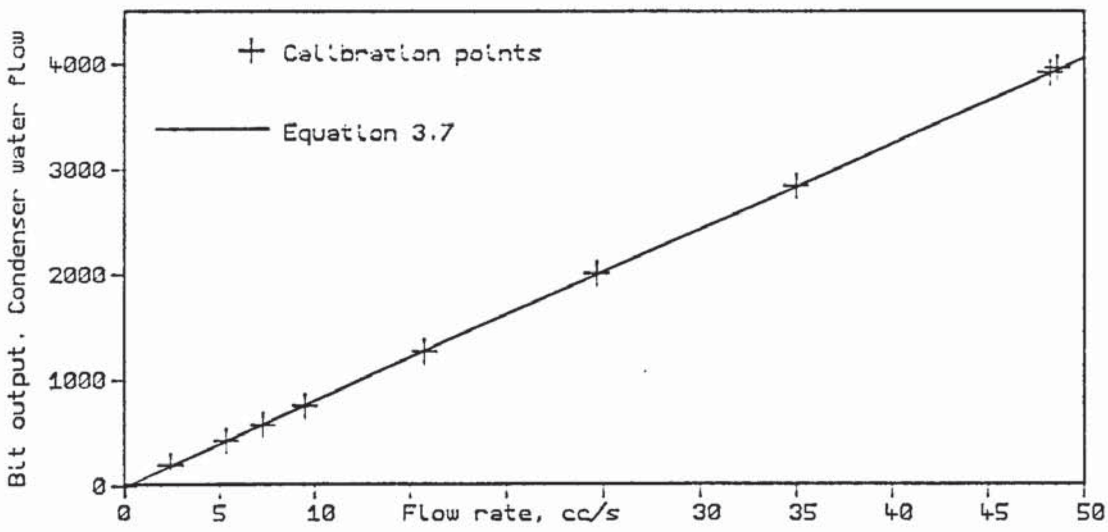

Figure 3.11b Condenser water flow meter calibration, 21/5/85

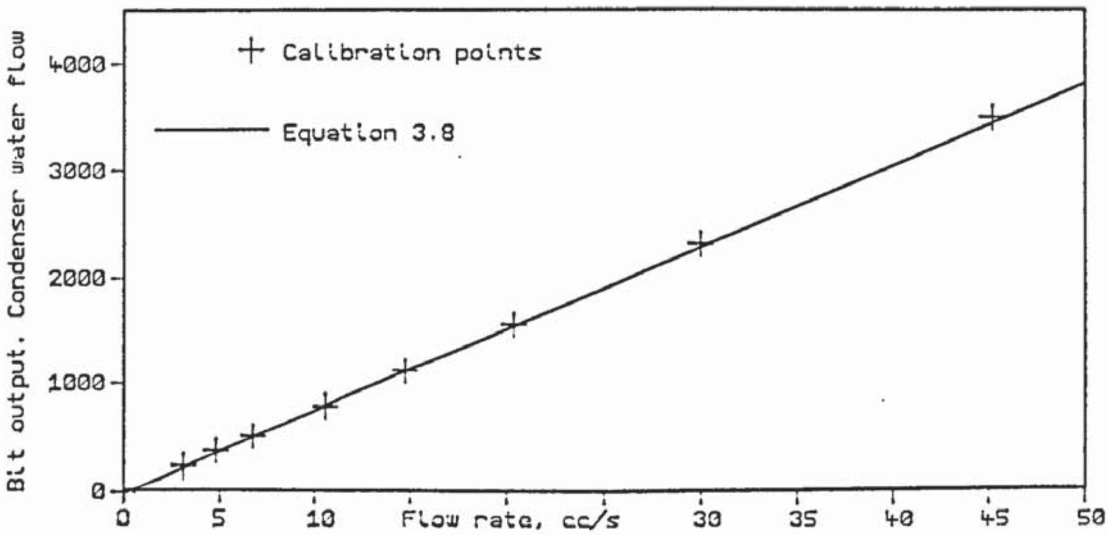

Figure 3.11c Condenser water flow meter calibration, 5/10/86

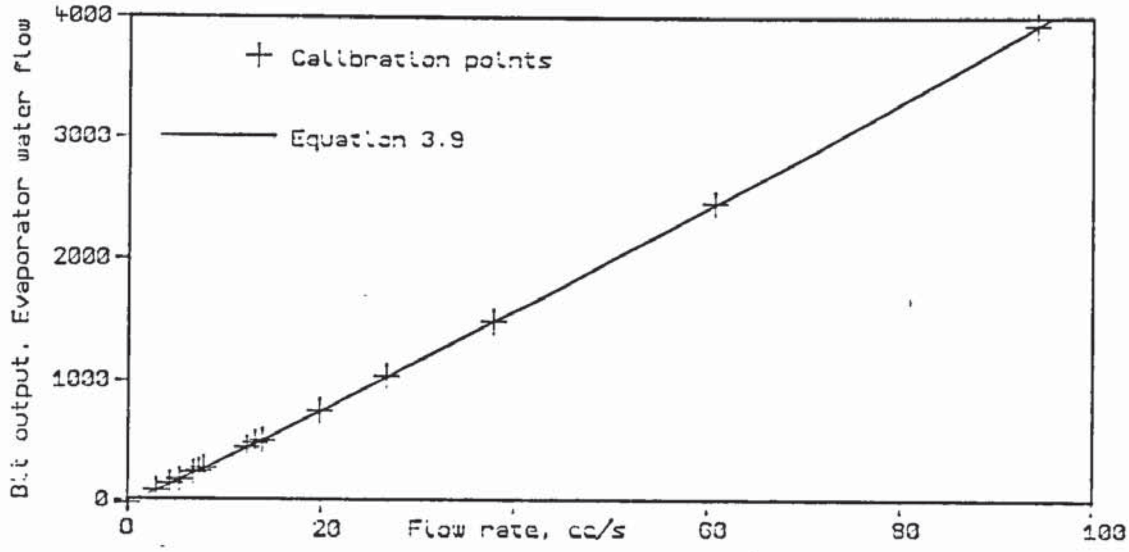

Figure 3.12a Evaporator water flow meter calibration, 21/2/85

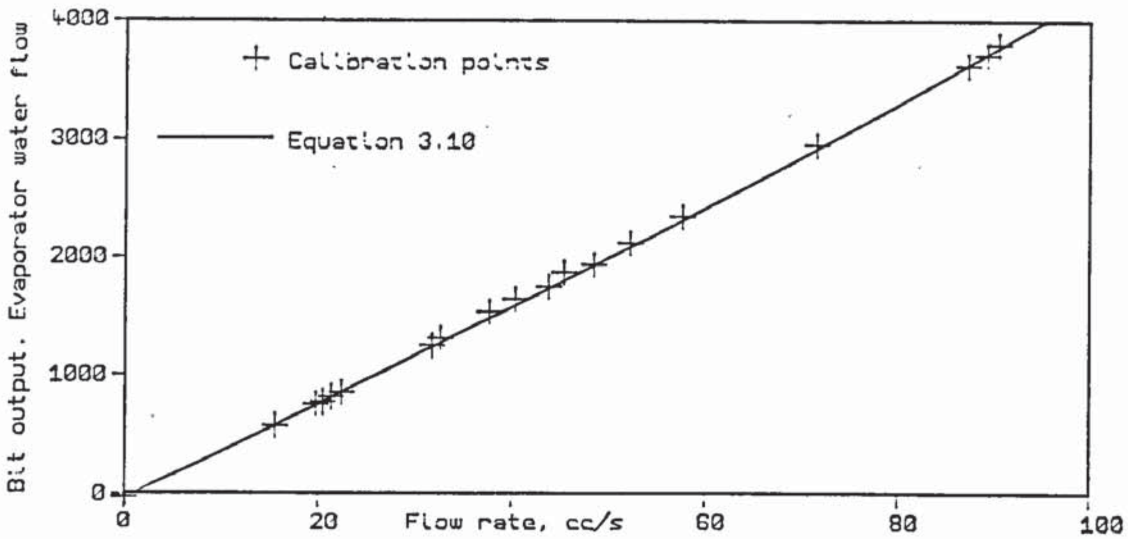

Figure 3.12b Evaporator water flow meter calibration, 21/5/85

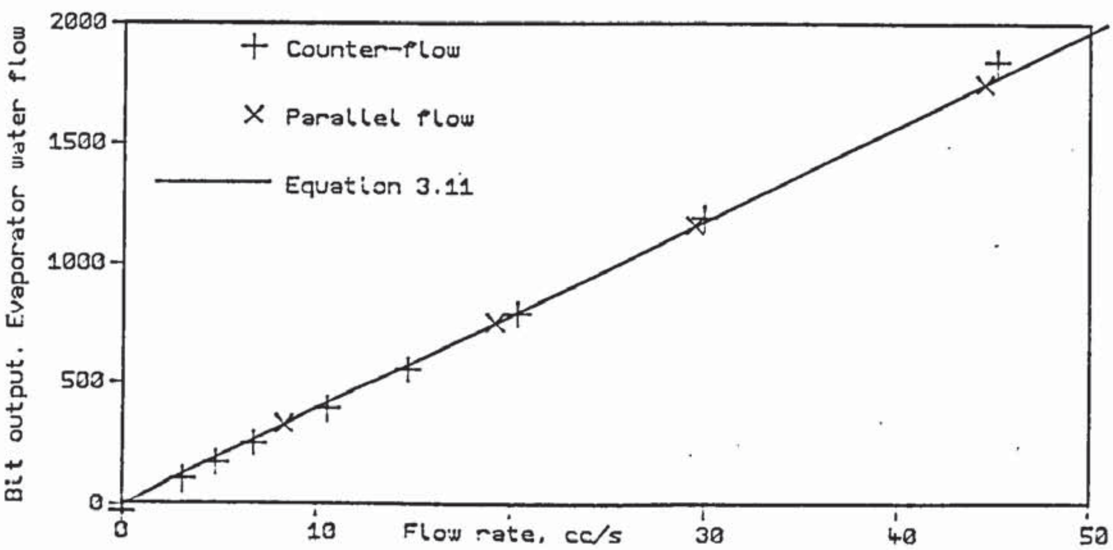

Figure 3.12c Evaporator water flow meter calibration, 5/10/86

3.9 The pressure transducers

The pressure transducers were made by Maywood Instruments of Basingstoke. Their "P102" was used (54). This transducer is based on a silicon strain gauge bridge bonded to a stainless steel diaphragm. It has a nominal pressure range of 0 to 200 psig. With a 10 Volt DC supply, the nominal output is 1 mVolt/psi. This output varies linearly with any variation in the supply voltage.

Before dis-assembling Mr. Othman's rig, his instrumentation was checked by running his data-logging programme after the heat pump had been quiescent for about a week. Although the freon circuit was at a uniform pressure throughout, the four pressures recorded by the computer showed a significant variation, the difference between highest and lowest being around 1 Bar. Mr. Othman's data logging programme had used the information on the calibration certificates furnished by Maywood. The observed discrepancies in the implied pressures were interpreted as the result of calibration drift. This problem has also been reported by McMullan & Morgan (14).

Because of this observation, it was considered desirable to be able to remove the pressure transducers for re-calibration, without having to let all the refrigerant out every time. For this reason, special couplings were made which included a Schraeder valve, so that the transducers could be removed without losing much refrigerant. Figure 3.13 includes the component parts of such a coupling laid out in order of assembly.

The transducers were calibrated on a 'Budenberg' pressure testing machine. By turning a handle, which drives a piston on a thread, a hydraulic pressure is developed in a cylinder of oil. The principle is similar to the master cylinder of a car's braking system. This pressure lifts a vertical shaft of known cross section, at the top of which weights are applied. In order to eliminate the effects of friction, the shaft is set spinning. By adjusting the oil pressure until the weights are lifted, a known pressure is obtained. The transducers were all calibrated by connecting them to this hydraulic system, and recording the ADC's bit output from each for a range of different pressures.

Figure 3.13. Pressure transducer coupling and thermowell assembly.

The pressure transducer outputs were plugged into channels 4, 5, 6 & 7 of the PCI1001. In order to avoid introducing errors due to the differences between the channels of the ADC, each transducer output remained always plugged into the same ADC channel. This obviated the need to separately calibrate each ADC channel.

The following table summarises the results of three calibrations at the beginning, middle and end of an eighteen month period.

Pressure transducer serial no.	ADC channel number	Bits at 0 bar gauge 18/2/85	Bits at 0 bar gauge 7/12/85	Bits at 0 bar gauge 4/10/86	Bits at 12 bar gauge 18/2/85	Bits at 12 bar gauge 7/12/85	Bits at 12 bar gauge 4/10/86
4800	4	78	85	194	3649	3685	3715
4941	5	-210	-224	-237	3247	3238	3224
4942	6	29	33	48	3482	3493	3508
4943	7	-62	-80	-103	3383	3370	3349

Table 3.4

Figure 3.14 is a sample calibration plot. No deviation from linearity was ever found in any calibration test, and the scatter about the best straight line was consistently small.

On a few occasions, a check was made of the calibration's sensitivity to temperature variations, from which it was concluded that there is no need to include any correction. The manufacturer's calibration certificates also support this conclusion.

The transducer locations are summarised in table 3.5 below.

serial no.	Location
4800	Discharge stub
4941	End of condenser
4942	Outlet from expansion valve
4943	Suction stub

Table 3.5

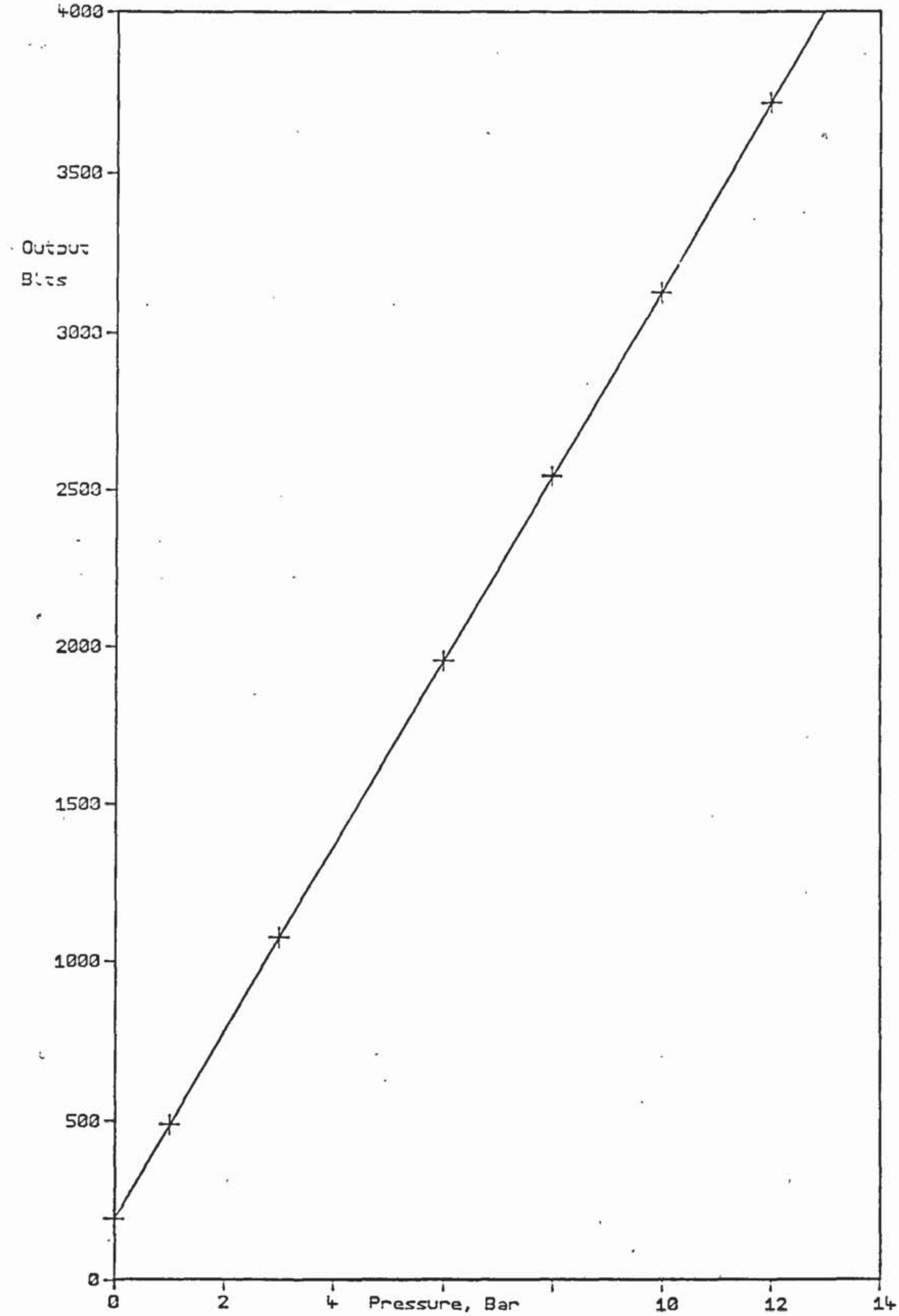

Figure 3.14. Pressure transducer 4800. Calibration of October 1986

This scheme was retained until October 1986, when it was intended to perform a systematic set of experiments including tests at a discharge pressure exceeding 13 Bar. In order to avoid exceeding the 4095 bit limit of the ADC, pressure transducers 4800 and 4943 were swopped over. This subterfuge thus exploited the negative offset in 4943's calibration to extend the range of measurable discharge pressure.

Immediately before the start of the first run in October 1986, a precautionary inspection of the pressure transducer outputs showed that the zero-point of 4800 had again shifted, this time by 50 bits, and the calibration equation was accordingly adjusted to;

$$P = 0.003328 \times (\text{Bits} - 244)$$

During the experiments of October 1986, the transducer outputs were constantly checked against the Bourdon gauges. It was found that the three transducers other than 4800 consistently reproduced the same pressure at the same Bourdon gauge reading. However, 4800 failed this test of consistency. This unsatisfactory behaviour of 4800 may have resulted from its long service in the discharge line where it was subjected to thermal cycling to over 100C. It is also important to point out that this diagnosis was only possible thanks to the Bourdon gauges and had nothing to do with the 'High-tech' features of the instrumentation. On the contrary, as will be further amplified in the following chapters, reliance on the automatic data-logging alone could produce misleading and unsatisfactory results.

In addition to the formal calibrations reported above, all data acquisition runs were preceeded by an inspection of all the transducer outputs while the rig was still quiescent, before turning the compressor on. In this way, the large change seen for 4800 between December 1985 and October 1986 was first noticed in April 1986, and an appropriate adjustment was made in the calibration programme.

3.10 The thermocouples

By running Othman's data logging programme with his rig quiescent, as described above, the opportunity was taken to check the consistency of his temperature measurements. All the thermocouples should have recorded close to room temperature. It was again found that there were significant differences between the measurements, and, at the time, this was assumed to be due to drift in the calibration of the thermocouples that had occurred since Othman's original construction of the rig. However this assumption is now thought to have been in error.

In chapter 6 of his thesis, Othman reports an operating condition for which the subcooled liquid refrigerant temperature falls below the condenser water entry temperature (45). For a perfectly insulated heat exchanger, this would be contradictory to the second law. This observation may have resulted from heat loss to ambient, because it was observed only for a high condensate temperature. However, at the time of reconstruction of the rig, it was thought that this anomalous observation might have been caused by a thermocouple calibration error.

Because of the suspicion that the thermocouple calibration can drift, thermowells were designed for the refrigerant side thermocouples. On figure 3.13, beside the exploded view of the pressure transducer coupling, one can see a similar lay-out of the thermowell components. This thermowell design satisfied the conflicting requirements of having thermal contact between the thermocouple and the refrigerant, while retaining the ability to remove the thermocouples for calibration without any interference of the refrigerant circuit.

The thermocouple leads were plugged into the PCI1002 which is an ADC designed specifically for copper-constantan thermocouples, having a built in reference junction, monitored by a platinum resistance thermometer (52). The PCI1002 includes 12 dedicated amplifiers, one for each thermocouple. It is then the amplifier outputs which are multiplexed to the ADC, figure 3.15.

In order to explain how the built-in reference junction is used, it is first necessary to explain the relationship between thermal EMF and temperature difference when the reference junction is not at 0C.

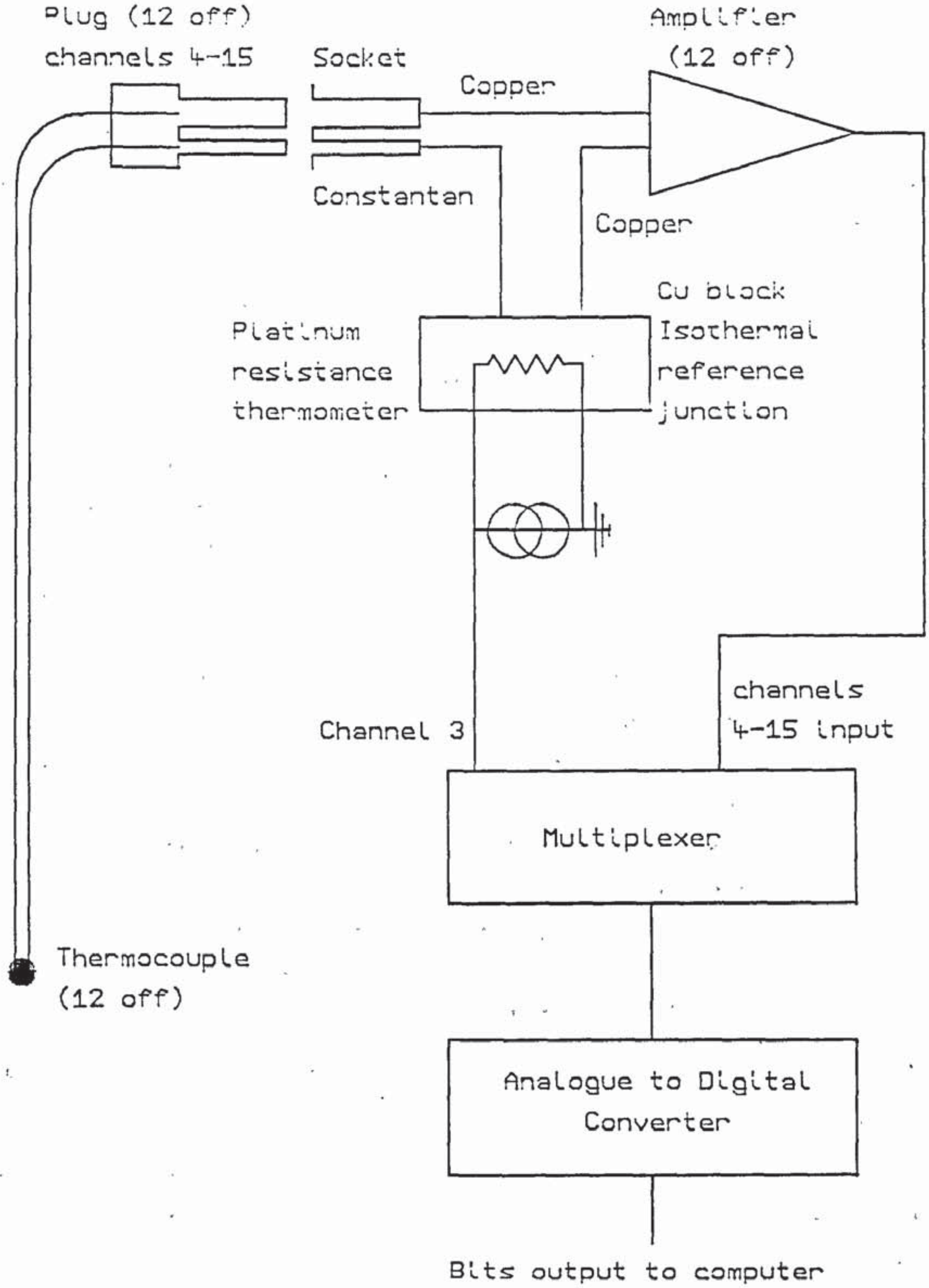

Figure 3.15. Principle of operation of the PCI1002

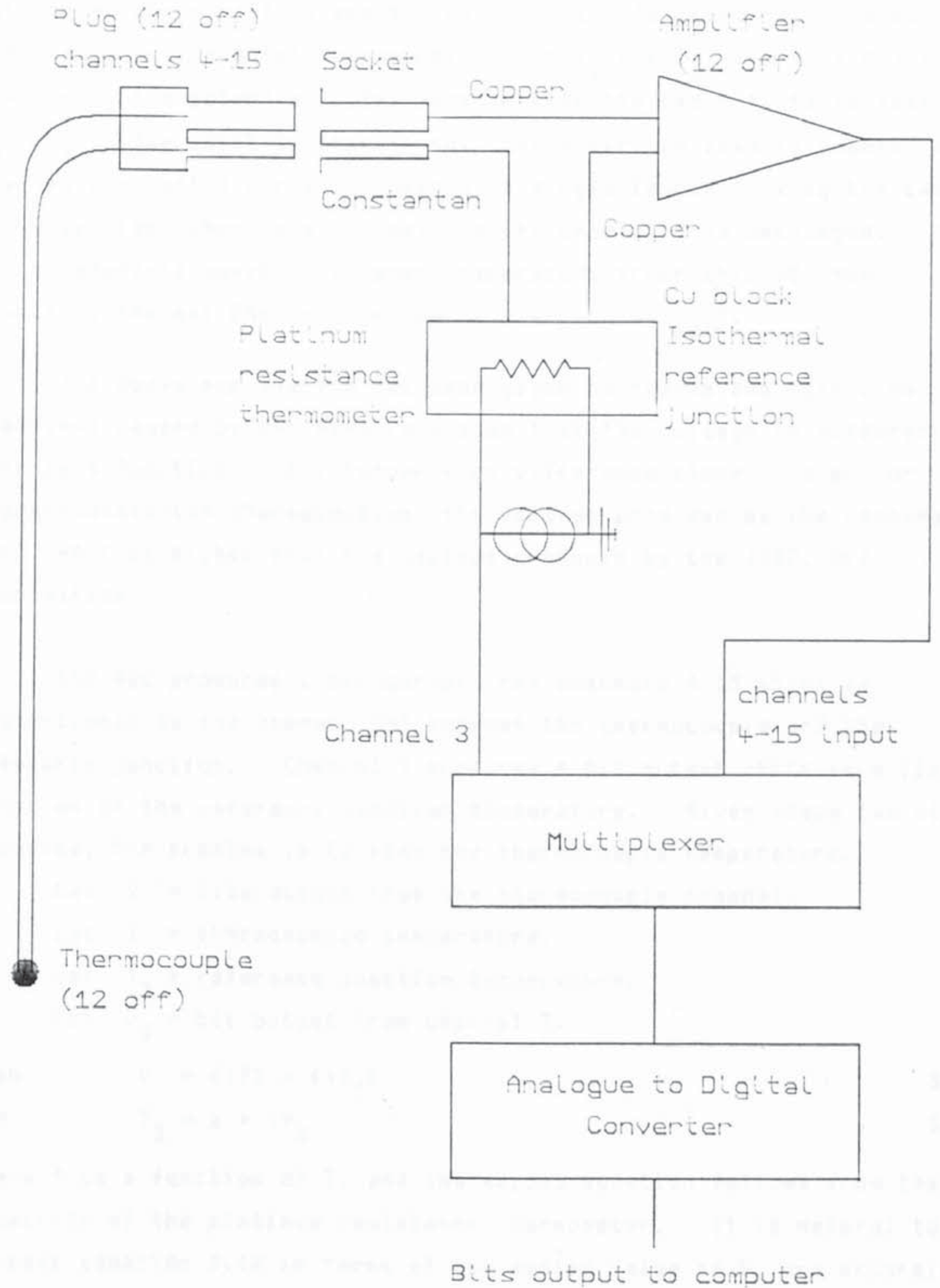

Figure 3.15. Principle of operation of the PCI1002

Consider two thermocouples at temperatures T_1 and T_2, which both have their reference junctions in an ice bucket at T_0 (0C), figure 3.16. Let the function V(T) be the thermal EMF as a function of temperature when using an ice point reference. Then $V_1 = V(T_1)$ and $V_2 = V(T_2)$. Obviously, the potential difference between the two outputs is just $V_2 - V_1$. The point is that if the common earthed lead is removed and the two constantan wires replaced by a single length linking the two thermocouples, then this potential difference will be unchanged. Thus, for a reference junction at some temperature other than 0C, the resulting thermal EMF is given by $V = V(T) - V(T_{ref})$.

The above explanation has been given to remove the confusion sometimes caused by the misaprehension that the voltage in differential mode is a function of the temperature difference alone. e.g. for copper-constantan thermocouples, the voltage produced by the combination (50C, 40C) is higher than the voltage produced by the (10C, 0C) combination.

The ADC produces a bit output from channels 4-15 which is proportional to the thermal EMF between the thermocouple and the reference junction. Channel 3 produces a bit output which is a linear function of the reference junction temperature. Given these two bit readings, the problem is to find the thermocouple temperature.

Let V = bits output from the thermocouple channel.

Let T = thermocouple temperature.

Let T_3 = reference junction temperature.

Let V_3 = bit output from channel 3.

Then $$V = f(T) - f(T_3) \tag{3.12}$$

and $$T_3 = a + bV_3 \tag{3.13}$$

where f is a function of T, and the second equation follows from the linearity of the platinum resistance thermometer. It is helpful to re-cast equation 3.13 in terms of the median value of V_3 and excursions from this value. Upon substituting into equation 3.12, one obtains

$$V = f(T) - f([a+b\bar{V}_3] + b[V_3 - \bar{V}_3]) \tag{3.14}$$

The second term of the RHS can be expanded to first order about this median value to produce

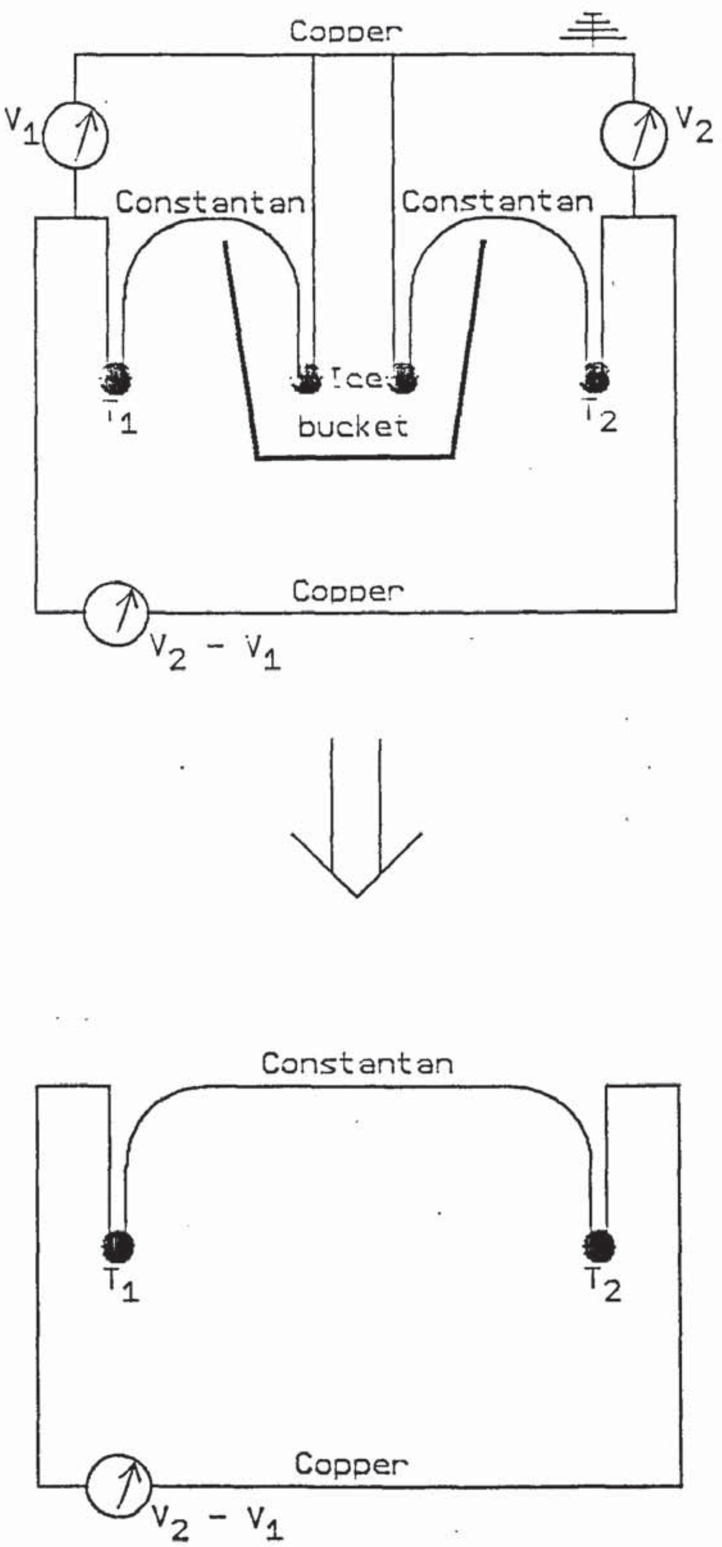

Figure 3.16. A way of regarding differential thermocouples

$$V = f(T) - f(a+b\bar{V}_3) - b(V_3 - \bar{V}_3)f'(a+b\bar{V}_3) \qquad 3.15$$

Recognising the function of a constant as another constant, this can be re-written as

$$V = f(T) - A - BV_3 \qquad 3.16$$

The constant A can be absorbed into function f to give the final form

$$V = F(T) - BV_3 \qquad 3.17$$

Thus, in order to extract the temperature from the ADC readings, an equation of the form

$$T = G(V + BV_3) \qquad 3.18$$

must be evaluated, where G is the inverse of function F.

To see why the argument of function G must be of this form, consider the effect of a rise in temperature of the reference junction, with a fixed thermocouple temperature. With increasing reference junction temperature, V falls, and V_3 increases. Since the thermocouple's temperature is unchanged, the argument of G must remain constant. Thus B must be the ratio of the thermocouple sensitivity to the resistance thermometer's sensitivity at the working temperature of the reference junction.

<u>Calibrating the reference junction</u>

The explanation above summarises the method which was used to find a value for B. This involved monitoring all the bit outputs while the reference junction temperature was rising, with the thermocouples immersed in water, steady at room temperature. The salient record is presented in table 3.6, below, which summarises the bit readings.

Channel	Bit readings At first	Later	Change	adjusted change
3	964.3	1044.9	80.5	80.5
4	-50.0	-88.0	38.0	33.0
5	-49.3	-85.9	36.6	31.6
6	-43.0	-80.8	37.8	32.8
7	-40.4	-78.0	37.6	32.6
8	-40.0	-77.0	37.0	32.0
9	-41.0	-76.0	35.0	30.0
10	-53.0	-90.8	37.8	32.8
11	-50.0	-87.9	37.9	32.9
12	-45.0	-83.0	38.0	33.0
13	-43.0	-80.0	37.0	32.0
14	-43.1	-79.0	35.9	30.9
15	-39.0	-75.2	36.2	31.2
Water Temperature	20.3C	20.0C		

Table 3.6

This table summarises two sets of bit readings resulting from a rise in temperature of the reference junction, with a near zero change in the thermocouple temperatures. Note that the 80 bit rise in the output from the resistance thermometer has been accompanied by a fall in the bit outputs from the thermocouple channels of 35-38 bits. Of this fall, 5 bits is accounted by the 0.3C drop in room temperature, because the thermocouple sensitivity at 20C is roughly 16 bits per degree. The last column of figures merely includes this correction. Thus, by inspection of these figures, one sees that an 80 bit rise on the reference channel is accompanied by a 32 bit drop on the thermocouple channels, which yields the result B=0.4.

This conclusion is supported by the makers' stated sensitivity of 40 bits per degree for the reference junction ouput. The nominal 16 bits per degree sensitivity of the thermocouple then also implies a sensitivity ratio of 0.4.

Calibrating the thermocouples

Having thus determined the co-efficient in the argument of function G, equation 3.18, the problem remained to determine calibration points, and obtain a suitable polynomial representation.

When the rig was first working, in February 1985, a set of thermocouples was made up and and calibrated by recording the bit outputs from every channel for a set of known temperatures. In October 1986 new thermocouples were made up and a similar calibration was performed. To avoid repetition, only the latter calibration is detailed below.

Six temperatures were used to calibrate the thermocouples, ranging from the ice point to the boiling point of water. The intermediate temperatures were 20.9C, 39.3C, 48.0C and 74C. From these points, a calibration equation was devised. The validity of extrapolating to lower temperatures was tested by immersing the thermocouples in a dewar of liquid R12, and deducing the temperature by applying the calibration equation to the observed bit output. A temperature of -31.9C was found, which is 2C below the boiling point of R12. However, a subsequent check on the behaviour of R12 in a dewar showed that its steady state temperature is indeed slightly lower than its boiling point, and so the calibration equation was accepted as satisfactory for the subsequent measurements.

Deriving the calibration equation

The raw data from the calibration tests is collated in table 3.7 below.

Bit readings

Temperatures	<-30C	0.0C	20.9C	38.4C	48.0C	74.0C	100C	
Channel								offset
3	1025	1028	1028	1025.7	1023.6	1026	1024	
4	-857	-389	-64	224.6	387.2	827.7	1305.6	22.2
5	-857	-389	-64	224.2	387.2	827.7	1305.6	22.2
6	-846	-378	-54	234.0	396.8	836.7	1313	33.2
7	-849	-381	-57	231	393.9	833.8	1310	30.2
8	-843	-375	-50.7	238	400.5	840.4	1317.3	36.2
9	-849	-381	-56.7	232	394.6	834.4	1310.5	30.2
10	-860	-392	-67.6	221	383.6	823.5	1300	19.2
11	-858	-390	-65	224	386.8	827.8	1305	21.2
12	-851	-384	-59.3	229	391.7	831.3	1307.5	27.2
13	-845.8	-377.8	-53	235.5	398.5	838.5	1314	33.4
14	-850.1	-382	-58	230.5	393.5	832.9	1311	29.2
15	-842	-374	-49	239.1	402	841.6	1320.5	37.2

Table 3.7

The 'offset' is a constant for each channel, and is defined by;

offset = bit reading + 0.4 x (channel 3 bit output) for the test at 0C.

By defining the 'reduced bit output' as;

reduced bit output = bit reading + 0.4 x (channel 3 output) - offset

this quantity has the useful feature of being identically 0 at 0C on all the channels. More importantly, thanks to good matching of the thermocouples and of the ADC channels, this derived quantity is essentially the same function of temperature for all the channels, as illustrated in table 3.8 below.

<u>Reduced bit outputs</u>

Temperatures	<-30C	0.0C	20.9C	38.4C	48.0C	74.0C	100C
Channel							
4	-469.2	0	325	612.7	774.4	1215.9	1693
5	-469.2	0	325	612.3	774.4	1215.9	1693
6	-469.2	0	324	611.1	773	1213.9	1689.4
7	-469.2	0	324	611.1	773.1	1214	1689.4
8	-469.2	0	324.3	612.1	773.7	1214.6	1690.7
9	-469.2	0	324.3	612.1	773.8	1214.6	1689.9
10	-469.2	0	324.4	612.1	773.8	1214.7	1690.4
11	-469.2	0	325	613.1	775	1217	1693.4
12	-468.2	0	324.7	612.1	773.9	1214.5	1689.9
13	-469.2	0	324.8	612.4	774.5	1215.5	1690.2
14	-469.3	0	324	611.6	773.7	1214.1	1691.4
15	-469.2	0	325	612.2	774.2	1214.8	1692.9
Value used for fit	-469.2	0	324.5	612	774	1215	1690.3

<u>Table 3.8</u>

The worst scatter between channels is seen at 100C, for which the range is 4 bits. However, the only thermocouples which need to be valid at 100 C are the ones recording the R12 discharge and condenser entry temperatures. These temperatures were recorded on channels 8 & 9. This is the reason for adopting 1690.3 as the representative reduced bit reading at 100C.

The manufacturers quote a standard fourth order polynomial fit for the temperature as a function of the thermal EMF, referenced to OC; -

$$T = a_1V + a_2V^2 + a_3V^3 + a_4V^4 \qquad 3.19$$

where T is in centigrade, V is the thermal EMF in microvolts, and

$a_1 = 0.0256613$, $a_2 = -6.19549\times10^{-7}$, $a_3 = 2.21816\times10^{-11}$, $a_4 = -3.55009\times10^{-16}$

for temperatures exceeding OC. For temperatures below OC, different co-efficients are specified;-

$a_1 = 0.0238371$, $a_2 = -2.98788\times10^{-6}$, $a_3 = -7.19458\times10^{-10}$, $a_4 = -1.00419\times10^{-13}$

The makers suggest an ADC calibration of 2.5 microvolt/bit, but a better fit was found using 2.53 microvolts/bit. Rather than retain the multiplication by 2.53 in the data logging programme, this co-efficient was absorbed into the co-efficients of the polynomial. The equation was further simplified by dropping the quartic term, and re-adjusting the remaining three co-efficients to recover the same standard of fit. The equation finally adopted was;

$$T = g_1b + g_2b^2 + g_3b^3 \qquad 3.20$$

where b is the reduced bit reading, $g_1 = 0.0655$, $g_2 = 4.83\times10^{-6}$ and $g_3 = 6.4\times10^{-10}$

Table 3.9, below, summarises the results of using either this empirical cubic function of the reduced bit output, or the standard quartic function of the microvolt output, using 2.53 microvolts/bit.

Measured Temperature	Reduced Bit reading	microvolts	Implied temperature quartic	cubic
<-30	-469.2	-1187.1	-31.5	-31.9
0.0	0	0.0	0.0	0.0
20.9	324.5	821.0	20.7	20.8
38.4	612.0	1548.4	38.3	38.4
48.0	774.0	1958.2	48.0	48.1
74.0	1215.0	3074.0	73.6	73.6
100.0	1690.3	4276.5	100.0	100.0
	2500	6325	142.6	143.6

Table 3.9

At the time, temperatures much in excess of 100C had not been anticipated. However, discharge temperatures approaching 140C have since been observed. Upon substituting 2500 bits into each calibration, the quartic implies a temperature of 142.6C, whereas the cubic implies 143.6C. This calibration error of 1C at the highest observed temperature is not considered serious.

Each amplifier's offset is adjusted using a 100 Kohm 10 turn potentiometer. With the inputs all shorted, the makers recommend setting all the offsets to the same value in order that a single calibration equation may be applied to all the thermocouples (51). It was found that upon setting the potentiometers accordingly, the offsets all drifted over the course of the following few days, each levelling off to a different steady state after about a week. It was thus recognised that it was not practical to pursue the makers' suggestion. This led to the individual treatment of each amplifier's offset, as explained above. The close grouping of the offsets shown in table 3.7 above, ranging from 19 bits to 37 bits, resulted from three iterations of attempting to set the potentiometers. At each attempt, all the channels which were within about 10 bits of each other would be left severely alone, and only the channels showing the biggest deviation were adjusted. After the first attempt to set the potentiometers, the scatter in the offsets a few days later was very much worse than that shown in table 3.7.

With the benefit of hindsight, having since found that the thermocouple calibration does not drift, it is now thought that the most likely reason to account for Othman's thermocouple calibration errors is the drift of the amplifier offsets that occurs over the days following their setting.

Chapter 4. The experimental investigation

4.1 Introduction

The purpose of this chapter is to briefly tell the story of the experimental investigation in order that each experiment may more easily be seen in context. More detailed accounts are given in the following chapters.

The heatpump was first functional in October 1984, but it was not possible to record reliable data until February 1985 because of a hardware problem with the thermocouple ADC.

The first data recorded indicated a power imbalance consistent with liquid freon return to the compressor, such as results from freon solution into the oil that returns from the evaporator (33,55,56,57). This precipitated an interest in two component - two phase thermodynamics, and a calculation was devised for the vapour pressure of an oil/freon mixture as a function of composition and temperature. The understanding gained during this study was applied to the empirical equations presented by Bambach (58), initially with a view to finding the molecular weight of his oil. The results were totally inconsistent, which was quite worrying, until it was realised that the problem lies with Bambach's equations, which are not thermodynamically consistent.

4.2 First attempt to determine the performance map

After this digression, an attempt was made to obtain performance measurements for wide ranges of 3 of the independent variables. At this stage, the heat pump was regarded as a system having 5 independent variables :-

The water entry temperatures to the condenser & evaporator.

The evaporator water flow rate.

The setting of the discharge pressure regulator.

The setting of the thermostatic expansion valve.

The first systematic set of measurements, performed between May 11 and June 9 1985, was intended principally to determine the dependence of capacity and C.O.P. on the evaporator water entry temperature & flow rate, and on the discharge pressure regulator setting.

Nine runs were executed, which each lasted between 12 and 20 hours. In preparation for each run, the evaporator water reservoir was heated to over 40C, using an immersion heater. In the course of each run, this reservoir was allowed to cool slowly by setting the immersion heater's power supply always slightly lower than the refrigerating capacity. In this way, on each run, the evaporator water supply temperature was varied continuously over the range of interest.

From the data acquired on this set of measurements, several phenomena were subsequently demonstrable:-

i) Hunting of the thermostatic expansion valve.

ii) Fixed orifice operation of the valve, under certain conditions.

iii) Step-like discontinuities in the time-dependence of the compressor's power requirement, with no corresponding change in any other measurement to account for it. This was particularly perplexing.

On account of this last observation, a new compressor was purchased. On 14 July 1985 a repeat of the run of 7 June constituted the first 15 hours operation of this new compressor. This repeat test reproduced the same overall behaviour, and also reproduced the power step.

The initial reaction was to press on regardless, and ignore the problem. A test was performed on 26 July 1985 intended to investigate the effect of varying the expansion valve's superheat setting. Quite unaccountably, it was found that the compressor's power requirement was 25 watts higher at the minimum superheat than at the higher superheat settings. This was a further manifestation of the seemingly bistable behaviour of the compressor's power requirement. Having tried to ignore the problem and perform an unrelated experiment, the result has been compromised by the influence of this uncontrolled variable of unknown origin.

4.3 Further pursuit of the power step

A simple instrument was constructed to monitor mains voltage and current consumption. Its outputs were taken to the two spare analogue input channels of the thermocouple ADC, as shown in figure 3.7. On subsequent tests in October 1985 it was established that these discontinuous changes in power consumption are not caused by variations in mains voltage. It was also verified that the start relay was functioning correctly, and that there was no leakage to the start winding or capacitor. By recording all the measurements every 3 seconds it was also demonstrated that the this transition in the power requirement occurs in less than 3 seconds.

Suspicion fell on the compressor's lubrication system. In pursuit of the various ideas implicating the lubrication system, the old compressor's can was cut open, and flanges were brazed on in order to make the compressor demountable. At the same time, the opportunity was taken to solder 6mm water pipes onto the can, with a view to a future experiment. During December 1985 the effects of various modifications to the oil delivery system were tried, but it was only at the end of December that a certain relevant feature of the compressor's design was observed. Thus, it was only the modifications tested subsequently that were designed with a full command of the salient facts.

4.4 More direct measurement of mechanical losses

Up to this point, all the measurements had involved recording the behaviour of the heat pump. It was realised that, having made the compressor accessible, a much more direct measure of the compressor's mechanical losses could be obtained by running it with the cylinder head absent, and monitoring the motor's power consumption. This avoided all the complications of trying to estimate the work of compression and the gas flow losses.

It was considered undesirable to dis-assemble and re-assemble the cylinder head any more often than was absolutely necessary. By this time, the new compressor had been dis-assembled, but had not been re-assembled. For this reason, these 'free running' tests, performed with the cylinder head absent, were all executed using the new compressor mounted in the old compressor's can, while the old compressor was preserved in its fully assembled state.

These tests were performed in air with the top half of the can replaced by a perspex cover. This arrangement was dictated by the need to have visual confirmation that oil was reaching the top of the crankshaft.

The power step was never observed during any of these tests. This fits with current thinking that the power step problem obeys a stability criterion involving bearing load and lubricant viscosity. For the free running tests the bearing load is minimal and there is no refrigerant dissolved in the oil.

One of the more important conclusions of the free running tests was that, contrary to supposition, the mechanical loss increases with increasing oil supply rate, provided that the minimum requirement is satisfied.

4.5 Compressor temperature variation

In February 1986 two runs were performed whose purpose was to investigate the dependence of the compressor's behaviour on its temperature. By running water through the sump heat exchanger, and through the pipes soldered onto the can, the compressor's temperature could be varied.

In preparation for this test, the evaporator's water reservoir was first cooled close to freezing by running the heat pump in the usual way. This 100L reservoir was then coupled to the compressor's pipework, while the evaporator was supplied, instead, with tap water. Over several hours the water reservoir warmed up and asymptotically approached a steady state, due to heat removal from the compressor. In order that this investigation should continue to a high temperature, an immersion heater was used to further heat the reservoir.

It has been reported that a compressor's volumetric efficiency can be adversely affected by condensation of the refrigerant during compression and discharge (59). The initial objective of this experiment was to ascertain whether this phenomenon is relevant to the Danfoss SC10H. Because of the presence of oil on the cylinder wall, condensation is thermodynamically permisible even if the wall temperature exceeds the condensing temperature at the cylinder pressure. The point at issue is whether the time scale of the compression stroke is short, or long, compared with the time scale for approach to equilibrium of the liquid and vapour phases. In the former case, the phenomenon can be ignored, and in the latter, instantaneous thermodynamic equilibrium would be a legitimate assumption. Comparable time scales would present a more complicated problem.

Thanks to the wide variation of the compressor's temperature, this test provided an opportunity to look for evidence to support, or refute, a capacity loss caused by condensation in the cylinder.

It has since been recognised that this experiment could cast light on the power-step problem. It was thought that persistence of the high power mode is aggravated by solution of refrigerant into the oil. It has been shown (60, Chapter 7) that in a hydrodynamically lubricated journal bearing, a region of negative pressure can exist in the lubricant. While a transient negative pressure can be supported by pure oil, there was considerable doubt about the behaviour of the lubricant in the compressor, because it is a mixture of oil and refrigerant, whose composition satisfies Raoult's law (41,42). This led to the speculation that if the refrigerant fraction was too high, the oil film in the bearing would cavitate due to flashing of the volatile component, caused by the negative pressure transients. Alternatively, the deleterious effect of refrigerant admixture may be due solely to the reduced lubricant viscosity.

Using worst case estimates for bearing load and lubricant viscosity, it has been ascertained that the Sommerfeld criterion (60, section 13.6) is never normally violated. i.e. theoretically, provided cavitation does not occur, the lubricant film never gets thin enough to allow asperity contact of the sliding surfaces. However, there is a further relevant criterion, which concerns dynamical stability of a journal bearing (60, Chapter 14). Normally, if the load on a journal bearing is constant, without any time dependence, then the position of the shaft w.r.t. the journal is also constant. However, if the lubricant viscosity falls too low, then instead of having a fixed vector from journal centre to shaft centre, this 'eccentricity' vector can describe a polygonal trajectory. This can be quite a violent and destructive phenomenon. (A similar phenomenon is the hazardous instability sometimes encountered when trying to widen a round hole using a larger drill bit.) The text-book treatment of this phenomenon is confined to the simplest possible system, a flywheel spinning about a horizontal rotation axis, so that the bearing is just loaded by the wheel's dead-weight. Even so, the stability analysis is still quite daunting. The criterion involves the load on the bearing and the lubricant viscosity, as one might expect. However, it also involves the inertia of the rotating component, because the key point about this instability is that the inertial force attributable to the rotator's translational acceleration overcomes the damping effect of the lubricant in the bearing. Because the text-book example has the nominal bearing load proportional to the inertial loading, the final algebraic form of the criterion involves g, the acceleration due to gravity, and is applicable only to this restricted set of problems.

For the compressor, the complicated time dependence of the load makes an analytic stability analysis impractical. However, consider the inertial loading of the journal bearings. The motor's rotor weighs almost 1Kg, and its total length exceeds its diameter. Thus, in operation, the rotor - crankshaft assembly is rotating about that principle rotation axis which has the minimum moment of inertia. It is a standard result of classical mechanics that for an unconstrained rotator, rotation about the axis of minimum moment of inertia is unstable (61).

While it is quite normal for electric motors to have such a rotor aspect ratio, any predilection for instability is inhibited by supporting the rotor with a bearing at each end. This is not the case for the compressor, whose rotor is supported by a bearing at one end only.

At this stage, then, there had been three ideas in contention to account for the high power mode;-

Cavitation of the lubricant film due to flashing of the R12.

Failure of hydrodynamic lubrication due to low viscosity.

Dynamical instability due to low lubricant viscosity.

As explained above, application of the Sommerfeld criterion had narrowed the field to the first and last of these possibilities.

If the first suggestion is correct, then persistence of the high power mode would be expected for a high refrigerant fraction, but not for a high oil temperature, even if the resulting viscosity was the same.

In contrast, if the last suggestion is correct, then the behaviour would be expected to be dependent on viscosity alone, irrespective of whether it was high temperature, or high refrigerant fraction that made the viscosity low.

Since the compressor's temperature was varied, both instances of low lubricant viscosity were established. Depending on whether or not the high power mode occurs at the high temperature, one or other of its two possible causes may be vindicated.

In addition to the above two considerations, it was also realised that the sump oil temperature variation is applicable to a further question concerning the motor's operation.

Danfoss have supplied performance data for the motor running at 80C (34). It is commonly assumed that electric motors work more efficiently if the temperature is held down, because this reduces the resistance of the stator, and of the rotor's squirrel cage. However, it is possible that any gain is offset by an increased current consumption. By subsequently examining the temperature dependence of the motor's current consumption, some light may be cast on this point.

4.6 Preliminary analysis

After performing these tests, a simple calculation was devised to extract estimates of volumetric efficiency and work of compression from the measurements. The calculation can be explained in a few sentences:-

From the measured pressure and temperature of the discharge gas, its density, enthalpy and entropy were found.

From the subcooled liquid enthalpy and measured condenser power, an estimate for the refrigerant flow rate was obtained.

By making the simplifing assumption that the cylinder gas at the suction pressure has the same entropy as the discharge gas, an estimate was obtained for the gas state at the start of the compression stroke. This method eliminated the need to attempt an independent estimate of the suction gas preheat.

Having thus estimated the mass flow rate, and the specific enthalpy increment on the compression stroke, there followed an estimate for the mechanical power required to compress the gas.

At the same time, having obtained estimates for the gas density at top & bottom dead centre, an independent estimate could be obtained for the refrigerant flow rate that would be expected. The above outline is summarised by the following equations

$$\dot{m} = \frac{\text{condenser power}}{h_{dis} - h_{sub}} \qquad 4.1$$

$$\text{Power reqired for compression} = \dot{m}(h_{dis} - h_{bdc}) \qquad 4.2$$

$$\text{'Ideal' mass flow rate} = f(\rho_{bdc}V_{bdc} - \rho_{dis}V_{dis}) \qquad 4.3$$

where V_{bdc}=10.7cc, V_{tdc}=0.5cc, f=compressor's frequency,

h_{sub}= subcooled liquid enthalpy, and

h_{bdc} is defined by the discharge entropy & suction pressure.

This calculation was necessary in order to obtain answers to the questions addressed by this experiment. By subtracting the work of compression from the measured power consumption, the total of all the losses is obtained. This is a necessary first step in the elucidation of the mechanical losses.

The question of condensation in the cylinder could be checked by finding the temperature dependence of the ratio of the observed refrigerant flow rate to the ideal value.

Having set up this calculation, it was applied to some of the data acquired during 1985. The most surprising observation was that the compressor's performance is disappointingly poor. The calculated work of compression was consistently around half of the total consumption, and the apparent refrigerant flow rate was nearly always less than 90% of the ideal value. Since the ideal figure already includes the effect of the re-expansion charge, it seemed very difficult to account for this 10%+ shortfall in capacity. Although it had always been realised that the compressor is not very efficient, it nonetheless came as something of a surprise to find that it was struggling even to reach 50%. Like the capacity shortfall, it seemed difficult to account for such large losses.

4.7 Compressor's losses

The compressor's losses, of both capacity and efficiency, may be accounted by the following features of its operation.

Electrical losses

i) Stator Joule heating

ii) Rotor Joule heating

Gas flow losses

i) Pressure loss through the suction system during intake.

ii) Pressure excess in the discharge plenum during discharge.

iii) Pressure drop accompanying flow through the valves.

iv) Reverse flow through the valves due to late closure.

v) Leakage past the piston on compression & discharge.

vi) Condensation in the cylinder.

Mechanical losses

i) Losses at the journal bearings, thrust bearing, & piston.

ii) Viscous drag due to oil in the gap between the motor's rotor & stator.

iii) Power required by the oil delivery system.

Heat exchange loss

The effect of the heat exchange that occurs inside the can between the discharge and suction gas is to make the actual cylinder gas entropy higher than the estimated value. This makes the specific work of compression higher, and introduces a capacity loss due to the reduced cylinder gas density.

This list has been compiled with the benefit of hindsight. At the time, not all of these points had been recognised. There was only a vague idea of their individual magnitudes, and this obscure picture was further confused by some misconceptions that have only since been recognised as such.

At one time, the viscous drag caused by oil in the rotor - stator gap had been considered as a possible cause of the bistability of the motor's power consumption. This idea required that an empty gap, and a filled gap should both be stable states, with an intermediate state being unstable, in order to account for this bistability. However, from the experimental measurements, it appears that the high power mode is made more persistent by a high load on the journal bearings, i.e. a high discharge pressure, whereas a low discharge pressure favours the low power mode. This observation suggests that the rotor - stator viscous drag is not responsible for the power step, since it cannot be influenced by the bearing load.

Around this time, March 1986, it was necessary to prepare the hardware for further anticipated experiments, without first making a detailed examination of the preceding measurements. This unsatisfactory circumstance had been precipitated by the imminent closure of the workshop, which dictated the need to complete all the foreseeable metalwork as a matter of urgency.

The new compressor was modified to facilitate total dis-assembly and re-assembly. This is normally precluded by the interference fit of the rotor onto the crankshaft. By running the compressor with the piston & con-rod omitted, and comparing the result with the previous free running tests, it had been hoped to obtain an experimental determination of the mechanical loss associated with these components. In preparation for this test, the sump had been filled with new oil which was ostensibly identical to the original oil, but it was subsequently found to be significantly different. Upon communicating with Du Pont (48) , who made the original oil, it was discovered that production of this lubricant had been transferred to a different manufacturer. This change of the lubricant compromised the validity of this test. However, the more important result was that the high power mode became much less persistent. It is well known in tribology that the properties of a lubricated interface can be radically altered by minute amounts of foreign material in the lubricant (62). This unexpected change in the behaviour of the compressor's power consumption may have been caused by this unintentional change in the lubricant. In response to this turn of events, it was decided to press on with the measurements that had been planned originally, before the power step was noticed.

4.8 Further experiments

During the second week of April 1986 some of the initial tests, performed with the old compressor during the Summer of 1985, were repeated with the new compressor, now modified as explained above. These tests included two repeats of the variation in TXV setting, first tried on 26/7/85. During two of these tests it was noticed that the output from the condenser's Pelton wheel flow meter was not always consistent with the flow rate recorded by the condenser water rotameter. At a low flow rate, it was noticed that the Pelton wheel flow meter would occasionally produce an absurdly high value, which increased with further fall in the true flow rate. For this reason, the practice of making manual flow rate measurements was adopted shortly afterwards.

Up till this point, the water regulator had not been set higher than 4, giving a discharge pressure of around 190psia. On 18/4/86 a discharge pressure of 220 psia was tried. Unfortunately, the output from the discharge pressure transducer exceeded the 4095 bit limit of the ADC.

Having thus lost the discharge pressure measurement, the scope for analysis of the results was rather limited.

On 20,21,22/4/86 three tests were performed for the purpose of demonstrating that subcooling of the liquid is reduced if there is insufficient refrigerant, or if the liquid reservoir is placed at the end of the condenser. In either case, reduced subcooling reduces the cycle's efficiency.

4.9 More novel tests

Fixed orifice expansion valve

A further test on the expansion valve setting was performed on 23/4/86. Of all the tests on the expansion valve that had been performed up till this point, the behaviour seen on the first test of 26/7/85 had never been reproduced. A likely reason for this anomaly was worked out, and on 27/4/86 a further experiment was performed to check the idea. This experiment included disconnecting the vapour pressure bulb from the suction line in order to force the expansion valve to remain fully open. This had an interesting effect on the system's behaviour, with implications beyond the context of this test alone.

Suction system by-pass

It was thought that the large shortfall of the measured capacity from its ideal value might be due mainly to pressure drops in the suction plenum system. In order to test this possibility, the suction system was by-passed by drilling two 8mm holes into each of the inner plenums. By making performance measurements with these holes either open, or plugged to restore the status quo, it was found that this labyrinth introduces a small penalty only at a high suction pressure. This ruled out the possibility of the suction system's accounting for the capacity shortfall.

Leakage past the piston

Up till this point it had been thought that leakage past the piston was negligible, because the results quoted in a paper on the subject (63) showed this. Then an account was found of a completely independent experimental measurement (64), for which the leakage was not negligible. The initial misconception had occurred because the compressor used in (63) had had a very narrow piston-bore clearance, whereas the investigation of (64) was more relevant to the Danfoss SC10H.

This presented the problem of devising a measurement of the leakage past the piston which could be quickly implemented using the available hardware. This requirement was met by removing the top of the compressor's can, and coupling the suction pipe directly to the casting's suction stub. Thus leakage past the piston emerged into the atmosphere, lost from the heat pump's circuit. This rate of loss was measured by monitoring the fall of the accumulator's liquid level, after steady-state operation had been established.

4.10 First attempt at modelling

Danfoss have a wholly empirical double quadratic correlation for the capacity and C.O.P. as functions of the evaporating and condensing temperatures (34). It was thought that it would be straightforward to write a compressor model with a minimal empirical content, and then demonstrate that this gave a better match to the measurements than Danfoss' empirical fit. After performing these calculations, it was indeed observed that there were significant differences between the model, and the empirical correlation, especially at extreme conditions, outwith the range of validity of the correlation. However, on appealing to the measured capacity as the ultimate arbiter of this competition, it was found that the scatter in the capacity measurements was of the same order as the difference between the sophisticated model, and the crude correlation. This problem is thought to have been a consequence of the unreliability of the Pelton wheel flow meters.

In response to this difficulty, an ambitious programme was devised to execute several experiments involving a large number of definitive performance measurements. In this final set of measurements the lessons learned up to this point were all implemented. A more complete account is given in chapter 8.

Chapter 5. The experiments of 1985

5.1 Introduction

Having outlined the experiments, the thinking behind them, and some of the more important results, the purpose of this chapter is to present more detailed accounts of the initial trials.

5.2 First attempted performance map determination

It was suggested that in order to acquire data over a wide range of evaporating temperatures in a single run, the evaporator could be supplied from a large water tank, which would initially be heated to a temperature of 40 - 50C. In the course of the run this would cool due to the heat removed by the evaporator. It was found that, as a consequence of the very high heat pump capacity at the high evaporating temperature, the initial rate of fall of the reservoir temperature was unacceptably high. The strategy was adopted of operating an immersion heater from a variac. By setting the heater power always slightly below the current refrigerating capacity, a controlled and slow rate of fall of reservoir temperature could be maintained.

A major penalty of this technique was that it resulted in the experimental runs taking a very long time. A 12 hour run would seem quick by comparison with the more common 15 - 18 hours.

During informal preliminary tests on the heatpump, it had sometimes been noticed that the liquid freon flow rate through the throttle valve varied cyclically from near zero to a litle over the mean flow rate, with a period of order 1 minute. The liquid freon flowmeter indicated this effect, which was confirmed by observing that the accumulator's liquid level drops at the peak flow rate, with a subsequent recovery at the low flow rate. This was interpreted as resulting from hunting of the TXV control loop.

In order to record this effect, it would be neccessary to write a complete set of data onto the disc every 3 seconds, this being the highest speed at which the data recording program could be run. Continuous recording at this rate would have resulted in each run using a lot of floppy discs. Apart from the obvious penalty of cost, this would have aggravated the problems of post-processing, filing and data retrieval. In view of these considerations, the following schedule was adopted for each run.

Preliminary to the run, the evaporator water reservoir was heated to around 45C. For the first 3 hours of the run, the variac was left at 70%, giving an immersion heater power of about 1.5 KW. Every 2 minutes during this period the ADCs were read 50 times, and the average bit reading of each channel recorded onto disc. This 3 hour recording was then followed by 12 minutes of time resolved recording, during which 300 data sets were written onto the disc. In order to distinguish the effect, if any, of the condenser water flow control loop, there followed a second time resolved recording for which the condenser water flow rate was manually set, using the rotameter's valve. Afterwards, the condenser water flow regulator was re-instated, the variac reset to a lower power, and the process repeated. In this way, the complete range of evaporator water supply temperature was covered in 4 or 5 such steps.

During the period of May - June 1985 a systematic set of experimental runs was executed in this way. At nominal evaporator water flow rates of 20, 50 & 90 cc/s, condenser water flow regulator settings of 3 and 4 were used. These corresponded to nominal discharge pressures of 150 and 200 psia. Lastly, the range of condensing pressure investigated was extended by a single run at 90cc/s evaporator water flow rate, and a discharge pressure regulator setting of 2.4, giving a nominal condensing pressure of 120 psia.

<u>Summary of runs in May & June 1985</u>

Date	Discharge pressure regulator setting	Evaporator water flow rate	Evaporator water temperature range
11/5/85	3	50	42-5
19/5/85	3	20	41-12
25/5/85	3	50	42-5
27/5/85	3	20	47-10
1/6/85	3	90	45-4
2/6/85	4	90	41-14
7/6/85	4	20	46-17
8/6/85	4	50	44-14
9/6/85	2.4	90	45-3

<u>Table 5.1</u>

Having varied three of the independent variables - evaporator water supply temperature, evaporator water flow rate, and the discharge pressure regulator setting, it was naively thought that it only remained to plot the graphs. In figure 5.1a a set of curves has been plotted for the condenser output power as a function of evaporator water entry temperature, with the evaporator water flow rate as parameter. For the five plots in figure 5.1a the discharge pressure regulator setting is 3. Figure 5.2a shows a complementary plot. Here, three results are plotted for an evaporator flow rate of 90cc/s, with the flow regulator setting as parameter.

Figures 5.1b & 5.2b present the corresponding plots of C.O.P. At this stage several points become apparent. Firstly, while it is arguably necessary to present figures 5.1 & 5.2 for the reader's information, by themselves these plots do very little to assist the understanding and diagnosis of the system. Secondly, these plots raise more questions than they answer. For instance, with increasing evaporator water temperature, some of these plots show capacity and COP levelling off, while under different conditions there is no sign of this effect. Additionally, the plots of COP show anomalous rises and falls which are not correlated with evaporating temperature. In order to understand the heat pump's behaviour, a more detailed examination of the data is necessary.

Behaviour of the discharge pressure regulator

It was observed that, by virtue of the finite gain of the discharge pressure control loop, as the capacity fell, so the discharge pressure fell slightly. For a change in capacity from 2kW to 500W, the effect was of order 5 - 10psi. Although a small effect, this was undesirable, since the fundamental independent variable is discharge pressure, not the water flow regulator setting.

5.3 TXV limited operation

A more important observation was that of saturation of the throttle valve. For a given condensing pressure, the mass flow rate which can be maintained by the compressor increases monotonically with evaporating pressure. However, for a fully open throttle, the flow rate through

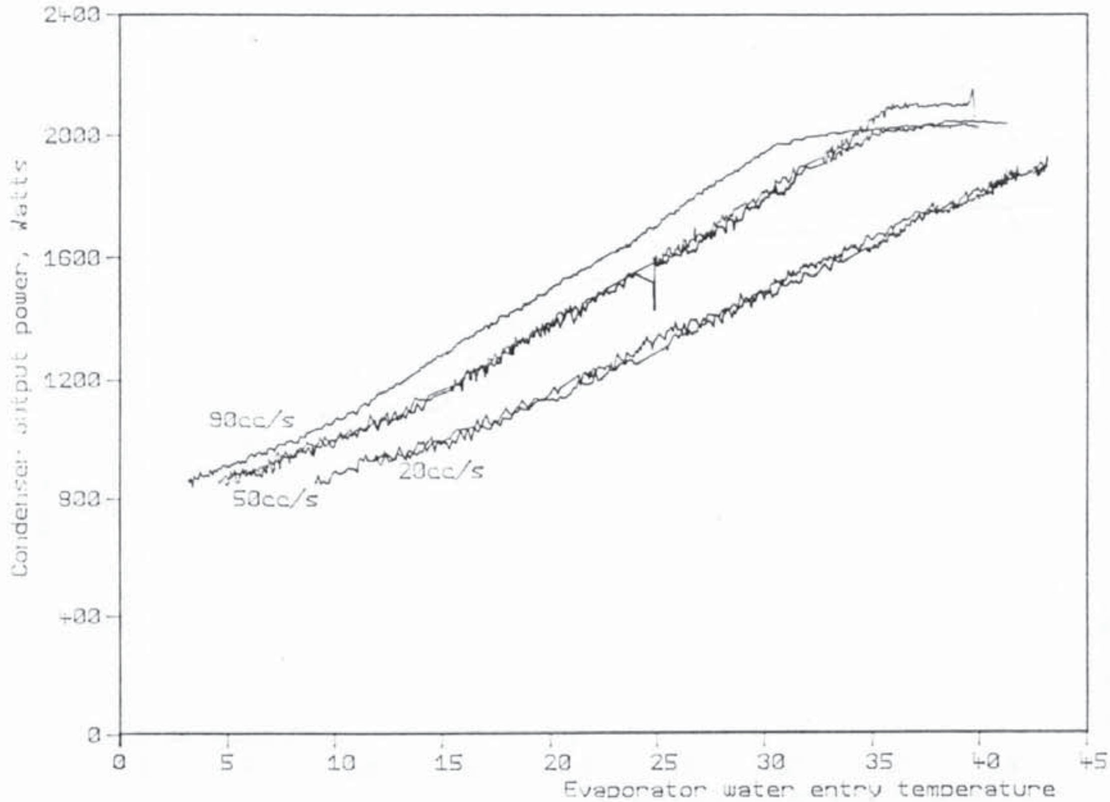

Figure 5.1a Dependence of capacity on evaporator water supply temperature & flow rate. Regulator setting = 3

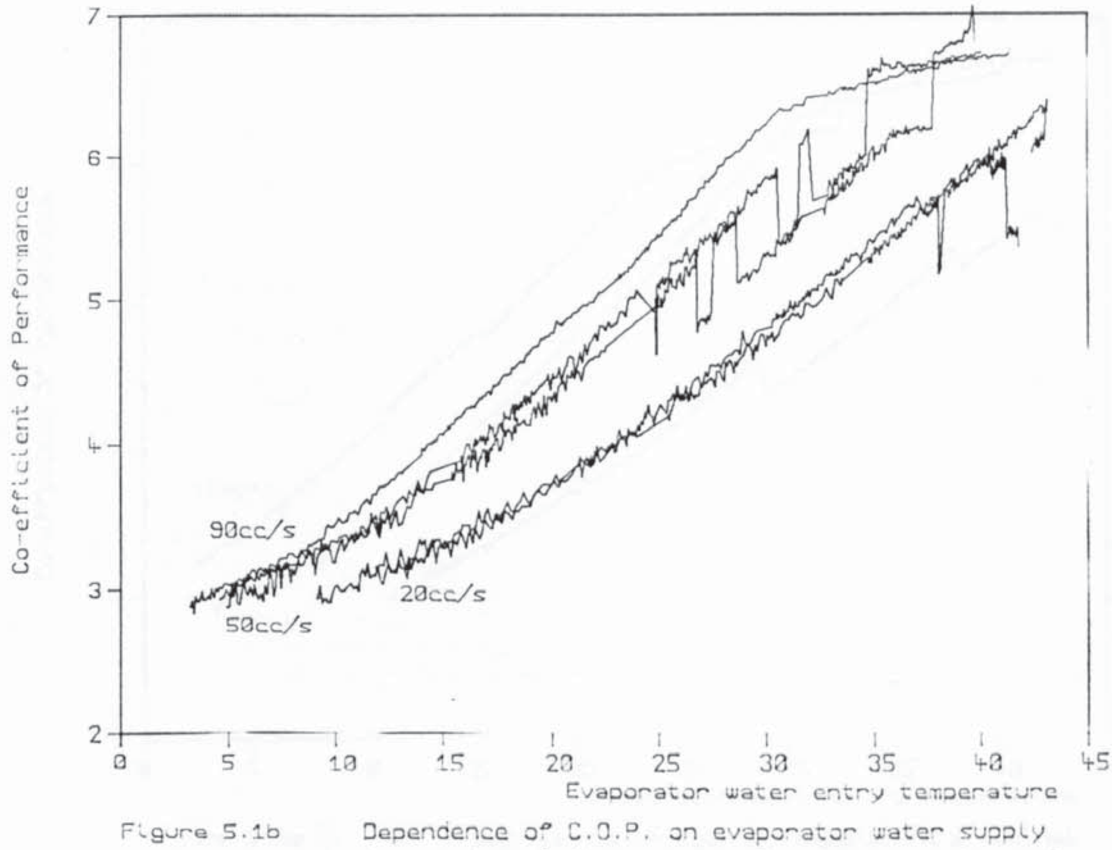

Figure 5.1b Dependence of C.O.P. on evaporator water supply temperature & flow rate. Regulator setting = 3

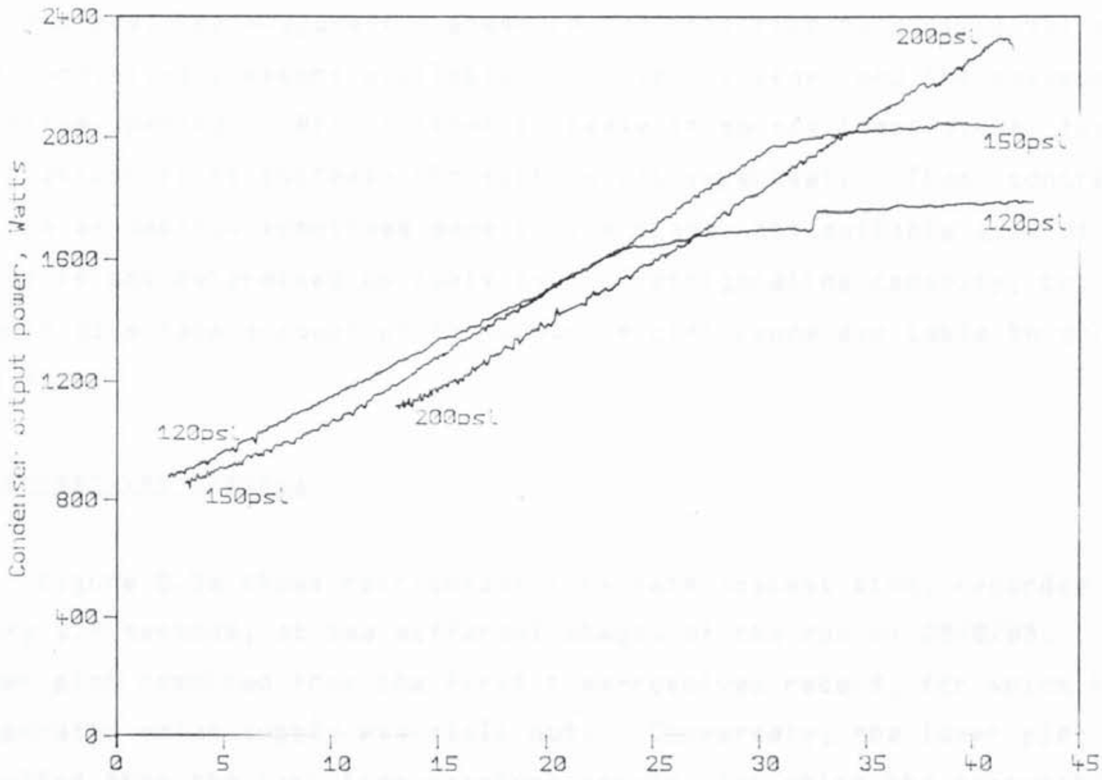

Figure 5.2a Capacity dependence on source temperature & nominal discharge pressure. Water flow rate = 90cc/s

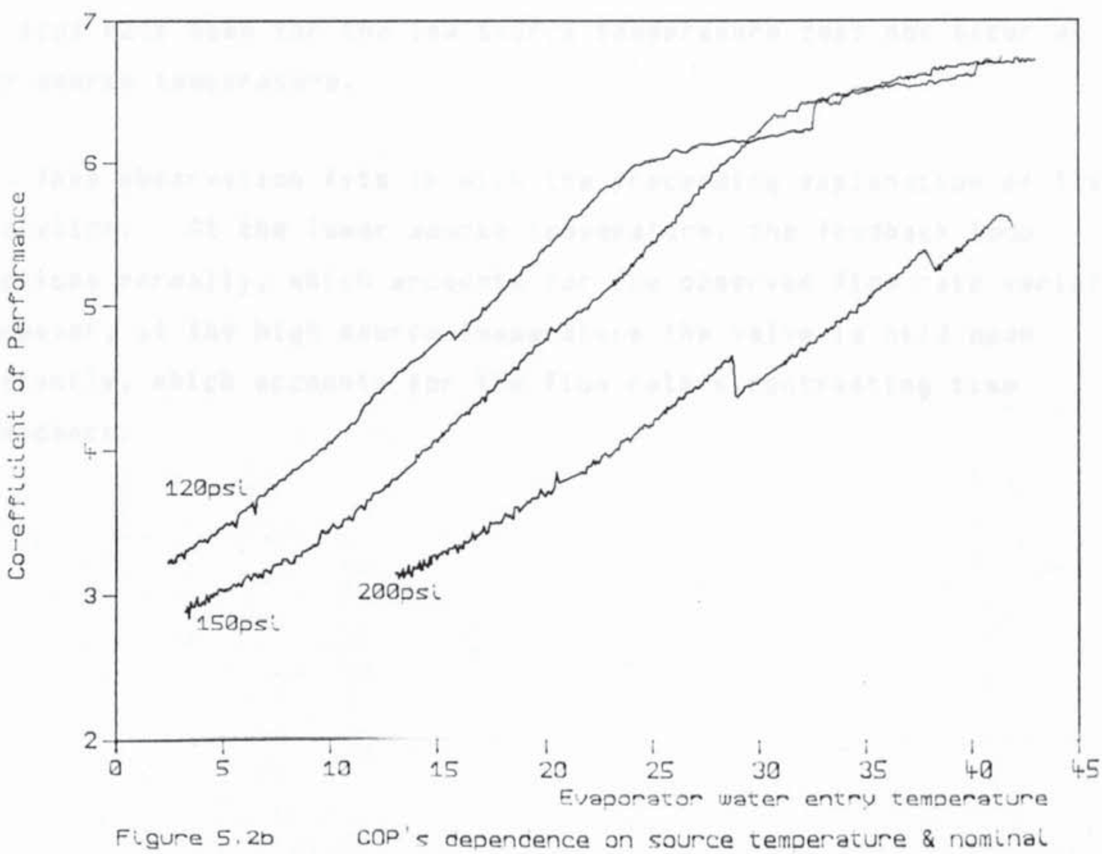

Figure 5.2b COP's dependence on source temperature & nominal discharge pressure. Water flow rate = 90cc/s

the throttle would fall with increasing pressure in the evaporator. The result of this is that with increasing evaporator source temperature, the evaporating pressure can only rise to a limit set by the condensing pressure available to drive the flow, and the maximum throttle opening. With further increase in source temperature, the only effect is to increase the suction gas superheat. Thus, contrary to the assumption sometimes made in the trade, the suitable size of valve is not determined uniquely by the refrigerating capacity, but should also take account of the pressure difference available to drive the flow.

Time-resolved records

Figure 5.3a shows refrigerant flow rate against time, recorded every 2.4 seconds, at two different stages of the run of 25/5/85. The upper plot resulted from the first time-resolved record, for which the evaporator water supply was still hot. Conversely, the lower plot resulted from the last time resolved record, for which the evaporator supply was cold. Figure 5.3b presents the corresponding plots for the run of 27/5/85. Sample data sets from these four time-resolved records are listed on tables 5.2 to 5.5. Note that the periodic variation of the flow rate seen for the low source temperature does not occur at the high source temperature.

This observation fits in with the preceeding explanation of TXV saturation. At the lower source temperature, the feedback loop functions normally, which accounts for the observed flow rate variation. However, at the high source temperature the valve is held open constantly, which accounts for the flow rate's contrasting time dependance.

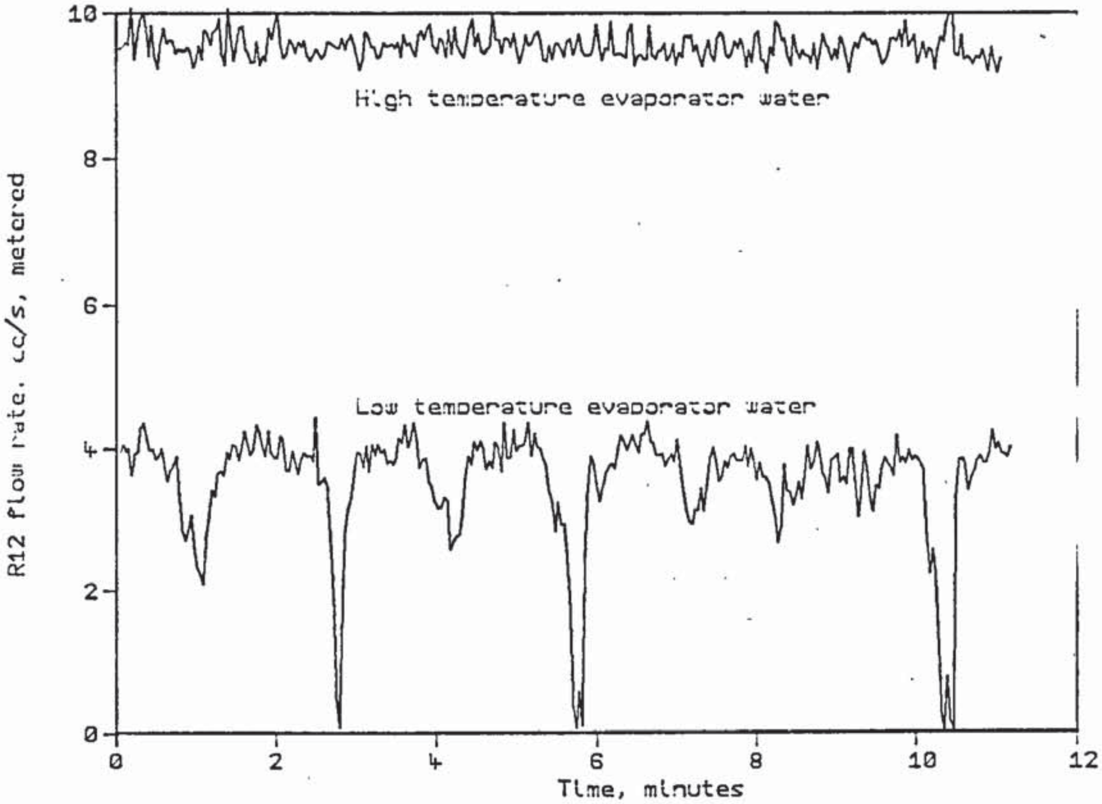

Figure 5.3a R12 flow rate. Time resolved plots from 25/5/85

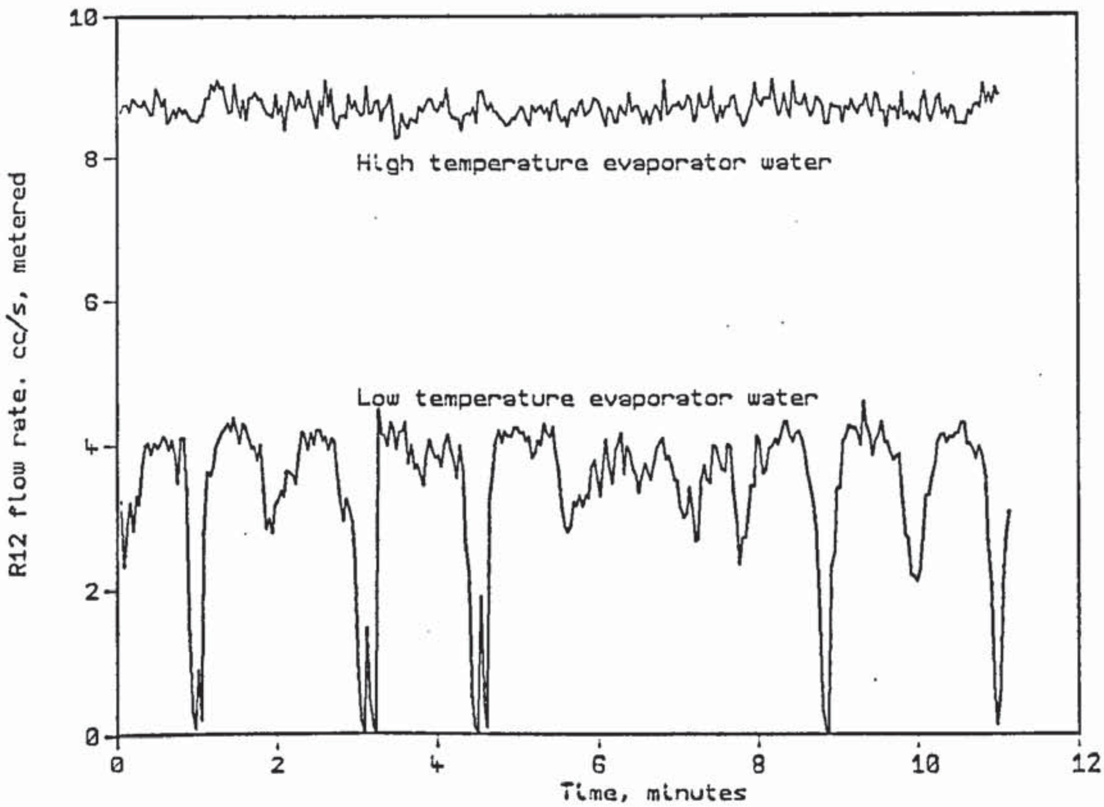

Figure 5.3b R12 flow rate. Time resolved plots from 27/5/85

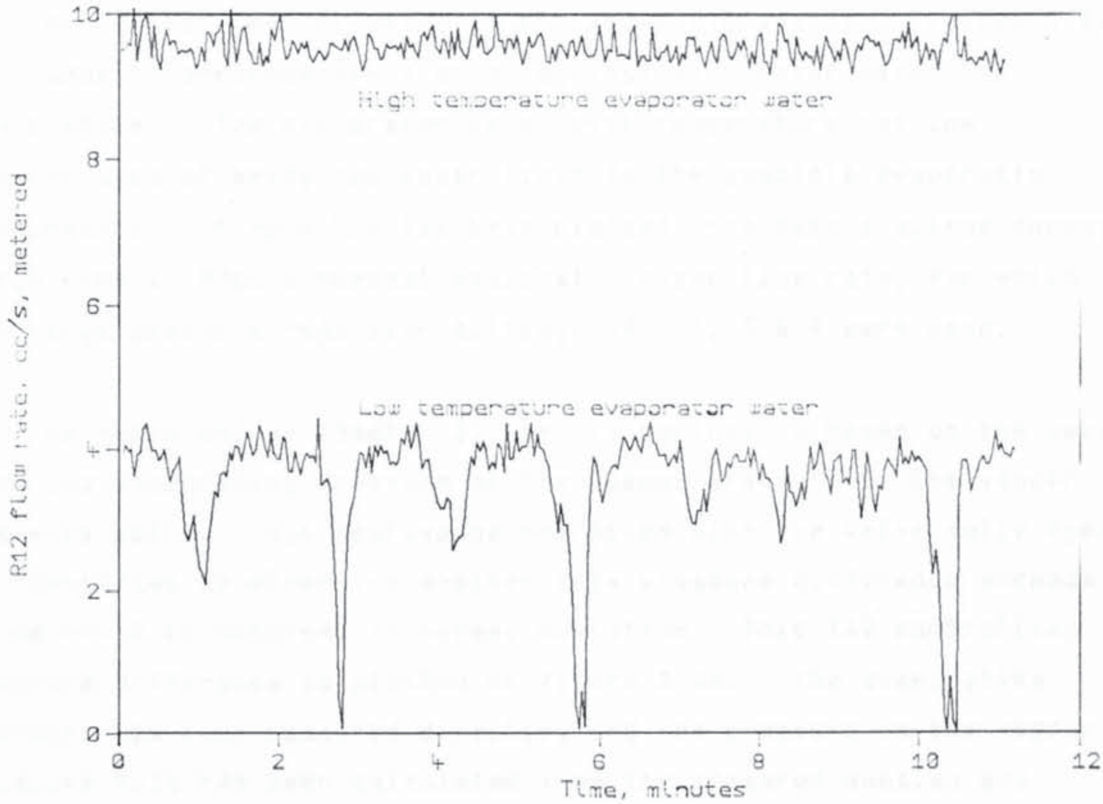

Figure 5.3a R12 flow rate. Time resolved plots from 25/5/85

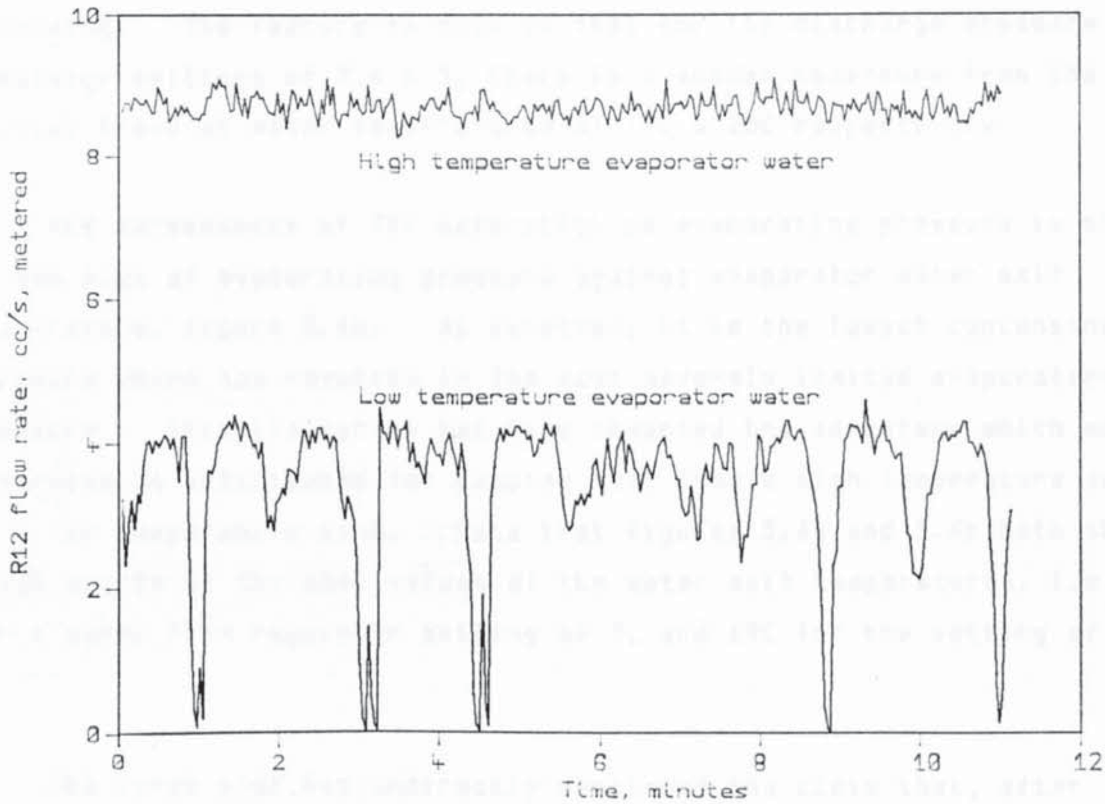

Figure 5.3b R12 flow rate. Time resolved plots from 27/5/85

Further consequences of TXV saturation

As further demonstration of the above explanation, figures 5.4a, b & c, show threeparameters plotted against evaporator water exit temperature. The evaporator water exit temperature has the significance of being the upper limit to the possible evaporating temperature. Figure 5.4 has been plotted from data acquired during the three runs at 90cc/s nominal evaporator water flow rate, for which discharge pressure regulator settings of 2.4, 3 & 4 were used.

As explained in chapter 3, the TXV control is based on the excess over the evaporating pressure of the vapour pressure in the vapour pressure bulb. Thus continuous operation with the valve fully open can be identified by observing whether this pressure difference exceeds that value which is observed in normal operation. This TXV controlling pressure difference is plotted on figure 5.4a. The evaporating pressure has been measured directly, and the pressure in the vapour pressure bulb has been calculated from the measured suction gas temperature. The discontinuity seen for the high discharge pressure (discharge pressure regulator set to 4) is of no significance, as it resulted from manual resetting of the regulator after time resolved recording. The feature to note is that for the discharge pressure regulator settings of 2.4 & 3, there is a sudden departure from the initial trend at water temperatures of 19C & 25C respectively.

The consequence of TXV saturation on evaporating pressure is shown in the plot of evaporating pressure against evaporator water exit temperature, figure 5.4b. As expected, it is the lowest condensing pressure which has resulted in the most severely limited evaporating pressure. This limitation has thus thwarted the advantage which would otherwise be anticipated for pumping heat from a high temperature source to a low temperature sink. Note that figures 5.4a and 5.4b both show break points at the same values of the water exit temperatures. i.e. 25C for a water flow regulator setting of 3, and 19C for the setting of 2.4.

The first plot has indirectly confirmed the claim that, after saturation of the TXV, further increase of source temperature only drives up the superheat. However, by plotting against water exit

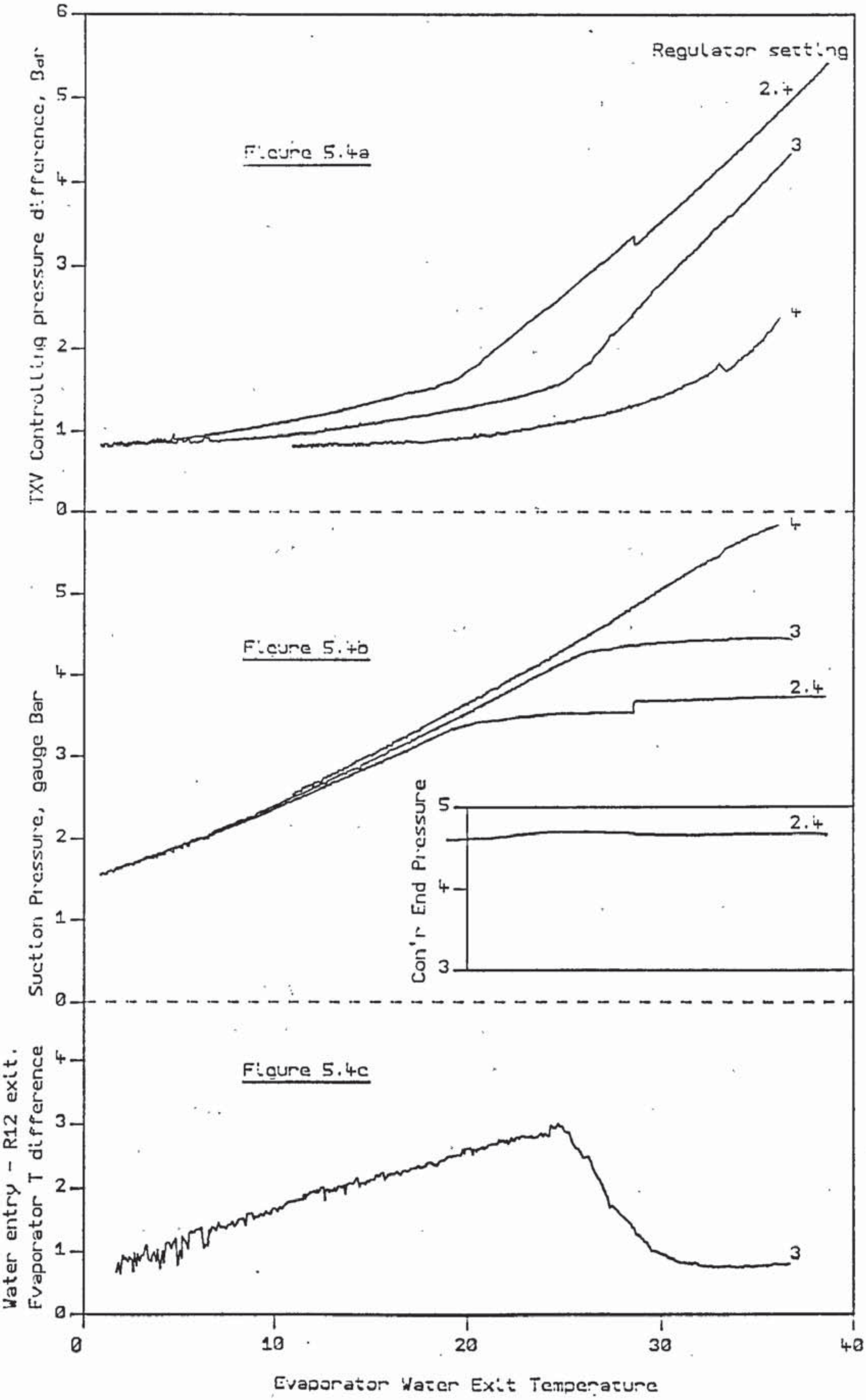

Figure 5.4. Further symptoms of TXV saturation

temperature the difference between the water entry temperature and the vapour exit temperature, a further important feature can be demonstrated. Figure 5.4c shows this evaporator end temperature difference plotted for the run at the intermediate discharge pressure (water flow regulator set to 3). At a low source temperature, the freon flow rate falls with falling temperature. With falling refrigerant flow rate, the freon vapour can more closely approach the water entry temperature. This accounts for the initially positive slope of this plot. However, at 25C, the break point shown in plots 5.4a & 5.4b, this evaporator end temperature difference peaks, and starts to fall with further increase of the water temperature. Figure 5.4b has shown that the evaporating pressure is approximately constant in this regime of high source temperature. Since the pressure at the condenser's end was also held constant, and since figure 5.4a indicates that the valve was held fully open by a highly superheated vapour pressure bulb, it follows that the refrigerant flow rate was approximately constant. This deduction has not involved any assumption about the compressor, and has followed solely from the observation that the conditions at the expansion valve were invariant in this operating regime. Thus figure 5.4c shows that at a temperature above the break point, further increase of the evaporator water temperature results in a closer approach of the suction gas temperature to the water entry temperature, while the refrigerant flow rate remains constant.

This is indicative that the length of the evaporator available for superheating increases with increasing source temperature. This makes sense, because, with an approximately constant boiling heat transfer co-efficient, *and* a fixed capacity, the wetted surface of the evaporator must fall with increasing source temperature, so leaving more available heat transfer surface for superheating. This interpretation of these observations would predict that by starting the run with a high source temperature, the initial effect of the falling source temperature would be to increase the amount of liquid in the evaporator, so causing a fall in the liquid level in the accumulator.

This interpretation has been supported by the observation that upon starting in the saturated TXV regime, the liquid level in the accumulator does indeed fall with falling source temperature.

5.4 Anomalous orifice flow

To return to figure 5.4b, the vigilant will have noticed that the run with the lowest condensing pressure shows a sudden, discontinuous drop in evaporating pressure, during operation of the TXV as a fixed orifice. (In figure 5.4 the arrow of time is from right to left.) Reference to a listing of the data quickly discounted the possibility that this resulted from inaccurate resetting of the water flow regulator after time resolved recording. In fact, this step occurred in the middle of one of the 3 hour recordings. Confirmation that this was not caused by a change in pressure upstream of the TXV is indicated by the inset on this plot, which shows the relevant plot of pressure at the condenser's end.

This apparently spontaneous discontinuity in evaporating pressure, seen for operation with a fixed orifice, is sufficiently interesting to warrant examination of other data recorded in this operating regime. Figure 5-5 shows the initial pressure histories of this, and five other runs.

The first plot on figure 5.5 shows evaporating pressure against time for the run in question. (9/6/85, 90cc/s evaporator water flow rate, discharge pressure regulator set to 2.4, nominal discharge pressure 120psia). For the sake of clarity, figure 5.4 did not include data recorded during the first three hours of this run, because there was very little variation in evaporator water entry temperature during this time. However, for the histories shown in figure 5.5, all points are shown, with the exception of the time-resolved records. It can be seen that on the run of 9/6/85 there was a discontinuous upward transition in evaporating pressure after 2 hours, followed by the downward transition 4 hours later. Tables 5.6 & 5.7 list all the data recorded at the upward and downward transitions respectively. These tables include the results of the calculation outlined in section 4.7.

By inspecting this data, one can see that these discontinuities in the evaporating pressure history are confirmed by the independent records of evaporating temperature, refrigerant flow rate, condenser power, and suction pressure. Co-incident with this 0.15 Bar change, there is a corresponding change of 0.15 Bar in the suction pressure and

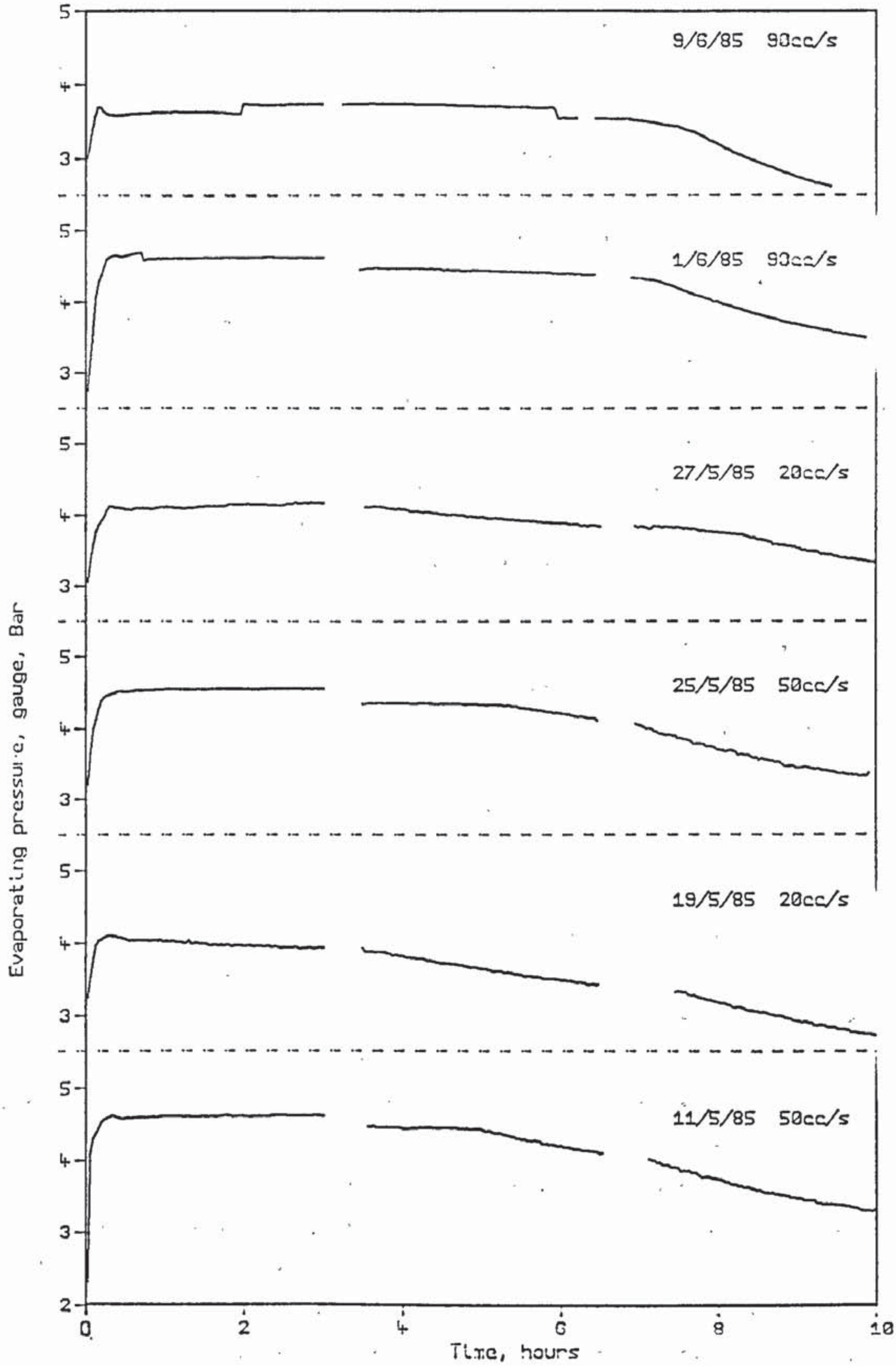

Figure 5.5 Search for evaporating pressure transitions

a change of 0.8C in the evaporating temperature. Additionally, the liquid freon flowmeter indicates a corresponding step of about 4%, which is in agreement with the change in condenser power. Furthermore, the calculated results indicate that the ratio (Apparent R12 flow rate)/(Ideal value) remains constant. This indicates that the measured change in condenser power is just what would be expected from the observed change in evaporating pressure. With all this independent confirmation, there can be no doubt that the observations are legitimate and not merely the result of an instrumental anomaly.

The other plots on figure 5.5 show the evaporating pressure histories of the five runs which had the water flow regulator set to 3, giving a nominal discharge pressure of 150psi. For ease of reference, they have been labelled with the date of execution and the nominal evaporator water flow rate. For the purpose of this search, it is only the trials which started with fixed orifice TXV operation that are relevant. The runs which had the discharge pressure regulator set to 4 are thus not relevant, because the TXV control loop was operative even at the highest evaporator water temperature.

From figure 5.5 one can see that the two runs at 20cc/s evaporator flow rate start at a lower evaporating pressure than the runs at 50cc/s. For the runs at 20cc/s the evaporator water exit temperature never exceeded 25C, whereas for the runs at 50cc/s it consistently exceeded 30C. Thus it is only the runs at 50cc/s & 90cc/s which operated initially in the fixed orifice regime.

Some of these plots show that upon resuming the data acquisition after the first break for time-resolved recording, the evaporating pressure starts lower. This is merely a consequence of having reset the discharge pressure regulator, resulting in an unintentional 0.3 bar reduction in the discharge pressure. The downward step in pressure seen at 30 minutes on 1/6/85 had a different, but no less artificial origin. In an attempt to restart the evaporator water flowmeter, which had got stuck, the evaporator water flow was stopped, and then suddenly restarted at a high flow rate. This perturbation of the system sent the discharge pressure regulator into an overshoot / undershoot cycle, to level off at a discharge pressure 0.2 bar lower than initially.

It has thus been concluded that there is no record other than that of 9/6/85 which shows a truly spontaneous discontinuity in the evaporating pressure.

Inspection of the data has revealed an important feature. For all the runs used to plot figure 5.5, the condensed freon was subcooled to a temperature of between 16C and 18C. For those runs at a nominal discharge pressure of 150psi, (regulator set to 3) which exhibited fixed orifice operation, the boiling point at the evaporating pressure was around 19 to 20C. Thus the freon flowing through the valve was single phase. However, the boiling point at the evaporating pressure on 9/6/85, for a nominal discharge pressure of 120 psi, was around 14C, so that the throttled refrigerant would have emerged partially vapourised.

The experimental results are thus indicative that when operating in the fixed orifice regime, observation of a double-valued evaporating pressure is conditional upon the orifice flow being two phase.

The most likely interpretation of this observation is that for two phase orifice flow, the flow rate can be intrinsically double-valued, even for fixed upstream and downstream pressures (65). This conclusion was reached after considering the possibility that the compressor's capacity as a function of suction pressure may have two stable intersections with a plot of orifice flow rate as a function of evaporating pressure. However, this possibility was rejected on the grounds that the orifice flow rate would need to be very sharply peaked in order to get two intersections separated by only 0.15 bar.

No other run showed this behaviour, because in order to see it, the two conditions must be met of having a saturated TXV, and two phase entry to the evaporator.

Interesting as this phenomenon is, for the current pursuit, it is of no practical importance, because in practice one would always seek to size the TXV to ensure that fixed orifice operation did not occur. However, there has been an important reason for the above consideration of this curiosity.

5.5 Bistability of the power consumption

Figure 5.6a shows the record of suction & discharge pressure for the run of 11/5/85. With the controlled fall in the source temperature, the suction pressure falls, and there is a small drop in discharge pressure due to the finite gain of the pressure regulating control loop. Figure 5.6b shows the corresponding record of power consumption. The striking features to note are the step-like discontinuities in power consumption. The immediate reaction to this was one of incredulity. However, from the plot of sump oil temperature against time, also shown on figure 5.6b, it can be seen that at every discontinuous change in power consumption there is a corresponding discontinuity in the first time derivative of oil temperature. This rules out dismissal of the effect as a spurious artefact. It is real. Figure 5.6c presents the records of discharge gas temperature, sump temperature, and the discharge - sump temperature difference. In order to use the power steps as fiducial marks, the power consumption record has also been superposed. One can see that the discharge temperature is correlated with the sump oil temperature. They tend to rise & fall together. However, the temperature difference record shows that at the transition from low to high power consumption, this temperature difference falls by about 1C in a time too short to be resolved in this plot. Similarly, at a downward transition in the power consumption, this temperature difference rises by about 1C. The gaps in these records, at 3 hour intervals, correspond to the time resolved data acquisition records. Figure 7a shows the suction and discharge pressure record for the period between 3 hours and 3 hours 25 minutes. Data was recorded during this period at a rate of 1 data set every 2.4 seconds. i.e. this is the first time resolved record. The short break in the middle corresponds to the change from use of the flow regulator to a manually set constant water flow rate to the condenser. Figure 5.7b shows the records of power consumption and sump temperature. Even at this high sampling rate, the transitions in power consumption are still step like. With this expanded time axis, it can be seen that at the upward transition in power consumption there is an initially steep rise in temperature, too steep to be accounted for by the 30 Watts extra heating, until the oil's temperature has risen by about 0.5C. The subsequent, lower gradient is consistent with the excess 30 Watts. At the downward transition, there is a similar fast fall of about 0.5C, followed by a less steep fall.

The purpose of the above observation is to put figure 5.7c into context. This shows the records of discharge temperature and discharge - sump temperature difference. Again, the power consumption plot has been superposed to show the exact correspondence between the power consumption transitions and these temperature records. Note that the short-term response of the discharge gas is precisely opposite to that of the sump. This accounts for the shape of the temperature difference plot. At the upward power transition the temperature difference drops by about 1C in a time scale of order 1 minute, this behaviour being reversed at the downward power step. The speed with which this temperature difference approaches its new steady state is fully an order of magnitude faster than the approach to steady state of either temperature separately.

While the above observation is not sufficient to prove any proposed explanation of the power transition, it demonstrates an additional feature for which any suggested mechanism must account. In this way the number of contending theories can be reduced.

Figure 5.8 shows the records for the run of 25/5/85 which correspond to figure 5.6. Figures 5.6a, 5.7a and 5.7d have shown that at a transition in the compressor's power consumption there is no corresponding change in the compressor's operating conditions or capacity. Thus these discontinuous changes in consumption indicate discontinuous changes solely in the compressor's losses. Although only of order 10% of the electrical consumption, the step size is closer to 20% of the losses, and must consequently be regarded as a significant phenomenon - whatever it is.

Sample data sets for all the trials mentioned in this chapter can be found on tables 5.2 to 5.15. The "calculated results" presented on these tables have resulted from the simple calculation outlined in section 4.6. Upon referring to tables 5.7 & 5.8, note that the total of the compressor's losses consistently amounts to 170 Watts in the low power mode, and nearly 200 Watts in the high power mode. Power transitions apart, it is significant that the losses are virtually constant in spite of the substantial variation in the work of compression.

The immediate reaction to the power-step problem was to rush out and buy a new compressor. This new compressor's power consumption was found to behave in the same way. Figure 5.9 shows the records for the run of 7/6/85, which was performed by the original compressor. The discharge pressure regulator was set to 4, for a nominal 200psi, and the evaporator water flow rate was nominally 20cc/s. A repeat of this run on 14/7/85 constituted the very first 15 hours of operation of the new compressor, and the records are shown in figure 5.10. It was assumed that because Mr. Othman had used the original compressor for all his experimental work, it must have been in operation for hundreds of hours. For this reason, the similarity of the two power consumption records led to the tentative conclusion that the observed behaviour is a permanent feature, unaffected by running-in of the compressor.

On 26 July 1985 a completely different test was performed, which was intended to investigate the effect of varying the superheat control of the TXV. In principle, reduction of the superheat is expected to improve capacity and C.O.P. by allowing the evaporating temperature to approach the source temperature more closely. This point will be considered further in section 7.4, which is dedicated to the tests on the expansion valve.

For the first 3 hours of this test, the heatpump was allowed to equilibrate to steady state operation at the same TXV setting as had been used previously. The TXV adjustor was then fully retracted to give minimum superheat, and the run was continued long enough to approach a new steady state, all the measurements being recorded every 2 minutes. After recording the new steady state, the adjustor was screwed in one turn, and the approach to a new steady state monitored. This was continued in one turn steps over the entire range of TXV adjustment. The records of power consumption and oil temperature can be seen by refferring forward to figure 7.11. The effect on oil temperature of changing the TXV setting is clearly recognisable. The key feature to note is the persistence of the high power mode during operation at the minimum superheat. The point is that upon trying to ignore the problem, an experiment designed to look at a completely different question was compromised by this additional uncontrolled variable of unknown origin.

This problem prompted the construction of a simple instrument to monitor mains voltage and compressor current consumption. The outputs were recorded using the two spare analogue inputs of the thermocouple ADC, as explained in chapter 3.

Further, shorter runs of the new compressor were performed. Their purpose was to obtain additional confirmation of the reproducibility of the effect and investigate possible causes. The first suggestion to be checked was that errant operation of the starter coil relay might account for the observations. This was quickly ruled out by manually isolating the starter coil immediately after starting up, and yet still observing the same effect. In every repeat attempted, the high power mode remained stable for some time after starting up, until the evaporator water supply temperature had fallen below a temperature of around 25C, although the exact water temperature at which the transition occurred varied from run to run. Figure 5.11 presents the records of one such test, for which the nominal discharge pressure was 150 psi. Having been performed with the new compressor, these records have been included for comparison with figures 5.6 & 5.8, which present similar data for the old compressor.

On 18/10/85 an attempt was made to force an upward power transition after observing the downward transition. Having started up as normal, at a high source temperature, the transition to the low power mode ocurred after 75 minutes, figure 5.12b. 30 minutes later, the power supplied to the heater in the evaporator's reservoir was increased, to raise the source temperature. This produced the rising suction pressure seen on figure 5.12a. In spite of the suction pressure's being restored to its original value, the high power mode did not recur. Figure 5.12c casts light on this point.

It is thought that the stability of the low power mode depends on the refrigerant fraction in the lubricant not being too high. From Raoult's law, a low refrigerant fraction is favoured by a high ratio of (vapour pressure at the oil temperature)/(suction pressure). Since the vapour pressure is an approximately exponential function of temperature, this ratio is approximately proportional to the temperature *difference* between the liquid in the evaporator and the oil in the sump. This temperature difference is plotted on an expanded scale as the uppermost trace on figure 5.12c. The effect of increasing the evaporator's source temperature is, at first, to make the oil's superheat fall, due to the rising evaporating temperature. However, with the onset of saturation of the TXV, just before 3 hours, further increase of the source temperature has only a marginal effect on the evaporating temperature, while the suction gas temperature continues to climb. This is the reason for the sudden onset of a rising oil temperature, after having been steady around 55C over the preceeding hour. With this rise in oil temperature, the oil's superheat first exceeds its highest previous value at 3 hours 40 minutes. In this test, there was thus a window of a little under 2 hours 30 minutes during which the equilibrium refrigerant fraction in the sump would have exceeded the lowest value present during operation in the high power mode, and yet the high power mode did not recur.

It was recognised that by starting with an initial evaporator supply temperature of 25C, and allowing the reservoir to cool freely, with no backup heating, it would be possible to observe the downward transition within one hour. This offered the potential to record throughout at a sampling rate of one data set every three seconds. The first such run was performed on 20/10/85. Figure 5.13 shows power and current consumption against time for this run. As noted earlier, even at this high sampling speed the transition is still step-like, occurring between one reading and the next. This behaviour is consistent with the hysteresis implied by the re-heat experiment. The downward current step of 65mA is consistent with the downward power step and known power factor. A further interesting feature is the dramatic change in the current's time dependence at the transition.

At this stage it was decided to cut open the old compressor's can and braze on flanges. This access to the compressor was needed to set up more detailed experiments, to be explained in the next chapter.

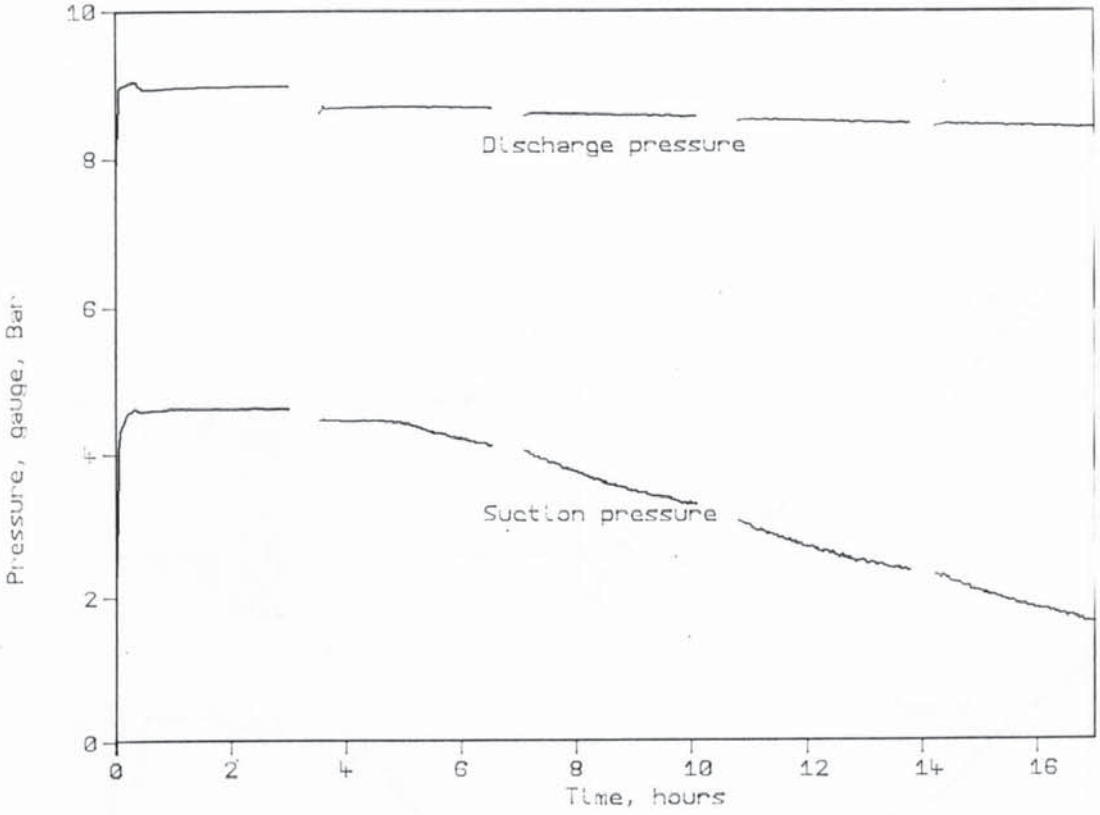

Figure 5.6a Discharge & suction pressure histories of 11/5/85

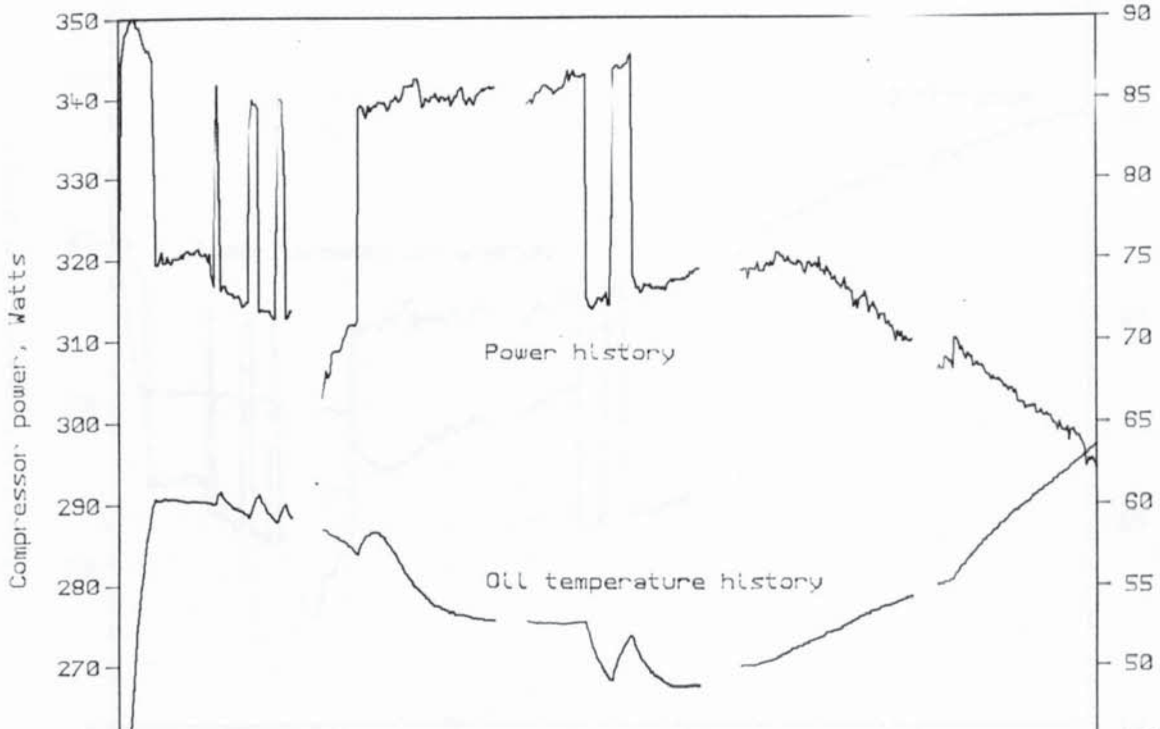

Figure 5.6b Compressor power & oil temperature of 11/5/85

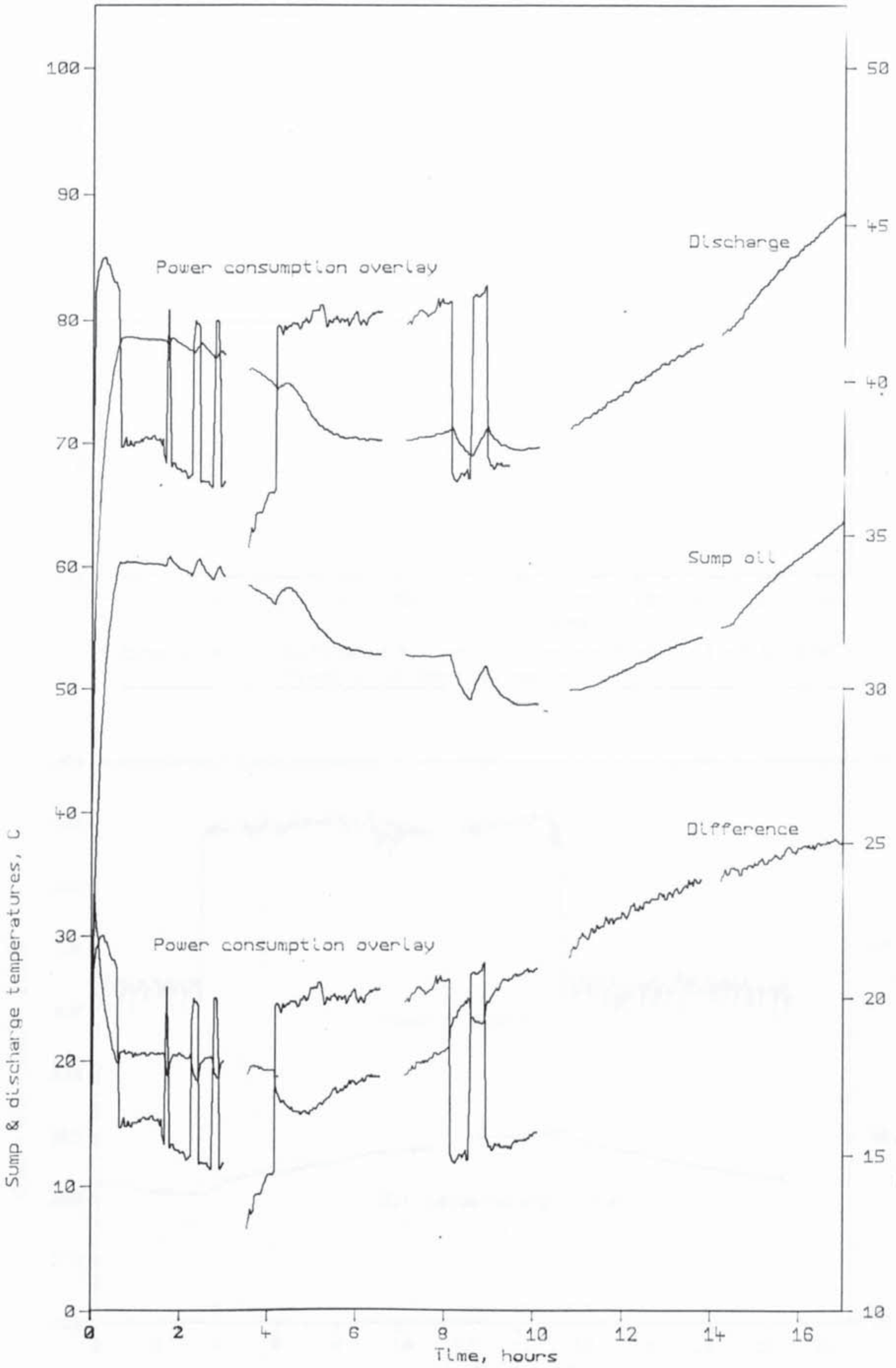

Figure 5.6c Discharge & sump temperature histories of 11/5/85

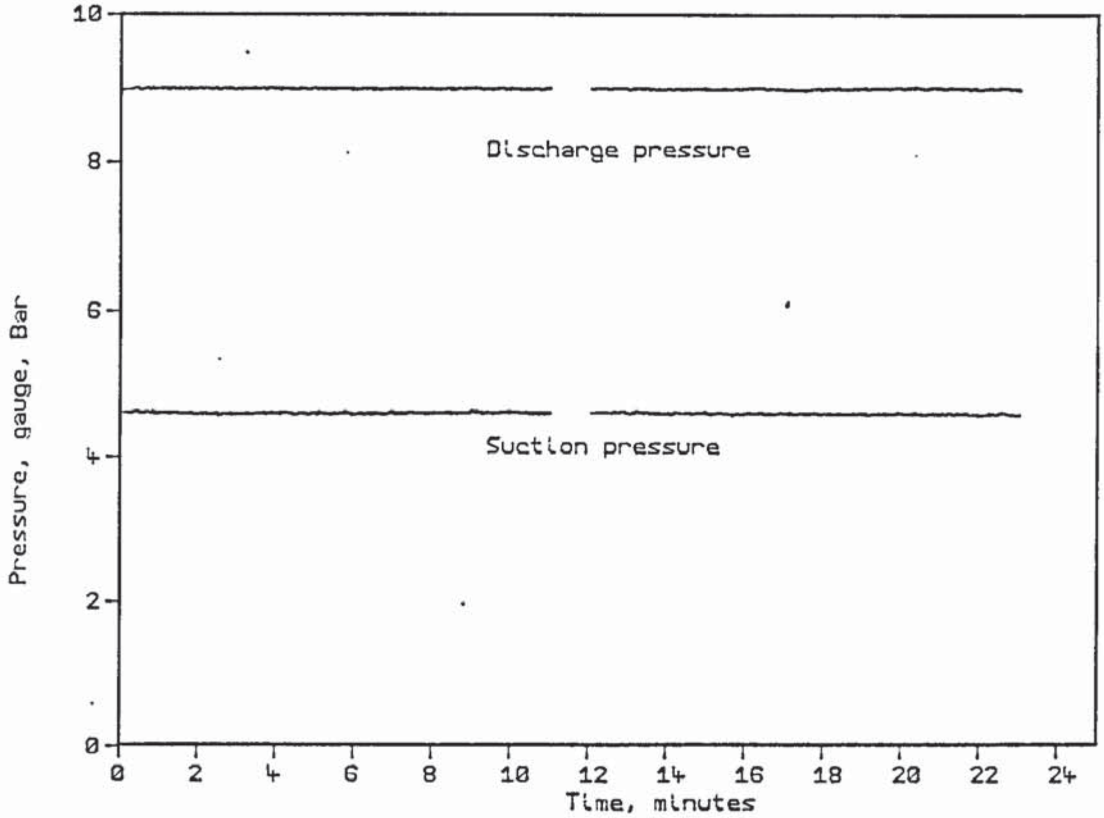

Figure 5.7a Discharge & suction pressure histories of 11/5/85
First time resolved record

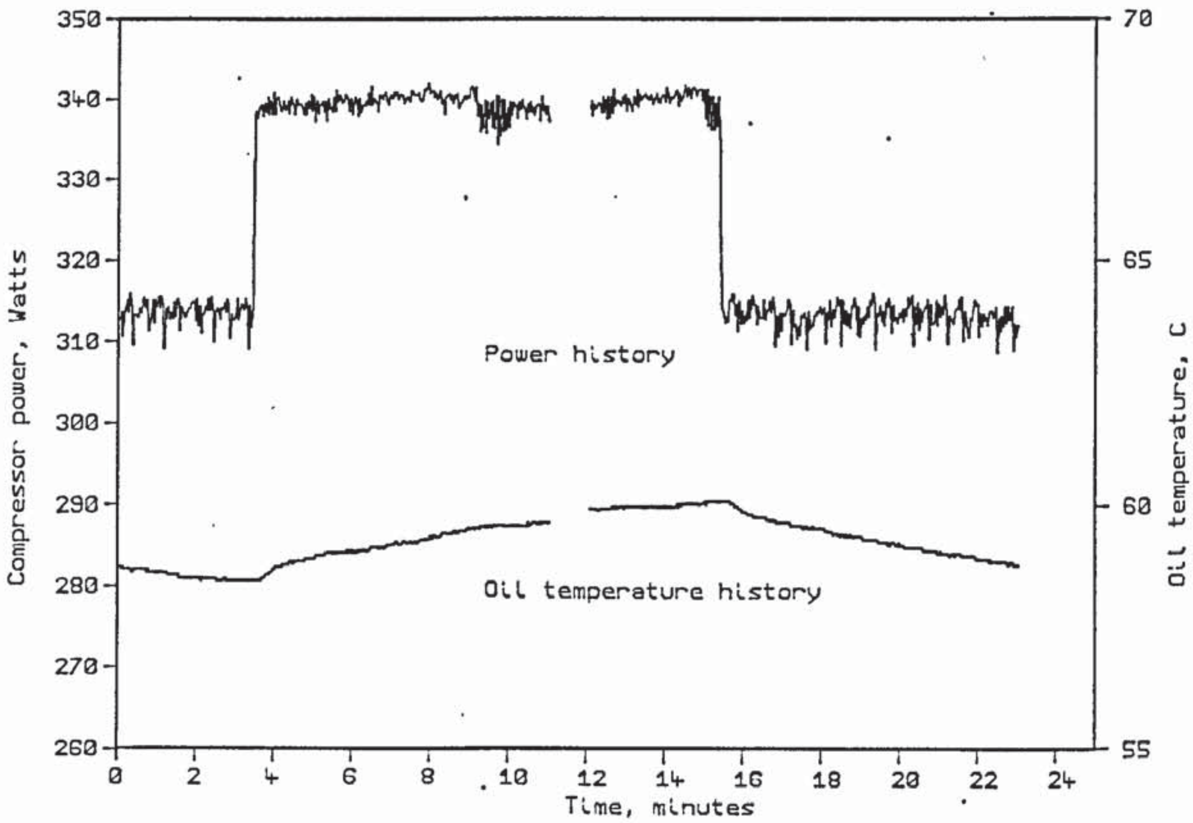

Figure 5.7b Compressor power & oil temperature of 11/5/85
First time resolved record

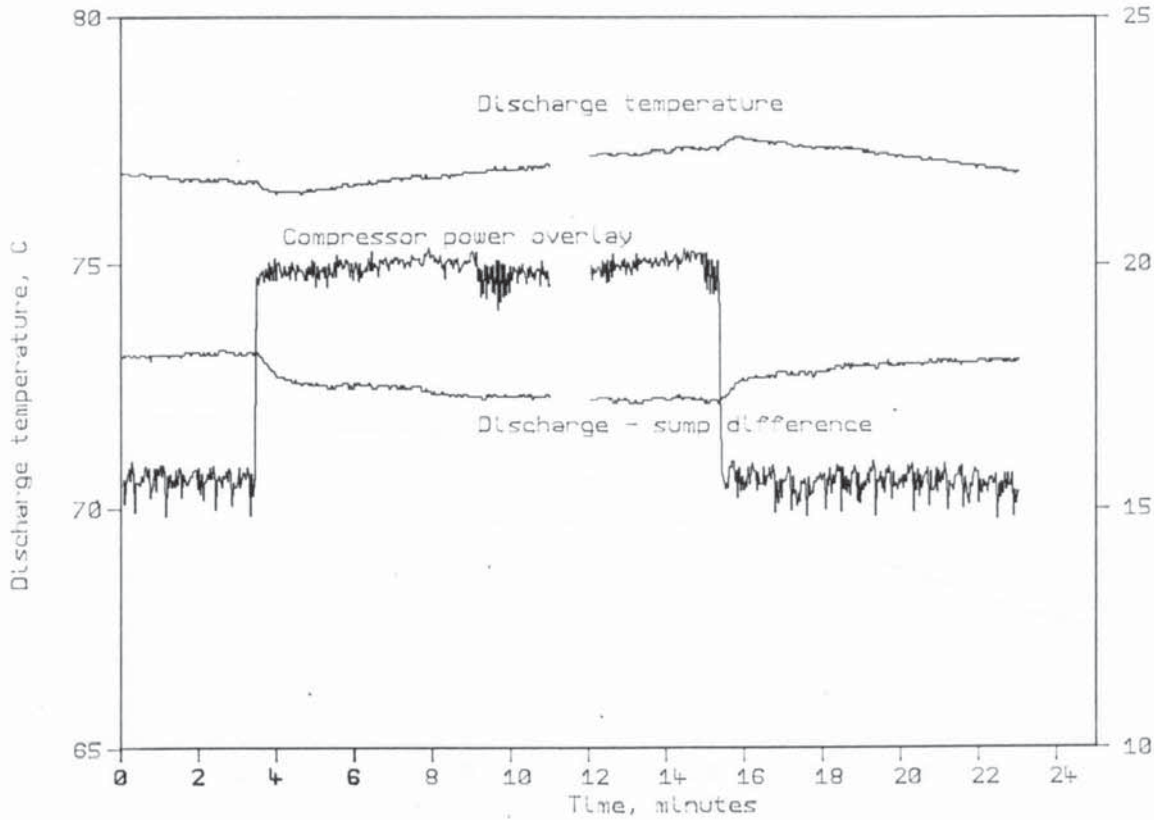

Figure 5.7c Discharge temperature, and discharge - sump oil temperature difference. 11/5/85 time resolved

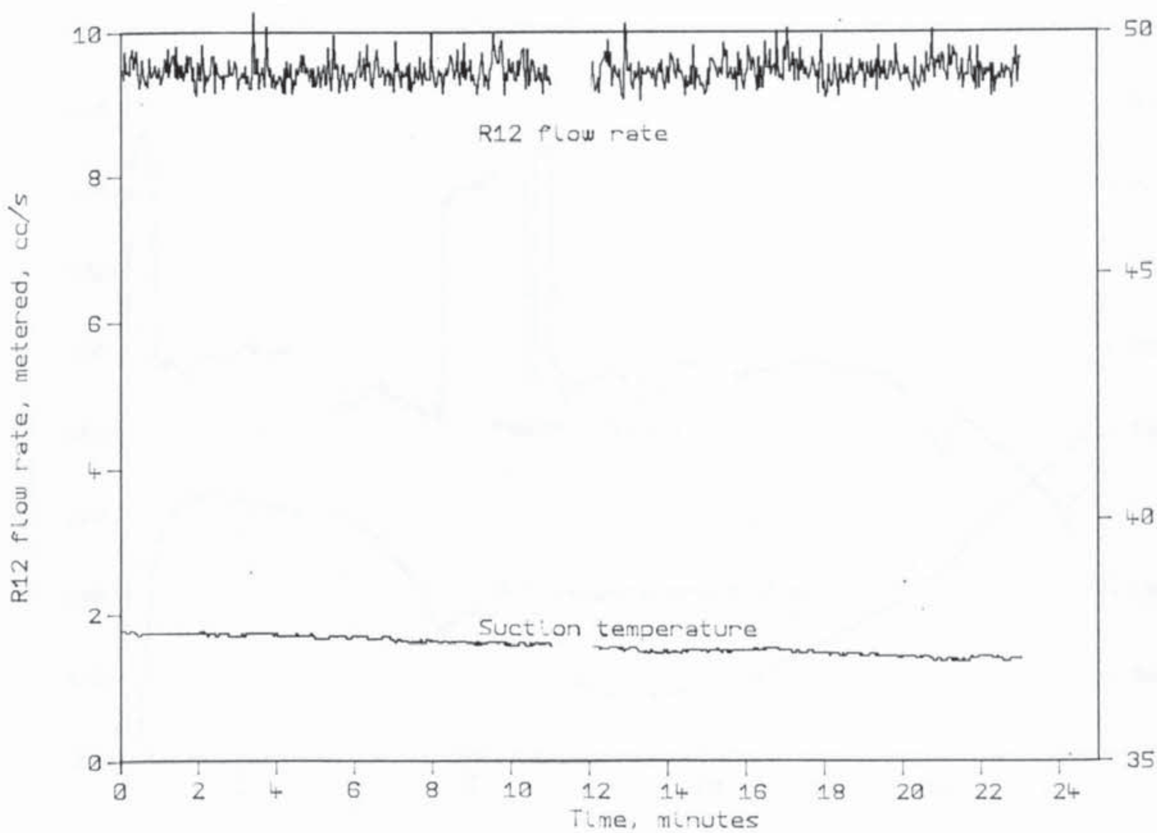

Figure 5.7d Time dependence of the metered R12 flow rate and suction temperature. 11/5/85 time resolved

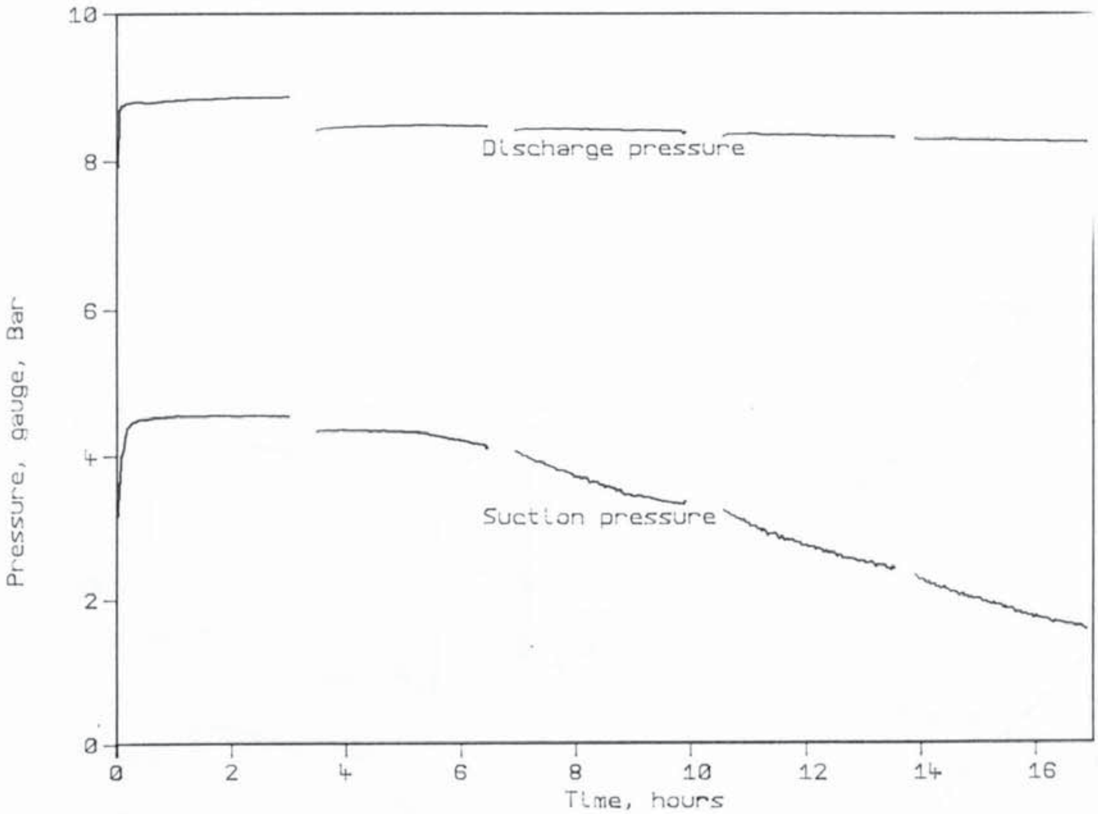

Figure 5.8a Discharge & suction pressure histories of 25/5/85

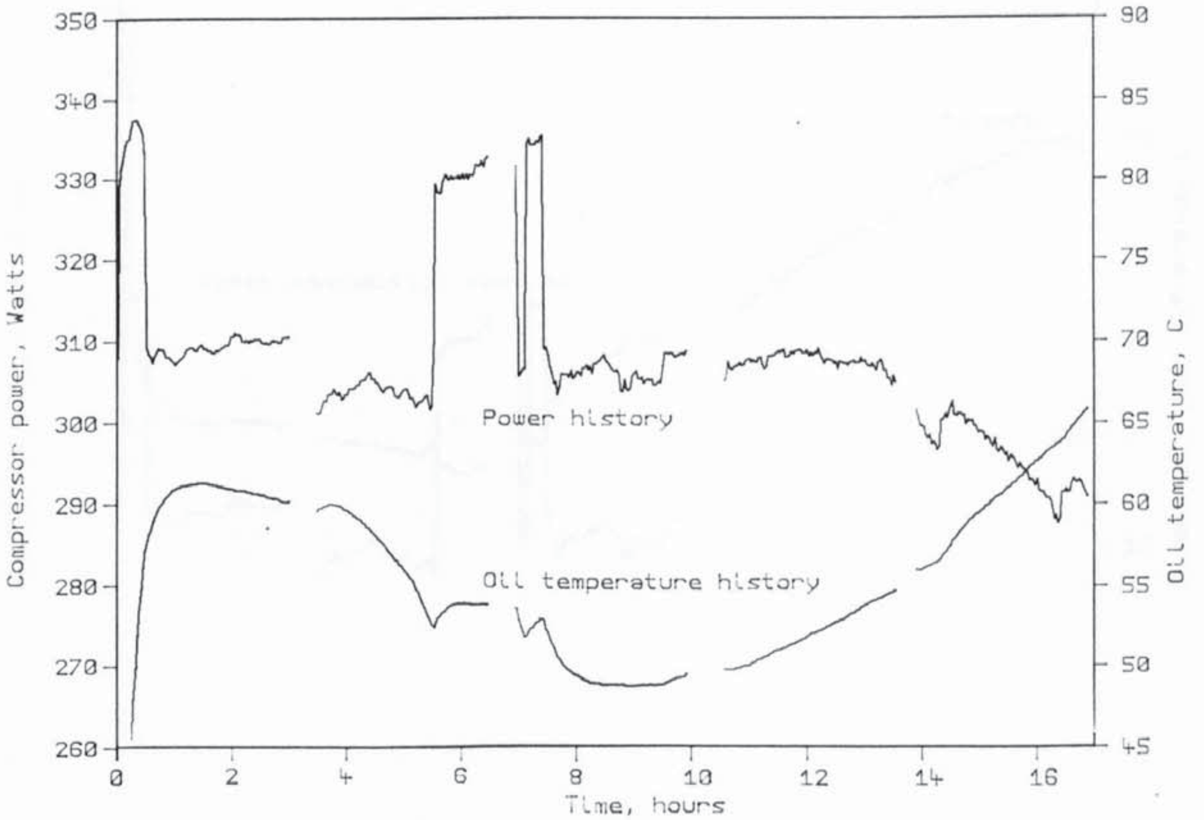

Figure 5.8b Compressor power & oil temperature of 25/5/85

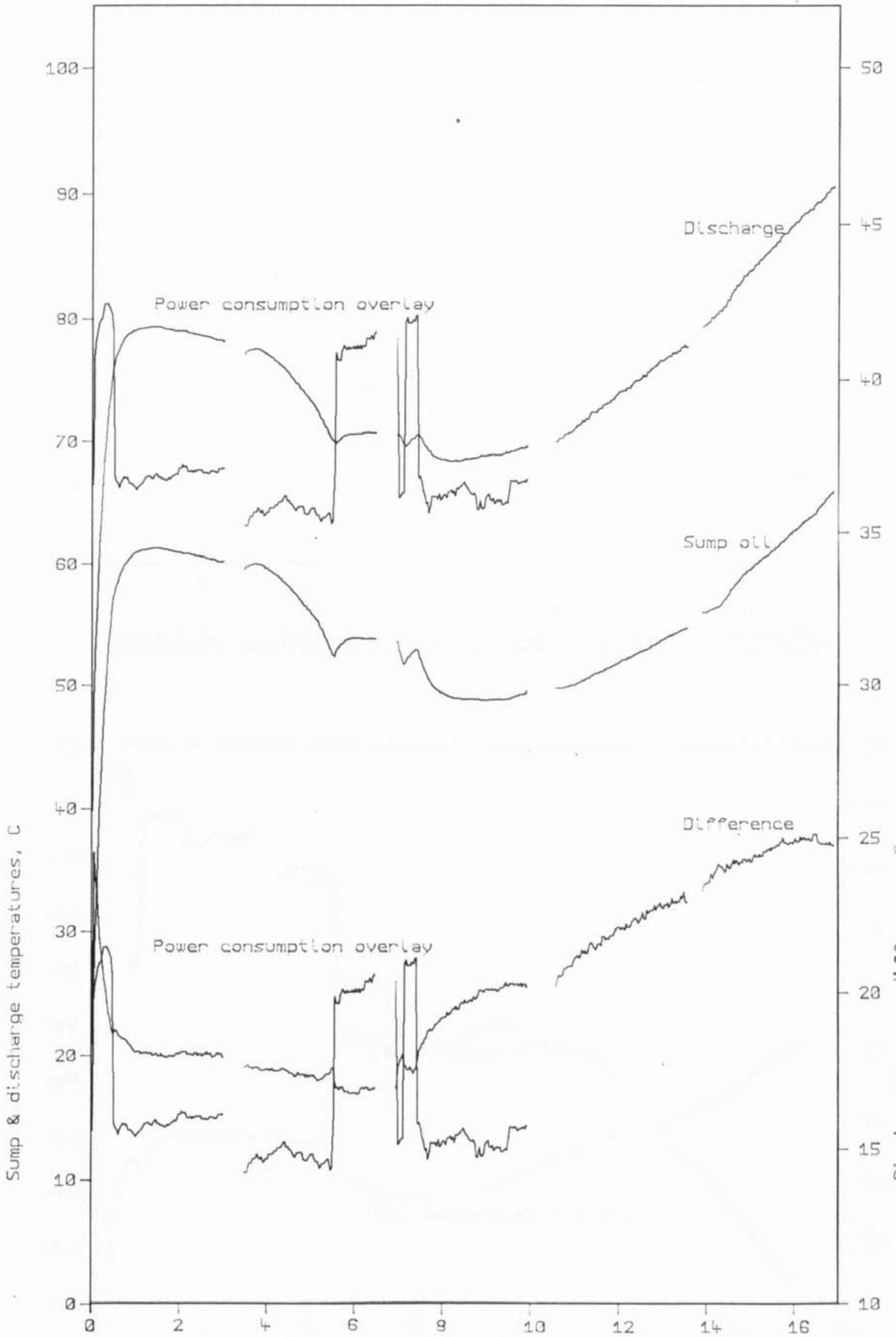

Figure 5.8c Discharge & sump temperature histories of 25/5/85

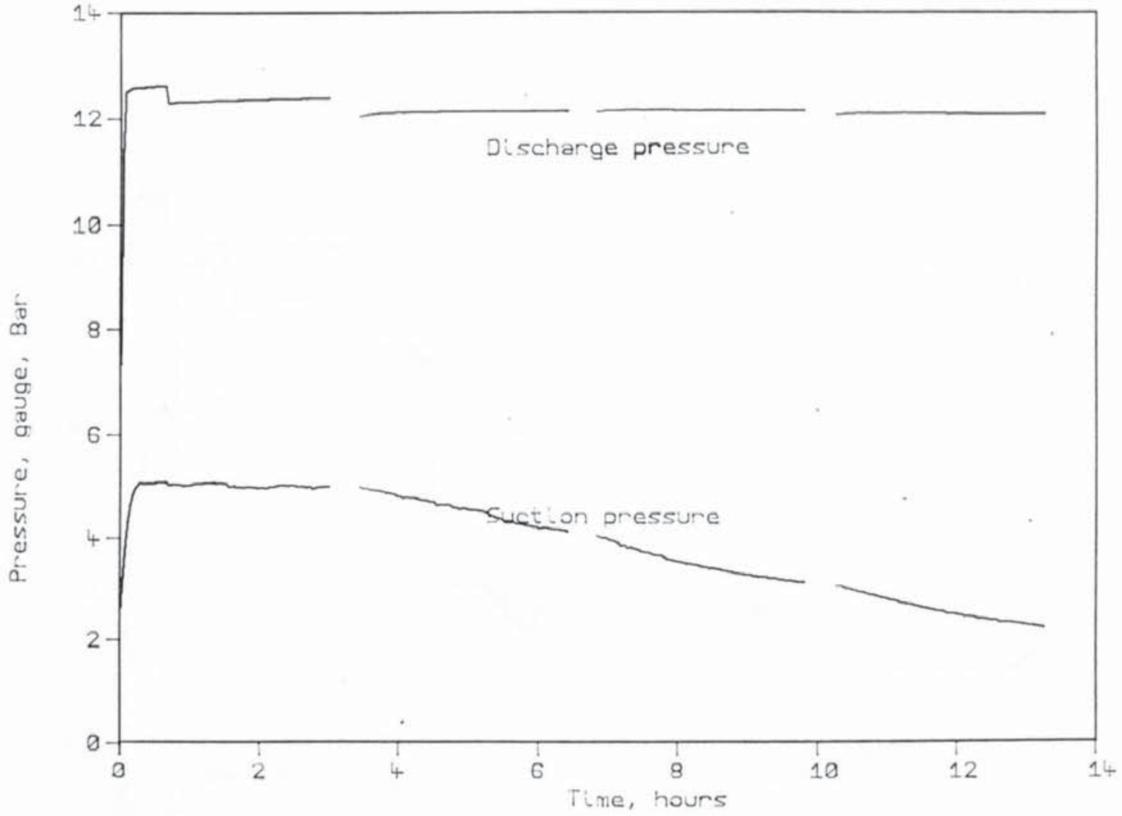

Figure 5.9a Discharge & suction pressure histories of 7/6/85

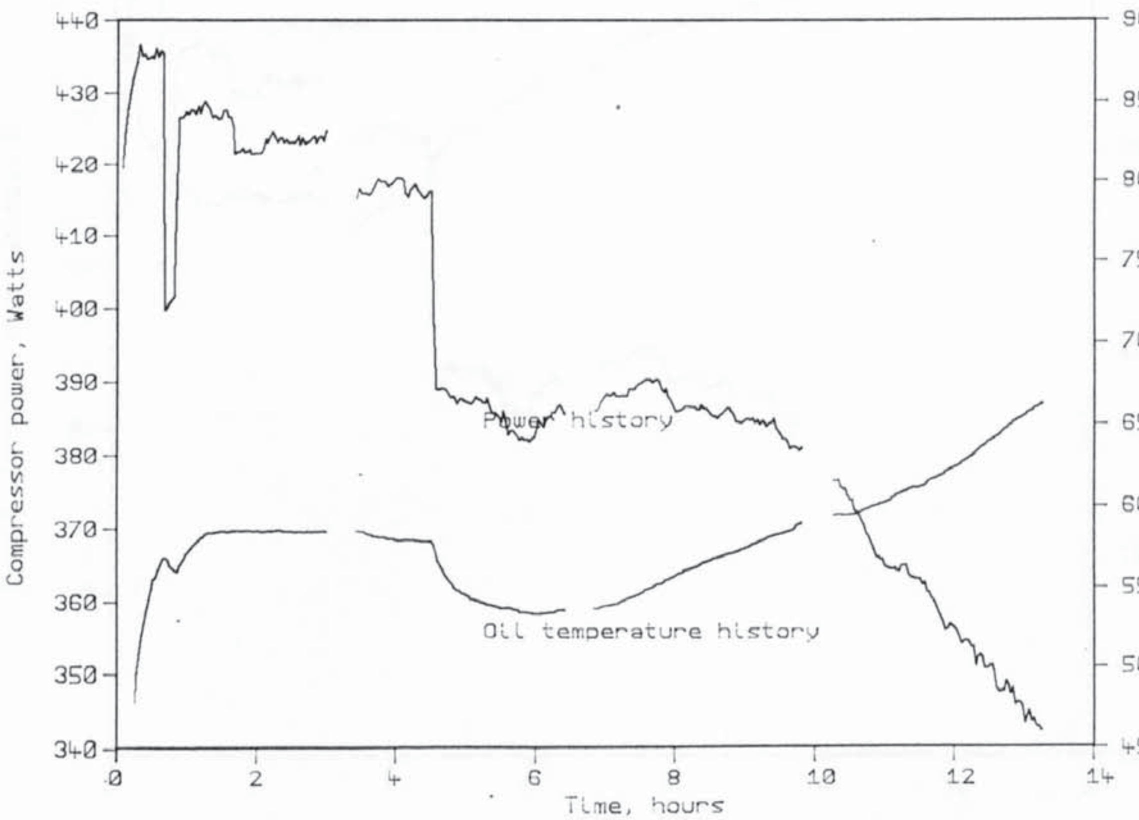

Figure 5.9b Compressor power & oil temperature of 7/6/85

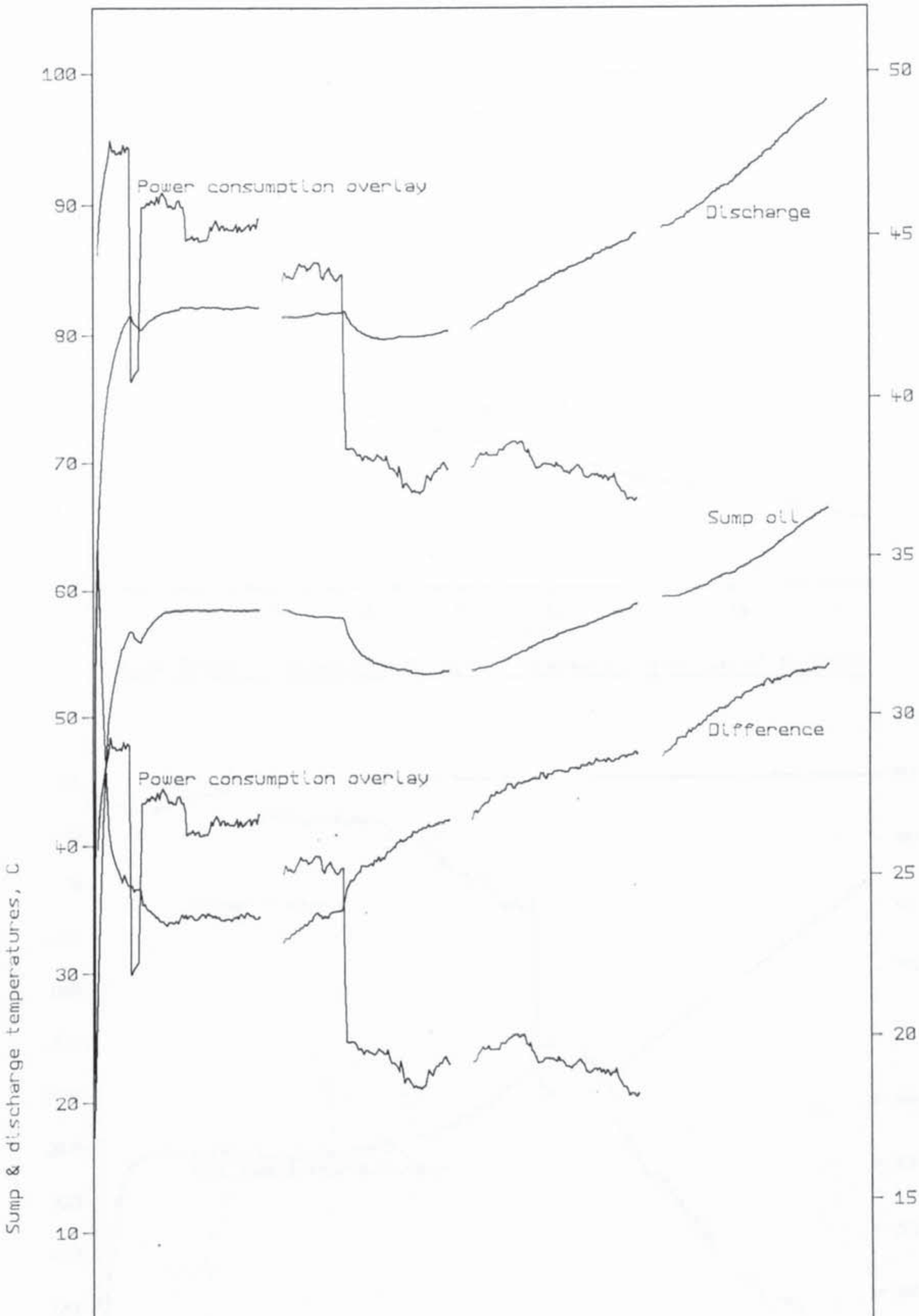

Figure 5.9c Discharge & sump temperature histories of 7/6/85

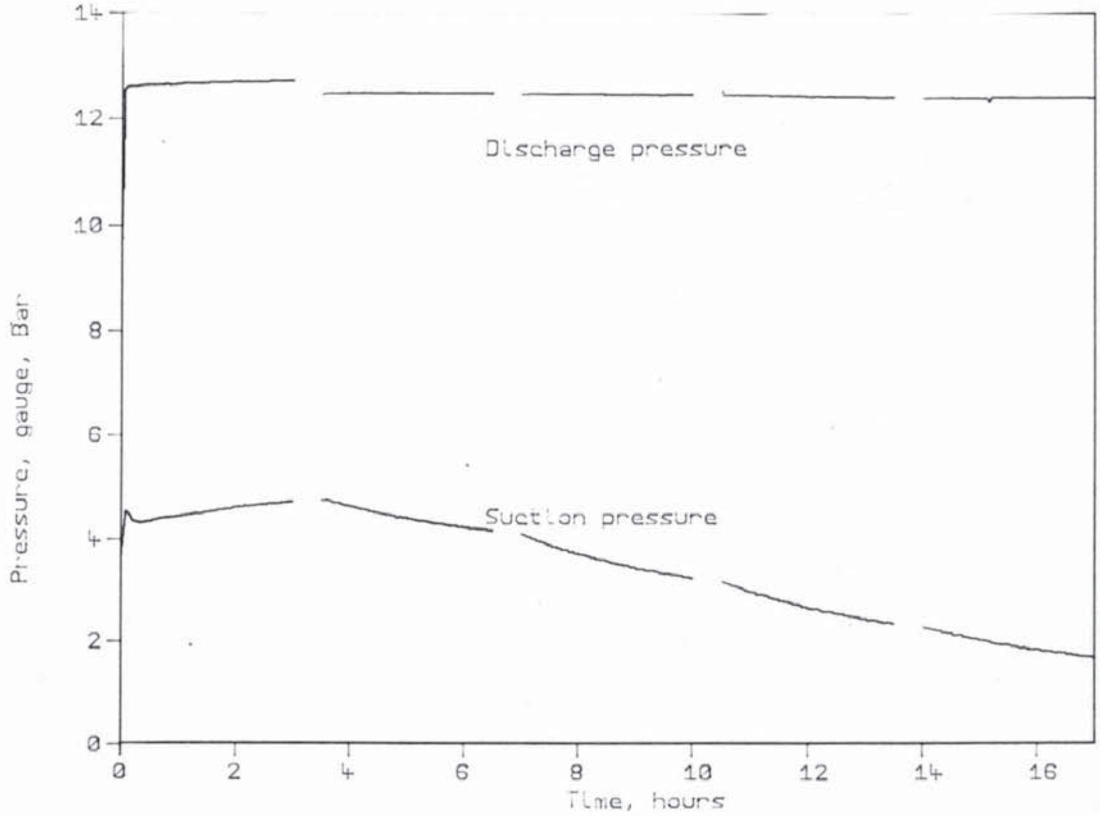

Figure 5.10a Discharge & suction pressure histories of 14/7/85

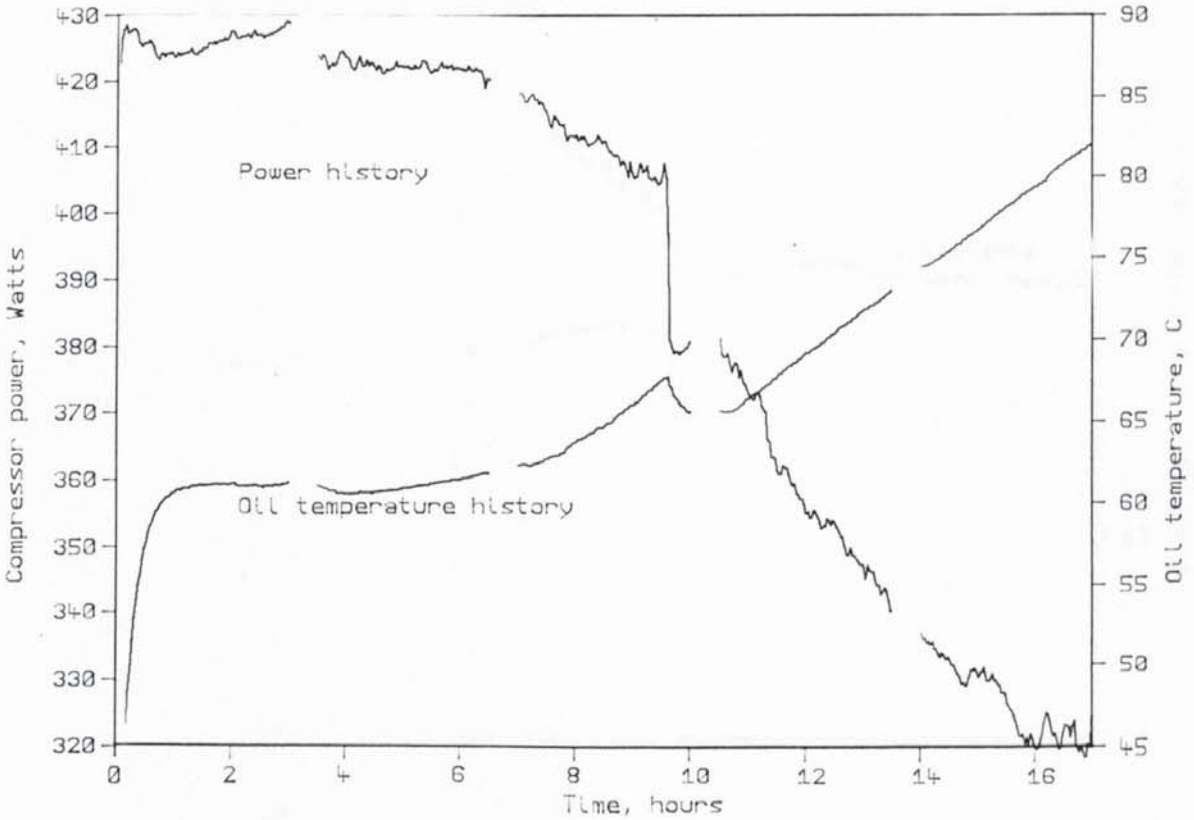

Figure 5.10b Compressor power & oil temperature of 14/7/85

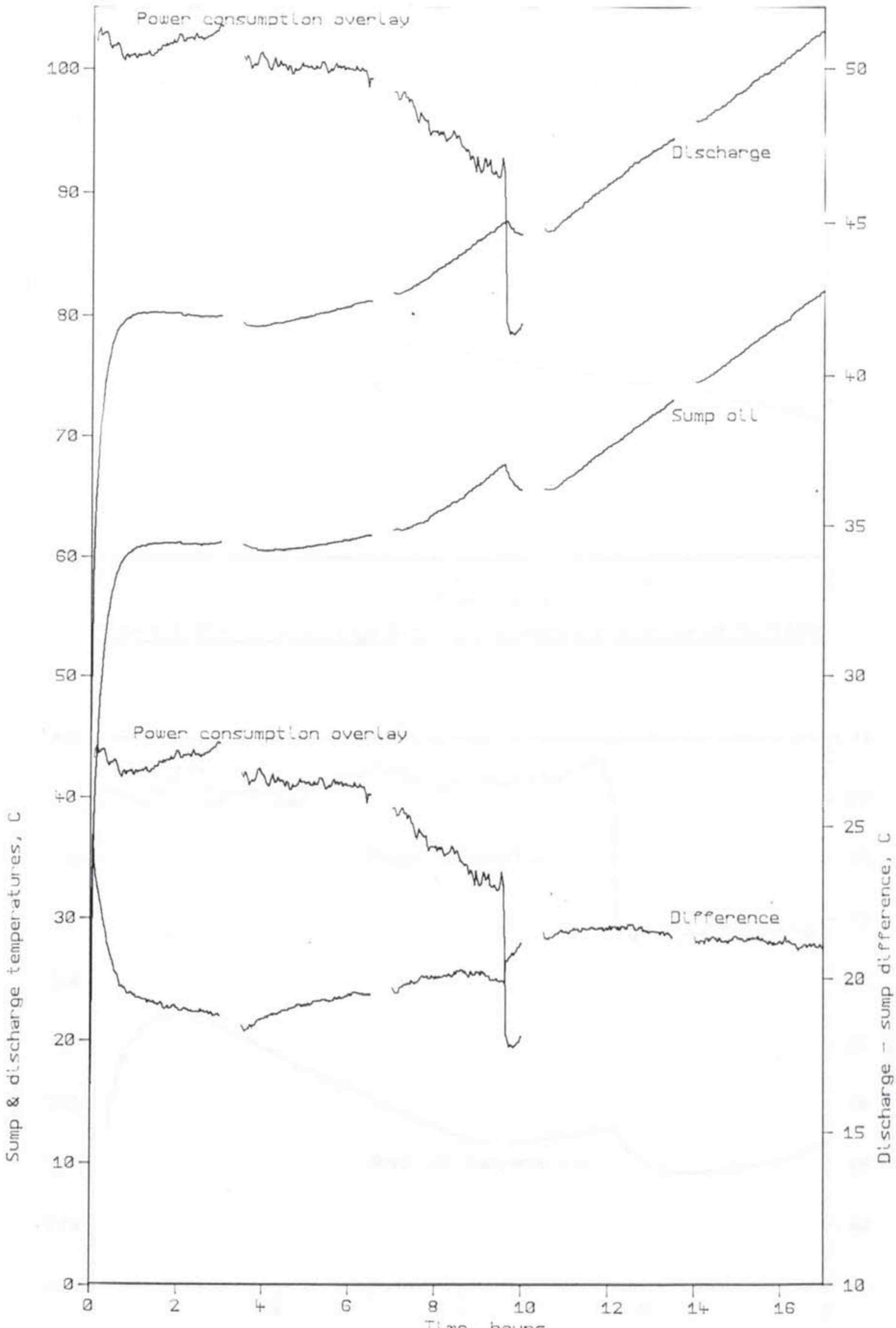

Figure 5.10c Discharge & sump temperature histories of 14/7/85

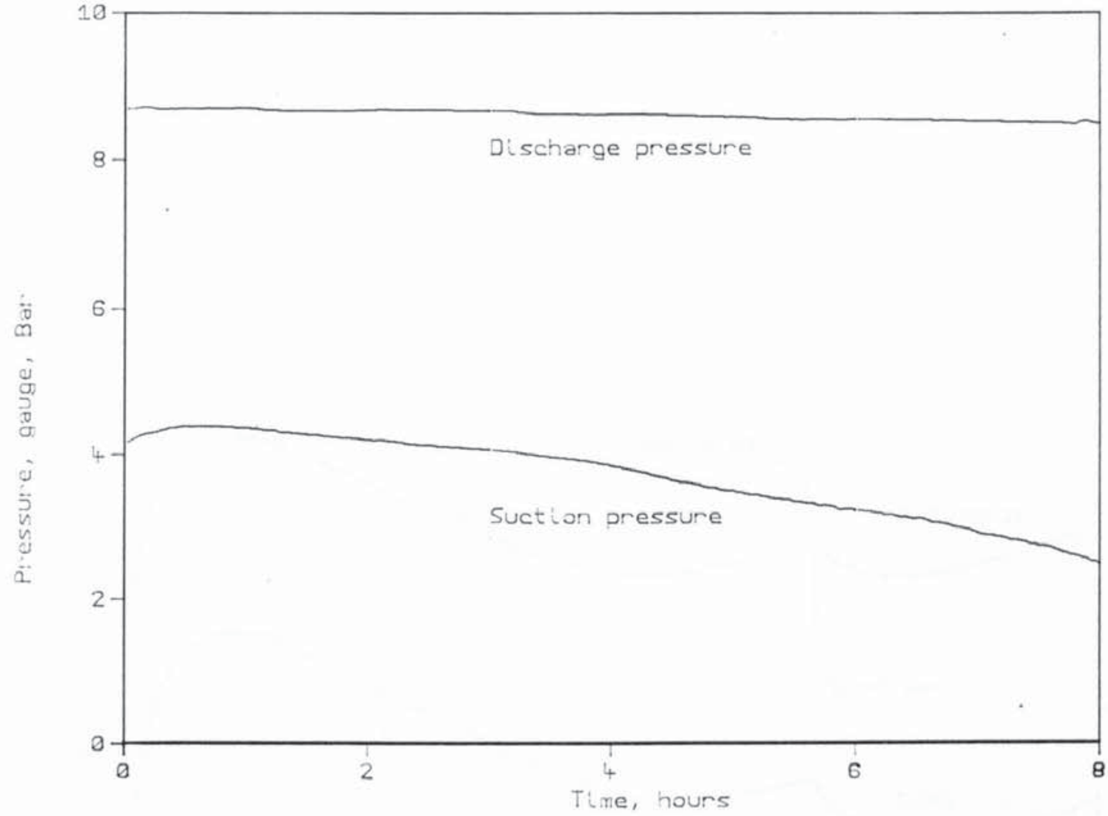

Figure 5.11a Discharge & suction pressure histories of 17/10/85

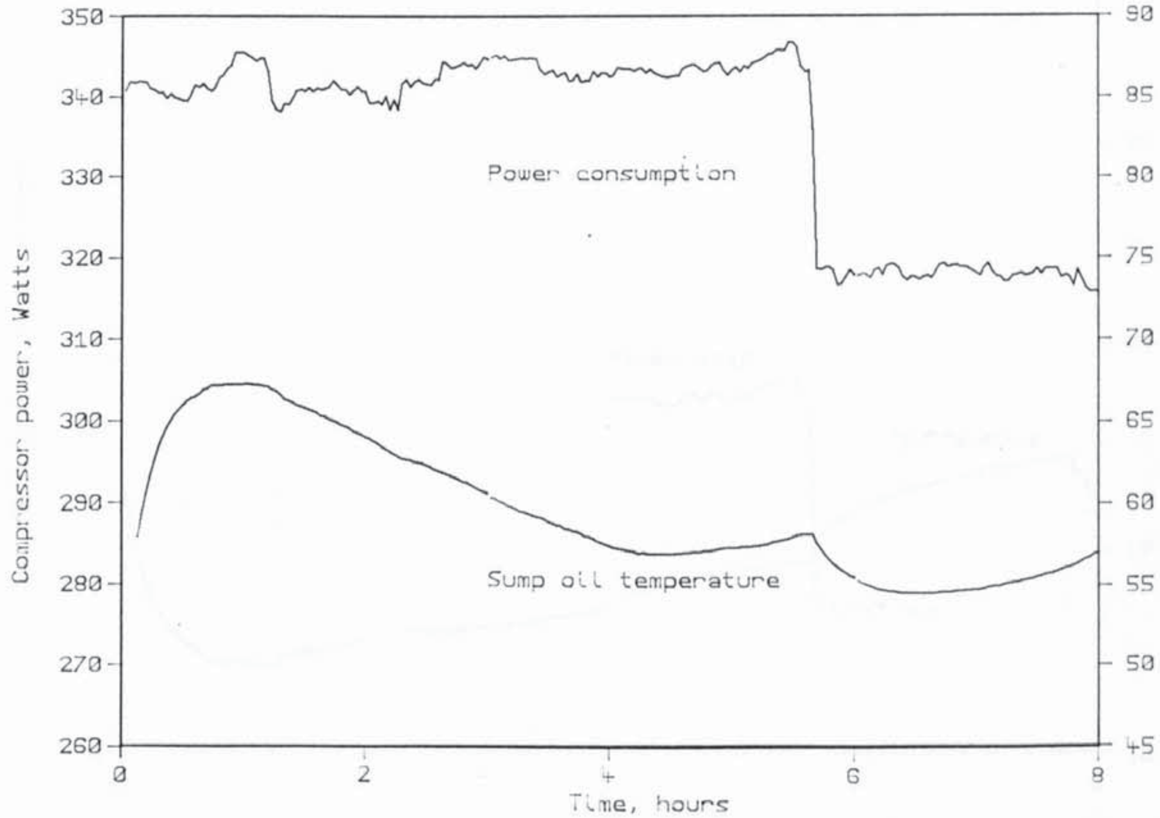

Figure 5.11b Compressor power & oil temperature of 17/10/85

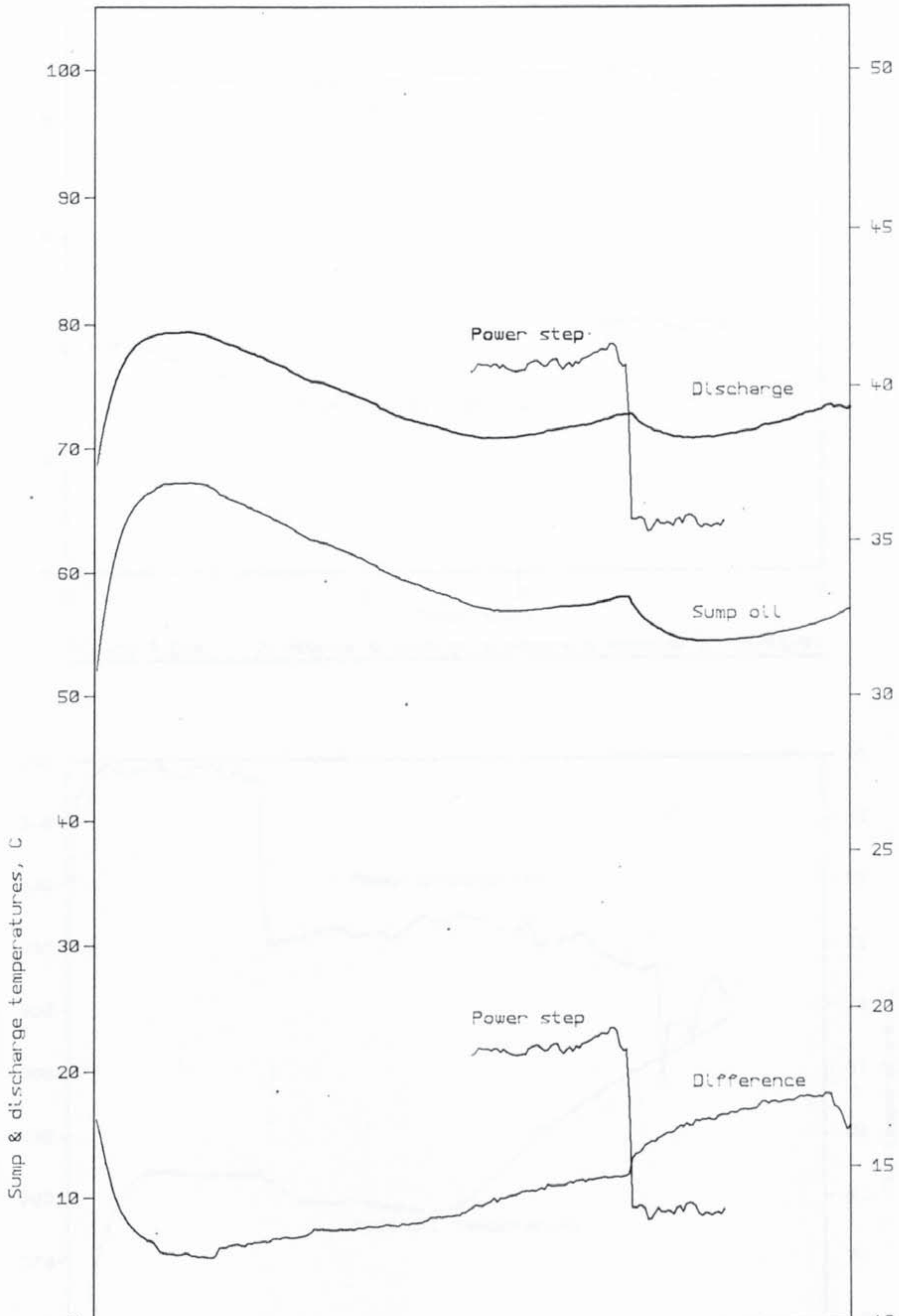

Figure 5.11c Discharge & sump temperature histories of 17/10/85

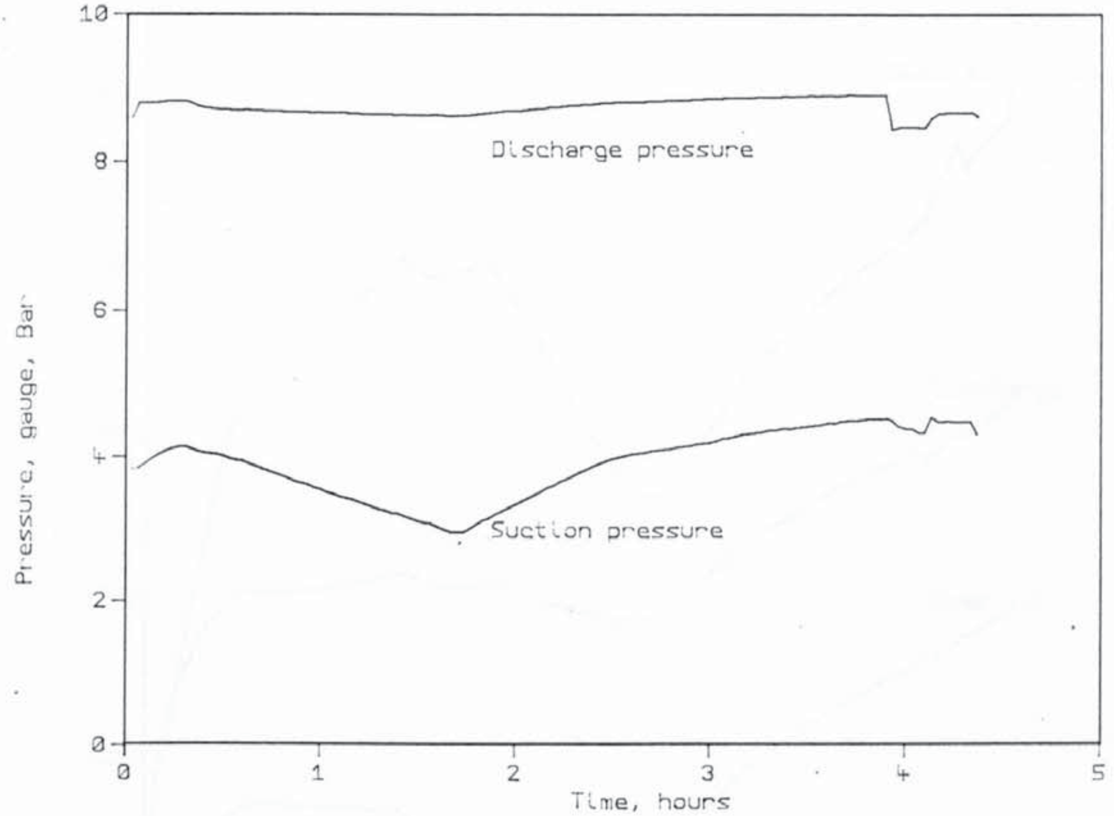

Figure 5.12a Discharge & suction pressure histories of 18/10/85

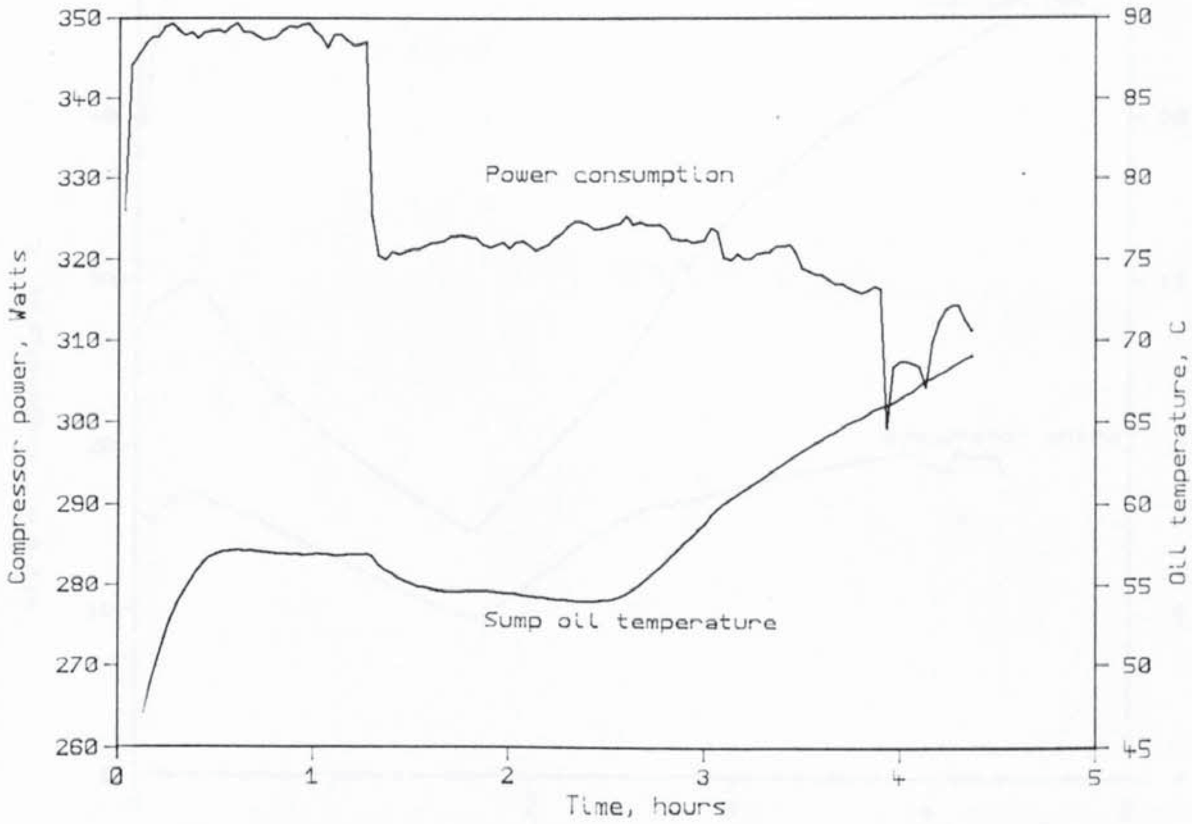

Figure 5.12b Compressor power & oil temperature of 18/10/85

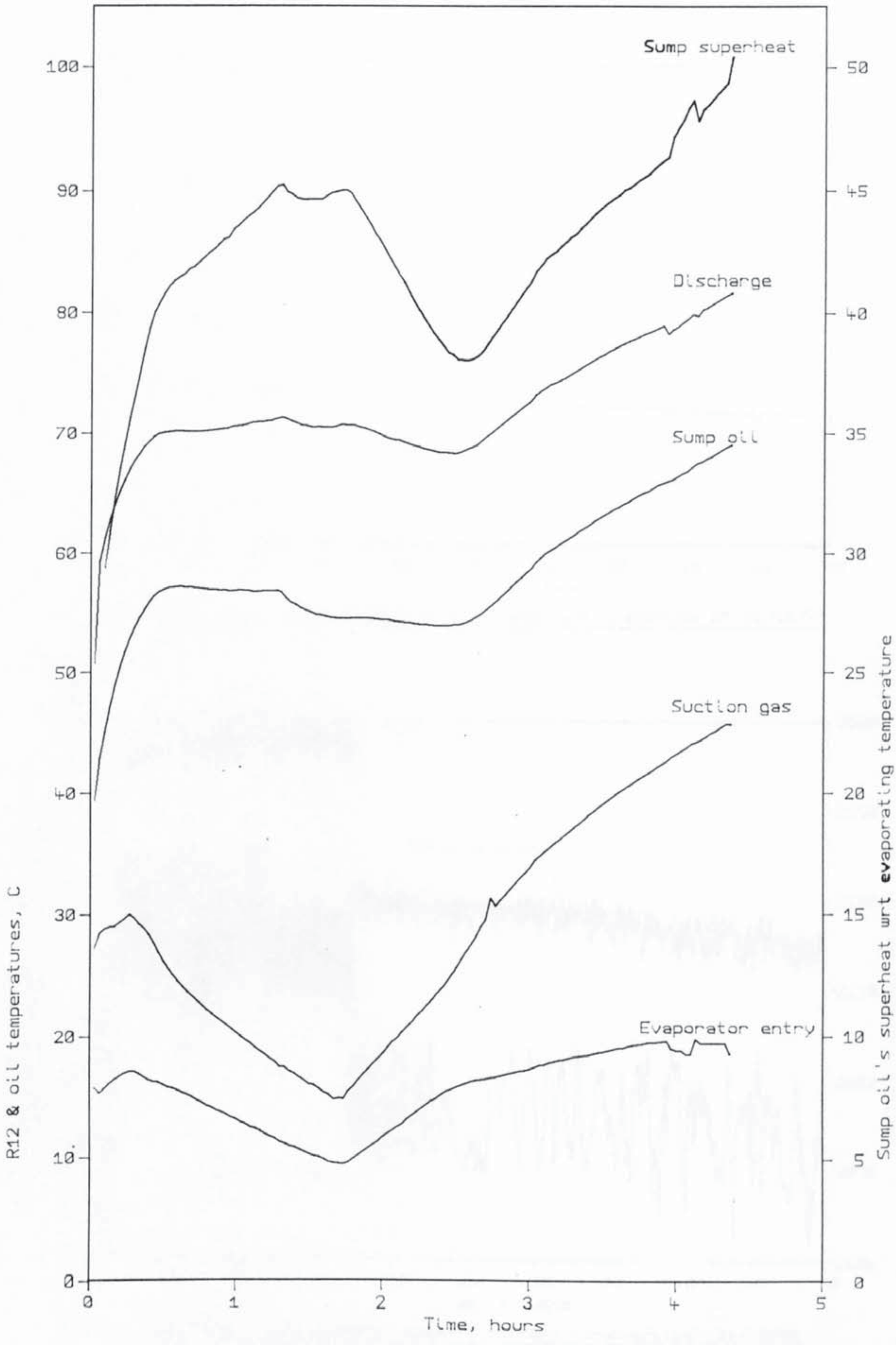

Figure 5.12c R12 & oil temperatures for re-heat trial, 18/10/85

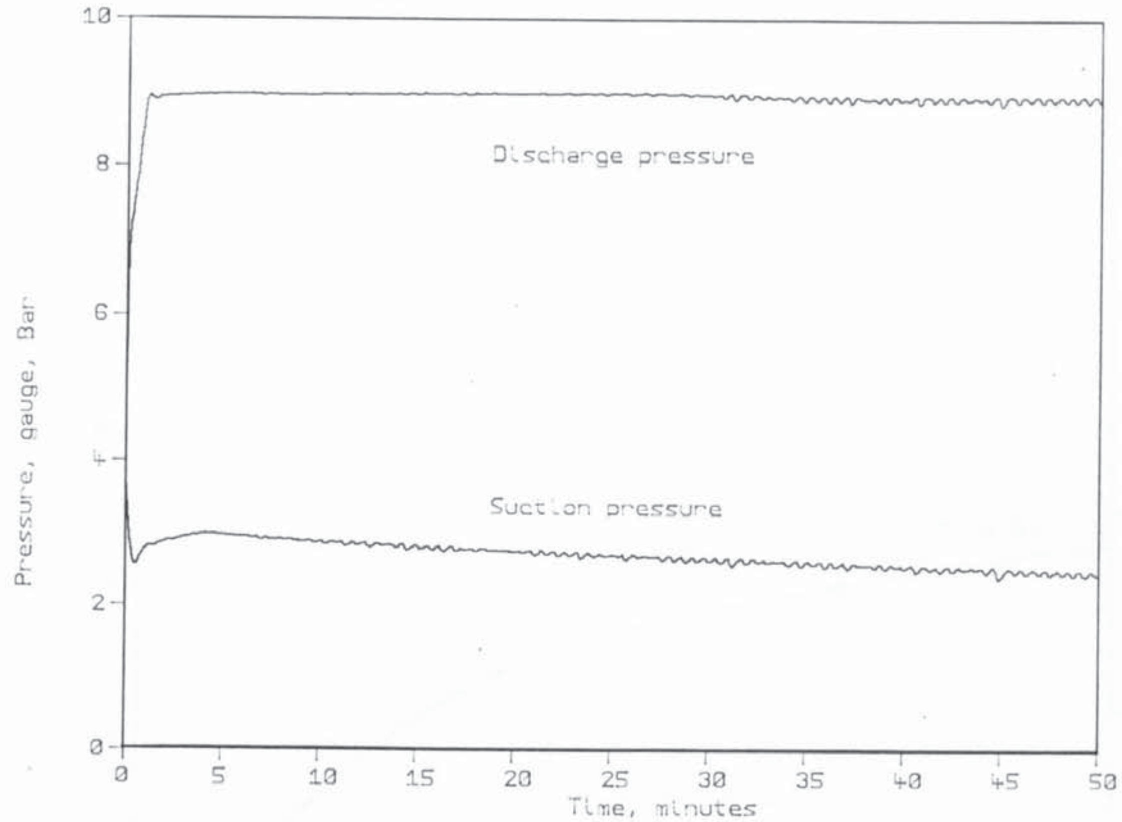

Figure 5.13a Discharge & suction pressure histories of 21/10/85

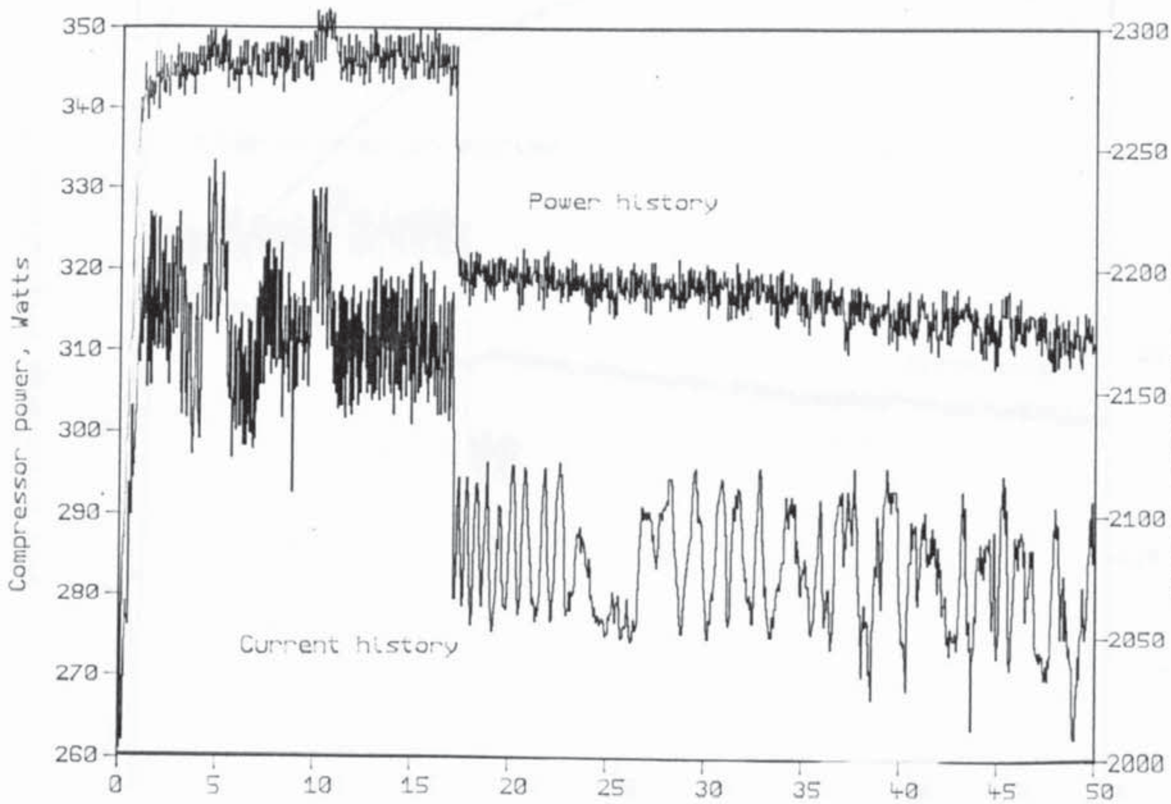

Figure 5.13b Compressor power & current consumption. 21/10/85

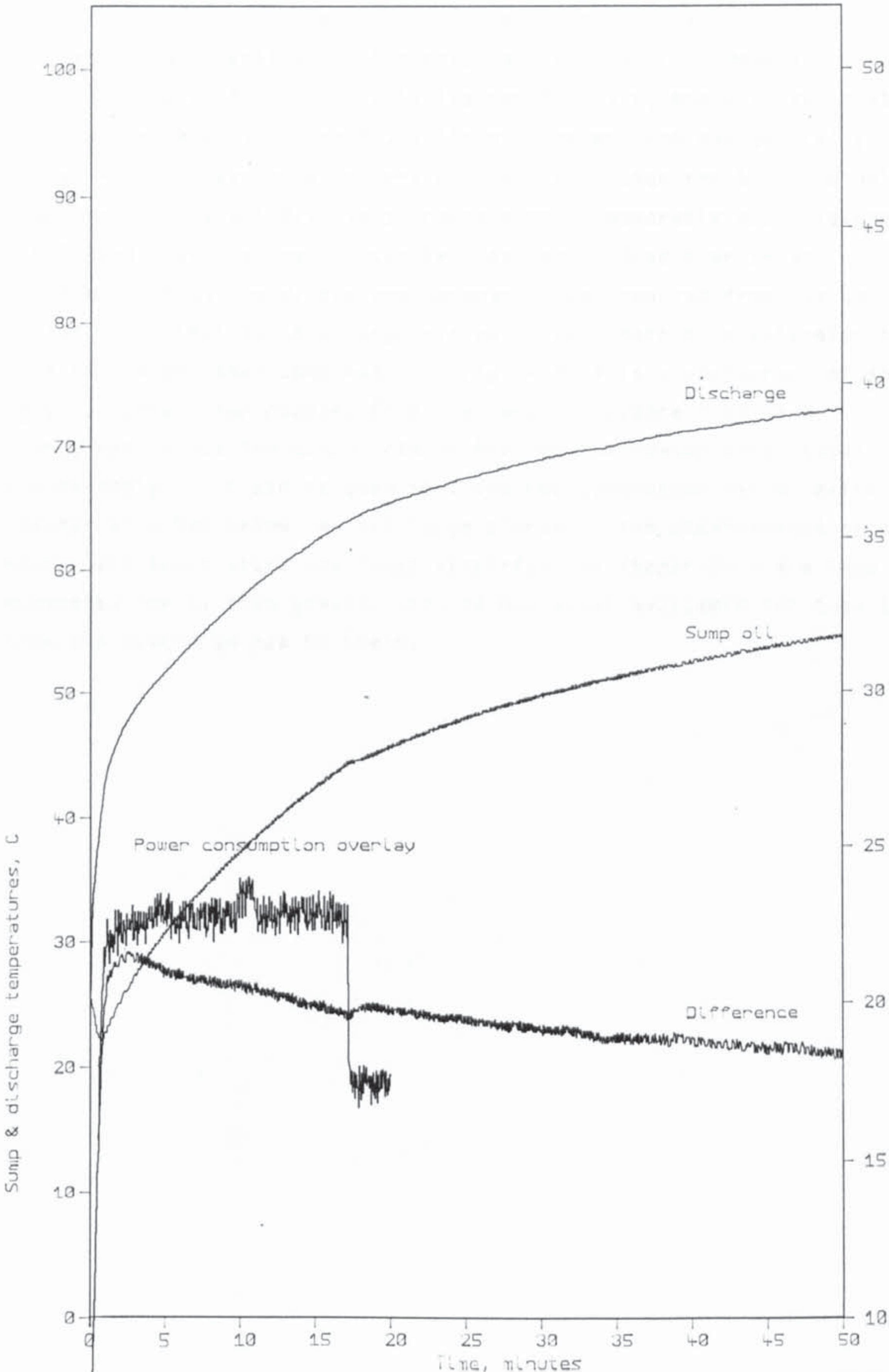

Figure 5.13c Discharge & sump temperature histories of 21/10/85

5.6 Differences between the new compressor and the original compressor

At the time of these trials, it was thought that the new compressor was identical to the original compressor. However, if one compares figures 5.10b & c, with figures 5.9b & c, one will see that for the new compressor, figure 5.10, the oil temperature was generally higher and the discharge temperature was lower than for the original compressor. Figure 5.11 is correspondingly comparable with figures 5.6 & 5.8, and a similar result can be observed. Some time after performing these tests, the new compressor was removed from its can, and it was found that its discharge system is very much more extensive than that of the original compressor. Figure 5.14 is a photograph of the original compressor removed from its can, and figure 5.15 is a photograph of all the components of the new compressor after total dis-assembly. It can be seen that the new compressor has an extra chamber attached below the discharge plenum. The observations of a higher oil temperature and lower discharge gas temperature are thus accounted for by this greater area of hot metal available for heat loss from the discharge gas to the oil.

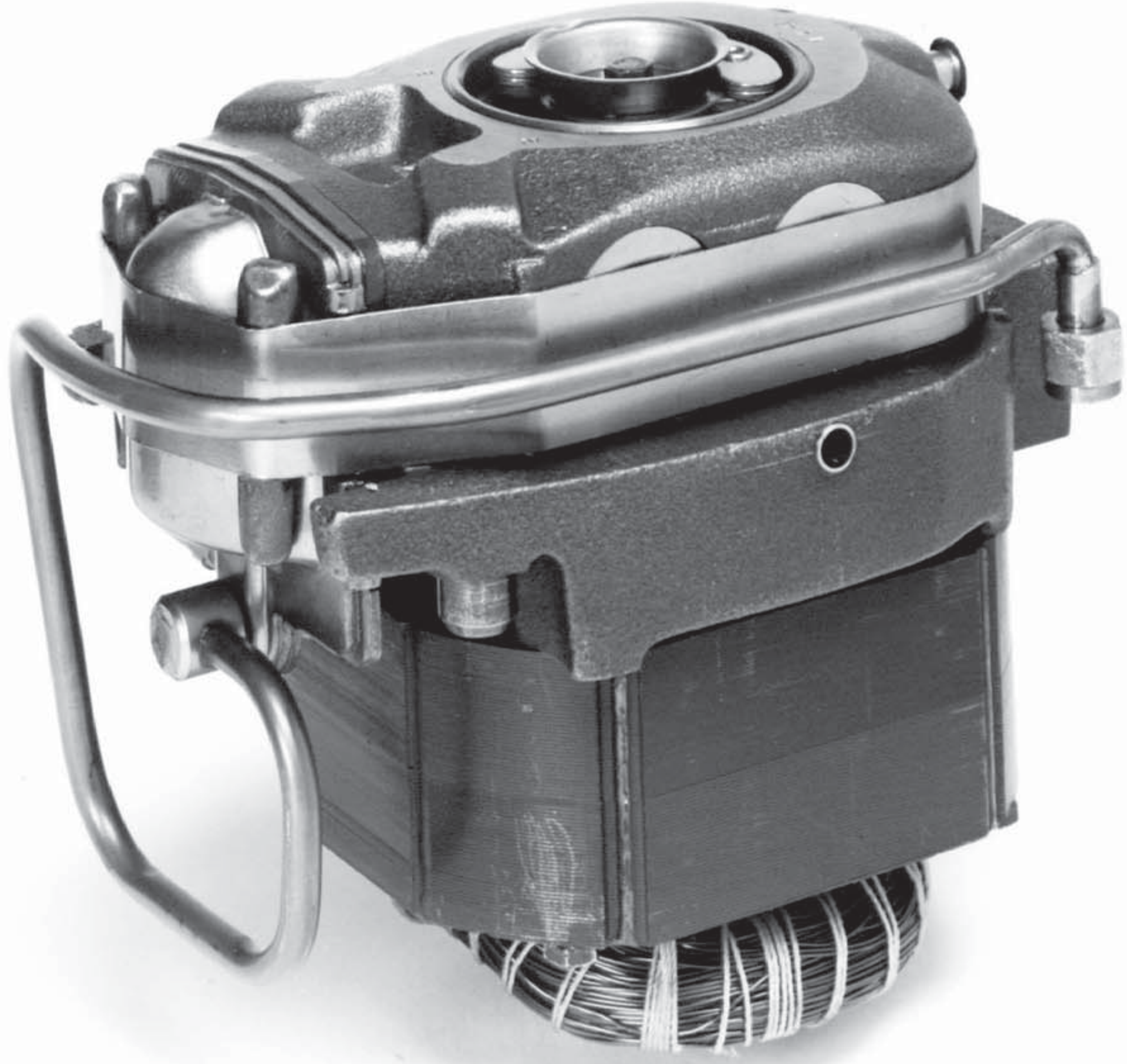

Figure 5.14. Old compressor removed from its can

Figure 5.15. New compressor fully dis-assembled.

Sample data sets from first time-resolved record of 25/5/85

Discharge pressure regulator set to 3.
Nominal evaporator water flow rate = 50cc/s. Variac at 80%.

Index	60.00	61.00	62.00	63.00	64.00	65.00	66.00
Time, seconds	132.62	134.82	137.05	139.25	141.47	143.65	145.87
Performance							
Cond. water in	16.10	16.02	16.10	16.08	16.04	16.10	16.02
water out	40.31	40.28	40.25	40.28	40.25	40.37	40.28
flow rate	20.73	20.76	20.59	20.50	21.02	20.95	20.77
Power	2099.65	2108.99	2080.81	2077.34	2129.86	2127.31	2110.24
Evap. water in	40.26	40.23	40.26	40.23	40.26	40.26	40.18
water out	30.73	30.71	30.73	30.65	30.79	30.67	30.71
flow rate	47.16	47.45	47.50	47.45	47.40	47.45	47.45
Power	1880.68	1892.21	1894.01	1904.28	1878.14	1904.18	1880.40
Compressor power	315.17	314.69	315.33	314.85	311.17	315.17	313.73
R12 metered rate	9.56	9.45	9.60	9.53	9.63	9.40	9.34
R12 Temperatures							
Sump Oil	59.98	59.95	59.98	59.95	59.98	59.98	59.95
Discharge	78.12	78.15	78.18	78.10	78.12	78.12	78.15
Condenser Start	78.59	78.57	78.59	78.57	78.59	78.59	78.57
Mid Condenser	28.74	28.72	28.74	28.72	28.74	28.80	28.78
Condenser End	17.36	17.33	17.42	17.33	17.36	17.36	17.40
Evaporator Start	20.63	20.54	20.69	20.60	20.69	20.63	20.60
Evaporator End	37.60	37.58	37.60	37.52	37.54	37.54	37.52
Suction	38.57	38.55	38.57	38.55	38.57	38.51	38.55
Pressures, gauge, Bar							
Discharge	8.98	8.99	8.98	9.00	9.01	9.00	9.00
Cond. End	5.89	5.89	5.89	5.89	5.90	5.89	5.89
Evap. Start	4.71	4.70	4.72	4.72	4.73	4.72	4.71
Suction	4.59	4.58	4.60	4.60	4.62	4.60	4.60
Calculated results							
C.O.P.	6.66	6.70	6.60	6.60	6.85	6.75	6.73
Tbdc	53.74	53.72	53.88	53.73	53.81	53.78	53.76
Apparent R12mdot	11.70	11.75	11.59	11.57	11.87	11.85	11.76
Ideal R12 mdot	12.98	12.97	13.01	13.01	13.06	13.02	13.01
R12 flow ratio	0.90	0.91	0.89	0.89	0.91	0.91	0.90
Minimum work	141.46	142.43	139.76	139.83	142.98	143.05	142.26
Comp. efficiency	0.45	0.45	0.44	0.44	0.46	0.45	0.45

Table 5.2

Sample data sets from last time-resolved record of 25/5/85

Discharge pressure regulator set to 3.
Nominal evaporator water flow rate = 50cc/s.   Immersion heater off.

Index	60.00	61.00	62.00	63.00	64.00	65.00	66.00
Time, seconds	134.28	136.48	138.72	140.97	143.20	145.43	147.67
Performance							
Cond. water in	18.49	18.49	18.49	18.49	18.49	18.49	18.43
water out	43.28	43.22	43.22	43.22	43.22	43.22	43.22
flow rate	8.04	8.25	8.28	7.92	7.99	8.04	8.12
Power	834.48	854.13	856.67	819.76	827.40	832.49	842.26
Evap. water in	3.96	3.96	3.96	3.96	3.90	3.96	3.96
water out	0.83	0.83	0.83	0.76	0.76	0.83	0.76
flow rate	42.75	42.65	42.50	42.67	43.06	42.84	42.89
Power	560.53	559.27	557.37	571.24	564.71	561.80	574.15
Compressor power	286.57	287.37	286.57	287.37	288.17	287.21	288.49
R12 metered rate	3.83	3.66	3.86	3.96	3.89	3.92	3.82
R12 Temperatures							
Sump Oil	67.03	67.03	67.03	67.03	67.03	67.03	67.03
Discharge	91.60	91.60	91.60	91.60	91.60	91.60	91.60
Condenser Start	92.28	92.28	92.28	92.28	92.28	92.28	92.28
Mid Condenser	35.55	35.55	35.55	35.55	35.49	35.49	35.55
Condenser End	19.68	19.68	19.80	19.74	19.74	19.68	19.68
Evaporator Start	-2.70	-2.63	-2.63	-2.56	-2.63	-2.63	-2.56
Evaporator End	2.17	2.11	2.04	2.04	2.04	1.98	1.91
Suction	6.16	6.16	6.16	6.16	6.10	6.16	6.16
Pressures, gauge, Bar							
Discharge	8.04	8.05	8.05	8.05	8.05	8.04	8.05
Cond. End	7.50	7.50	7.51	7.50	7.50	7.50	7.50
Evap. Start	1.67	1.69	1.68	1.68	1.68	1.68	1.68
Suction	1.58	1.59	1.59	1.58	1.58	1.58	1.59
Calculated results							
C.O.P.	2.91	2.97	2.99	2.85	2.87	2.90	2.92
Tbdc	41.51	41.68	41.61	41.52	41.52	41.54	41.63
Apparent R12mdot	4.43	4.54	4.55	4.35	4.40	4.42	4.47
Ideal R12 mdot	5.54	5.57	5.56	5.54	5.54	5.54	5.56
R12 flow ratio	0.80	0.81	0.82	0.79	0.79	0.80	0.80
Minimum work	120.64	123.04	123.66	118.51	119.61	120.27	121.47
Comp. efficiency	0.42	0.43	0.43	0.41	0.42	0.42	0.42

Table 5.3

Sample data sets from first time-resolved record of 27/5/85

Discharge pressure regulator set to 3.
Nominal evaporator water flow rate = 20cc/s. Variac at 80%.

Index	60.00	61.00	62.00	63.00	64.00	65.00	66.00
Time, seconds	132.13	134.33	136.55	138.75	140.93	143.13	145.33
Performance							
Cond. water in	16.75	16.68	16.75	16.71	16.68	16.75	16.71
water out	40.08	40.08	40.08	40.05	40.08	40.08	40.11
flow rate	18.94	19.42	19.23	19.21	19.46	19.21	19.42
Power	1850.09	1902.06	1877.72	1876.68	1905.67	1876.52	1901.95
Evap. water in	43.06	43.06	43.06	43.08	43.06	43.06	43.08
water out	23.88	23.94	23.94	23.97	23.94	23.94	23.91
flow rate	20.49	21.17	20.31	20.69	20.77	20.41	21.04
Power	1644.61	1693.70	1625.20	1655.34	1661.48	1633.26	1688.98
Compressor power	308.14	307.50	308.14	302.87	307.18	305.74	306.70
R12 metered rate	8.87	8.68	8.85	8.73	8.72	8.96	8.76
R12 Temperatures							
Sump Oil	55.47	55.47	55.47	55.50	55.47	55.53	55.50
Discharge	74.40	74.40	74.40	74.48	74.40	74.40	74.42
Condenser Start	74.98	74.93	74.98	74.95	74.98	74.98	75.00
Mid Condenser	28.63	28.63	28.57	28.59	28.57	28.57	28.59
Condenser End	20.76	20.76	20.76	20.84	20.88	20.88	20.84
Evaporator Start	16.97	16.97	17.10	17.12	17.16	17.10	17.12
Evaporator End	31.52	31.70	31.46	31.54	31.33	31.27	31.23
Suction	32.06	32.12	32.19	32.21	32.19	32.19	32.21
Pressures, gauge Bar							
Discharge	8.74	8.74	8.77	8.77	8.78	8.78	8.79
Cond. End	5.66	5.66	5.66	5.65	5.64	5.64	5.64
Evap. Start	4.22	4.23	4.27	4.26	4.28	4.27	4.28
Suction	4.12	4.12	4.16	4.16	4.18	4.17	4.18
Calculated results							
C.O.P.	6.00	6.19	6.09	6.20	6.20	6.14	6.20
Tbdc	47.62	47.66	47.83	47.84	47.90	47.81	47.88
Apparent R12mdot	10.64	10.94	10.80	10.80	10.97	10.80	10.95
Ideal R12 mdot	12.04	12.06	12.15	12.14	12.19	12.17	12.19
R12 flow ratio	0.88	0.91	0.89	0.89	0.90	0.89	0.90
Minimum work	140.64	144.39	141.47	141.91	143.23	141.57	143.14
Comp. efficiency	0.46	0.47	0.46	0.47	0.47	0.46	0.47

Table 5.4

Sample data sets from last time-resolved record of 27/5/85

Discharge pressure regulator set to 3.
Nominal evaporator water flow rate = 20cc/s.   Immersion heater off.

Index	60.00	61.00	62.00	63.00	64.00	65.00	66.00
Time mins	133.68	135.92	138.15	140.38	142.60	144.83	147.05

Performance

Cond. water in	18.80	18.80	18.80	18.80	18.80	18.80	18.80
water out	44.58	44.69	44.75	44.87	44.93	45.11	45.17
flow rate	7.81	9.09	7.50	7.49	7.10	7.31	7.45
Power	842.49	984.96	814.88	817.24	776.05	804.32	822.41
Evap. water in	8.86	8.80	8.80	8.80	8.80	8.80	8.80
water out	1.15	1.15	1.15	1.22	1.15	1.15	1.09
flow rate	18.27	18.29	18.80	18.17	18.07	17.99	18.07
Power	589.25	585.16	601.33	576.15	577.87	575.44	582.80
Compressor power	290.57	289.13	290.41	290.09	289.13	290.09	290.89
R12 metered rate	3.49	3.91	4.21	4.16	3.95	4.19	4.03

R12 Temperatures

Sump Oil	66.53	66.53	66.53	66.53	66.53	66.53	66.53
Discharge	91.76	91.71	91.71	91.71	91.76	91.76	91.76
Condenser Start	92.38	92.38	92.44	92.38	92.44	92.44	92.44
Mid Condenser	36.82	36.82	36.76	36.70	36.70	36.70	36.70
Condenser End	19.80	19.74	19.74	19.74	19.74	19.74	19.74
Evaporator Start	-2.30	-2.36	-2.30	-2.30	-2.30	-2.30	-2.23
Evaporator End	3.55	3.55	3.62	3.62	3.62	3.62	3.62
Suction	6.61	6.61	6.68	6.74	6.74	6.74	6.81

Pressures, gauge, Bar

Discharge	8.31	8.31	8.29	8.28	8.29	8.29	8.29
Cond. End	7.81	7.80	7.78	7.77	7.77	7.76	7.76
Evap. Start	1.71	1.70	1.69	1.71	1.71	1.71	1.72
Suction	1.61	1.60	1.59	1.61	1.61	1.61	1.62

Calculated results

C.O.P.	2.90	3.41	2.81	2.82	2.68	2.77	2.83
Tbdc	40.86	40.74	40.73	40.95	41.02	41.04	41.18
Apparent R12mdot	4.48	5.24	4.33	4.34	4.13	4.28	4.37
Ideal R12 mdot	5.60	5.59	5.57	5.60	5.61	5.61	5.63
R12 flow ratio	0.80	0.94	0.78	0.78	0.74	0.76	0.78
Minimum work	123.41	144.41	119.51	119.36	113.28	117.38	119.67
Comp. efficiency	0.42	0.50	0.41	0.41	0.39	0.40	0.41

Table 5.5

Data sets from 9/6/85 showing upward evaporating pressure transition

	Before transition				After transition		
Index	56.00	57.00	58.00	59.00	60.00	61.00	62.00
Time mins	111.49	113.48	115.49	117.48	119.49	121.48	123.49
Performance							
Cond. water in	15.57	15.55	15.53	15.50	15.49	15.47	15.45
water out	25.44	25.45	25.44	25.42	25.55	25.52	25.51
flow rate	42.07	41.94	41.86	41.83	42.34	42.39	42.47
Power	1737.60	1738.82	1736.22	1735.89	1781.79	1782.84	1789.28
Evap. water in	42.83	42.85	42.85	42.88	42.89	42.90	42.89
water out	38.61	38.62	38.63	38.66	38.53	38.54	38.55
flow rate	91.36	91.21	91.20	91.13	91.00	90.83	91.15
Power	1612.85	1615.61	1611.25	1610.31	1660.83	1657.22	1653.61
Compressor power	266.27	265.78	265.46	265.07	264.98	264.11	265.29
R12 metered rate	8.02	7.88	7.94	8.07	8.27	8.28	8.28
R12 Temperatures							
Sump Oil	65.41	65.44	65.47	65.53	65.58	65.53	65.47
Discharge	80.50	80.53	80.51	80.53	80.33	80.15	80.11
Condenser Start	80.36	80.39	80.38	80.39	80.21	80.00	79.96
Mid Condenser	20.68	20.68	20.65	20.64	20.60	20.59	20.56
Condenser End	16.21	16.17	16.15	16.14	16.11	16.10	16.09
Evaporator Start	13.88	13.82	13.86	13.87	14.52	14.68	14.62
Evaporator End	41.61	41.63	41.64	41.66	41.67	41.68	41.66
Suction	42.70	42.73	42.73	42.75	42.76	42.73	42.72
Pressures, gauge, Bar							
Discharge	6.66	6.65	6.65	6.64	6.73	6.72	6.73
Cond. End	4.68	4.68	4.68	4.68	4.66	4.66	4.66
Evap. Start	3.70	3.70	3.70	3.70	3.85	3.84	3.83
Suction	3.60	3.60	3.60	3.60	3.73	3.73	3.72
Calculated results							
C.O.P.	6.53	6.54	6.54	6.55	6.72	6.75	6.74
Tbdc	59.70	59.76	59.77	59.80	60.27	60.13	60.01
Apparent R12mdot	9.42	9.42	9.41	9.41	9.66	9.68	9.71
Ideal R12 mdot	10.39	10.39	10.39	10.39	10.71	10.72	10.70
R12 flow ratio	0.91	0.91	0.91	0.91	0.90	0.90	0.91
Minimum work	104.41	104.31	104.01	103.96	102.98	102.82	103.62
Comp. efficiency	0.39	0.39	0.39	0.39	0.39	0.39	0.39

Table 5.6

Data sets from 9/6/85 showing downward evaporating pressure transition

	Before transition				After transition		
Index	169.00	170.00	171.00	172.00	173.00	174.00	175.00
Time mins	350.47	352.47	354.47	356.48	358.47	360.48	362.47
Performance							
Cond. water in	15.77	15.78	15.78	15.78	15.78	15.80	15.81
water out	25.63	25.64	25.63	25.60	25.51	25.52	25.54
flow rate	42.55	42.56	42.57	42.38	41.64	41.58	41.61
Power	1756.16	1756.92	1756.56	1741.49	1696.55	1691.28	1694.97
Evap. water in	32.98	32.84	32.72	32.58	32.47	32.34	32.23
water out	28.91	28.77	28.64	28.55	28.52	28.40	28.27
flow rate	91.28	91.16	91.31	91.31	91.08	90.90	90.96
Power	1558.45	1554.53	1556.56	1542.11	1505.66	1501.17	1508.17
Compressor power	272.18	271.93	272.73	272.48	271.80	271.33	271.48
R12 metered rate	8.48	8.37	8.55	8.22	8.08	8.16	8.11
R12 Temperatures							
Sump Oil	58.25	58.11	57.99	57.88	57.81	57.81	57.80
Discharge	72.67	72.53	72.43	72.33	72.55	72.57	72.55
Condenser Start	72.70	72.56	72.45	72.34	72.57	72.61	72.59
Mid Condenser	20.73	20.74	20.75	20.76	20.79	20.81	20.82
Condenser End	16.29	16.30	16.30	16.30	16.31	16.31	16.33
Evaporator Start	14.09	14.11	14.11	13.97	13.21	13.20	13.25
Evaporator End	32.23	32.09	31.97	31.84	31.75	31.65	31.53
Suction	33.18	33.05	32.92	32.80	32.74	32.64	32.53
Pressures, gauge, Bar							
Discharge	6.76	6.76	6.76	6.73	6.66	6.66	6.67
Cond. End	4.68	4.68	4.68	4.68	4.69	4.69	4.70
Evap. Start	3.80	3.80	3.80	3.76	3.65	3.66	3.66
Suction	3.68	3.68	3.68	3.64	3.54	3.54	3.54
Calculated results							
C.O.P.	6.45	6.46	6.44	6.39	6.24	6.23	6.24
Tbdc	52.15	52.00	51.87	51.57	51.27	51.32	51.28
Apparent R12mdot	9.82	9.83	9.83	9.75	9.49	9.46	9.48
Ideal R12 mdot	10.91	10.92	10.92	10.82	10.56	10.57	10.57
R12 flow ratio	0.90	0.90	0.90	0.90	0.90	0.89	0.90
Minimum work	104.31	104.38	104.48	104.68	104.78	104.29	104.62
Comp. efficiency	0.38	0.38	0.38	0.38	0.39	0.38	0.39

Table 5.7

Sample data sets from 11/5/85. Nominal discharge pressure = 150psia

Note that the 2 examples here of the high power mode indicate total losses of almost 200 Watts, while the other data sets indicate a near-constant total loss of 170 Watts.

Index	40.00	80.00	170.00	230.00	290.00	360.00	450.00
Time mins	79.53	159.52	371.18	524.54	686.54	826.54	1031.55
Performance							
Cond. water in	15.15	15.26	15.25	15.67	16.05	16.55	17.04
water out	40.74	40.70	39.28	40.40	42.22	43.67	45.40
flow rate	20.22	20.25	19.25	16.17	12.96	10.27	7.14
Power	2165.71	2156.52	1936.10	1673.90	1419.67	1165.33	847.35
Evap. water in	41.87	40.63	33.18	27.10	20.39	15.30	4.92
water out	32.38	31.08	24.80	20.05	14.54	10.42	1.54
flow rate	48.96	48.09	47.77	47.36	46.42	45.16	42.38
Power	1944.91	1922.21	1674.25	1396.59	1135.65	923.47	600.68
Compressor power	320.69	313.07	339.12	343.86	320.77	309.90	294.09
R12 metered cc/s	9.40	9.46	8.92	7.66	6.56	5.41	-0.01
R12 Temperatures							
Sump Oil	60.25	59.20	52.92	50.89	50.48	54.32	64.11
Discharge	78.43	77.31	70.25	70.11	72.82	78.15	89.25
Condenser Start	78.49	77.39	70.52	70.53	73.33	78.55	89.09
Mid Condenser	28.61	28.70	28.66	30.86	33.29	35.19	37.01
Condenser End	16.45	16.59	16.50	16.96	17.38	17.84	17.86
Evaporator Start	18.00	18.01	15.57	12.27	7.55	4.31	-2.66
Evaporator End	40.00	38.32	25.62	20.27	15.42	11.64	2.52
Suction	40.00	38.35	25.97	20.33	15.00	11.10	5.04
Pressures, gauge, Bar							
Discharge	8.98	8.99	8.68	8.58	8.52	8.47	8.39
Cond. End	5.94	5.95	5.97	6.44	6.97	7.43	7.94
Evap. Start	4.72	4.72	4.25	3.62	2.92	2.45	1.68
Suction	4.62	4.62	4.16	3.54	2.85	2.37	1.61
Calculated results							
C.O.P.	6.75	6.89	5.71	4.87	4.43	3.76	2.88
Tbdc	54.29	53.12	44.06	39.42	35.99	36.48	38.06
Apparent R12mdot	12.01	12.02	11.08	9.60	8.06	6.49	4.52
Ideal R12 mdot	13.03	13.11	12.30	10.79	9.03	7.71	5.65
R12 flow ratio	0.92	0.92	0.90	0.89	0.89	0.84	0.80
Minimum work	144.00	143.73	140.86	144.14	148.09	138.47	124.09
Total losses	176.69	169.34	198.26	199.72	172.68	170.62	170.00
Comp. efficiency	0.45	0.46	0.42	0.42	0.46	0.45	0.42

Table 5.8

Sample data sets from first time-resolved record of 11/5/85

Index	1.00	100.00	200.00	300.00	400.00	500.00	600.00
Time mins	2.92	220.00	440.32	660.60	220.15	440.28	660.38
Performance							
Cond. water in	15.22	15.22	15.22	15.22	15.22	15.22	15.22
water out	40.72	40.67	40.67	40.72	40.72	40.78	40.61
flow rate	20.05	20.44	20.15	20.11	20.09	19.99	19.99
Power	2140.22	2177.15	2145.71	2146.79	2144.16	2138.63	2123.70
Evap. water in	40.20	40.14	40.08	40.02	39.96	39.90	39.84
water out	30.67	30.67	30.67	30.61	30.43	30.49	30.24
flow rate	48.14	48.11	48.28	48.19	48.33	47.97	48.21
Power	1919.95	1907.02	1901.61	1898.12	1928.62	1890.20	1936.69
Comp. Voltage	0.00	0.00	0.00	0.00	0.00	0.00	0.00
Current	0.00	0.00	0.00	0.00	0.00	0.00	0.00
Power	312.77	339.29	340.09	337.37	315.01	314.85	311.97
R12 metered rate	9.49	9.44	9.54	9.30	9.36	9.63	9.65
R12 Temperatures							
Sump Oil	58.72	58.44	59.24	59.64	60.03	59.29	58.78
Discharge	76.84	76.51	76.73	76.95	77.51	77.23	76.84
Condenser Start	76.92	76.59	76.81	77.09	77.59	77.31	76.92
Mid Condenser	28.74	28.68	28.68	28.68	28.68	28.74	28.62
Condenser End	16.60	16.54	16.54	16.54	16.60	16.54	16.48
Evaporator Start	17.91	17.97	18.04	18.04	17.91	17.97	17.84
Evaporator End	37.66	37.60	37.42	37.36	37.30	37.24	37.12
Suction	37.67	37.67	37.55	37.43	37.37	37.31	37.19
Pressures, gauge, Bar							
Discharge	8.98	9.00	9.00	9.00	8.97	9.00	8.97
Cond. End	5.95	5.95	5.96	5.95	5.95	5.95	5.95
Evap. Start	4.70	4.72	4.73	4.72	4.68	4.71	4.68
Suction	4.60	4.62	4.63	4.62	4.59	4.62	4.59
Calculated results							
C.O.P.	6.84	6.42	6.31	6.36	6.81	6.79	6.81
Tbdc	52.55	52.28	52.59	52.74	53.19	52.98	52.52
Apparent R12mdot	11.96	12.18	11.99	11.98	11.94	11.93	11.85
Ideal R12 mdot	13.09	13.11	13.12	13.09	13.01	13.10	13.06
R12 flow ratio	0.91	0.93	0.91	0.92	0.92	0.91	0.91
Minimum work	143.30	145.26	142.66	143.11	143.81	142.83	142.34
Comp. efficiency	0.46	0.43	0.42	0.42	0.46	0.45	0.46

Table 5.9

Sample data sets from 25/5/85. Nominal discharge pressure = 150psi

Index	50.00	140.00	160.00	190.00	270.00	360.00	450.00
Time mins	99.71	307.52	347.53	434.53	594.53	812.54	1012.55
Performance							
Cond. water in	15.69	15.91	16.03	16.04	16.57	17.39	18.42
water out	39.81	37.19	37.31	38.14	39.80	42.21	44.35
flow rate	20.75	22.62	21.94	19.68	15.63	11.41	7.87
Power	2094.87	2014.43	1953.52	1820.18	1519.80	1185.33	854.22
Evap. water in	41.39	35.64	34.05	31.09	24.78	15.74	4.61
water out	31.81	26.82	25.53	23.27	18.35	10.76	1.35
flow rate	47.33	47.78	47.66	47.48	47.07	45.09	43.11
Power	1898.85	1764.62	1699.30	1554.83	1267.97	939.45	586.73
Compressor power	308.54	302.90	329.83	334.48	308.74	304.90	290.84
R12 metered cc/s	9.40	9.28	9.11	8.55	7.64	-0.00	-0.00
R12 Temperatures							
Sump Oil	61.17	55.38	53.74	52.41	49.47	54.79	65.81
Discharge	79.14	72.62	70.54	69.97	69.66	77.70	90.56
Condenser Start	79.55	73.09	71.05	70.59	70.51	78.72	91.28
Mid Condenser	28.25	26.85	27.15	28.23	29.51	34.07	36.49
Condenser End	17.02	17.05	17.18	17.26	24.57	18.73	19.70
Evaporator Start	20.48	18.77	18.03	16.00	12.20	5.55	-2.17
Evaporator End	39.25	31.03	27.32	24.30	19.13	11.56	2.32
Suction	40.22	31.97	28.08	24.52	19.88	11.94	5.79
Pressures, gauge, Bar							
Discharge	8.85	8.49	8.48	8.43	8.38	8.31	8.24
Cond. End	5.80	5.55	5.61	5.83	5.76	7.12	7.72
Evap. Start	4.68	4.45	4.35	4.04	3.47	2.55	1.68
Suction	4.56	4.33	4.23	3.93	3.37	2.45	1.58
Calculated results							
C.O.P.	6.79	6.65	5.92	5.44	4.92	3.89	2.94
Tbdc	55.11	48.61	45.84	43.11	38.32	37.60	39.68
Apparent R12mdot	11.59	11.42	11.18	10.44	9.08	6.62	4.56
Ideal R12 mdot	12.86	12.62	12.45	11.73	10.41	7.91	5.57
R12 flow ratio	0.90	0.91	0.90	0.89	0.87	0.84	0.82
Minimum work	139.22	134.97	134.87	137.14	139.96	136.11	125.21
Total losses	169.32	167.93	194.96	197.34	168.78	168.79	165.62
Comp. efficiency	0.45	0.45	0.41	0.41	0.45	0.45	0.43

Table 5.10

Sample data sets from 7/6/85. Nominal discharge pressure = 200psi

Index	90.00	100.00	125.00	180.00	240.00	300.00	360.00
Time mins	179.48	224.47	274.48	384.49	528.50	674.50	794.51
Performance							
Cond. water in	19.09	19.16	19.04	19.21	19.62	19.92	20.02
water out	59.30	57.94	58.49	59.10	60.49	61.80	63.53
flow rate	11.10	11.55	11.03	9.81	8.25	6.72	5.34
Power	1868.24	1874.87	1821.53	1637.70	1411.23	1178.26	972.47
Evap. water in	46.42	45.64	43.53	38.77	30.27	22.62	16.37
water out	28.30	27.72	26.28	22.84	16.90	11.76	7.36
flow rate	22.38	22.41	22.28	21.53	20.98	20.03	19.22
Power	1697.50	1680.18	1608.01	1435.96	1174.34	910.87	724.78
Compressor power	424.85	418.14	389.19	385.82	385.91	365.16	342.38
R12 metered cc/s	10.08	9.80	9.24	8.24	6.93	5.31	4.37
R12 Temperatures							
Sump Oil	58.43	58.06	57.02	53.57	57.09	60.87	66.30
Discharge	82.15	81.45	81.68	80.36	85.54	90.96	97.89
Condenser Start	82.57	81.89	82.21	81.07	86.38	91.74	98.43
Mid Condenser	44.95	43.90	45.18	47.10	49.46	50.71	51.52
Condenser End	35.43	33.62	31.04	27.88	22.59	22.77	22.77
Evaporator Start	22.71	22.03	20.44	17.12	11.66	7.47	3.34
Evaporator End	28.85	28.62	27.16	24.03	18.46	13.32	9.71
Suction	31.16	30.23	27.98	23.80	16.81	11.43	8.43
Pressures, gauge, Bar							
Discharge	12.39	12.11	12.14	12.13	12.13	12.09	12.06
Cond. End	8.76	8.56	9.05	9.77	10.80	11.24	11.53
Evap. Start	5.11	5.00	4.74	4.22	3.41	2.80	2.31
Suction	5.00	4.89	4.64	4.12	3.31	2.71	2.21
Calculated results							
C.O.P.	4.40	4.48	4.68	4.24	3.66	3.23	2.84
Tbdc	47.25	46.80	45.17	40.01	38.50	38.27	39.83
Apparent R12mdot	11.61	11.54	11.02	9.78	7.98	6.52	5.23
Ideal R12 mdot	13.94	13.70	13.12	11.93	9.72	8.11	6.78
R12 flow ratio	0.83	0.84	0.84	0.82	0.82	0.80	0.77
Minimum work	187.66	185.97	187.73	183.96	181.10	170.78	155.97
Total losses	237.19	232.17	201.46	201.86	204.81	194.37	186.41
Comp. efficiency	0.44	0.44	0.48	0.48	0.47	0.47	0.46

Table 5.11

Sample data sets from first use of new compressor, 14/7/85

Discharge pressure regulator set to 4.
Nominal evaporator water flow rate = 20cc/s.

Index	50.00	130.00	200.00	255.00	265.00	360.00	450.00
Time mins	99.55	289.56	459.55	569.56	589.55	809.56	1019.57
Performance							
Cond. water in	21.13	21.93	21.86	22.19	22.24	22.42	22.38
water out	59.98	59.10	60.54	61.76	61.47	63.59	65.91
flow rate	11.32	11.61	9.58	8.36	8.52	5.87	4.52
Power	1840.96	1805.60	1551.15	1384.66	1399.35	1012.30	824.44
Evap. water in	42.90	41.33	34.92	29.38	28.68	17.33	7.98
water out	26.66	25.90	21.64	17.76	17.20	9.03	1.60
flow rate	23.95	24.59	24.22	23.91	23.85	21.79	20.39
Power	1628.57	1587.62	1345.52	1163.09	1145.20	756.77	544.30
Compressor power	425.55	422.28	414.38	404.77	378.74	340.46	324.51
R12 metered cc/s	8.80	8.58	7.54	6.63	6.32	4.38	3.15
R12 Temperatures							
Sump Oil	61.10	60.72	62.83	67.50	66.01	72.98	82.02
Discharge	80.27	79.87	82.84	87.38	86.77	94.32	103.03
Condenser Start	80.61	80.27	83.41	88.05	87.43	95.18	103.97
Mid Condenser	48.22	47.67	49.38	50.61	50.74	52.31	53.01
Condenser End	24.16	24.66	24.54	24.80	24.84	24.84	24.89
Evaporator Start	19.74	19.05	15.37	12.05	11.66	4.76	-1.21
Evaporator End	26.74	26.28	22.12	18.97	18.66	11.46	3.54
Suction	26.72	25.77	21.11	17.45	16.87	9.68	4.95
Pressures, gauge, Bar							
Discharge	12.69	12.48	12.46	12.45	12.45	12.40	12.39
Cond. End	10.29	10.17	10.72	11.12	11.17	11.79	12.03
Evap. Start	4.67	4.55	3.95	3.45	3.39	2.44	1.79
Suction	4.55	4.42	3.83	3.32	3.27	2.32	1.66
Calculated results							
C.O.P.	4.33	4.28	3.74	3.42	3.70	2.97	2.54
Tbdc	41.09	40.49	39.02	39.35	38.24	36.35	36.66
Apparent R12mdot	10.83	10.65	9.01	7.89	8.00	5.59	4.39
Ideal R12 mdot	12.96	12.65	11.07	9.67	9.59	7.11	5.38
R12 flow ratio	0.84	0.84	0.81	0.82	0.83	0.79	0.82
Minimum work	194.01	192.68	185.55	182.91	186.93	163.02	152.38
Total losses	231.53	229.60	228.84	221.86	191.81	177.44	172.13
Comp. efficiency	0.46	0.46	0.45	0.45	0.49	0.48	0.47

Table 5.12

Sample data sets from run of 17/10/85

New compressor. Nominal discharge pressure 150psi.
Nominal evaporator water flow rate 50 cc/s.

Index	35.00	69.00	103.00	138.00	172.00	206.00	240.00
Time mins	69.92	137.91	205.92	275.93	343.94	411.94	479.92
Performance							
Cond. water in	17.87	18.69	18.07	19.08	18.49	19.37	19.93
water out	38.25	38.48	38.69	39.34	39.98	40.14	41.69
flow rate	24.04	23.33	21.34	19.90	17.56	16.61	13.55
Power	2051.09	1931.85	1841.09	1687.64	1579.40	1444.10	1234.56
Evap. water in	38.74	34.25	31.11	27.25	24.26	21.10	15.89
water out	30.91	26.77	24.17	21.00	18.43	15.79	11.41
flow rate	53.80	52.53	52.86	52.75	52.53	52.28	51.28
Power	1762.49	1646.21	1534.99	1379.47	1280.39	1160.31	961.39
Comp. Voltage	2843.78	2752.54	2819.82	2818.14	2803.08	2767.42	2784.94
Current	2174.36	2117.54	2147.51	2165.27	2036.63	2028.64	2019.17
Power	344.79	341.76	343.34	343.64	318.38	318.87	315.68
R12 metered cc/s	8.67	8.45	8.27	7.70	7.12	6.59	5.63
R12 Temperatures							
Sump Oil	67.07	62.59	58.96	56.93	57.12	54.62	57.02
Discharge	79.15	75.44	72.17	71.16	72.53	71.43	73.30
Condenser Start	79.17	75.51	72.33	71.39	72.85	71.81	74.41
Mid Condenser	28.17	28.63	28.55	30.26	31.50	32.79	34.78
Condenser End	18.80	20.33	20.83	21.02	19.84	20.38	20.86
Evaporator Start	18.27	17.06	15.91	13.75	11.63	9.61	6.24
Evaporator End	36.96	31.09	25.62	21.13	18.43	16.02	12.07
Suction	37.44	31.69	26.50	21.88	19.05	16.33	24.50
Pressures, gauge, Bar							
Discharge	8.68	8.68	8.63	8.61	8.56	8.53	8.49
Cond. End	5.77	5.80	5.72	6.13	6.45	6.76	7.22
Evap. Start	4.53	4.32	4.13	3.78	3.45	3.13	2.62
Suction	4.36	4.16	3.98	3.63	3.30	2.98	2.49
Calculated results							
C.O.P.	5.95	5.65	5.36	4.91	4.96	4.53	3.91
Tbdc	54.46	49.26	44.82	41.03	39.79	35.83	32.89
Apparent R12mdot	11.46	11.05	10.70	9.86	9.11	8.39	7.11
Ideal R12 mdot	12.32	12.04	11.76	10.95	10.14	9.40	8.14
R12 flow ratio	0.93	0.92	0.91	0.90	0.90	0.89	0.87
Minimum work	142.33	143.57	143.80	145.84	147.84	147.94	144.23
Total losses	202.46	198.19	199.54	197.80	170.54	170.93	171.46
Comp. efficiency	0.41	0.42	0.42	0.42	0.46	0.46	0.46

Table 5.13

Sample data sets from run of 18/10/85. The "re-heat" trial

Nominal discharge pressure = 150psi.
Nominal evaporator water flow rate = 50cc/s.

Index	17.00	34.00	51.00	68.00	85.00	102.00	119.00
Time mins	33.91	67.92	101.92	135.91	169.89	203.90	237.90
Performance							
Cond. water in	18.75	19.20	18.66	19.18	18.96	18.70	18.70
water out	39.02	40.36	41.04	39.91	39.17	38.95	35.82
flow rate	21.36	18.18	15.33	19.69	22.42	23.98	28.75
Power	1812.06	1610.01	1435.54	1708.40	1895.90	2032.39	2060.14
Evap. water in	30.04	24.88	20.55	27.71	34.08	39.69	44.26
water out	23.84	19.43	15.71	21.67	27.13	32.17	36.45
flow rate	57.76	56.57	56.16	56.99	57.57	58.07	57.49
Power	1498.50	1291.59	1136.76	1438.56	1674.93	1828.80	1877.75
Comp. Voltage	2803.56	2778.86	2797.26	2800.48	2809.04	2808.54	2745.26
Current	2127.26	2095.26	2035.52	2058.16	2069.54	2051.10	1981.32
Power	348.87	347.97	322.75	323.14	322.49	321.60	306.64
R12 metered cc/s	8.17	7.29	6.54	7.83	8.45	8.73	8.62
R12 Temperatures							
Sump Oil	57.19	56.82	54.56	54.07	56.88	62.42	66.19
Discharge	70.18	70.96	70.79	68.72	71.16	75.99	78.66
Condenser Start	70.69	71.69	71.66	69.39	71.72	76.44	79.06
Mid Condenser	29.06	31.50	33.23	30.47	29.27	29.10	27.35
Condenser End	21.87	20.79	19.82	22.47	21.54	19.74	19.44
Evaporator Start	15.82	12.51	9.52	14.29	16.99	18.54	19.00
Evaporator End	24.38	18.97	15.32	21.76	31.41	38.09	42.98
Suction	24.98	19.09	15.02	22.15	31.66	38.25	43.11
Pressures, gauge, Bar							
Discharge	8.70	8.66	8.62	8.77	8.84	8.89	8.46
Cond. End	5.81	6.42	6.84	6.10	5.87	5.93	5.66
Evap. Start	4.11	3.58	3.12	3.86	4.30	4.56	4.59
Suction	3.95	3.43	2.97	3.71	4.14	4.39	4.41
Calculated results							
C.O.P.	5.19	4.63	4.45	5.29	5.88	6.32	6.72
Tbdc	42.30	38.91	34.64	38.57	44.07	50.58	55.35
Apparent R12mdot	10.68	9.39	8.32	10.17	11.11	11.56	11.54
Ideal R12 mdot	11.79	10.48	9.39	11.32	12.24	12.60	12.49
R12 flow ratio	0.91	0.90	0.89	0.90	0.91	0.92	0.92
Minimum work	144.71	147.62	148.33	148.08	146.17	145.06	135.71
Total losses	204.16	200.34	174.42	175.06	176.32	176.53	170.94
Comp. efficiency	0.41	0.42	0.46	0.46	0.45	0.45	0.44

Table 5.14

Sample data sets from run of 21/10/85

New compressor. Time resolved. Downward power step after 18 minutes.

Index	335.00	340.00	345.00	350.00	990.00	995.00	1000.00
Time mins	17.90	18.17	18.43	18.70	53.02	53.28	53.55
Performance							
Cond. water in	22.67	22.67	22.67	22.67	19.72	19.72	19.74
water out	41.91	41.85	41.91	41.85	43.84	43.67	43.75
flow rate	16.32	16.13	16.13	15.99	11.68	12.32	11.45
Power	1314.31	1295.08	1299.09	1283.95	1179.47	1235.21	1150.83
Evap. water in	18.80	18.74	18.74	18.67	15.38	15.32	15.34
water out	14.12	13.93	14.00	14.00	11.11	11.18	11.01
flow rate	52.28	52.27	52.67	52.76	51.66	51.85	52.09
Power	1023.53	1050.98	1045.05	1033.11	922.77	898.61	944.37
Comp. Voltage	2781.00	2782.00	2785.00	2786.00	2805.00	2815.00	2822.00
Current	2166.42	2185.26	2064.69	2093.58	2049.62	2099.86	2082.27
Power	347.75	345.04	322.51	317.88	314.85	311.65	310.53
R12 metered cc/s	6.63	6.15	6.58	6.37	6.36	4.70	6.23
R12 Temperatures							
Sump Oil	43.87	44.10	44.52	44.64	54.57	54.40	54.42
Discharge	63.69	63.86	64.04	64.21	72.74	72.85	72.87
Condenser Start	64.69	64.86	64.97	65.20	73.83	73.88	73.91
Mid Condenser	35.61	35.97	35.79	35.73	36.86	37.04	36.82
Condenser End	24.41	24.41	24.28	24.28	21.15	21.22	21.18
Evaporator Start	8.87	8.80	8.80	8.80	6.24	6.24	6.20
Evaporator End	13.91	13.78	13.91	13.71	11.38	10.99	11.21
Suction	13.60	12.90	13.21	13.21	10.45	9.81	10.22
Pressures, gauge, Bar							
Discharge	8.97	8.98	9.01	8.97	8.92	8.96	8.90
Cond. End	7.32	7.44	7.40	7.37	7.64	7.72	7.63
Evap. Start	2.98	2.92	2.96	2.94	2.63	2.62	2.61
Suction	2.83	2.78	2.81	2.79	2.47	2.46	2.46
Calculated results							
C.O.P.	3.78	3.75	4.03	4.04	3.75	3.96	3.71
Tbdc	24.71	24.27	24.68	24.83	30.17	30.05	30.26
Apparent R12mdot	8.09	7.97	7.99	7.88	6.84	7.17	6.67
Ideal R12 mdot	9.34	9.19	9.30	9.25	8.12	8.11	8.09
R12 flow ratio	0.87	0.87	0.86	0.85	0.84	0.88	0.82
Minimum work	149.52	149.72	149.06	147.50	144.38	152.02	141.16
Total losses	198.23	195.32	173.45	170.39	170.47	159.64	169.38
Comp. efficiency	0.43	0.43	0.46	0.46	0.46	0.49	0.45

Table 5.15

Chapter 6. Experiments on the lubrication system

6.1. Introduction

In order to experiment with the compressor's lubrication system, the original compressor was made demountable by cutting open its can and brazing on flanges. This metal work was completed early in December 1985. During the following two months 30 short tests were performed which investigated the effect on the compressor's power consumption of various modifications to the lubrication system. Each test had the discharge pressure regulator set to 3, for a nominal 150 psi discharge pressure. The evaporator water started at 25C, at a flowrate of 50cc/s, and data was recorded for 1 hour.

Originally, all these tests were recorded by the Commodore PET at the rate of 1 dataset every 3 seconds. It was found that transferring data onto BBC Acorn compatible discs was very time wasting. For this reason, the compromise was made of reducing the large files of 1000 data sets to 50 data sets before transferring. Consequently, the time resolution of the records presented here is not as good as in the original data.

Figure 6.1 shows the crankshaft, rotor, oil impeller assembly of the compressor, and indicates the positions of the journal bearings. The crankshaft is supported in two journal bearings. The con-rod end forms a third journal bearing around the crank. Additionally, the dead weight of the crankshaft & rotor is supported by a thrust bearing formed between the plate bolted onto the crankshaft's top end, and the journal end upon which this plate rests. These four sliding interfaces are all supplied with oil which is forced up through ducts in the crankshaft by an impeller mounted below the rotor, dipping into the sump. The last sliding interface is that of the piston in its bore, which is lubricated by the combined effects of the oil spraying from the crankshaft, and entrainment in the suction gas. This collection of 5 sites at which a mechanical loss occurs is further complicated by the uncertainty concerning whether sufficient oil can be held in the gap between the rotor and the stator to cause an added viscous loss. In making any modification to the lubrication system, there are thus 6 sites of mechanical loss, which all respond separately to the modification.

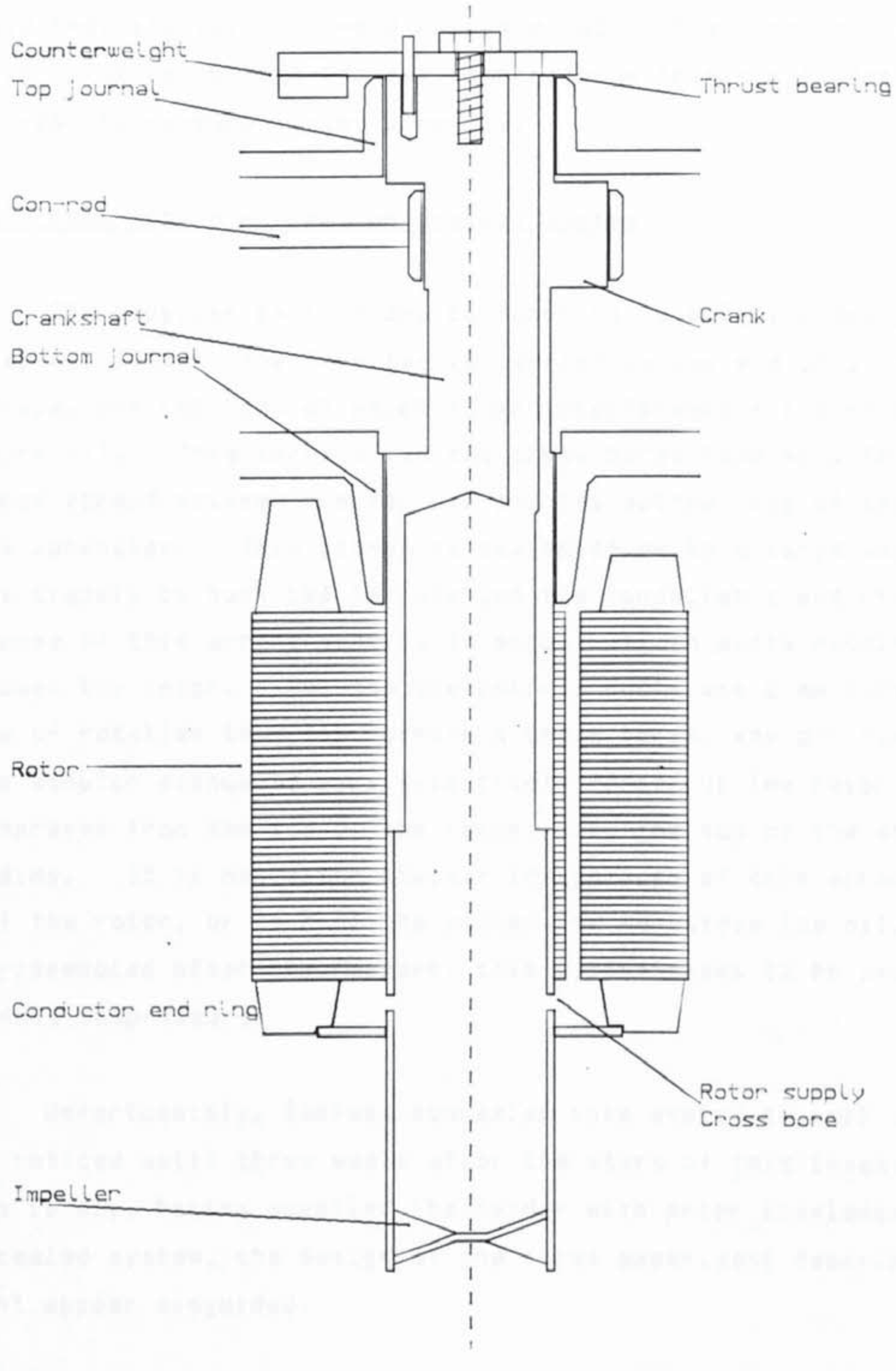

Figure 6.1. Sectional view of rotating assembly, including the bearings

This has made interpretation of the results very difficult, because it is only the total power consumption that has been measured, not the loss at each bearing separately.

In an attempt to eliminate some of the complicating features of these experiments, they were complemented by the "free running" tests, which involved running the new compressor with its cylinder head absent, in order to measure losses directly.

6.2 Description of the lubrication system

The impeller is intended to function as a fan, producing an upward axial oil flow. The impeller is carried in the end of a thin-walled ferrule, the top 2cms of which is an interference fit into the rotor, figure 6.1. This ferrule has two cross bores leading into an annular plenum formed between the ferrule and the bottom ring of the squirrel cage conductor. This plenum is sealed below by a large washer, which fits tightly to both the ferrule and the conductor's end ring. The purpose of this arrangement is to supply oil to ducts running vertically through the rotor. Because the rotor's ducts are 2 mm further from the axis of rotation than the ferrule's cross bores, any oil running into this annular plenum is very effectively forced up the rotor's ducts to be sprayed from the top of the rotor, onto the top of the stator's winding. It is not clear whether the purpose of this arrangement is to cool the rotor, or to cool the stator, or to outgas the oil. Having dis-assembled other compressors, this system seems to be peculiar to Danfoss compressors.

Unfortunately, Danfoss concealed this system so well that it was not noticed until three weeks after the start of this investigation. This is why, having supplied the reader with prior knowledge of this concealed system, the design of the first experiment described below might appear misguided.

6.3 Excluding oil from the motor

From the rotor - stator gap width of 0.2mm, the rotor's surface speed of 10m/s, and its curved surface area of 150 cm^2, a maximum possible viscous loss of 30 Watts was estimated. If a mechanism could exist whereby an empty gap and a filled gap were both stable states, then the observed discontinuities in the losses would be explained.

The oil sprayed from the crankshaft drains away through holes in the floor of the casting, directly above the rotor - stator gap. In order to test the possibility that this was causing an added viscous loss, these drain holes were blanked off, and alternative ducts installed. This modification required some devious machining. The open end of one of the new ducts can be seen on figure 5.14 at the side of the casting.

The resulting power v time plot is shown as the first record in figure 6.2. It would appear that this modification to the compressor has made no difference to the occurrence of the power step. As explained above, three weeks later it was realised that this test had not involved a significant reduction in the amount of oil sprayed onto the top of the rotor. The experimental result of no change was thus sensible. However, at the time, this null result provoked a consideration of possible alternative reasons for the power step.

This first record of power consumption shows one significant difference from preceeding experience. The power step is now barely 20 Watts, compared with the 27 Watts seen on the trials in the Summer of 1985. On subsequent tests, steps of between 15 and 20 Watts have consistently been observed shortly after starting up, but never a 27 Watt step. This appears to be due to a fall in the losses associated with the high power mode, rather than a rise in the losses associated with the low power mode. This change in behaviour seems to have been caused by the work that was done on the compressor. For instance, in order to fit the covers over the original oil drain holes, it was necessary to remove the top journal, and replace it later. This dis-assembly and re-assembly of the top journal bearing would be expected to change the mechanical losses.

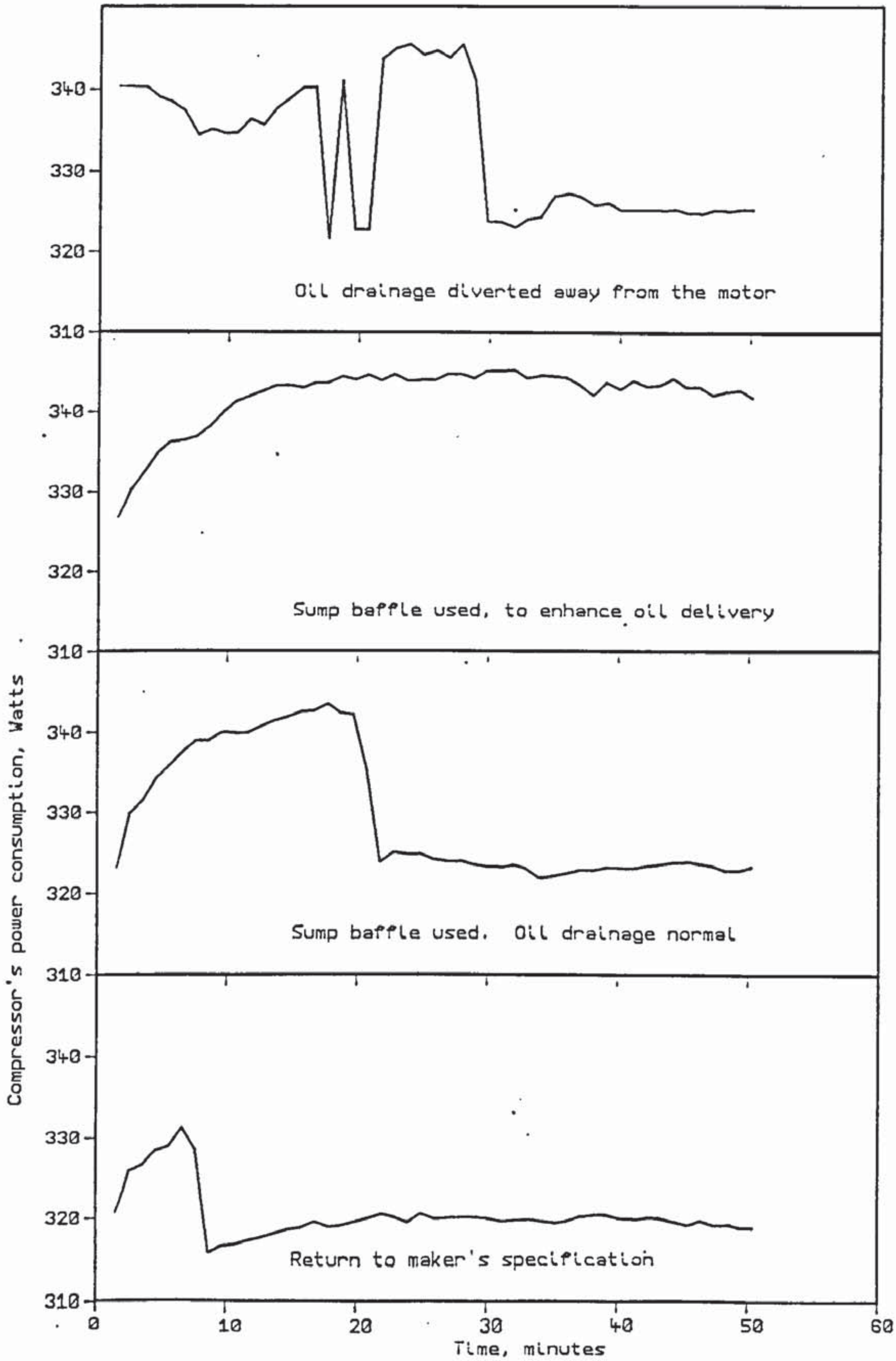

Figure 6.2 Initial experiments with the lubrication system

6.4 Improved oil delivery

Upon observing the free running of a compressor, for which the top of the can had been replaced with a clear perspex lid, it had been noticed that there is a sudden onset of oil spray from the ducts at the top of the crankshaft, after a prolonged period after startup during which no oil spray was visible. For a compressor idling in air this observation was quite reproducible. The onset of oil spray from the top of the crankshaft normally occurred about 20 minutes after switching on, at an oil temperature of around 50C, for which the viscosity is 16 centipoise.

Normal functioning of the oil impeller would fail if the liquid in its vicinity was to acquire an angular speed close to that of the crankshaft, as there would then be insufficient speed of the impeller blades w.r.t. the liquid to drive it up.

This was the thinking behind a back-of-the-envelope calculation which indicated that there is a critical viscosity, below which normal operation can occur, and above which the liquid would tend to be driven up to the angular speed of the crankshaft. This seemed to be consistent with the observed behaviour, idling in air, and offer a possible explanation for the power step as being due to a failure of the impeller to deliver oil to the bearings.

Although this picture was very appealing, there is at least one objection to it. For Alkylbenzene in equilibrium with R12 at 3 Bar, the viscosity cannot exceed 5 centipoise (66, fig 31). This is a consequence of the inverse relationship between liquid refrigerant fraction and temperature. With increasing R12 pressure, the maximum possible viscosity gets less. Since, in the heat pump, the compressor has normally been started in an atmosphere of around 4 Bar, there is reason to suspect that the observed behaviour of the compressor idling in air may be irrelevant to the resolution of the power step mystery.

In order to obtain some experimental confirmation or otherwise that the power step could be explained by the observed behaviour of a compressor idling in air, a baffle arrangement was set up around the impeller, whose purpose was to inhibit the acquisition of angular speed by the oil in the neighbourhood of the impeller. After placing the compressor in the can, before completing the installation, the motor was started to ascertain that this modification did indeed result in fully developed oil flow from the outset. It was found that the baffle's effect surpassed expectation, a heavy oil spray being produced from the top of the crankshaft, almost from the first turn of the compressor. Having thus verified that the baffle had had the desired effect, the re-installation procedure was completed.

The power v time plot for the following run is shown as the second record in figure 6.2. In this run the high power mode was persistent, and outlasted the run. This result was of sufficient concern to warrant repeating this test, but with the original oil drain holes restored. The resulting power consumption record is shown next in figure 6.2. The high power mode again occurred, but this time lasted only 20 minutes. These two tests together are suggestive that increasing the oil delivery in this way has not merely made no difference, but has made the problem slightly worse.

These results prompted a return to the status quo. The last record on figure 6.2 shows the power consumption record obtained after restoring the compressor to the maker's specification. After 10 minutes, this settled down to a steady 320 Watts. For the operating conditions of this test, the work of compression is virtually constant throughout, at a value of 150 watts. A 320 Watt consumption thus corresponds to a loss of 170 watts, which agrees with the tests performed in May 1985 at the same suction and discharge pressures.

6.5 A novel oil delivery system

At this stage, having absolutely no understanding of the previous results, it was recognised as desirable to use an oil induction system which was more amenable to analytic inspection and estimation of the oil delivery rate.

Figure 6.3 shows the modified rotor - crankshaft - impeller assembly in section. The modification involved cementing a washer over the end of the ferrule which contains the impeller, and setting up a support for the duct mounted below the hole in the washer. The unmodified impeller is essentially acting as a fan to produce axial flow. The modified system functions instead as a centrifugal pump, whose principle of operation is explained below.

The principal gravitational equipotential surface perceived inside a rotating frame is a paraboloid given by

$$h = \frac{(\omega r)^2}{2g} \qquad 6.1$$

where h is height, r is the distance from the axis of rotation, and ω is the angular speed.

The entry hole in the washer is just 3 mm in radius. The bores in the crankshaft are offset from the axis of rotation by 9mm. Consequently, by virtue of the crankshaft's angular speed of 3000 RPM, the apparent gravitational potential at the top of the crankshaft's bores is actually 20 cms *lower* than at the outer edge of the entry hole. Thus, from the point of view of oil entering at the bottom, it runs *downhill* to the top of the crankshaft.

The "feeder" shown just entering the hole in the washer is a short piece of copper tube which is mounted on a rigid framework secured to the compressor by the same bolts as hold the motor's stator in place. This is a necessary additional feature without which the oil in the vicinity of the entry hole tends to be forced away, because of the high angular speed which it acquires through viscous drag.

For this configuration it was possible to obtain an estimate of the oil delivery rate. By measuring the depth of oil in the sump, the free surface was estimated to be 15 mm above the top of the feeder. Assuming that the centrifugal pump is capable of maintaining the top of the feeder clear of oil, one can estimate that the oil flows up the feeder at a speed of about 50cm/s. The estimate of delivery rate is then obtained by multiplying by the cross-sectional area of the feeder.

For the first trial of this type, the feeder csa was 15mm^2, giving a delivery rate estimate of 7 cc/s. The resulting power v time plot is shown as the first record, at the top of figure 6.4.

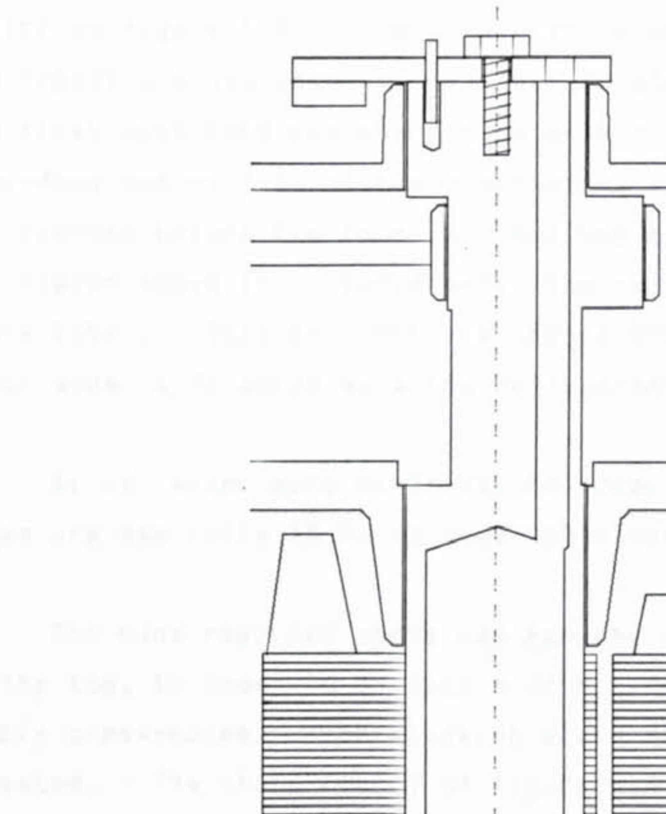

Figure 6.3. Centrifugal pump improvisation

The original time resolved record showed that between 3 and 4 minutes the power consumption was steady at 303 Watts, until the abrupt transition to the high power mode. (This feature has been slightly blurred by the data reduction.) The downward transition then occurred at 45 minutes. A simple repeat of this test is shown as the second record on figure 6.4. The only significant point of difference is that the repeat did not show any tendency to start in the low power mode. The first test here was started up within minutes of completing the pump-down and re-fill of the compressor, after re-installation. i.e. it was started before the lubricant had had time to reach equilibrium with the vapour above it. Conversely, the repeat was performed several hours later. This is further evidence that the occurrence of the low power mode is favoured by a low refrigerant fraction in the lubricant.

It is rather more difficult to account for the fact that both modes are now fully 15 Watts lower than observed previously.

The runs reported above had had the crankshaft bores blanked off at the top, in order to develop a true hydrostatic head at the bearing supply cross-bores. The blanking plate was removed and the run repeated. The third record on figure 6.4 shows the result. For this oil delivery method, it appears to make no difference whether or not the crankshaft's bores are left open at the top.

The results of these first tests with the improvised centrifugal pump & feeder presented an agonisingly tantalising problem. In the low power mode, the lowest observed value of the compressor's total loss is 150 Watts. This is 20 Watts lower than for the unmodified compressor in the low power mode at the same suction and discharge pressure. The problem was that, having no understanding of the results so far, it was not possible to devise a way of stabilising the low power mode at this new, lower level.

There followed an excursion into the design and testing of new impellers, the results of which added further to the confusion. Then, on 29 December 1985, the presence of the rotor's ducts was recognised, and some of the results, especially the very first null result, started to make more sense. This prompted a return to the improvised centrifugal pump and feeder.

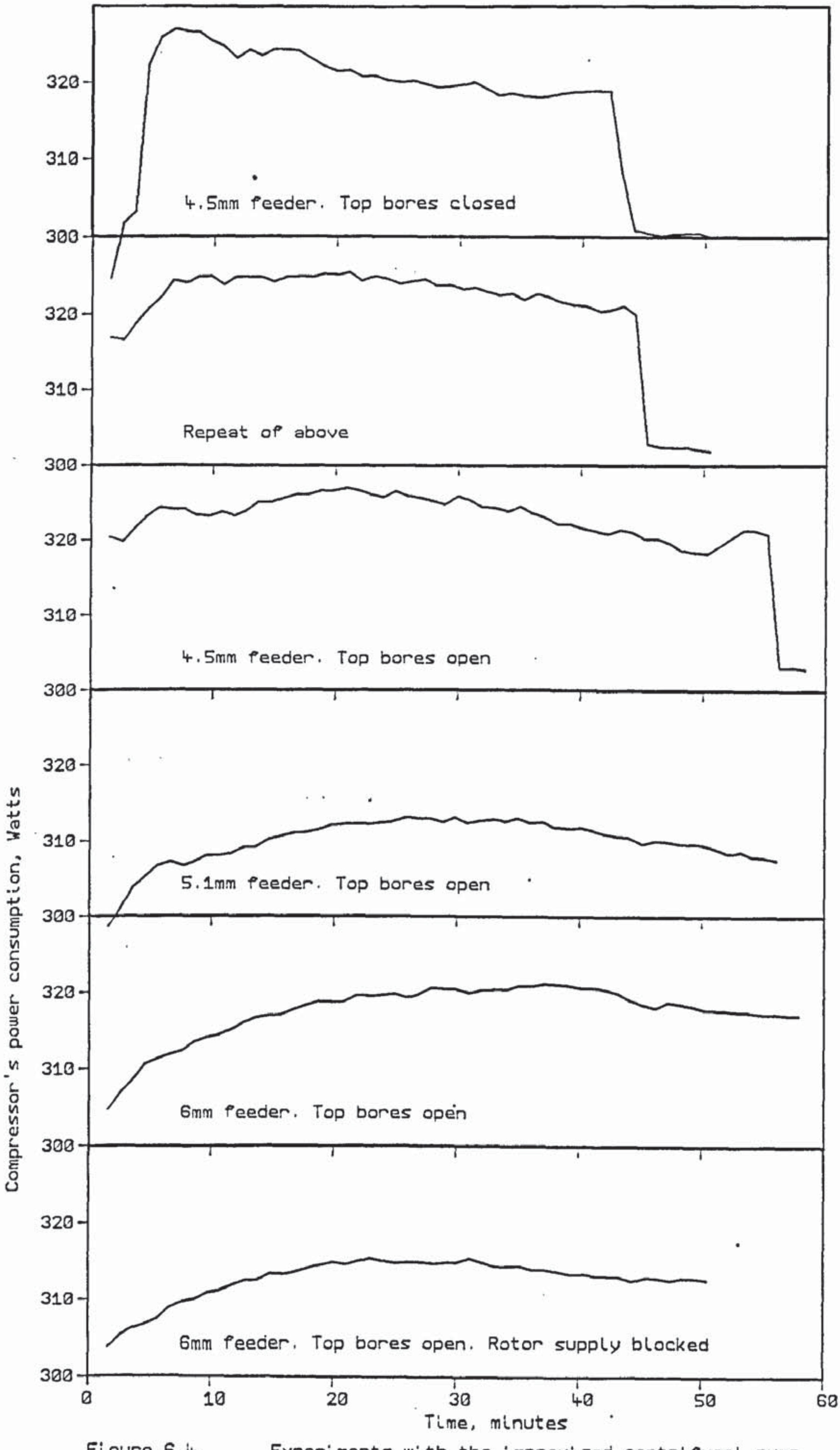

Figure 6.4 Experiments with the improvised centrifugal pump

It was realised that of the estimated 7cc/s pumped by the first trial, most was shunted by the supply to the rotor's ducts, perhaps starving the bearings of oil. Upon resurrecting this experiment, the first trial involved filing out the feeder to a larger internal diameter, with no other change. This gave an increased flow cross section of 20 mm^2, to give an estimated delivery of 10 cc/s. The resulting power consumption is shown as the fourth record on figure 6.4.

This consumption of 310 Watts splits the difference between the high and low power modes seen with the smaller feeder. The favoured interpretation is that the increased oil delivery rate has stabilised the low power mode at a slightly higher level.

The feeder internal diameter was raised to 6 mm, for an estimated 14 cc/s delivery rate, and the resulting power record is shown second last on figure 6.4. This consumption of 320 Watts is back up to the level of the unmodified system.

The results of these experiments with the improvised centrifugal pump and feeder thus seem to be indicating that, after satisfying a certain minimum oil delivery rate, the effect of further increasing the oil delivery rate is to *increase* the losses from 150 Watts to a limit of not less than 170 Watts.

The last trace on figure 6.4 shows the result of blocking off the rotor supply ducts. It may be invalid to interpret the resulting 6 Watt reduction in consumption as due solely to elimination of viscous drag at the rotor - stator gap, because this modification would have had the side effect of increasing the delivery to the bearings, and, at this stage, the effect of this on the loss at the bearings is unknown.

6.6 Customised centrifugal pump

The principle of operation of a centrifugal pump requires only that a narrow, hollow, inverted cone spins in the sump. It is not necessary to bludgeon the oil with Danfoss' large impeller. After the first trials with the improvised centrifugal pump, in the absence of a clear understanding to point the right direction, it seemed worthwhile to replace the original impeller with the minimum necessary hardware, in the hope that a less inelegant assembly might confer a corresponding performance improvement.

A centrifugal pump was machined out of a perspex billet. Perspex was chosen, because it can be cut by mild steel. In order to get the desired internal taper, a conical reamer was made out of a mild steel billet. The finished article had an entry hole 6 mm in diameter, and tapered up with a cone angle of 4 degrees. The centrifugal pumping principle depends on the oil's angular speed remaining close to that of the crankshaft during its transit from the entry hole, upward and outward to the bearings. To augment the requisite torsional coupling to the oil, vertical vanes were cemented against the internal conical surface. From the view point of an observer inside the crankshaft, these vertical vanes exert a reaction against the Coriolis force produced by the radial component of the oil's velocity.

6.7 Trials with the customised oil pump

Figure 6.5 shows the crankshaft, impeller assembly with this new impeller. Note that there was no provision for oil supply to the rotor's ducts. This was because the rotor duct supply had still not been noticed at this stage. There are two significant consequences of this oversight. Since the rotor ducts shunt a very large fraction of the oil supplied by the impeller, the omission of this system meant that the supply to the bearings was significantly greater than for the first tests with the improvised centrifugal pump. Secondly, because the direct feed to the top of the rotor has been omitted, it is realistic to expect viscous loss at the rotor-stator gap to be negligible. The resulting power record is shown at the top of figure 6.6. This test was repeated after bolting on the same, small feeder as used in the first such test, and the resulting power consumption is shown as the second trace on figure 6.6. Using the small feeder has pushed the consumption up 5 Watts, which may be consistent with the anticipated increase in the oil flow rate.

This higher consumption of 320 Watts just corresponds to the status quo, as observed either with the unmodified lubrication system, or with the 6 mm feeder, with the rotor supply retained. Two

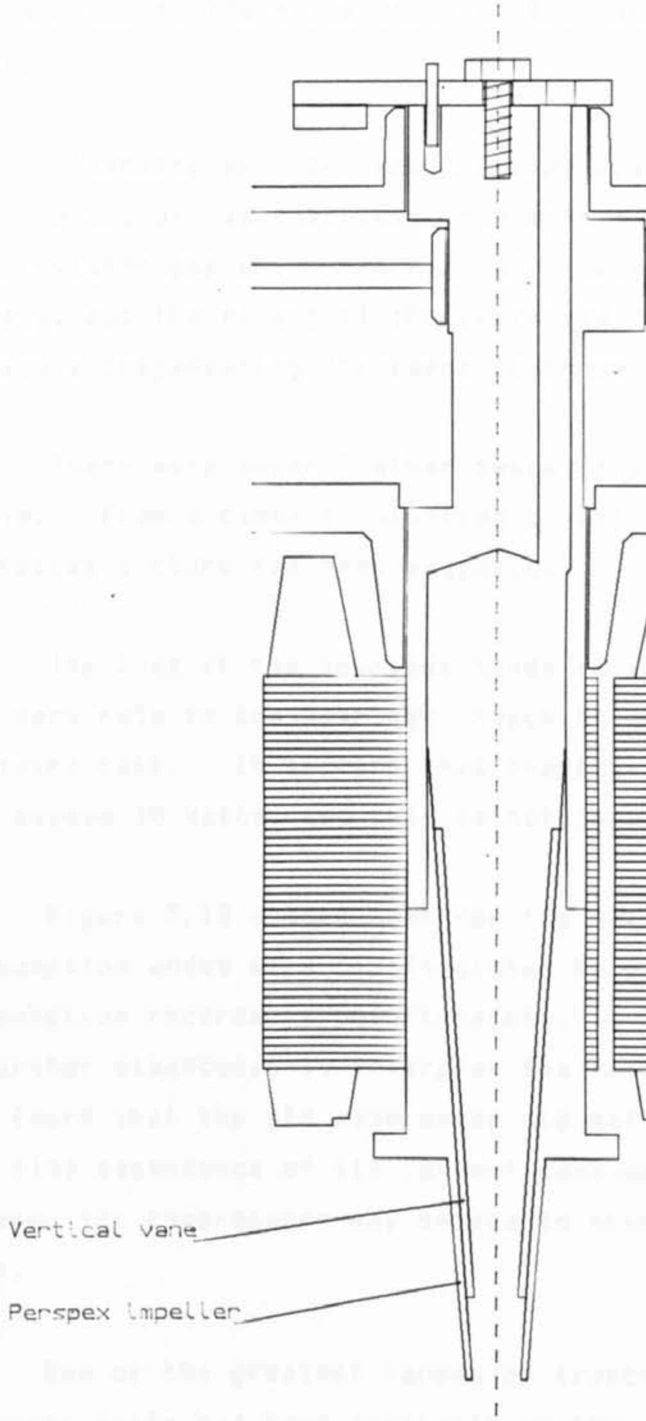

Figure 6.5. Perspex impeller fitted

interpretations are possible. It may be that for the unmodified compressor the rotor-stator gap does not retain enough oil to present a significant viscous loss, and that the test in question has produced the same power consumption because the supply to the bearings is as high as normal, due to the elimination of the shunt presented by the rotor's ducts.

Alternatively, the observations also support the suggestion that for the unmodified compressor there is a loss due to oil in the rotor-stator gap which has been eliminated by omitting the rotor's oil supply, but the effect of the increased oil supply to the bearings has caused a compensating increment in these other losses.

There were several other tests in addition to those explained above. From a close examination of all the results, the following, tentative picture has been suggested.

The loss at the bearings tends to increase with increasing oil delivery rate to the bearings, reaching an upper limit at a high delivery rate. It appears that the loss at the rotor - stator gap does not exceed 10 Watts, and this is not involved in the power step.

Figure 5.13 showed that for the new compressor the two power consumption modes were distinguished by clearly different current consumption records. Unfortunately, it was not possible to use this as a further diagnostic to interpret the tests described here, because it was found that the old compressor did not exhibit such a clear change in the time dependence of its current consumption. This difference between the compressors may be due to their different discharge systems (67).

One of the greatest causes of frustration is that if all the relevant facts had been available at the outset, instead of only being discovered half way through, more conclusive results could have been obtained.

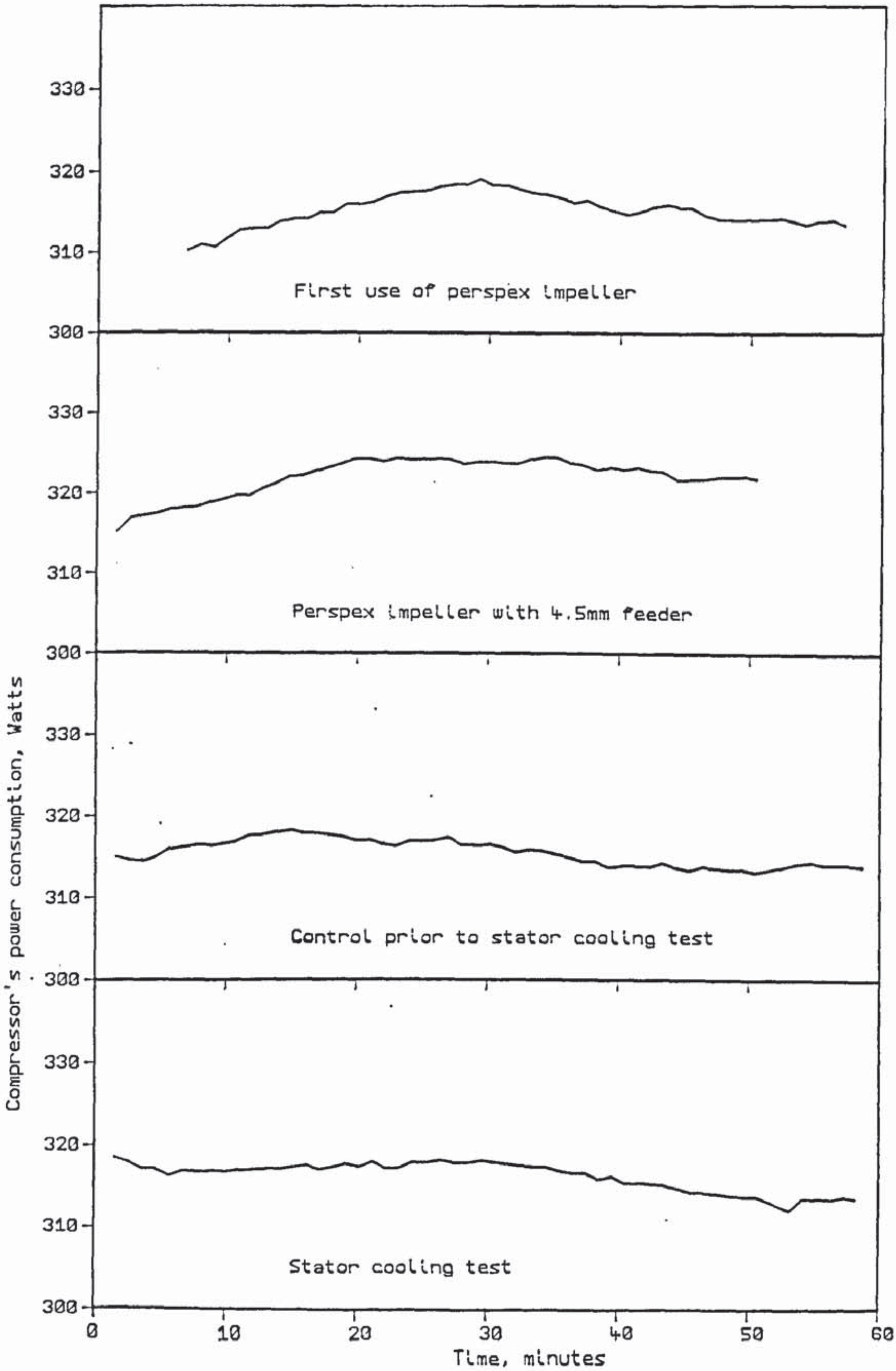

Figure 6.6 Experiments with the perspex impeller

6.8 Direct suction gas cooling of the stator

The observation of Danfoss' arrangement for spraying oil onto the stator's winding had raised the question of whether any performance improvement can result from cooling the stator.

Towards the end of January 1986, two plate heat exchangers were made, which were designed to be clamped onto the stator. Each heat exchanger was machined out of a rectangular block of brass 7 cm x 5 cm and 3 mm thick. Into one side of this block, 30 parallel grooves were milled, running in the short direction, so that when clamped onto the stator's core, it formed 30 vertical, rectangular section ducts, the stator itself forming one wall of each duct. These 30 slots were all joined together at the top, and supplied from a manifold. The heat exchangers' two manifolds were supplied in parallel from the suction stub using 8 mm plastic hose inside the can.

For the purpose of this experiment, the perspex impeller was particularly suited, because it does not stir the oil in the sump as much as Danfoss' original impeller.

On 26/1/86 the control trial was performed. This differed from the first use of the perspex impeller on two points. Firstly, the crankshaft's ducts had been blanked off at the top to prevent any oil spray from the top of the crankshaft. The other difference was that the plate heat exchangers had been attached to the stator, but had not been connected to the suction stub.

The resulting power consumption record is shown as the third record on figure 6.6. This reproduces the first trial quite well.

On 27/1/86 the trial of interest was performed, differing from the previous control only in having the plate heat exchangers connected. The power consumption record, shown last on figure 6.6, is practically unaltered.

It was found that using the stator heat exchangers made its resistance 0.5 ohm lower at the end of this trial than at the end of the control test. From the resistance measurements, winding temperatures of 66C and 48C were estimated. The discharge gas temperature and capacity were unaltered, which implies that the suction gas enthalpy increment before entry into the cylinder was also unaffected.

Apart from the winding resistance measurement, only two measurements showed any difference. There was a hint that the cooler stator resulted in an increase of about 15mA in the current consumption, and the sump oil temperature was brought down from 48C, for the control, to 43C for the cooled stator. These differences are both undesirable.

6.9 The free-running tests

In order to eliminate some of the problems of interpretation associated with the above tests, the new compressor was used with its cylinder head absent. These tests were performed in air, with a perspex cover replacing the top half of the can, in order to observe whether oil reached the top of the crankshaft's bores.

Half way through this investigation, it was realised that the purpose of the oil flow through the rotor ducts may be to cool the stator, and the idea was formed of estimating the stator's temperature by measuring its resistance at the end of a test. It was found that the stator's temperature is insensitive to the omission or inclusion of the flow through the rotor's ducts, but the oil temperature tends to be increased if the rotor duct flow is included. This question was more effectively and systematically investigated in the heat pump tests of October 1986, thus superseding this part of the free-running investigation.

However, there remain three results which are worth recording. On 8/1/86 a benchmark test was performed. This involved running the compressor from cold for an hour, while the oil temperature & power consumption were recorded. This was repeated on 9/1/86. At this stage, the compressor's lubrication system remained unaltered. In all these tests, the general behaviour was the same. The power consumption would start high, usually in excess of 200 watts. In the course of the run the power would fall, gradually approaching an asymptote, with increasing oil temperature. For the sake of making fair comparisons, quoted values of power consumption refer to an oil temperature of 60C.

For the first test and its repeat, power consumptions of 126 Watts and 121 Watts were recorded.

Later on 9/1/86 the first modification was tried. The outlets to the rotor's ducts were blanked off, and the effect of this modification was tested. This was repeated, without further change on 10/1/86. These tests resulted in power consumptions of 108 Watts & 111 Watts.

On 12/1/86 a second modification was introduced. An improvised centrifugal pump was set up, by the method of figure 6.6, but with a feeder internal diameter of 3.2mm, giving a flow cross section of just 8 mm^2. This resulted in a consumption of 100 Watts.

On 14/1/86 a feeder of 4.5 mm internal diameter was used, and this resulted in a consumption of 103 Watts.

According to data supplied by Danfoss (34), the motor's electrical loss is 70 Watts, when idling like this. The lowest observed power thus indicates a loss at the bearings of 30 watts. The effect of increasing the oil flow rate is to reduce the temperature of the oil in the bearing, and so increase the viscous loss at the bearings. This would account for the above observations. Finally, the 10 - 15 Watt reduction obtained solely by blanking off the rotor ducts is consistent with a viscous drag at the rotor-stator gap.

In the middle of March 1986 it was realised that an effective way to check this last point would be to set out deliberately to force oil into the rotor-stator gap, and see if this made the idling power requirement any higher than for the benchmark test.

During March the new compressor was totally stripped down and re-assembled. Since the idling power could not be assumed to have been unaltered by this work, the benchmark test was repeated on 24/3/86 and a power consumption of 131 watts was recorded. Then, the stator was unbolted, and nylon string was wound round and round the top of the stator winding, to make it impossible for oil sprayed from the rotor to drain down the outside of the stator. The idea was to make sure that all the oil sprayed out by the rotor would be forced down into the rotor-stator gap. This was tested later on 24/3/86, and the power consumption was, again, 131 watts.

These idling tests thus seem to make sense. They indicate an upper limit on rotor-stator drag of 20 watts, and seem also to support the direct relationship between oil delivery rate and mechanical losses.

From the geometrical specifications of the journal bearings, it has been estimated that, for pure hydrodynamic lubrication, the viscous loss in Watts is given by 4x the lubricant viscosity in centipoise. The lowest observed loss of 30 watts thus implies an oil viscosity of 7.5 centipoise. From the known temperature dependence of Alkylbenzene's viscosity this implies a bearing temperature of 73C. i.e. For the low oil delivery rate the bearings are 13C hotter than the sump. At the high oil delivery rate, the 40 Watt loss implies a bearing temperature of 63C - just 3C hotter than the sump. This effect of oil supply rate on the bearings' temperature was also considered by Cameron (68).

Since the power reduction obtained by reducing the oil supply rate is merely the result of thinner oil at the higher bearing temperature, one recognises that this incurs the penalty of a reduced safety margin against the failure of hydrodynamic lubrication. This may be the reason for the persistance of the high power mode during the first tests to use the improvised centrifugal pump. The only potential which exists to reduce losses without incurring such a penalty is the elimination of the rotor-stator viscous drag. However, it appears that for normal operation, working in a refrigerant atmosphere, this loss is less significant than that observed in the free running tests.

For oil in equilibrium with an R12 atmosphere there is an optimum temperature for which the viscosity is maximised, below which the effect of the increasing liquid R12 fraction more than offsets the tendency of the oil viscosity to increase. The observation of a persistent high power mode on the occasion of the sump baffle test may thus be consistent with the bearing temperature having been held down by the resulting high oil flow rate.

Chapter 7. Heat pump tests of 1986

7.1 Oil temperature test

Searching for the power step

Figures 7.1a & b show oil temperature & power against time for the run of 15/2/86. The oil temperature was steadily increased during this test. Unfortunately, as one can see from the plot of power consumption, no transition between modes has occurred, so that it has not been possible to categorically support or refute either of the proposed explanations suggested in chapter 4.

If a higher discharge pressure had been used, it might have been possible to precipitate the transitions of interest. The conservative choice of discharge pressure, about 9.7 Bar absolute, had been borne of concern that had too high a discharge pressure been chosen, the high power mode might have been permanent, so that there would have been no diagnostic transition with which to distinguish the modes. It is just unfortunate that this choice of discharge pressure has been too conservative.

This test was not repeated at a higher discharge pressure, because at the time of its execution, it was only the question of condensation in the cylinder that had been considered. This test's potential relevance to the power step problem was not realised until much later.

Figures 7.2a, b & c show the compressor power consumption plotted against oil temperature, and the breakdown into minimum work & losses, calculated by the method described in section 4.6. The wide scatter shown on figures 7.2b & c is probably due to the variability of the output from the condenser's Pelton wheel flowmeter. However, one can pick out the median trend by eye, and see that the compressor's efficiency is improving with increasing temperature. This demonstration makes the common practice of routing the discharge gas through the sump heat exchanger more understandable.

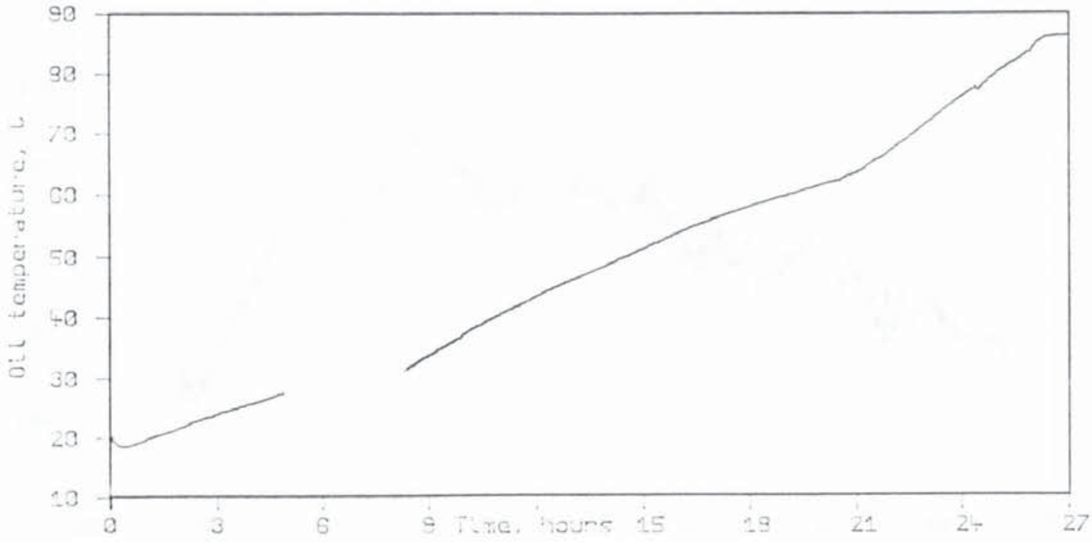

Figure 7.1a. Oil temperature history. 15/2/86

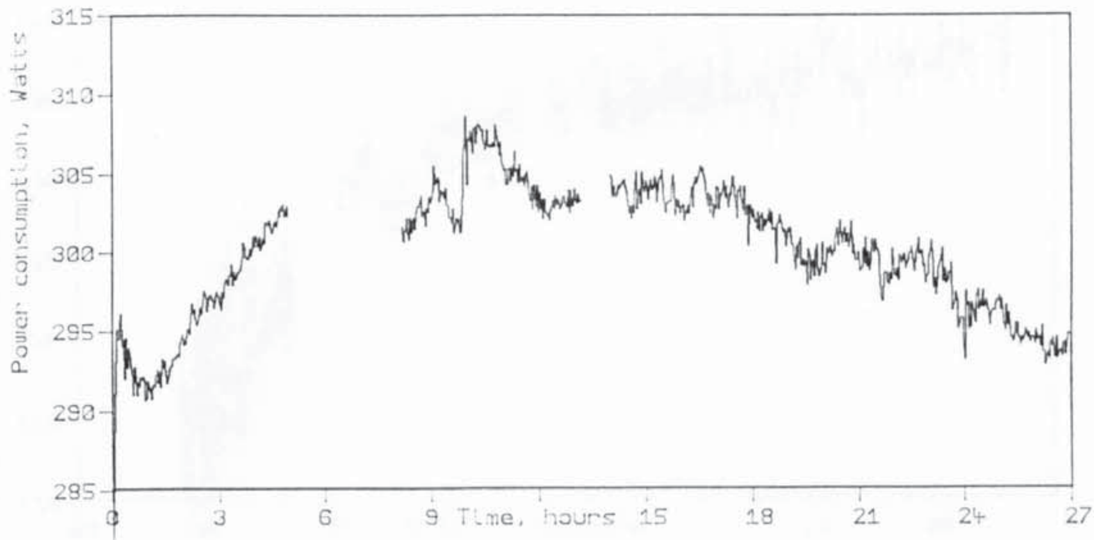

Figure 7.1b. Compressor power history. 15/2/86

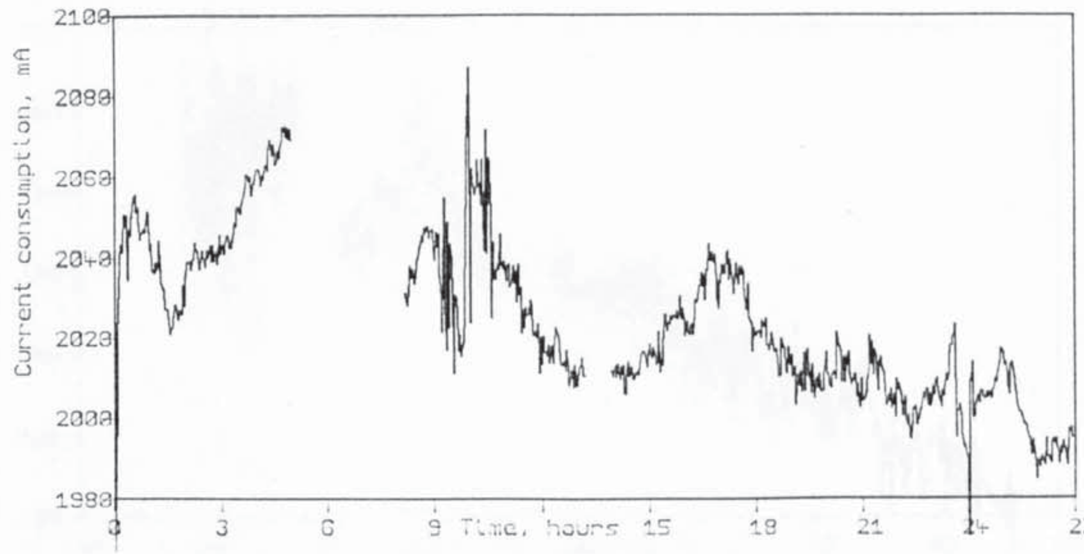

Figure 7.1c. Current consumption history. 15/2/86

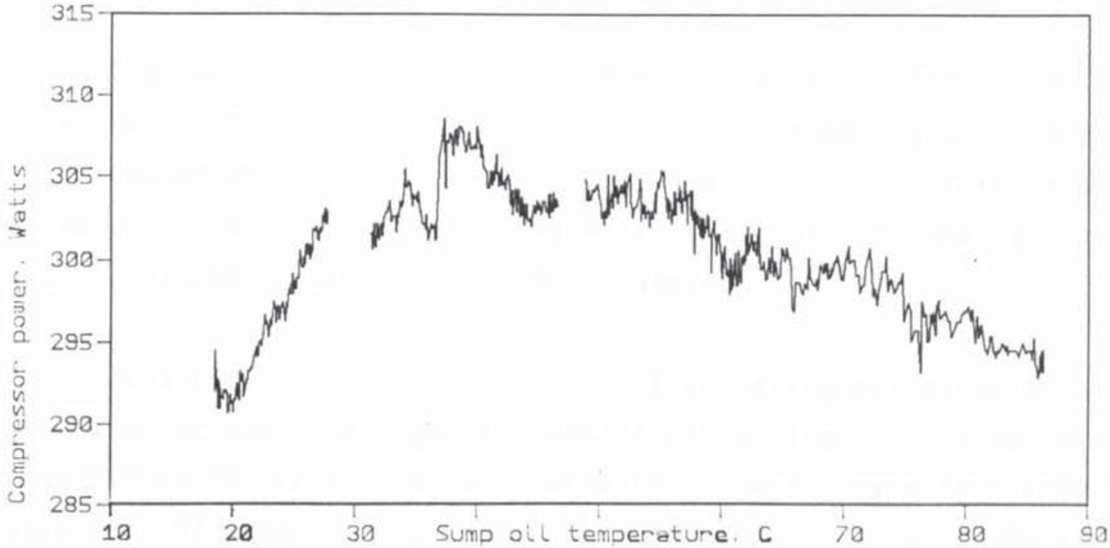

Figure 7.2a. Temperature dependence of compressor power

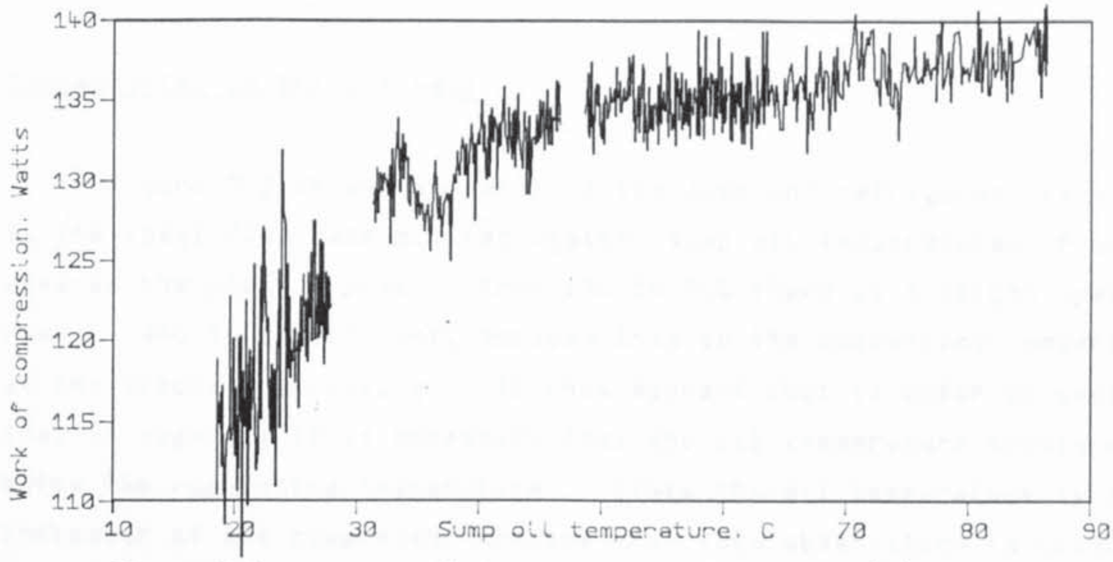

Figure 7.2b. Minimum power requirement. 15/2/86

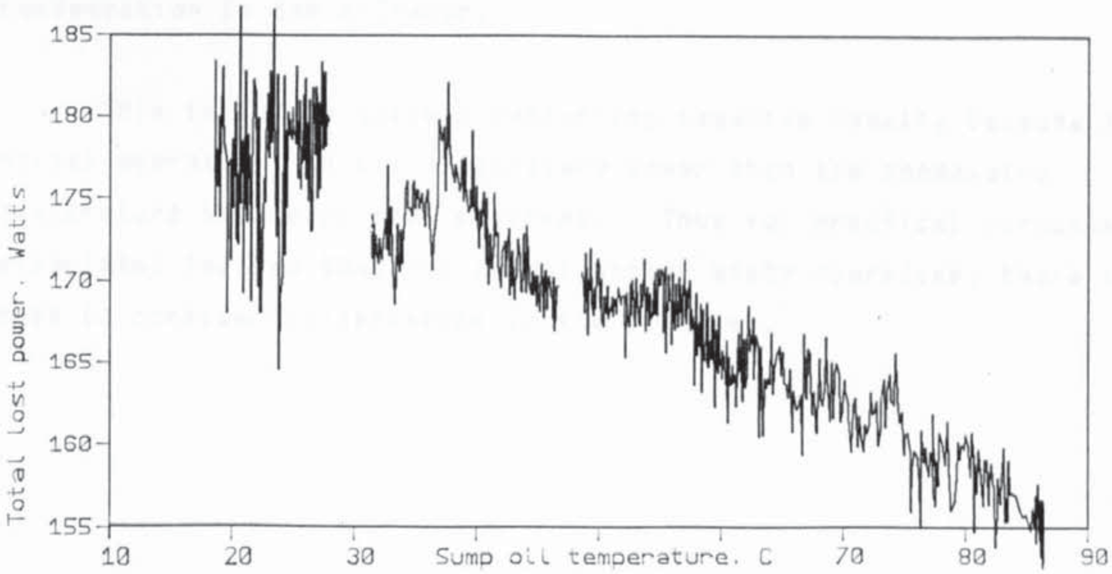

Figure 7.2c. Temperature dependence of compressor losses

Current consumption

Figure 7.1c shows current consumption against time. As anticipated, there is a downward trend with increasing oil temperature. The scatter on this plot is mainly caused by variations in mains voltage. This has been ascertained by inspection of the raw data, which includes a record of mains voltage.

At a power consumption of 300 Watts, having picked data recorded at a similar mains voltage, the effect of raising the oil temperature from 20C to 80C is to produce a drop in current consumption from 2.05 Amps to 1.99 Amps. This result is qualitatively as anticipated, and shows a reassuringly small sensitivity to temperature.

Condensation in the cylinder

Figure 7.3 shows the ratio of the apparent refrigerant flow rate to the ideal flow rate plotted against sump oil temperature. From 40C upwards the plot is flat. From 15C to 40C there is a slight upward ramp. 40C is significant, because this is the condensing temperature at the discharge pressure. It thus appears that in order to avoid a loss of capacity it is necessary that the oil temperature should not be below the condensing temperature. Since the oil temperature is an indicator of the compressor temperature, this observation is consistent with the small loss seen at the lowest temperatures being the result of condensation in the cylinder.

This is really quite a comforting negative result, because in normal operation, an oil temperature lower than the condensing temperature has never been observed. Thus for practical purposes, this experiment implies that for normal steady state operation, there is no need to consider condensation in the cylinder.

Sump lubricant composition and subcooling

As explained in chapter 4, the purpose of the initially low sump temperature was to obtain a high refrigerant fraction in the lubricant. However, the inevitable consequence of contriving to get a significant amount of refrigerant mixed into the sump oil is to make less refrigerant available to the rest of the circuit. This raised the possibility that there would be no surplus refrigerant available to ensure complete liquid filling of the subcooler. The subcooler is the last two metres of the condenser, downstream from the accumulator, immediately before the expansion valve. Ordinarily, the refrigerant charge is chosen to ensure liquid in the accumulator, and so ensure liquid filling of the condenser's last two metres.

Figure 7.4 shows the R12 liquid temperature at the end of the condenser as a function of sump oil temperature, with the corresponding condenser water entry temperature superposed. The pressure at the condenser's end was never lower than 8.5Bar, absolute. At this pressure liquid - vapour equilibrium occurs at 35C. Since the highest recorded R12 condenser end temperature was 24C, it follows that the liquid was always subcooled. It has been necessary to check this point because, without liquid subcooling, the condenser end enthalpy is indeterminate. Thus, for validity of the calculated R12 flow rate, one requires subcooling to have occurred.

The condenser water supply temperature was steady around 9.5C throughout the test, and one can see that the subcooled R12 - water entry temperature difference approaches a steady value of about 3K for oil temperatures in excess of 25C. At the lowest oil temperature, the liquid filling of the subcooler increases with increasing oil temperature, due to the sump's reduced share of the refrigerant charge. With increasing liquid fill of the subcooler, the condenser end liquid R12 can more closely approach the water entry temperature. This dependence on oil temperature persists until the subcooler is full, at which point any further release of refrigerant from the sump merely increases the charge in the accumulator. From figure 7.3, this state appears to have been reached at an oil temperature of around 25C.

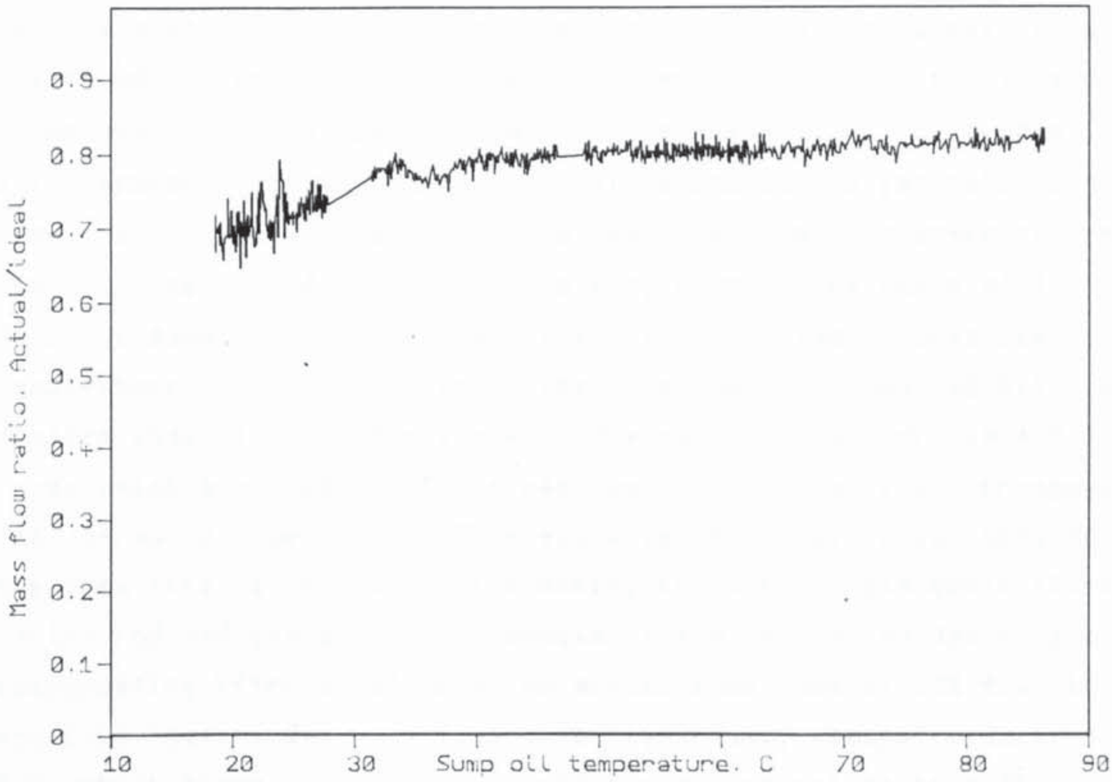

Figure 7.3. Mass flow efficiency v oil T

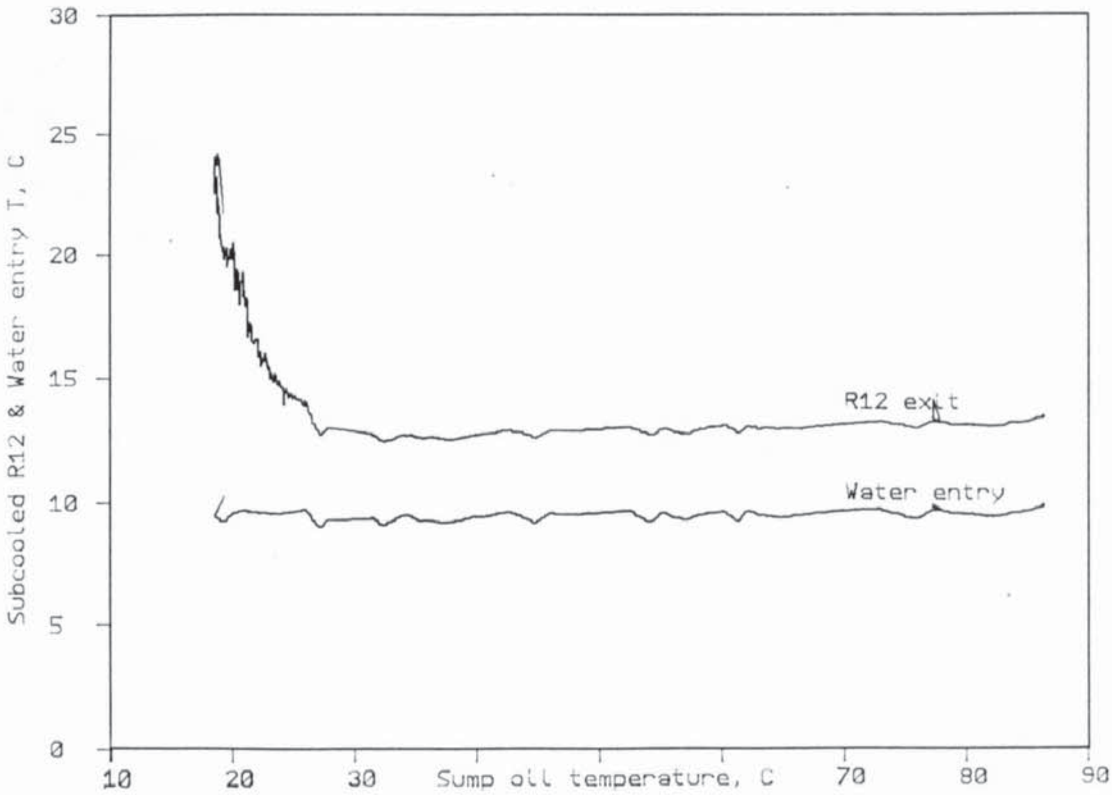

Figure 7.4. R12 subcooling. Dependence on oil T.

R12 flow rate dependence on compressor temperature

In section 4.6 it was explained that an estimate for the cylinder gas state at BDC can be found by assuming the suction pressure, and the discharge gas entropy. Figure 7.5 shows 'Tbdc' and the discharge temperature plotted against sump oil temperature. The correlation with oil temperature is inescapable. This supports the generally accepted view that the suction gas picks up heat from the compressor before reaching the cylinder. Over the sump temperature range of 40C to 80C, Tbdc increases from 25C to 60C, i.e a 12% increase in absolute temperature. Figure 7.6 shows the experimentally deduced R12 flow rate plotted against oil temperature. One can see that for the 40C to 80C range which produced a 12% increase in Tbdc, there is a corresponding fall of 8% in flow rate. This supports the simple understanding that the flow rate is reduced by increasing the suction gas temperature, due to the reduced gas density. However there is also evidence of other compensating effects reducing the anticipated loss of 12% down to an observed loss of 8%. This is more rigourously demonstrated in figure 7.3, which shows a very slight upward ramp, amounting to a 3% increase in the ratio of observed to ideal R12 flow rate, for the sump temperature range of 40C to 85C.

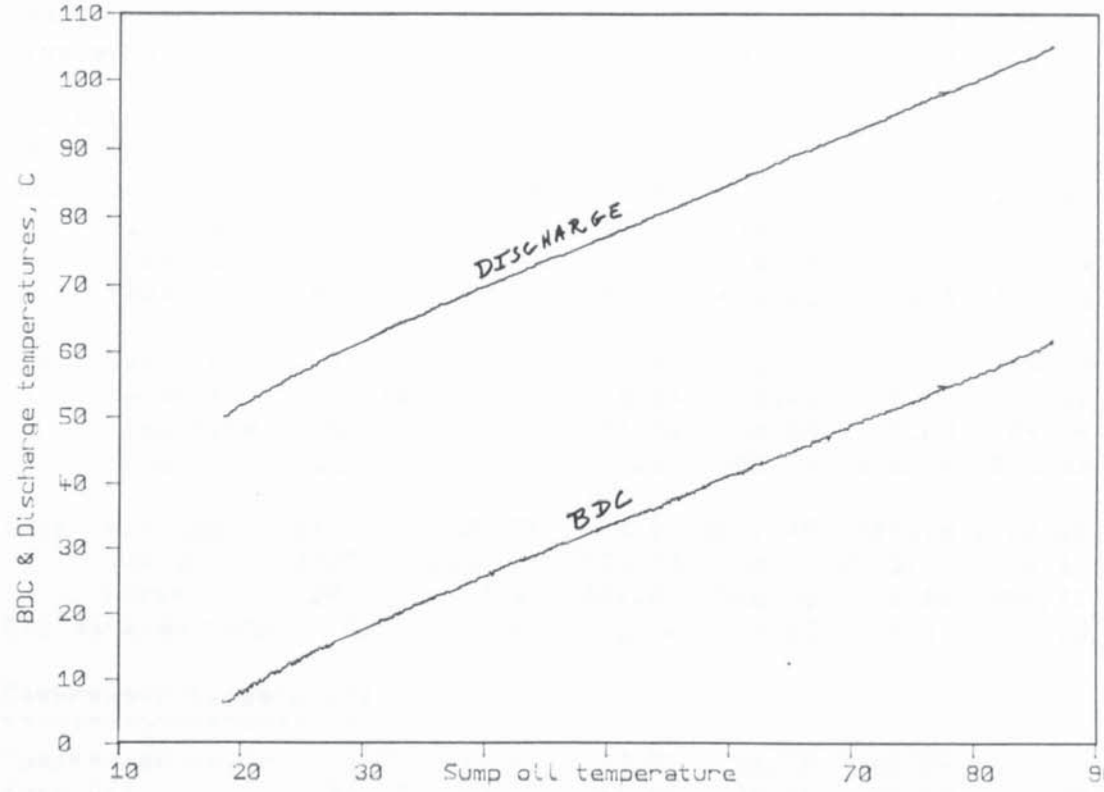

Figure 7.5. Cylinder temperatures v oil T

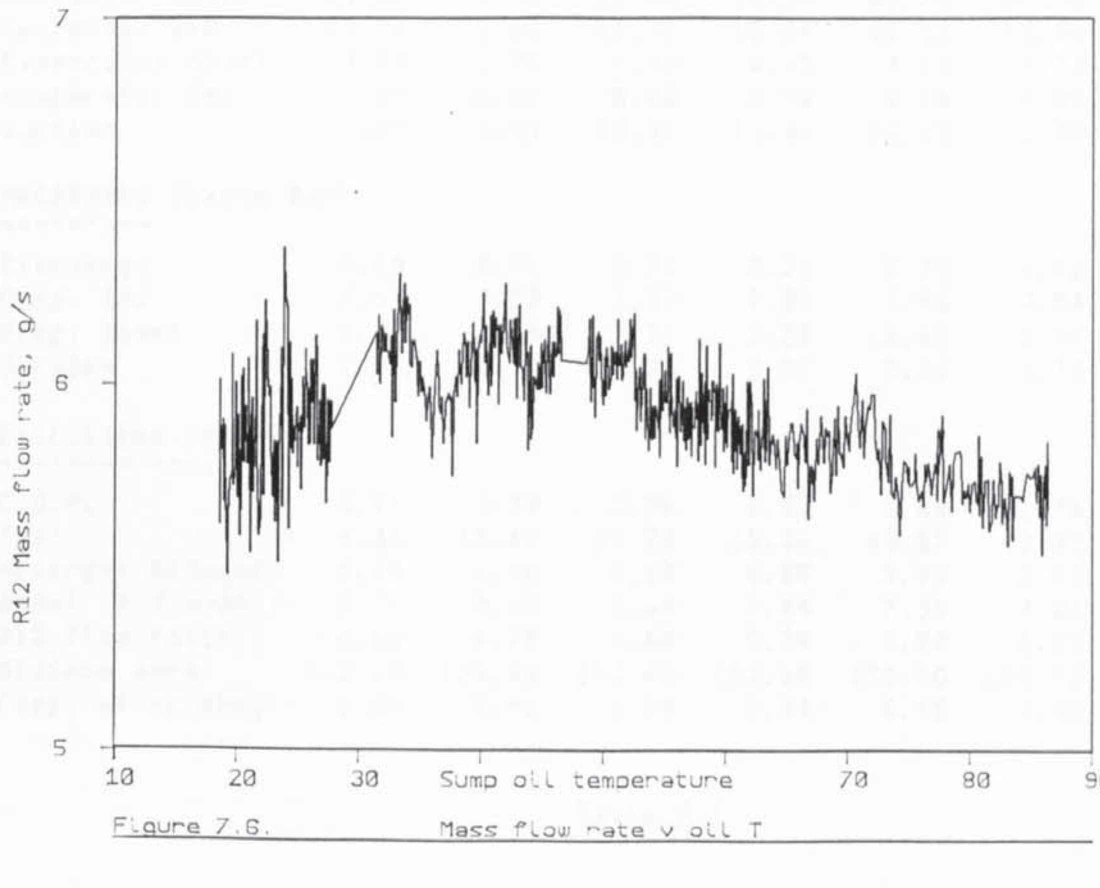

Figure 7.6. Mass flow rate v oil T

15/2/86 Oil temperature test specimen datasets

Filename :1.ALL_OTT

Index	100.00	300.00	500.00	700.00	900.00	1100.00	1300.00
Time mins	315.18	515.17	905.83	1151.59	1351.59	1551.70	1752.79
PERFORMANCE							
Cond. water in	9.71	9.36	9.60	9.64	9.64	9.65	9.53
water out	43.25	43.84	45.22	46.37	47.06	47.98	49.66
flow rate	6.48	7.02	7.27	6.99	7.04	7.04	6.72
Power	909.48	1013.40	1083.16	1075.21	1103.24	1129.16	1128.88
Evap. water in	13.02	13.31	13.42	13.21	13.17	13.13	12.86
water out	8.68	8.40	8.81	8.88	8.94	9.00	8.91
flow rate	47.46	43.46	47.26	48.84	49.60	49.14	48.79
Power	860.57	892.94	912.51	885.88	878.44	850.06	807.89
Comp. Voltage	2791.10	2823.20	2774.20	2801.45	2785.15	2788.85	2799.50
Current	2027.82	2069.21	2023.74	2024.37	2015.70	2004.46	1998.75
Power	292.50	302.12	304.01	302.92	301.40	300.42	294.29
R12 metered rate	5.91	5.57	5.60	5.62	5.31	5.28	5.09
Compressor temperature							
Compressor water	3.97	11.05	32.57	48.35	58.28	71.73	91.86
Sump Oil	21.13	27.79	41.91	52.76	59.52	68.38	82.56
R12 TEMPERATURES							
Discharge	52.99	59.67	71.17	79.34	84.50	91.21	102.23
Condenser Start	53.09	58.54	69.05	76.60	81.38	87.52	97.53
Condenser End	17.26	13.10	12.92	13.04	13.11	13.18	13.16
Evaporator Start	3.93	3.96	4.44	4.45	4.74	4.78	4.48
Evaporator End	9.26	8.07	8.48	8.96	8.45	9.05	9.35
Suction	9.87	9.51	10.81	11.86	12.03	12.90	14.16
PRESSURES (gauge Bar)							
Discharge	8.65	8.71	8.71	8.71	8.72	8.73	8.71
Cond. End	7.64	7.83	7.86	7.89	7.90	7.94	7.99
Evap. Start	2.27	2.25	2.27	2.28	2.32	2.34	2.31
Suction	2.26	2.25	2.26	2.27	2.31	2.33	2.30
Calculated results							
C.O.P.	3.11	3.35	3.56	3.55	3.66	3.76	3.84
Tbdc	9.31	15.65	27.24	35.38	40.87	47.59	58.09
Apparent R12mdot	5.65	6.00	6.12	5.89	5.93	5.93	5.71
Ideal R12 mdot	8.31	8.03	7.67	7.44	7.39	7.26	6.93
R12 flow ratio	0.68	0.75	0.80	0.79	0.80	0.82	0.82
Minimum work	112.68	124.48	133.40	132.68	135.00	137.92	138.90
Comp. efficiency	0.39	0.41	0.44	0.44	0.45	0.46	0.47

Table 7.1

7.2 Dis-assembly and re-assembly of the new compressor

In order to dis-assemble the crankshaft and piston from Danfoss' SC10H, it is first necessary to remove the rotor from the crankshaft. This is difficult, because it seems that Danfoss shrink fit the rotor onto the crankshaft. This difficulty was overcome, and the new compressor was fully dis-assembled, as seen in figure 5.15.

In order to facilitate subsequent dis-assembly and re-assembly, a male thread was cut on the crankshaft, and a corresponding female thread was cut inside a mild steel sleeve. The rotor was then bored out to the outer diameter of this sleeve. The sleeve was then pressed into the rotor. A new impeller was made up which screwed into the open end of the rotor's threaded insert. By tightening this against the end of the crankshaft, the thread could be locked. See figure 7.7a & b.

It was not clear whether this modification to the rotor would aggravate its losses. Figure 7.8 shows that in boring out the rotor to accomodate this insert, the hole in the rotor has just been opened up sufficiently to breach the rotor's oil ducts. It is not obvious that enough of the magnetic field gets past these ducts for the presence of this solid steel insert to cause an eddy current loss. This observation raises the possibility that one of the purposes of these ducts has been to reduce the eddy current loss associated with the shrink fit onto the crankshaft, by reducing the strength of the field at the crankshaft. If this consideration influenced the design, then it begs the question of whether such a reduction in eddy current loss can offset the additional penalty caused by the reduced cross-section of steel available to carry the magnetic flux across the rotor.

After re-assembling the compressor, several tests were performed to see whether this modification had altered the motor's performance. Upon comparing the results with previous tests, there appeared to be no evidence of any change. However, in the course of making these measurements, it was found that the condenser water flow measurement had become unacceptably unreliable, and for this reason presentation of data justifying this claim is deferred to a discussion of tests which included a more reliable condenser water flow rate measurement.

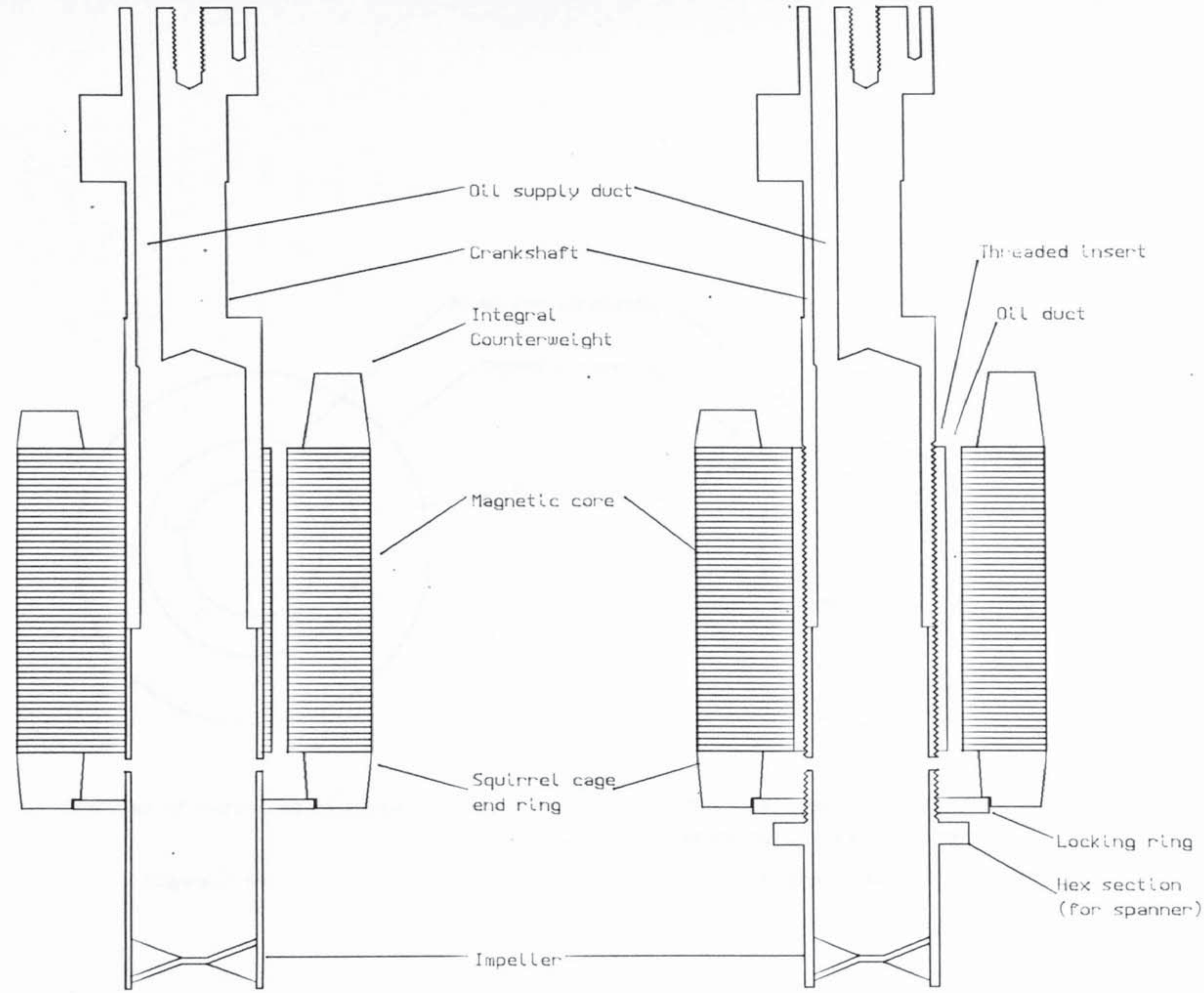

Figure 7.7a. Crank assembly, as received

Figure 7.7b. Modified crank assembly

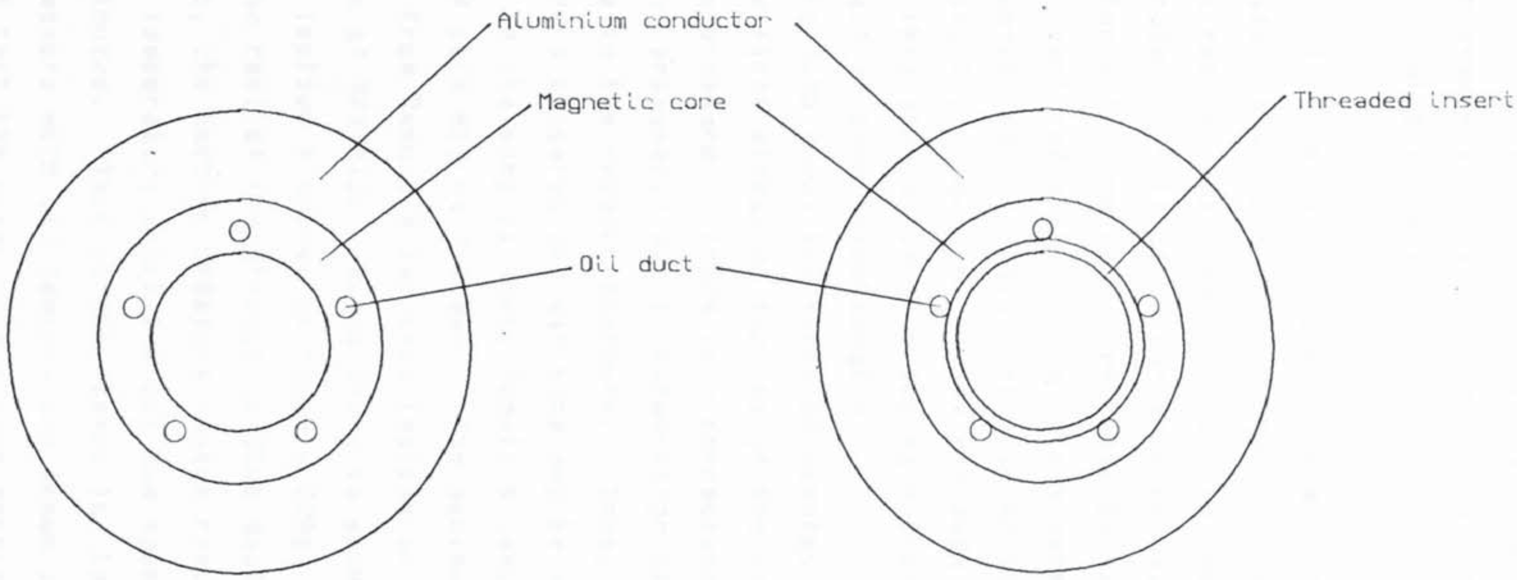

End view of rotor, as received

Figure 7.8a

Modified rotor end view after pressing in threaded insert

Figure 7.8b

On 18/4/86 the first attempt was made to increase the range of discharge pressure studied. As explained in chapter 4, the discharge pressure measurement was lost. However, on the basis of the recorded pressure at the condenser's end, it has been possible to estimate the discharge pressure as 14 bar, gauge. This has been used to obtain the calculated results in table 7.2.

Figure 7.9a shows the power consumption, evaporating pressure and oil temperature histories for this test. In spite of the high discharge pressure, the transition to the low power mode occurs after only 15 minutes. This is in marked contrast to the run of 14/7/85, for instance, for which the high power mode persisted for almost 10 hours. This significant reduction in the persistence of the high power mode seemed to co-incide with this first use of the new compressor after re-assembling it. However, it has not been possible to determine the reason for this change, because too many things all changed at the same time, not all of them intentionally.

Figure 7.9b shows the first 30 minutes on a greatly expanded time axis. The first effect of turning on the compressor was to lower the suction gas pressure. There is a corresponding drop in the sump oil temperature, presumably due to evaporation of the dissolved refrigerant in response to the reduced pressure. Thus, at the minimum temperature and pressure a conservative estimate may be obtained for the mass of liquid R12 in the sump by using Raoult's law. At 18C the vapour pressure of pure R12 is 5.3 Bar. The minimum suction pressure is about 3.6 Bar. From Raoult's law this implies an equilibrium molar composition of 2/3 R12. Since there is about 2 moles of oil in the sump, this implies 4 moles, or roughly 500g, of liquid R12 in the sump. Because the rest of the circuit is thus depleted of this 500g of refrigerant, the suction pressure cannot reach the value permitted by the source temperature until the oil has been boiled out, which took about 15 minutes. This is the reason for the correlation of the suction pressure with oil temperature shown in figure 7.9b. It is also significant that the power consumption apparently drops to the low power mode in response to the boiling out of the oil.

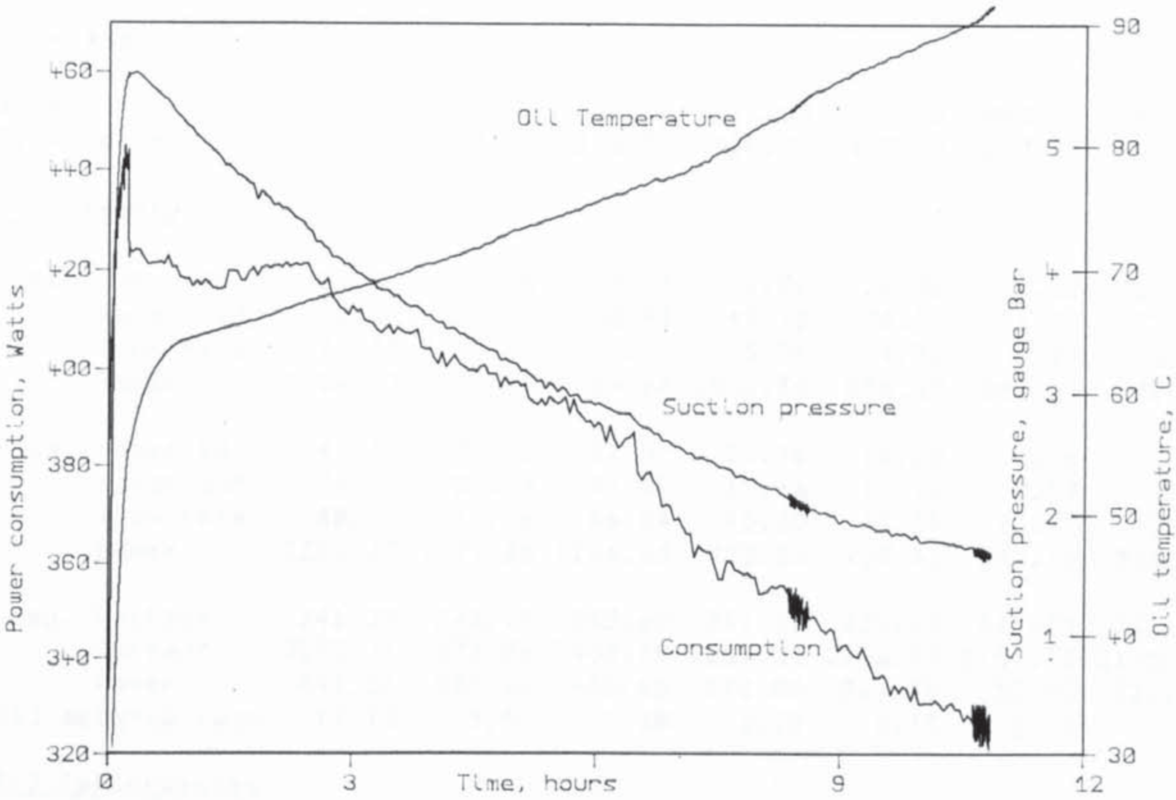

Figure 7.9a 18/4/86 High pressure test

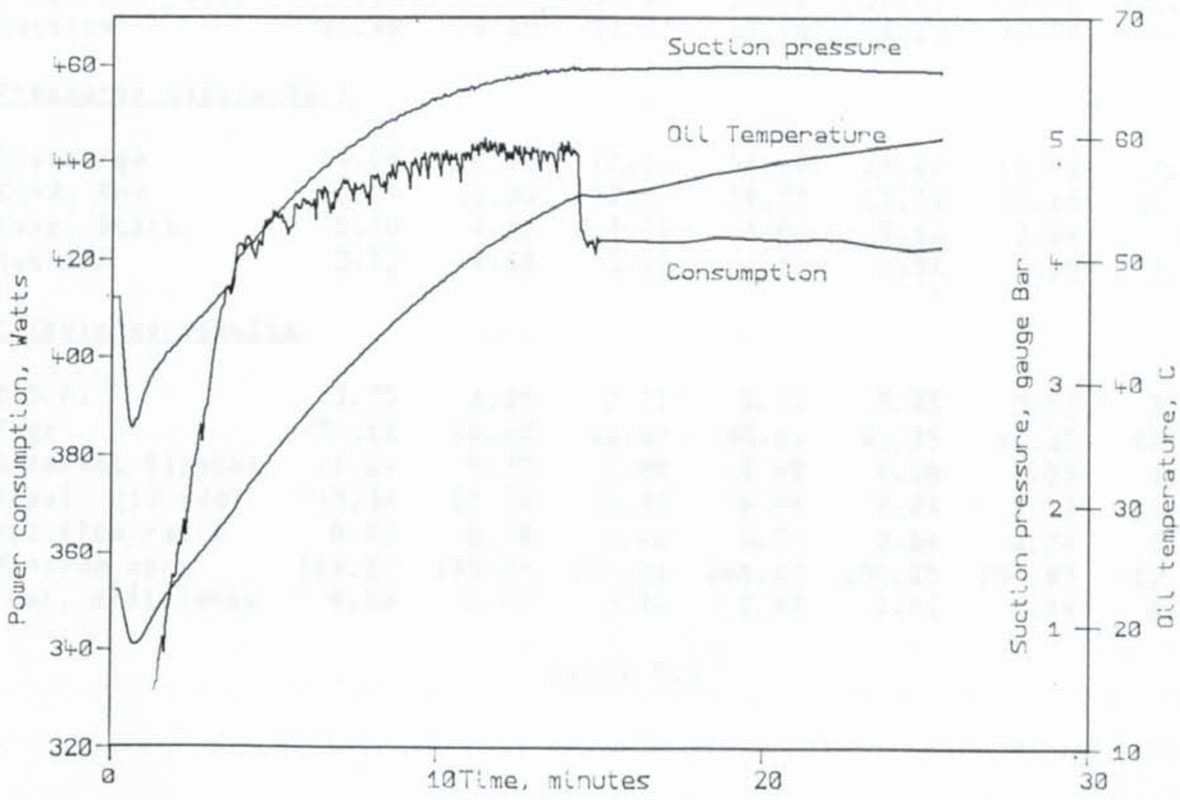

Figure 7.9b 18/4/86 High pressure test

18/4/86 Specimen data sets for first test of discharge P > 200psia

Filename	:3.HiPress						
Index	200.00	390.00	500.00	610.00	700.00	890.00	1155.00
Time, mins	9.98	105.40	216.93	328.03	420.08	507.03	591.74
Performance							
Cond. water in	25.27	18.88	19.97	20.26	20.06	20.63	21.29
water out	63.53	68.11	68.99	69.75	70.79	71.72	72.13
flow rate	10.33	7.93	6.77	5.24	4.22	3.94	3.68
Power	1654.37	1634.54	1389.64	1086.50	896.80	842.53	782.36
Evap. water in	42.10	34.45	27.02	20.48	14.88	9.26	5.33
water out	34.50	27.34	21.07	15.66	10.95	5.99	2.44
flow rate	48.72	47.78	46.84	45.80	44.30	43.72	42.50
Power	1548.63	1421.25	1166.65	923.83	728.61	597.16	514.51
Comp. Voltage	246.23	243.18	242.62	241.50	238.93	241.23	242.81
Current	2572.11	2473.89	2408.39	2287.31	2196.19	2151.35	2105.13
Power	441.36	420.66	408.15	393.50	369.38	353.02	333.46
R12 metered rate	12.73	9.50	7.28	6.30	5.10	5.36	0.02
R12 Temperatures							
Sump Oil	47.92	65.88	69.78	74.27	77.74	83.48	87.95
Discharge	75.67	90.97	96.42	101.25	104.55	108.73	112.22
Condenser Start	75.03	89.39	93.92	97.53	99.86	102.76	104.75
Mid Condenser	53.80	56.23	58.05	58.97	59.53	59.73	59.94
Condenser End	48.44	35.86	26.88	24.17	23.85	24.05	24.69
Evaporator Start	25.52	21.49	15.67	10.75	6.61	2.42	-0.14
Evaporator End	40.44	27.53	20.89	15.34	10.97	6.18	2.88
Suction	40.48	28.00	21.38	17.16	14.02	11.89	10.78
Pressures (gauge Bar)							
Discharge	14.00	14.00	14.00	14.00	14.00	14.00	14.00
Cond. End	10.79	11.85	12.81	13.29	13.50	13.64	13.71
Evap. Start	5.40	4.72	3.78	3.08	2.56	2.09	1.84
Suction	5.32	4.68	3.75	3.07	2.56	2.10	1.84
Calculated results							
C.O.P.	3.75	3.89	3.41	2.76	2.43	2.39	2.35
Tbdc	37.16	48.45	46.86	45.62	43.79	42.67	42.76
Apparent R12mdot	11.87	9.98	7.88	5.98	4.88	4.53	4.19
Ideal R12 mdot	15.34	12.78	10.35	8.59	7.34	6.20	5.54
R12 flow ratio	0.77	0.78	0.76	0.70	0.66	0.73	0.76
Minimum work	194.62	198.34	189.21	165.60	150.25	154.83	152.68
Comp. efficiency	0.44	0.47	0.46	0.42	0.41	0.44	0.46

Table 7.2

7.3 Siting of the liquid reservoir

A set of three tests was performed on 20,21 & 22/4/86, whose purpose was to demonstrate how the subcooling depends on the siting of the liquid accumulator, and on the refrigerant charge.

It was with these three tests that the practice was adopted of making manual measurements of the condenser water flow rate, using a stopwatch, and a flask of known volume.

Effect of insufficient R12 charge

On 20/4/86 data was recorded in the normal way at a nominal evaporator water flow rate of 20cc/s, and a condenser water flow regulator setting of 4 The liquid accumulator was sited 2m. upstream from the condenser's end, as usual. However, throughout the run no liquid was ever visible in the accumulator, showing that the 2 phase - subcooling boundary was downstream from it. Figure 7.10a shows, plotted against evaporating temperature, the R12 exit temperature, and the condenser water entry temperature. For a long subcooling length, the liquid R12 temperature would closely approach the water entry temperature.

This plot shows that there was no subcooling until the evaporating temperature had fallen below 14C. Over the range from 20C to 14C evaporating temperature, the refrigerant flow rate falls, which results in a lower pressure drop in the condenser. The resulting rise in the pressure at the condenser's end accounts for the rise in condenser end temperature down to 14C evaporating. With further fall in the evaporating temperature, subcooling became possible due to the falling mass of refrigerant in the evaporator, making more refrigerant available to the condenser, so permitting a partial liquid fill of the subcooler.

Having thus obtained a demonstration of the effect of insufficient refrigerant charge, on 21/4/86 the test was repeated, but only after adding a further 140g of R12 to the rig. A few minutes after starting, liquid was first visible in the accumulator, and from then till the end of the run the accumulator was never empty. Figure 7.10b presents the plot of the condenser end temperatures corresponding to figure 7.10a.

It is evident from these two plots that the increased refrigerant charge has allowed more effective subcooling of the liquid. From the observed presence of liquid in the accumulator, it is obvious that the increased refrigerant charge has resulted in the complete liquid fill of the 2m of condenser downstream from the accumulator, and it is this increase in the subcooling length that has resulted in the closer approach of the condensed refrigerant to the water entry temperature.

Effect of accumulator position

Having obtained this demonstration of the dependence of subcooling on the liquid-filled length, the obvious next step was to reset the accumulator's valves to put it at the end of the condenser. Thus on 22/4/86 the previous run was repeated, save for this one difference. Figure 7.10c shows the condenser end temperatures as before. It is clear that effective subcooling has not occurred. By siting the accumulator at the condenser's end, in this way, it is not possible to have any liquid fill at the end of the condenser, unless the accumulator fills completely. This position of the accumulator thus makes effective subcooling of the condensate impossible.

In conclusion then, it would appear to be desirable always to include a dedicated subcooler downstream from the accumulator, before the expansion valve. In order for this to work effectively, the refrigerant charge should be chosen to ensure the presence of liquid in the accumulator.

Sample data sets from these tests are presented in tables 7.3, 7.4 & 7.5. At each test, 4 manual measurements were made of the condenser water flow rate, and the result of using this measurement is shown in the last four columns of each of these tables. The first three columns show the results implied by the pelton wheel flowmeter. One can see by inspection that the manual measurement results in a good reproducibility of the calculated compressor efficiency, and R12 flow ratio, both showing a monotonic downward trend with falling suction pressure. By contrast, the pelton wheel measurement produces erratic and potentially misleading results for the compressor's performance.

The test of 21/4/86 was a repeat of the test of 14/7/85, the very first use of the new compressor. Sample data sets are presented in table 7.6. By comparing the compressor's performance figures, one can see that there is no evidence of the modification to the rotor having increased the losses.

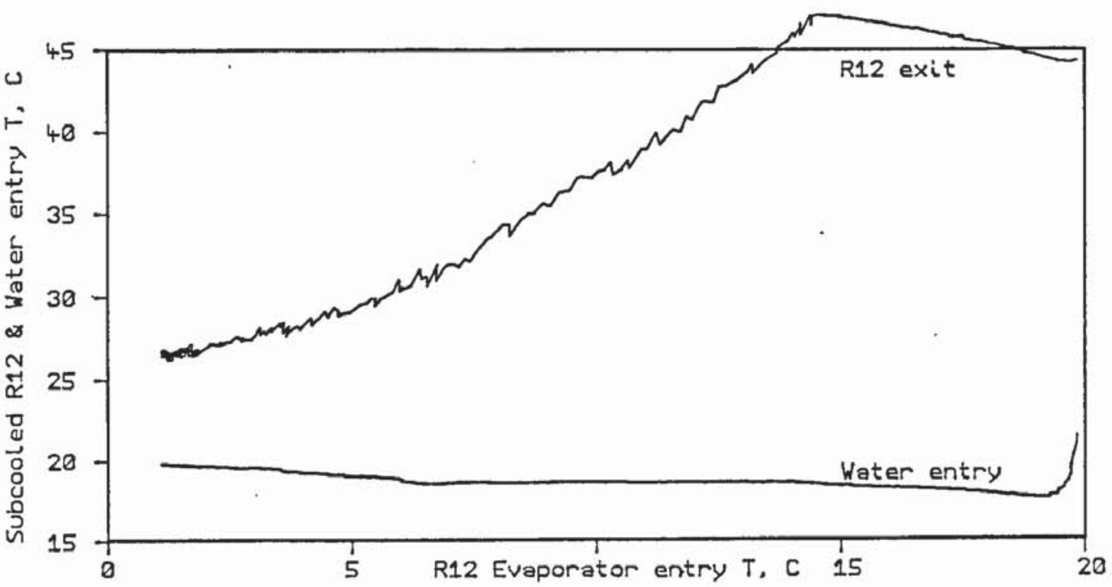

Figure 7.10a. Insufficient R12 charge

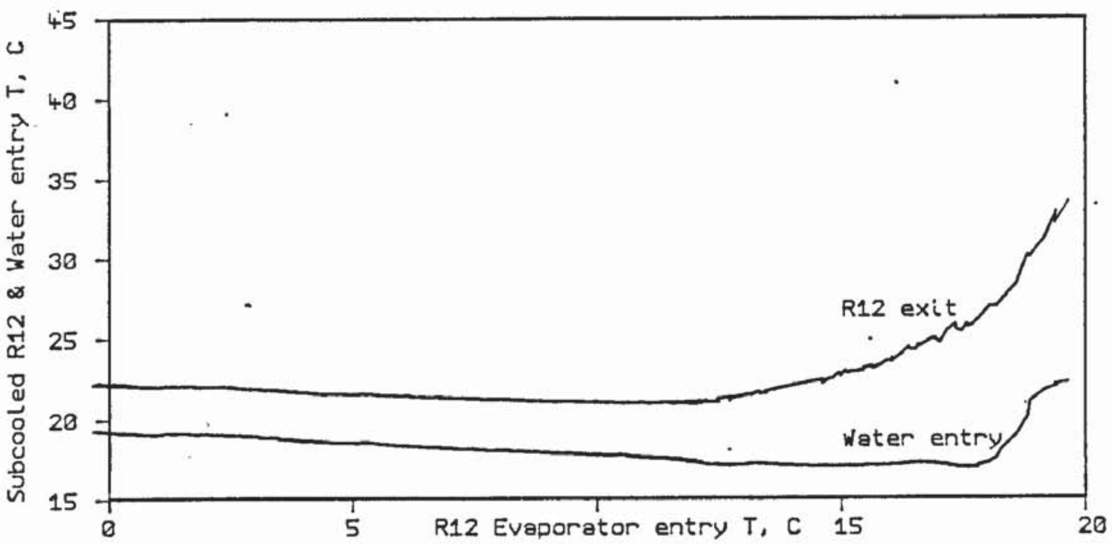

Figure 7.10b. 140g R12 added

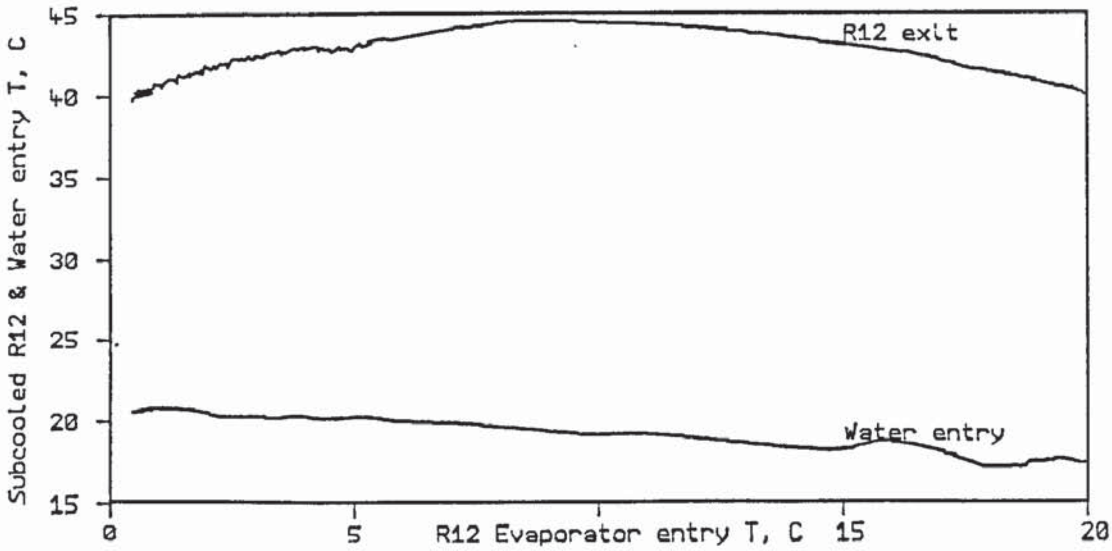

Figure 7.10c. Accumulator at condenser's end

20/4/86 Insufficient R12. Specimen data sets. (Rebuilt new compressor)

Filename :3.P.20046

In this table the use of the condenser water flowmeter measurement is compared with a manual measurement of the flow rate.

	Flowmeter's result			Manual measurement			
Index	570.00	675.00	735.00	570.00	635.00	675.00	735.00
Time, mins	300.45	406.18	466.18	300.45	365.45	406.18	466.18
Performance							
Cond. water in	18.68	19.03	19.54	18.68	18.66	19.03	19.54
water out	62.05	62.98	63.53	62.05	62.58	62.98	63.53
flow rate	6.22	3.97	4.31	6.71	5.65	5.25	4.72
Power	1129.82	730.56	793.44	1217.98	1038.72	965.84	869.19
Evap. water in	25.88	17.32	13.80	25.88	20.23	17.32	13.80
water out	15.80	9.26	6.60	15.80	11.52	9.26	6.60
flow rate	21.43	21.16	21.06	21.43	21.34	21.16	21.06
Power	903.51	713.89	635.32	903.51	777.04	713.89	635.32
Comp. Voltage	244.84	240.34	239.94	244.84	242.84	240.34	239.94
Current	2277.71	2139.42	2098.98	2277.71	2205.80	2139.42	2098.98
Power	371.50	339.95	323.07	371.50	353.03	339.95	323.07
R12 metered rate	0.05	4.68	4.25	0.05	4.72	4.68	4.25
R12 Temperatures							
Sump Oil	65.55	71.22	74.48	65.55	69.03	71.22	74.48
Discharge	90.77	96.86	99.57	90.77	94.59	96.86	99.57
Condenser Start	88.68	93.31	95.40	88.68	91.55	93.31	95.40
Mid Condenser	51.37	52.52	52.84	51.37	52.18	52.52	52.84
Condenser End	40.91	29.83	27.93	40.91	32.91	29.83	27.93
Evaporator Start	11.82	5.57	3.34	11.82	7.61	5.57	3.34
Evaporator End	16.58	10.37	7.71	16.58	12.50	10.37	7.71
Suction	17.27	12.96	11.47	17.27	14.18	12.96	11.47
Pressures, gauge, Bar							
Discharge	11.98	11.91	11.90	11.98	11.95	11.91	11.90
Cond. End	10.79	11.39	11.54	10.79	11.12	11.39	11.54
Evap. Start	3.22	2.45	2.19	3.22	2.71	2.45	2.19
Suction	3.19	2.44	2.18	3.19	2.69	2.44	2.18
Calculated results							
C.O.P.	3.04	2.15	2.46	3.28	2.94	2.84	2.69
Tbdc	43.14	41.86	41.63	43.14	42.16	41.86	41.63
Apparent R12mdot	7.04	4.17	4.44	7.59	6.08	5.51	4.86
Ideal R12 mdot	9.24	7.33	6.68	9.24	7.96	7.33	6.68
R12 flow ratio	0.76	0.57	0.66	0.82	0.76	0.75	0.73
Minimum work	166.06	117.33	133.29	179.02	161.29	155.12	146.01
Comp. efficiency	0.45	0.35	0.41	0.48	0.46	0.46	0.45

Table 7.3

21/4/86 More R12 added

Filename :3.P.21046

In this table the use of the condenser water flowmeter measurement is compared with a manual measurement of the flow rate.

	Flowmeter's result			Manual measurement			
Index	430.00	647.00	750.00	430.00	537.00	647.00	750.00
Time, mins	194.38	411.84	519.74	194.38	301.38	411.84	519.74
Performance							
Cond. water in	17.17	18.56	19.16	17.17	17.78	18.56	19.16
water out	59.93	62.22	63.20	59.93	60.99	62.22	63.20
flow rate	8.89	4.69	4.51	8.54	7.21	5.60	4.54
Power	1591.15	856.57	832.21	1528.24	1304.09	1023.22	836.91
Evap. water in	32.70	17.86	11.59	32.70	26.08	17.86	11.59
water out	19.24	9.33	4.72	19.24	14.89	9.33	4.72
flow rate	21.22	21.32	20.94	21.22	21.33	21.32	20.94
Power	1195.31	761.45	601.54	1195.31	998.56	761.45	601.54
Comp. Voltage	240.40	241.07	239.26	240.40	242.29	241.07	239.26
Current	2253.47	2148.65	2065.69	2253.47	2231.74	2148.65	2065.69
Power	367.38	334.87	314.19	367.38	360.32	334.87	314.19
R12 metered rate	7.51	4.77	3.77	7.51	6.06	4.77	3.77
R12 Temperatures							
Sump Oil	62.63	72.23	77.13	62.63	66.64	72.23	77.13
Discharge	87.48	97.74	101.98	87.48	92.27	97.74	101.98
Condenser Start	85.86	94.17	97.17	85.86	89.95	94.17	97.17
Mid Condenser	49.93	52.16	52.65	49.93	51.20	52.16	52.65
Condenser End	21.45	21.56	22.13	21.45	21.08	21.56	22.13
Evaporator Start	13.08	5.27	1.39	13.08	10.17	5.27	1.39
Evaporator End	19.98	10.15	6.02	19.98	15.65	10.15	6.02
Suction	19.83	12.76	10.52	19.83	16.27	12.76	10.52
Pressures							
Discharge	11.98	11.92	11.87	11.98	11.97	11.92	11.87
Cond. End	10.72	11.49	11.66	10.72	11.16	11.49	11.66
Evap. Start	3.62	2.46	2.02	3.62	3.09	2.46	2.02
Suction	3.57	2.44	2.00	3.57	3.04	2.44	2.00
Calculated results							
C.O.P.	4.33	2.56	2.65	4.16	3.62	3.06	2.66
Tbdc	43.22	42.68	41.87	43.22	43.30	42.68	41.87
Apparent R12mdot	8.96	4.66	4.48	8.60	7.20	5.56	4.51
Ideal R12 mdot	10.28	7.30	6.21	10.28	8.86	7.30	6.21
R12 flow ratio	0.87	0.64	0.72	0.84	0.81	0.76	0.73
Minimum work	192.93	131.62	141.04	185.30	176.03	157.23	141.84
Comp. efficiency	0.53	0.39	0.45	0.50	0.49	0.47	0.45

Table 7.4

22/4/86 Accumulator at condenser's end

Filename :3.P.NoSubC1

In this table the condenser's Pelton wheel flow measurement is compared with a manual measurement of the flow rate.

		Flowmeter's result			Manual measurement		
Index	485.00	724.00	840.00	485.00	587.00	724.00	840.00
Time, mins	203.91	470.33	586.96	203.91	306.48	470.33	586.96
Performance							
Cond. water in	18.35	20.34	20.80	18.35	19.22	20.34	20.80
water out	60.95	64.02	65.09	60.95	62.32	64.02	65.09
flow rate	7.10	4.32	4.50	7.67	6.26	4.50	3.95
Power	1265.14	790.12	834.12	1367.48	1129.40	822.76	732.17
Evap. water in	31.60	13.64	9.05	31.60	24.20	13.64	9.05
water out	19.72	7.00	3.37	19.72	14.72	7.00	3.37
flow rate	21.23	20.97	21.14	21.23	21.24	20.97	21.14
Power	1055.38	582.30	502.94	1055.38	843.09	582.30	502.94
Comp. Voltage	243.50	239.23	244.41	243.50	241.64	239.23	244.41
Current	2316.01	2107.58	2081.77	2316.01	2242.79	2107.58	2081.77
Power	369.16	326.35	318.74	369.16	357.86	326.35	318.74
R12 metered rate	5.66	0.01	0.02	5.66	0.03	0.01	0.02
R12 Temperatures							
Sump Oil	62.11	73.82	78.99	62.11	65.61	73.82	78.99
Discharge	86.58	99.30	103.63	86.58	91.30	99.30	103.63
Condenser Start	85.20	95.48	98.74	85.20	89.09	95.48	98.74
Mid Condenser	49.86	52.64	52.86	49.86	51.30	52.64	52.86
Condenser End	43.06	42.73	40.23	43.06	44.42	42.73	40.23
Evaporator Start	15.18	3.83	0.79	15.18	10.59	3.83	0.79
Evaporator End	20.57	7.74	4.28	20.57	15.48	7.74	4.28
Suction	20.60	11.46	9.86	20.60	16.41	11.46	9.86
Pressures, gauge, Bar							
Discharge	11.97	11.90	11.91	11.97	11.95	11.90	11.91
Cond. End	10.22	11.44	11.60	10.22	10.84	11.44	11.60
Evap. Start	3.75	2.30	1.98	3.75	3.12	2.30	1.98
Suction	3.70	2.27	1.96	3.70	3.08	2.27	1.96
Calculated results							
C.O.P.	3.43	2.42	2.62	3.70	3.16	2.52	2.30
Tbdc	43.49	42.38	42.81	43.49	42.74	42.38	42.81
Apparent R12mdot	8.13	4.82	4.94	8.78	7.18	5.02	4.33
Ideal R12 mdot	10.63	6.88	6.07	10.63	8.98	6.88	6.07
R12 flow ratio	0.76	0.70	0.81	0.83	0.80	0.73	0.71
Minimum work	169.56	141.88	158.07	183.28	173.41	147.74	138.75
Comp. efficiency	0.46	0.43	0.50	0.50	0.48	0.45	0.44

Table 7.5

14/7/85 First 16 hours operation of new compressor

Water flow regulator set to 4. Suction pressure varied from high to low.

This is the reference run against which subsequent tests should be compared.

Filename :3.14/7/85

	High power mode			Low power mode			
Index	90.00	180.00	258.00	260.00	270.00	360.00	450.00
Time mins	179.54	389.56	575.55	579.55	599.55	809.56	1019.57
Performance							
Cond. water in	21.59	21.94	22.21	22.23	22.26	22.42	22.38
water out	59.56	59.75	61.72	61.59	61.44	63.59	65.91
flow rate	12.17	10.78	8.41	8.62	8.54	5.87	4.52
Power	1934.20	1705.34	1389.85	1419.35	1401.01	1012.30	824.44
Evap. water in	44.56	38.25	29.17	29.03	28.32	17.33	7.98
water out	27.80	23.94	17.68	17.51	17.02	9.03	1.60
flow rate	24.28	24.63	23.87	24.06	24.16	21.79	20.39
Power	1703.65	1474.22	1148.22	1160.08	1141.83	756.77	544.30
Comp. Power	428.81	420.45	405.42	380.79	380.65	340.46	324.51
R12 metered rate	8.94	8.07	6.26	6.36	6.36	4.38	3.15
R12 Temperatures							
Sump Oil	61.20	61.75	67.69	67.12	65.46	72.98	82.02
Discharge	79.98	81.24	87.57	87.72	86.64	94.32	103.03
Condenser Start	80.31	81.72	88.21	88.37	87.32	95.18	103.97
Mid Condenser	47.79	48.51	50.66	50.67	50.78	52.31	53.01
Condenser End	24.56	24.63	24.83	24.84	24.85	24.84	24.89
Evaporator Start	20.79	17.42	12.03	11.87	11.40	4.76	-1.21
Evaporator End	27.53	24.06	18.73	18.65	18.55	11.46	3.54
Suction	27.91	23.54	17.29	17.18	16.80	9.68	4.95
Pressures, gauge, Bar							
Discharge	12.74	12.48	12.45	12.46	12.46	12.40	12.39
Cond. End	10.16	10.44	11.14	11.15	11.20	11.79	12.03
Evap. Start	4.86	4.28	3.44	3.42	3.36	2.44	1.79
Suction	4.73	4.16	3.32	3.30	3.23	2.32	1.66
Calculated results							
C.O.P.	4.51	4.06	3.43	3.73	3.68	2.97	2.54
Tbdc	41.93	39.94	39.50	39.46	37.74	36.35	36.66
Apparent R12mdot	11.42	9.99	7.91	8.08	8.01	5.59	4.39
Ideal R12 mdot	13.43	11.95	9.65	9.63	9.51	7.11	5.38
R12 flow ratio	0.85	0.84	0.82	0.84	0.84	0.79	0.82
Minimum work	197.81	191.48	183.82	188.48	188.59	163.02	152.38
Comp. efficiency	0.46	0.46	0.45	0.49	0.50	0.48	0.47

Table 7.6

7.4 Tests on the expansion valve setting

It is standard practice to set the TXV for 6C suction gas superheat. If the superheat is furnished by the available ambient source, then this reduces by 6C the theoretical upper limit to the evaporating temperature. So runs the thermodynamic argument in favour of zero superheat.

From a consideration of the relevant two-component two-phase thermodynamics of the oil - refrigerant mixture in the suction line, Hughes et al (57) obtained a thermodynamic justification for non zero superheat, and deduced, for instance, that for 2% oil circulation, the optimum superheat is around 2K. For the Danfoss reciprocating compressor, measurements of the oil circulation fraction have consistently shown it not to exceed 2%. Thus, for the Danfoss SC10H, the theoretical argument in favour of zero superheat is only slightly affected by this optimisation condition.

Before presenting the experimental results, it is helpful to consider the principle of operation of the TXV, and the anticipated effect of changing its setting.

The opening or closing of the valve is dictated by the difference between the saturated vapour pressure of the freon in the vapour pressure bulb, and the evaporating pressure inside the evaporator. The vapour pressure bulb is clamped onto the suction line. Ideally, it should be in good thermal contact with the suction pipe, and insulated from ambient. As long as the freon in the suction line is sufficiently superheated over its evaporating temperature, the vapour pressure inside the bulb holds the TXV open. Normally, the liquid flow rate through the valve exceeds the pumping rate that the compressor can maintain. This results in a gradual advance of the liquid level in the evaporator, as long as the valve is open. This has the effect of gradually increasing the wetted surface area at which boiling can take place, and reducing the available surface for superheating. There comes a point when the superheat of the vapour is no longer capable of maintaining sufficient pressure in the vapour pressure bulb to hold the valve open. The effect of the valve closing is to reduce the wetted surface area, and increase the area available for superheating.

The most important feature to note is that this control system is based on limiting the amount of evaporator surface available for superheating. By turning down the required superheat, one gains an increment in the available surface area for evaporation, with concomitant improvements in suction pressure, density, R12 flow rate, capacity and C.O.P. The magnitude of these anticipated improvements is dependent on the fraction of the evaporator's surface normally used for superheating. If this fraction is small, then only marginal improvements would be anticipated.

For the purpose of quantifying the above points, several runs have been executed to test the effects of varying the TXV setting.

<u>The experiments</u>

The first experiment was performed on 26/7/85. The run was started with 3 hours operation at the normal TXV setting, in order to approach steady state operation. Then the TXV was adjusted for minimum superheat, in order to see what difference resulted. After sufficient operation to reach a new steady state, the TXV was adjusted up by one turn of the adjustor, and data again recorded for a sufficiently long time to obtain steady state operation. This process was repeated until the highest possible superheat setting had been reached. Figures 7.11a, b & c illustrate the response of four key parameters to these changes. Upon reducing the superheat setting to its minimum, the liquid accumulator emptied and remained empty until a further 93g of R12 was added, the effect of which can be seen on the record of the sump and discharge temperatures.

A further 4 similar runs were performed in April 1986. The results of all 5 runs are in accord for non zero superheat, but at the minimum superheat setting the oil temperature & discharge temperature have not been reproducible. With the TXV adjustor screwed in by 3 turns, which gives about 8C superheat, the sump and discharge temperatures both reproduce to within 4C, but at the minimum superheat, there has been a variation of over 20C, as shown on table 7.7.

Sump oil temperatures, C.

TXV Setting	0	+1	+2	Normal	+3	+4
26/7/85	34.4	36.4	53.8	57.5	63.4	71.0
10/4/86	57.0	56.1	59.0	61.5	63.4	69.9
13/4/86	45.9	44.8	56.6	59.2	62.9	69.9
23/4/86	44.2	44.7	54.6	57.3	60.2	66.4
27/4/86	51.3			60.1		

Table 7.7

The discharge gas has consistently been found to be about 20C hotter than the sump oil, and shows the same variations.

Apart from these differences, of which more will be said later, it is important to see whether the anticipated effects of turning down the superheat have been realised.

Consider the run of 23/4/86. Figures 7.12a, b & c show how the operating conditions were varied in the course of this test. The complete data sets, corresponding to steady state operation at each specification of interest, are presented in table 7.8. The first two columns indicate the result of operation at the normal superheat, and minimum superheat respectively. The improvements in evaporating pressure, capacity and C.O.P., which had been anticipated, turn out to be marginal, if not non-existent. There is a slight improvement in R12 flow rate, of about 4%, as shown by the 'apparent' value, which is more reliable than the metered value. However, this 4% gain in flow rate has been offset by the reduced discharge gas enthalpy, so producing no overall improvement in output power. The improvement in the flow rate has been produced by the combined effects of a slight increase in suction pressure, and a lower compressor temperature, which both enhance the suction gas density. In order to see the effect of the lower compressor temperature, note the results for 'Tbdc', which are well corelated with sump oil temperature.

The unremarkable results seen for the reduction to minimum superheat do not invalidate or contradict the earlier qualitative outline of the relevant theory. This merely shows that at the normal superheat setting, the fraction of the evaporator used for superheating is not large, with a consequently modest further improvement obtained by making this superheating region available for evaporation.

In contrast, the system's response to an increase in the superheat setting vindicates the theory totally. Evaporating temperature, pressure, R12 flow rate, capacity and C.O.P. all fall with increasing superheat.

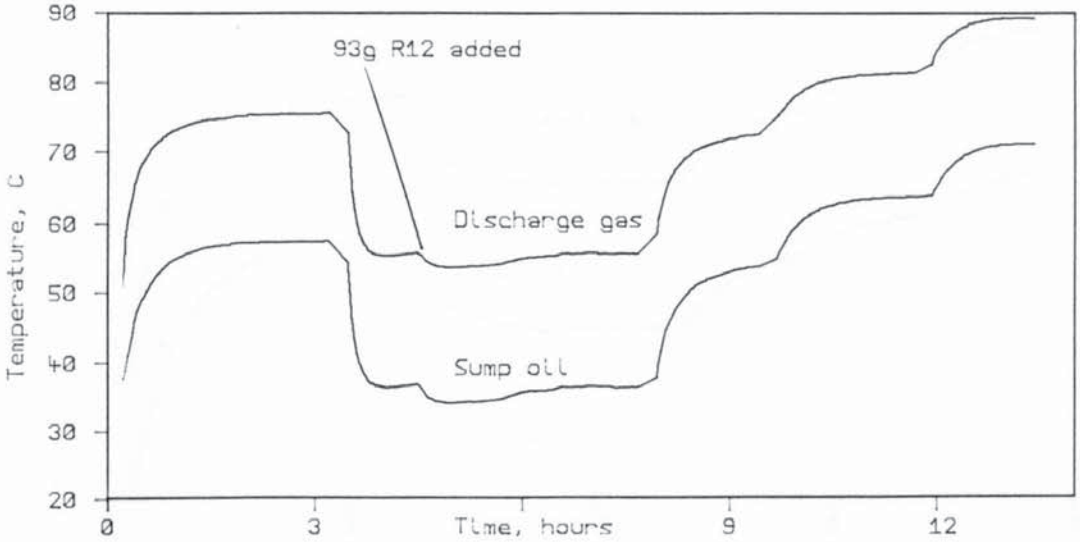

Figure 7.11a Discharge & oil temperature. 26/7/85

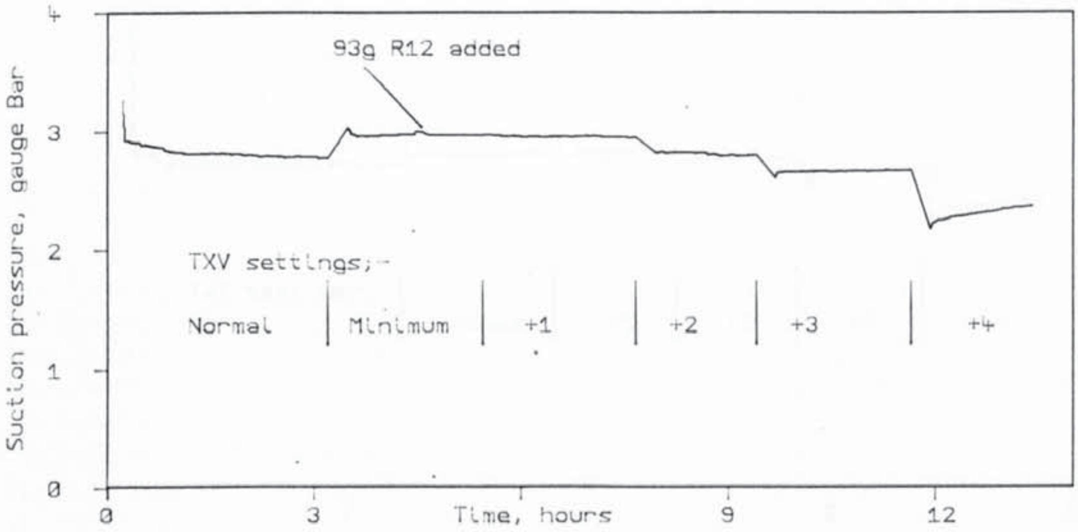

Figure 7.11b Suction pressure history. 26/7/85

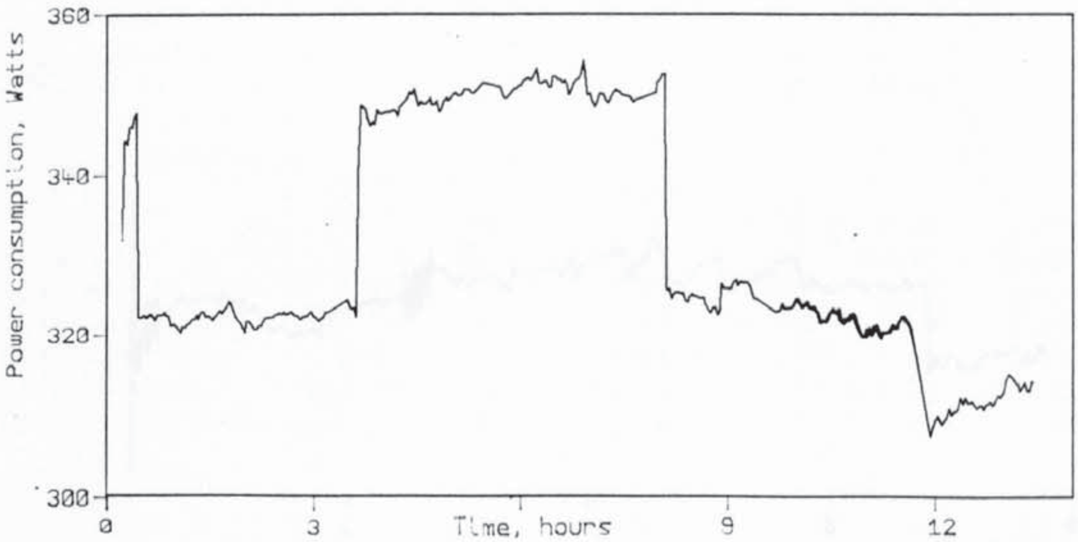

Figure 7.11c Compressor power consumption. 26/7/85

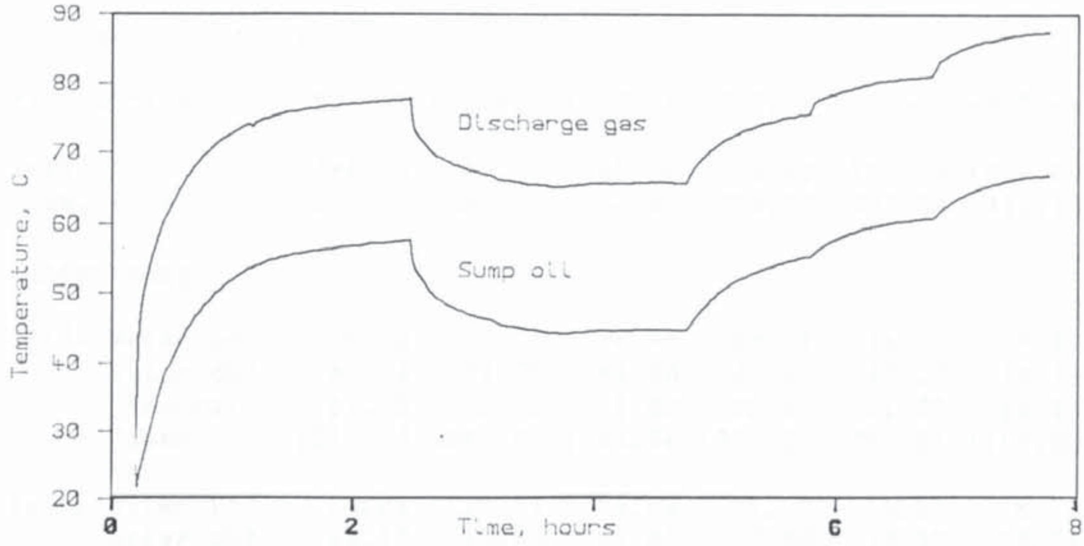

Figure 7.12a Discharge & oil temperature. 23/4/86

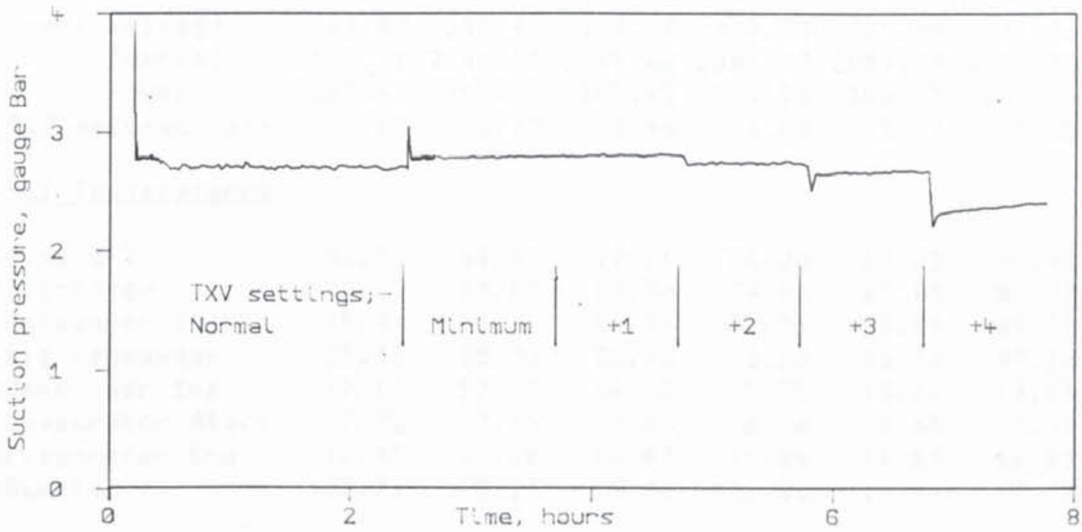

Figure 7.12b Suction pressure history. 23/4/86

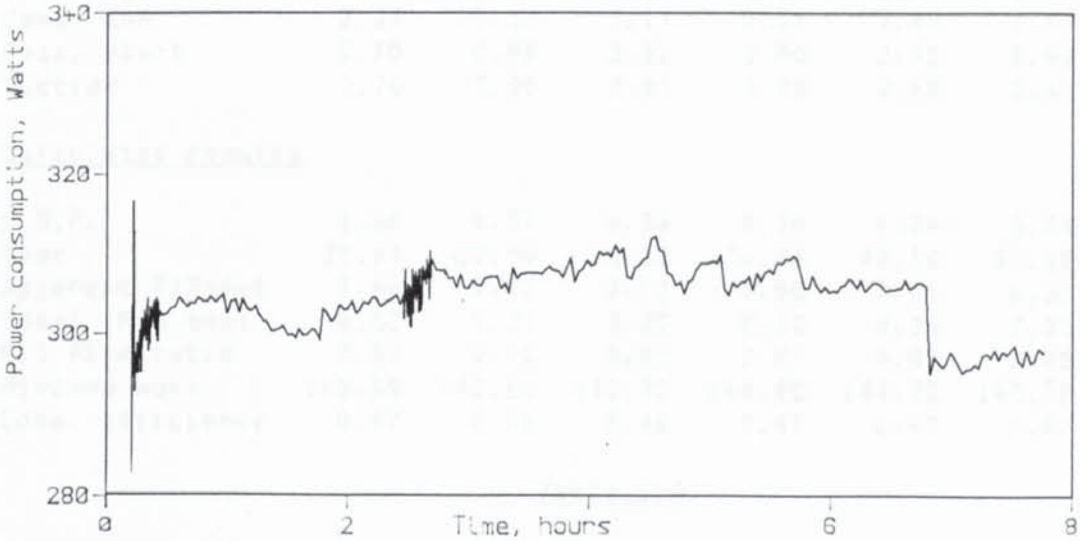

Figure 7.12c Compressor power consumption. 23/4/86

23/4/86 First TXV test with manual condenser capacity measurements

Filename :3.P.A11TXV

TXV setting	Normal	Minimum	+1 Turn	+2 Turn	+3 Turn	+4 Turn
Index	396.00	769.00	835.00	888.00	951.00	1009.00
Time, mins	110.60	199.61	266.68	320.17	384.54	443.10
Performance						
Cond. water in	15.65	15.72	16.44	16.13	16.76	17.46
water out	42.44	41.35	41.38	42.43	43.17	44.19
flow rate	11.75	12.53	12.85	12.11	11.77	10.44
Power	1317.18	1343.89	1341.26	1333.26	1300.85	1167.88
Evap. water in	15.86	15.98	16.08	15.97	16.02	16.76
water out	13.17	13.35	13.43	13.28	13.39	14.37
flow rate	91.48	91.63	91.25	91.66	91.64	91.08
Power	1026.55	1008.60	1011.49	1031.99	1008.63	908.27
Comp. Voltage	242.33	244.49	239.87	245.73	239.64	241.96
Current	2100.11	2144.00	2091.82	2084.22	2051.44	1977.52
Power	302.67	307.87	307.83	306.96	306.97	296.08
R12 metered rate	6.15	6.52	6.46	6.08	5.91	5.25
R12 Temperatures						
Sump Oil	56.93	44.35	44.61	54.30	60.23	66.43
Discharge	77.19	65.02	65.36	74.86	80.83	87.27
Condenser Start	75.41	64.31	64.64	73.36	78.89	84.58
Mid Condenser	35.42	35.03	35.18	35.68	36.18	37.13
Condenser End	17.17	17.39	18.05	17.75	18.34	18.89
Evaporator Start	7.78	7.98	7.99	8.04	7.65	5.75
Evaporator End	12.43	10.68	10.92	11.84	14.53	16.81
Suction	13.71	8.23	8.36	11.81	16.61	19.78
Pressures, gauge, Bar						
Discharge	8.45	8.51	8.53	8.55	8.54	8.50
Cond. End	7.24	7.13	7.17	7.31	7.42	7.67
Evap. Start	2.75	2.85	2.86	2.80	2.73	2.46
Suction	2.70	2.80	2.81	2.75	2.68	2.41
Calculated results						
C.O.P.	4.35	4.37	4.36	4.34	4.24	3.94
Tbdc	39.14	27.80	28.10	36.86	42.10	45.68
Apparent R12mdot	7.40	7.93	7.93	7.58	7.25	6.38
Ideal R12 mdot	8.53	9.21	9.22	8.73	8.36	7.55
R12 flow ratio	0.87	0.86	0.86	0.87	0.87	0.85
Minimum work	143.39	142.60	142.93	144.98	144.73	140.20
Comp. efficiency	0.47	0.46	0.46	0.47	0.47	0.47

Table 7.8

26/7/85 First trial of different TXV settings

Filename :1.ALLTXV

TXV setting	Normal	Minimum	+1 Turn	+2 Turn	+3 Turn	+4 Turn
Index	90.00	150.00	210.00	255.00	315.00	360.00
Time mins	179.73	314.73	447.73	552.73	686.73	791.73
Performance						
Cond. water in	20.72	20.64	20.67	20.68	20.93	21.18
water out	44.92	42.52	42.76	44.69	45.92	47.21
flow rate	12.94	14.34	14.19	13.14	12.19	10.49
Power	1311.06	1313.13	1312.20	1320.95	1275.24	1142.86
Evap. water in	15.95	16.49	16.43	15.98	16.04	17.44
water out	13.30	13.95	13.89	13.35	13.48	15.15
flow rate	90.62	90.89	90.22	90.42	90.97	91.25
Power	1007.65	966.19	957.73	997.19	974.71	876.04
Comp. Voltage	0.00	0.00	0.00	0.00	0.00	0.00
Current	0.00	0.00	0.00	0.00	0.00	0.00
Power	323.04	351.49	349.44	324.69	320.85	314.10
R12 metered rate	5.99	6.57	6.54	6.05	5.76	5.03
R12 Temperatures						
Sump Oil	57.46	34.43	36.44	53.82	63.39	71.00
Discharge	75.66	53.75	55.56	72.45	81.34	89.26
Condenser Start	76.07	55.19	56.95	72.96	81.61	89.35
Mid Condenser	37.06	35.95	36.27	37.03	37.68	38.64
Condenser End	21.88	22.07	21.79	21.80	22.06	22.29
Evaporator Start	8.34	9.50	9.33	8.43	7.71	5.55
Evaporator End	13.25	11.77	11.71	12.38	15.25	17.66
Suction	13.22	9.78	9.73	11.41	16.39	19.78
Pressures, gauge, Bar						
Discharge	9.14	9.01	9.11	9.10	9.18	9.15
Cond. End	7.73	7.45	7.54	7.74	7.89	8.16
Evap. Start	2.89	3.09	3.07	2.92	2.80	2.50
Suction	2.77	2.97	2.95	2.80	2.67	2.37
Calculated results						
C.O.P.	4.06	3.74	3.75	4.07	3.97	3.64
Tbdc	35.24	15.87	17.07	32.56	39.75	44.37
Apparent R12mdot	7.57	8.34	8.26	7.73	7.20	6.26
Ideal R12 mdot	8.75	10.15	10.02	8.94	8.34	7.40
R12 flow ratio	0.87	0.82	0.82	0.86	0.86	0.85
Minimum work	152.30	141.84	143.71	151.52	152.50	147.58
Comp. efficiency	0.47	0.40	0.41	0.47	0.48	0.47

Table 7.9

The first trial, 26/7/85

Table 7.9 presents all the measurements performed for the run of 26/7/85, and figure 7.11a, b & c shows the histories of some of the parameters of interest. Comparison with table 7.8 provides an insight into the nature of the differences between this run and that of 23/4/86, and permits identification of the most likely cause.

Upon turning the superheat down from its normal setting to its minimum, the changes seen on 26/7/85 were more pronounced than on 23/4/86. Table 7.10 below lists the observed changes that occurred on turning the TXV from its normal setting down to minimum superheat. It compares the observations of 23/4/86 with those of 26/7/85.

	26/7/85	23/4/86
Evaporator power	Fall of 53 Watts	Fall of 4 Watts
Compressor power	Rise of 28 Watts	Rise of 4 Watts
Sump & Discharge Temperatures	Fall of 22K	Fall of 12K
Evaporator's R12 entry - water exit T difference	Fall of 0.5C	Fall of 0.1C

Table 7.10

On 23/4/86 the evaporator power was essentially unaffected by turning to minimum superheat, and the 0.1C fall in the water/freon temperature difference is accountable by the increment in the wetted surface area of the evaporator. By contrast, on 26/7/85 the drop of 0.5K in this temperature difference is accountable by the reduction of 50 Watts in the evaporator power.

Upon considering these, and the other differences summarised in table 7.10, it was realised that all the observations were consistent with the vapour pressure bulb more closely matching the suction line temperature on 23/4/86 than on 26/7/85.

One cannot take it for granted that the vapour pressure bulb matches the suction gas temperature. The thermal resistances from suction gas to vapour pressure bulb, and from vapour pressure bulb to ambient, constitute a potentiometer. Ideally, the first resistance should be zero, and the latter should be infinite. Suppose that on two different occasions this potentiometer's resistance ratio is first 4, and latterly 8. Assuming a room temperature of 20C, and an evaporating temperature of 10C, table 7.11 summarises the suction gas temperatures at which the vapour pressure bulb will open the valve, for nominal superheat settings of 6C and 2C respectively:

Resistance ratio	4		8	
Nominal superheat setting	6	2	6	2
Evaporating temperature	10	10	10	10
V. P. bulb temperature	16	12	16	12
Room temperature	20	20	20	20
Suction line temperature at which valve can open	15	10	15.5	11

Table 7.11

The point of this numerical illustration is to show that if the superheat is normal, then the system is not sensitive to variations in this resistance ratio. i.e. the normal superheat setting gives some immunity to the variability of the coupling of the vapour presure bulb to the suction line. However, at the low superheat setting, this change in resistance ratio makes the difference between 1C superheat and zero superheat. i.e. the difference between functioning of the control loop, and no control at all, because at zero superheat, liquid and vapour cannot be distinguished by a control loop actuated by temperature alone.

The observations of the difference between the test on 26/7/85, and the subsequent attempts to repeat it, are consistent with liquid return to the sump on the first test, when set to minimum superheat, which did not occur to as great an extent on the subsequent repeats.

This liquid return can account for both the fall in the evaporator power, and the fall in the sump oil temperature. The transition of the compressor's power consumption to the high power mode is then also accounted for as a consequence of the dilution of the oil by the refrigerant.

Fixed orifice expansion valve. 27/4/86

Having thus recognised the possibility of the TXV feedback loop failing on attempting to minimise the superheat, and leaving the valve continuously fully open, it was natural to devise a test in which this operating condition was deliberately established, in order to observe the system's response.

After establishing steady state operation at the normal superheat, the TXV was adjusted for minimum superheat, and a new steady state established. Up to this point, then, the run of 23/4/86 had been repeated. After establishing steady state operation at the minimum superheat, the vapour pressure bulb was removed from the suction line, in order to let it approach room temperature, and so ensure that the valve would be held fully open. After establishing a steady state at this operating condition, more freon was added, and a new steady state was approached. Relevant histories are plotted in figures 7.13a, b & c. The complete data sets are presented in table 7.12, where the first two columns refer to the status quo, the next two have minimum superheat, columns five & six have the vapour pressure bulb removed from the suction line, and the last column shows the result of adding more R12.

The most striking features of operation with a fixed orifice are;-

i) Reduced evaporator and condenser power.
ii) A spectacular fall in oil temperature.
iii) Discharge gas close to saturation.
iv) Near zero liquid subcooling.

This last point is quite significant. In the absence of externally imposed control, matching of the flow rate through the valve to that maintained by the compressor is recovered by virtue of the flow properties of a two phase mixture mixture through an orifice. The purpose of adding more freon was to see if any subcooling could be obtained. It had the effect of further lowering the sump temperature, without affecting the R12 condenser end temperature. This shows that the sump was acting as a liquid accumulator, serving to starve the system of freon, until the resulting two phase orifice flow matched the compressor's pumping rate.

The last column of table 7.12 shows an estimated R12 temperature at bdc lower than the evaporating temperature. This is impossible. This has occurred because, in this data set, the compressor's temperature is so low that the discharge gas is emerging with a lower entropy than that of saturated vapour at the suction pressure. This does not necessarily mean that the vapour is wet at the start of the compression stroke, because heat loss from the internal discharge pipe means that the gas' entropy on the compression stroke is higher than the discharge gas' entropy.

If one considers the compressor's performance figures, one sees that the mass flow efficiency and thermodynamic efficiency are consistent at both normal and minimum superheat. However, upon unclipping the vapour pressure bulb to force fixed orifice operation, these indicators of compressor efficiency both fall significantly.

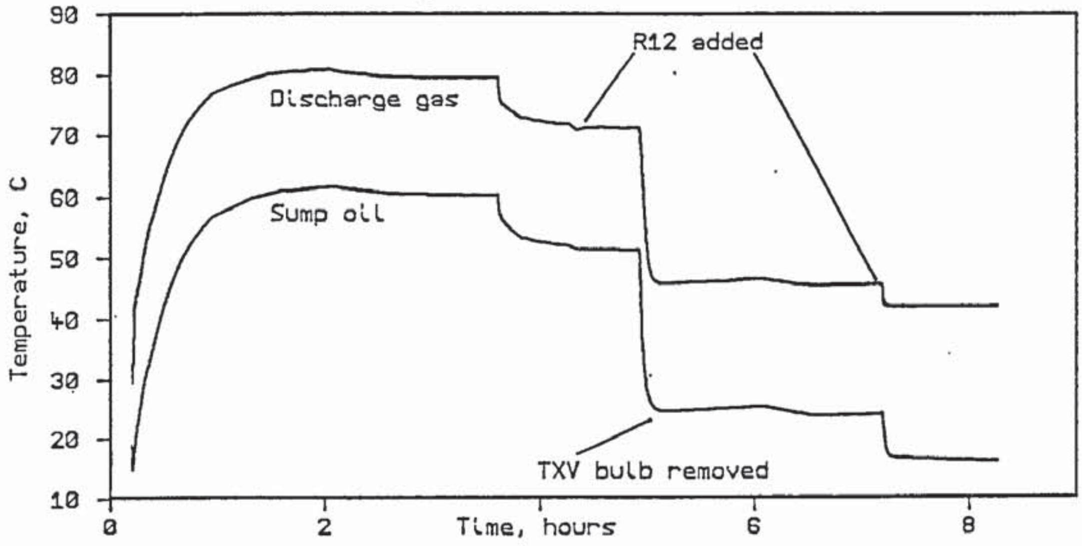

Figure 7.13a Discharge & oil temperature. 27/4/86

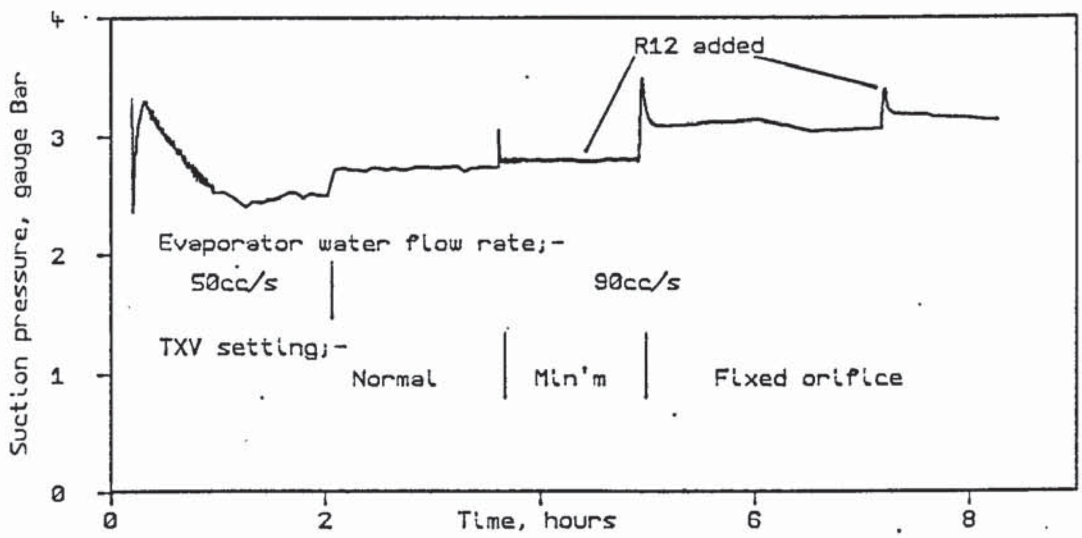

Figure 7.13b Suction pressure history. 27/4/86

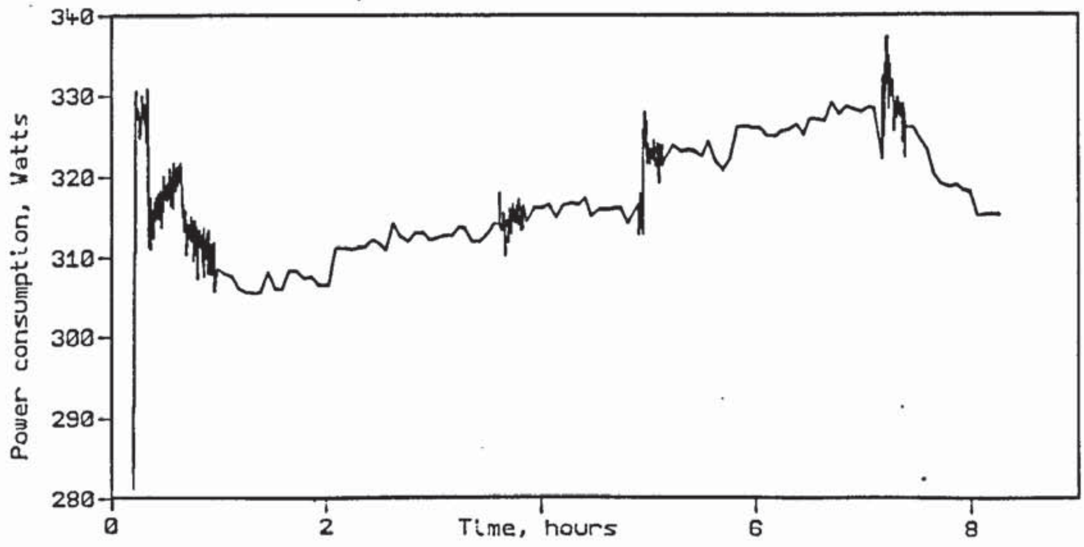

Figure 7.13c Compressor power consumption. 27/4/86

27/4/86 Further testing of TXV, including fixed orifice operation

Manual condenser water flow rate measurement throughout.
Filenames :1.P.TVstart :3.P.OrfTest

TXV setting	Normal		Minimum		vP Bulb Removed		R12 added
Index	1053.00	1125.00	20.00	45.00	408.00	469.00	837.00
Time, mins	99.38	177.53	239.19	264.19	344.44	406.14	491.41
Performance							
Cond. water in	16.41	16.09	16.05	16.08	15.93	16.06	16.46
water out	44.27	43.75	42.90	42.72	40.56	40.62	39.59
flow rate	10.34	11.41	11.93	12.04	12.01	11.46	10.70
Power	1205.73	1320.56	1340.75	1342.23	1238.30	1177.94	1035.87
Evap. water in	16.20	15.91	16.04	16.09	17.31	16.24	15.65
water out	11.27	13.31	13.42	13.48	14.99	14.10	13.84
flow rate	44.51	92.82	92.90	93.29	93.47	93.35	93.54
Power	918.19	1010.74	1017.53	1016.74	905.12	837.98	705.71
Comp. Voltage	241.70	241.36	241.80	242.18	241.85	243.38	240.69
Current	2060.10	2075.61	2090.31	2099.23	2140.30	2168.69	2146.08
Power	307.67	312.79	315.43	316.05	325.28	327.91	315.22
R12 metered rate	5.90	6.40	6.66	6.81	3.68	4.14	3.66
R12 Temperatures							
Sump Oil	61.41	60.16	52.02	51.21	25.53	24.12	16.00
Discharge	80.82	79.40	71.67	70.98	46.32	45.42	41.82
Condenser Start	78.53	77.43	70.21	69.55	46.95	45.89	42.07
Mid Condenser	37.44	36.71	36.35	36.36	33.55	33.93	33.55
Condenser End	18.19	17.87	17.96	17.85	27.47	28.21	27.92
Evaporator Start	6.23	8.23	8.52	8.63	10.21	9.64	10.35
Evaporator End	10.72	12.35	10.84	10.76	12.38	11.67	11.84
Suction	12.41	13.98	8.39	8.41	10.55	9.82	10.18
Pressures (gauge Bar)							
Discharge	8.65	8.68	8.71	8.71	8.71	8.71	8.69
Cond. End	7.68	7.50	7.41	7.43	6.42	6.49	6.47
Evap. Start	2.55	2.79	2.84	2.85	3.19	3.11	3.18
Suction	2.52	2.75	2.80	2.81	3.14	3.06	3.13
Calculated results							
C.O.P.	3.92	4.22	4.25	4.25	3.81	3.59	3.29
Tbdc	39.89	40.77	33.51	32.89	11.28	9.59	6.64
Apparent R12mdot	6.73	7.40	7.75	7.77	8.46	8.14	7.29
Ideal R12 mdot	7.98	8.57	8.96	9.00	11.01	10.84	11.26
R12 flow ratio	0.84	0.86	0.86	0.86	0.77	0.75	0.65
Minimum work	141.80	145.85	146.23	146.01	128.41	125.62	107.93
Comp. efficiency	0.46	0.47	0.46	0.46	0.39	0.38	0.34

Table 7.12

Conclusions from TXV tests

The main purpose of the thermostatic expansion valve is to prevent liquid return to the compressor, in order to avoid losing evaporator power, and to avoid diluting the oil with refrigerant. Additionally, it has been shown that effective subcooling is also dependent on the effective operation of this control loop.

The conventionally accepted standard of 6C superheat is borne more of the requirement for robustness of the control loop against perturbations, than of considerations for thermodynamic optimisation.

It also appears that in spite of the thermodynamic arguments in favour of minimum superheat, in practice there appears to be very little sensitivity of the heatpump's output to the superheat setting for settings at or below the norm. This is interpreted as being due to the small fraction of the evaporator normally used for superheating. The theoretical advantages of minimising the superheat could only be realised by an evaporator sized to allow a much closer approach of the evaporating temperature to the source temperature.

The above observations suggest the following rule of thumb for the TXV superheat setting; - With the TXV set for minimum superheat, find the temperature difference between the ambient source and the boiling R12. Set the TXV for a superheat of this value.

7.5 The effect of by-passing the suction system

So far, all the tables of results have shown that the ratio of the apparent gas flow rate to the ideal value has never been over 90%, and is more typically around 80%. In section 4.7 a long list of non-idealities was presented, some of which are relevant to this capacity shortfall. In May 1986 it was thought that the pressure drop associated with the suction system's narrow bores might be a likely contender to account for a significant part of this capacity shortfall. For this reason, 2 holes, each 8mm in diameter, were drilled through the old compressor's casting into each of the innermost plenums. Since the maker's bores from the outer plenum to each inner plenum are just 5mm in diameter, these by-pass holes presented a flow area 5x more than for the unmodified suction system, giving a reduction in the pressure drop by a factor of 25 for the same flow rate. These by-pass holes were drilled, from below, through the floor of each inner plenum. This position was chosen in order to avoid oil running in through these holes, as could happen for holes through either the top or sides of the casting, due to the oil spray from the top of the crankshaft. For the same reason, the precaution was taken of blocking the duct inside the impeller which supplies oil to the rotor's ducts, as there would otherwise have been a copious oil spray from the top of the rotor, which is situated immediately below the new by-pass holes.

Three tests were performed. On 18/5/86 PTFE plugs were inserted into the by-pass holes in order to restore the suction system to normal, and the heat pump's performance was recorded in the usual way for a wide range of evaporator water supply temperatures. On 19/5/86 the plugs were removed, and the same performance measurement repeated. On 20/5/86 the plugs were replaced; the lubrication system was restored to the status quo, and the same measurement was again repeated.

By comparing the first and last tests, the effect of the modification to the oil distribution system may be elucidated, and by comparing the first and second test, the effect of the suction system by-pass may be determined.

From attempts to devise a mathematical model of the compressor, it had been recognised that the behaviour of the gas flow in the plenum system is dictated mainly by the crank angle at the first opening of the suction valve. This is essentially a function of compression ratio alone. For the purpose of this test, it was thus desirable to cover a wide range of compression ratio. For this reason the water regulator was set to 4, giving about 200 psi discharge, and the evaporator water reservoir was run down from 40C to 2C in the course of the test.

During each of these three tests over 30 manual measurements were made of the condenser water flow rate. These data sets are presented in full at the end of this chapter. The following presentation of the results has been based exclusively on these manual flow measurements, because the scatter on the Pelton wheel flow measurements exceeds the differences of interest.

Results of suction by-pass test

Figure 7.14a shows the ratio of apparent to ideal R12 flow rate plotted as a function of suction pressure, for the first two tests. i.e. with & without the by-pass holes plugged. At the highest suction pressure the by-pass holes furnish a small gain in capacity, as anticipated, but this improvement declines with falling suction pressure. Figure 7.14a also demonstrates that the penalty introduced by the suction system only accounts for a small fraction of the capacity's shortfall from the ideal value.

With falling suction pressure, the drop-off in the improvement came as a surprise, and raised the doubt that perhaps the effect of the by-pass was being obscured by added oil entrainment, since there had been no attempt to prevent the oil spray from the top of the crankshaft. However, the validity of the result, that the suction system degrades the capacity only at a high suction pressure, was later confirmed in the final set of experiments.

Figure 7.14b shows the compressor power consumption for these same two runs. Note that apart from the cross over at about 1.7 Bar suction pressure, the power consumption with the by-pass open never exceeds the power consumption with the by-pass plugged. This is in spite of the fact that the capacity is slightly better with the by-pass open. This point is more forcibly made in figure 7.14c which shows the compressor's

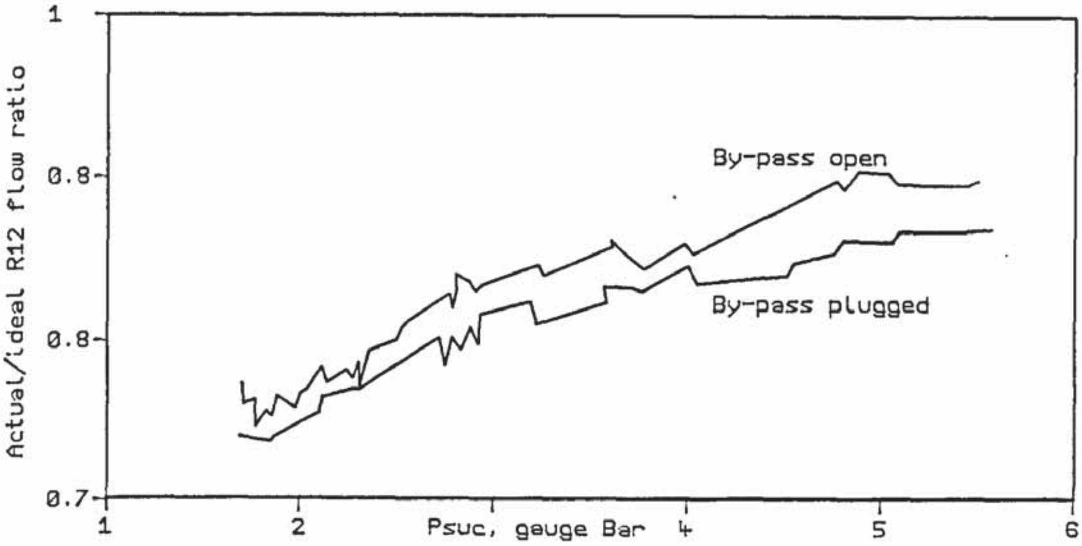

Figure 7.14a Suction by-pass test, 18 & 19/5/86

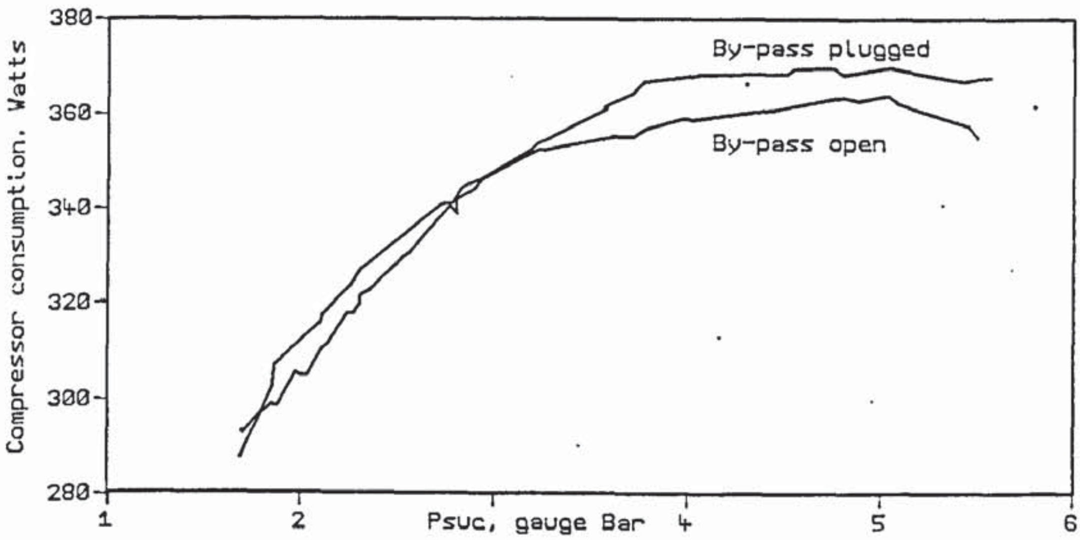

Figure 7.14b Suction by-pass test, 18 & 19/5/86

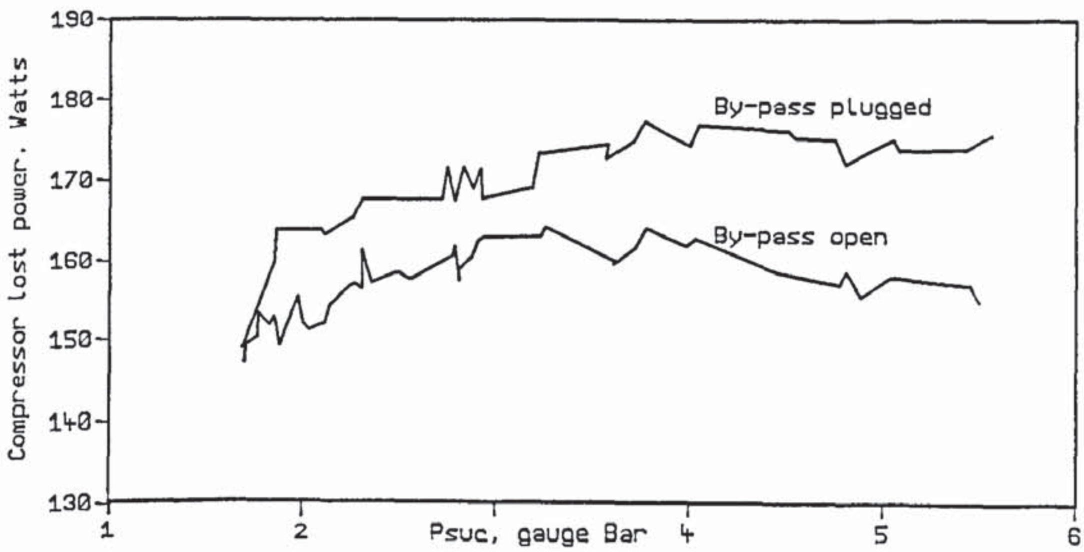

Figure 7.14c Suction by-pass test, 18 & 19/5/86

total losses plotted against suction pressure for these two runs. The difference between these two plots constitutes an experimental measurement of the power loss caused by the suction system. One can see that at 5 Bar there is about 15 Watts loss, which tapers off to about 10 Watts at 2 Bar.

Effect of modifying the oil delivery system

Figure 7.15a shows the ratio of apparent to ideal R12 flow rate plotted as a function of suction pressure, for the first and last tests. i.e. with & without the rotor's oil ducts plugged. There is some evidence here that the capacity is marginally better if the oil spray from the rotor's top is retained. The total power consumption and calculated total loss are compared in figures 7.15b & c respectively.

The possibility exists that by spraying oil from the top of the rotor onto the top of the stator's windings, the mechanical losses are aggravated due to the viscous drag of the oil that runs into the rotor - stator gap. The purpose of this experiment was to further test this question.

Figure 7.15c indicates that, in spite of the plausibility of the above suggestion, the presence or absence of oil spray from the top of the rotor has had very little effect on the compressor's total losses.

7.6 Improvised piston leakage measurement

As explained in section 4.9, the results reported in (63) had led to the misconception that leakage past the piston does not cause a significant loss of capacity. When it was realised that, for a more representative piston-bore clearance (64), leakage is not negligible, the need for a leakage measurement was recognised.

For this test, the compressor was mounted in the bottom half of the can, and the suction pipe was coupled directly to the casting's suction stub. This arrangement ensured that any refrigerant leaking past the piston would be lost from the circuit. The loss rate was then subsequently found from a plot of accumulator liquid level against time.

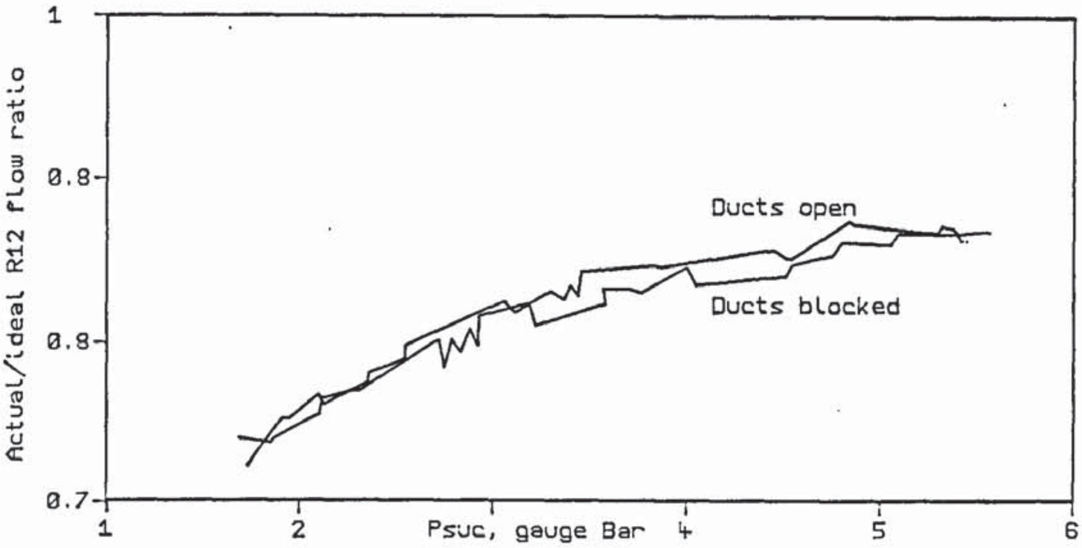

Figure 7.15a Rotor oil duct test, 18 & 20/5/86

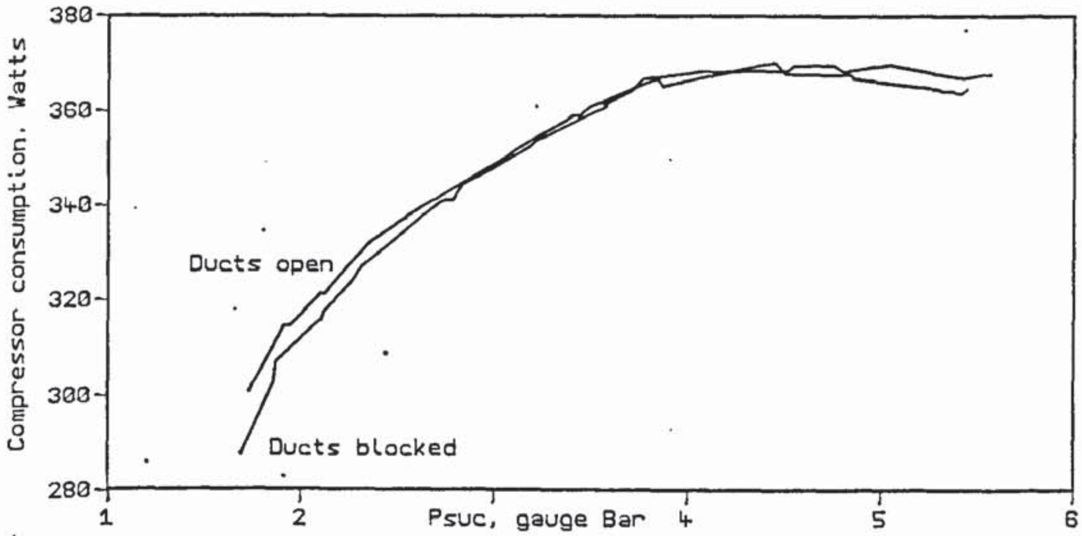

Figure 7.15b Rotor oil duct test, 18 & 20/5/86

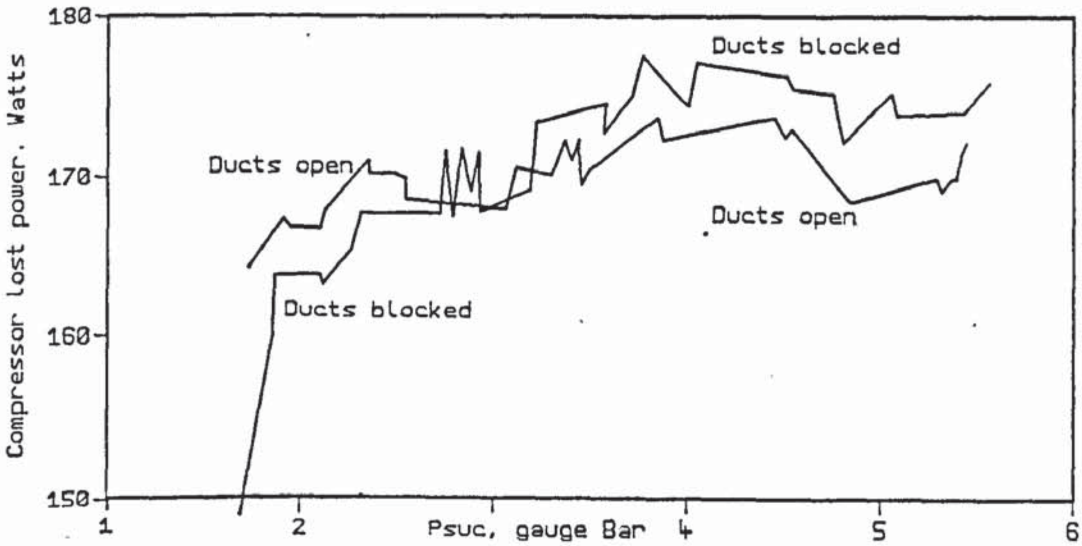

Figure 7.15c Rotor oil duct test, 18 & 20/5/86

The new compressor was used in this test, because the old compressor had had holes drilled into its inner suction plenums.

In normal operation, there can be no leakage on the suction stroke, because the can is pressurised by the suction gas.

In order to avoid deviating too much from normality, it was desirable to obtain as low a suction pressure as possible. The other reason for wishing to minimise leakage on the suction stroke was to minimise the total leakage rate, and so improve the chances of approaching steady state operation while there was still enough liquid left in the accumulator to make the measurement.

For this reason, before removing the old compressor, which was still set up from the previous test, it was used to refrigerate the evaporator water reservoir.

Having obtained the desired low evaporator water reservoir temperature, the old compressor was removed, and the new one was installed, as described above.

There followed two attempts to perform the measurement. The first attempt failed for a very illuminating reason. Upon starting the compressor, for the first few minutes after start up, an alarming amount of liquid freon was returned to the compressor as large, intermittent slugs, visible through the transparent hose used to couple the suction line to the intake. The compressor's casting quickly became very cold to the touch, and a mist of refrigerant was blown past the cylinder head gaskets as the cylinder head lifted at each liquid slug. (The cylinder head's ability to lift is a built-in safety feature of the design.)

It was realised that this liquid slugging problem resulted from the hunting of the TXV feedback loop. In principle, if the expansion valve is admitting too high a liquid flow rate, then this should cause the vapour pressure bulb temperature to fall, which closes the valve. However, in reality the response of the vapour pressure bulb is delayed by the heat capacity of the suction pipe, the heat capacity of the vapour pressure bulb and the capacity of the evaporator, since a significant amount of liquid must flow into the evaporator before the surface area available for superheating can be reduced. It is this delay that makes the loop hunt. Without this delay, a uniform steady state would become established.

This observation was significant because it had not previously been realised that, in normal operation, significant amounts of liquid refrigerant could be returned to the sump as a consequence of the hunting of the TXV feedback loop. The only way of checking whether this occurred on past tests is to examine the sump oil temperature history. However, for most of the past tests, the heat pump was started in the saturated TXV regime (section 5.3), for which the return of liquid slugs to the sump is impossible.

For the second attempt to make this piston leakage measurement, the superheat setting was turned up. As well as eliminating the problem of liquid slugs returning to the compressor, this gave a further depression of the suction pressure. Before starting the run, the circuit was generously topped up with R12. Shortly after starting the compressor, the accumulator filled completely with liquid, so that the 2 phase - liquid boundary must have been upstream from the accumulator. After a few minutes, vapour was again visible at the top of the accumulator, and over the following 8 minutes the fall in the accumulator's liquid level was recorded.

Figure 7.16 shows the accumulator liquid level plotted against time. From the slope of this plot, the accumulator's cross section of 6.4cm^2, and a density of 1.3g/cc, a leakage rate past the piston of 0.24 g/s has been deduced. From this measurement it has been possible to determine the one parameter in a mathematical model of leakage past the piston, and so obtain a means of estimating this loss at any other operating condition.

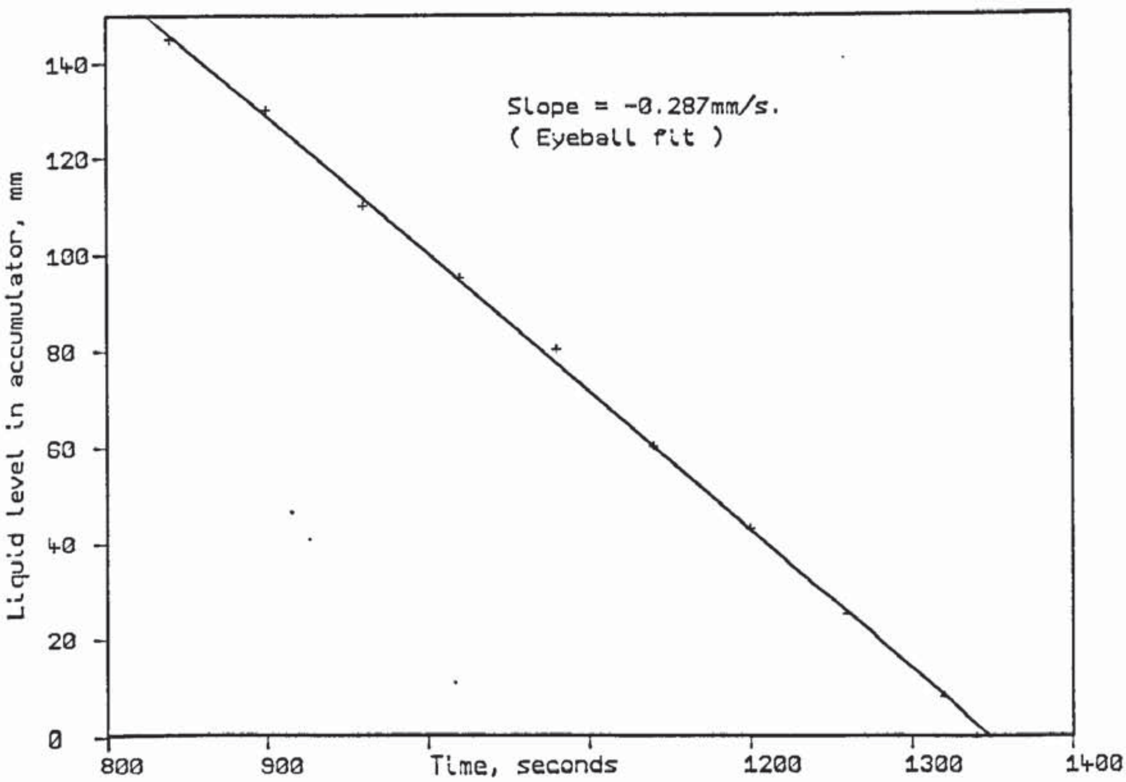

Figure 7.16 Improvised piston leakage measurement

28/5/86 Improvised leakage test. Sample data sets.

	:3.pr25056			:3.2r25056			
Index	40.00	60.00	80.00	100.00	20.00	50.00	80.00
Time, mins	9.91	14.91	19.91	24.91	32.41	39.91	47.40
Performance							
Cond. water in	18.83	19.24	18.89	18.10	18.07	18.47	19.24
water out	40.56	42.72	43.35	43.93	45.20	46.79	55.75
flow rate	6.51	6.30	6.73	6.51	5.34	3.49	-0.31
Power	592.04	619.06	689.08	703.32	605.76	413.64	-47.10
Evap. water in	7.47	7.19	6.88	6.60	6.21	5.91	8.04
water out	5.80	5.52	5.25	5.00	4.69	4.96	5.76
flow rate	91.31	90.81	90.81	90.15	90.14	90.33	-0.65
Power	639.59	636.34	621.91	603.05	574.05	360.44	-6.19
Comp. Voltage	241.63	241.97	242.52	240.26	240.05	240.38	241.12
Current	2306.34	2217.17	2149.09	2099.10	2069.21	2047.86	253.03
Power	345.49	327.40	308.49	299.86	292.04	284.75	9.97
R12 metered rate	-0.10	-0.11	-0.11	-0.11	-0.11	-0.11	-0.10
R12 Temperatures							
Sump Oil	23.33	36.40	46.01	52.31	59.50	65.04	59.75
Discharge	46.72	62.87	68.59	72.93	77.37	81.28	61.55
Condenser Start	44.40	60.75	66.24	70.34	74.34	77.65	54.35
Mid Condenser	22.02	39.67	39.88	39.95	40.02	39.99	33.22
Condenser End	18.70	19.25	19.85	19.69	32.58	38.43	33.01
Evaporator Start	-2.44	-2.04	-2.15	-2.26	-2.42	-5.59	3.56
Evaporator End	7.81	7.75	7.45	7.18	6.85	6.66	9.41
Suction	7.75	9.23	9.10	8.91	8.80	8.78	13.09
Pressures, gauge, Bar							
Discharge	9.10	9.07	9.09	9.07	9.05	8.95	6.93
Cond. End	8.61	8.44	8.43	8.43	8.30	8.31	6.97
Evap. Start	1.54	1.64	1.62	1.60	1.59	1.23	2.39
Suction	1.50	1.58	1.57	1.56	1.55	1.20	0.21
Calculated results							
C.O.P.	1.71	1.89	2.23	2.34	2.07	1.45	0.00
Tbdc	-8.78	8.88	14.27	18.47	22.81	21.78	-8.39
Apparent R12mdot	3.89	3.77	4.11	4.11	3.75	2.61	-0.32
Ideal R12 mdot	6.40	6.17	6.00	5.88	5.76	4.84	2.79
R12 flow ratio	0.61	0.61	0.68	0.70	0.65	0.54	-0.11
Minimum work	94.81	97.24	109.32	111.78	104.02	80.61	-11.25
Comp. efficiency	0.27	0.30	0.35	0.37	0.36	0.28	-1.13

7.7 Conclusions and further implications.

In retrospect, one sees that in spite of the diversity of the experiments which have been described here, there is the common thread of the performance degradation that results from liquid R12 in the sump. It should be stressed that these experiments were not devised in anticipation of this phenomenon. On the contrary, before performing these tests it had been believed that the TXV feedback loop ensures that no liquid returns to the sump other than that dissolved in the returning oil.

Additionally, it had not been realised that liquid R12 in the sump degrades the performance by starving the circuit of refrigerant. This results in reduced subcooling, or even incomplete condensation. This operating condition always exists on starting up, because during periods of quiescence the refrigerant is gradually absorbed by the oil until thermodynamic equilibrium is reached between the vapour and the liquid phase. In this state most of the charge may be in the sump.

The problem of boiling out the sump quickly after start-up was probably the original impetus to the now accepted convention of heating the sump with the discharge gas. However, the correlation of gas temperature with oil temperature shown by figure 7.5, shows that heating the oil incurs the penalty of increasing the suction gas preheat, which in turn increases the discharge gas temperature. If the oil is being heated by the discharge gas, then this presents a potentially aggressive positive feedback loop. This loop may be broken either by using an alternative heat source for the oil, or by reducing the intimacy of the thermal contact between the oil and the suction gas.

By using very simple calculations to interpret the measurements, as explained in chapter 4, it has been shown that the compressor's efficiency has considerable room for improvement.

Section 4.7 introduced a list of non-idealities accounting for the compressor's poor efficiency. Three of these features have been the subject of an experimental measurement, namely the loss of both capacity and power caused by the suction system; the viscous power loss caused by the ingress of oil into the rotor-stator gap; and the capacity loss caused by leakage past the piston. While these three effects are big enough to be measurable, and account for some of the compressor's losses, they come nowhere near accounting totally for the compressor's losses. Up till this point, it had been thought that the capacity shortfall might be mainly accountable by the pressure drop in the suction system. It was as a result of performing the experiment that this suspicion was refuted.

A major factor contributing to the compressor's losses is the poor efficiency of the motor, as shown by the performance figures supplied by Danfoss. However, in view of the earlier comments concerning the desirability of a heat source for the oil other than the discharge gas, it becomes understandable that an iterative evolutionary development, driven by the need for reliability rather than efficiency, would result in this choice of motor.

18/5/86 Rotor oil ducts plugged. Suction by-pass holes plugged

	:3.P.Control						
Index	341.00	350.00	375.00	378.00	406.00	409.00	441.00
Time, mins	57.97	66.97	91.97	94.97	122.97	125.97	157.96

PERFORMANCE

Cond.	water in	16.15	16.45	16.77	16.83	17.12	17.16	17.37
	water out	55.13	55.63	56.41	56.49	57.01	57.13	57.57
	flow rate	14.08	13.81	12.99	12.82	12.20	11.93	11.32
	Power	2297.10	2264.27	2155.54	2128.08	2036.91	1995.97	1904.72
Evap.	water in	38.87	37.83	35.27	35.03	32.75	32.55	30.48
	water out	33.59	32.67	30.50	30.29	28.33	28.15	26.35
	flow rate	91.20	90.60	91.30	91.19	91.14	91.18	90.92
	Power	2015.57	1957.71	1825.16	1807.80	1688.01	1677.88	1572.29
Comp.	Voltage	239.38	238.21	240.92	240.55	239.62	240.44	241.07
	Current	2233.93	2227.78	2240.78	2238.90	2243.79	2243.79	2223.45
	Power	367.95	366.86	369.66	369.85	368.30	369.73	369.35
R12 metered rate		11.13	11.17	10.44	10.62	10.29	10.16	9.75

R12 TEMPERATURES

Sump Oil	49.61	51.18	52.56	52.64	53.22	53.05	53.36
Discharge	75.89	77.59	79.65	79.90	80.68	81.00	81.55
Condenser Start	75.44	77.08	78.97	79.19	79.88	80.17	80.63
Mid Condenser	42.72	43.79	45.75	45.87	46.84	47.06	47.82
Condenser End	23.47	22.17	20.42	20.41	20.58	20.59	20.82
Evaporator Start	25.76	24.99	23.16	23.00	21.81	21.44	20.11
Evaporator End	35.56	34.03	31.04	30.90	28.27	28.92	26.59
Suction	35.80	34.26	31.38	31.24	28.89	28.94	27.01

PRESSURES (gauge Bar)

Discharge	12.39	12.38	12.39	12.39	12.37	12.38	12.38
Cond. End	8.49	8.90	9.62	9.66	9.96	10.03	10.26
Evap. Start	5.64	5.51	5.15	5.11	4.89	4.84	4.63
Suction	5.57	5.43	5.09	5.05	4.80	4.75	4.54

Calculated results

C.O.P.	6.24	6.17	5.83	5.75	5.53	5.40	5.16
Tbdc	44.57	45.49	45.27	45.31	44.44	44.36	43.46
Apparent R12mdot	13.75	13.35	12.48	12.31	11.75	11.50	10.97
Ideal R12 mdot	15.87	15.41	14.40	14.31	13.64	13.48	12.94
R12 flow ratio	0.87	0.87	0.87	0.86	0.86	0.85	0.85
Minimum work	191.68	192.85	195.86	194.64	196.20	194.50	193.83
Comp. efficiency	0.52	0.53	0.53	0.53	0.53	0.53	0.52

18/5/86 Rotor oil ducts plugged. Suction by-pass holes plugged

	:3.P.Control						
Index	447.00	497.00	538.00	542.00	568.00	570.00	608.00
Time, mins	163.96	214.81	255.81	259.81	285.81	287.81	329.77
PERFORMANCE							
Cond. water in	17.34	17.91	18.19	18.18	18.13	18.16	18.22
water out	57.66	58.42	58.94	59.00	59.05	59.24	59.60
flow rate	11.11	10.00	9.29	9.19	8.88	8.77	7.87
Power	1874.82	1695.63	1584.61	1570.25	1520.73	1507.95	1363.81
Evap. water in	30.17	26.40	24.09	23.89	22.62	22.55	19.37
water out	26.08	22.86	20.75	20.59	19.45	19.36	16.53
flow rate	91.19	91.02	90.78	90.40	90.06	90.04	89.53
Power	1563.87	1351.31	1269.49	1248.24	1195.30	1201.09	1064.61
Comp. Voltage	241.29	242.93	242.62	241.28	239.30	239.35	239.63
Current	2247.94	2258.18	2236.45	2253.28	2215.60	2219.43	2222.76
Power	368.49	367.11	366.52	364.11	361.27	360.91	353.62
R12 metered rate	9.45	8.61	7.80	7.71	7.57	7.70	6.58
R12 TEMPERATURES							
Sump Oil	53.45	53.95	54.54	54.53	54.85	54.92	55.90
Discharge	81.68	83.63	84.88	85.02	85.78	85.87	87.89
Condenser Start	80.75	82.41	83.52	83.61	84.18	84.30	85.79
Mid Condenser	47.93	49.34	50.02	50.15	50.57	50.48	51.34
Condenser End	20.78	21.24	21.31	21.23	21.11	21.06	20.09
Evaporator Start	19.91	16.88	15.16	14.98	14.36	14.30	11.69
Evaporator End	25.92	22.57	19.92	20.15	18.46	18.48	15.61
Suction	26.39	22.83	20.30	19.99	18.42	19.03	16.31
PRESSURES (gauge Bar)							
Discharge	12.38	12.37	12.36	12.35	12.35	12.34	12.32
Cond. End	10.30	10.75	10.98	11.02	11.17	11.13	11.45
Evap. Start	4.59	4.11	3.64	3.79	3.64	3.65	3.28
Suction	4.51	4.03	3.76	3.71	3.57	3.58	3.21
Calculated results							
C.O.P.	5.09	4.62	4.32	4.31	4.21	4.18	3.86
Tbdc	43.33	41.78	40.91	40.64	40.17	40.41	39.33
Apparent R12mdot	10.79	9.71	9.03	8.94	8.63	8.55	7.64
Ideal R12 mdot	12.85	11.59	10.88	10.74	10.37	10.39	9.44
R12 flow ratio	0.84	0.84	0.83	0.83	0.83	0.82	0.81
Minimum work	192.17	191.58	188.96	189.12	188.53	186.34	180.27
Comp. efficiency	0.52	0.52	0.52	0.52	0.52	0.52	0.51

18/5/86 Rotor oil ducts plugged. Suction by-pass holes plugged

	:3.P.Control						
Index	612.00	652.00	657.00	661.00	671.00	680.00	690.00
Time, mins	333.77	373.77	378.77	382.77	392.77	401.77	411.77
PERFORMANCE							
Cond. water in	18.25	18.48	18.49	18.50	18.52	18.57	18.47
water out	59.70	60.18	60.32	60.23	60.33	60.53	60.59
flow rate	7.94	7.30	7.10	7.14	6.90	6.86	6.62
Power	1376.95	1274.11	1242.98	1247.32	1207.50	1204.92	1167.23
Evap. water in	19.09	16.61	16.33	16.11	15.62	15.17	14.74
water out	16.28	14.05	13.80	13.62	13.16	12.78	12.36
flow rate	89.24	89.24	89.24	89.29	89.28	88.88	88.72
Power	1048.80	955.04	944.94	930.59	921.89	891.41	883.54
Comp. Voltage	238.40	241.17	241.92	242.02	242.69	241.60	242.06
Current	2183.82	2180.55	2182.75	2182.06	2177.54	2168.43	2171.51
Power	352.25	346.12	345.84	345.33	344.14	340.96	340.92
R12 metered rate	6.67	6.15	5.99	6.00	5.77	5.96	5.70
R12 TEMPERATURES							
Sump Oil	56.06	57.58	57.95	58.10	58.55	58.86	59.32
Discharge	88.10	90.38	90.69	90.89	91.50	91.93	92.39
Condenser Start	85.97	87.66	87.96	88.12	88.57	88.90	89.32
Mid Condenser	51.42	51.87	51.91	52.00	52.06	52.07	52.21
Condenser End	20.03	19.62	19.62	19.56	19.51	19.50	19.34
Evaporator Start	11.47	9.46	9.32	9.05	8.64	8.32	7.98
Evaporator End	15.23	13.03	12.86	12.64	12.14	11.90	11.46
Suction	16.06	14.07	14.21	14.00	13.51	13.42	12.93
PRESSURES (gauge Bar)							
Discharge	12.31	12.29	12.29	12.30	12.29	12.26	12.28
Cond. End	11.47	11.67	11.67	11.71	11.73	11.74	11.79
Evap. Start	3.25	2.99	2.97	2.94	2.89	2.84	2.80
Suction	3.18	2.92	2.91	2.88	2.83	2.78	2.75
Calculated results							
C.O.P.	3.91	3.68	3.59	3.61	3.51	3.53	3.42
Tbdc	39.27	39.16	39.36	39.19	39.32	39.38	39.40
Apparent R12mdot	7.71	7.06	6.88	6.90	6.66	6.64	6.41
Ideal R12 mdot	9.36	8.67	8.63	8.54	8.40	8.28	8.18
R12 flow ratio	0.82	0.82	0.80	0.81	0.79	0.80	0.78
Minimum work	183.09	178.30	174.32	176.21	172.35	173.39	169.28
Comp. efficiency	0.52	0.52	0.50	0.51	0.50	0.51	0.50

18/5/86 Rotor oil ducts plugged. Suction by-pass holes plugged

	:3.P.Control						
Index	753.00	758.00	789.00	795.00	858.00	865.00	926.00
Time, mins	478.36	483.36	514.35	520.36	583.36	590.36	651.35
PERFORMANCE							
Cond. water in	19.00	19.02	19.12	19.11	19.20	19.20	19.45
water out	61.23	60.76	61.42	61.45	62.17	62.48	63.39
flow rate	5.65	5.62	5.24	5.13	4.53	4.46	4.13
Power	998.66	981.95	927.13	908.82	814.44	808.65	759.80
Evap. water in	9.95	9.62	7.77	7.43	4.50	4.19	2.11
water out	7.99	7.68	5.99	5.66	2.93	2.65	0.72
flow rate	87.34	87.02	86.11	85.96	85.30	84.38	83.33
Power	719.46	707.89	641.16	634.59	559.59	544.68	485.88
Comp. Voltage	242.30	242.07	242.31	241.64	245.82	242.26	239.02
Current	2116.06	2113.99	2089.05	2084.91	2088.49	2076.24	1979.97
Power	326.72	323.44	317.18	315.40	306.80	302.11	287.64
R12 metered rate	4.68	4.44	4.17	4.08	3.73	3.70	-0.03
R12 TEMPERATURES							
Sump Oil	62.24	62.50	64.14	64.50	67.67	68.13	70.84
Discharge	96.45	96.68	98.47	98.78	101.80	102.13	104.53
Condenser Start	92.47	92.57	93.97	94.18	96.27	96.60	98.28
Mid Condenser	52.65	52.67	52.47	52.59	51.36	51.16	43.06
Condenser End	19.48	19.49	19.48	19.48	19.49	19.50	19.69
Evaporator Start	4.38	4.16	2.69	2.50	0.32	0.12	-1.48
Evaporator End	6.95	6.61	5.11	4.86	2.13	2.01	0.76
Suction	10.22	9.90	8.94	8.88	7.20	7.97	8.06
PRESSURES (gauge Bar)							
Discharge	12.25	12.27	12.24	12.25	12.23	12.21	12.16
Cond. End	11.99	12.04	12.07	12.08	12.15	12.13	12.14
Evap. Start	2.36	2.30	2.16	2.14	1.90	1.89	1.72
Suction	2.31	2.26	2.11	2.09	1.86	1.85	1.69
Calculated results							
C.O.P.	3.06	3.04	2.92	2.88	2.65	2.68	2.64
Tbdc	38.80	38.42	38.54	38.62	38.68	38.92	39.23
Apparent R12mdot	5.42	5.33	5.00	4.90	4.35	4.31	4.03
Ideal R12 mdot	7.04	6.92	6.54	6.49	5.89	5.86	5.44
R12 flow ratio	0.77	0.77	0.76	0.75	0.74	0.74	0.74
Minimum work	158.87	157.98	153.82	151.44	143.04	142.25	138.67
Comp. efficiency	0.49	0.49	0.48	0.48	0.47	0.47	0.48

19/5/86 Suction by-pass holes open. Rotor oil ducts plugged

	:3.P.SucTest						
Index	401.00	405.00	433.00	437.00	451.00	454.00	456.00
Time, mins	118.29	122.29	150.29	154.29	168.29	171.29	173.29
PERFORMANCE							
Cond. water in	17.92	18.12	16.92	16.98	17.48	17.59	17.68
water out	53.80	54.03	55.32	55.38	55.67	55.76	55.79
flow rate	15.38	15.29	13.77	13.76	13.51	13.16	13.16
Power	2309.06	2297.85	2213.22	2212.01	2159.50	2102.72	2098.81
Evap. water in	38.33	37.87	34.97	34.63	33.39	32.82	32.40
water out	32.91	32.50	29.91	29.65	28.58	28.10	27.76
flow rate	88.46	88.72	88.69	88.91	88.72	88.70	88.65
Power	2006.64	1992.32	1878.17	1853.84	1785.82	1751.48	1720.29
Comp. Voltage	239.11	240.37	241.79	242.60	239.08	239.63	240.64
Current	2241.34	2250.95	2243.86	2265.52	2240.40	2235.44	2229.98
Power	355.33	357.74	362.35	363.98	362.71	363.51	363.19
R12 metered rate	11.35	11.20	10.52	10.50	10.09	10.19	9.87
R12 TEMPERATURES							
Sump Oil	47.82	48.93	51.72	51.82	51.86	51.74	51.71
Discharge	75.26	76.30	79.89	80.10	80.70	80.82	80.90
Condenser Start	74.54	75.63	79.04	79.23	79.73	79.82	79.85
Mid Condenser	43.04	43.49	45.61	45.84	46.56	46.84	46.97
Condenser End	26.76	25.75	21.57	21.49	21.34	21.23	21.24
Evaporator Start	25.84	25.51	23.48	23.26	22.37	21.93	21.68
Evaporator End	34.79	34.16	30.60	30.19	28.79	27.95	27.63
Suction	35.32	34.67	31.26	30.83	29.54	28.70	28.40
PRESSURES (gauge Bar)							
Discharge	12.41	12.43	12.46	12.46	12.46	12.45	12.46
Cond. End	8.50	8.70	9.52	9.59	9.84	9.95	10.00
Evap. Start	5.61	5.55	5.18	5.14	4.98	4.90	4.86
Suction	5.50	5.45	5.08	5.04	4.88	4.81	4.77
Calculated results							
C.O.P.	6.50	6.42	6.11	6.08	5.95	5.78	5.78
Tbdc	43.40	44.07	45.23	45.16	44.74	44.34	44.14
Apparent R12mdot	14.16	13.94	12.90	12.87	12.53	12.19	12.16
Ideal R12 mdot	15.78	15.57	14.39	14.27	13.86	13.66	13.56
R12 flow ratio	0.90	0.89	0.90	0.90	0.90	0.89	0.90
Minimum work	200.02	200.28	203.99	205.65	206.91	204.54	205.88
Comp. efficiency	0.56	0.56	0.56	0.56	0.57	0.56	0.57

19/5/86 Suction by-pass holes open. Rotor oil ducts plugged

	:3.P.SucTest						
Index	470.00	489.00	492.00	503.00	506.00	514.00	525.00
Time, mins	187.29	206.29	209.29	220.29	223.29	231.29	242.91
PERFORMANCE							
Cond. water in	18.06	18.59	18.66	18.85	18.93	19.13	19.01
water out	56.28	57.20	57.16	57.68	57.73	57.92	58.05
flow rate	12.05	10.64	10.64	9.90	9.84	9.72	9.63
Power	1927.74	1719.63	1714.50	1608.60	1597.91	1578.30	1573.52
Evap. water in	29.69	26.51	26.03	24.37	23.95	23.13	23.06
water out	25.54	22.79	22.34	20.94	20.55	19.82	19.75
flow rate	89.57	89.87	89.84	90.49	90.16	90.50	90.24
Power	1556.23	1399.05	1386.09	1302.40	1282.45	1252.87	1251.77
Comp. Voltage	240.83	240.39	240.82	239.94	239.15	239.98	240.30
Current	2249.76	2237.58	2236.51	2232.05	2236.13	2222.76	2224.07
Power	360.79	358.79	359.01	356.80	355.18	355.38	355.13
R12 metered rate	9.14	8.48	8.18	7.73	7.66	7.35	7.49
R12 TEMPERATURES							
Sump Oil	51.41	51.61	51.68	52.02	52.18	52.54	53.01
Discharge	81.56	82.98	83.18	84.04	84.26	84.98	85.44
Condenser Start	80.38	81.65	81.84	82.55	82.78	83.40	83.79
Mid Condenser	48.11	49.30	49.44	49.92	50.10	50.37	50.43
Condenser End	21.44	21.86	21.91	22.06	22.11	22.26	22.20
Evaporator Start	19.63	17.33	16.76	15.81	15.50	14.89	14.82
Evaporator End	24.72	21.86	20.99	19.56	19.37	18.63	18.62
Suction	25.64	22.85	22.19	20.83	20.48	19.84	19.97
PRESSURES (gauge Bar)							
Discharge	12.44	12.40	12.40	12.37	12.36	12.37	12.39
Cond. End	10.36	10.72	10.77	10.92	10.97	11.07	11.09
Evap. Start	4.53	4.12	4.07	3.86	3.80	3.68	3.69
Suction	4.44	4.03	3.98	3.78	3.71	3.60	3.61
Calculated results							
C.O.P.	5.34	4.79	4.78	4.51	4.50	4.44	4.43
Tbdc	42.55	40.96	40.81	40.11	39.88	39.65	40.11
Apparent R12mdot	11.16	9.91	9.88	9.25	9.18	9.05	9.00
Ideal R12 mdot	12.72	11.62	11.50	10.96	10.81	10.50	10.50
R12 flow ratio	0.88	0.85	0.86	0.84	0.85	0.86	0.86
Minimum work	201.87	195.74	196.95	192.45	193.35	195.54	194.88
Comp. efficiency	0.56	0.55	0.55	0.54	0.54	0.55	0.55

19/5/86 Suction by-pass holes open. Rotor oil ducts plugged

	:3.P.SucTest						
Index	570.00	574.00	617.00	620.00	625.00	637.00	642.00
Time, mins	289.62	293.62	336.62	339.62	344.62	356.62	361.62
PERFORMANCE							
Cond. water in	18.89	19.01	19.61	19.61	19.59	19.59	19.61
water out	58.85	58.92	59.62	59.68	59.72	59.83	59.92
flow rate	8.45	8.47	7.69	7.58	7.55	7.43	7.35
Power	1413.50	1414.82	1287.85	1271.33	1267.94	1251.64	1240.29
Evap. water in	19.86	19.56	16.94	16.78	16.51	15.90	15.66
water out	16.94	16.69	14.33	14.17	13.95	13.39	13.17
flow rate	90.12	90.30	89.62	89.43	89.41	89.35	88.59
Power	1104.79	1086.36	978.68	976.91	960.61	939.83	924.08
Comp. Voltage	241.82	241.87	241.60	240.85	242.05	241.91	238.52
Current	2207.31	2205.74	2184.01	2179.11	2162.40	2171.70	2151.79
Power	352.37	352.40	346.20	344.49	343.47	341.78	338.79
R12 metered rate	6.70	6.62	6.05	5.87	5.72	5.74	5.90
R12 TEMPERATURES							
Sump Oil	54.56	54.70	56.38	56.60	56.61	57.06	57.28
Discharge	88.03	88.31	90.78	91.00	91.10	91.75	91.91
Condenser Start	85.98	86.27	88.34	88.51	88.59	89.12	89.18
Mid Condenser	51.30	51.33	52.00	52.05	52.11	52.23	52.26
Condenser End	22.04	22.13	22.56	22.54	22.52	22.49	22.48
Evaporator Start	12.22	12.01	9.91	9.76	9.53	9.04	8.91
Evaporator End	15.54	15.25	13.06	12.95	12.63	12.14	11.81
Suction	17.43	17.27	15.45	15.07	14.98	14.49	14.61
PRESSURES (gauge Bar)							
Discharge	12.37	12.38	12.36	12.35	12.36	12.35	12.35
Cond. End	11.36	11.39	11.58	11.60	11.64	11.67	11.67
Evap. Start	3.33	3.30	3.00	2.97	2.93	2.87	2.87
Suction	3.25	3.23	2.94	2.90	2.87	2.80	2.80
Calculated results							
C.O.P.	4.01	4.01	3.72	3.69	3.69	3.66	3.66
Tbdc	39.62	39.64	39.44	39.36	39.08	39.11	39.30
Apparent R12mdot	8.00	8.00	7.23	7.13	7.11	7.00	6.94
Ideal R12 mdot	9.53	9.46	8.68	8.60	8.51	8.34	8.34
R12 flow ratio	0.84	0.85	0.83	0.83	0.84	0.84	0.83
Minimum work	187.95	189.26	183.07	181.86	182.78	182.77	181.05
Comp. efficiency	0.53	0.54	0.53	0.53	0.53	0.53	0.53

19/5/86 Suction by-pass holes open. Rotor oil ducts plugged

	:3.P.SucTest						
Index	647.00	650.00	677.00	682.00	686.00	708.00	712.00
Time, mins	366.62	369.62	398.03	403.03	407.03	429.03	433.03
PERFORMANCE							
Cond. water in	19.59	19.58	19.56	19.57	19.57	19.67	19.72
water out	60.08	60.02	60.71	60.62	60.64	61.44	60.72
flow rate	7.16	7.22	6.54	6.45	6.33	5.91	5.77
Power	1213.65	1222.19	1126.43	1108.29	1088.28	1033.33	990.31
Evap. water in	15.44	15.30	13.06	12.69	12.38	10.83	10.57
water out	12.99	12.87	10.89	10.54	10.25	8.85	8.60
flow rate	88.84	89.05	89.54	89.35	89.46	89.20	88.97
Power	908.25	905.94	814.66	805.14	794.66	740.81	735.63
Comp. Voltage	240.55	241.30	240.71	241.47	241.63	242.57	242.21
Current	2168.43	2166.49	2129.87	2131.26	2126.73	2110.28	2109.09
Power	339.93	340.48	330.41	329.61	328.03	322.44	321.30
R12 metered rate	6.04	5.91	5.42	5.03	4.73	4.69	4.55
R12 TEMPERATURES							
Sump Oil	57.42	57.56	58.88	59.16	59.33	60.65	60.89
Discharge	92.18	92.31	94.13	94.45	94.70	96.34	96.57
Condenser Start	89.39	89.52	90.90	91.14	91.32	92.58	92.80
Mid Condenser	52.31	52.33	52.58	52.74	52.78	52.90	53.00
Condenser End	22.45	22.44	22.11	22.07	22.04	21.69	21.67
Evaporator Start	8.62	8.57	6.90	6.65	6.40	5.13	5.00
Evaporator End	12.11	11.73	9.97	9.48	9.02	8.02	7.47
Suction	14.34	14.37	12.93	11.97	12.44	11.92	11.16
PRESSURES (gauge Bar)							
Discharge	12.34	12.35	12.30	12.34	12.34	12.31	12.31
Cond. End	11.68	11.69	11.79	11.86	11.88	11.92	11.96
Evap. Start	2.85	2.83	2.62	2.58	2.55	2.41	2.36
Suction	2.78	2.77	2.56	2.52	2.49	2.35	2.30
Calculated results							
C.O.P.	3.57	3.59	3.41	3.36	3.32	3.20	3.08
Tbdc	39.35	39.32	39.10	38.90	38.85	39.01	38.68
Apparent R12mdot	6.78	6.83	6.24	6.13	6.02	5.67	5.43
Ideal R12 mdot	8.27	8.24	7.69	7.60	7.53	7.15	7.03
R12 flow ratio	0.82	0.83	0.81	0.81	0.80	0.79	0.77
Minimum work	177.99	179.72	172.48	171.30	169.17	165.02	159.74
Comp. efficiency	0.52	0.53	0.52	0.52	0.52	0.51	0.50

19/5/86 Suction by-pass holes open. Rotor oil ducts plugged

	:3.P.SucTest						
Index	717.00	721.00	726.00	752.00	757.00	779.00	784.00
Time, mins	438.03	442.03	447.03	473.03	478.03	500.03	505.03
PERFORMANCE							
Cond. water in	19.74	19.78	19.80	19.90	19.97	20.22	20.27
water out	61.15	60.83	60.89	61.48	61.95	62.28	61.67
flow rate	5.81	5.73	5.71	5.39	5.35	5.10	5.10
Power	1006.95	984.45	981.85	937.93	939.99	897.88	883.66
Evap. water in	10.26	10.00	9.69	8.20	7.94	6.87	6.65
water out	8.32	8.07	7.78	6.43	6.21	5.20	4.98
flow rate	88.79	88.44	88.52	88.49	88.31	87.40	87.56
Power	722.67	713.02	705.76	656.07	641.93	611.59	610.55
Comp. Voltage	242.04	241.81	242.12	242.79	242.92	241.61	242.68
Current	2107.45	2090.88	2095.71	2082.40	2076.31	2095.46	2044.22
Power	319.44	317.51	317.72	311.33	310.37	304.79	304.80
R12 metered rate	4.43	4.14	4.32	4.25	4.03	3.85	3.56
R12 TEMPERATURES							
Sump Oil	61.16	61.37	61.62	62.97	63.23	64.42	64.64
Discharge	96.84	97.12	97.46	98.98	99.27	100.50	100.78
Condenser Start	92.96	93.16	93.46	94.64	94.81	95.74	96.03
Mid Condenser	53.05	53.12	53.12	53.21	53.21	53.27	53.39
Condenser End	21.64	21.60	21.59	21.45	21.45	21.48	21.53
Evaporator Start	4.76	4.57	4.31	3.28	2.97	2.23	2.06
Evaporator End	7.27	7.01	6.64	5.31	5.35	4.32	3.88
Suction	11.29	10.80	10.80	10.42	10.14	9.76	9.63
PRESSURES (gauge Bar)							
Discharge	12.32	12.33	12.32	12.30	12.30	12.27	12.31
Cond. End	11.98	12.01	12.01	12.04	12.05	12.07	12.12
Evap. Start	2.35	2.32	2.29	2.19	2.16	2.08	2.04
Suction	2.30	2.27	2.24	2.13	2.11	2.03	2.00
Calculated results							
C.O.P.	3.15	3.10	3.09	3.01	3.03	2.95	2.90
Tbdc	38.86	38.77	38.78	39.11	39.10	39.44	39.16
Apparent R12mdot	5.52	5.39	5.37	5.10	5.10	4.86	4.78
Ideal R12 mdot	7.01	6.94	6.86	6.59	6.52	6.31	6.23
R12 flow ratio	0.79	0.78	0.78	0.77	0.78	0.77	0.77
Minimum work	162.72	160.14	160.65	156.77	158.01	153.45	152.37
Comp. efficiency	0.51	0.50	0.51	0.50	0.51	0.50	0.50

19/5/86 Suction by-pass holes open. Rotor oil ducts plugged

	:3.P.SucTest						
Index	788.00	822.00	828.00	834.00	840.00	863.00	868.00
Time, mins	509.03	543.03	549.03	555.03	561.03	584.03	589.03
PERFORMANCE							
Cond. water in	20.30	20.50	20.52	20.54	20.54	20.55	20.53
water out	61.63	62.05	62.02	62.14	62.39	62.08	62.97
flow rate	5.00	4.84	4.74	4.70	4.66	4.52	4.51
Power	864.98	841.83	823.43	818.47	816.26	785.59	801.18
Evap. water in	6.46	5.06	4.83	4.62	4.40	3.63	3.48
water out	4.84	3.52	3.29	3.08	2.89	2.15	2.02
flow rate	88.37	87.02	87.05	87.07	87.05	86.55	86.38
Power	599.59	559.85	561.39	560.47	549.90	536.66	528.69
Comp. Voltage	243.30	241.58	241.83	242.35	242.17	241.47	240.96
Current	2069.65	2060.61	2046.66	2053.89	2047.36	2033.10	2039.07
Power	305.53	298.63	298.83	299.04	298.02	296.25	295.97
R12 metered rate	3.93	3.12	3.42	3.19	3.11	3.13	2.99
R12 TEMPERATURES							
Sump Oil	64.83	66.12	66.39	66.63	66.85	67.59	67.77
Discharge	101.08	102.45	102.68	102.87	103.20	103.97	104.16
Condenser Start	96.25	97.25	97.42	97.63	97.88	98.37	98.47
Mid Condenser	53.32	53.54	53.44	53.50	53.49	53.54	53.51
Condenser End	21.53	21.57	21.56	21.56	21.52	21.47	21.45
Evaporator Start	1.84	0.90	0.64	0.49	0.31	-0.31	-0.45
Evaporator End	4.09	2.59	2.32	2.06	2.01	1.27	1.24
Suction	10.00	8.13	9.15	8.99	9.04	8.57	8.38
PRESSURES (gauge Bar)							
Discharge	12.28	12.32	12.28	12.30	12.29	12.28	12.28
Cond. End	12.10	12.18	12.14	12.16	12.17	12.17	12.17
Evap. Start	2.02	1.92	1.90	1.89	1.87	1.81	1.81
Suction	1.97	1.88	1.86	1.85	1.83	1.77	1.76
Calculated results							
C.O.P.	2.83	2.82	2.76	2.74	2.74	2.65	2.71
Tbdc	39.25	39.24	39.35	39.34	39.44	39.39	39.51
Apparent R12mdot	4.67	4.53	4.43	4.40	4.38	4.20	4.28
Ideal R12 mdot	6.16	5.92	5.87	5.84	5.79	5.63	5.61
R12 flow ratio	0.76	0.77	0.75	0.75	0.76	0.75	0.76
Minimum work	149.78	149.23	146.34	145.87	146.03	142.48	145.51
Comp. efficiency	0.49	0.50	0.49	0.49	0.49	0.48	0.49

19/5/86 Suction by-pass holes open. Rotor oil ducts plugged

	:3.P.SucTest	
Index	883.00	890.00
Time, mins	604.03	611.03

PERFORMANCE

Cond. water in	20.54	20.54
water out	61.84	62.59
flow rate	4.50	4.48
Power	777.97	788.44
Evap. water in	3.00	2.83
water out	1.58	1.41
flow rate	86.07	86.33
Power	514.25	514.68
Comp. Voltage	241.69	242.51
Current	2036.05	2034.80
Power	292.72	293.01
R12 metered rate	0.95	1.59

R12 TEMPERATURES

Sump Oil	68.51	68.83
Discharge	104.91	105.17
Condenser Start	99.00	99.20
Mid Condenser	53.64	53.64
Condenser End	21.39	21.38
Evaporator Start	-0.83	-1.07
Evaporator End	0.81	0.93
Suction	9.21	9.15

PRESSURES (gauge Bar)

Discharge	12.30	12.31
Cond. End	12.22	12.23
Evap. Start	1.74	1.73
Suction	1.70	1.69

Calculated results

C.O.P.	2.66	2.69
Tbdc	39.34	39.45
Apparent R12mdot	4.15	4.20
Ideal R12 mdot	5.46	5.44
R12 flow ratio	0.76	0.77
Minimum work	143.36	145.62
Comp. efficiency	0.49	0.50

20/5/86 Suction by-pass holes plugged. Rotor oil ducts open

	:3.P.StatQuo						
Index	425.00	427.00	430.00	432.00	435.00	438.00	477.00
Time, mins	140.95	142.95	145.95	147.95	150.95	153.95	192.95
PERFORMANCE							
Cond. water in	20.35	19.43	18.58	18.29	18.03	17.92	18.39
water out	55.25	55.32	55.52	55.66	55.83	55.97	56.87
flow rate	14.79	14.37	14.04	13.89	13.70	13.51	12.66
Power	2160.56	2158.75	2171.29	2172.68	2167.62	2151.52	2038.78
Evap. water in	37.38	37.17	36.87	36.68	36.39	36.12	32.86
water out	32.51	32.31	32.03	31.86	31.60	31.34	28.50
flow rate	91.52	91.31	91.38	91.65	91.72	91.42	91.52
Power	1863.76	1858.05	1853.78	1848.36	1836.97	1828.82	1671.18
Comp. Voltage	240.24	240.02	240.92	240.71	240.59	242.67	242.08
Current	2307.85	2306.34	2302.20	2310.24	2312.56	2307.22	2319.03
Power	364.69	363.78	363.82	364.33	364.31	364.80	367.00
R12 metered rate	11.06	11.08	11.02	10.71	10.71	10.70	9.96
R12 TEMPERATURES							
Sump Oil	53.73	54.01	54.40	54.53	54.67	54.83	55.38
Discharge	78.65	78.87	79.16	79.33	79.53	79.76	81.23
Condenser Start	77.91	78.09	78.40	78.61	78.78	78.98	80.23
Mid Condenser	43.90	43.94	43.99	44.06	44.31	44.52	46.58
Condenser End	29.64	28.90	28.23	27.99	27.30	26.93	24.14
Evaporator Start	25.81	25.65	25.47	25.36	25.09	24.86	22.30
Evaporator End	34.24	33.95	33.50	33.12	32.44	32.49	28.82
Suction	34.86	34.55	34.10	33.81	33.19	33.03	29.50
PRESSURES (gauge Bar)							
Discharge	12.40	12.38	12.39	12.38	12.37	12.40	12.38
Cond. End	8.69	8.70	8.72	8.73	8.83	8.93	9.68
Evap. Start	5.56	5.53	5.50	5.48	5.43	5.40	4.95
Suction	5.45	5.42	5.39	5.37	5.32	5.29	4.85
Calculated results							
C.O.P.	5.92	5.93	5.97	5.96	5.95	5.90	5.56
Tbdc	46.56	46.66	46.76	46.83	46.72	46.68	45.33
Apparent R12mdot	13.26	13.18	13.18	13.16	13.06	12.93	11.98
Ideal R12 mdot	15.37	15.29	15.20	15.13	14.99	14.91	13.74
R12 flow ratio	0.86	0.86	0.87	0.87	0.87	0.87	0.87
Minimum work	192.41	192.30	193.82	194.38	195.14	194.85	198.54
Comp. efficiency	0.53	0.53	0.53	0.53	0.54	0.53	0.54

20/5/86 Suction by-pass holes plugged. Rotor oil ducts open

	:3.P.StatQuo						
Index	479.00	514.00	519.00	527.00	574.00	578.00	620.00
Time, mins	194.95	229.95	234.95	242.95	291.32	295.32	337.32
PERFORMANCE							
Cond. water in	18.42	18.55	18.61	18.60	18.85	18.85	19.42
water out	56.88	57.42	57.45	57.59	58.55	58.67	59.33
flow rate	12.66	11.63	11.59	11.49	9.90	9.82	8.97
Power	2038.04	1891.60	1884.08	1875.32	1644.70	1636.54	1498.42
Evap. water in	32.70	30.48	30.21	29.82	25.29	24.94	21.75
water out	28.36	26.46	26.24	25.90	21.83	21.55	18.68
flow rate	91.72	91.37	91.38	91.79	90.52	91.05	90.30
Power	1664.85	1538.95	1517.81	1504.63	1310.75	1292.19	1158.18
Comp. Voltage	244.18	241.79	241.69	243.97	239.87	242.54	242.29
Current	2323.86	2283.86	2274.82	2303.45	2254.28	2260.75	2232.36
Power	367.78	367.91	367.76	370.18	365.11	366.82	360.77
R12 metered rate	9.91	9.34	9.21	9.09	8.06	7.87	7.05
R12 TEMPERATURES							
Sump Oil	55.39	55.63	55.67	55.84	56.18	56.26	57.02
Discharge	81.32	82.28	82.42	82.53	84.56	84.79	86.57
Condenser Start	80.31	81.15	81.28	81.40	83.12	83.37	84.86
Mid Condenser	46.66	47.88	48.00	48.17	49.77	49.81	50.67
Condenser End	23.91	22.52	22.44	22.27	22.20	22.18	22.66
Evaporator Start	22.13	20.30	20.12	19.76	16.02	15.79	13.43
Evaporator End	28.67	26.28	25.87	25.84	21.29	20.82	17.59
Suction	29.33	26.91	26.33	26.05	21.58	21.02	17.74
PRESSURES (gauge Bar)							
Discharge	12.40	12.39	12.39	12.40	12.35	12.36	12.36
Cond. End	9.73	10.21	10.26	10.33	10.84	10.86	11.16
Evap. Start	4.94	4.63	4.59	4.54	3.96	3.93	3.55
Suction	4.84	4.54	4.50	4.45	3.87	3.84	3.49
Calculated results							
C.O.P.	5.54	5.14	5.12	5.07	4.50	4.46	4.15
Tbdc	45.25	44.13	44.04	43.72	41.51	41.47	40.30
Apparent R12mdot	11.96	10.97	10.92	10.85	9.43	9.38	8.55
Ideal R12 mdot	13.69	12.89	12.80	12.66	11.15	11.07	10.15
R12 flow ratio	0.87	0.85	0.85	0.86	0.85	0.85	0.84
Minimum work	199.23	194.89	195.27	196.46	192.85	193.08	190.34
Comp. efficiency	0.54	0.53	0.53	0.53	0.53	0.53	0.53

20/5/86 Suction by-pass holes plugged. Rotor oil ducts open

	:3.P.StatQuo						
Index	623.00	626.00	629.00	632.00	639.00	648.00	666.00
Time, mins	340.32	343.32	346.32	349.32	356.32	365.32	385.12
PERFORMANCE							
Cond. water in	19.48	19.54	19.56	19.59	19.64	19.66	19.94
water out	59.42	59.40	59.42	59.51	59.60	59.78	60.13
flow rate	8.87	8.73	8.71	8.68	8.51	8.38	7.85
Power	1482.68	1456.28	1453.09	1450.34	1423.25	1407.43	1320.72
Evap. water in	21.58	21.37	21.18	20.98	20.57	20.03	18.20
water out	18.53	18.35	18.18	18.00	17.60	17.15	15.54
flow rate	90.09	89.83	89.90	90.07	89.75	89.77	89.70
Power	1146.40	1134.22	1130.87	1120.48	1112.85	1083.60	998.24
Comp. Voltage	241.22	237.78	239.98	240.03	239.46	239.99	240.22
Current	2212.46	2203.79	2207.62	2220.81	2241.34	2204.42	2193.81
Power	359.38	358.30	359.02	358.73	357.80	356.25	351.79
R12 metered rate	7.13	6.84	7.02	6.74	6.86	6.73	6.05
R12 TEMPERATURES							
Sump Oil	57.05	57.12	57.25	57.33	57.52	57.86	58.72
Discharge	86.70	86.82	87.00	87.12	87.45	87.93	89.21
Condenser Start	84.96	85.08	85.22	85.36	85.58	85.90	86.96
Mid Condenser	50.76	50.84	50.87	50.90	51.00	51.17	51.55
Condenser End	22.66	22.72	22.77	22.76	22.82	22.83	23.04
Evaporator Start	13.10	13.25	13.07	12.91	12.64	12.06	10.99
Evaporator End	17.61	17.26	17.21	16.93	16.53	16.17	14.36
Suction	17.37	17.60	17.68	17.35	17.13	16.65	15.16
PRESSURES (gauge Bar)							
Discharge	12.35	12.33	12.35	12.34	12.34	12.34	12.31
Cond. End	11.18	11.19	11.20	11.22	11.25	11.30	11.41
Evap. Start	3.50	3.49	3.50	3.45	3.42	3.35	3.16
Suction	3.45	3.43	3.44	3.39	3.36	3.29	3.11
Calculated results							
C.O.P.	4.13	4.06	4.05	4.04	3.98	3.95	3.75
Tbdc	40.10	40.16	40.29	40.08	40.13	40.01	39.72
Apparent R12mdot	8.46	8.30	8.28	8.26	8.10	8.00	7.48
Ideal R12 mdot	10.04	10.00	10.01	9.90	9.81	9.63	9.15
R12 flow ratio	0.84	0.83	0.83	0.83	0.83	0.83	0.82
Minimum work	189.85	186.86	186.67	187.68	185.52	186.07	181.14
Comp. efficiency	0.53	0.52	0.52	0.52	0.52	0.52	0.51

20/5/86 Suction by-pass holes plugged. Rotor oil ducts open

	:3.P.StatQuo						
Index	669.00	726.00	731.00	738.00	760.00	765.00	810.00
Time, mins	388.12	445.11	450.11	457.11	479.11	484.11	529.11
PERFORMANCE							
Cond. water in	19.99	20.43	20.40	20.39	20.41	20.55	20.74
water out	60.25	61.47	61.44	61.64	61.99	62.06	62.67
flow rate	7.79	6.36	6.29	6.14	5.79	5.74	5.16
Power	1312.71	1092.37	1080.48	1060.01	1007.53	997.15	905.46
Evap. water in	17.87	12.83	12.45	11.95	10.43	10.15	7.60
water out	15.26	10.68	10.32	9.86	8.46	8.19	5.84
flow rate	89.53	88.15	88.49	88.40	87.57	87.58	86.13
Power	979.35	794.11	788.26	775.26	721.97	716.51	634.54
Comp. Voltage	240.25	240.62	242.02	242.71	240.64	241.19	240.01
Current	2197.38	2159.96	2135.84	2155.94	2112.23	2111.85	2093.01
Power	350.13	337.34	337.10	335.79	332.14	331.69	321.16
R12 metered rate	6.39	5.01	4.79	5.12	4.61	4.73	3.96
R12 TEMPERATURES							
Sump Oil	58.87	62.41	62.72	63.12	64.57	64.82	67.26
Discharge	89.39	94.02	94.45	94.97	96.57	96.80	99.56
Condenser Start	87.06	90.66	91.04	91.50	92.65	92.89	94.99
Mid Condenser	51.64	52.42	52.44	52.50	52.69	52.72	52.97
Condenser End	23.02	23.31	23.30	23.25	23.27	23.34	23.54
Evaporator Start	10.61	6.75	6.56	6.16	5.00	4.81	2.94
Evaporator End	14.41	9.90	9.31	8.93	7.74	7.38	5.17
Suction	15.34	11.09	11.42	11.17	9.40	10.14	8.23
PRESSURES (gauge Bar)							
Discharge	12.30	12.26	12.28	12.25	12.25	12.26	12.24
Cond. End	11.45	11.74	11.76	11.77	11.84	11.84	11.94
Evap. Start	3.11	2.59	2.59	2.53	2.40	2.40	2.17
Suction	3.05	2.54	2.54	2.48	2.35	2.34	2.12
Calculated results							
C.O.P.	3.75	3.24	3.21	3.16	3.03	3.01	2.82
Tbdc	39.39	38.96	39.28	39.31	39.45	39.53	39.71
Apparent R12mdot	7.43	6.10	6.02	5.89	5.57	5.51	4.97
Ideal R12 mdot	9.01	7.65	7.63	7.49	7.14	7.11	6.53
R12 flow ratio	0.82	0.80	0.79	0.79	0.78	0.77	0.76
Minimum work	182.05	168.67	167.12	165.51	161.89	160.66	153.23
Comp. efficiency	0.52	0.50	0.50	0.49	0.49	0.48	0.48

20/5/86 Suction by-pass holes plugged. Rotor oil ducts open

	:3.P.StatQuo			
Index	815.00	865.00	874.00	942.00
Time, mins	534.11	584.11	593.11	662.50
PERFORMANCE				
Cond. water in	20.75	20.91	20.88	20.75
water out	62.92	63.31	63.46	64.18
flow rate	5.13	4.71	4.64	4.06
Power	905.29	835.98	826.78	737.86
Evap. water in	7.34	5.10	4.76	2.48
water out	5.61	3.50	3.19	1.12
flow rate	86.43	85.07	85.29	84.32
Power	624.17	570.30	560.50	481.05
Comp. Voltage	240.30	239.56	241.42	241.99
Current	2093.07	2067.51	2080.77	2036.80
Power	320.89	314.32	314.24	300.74
R12 metered rate	4.22	3.69	3.63	-0.03
R12 TEMPERATURES				
Sump Oil	67.52	69.56	69.96	72.71
Discharge	99.90	102.17	102.46	104.97
Condenser Start	95.29	96.99	97.13	98.74
Mid Condenser	52.97	53.12	53.13	53.29
Condenser End	23.54	23.70	23.65	23.53
Evaporator Start	2.69	1.08	0.83	-0.95
Evaporator End	4.94	3.04	2.72	0.91
Suction	8.43	6.92	7.02	3.19
PRESSURES (gauge Bar)				
Discharge	12.24	12.23	12.23	12.20
Cond. End	11.94	12.00	12.01	12.08
Evap. Start	2.14	1.98	1.95	1.77
Suction	2.09	1.94	1.91	1.73
Calculated results				
C.O.P.	2.82	2.66	2.63	2.45
Tbdc	39.74	40.04	39.93	40.06
Apparent R12mdot	4.96	4.55	4.50	3.98
Ideal R12 mdot	6.46	6.05	5.98	5.52
R12 flow ratio	0.77	0.75	0.75	0.72
Minimum work	154.02	147.37	146.75	136.36
Comp. efficiency	0.48	0.47	0.47	0.45

Chapter 8 The Final set of Experiments

8.1 Purpose of final tests

As explained in the previous chapter, by the Summer of 1986 understanding of the system had progressed to the recognition of several hitherto unrecognised questions. However, experiments designed to clarify these matters had not all been totally conclusive due to incomplete understanding of the system, and unreliability of the key capacity measurements.

The single most serious shortcoming in the data was the absence of systematic performance measurements over the complete ranges of evaporating and condensing temperature. The tests of the Summer of 1985, designed to furnish this data, had been compromised by the unreliability of the pelton-wheel flow meters. This dictated the need for definitive capacity measurements to be based on manual measurement of the condenser water flow rate. Because of the time taken to make a reliable manual flow measurement, it was recognised that slow variation of the source temperature would yield only equivocal data. Thus it was considered more satisfactory to aim for characterisation of a few discrete steady state operating conditions, rather than repeat the experimental technique of the original tests.

The thinking behind the original measurements had been based on an approach to the heat pump as a system of five independent variables and a large number of dependent variables. The five independent variables were regarded as the TXV setting, the two water entry temperatures, the evaporator water flow rate, and lastly, either the condenser water flow rate, or the discharge pressure regulator setting. It has since been recognised that this thinking is unnecessarily pedantic.

As illustrated in chapter 2, if the refrigerant flow rate is known, then the limiting performance of the heat exchangers can be found from straightforward calculations based solely on the first law of thermodynamics, and Clausius' statement of the second law. Consequently, however intricate the heat transfer calculations may be, the calculation of the state of the refrigerant at the end of either heat exchanger becomes extremely model insensitive as the limiting performance is approached. Thus one sees that in deriving a complete system model, the single most important calculation is that for the refrigerant flow rate, since it is this which dictates the capacity. This depends, in turn, on having a valid compressor model.

For the compressor, there are just 3 independent variables, the suction pressure & temperature, and the discharge pressure. There are only two key dependent variables, namely power consumption, and freon flow rate.

With this conceptual simplification, the purpose of the capacity measurements was reduced to acquisition of data for the dependence of the freon flow rate on the discharge pressure and suction state, against which a model could be validated. For this purpose, the heat exchangers were regarded as calorimeters, on the basis of which the freon flow rate would be estimated. In this way, the formidable experimental task of systematically exploring a five dimensional matrix was reduced to the very much more tractable exercise of establishing and recording steady state operation at a small number of combinations of evaporating pressure & condensing pressure.

A standard set of evaporating & condensing pressures was adopted. These were read from the Bourdon gauges. Although the Bourdon gauges are inaccurate and non-linear, they offer a very important advantage over the transducers - their calibration is reproducible and does not drift. Setting the operating conditions using these gauges ensured true reproduction of the same set of pressures from one run to the next. As mentioned in chapter 3, cross-reference to the pressure transducer readings made it possible to distinguish the one pressure transducer (Serial number 4800) whose calibration was unreliable and drifting, and to observe that the other transducers' calibrations were not drifting.

Table 8.1 indicates the nominal bourdon gauge settings that were used, and the region of the (discharge pressure, suction pressure) plane which was investigated. Note that some combinations are inaccesible. For instance, it was not possible to have a discharge pressure of 90psi with a suction pressure of 40psi, because, for such a small pressure difference, the throttle valve cannot admit the necessary liquid flow rate, as explained in chapter 5. At the other extreme, no attempt was made to investigate the 6psig/220psia combination for fear of overheating the compressor. At very low suction pressures, the lower limit to accesssible discharge pressure was set by the condenser water incoming temperature.

When using the 100L water tank to supply the evaporator, approach to a low evaporating temperature had been painfully slow, due to the time taken to refrigerate the tank. For this reason, the 100 litre tank was replaced by a 2 litre electric kettle. From room temperature, a low temperature could be reached within minutes, instead of hours. Upon reaching the desired evaporating pressure, the water temperature was steadied by supplying current from a variac to the kettle's heating element. By monitoring the current & voltage, an independent check was obtained of the evaporator power.

It had been recognised that there was a need for performance data at evaporating temperatures much lower than had been obtained during the initial tests. In order to further assist the pursuit of such conditions, the evaporator was re-configured in parallel flow. Thus the suction gas would depend for its superheat on the water exit, instead of the incomer. This yields a further depression of the evaporating temperature. This feature was exploited by using a very high superheat setting to further drive down the evaporating temperature, without freezing the water side. Using this subterfuge, the lowest recorded evaporating temperature was -26C.

In addition to determination of a definitive compressor performance map on the (Pc,Pe) plane, several other questions remained in need of definitive experimental treatment. In particular, the free running tests had implied that the compressor's losses could be significantly reduced by confining the oil delivery system to bearing lubrication alone. This raised several questions -

i) In service, with an atmosphere of R12 and its effect on oil viscosity, would a similar improvement be seen ?

ii) Would elimination of the flow through the rotor, and spray onto the stator, result in a significantly raised winding temperature, or reduced oil temperature ?

iii) How would elimination of the extraneous oil flows within the compressor affect the extent of oil contamination of the discharge gas ?

These questions dictated the need to measure the stator winding temperature, and the oil circulation fraction, in addition to the established measurements. The winding temperature was inferred from a resistance measurement made immediately after recording each steady state. The oil circulation fraction was measured, as before, by gravimetric analysis of a liquid sample taken from the condenser.

Two further matters required definitive treatment. There had been an attempt to determine the change in capacity which resulted from drilling large holes into the innermost plenums, in order to by-pass the suction side orifices. The result of this first test had been equivocal, because of uncertainty about the effect of this alteration on oil entrainment into the suction gas. By returning to this investigation, but with the oil delivery system reduced to bearing lubrication only, this complication was avoided.

The conventional wisdom regarding oil admixture in the refrigerant is that it reduces the refrigerating capacity, due to return to the sump of the liquid refrigerant that remains in solution with the oil. The freon fraction in the liquid phase is inversely related to the suction gas superheat, but for a fixed source temperature, the effect of increasing the superheat is to tend to drive down the evaporating pressure. These opposing consequences of raising the superheat furnish the basis of the superheat optimisation derived by McMullan et al (57). However, from the viewpoint of designing an experimental investigation, the simultaneous change of two key parameters upon changing the superheat is undesirable. For instance, with a fixed source temperature, increasing the superheat results in a rise in sump oil temperature. Some of this rise results from the reduction in the cooling effect of the liquid R12 returning with the oil, but the fall in suction pressure also contributes, due to the resultant reduction in the freon flow rate. From this experiment alone, there is no way of ascertaining the relative importance of these two effects separately.

For the final set of tests, as explained above, instead of treating the source temperature as the independent variable, the suction pressure was standardised. The effect on the mixture in the suction pipe of varying the superheat could then be investigated without the complication of a dependent suction pressure. Note that this investigation is intimately complementary to the questions raised by minimising the oil delivery system inside the compressor.

With the above considerations in mind, then, in October 1986 the original compressor was used to perform five runs, which were designed to furnish the desired information about the compressor and the effects on system performance of the compressor modifications mentioned above.

<u>Operating conditions investigated by runs 1 to 5 on the (Pc,Pe) plane</u>

Evaporating Pressure	0psig	6psig	20psig	40psig	64psig	78psig
Discharge Pressure, psia						
78	4	2 4				
90		2	1 2 3			
110		2 4		1 2 3		
150		2 4 5	1 2 3 5	1 2 3 5	1 2 3 5	
220			1 2 3	1 2 3	1 2 3	1 3

<u>Table 8.1</u>

8.2 The Experiments

In preparation for the final set of experiments, new thermocouples were made up and calibrated as described in chapter 3. In order to obtain the best possible thermal contact between the thermocouple tip and refrigerant, they were installed directly into the pipework, without any intervening thermowell. This was the only significant instrumentation difference between the final set of tests and the original tests.

The purpose of the first run was to obtain definitive data for the system's performance, without any alteration of the compressor, and for the normal setting of the expansion valve superheat. Specifications for nine operating conditions were obtained for evaporating pressures of 20psig to 78psig, and condensing pressures from 90psia to 220psia.

There were two purposes of the second run, for which the superheat was set high. By setting the superheat high, it is ensured that the liquid freon fraction in any oil returning to the compressor is minimised. By subsequently comparing the measurements of this run with those of the first run it is possible to assess the significance of this liquid freon return. The second purpose was to extend the data to still lower evaporating pressures. 6psig was adopted as the lower practical limit for making systematic sets of measurements. With the normal superheat setting, it is impossible to get this low, because the evaporator freezes.

In preparation for the third run, the compressor was removed, and the lubrication system was reduced to bearing lubrication only. Supply to the rotor's ducts was eliminated, and the crankshaft bores were sealed off at the top to prevent the escape of oil from the top end of the crankshaft. In order to ensure adequate lubrication of the bearings, the original impeller was replaced by a centrifugal pump which, unlike the original impeller, guarantees a hydrostatic head of oil at the bearing supply cross bores without the need for a high oil throughput rate.

The purpose of the third run was to provide a definitive assessment of the differences which result from eliminating all non-essential oil flows inside the compressor. For this reason, after re-assembly, evacuation & re-charging of the system, the same set of (Pe,Pc) conditions as used in the first run was repeated.

For the fourth run, the superheat was set high in order to extend this comparison to the low evaporating pressure of 6psig. Three of the conditions recorded on run 2 were repeated, and finally steady state operation was established and recorded at an evaporating pressure of 0psig, this marking the lower limit to accessible evaporating pressure. Upon attempting to obtain a lower evaporating pressure, it was found that the flow of refrigerant through the TXV would suddenly stop completely, with a subsequent very rapid evacuation of the evaporator by the compressor, down to a partial vacuum of about 4psia. This behaviour of the flow through the TXV may be due to occlusion of the orifice by oil freezing there. This fourth run thus served the two purposes of extending to an evaporating pressure of 6psig the comparison of modified v unmodified lubrication system, and extending to 0psig the range of evaporating pressure tested.

In preparation for the fifth run the compressor was again removed, and the system of plenums and orifices on the suction side was bypassed by removing the plugs that had been inserted into the holes drilled through the casting into the innermost plenums. These holes had been drilled in preparation for an earlier attempt to determine the effect on performance of the suction labyrinth. On that occasion a run was executed first with the status quo retained by leaving the holes plugged, and then repeated with the plugs removed. Unfortunately, the interpretation of the result had been unclear, because there was doubt about the effect of this alteration on the entrainment of oil by the suction gas. For the current set of experiments, having minimised the oil delivery system, this complication was avoided. After re-assembly, evacuation and recharging, four of the operating conditions tested on runs 3 and 4 were repeated. Specifically, for a discharge pressure of 150 psia, the four evaporating pressures 6, 20, 40 & 64psig were tested.

Chapter 9 A mathematical model to interpret the results

9.1 Introduction

It is difficult to draw definite conclusions from the raw data alone, because of the influence of all the small, uncontrolled differences that may exist between ostensibly comparable tests. Apart from the inevitable small errors in trying to reproduce the suction and discharge pressures of a previous test, there are also uncontrolled variations introduced by mains voltage, condenser water entry temperature and room temperature.

This problem has been resolved by developing a mathematical model for the specific purpose of interpreting the experimental measurements, henceforth referred to as the 'Interpretive model'. However, the model's real purpose goes beyond systematic collation of the measurements.

In chapter 2 it was shown that optimising a system within the constraints of currently available hardware can produce, at best, only a marginal improvement, because of the dominant influence of the compressor's losses. For this reason the ultimate objective is regarded as the development of a heatpump specification which will perform significantly better than what is currently conventional. In order to fulfill this objective, it is first necessary to quantify all the losses, in order that they may be appropriately addressed in a new design proposal. Secondly, it is necessary to develop a calculation which can predict the performance of a compressor even in the absence of any performance data. This is not immediately possible because there are three features of the compressor's behaviour, vital to the performance prediction, which are not sufficiently well specified to be reliably estimated by an ab-initio calculation, as outlined below.

Heat loss, & suction gas preheat

The preheat of the suction gas on its journey from the suction pipe to the cylinder cannot be reliably estimated. This is because several calculational uncertainties are all compounded in trying to make this estimate. While estimates for heat loss from the compressor to ambient, conduction from the case down the suction pipe, and the discharge to suction transfer are all separately uncertain, a worse problem still is presented by the uncertain cooling effect of the mixed oil & freon liquid phase which returns with the suction gas.

Mechanical losses

By considering Sommerfeld's criterion (60) for the three journal bearings, it would appear that they operate always in the regime of pure hydrodynamic lubrication, and the total loss in Watts has been estimated as 4 times the lubricant viscosity in centipoise. Unfortunately, the lubricant viscosity is not known because there is no measurement of the bearings' temperature, and there is uncertainty about the effect on viscosity of equilibration with the surrounding atmosphere of freon. The thrust bearing at the top of the crankshaft presents the same problem. Additionally, there is no way of knowing whether the gap between the rotor and stator produces a viscous drag due to ingress of oil, or if it runs free. Finally, recalling the experimental 'power-step' problem, re-inforces the view that these mechanical losses cannot be calculated.

Valve timing and leakage past the valves

There is a capacity loss due to the time taken for the valves to close, during which reverse flow can occur. This has been the subject of several attempted calculations, none of which were considered to be very satisfactory. A more detailed account is given in appendix 3.

The interpretive model's final form emerged in February 1988 after evolving through many versions from a model first written in 1984. During this development, the underlying philosophy was very conventional. The independent variables were regarded as the inputs to the model, and the modelling objective was to reproduce the measured, dependent variables. It was eventually realised that this strategy conflicts with the requirements intimated above, and that sticking to this modelling philosophy could produce misleading results.

For instance, in one version of the model the refrigerant flow rate was calculated by integrating the equations of motion of the valves and the gas, in order to obtain the charge at the beginning and end of the discharge stroke, from which the mass displacement per stroke follows. This version produced an estimate of the mechanical losses by subtracting the calculated indicated work from the measured power consumption. This calculation appeared to produce the result that minimising the oil flows inside the compressor makes the mechanical losses less. However, a more detailed inspection of the figures showed that, in fact, the minimised oil distribution results in a slight loss of capacity - about 2% lower than for the unmodified compressor. Since this calculation would generate identical capacities, irrespective of modifications to the lubrication system, its figure for the indicated work was 2% too high in the case of the modified system, so leading to the erroneous implication that this modification made the mechanical losses less.

The essential point is that this conventional approach to modelling is a very inefficient way to answer the questions of interest, because it does not use the measurements directly.

Because it would be totally impractical to give an account of the model's development, the explanations which follow are confined to the model's final form.

To sum up, there have been essentially four objectives in devising the interpretive model;-

i) To furnish a systematic collation and interpretation of the experiments.

ii) To quantify the loss of capacity associated with each non-ideality.

iii) To quantify the wasted electrical power associated with each degradative phenomenon.

iv) To furnish data for those features of the compressor's operation that cannot be satisfactorily estimated from an ab-initio calculation.

9.2 Flow Rate Calculation

The interpretive model's starting point is to find the refrigerant flow rate from the measurements.

This calculation is based on the measured condenser power, because this measurement is particularly reliable, being based on a manual water flow rate measurement good to 1%, or better, and a temperature increment good to 0.1K.

In order to obtain the best possible calculation of the refrigerant flow rate, it is necessary to include an estimate for the heat loss from the condenser. The key to making this estimate is to first deduce the condenser's temperature distribution.

Figure 9.1 illustrates the condenser's temperature distribution. T_1, T_2, T_3, T_4 are the refrigerant temperatures, as indicated, and T_a, T_b, T_c, T_d are the water temperatures. Because most of the pressure drop occurs in the two phase region, T_2 is deduced from the measured discharge pressure, and T_3 is found from the measured pressure at the condenser's end. Thus the 4 key temperatures on the refrigerant side are found immediately from the measurements. The three separate contributions to the refrigerant's total enthalpy change - desuperheating, condensing and subcooling - then follow. Having found these enthalpy changes, the water temperatures T_b & T_c then follow from the first law. Note that at this stage, thanks to the use made of the measurements, the problem is very nearly solved having done nothing more difficult than calculate functions of state for saturated liquid & vapour, and invoke energy conservation.

Having thus found all 8 key temperatures, an average temperature is found for each of the three regions. For the subcooling and condensing regions the simple arithmetic mean of the 4 vertex temperatures is used. For the desuperheating region an algebraically more complicated mean is used, which takes proper account of the exponential variation of the temperature with distance along the desuperheating region.

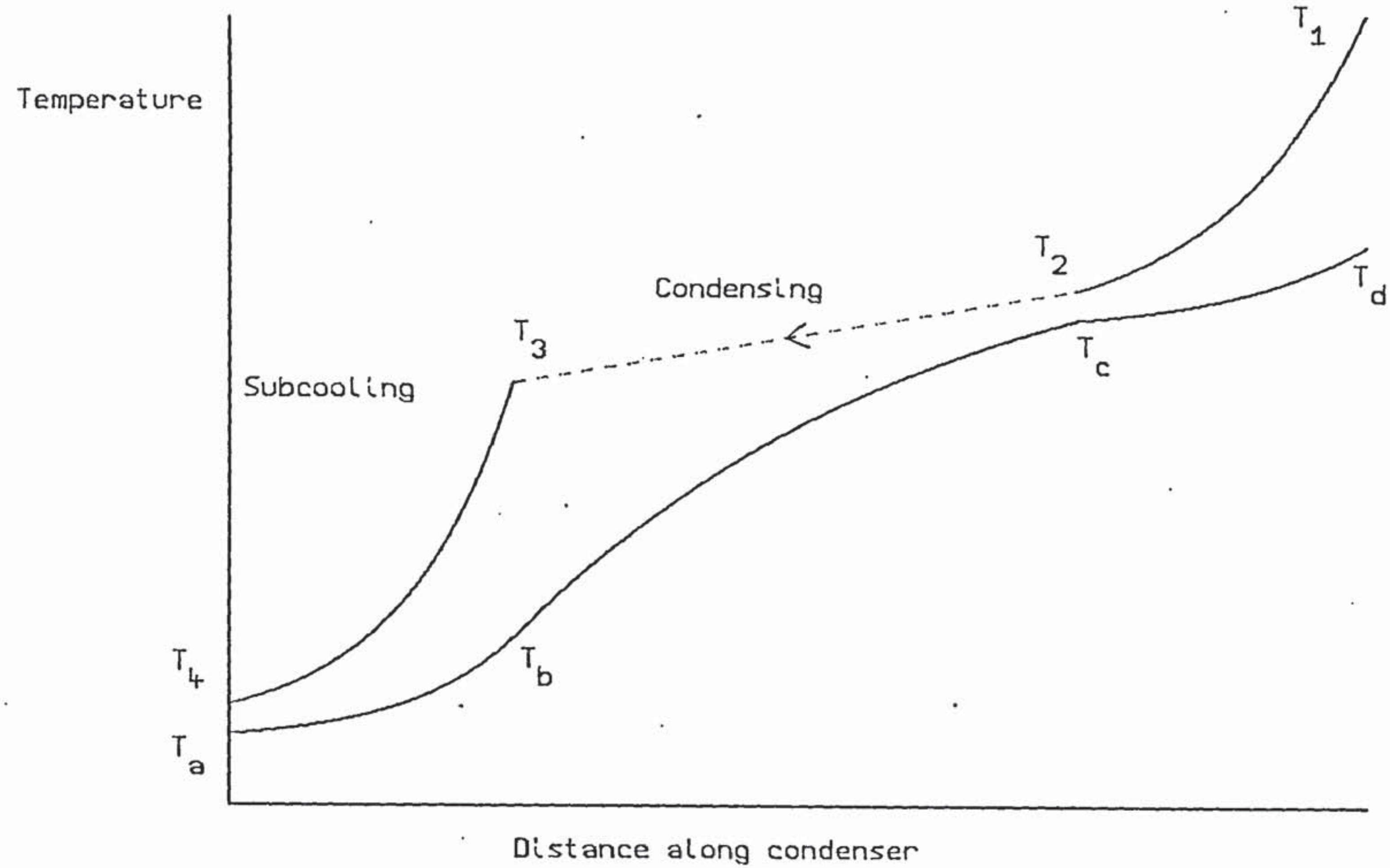

Figure 9.1. Condenser temperature distribution

In order to make the estimate of the condenser's heat loss to ambient, it only remains to determine the length of each region. The subcooling region has been taken to be 2m long, on the grounds that most of the tests had liquid visible in the reservoir, which is 2m. upstream from the condenser's end. For the desuperheating section, the LMTD is found from the 4 vertex temperatures, from which the length is found after calculating the heat transfer co-efficient using Reynold's analogy. The length of the condensing region is then found by subtracting these two lengths from the condenser's total length of 15m. The total heat loss to ambient is then found by evaluating the expression;-

$$\text{Heat loss} = U[(\bar{T}_{deS}-T_{Amb})L_{deS}+(\bar{T}_{Con}-T_{Amb})L_{con}+(\bar{T}_{sub}-T_{Amb})L_{sub}] \qquad 9.1$$

The linear heat transfer co-efficient, U, has been taken as 0.1W/mK. A precedent for this order of magnitude was established in a test which involved running warm water through the condenser, and measuring its drop in temperature, from which a total loss of 2W/K was deduced, corresponding to a U value of 0.13W/mK. The condenser's insulation has since been augmented, which is the reason for the more conservative 0.1W/mK having been adopted.

An important feature of the above method is that it uses the measurements to obviate a consideration of two phase flow and heat transfer. A comparatively simple single phase heat transfer calculation has been sufficient to make the problem determinate.

In addition to this estimate for the heat loss to ambient, it has also been found necessary to make a correction for the direct heat transfer from the compressor to the condenser. The compressor is mounted very close to the subcooling region of the condenser, as seen on figure 3.1, so that some of the heat loss from the compressor is picked up in the condenser. This point was recognised while trying to tune the penultimate form of the model, in which the refrigerant flow rate was calculated from an empirical treatment of the valve timing. It was found that with a generally good match to the measurements, the calculated refrigerant-side condenser power was consistently 10 - 15 Watts low for most of the tests that had an output power of less than 500 Watts. In one such case, the discrepancy of 4% was well outside the experimental uncertainty. It was from a consideration of this difficulty that the need was recognised to allow for the direct compressor-to-condenser transfer.

The compressor's total heat loss can be estimated from the difference between the measured input power and the refrigerant's product of (flow rate) x (enthalpy lift). This has furnished a fair impression of the efficacy of the compressor's insulation, from which an estimate of 0.12 W/K has been obtained for the total conductance between the compressor and the subcooling region. Thus the refrigerant flow rate is ultimately evaluated from the equation

$$\dot{m} = \frac{1}{h_{cs} - h_{ce}} \left[\begin{array}{l} \text{Measured condenser power} \\ + \text{ loss to ambient} \\ - \text{ transfer from compressor} \end{array} \right] \qquad 9.2$$

where h_{cs} = specific enthalpy at the condenser's start,

and h_{ce} = specific enthalpy at the condenser's end.

In practice, the estimate for the compressor - condenser heat transfer is compared with (compressor's total heat loss)/8, and the lower of the two figures is used. This avoids overestimating the effect for those trials in which the compressor's loss was unusually low.

9.3 Compressor capacity calculation

In the simple calculation introduced in section 4.6, the R12 flow rate implied by the condenser energy balance was put into perspective by expressing it as a fraction of the ideal flow rate. The shortfall from the ideal value results from several combined effects, as listed in section 4.7. It is desirable to obtain a more detailed breakdown, and estimate the individual significance of each non-ideality, rather than stop at a determination of their aggregate effect.

The strategy is to work out which phenomena can be modelled most reliably, and which present the greatest modelling uncertainties. Then, by calculating the effects of all the phenomena amenable to modelling, the effect of the latter category can be deduced by comparison with the measurements. This work is all done automatically by the calculation, which is written to take the measurements as inputs, and generate answers to the questions of interest.

The gas flow rate maintained by the compressor is given by

$$\dot{m} = f(m_4 - m_2 - m_{leak}) \qquad 9.3$$

where f = compressor's frequency - revolutions/s.

m_4= enclosed mass when the suction valve closes.

m_2= enclosed mass when the discharge valve closes.

m_{leak}= Leakage past the piston during compression & discharge.

It has been found that rather than work in terms of the gas masses, it is more helpful to work in terms of the gas volume at 2 reference states. The reference states are denoted by the subscripts "svc" & "dvo", the mnemonics being "suction valve closing" & "discharge valve opening". The dvo state is defined by the discharge pressure & cylinder gas entropy, while the svc state is defined by the cylinder gas entropy & suction pressure. The simplifying assumption is made that the specific entropy remains constant during the compression stroke. This entropy is found from hdvo & the discharge pressure, Pdis. hdvo is found by estimating the total specific enthalpy change that occurs between the cylinder gas first reaching the discharge pressure, and its arrival at the condenser. The condenser start temperature is more reliably measured than the discharge temperature. This is the reason for using the condenser start enthalpy as the reference from which to estimate hdvo.

Using the gas density in these 2 reference states, equation 9.3 is re-expressed in terms of gas volumes as;-

$$\dot{m} = f(\rho_{svc}V_{svc} - \rho_{dvo}V_{dvc} - \rho_{dvo}V_{leak}) \qquad 9.4$$

where "dvc" means "discharge valve closing.

Because the pressure in the cylinder does not necessarily match the suction pressure when the suction valve closes, Vsvc is not the enclosed cylinder volume at closure of the suction valve. Vsvc is simply the volume that would be occupied by the cylinder charge if it was at the suction pressure. The other Vs of equation 9.4 have a corresponding physical significance. The actual enclosed cylinder volumes at the opening and closing of the valves will be indicated with a numeric subscript.

As illustration of the usefulness of this formulation, in terms of these two reference states, the theoretical minimum power requirement for compression is given identically by $\dot{m}(h_{dvo} - h_{svc})$.

The original reason for working in terms of gas volumes, rather than masses, was that upon refining the estimate of cylinder gas entropy, the mass flow rate could be re-adjusted simply by recalculating the reference densities. This gave a tremendous saving in computing time when using the earlier version of the model.

For the final version of the model, although the mass flow rate is fixed by the condenser measurements, it is still preferable to work in terms of gas volumes because this makes it possible to draw meaningfull comparisons between completely different operating conditions.

If the known refrigerant flow rate and reference densities are substituted into equation 9.4 above, the three volumes remain as unknowns. Calculations have been developed for leakage past the piston, and for the build up of pressure in the discharge plenum during the discharge stroke. In the course of attempting to calculate the valves' displacement histories, it was noticed that the enclosed cylinder volume at closure of the discharge valve was normally around 0.6cc, i.e. 0.1cc more than the dead volume. When the valve is open, its being open adds 0.1cc to the enclosed cylinder volume, so that the effective dead space may realistically be taken as 0.6cc rather than the geometric minimum of 0.5cc. In this way Vdvc is found from the discharge plenum density, and this assumed value of the enclosed volume at closure of the discharge valve. Equation 9.4 then furnishes a value for Vsvc. The cylinder volume at bdc is 10.7cc. Thus the shortfall in Vsvc from this limit indicates the net effect on capacity of the suction valve timing and the suction plenum system.

In the following sections the calculations outlined above are explained in greater detail.

9.4 Modelling of Discharge System

The interpretive model is dependent on the deduction of the cylinder gas specific entropy from the measured state of the gas at the start of the condenser. In view of the vital nature of this calculation, a fully detailed explanation follows.

The calculation produces an answer for the overall change in specific enthalpy of the gas from the cylinder gas' first reaching the discharge pressure, to the arrival of the gas at the start of the condenser. This enthalpy change is regarded as the sum of seven terms:

$\Delta h =$	Excess Pdv work on the discharge stroke	(a)	9.5
	- Heat loss from plenum to suction gas	(b)	
	- Heat loss from internal pipe to suction gas	(c)	
	- Heat transfer to can from internal pipe	(d)	
	- Heat transfer to can via discharge stub	(e)	
	- Heat transfer to can from external pipe	(f)	
	- Heat loss to ambient from external pipe	(g)	

The first term is calculated by the valve & gas dynamic model of the discharge stroke, explained in section 9.7. The purpose of the present section is to explain how the heat transfer terms are calculated. For heat transfer to the suction gas, terms b & c, the plenum and discharge pipe are assumed to be at the same temperature as the enclosed gas, and an estimate is made for the rate of transfer of heat to the suction gas that would result from free convection only. Correlations quoted in "Handbook of heat transfer", by Rhosenow & Hartnett (69), have been used to make this estimate.

The origin of terms d, e & f may be understood by considering figure 9.2, which schematically illustrates the principle features of this part of the heat transfer model. Over part of its length, a gas carrying pipe is heatsinked by some heavy metalwork, namely the discharge stub & can. The compressor's can is modelled as a steel disc of thickness equal to the true wall thickness, with the boundary condition that at the disc's outer edge, its temperature equals that of the sump. For this disc, the overall thermal conductance from

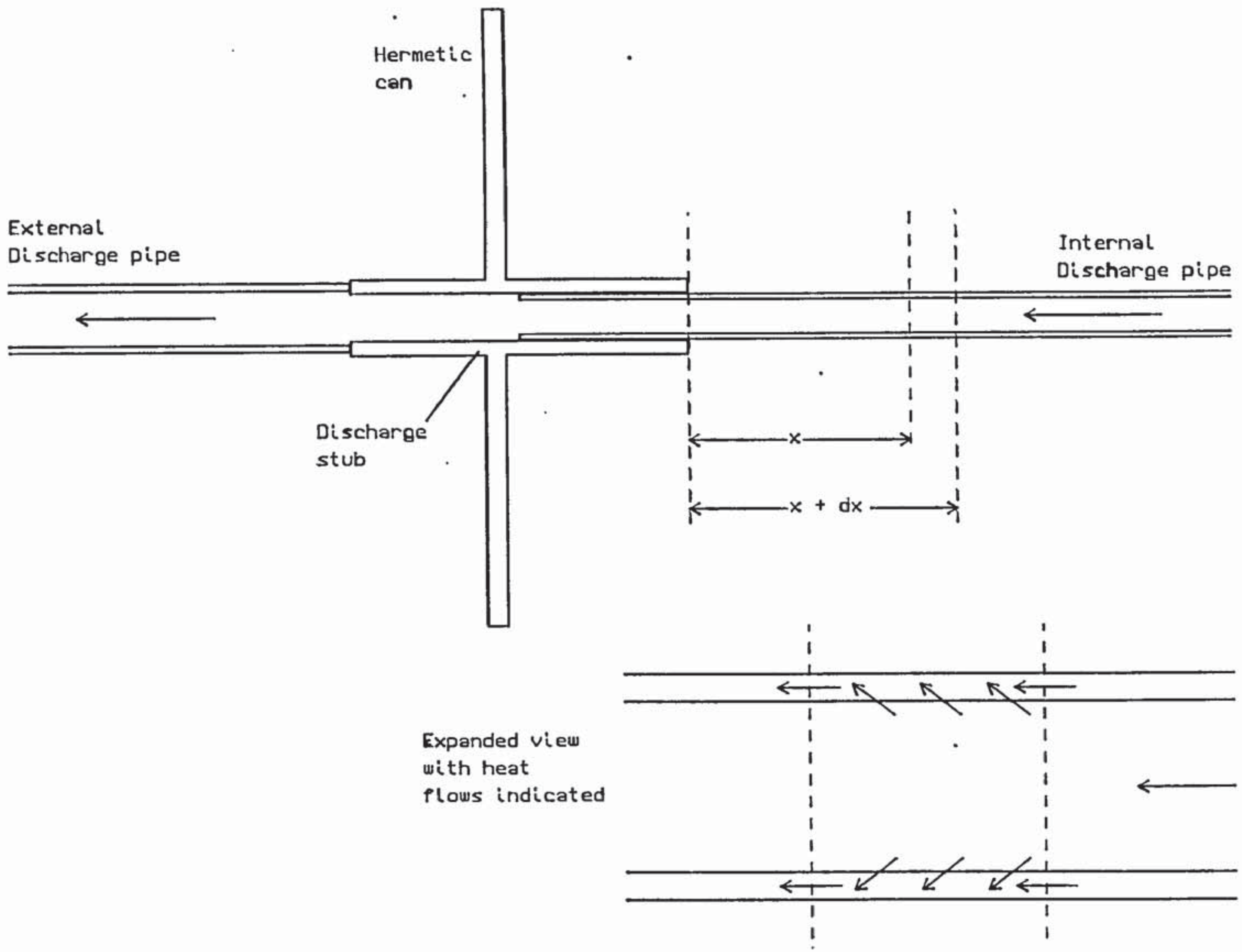

Figure 9.2. Discharge system model for heat loss estimate

discharge stub to outer edge is given by

$$2\pi(\text{ Thermal conductivity })(\text{ wall thickness })/(\text{ Ln}(b/a)\text{ }) \qquad 9.6$$

Where "b/a" is just the ratio of outer radius to inner radius. Substituting 54W/mK for the conductivity of steel, 3mm for the wall thickness, and taking the logarithm as nominally 2, yields a figure of 0.5W/K for the thermal conductance from discharge stub to sump oil. The stub itself is regarded as isothermal and of length 5cms. For the gas flowing through the stub, the conductance from gas to stub is just π(Gas conductivity)(Length)Nu. However, there is an additional heat flow to the stub from the pipework on either side. The derivation of the appropriate equations is explained below.

Consider first the internal discharge pipe, for which the gas flow is towards the discharge stub. At any point on this pipe the heat flow along it towards the stub is given by the product of the metal's conductivity, k, the cross sectional area of the metal, A, and the local temperature gradient. Additionally, there is a temperature difference between the pipe wall and the gas inside, which results in a transfer of heat from the gas to the pipe. Consider a length element from x to x + dx, where x is the distance from the discharge stub. If U is the heat transfer co-efficient/unit length from gas to pipe, then for this element, the heat transfer rate to the pipe is given by $(T_g - T_p)Udx$. In the steady state, this must equal the increment in the heat flow rate along the pipe towards the stub upon going from x + dx to x. i.e.;-

$$kA\left[\left.\frac{dT_p}{dx}\right|_{x} - \left.\frac{dT_p}{dx}\right|_{x+dx}\right] = U(\,T_g - T_p\,)dx \qquad 9.7$$

which reduces to;-

$$-kA\,\frac{d^2T_p}{dx^2} = U(\,T_g - T_p\,) \qquad 9.8$$

In order to make this differential equation soluble, it is necessary to re-express T_g in terms only of T_p. A long way from the stub, it is assumed that the pipe and the gas are at the same temperature, T_o. At x the heat flow along the pipe has been furnished entirely by transfer of heat from the gas. Therefore, one can write

$$kA\,\frac{dT_p}{dx} = \dot{m}C_p(\,T_o - T_g\,) \qquad 9.9$$

Using this to eliminate Tg from equation 9.7 produces the homogeneous second order differential equation;-

$$\frac{d^2(T_p-T_o)}{dx^2} = \frac{U}{\dot{m}C_p}\,\frac{d(T_p-T_o)}{dx} + \frac{U}{kA}(T_p-T_o) \qquad 9.10$$

At x = 0 the boundary condition is $T_p = T_{stub}$. The solution is thus

$$(T_p-T_o) = (T_{stub}-T_o)\exp(-\alpha x) \qquad 9.11$$

$$\text{where } \alpha = \frac{1}{2}\left[-\frac{U}{\dot{m}C_p} + \sqrt{\frac{U}{\dot{m}C_p}^2 + \frac{4U}{kA}}\right] \qquad 9.12$$

The total rate of transfer of heat is found by evaluating the temperature gradient at x = 0.

i.e. Conduction loss along inner pipe = $kA(T_{stub} - T_o)(-\alpha)$ 9.13

It is computationally inconvenient to retain T_o explicitly. For the purpose of writing the algorithm, T_o has been eliminated, and equation 9.13 has been cast in terms of the gas temperature at the discharge stub. The result is

$$\text{Conduction loss along inner pipe} = \frac{T_{dis} - T_{stub}}{(1/kA\alpha) - (1/\dot{m}C_p)} \qquad 9.14$$

For the outer discharge pipe, because the gas is flowing away from the stub, the differential equation derived for heat transfer to the discharge stub has a sign different. The results for temperature distribution and power loss can be expressed by equations identical to 9.11 & 9.14 above, but with α given by

$$\alpha_{outer} = \frac{1}{2}\left[\frac{U}{\dot{m}C_p} + \sqrt{\frac{U}{\dot{m}C_p}^2 + \frac{4U}{kA}}\right] \qquad 9.15$$

where U, k & A refer to the outer pipe, in this case.

For the total heat transfer to the can, then, one can extract the factor $(T_{dis} - T_{stub})$, and write

$$(T_{dis}-T_{stub})\left[\frac{1}{(1/kA\alpha)_{inner}-(1/\dot{m}C_p)}+UL+\frac{1}{(1/kA\alpha)_{outer}-(1/\dot{m}C_p)}\right] \qquad 9.16$$

where L = length of discharge stub = 5cms.

The term in square brackets is functionally equivalent to a thermal conductance from the discharge gas to the stub. Having estimated that the conductance from discharge stub to sump is 0.5W/K, the normal method is used to combine these two conductances in series, and so deduce the temperature of the stub, using the ratio of the thermal resistance between the stub and the sump to the overall thermal resistance from the discharge gas to the sump. Having found the stub temperature, these three heat transfer rates are individually calculable.

Lastly, the heat loss from the external discharge pipe to ambient is calculated. An estimate of 5K/W has been obtained for the thermal resistance presented by the insulation on the discharge pipe. At this stage in the calculation the linear heat transfer co-efficient from gas to pipe wall has already been calculated. This is combined with the insulation's resistance to obtain an overall heat transfer co-efficient from the discharge gas to ambient, from which the rate of loss of heat is evaluated.

The discharge pipework heat transfer model is implemented in the procedure "mdot", listed on page 333. This obtains self-consistent values for the R12 flow rate, discharge state and compressor heat loss. It evaluates terms d, e, f & g of equation 9.5. The discharge gas enthalpy is found by adding terms f & g to the condenser start enthalpy. Knowing both the enthalpy and the pressure, the discharge temperature and density are then found.

Term 'a' in equation 9.5 constitutes the sole coupling of the thermodynamic calculation - i.e. finding the cylinder entropy - to the hydrodynamc calculation, which finds the gas flow losses. Although the discharge gas state is found once and for all by the procedure 'mdot', hdvo has to be recalculated at each improvement in the estimate of this coupling term until internal consistency is obtained. Thus hdvo is found in the procedure 'cylrEntropy' by adding the remaining terms of equation 9.5 to the discharge enthalpy.

The cylinder gas specific entropy is then evaluated from s(T,v), after first solving for temperature and specific volume. This procedure is listed on page 334.

Fine tuning

It might seem odd that the discharge gas temperature should be calculated rather than using the temperature recorded by the discharge thermocouple. The reasons behind this are explained below.

During the first attempts to match the measurements, the following test of consistency was applied. Using the measured gas temperatures at each end of the external discharge pipe, the gas specific enthalpy drop was calculated. The implied heat loss from the discharge pipe then followed upon multiplying by the calculated mass flow rate. It was anticipated that these heat loss estimates would be consistent with an approximately constant thermal resistance between the discharge gas and ambient. In the event, it was found that this implied thermal resistance varied systematically with gas flow rate, being tolerably constant at a high gas flow rate, but rising with diminishing gas flow rate. This apparent dependence on gas flow rate was much stronger than could be accounted for by the variation in the thermal resistance of the gas metal interface, because the discharge pipe is well lagged, and so the controlling thermal resistance is that of the lagging.

It was recognised that these observations were consistent with incomplete isolation of the discharge thermocouple from its associated pipework. The heat transfer co-efficient between the gas and the thermocouple tip is dependent on the gas flow rate, but the thermal conductance between the thermocouple tip and the pipework is approximately constant. Ordinarily, this would not create a serious error, because the pipework temperature is usually close to the enclosed gas temperature. However, the discharge thermocouple is unusual in being mounted directly on the compressor's discharge stub, and is thus partially heatsinked by the compressor's can.

The resistance of the pipe's insulation was originally estimated as 3.6K/W by requiring that, at the highest freon flow rate, the calculated and measured discharge temperatures should be in agreement. This gave a worst case of 7K for the excess of the calculated discharge temperature over the measurement. This was considered unlikely. It was also found that the deduced heat loss from the compressor was not sensibly corellated with the sump oil temperature, being sometimes anomalously low. It was realised that these observations were consistent with the discharge pipe heat loss being over-estimated. It was observed that taking the estimate for the insulation's resistance as high as 5K/W produced a worst discrepancy at the high flow rates of having the calculated discharge temperature 0.3K lower than the measurement. Adopting this higher figure has resulted in a more realistically correlated heat loss from the compressor, and the more credible worst error, at the lowest flow rate, of 3.3K for the discharge thermocouple.

It is worth pointing out that it is intrinsically helpful to have obtained an estimate for the magnitude of this systematic measurement error.

Can gas temperature

The deduced value of the calculated mechanical loss is directly dependent on the estimate for the cylinder gas entropy. Because the flow rate is fixed by the measurements, the calculated total indicated work increases with increasing cylinder gas entropy. The mechanical loss is ultimately deduced by subtracting this indicated work from the measured power consumption, after making an allowance for the motor's electrical losses. The lowest power consumption ever observed for the compressor was 92 Watts, when it was running in a vacuum. Since the makers specify an electrical loss of 71 Watts for near-zero shaftwork, it follows that the lower credible limit to the mechanical loss is 20 Watts.

When first written, the free convection estimates for heat loss to the can gas had assumed a can gas temperature midway between the suction gas temperature and Tsvc. For some of the trials at a low suction pressure the resulting inferred mechanical loss had been rather too low for comfort. This led to the recognition that the assumed value for the can gas temperature was probably too low, which was leading to an over-estimate for the heat loss from the discharge system, thereby producing an over-estimate of the cylinder entropy. Revising the estimated can gas temperature to Tsvc produced the desired improvement in the consistency of the estimated mechanical loss.

It was mentioned in section 9.2 that the penultimate form of the model had employed an empirical correlation for the valve timing, and that the best fit had produced a slightly pessimistic capacity for tests at a low suction pressure. The above adjustment of the free convection estimate reduced this discrepancy, due to its producing a reduced estimate of cylinder gas entropy, with a consequent increase in calculated gas density and flow rate.

It is only the tests at the lowest suction pressure that are sensitive to this part of the model, because the two features are combined of a low flow rate, and a large temperature difference between the discharge and suction gas.

As explained in section 9.2, the remaining discrepancy was subsequently resolved by taking account of the direct heat transfer from the compressor to the condenser.

9.5 Leakage past the piston

Using a telescopic gauge and a micrometer, a direct measurement of 10um has been obtained for the clearance between the bore and the piston. The piston has a length of 2cms and a circumference of 10cms.

Consider figure 9.3 which shows, in section, the flow of a fluid through a narrow gap of length l, driven by the pressure difference $(P_c - P_{suc})$. By equating the resultant force on a thin fluid element caused by viscous shear, to the force produced by the pressure drop, one obtains

$$\eta l \left(\frac{dv}{dz}\bigg|_z - \frac{dv}{dz}\bigg|_{z+dz} \right) = (P_c - P_{suc})dz \qquad 9.17$$

This reduces to

$$-\eta l \frac{d^2v}{dz^2} = (P_c - P_{suc}) \qquad 9.18$$

Noting the boundary conditions that v=0 at z = 0 and at z = g, the gap width, the solution can be written down

$$v = \frac{(P_c - P_{suc})}{2\eta l} z(g - z) \qquad 9.19$$

The mass flow rate is found by integrating across this velocity profile. If L is the piston's circumference, the result is

$$\dot{m} = \frac{L(P_c - P_{suc})\rho g^3}{12\eta l} \qquad 9.20$$

This equation is valid for incompressible flow, but for the gas there is a decompression through a large pressure ratio, with a correspondingly large change in density.

Consider now a small section through the gap, dl. One can use equation 9.20 above to legitimately write

$$\frac{dP}{dl} = \frac{12\eta\dot{m}}{Lg^3\rho} \qquad 9.21$$

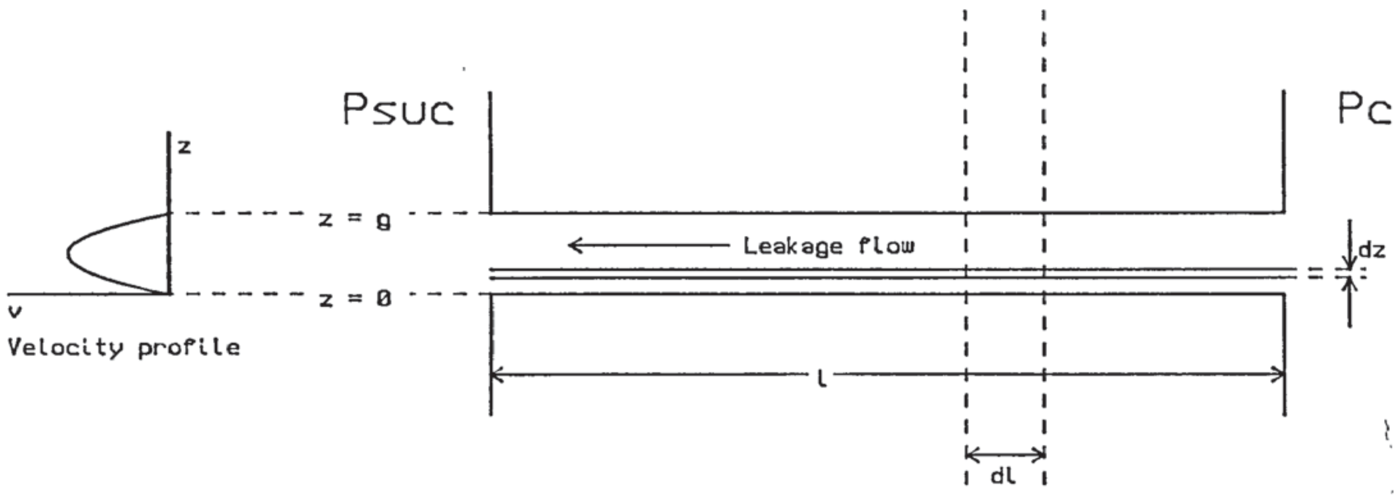

Figure 9.3. Deriving the leakage rate equation

By expressing ρ as a linear function of P, $\rho = \bar{\rho} + \lambda(P - \bar{P})$, this becomes

$$[\bar{\rho} + \lambda(P - \bar{P})]dP = \frac{12\eta\dot{m}}{lg^3} dl \qquad 9.22$$

This can be integrated on sight to yield

$$\rho(P_c - P_{suc}) + (\lambda/2)[(P_c - 2\bar{P})P_c - (P_{suc} - 2\bar{P})P_{suc}] = \frac{12\eta\dot{m}l}{Lg^3} \qquad 9.23$$

If the substitution $\bar{P} = (P_c + P_{suc})/2$ is made, this reduces to

$$\bar{\rho}(P_c - P_{suc}) = \frac{12\eta\dot{m}l}{Lg^3} \qquad 9.24$$

Therefore the mass leakage rate is given by

$$\dot{m} = \frac{g^3 L\bar{\rho}(P_c - P_{suc})}{12\eta l} \qquad 9.25$$

where $\bar{\rho}$ is defined as the gas density at the mean pressure.

The calculation of mass loss on the compression stroke is entered after completing the suction stroke calculation. i.e. at closure of the suction valve. At each time step the enclosed volume is recalculated, and the gas specific volume is updated. From the new specific volume, a new temperature is found by solving s(T,v) iteratively, using the simple Newton Raphson method. Having updated T & v, the cylinder pressure is evaluated. Calculation of the kinematic viscosity requires a temperature and a density. The mean of the current cylinder gas temperature and Tsvc is used for the temperature, and an appropriate mean density is evaluated similarly. These mean values are then used to calculate the gas' kinematic viscosity. Having found the cylinder pressure and an appropriate value for kinematic viscosity, the current leakage rate is evaluated, and the cylinder charge is updated. This process is repeated until the cylinder pressure is first found to exceed the discharge pressure. The cylinder charge and crank angle upon first reaching the discharge pressure are then found by interpolating between the results of the last 2 time steps, in preparation for entry into the discharge stroke calculation. This procedure also integrates the leakage during the re-expansion stroke, starting at closure of the discharge valve, and concluding when the cylinder pressure first drops to the suction pressure.

Although the clearance has been measured as 10um, it does not follow that this is the appropriate value to use in equation 9.25. Partial sealing of the gap with oil would reduce the leakage; eccentricity of the piston in its bore would increase it and, lastly, the measurement may be low, being in disagreement with the maker's specification of 14 - 18um (70).

As explained in section 7.6, a one-off measurement was made of the leakage past the piston, and a figure of 0.24g/s was found. From this test, the appropriate value of the gap has been found by requiring that the calculation should reproduce the observed leakage at the same operating condition. Co-incidentally, the appropriate value has turned out to be 10um. - the nominal measurement.

9.6 Suction stroke algorithm

The original purpose of the suction stroke algorithm was to find the mass of gas in the cylinder when the suction valve shuts, from which Vsvc followed. This required a numerical integration of the equations of motion of the gas in the plenums. In the final form of the model, because the mass flow rate is known at the outset, the cylinder charge at the end of the suction stroke becomes determinate once the leakage, and the re-expansion charge have been evaluated. However, the suction stroke algorithm has been retained, essentially in its original form, in order to calculate the losses associated with the suction system. The only difference has been that instead of finding the closure of the valve from a numerical integration of the valve's equation of motion, the valve is artificially constrained to remain fully open until the cylinder charge has fallen to its pre-determined value, shortly after bottom dead centre. In this way the valve lateness needed to match the measured condenser power is found automatically, rather than attempting to calculate the valve's closure independently.

Figure 9.4 shows a plan view of a section through the casting, illustrating the three suction plenums, and the path taken by the gas in moving from the general atmosphere within the can to the cylinder. Note that the 2 inner plenums and the 2 bores from outer to inner plenums are in parallel. This is the justification for treating the suction system as 2 plenums in series connected by a single bore. The model's inner plenum has a volume equal to the sum of the casting's 2 inner plenums, and the single bore in the model has a cross sectional area double that of one of the bores through the casting. This is illustrated in figure 9.5.

Before launching into the relevant algebra, it is helpful to explain qualitatively how the algorithm works. The suction stroke algorithm is entered at the end of the re-expansion stroke, which is defined as the instant when the gas pressure within the cylinder equals the pressure in the inner plenum, thus removing any internal pressure to hold the valve shut.

In an earlier version of the model, the calculation of the pressure history in both suction plenums was continued for the period

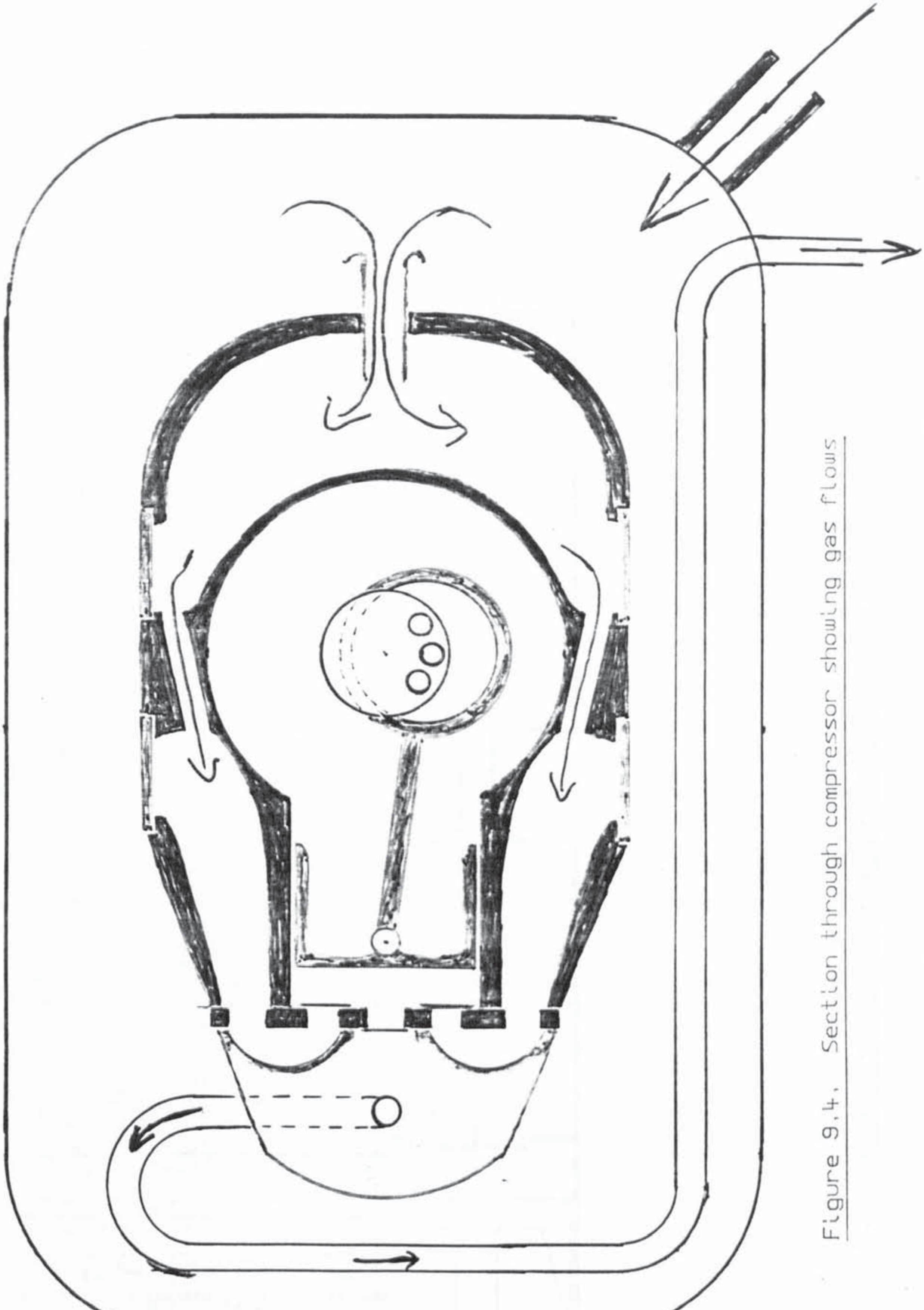

Figure 9.4. Section through compressor showing gas flows

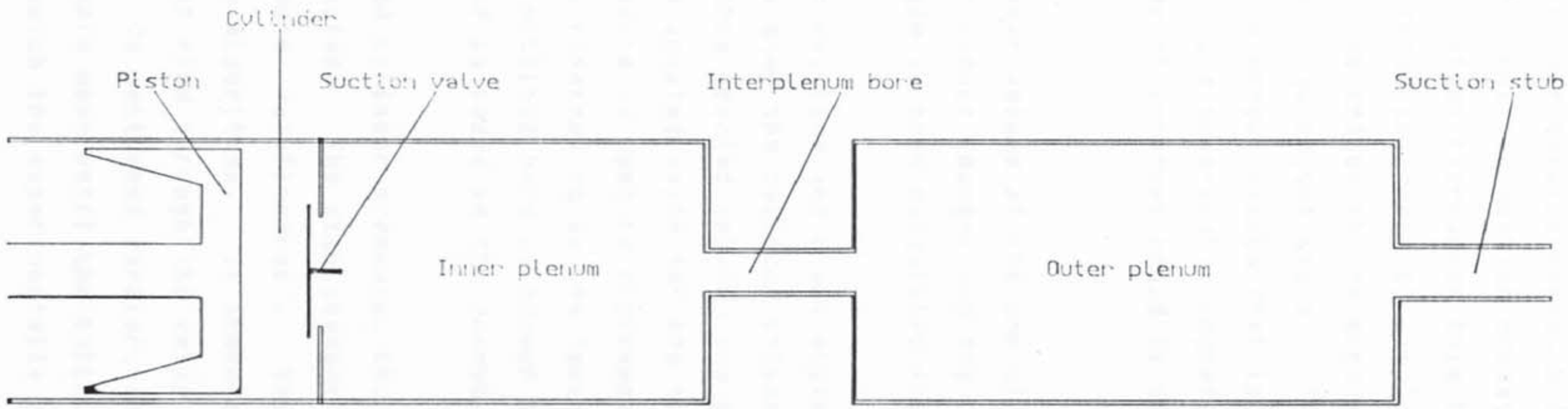

Figure 9.5. Equivalent suction system for sucton stroke calculation

between the suction valve's closing, and its next re-opening. Thus the cylinder pressure at the calculated end of the re-expansion stroke was not equal to the suction pressure. During this period the pressure in the plenums does not asymptotically approach the suction pressure. Instead it oscillates about the suction pressure with a decaying amplitude. The calculation reproduces this behaviour, qualitatively. However, it was considered desirable to simplify the model by making the approximation that at the end of the re-expansion stroke the plenum system has returned to a quiescent state. This was considered preferable, because the danger exists that in trying to track an oscillatory system using a numerical integration, the calculation of the conditions at the time of interest could be diametrically opposed to reality.

Thus, the cylinder volume at the end of the re-expansion stroke is calculated from the cylinder charge, and the reference density ρ_{svc}. The initial crank angle is then calculated from this volume.

From this point on, time and crank angle are incremented in small steps. At each time step the cylinder volume is found from the new crank angle. From this updated volume, the gas density is updated, from which follows an updated value for the cylinder pressure. This updated cylinder pressure is used to increment the numerical integration of the gas flow loss, referred to as the 'excess PdV work'. The calculation sequence outlined here is common to both the suction and discharge strokes, and is coded in the procedure 'IncrementPhi'.

From the updated cylinder pressure, the pressure difference acting on the valve is evaluated. The displacement of the valve is then updated in the procedure 'ValvFlowArea'. This is also used by both the suction and discharge algorithms. It produces an updated value for the area available for gas flow through the valve by integrating the valve's equation of motion. As mentioned earlier, once the valve is open, it is constrained to remain open until the cylinder charge has fallen to the value needed to match the experimentally determined flow rate.

This chimera of a valve dynamic model, with its 'correct' treatment of valve opening and empirical treatment of closing, has been borne of the need to include the indicated work increment caused by the delay in the opening of the suction valve, while avoiding the problems associated with trying to calculate the valve's closure from its equations of motion. The need for a hybrid valve dynamic model has been recognised by other workers (71). Modelling the valve dynamics has been the subject of some effort, which is explained in more detail in appendix 3.

Using the pressure difference across the valve, and the area available for flow through it, the mass flow rate of gas into the cylinder is evaluated, and the cylinder charge is updated, in readiness for the next time step. This completes the calculational cycle for the cylinder charge.

For a consistent calculation of the pressure difference across the valve it is also necessary that the plenums' charges, densities and pressures be updated at each time step. The rate of change of mass in the inner plenum is evaluated at each time step by subtracting the flow rate through the valve from the flow rate through the interplenum bore. This allows the mass, density and gas pressure in the inner plenum to be updated. Similarly, the charge, density and pressure in the outer plenum are all updated using the difference between the flow rate through the suction stub and the flow rate through the interplenum bore.

There is just one subtle feature of the modelling, which concerns the relationship between the plenum pressures and the flow rates in and out of the plenums. An explanation follows.

The bore from outer plenum to inner plenum has a non-negligible length. Because of its comparatively small cross sectional area, the gas within it can reach quite a high speed. The result of this is that the bore can store a non-negligible amount of momentum. The point is that in the calculation one cannot legitimately set the instantaneous flow rate through the bore equal to that steady state flow which would result from the current value of the pressure difference across it. Instead, the pressure difference needed to maintain the current flow rate is compared with the current pressure difference. The calculated shortfall or excess is then used to calculate the rate of change of mass flow rate, using the appropriate form of Newton's second law, derived below. From this calculated acceleration, the mass flow rate itself is updated at each time step. The flow through the short stub into the outer plenum is modelled similarly.

Consider figure 9.5. The following symbolism has been adopted

$\dot{m}_s$ - Inward flow through outer stub

$\dot{m}_b$ - Flow through bore from outer to inner plenum.

$\dot{m}_v$ - Flow through valve into cylinder.

P_{suc} - suction gas pressure in can.

P_o - pressure in outer plenum

P_i - pressure in inner plenum

P_c - pressure in cylinder

The short bore has cross sectional area of A, length of L, and encloses gas of density ρ.

Mass of gas enclosed in short bore = ρAL 9.26

Gas speed through short bore = $\dot{m}_b/\rho A$ 9.27

Therefore momentum stored in short bore = $\dot{m}_b L$ 9.28

Unbalanced force acting on short bore = $A(P_o-P_i-\dot{m}_b\ \dot{m}_b\ /2\rho A^2)$ 9.29

where simple orifice flow has been used for the pressure difference that would be needed to maintain m_b continuously.

Since the rate of change of momentum = unbalanced force, one deduces

$$L\frac{d\dot{m}_b}{dt} = A(P_o - P_i - \dot{m}_b\ \dot{m}_b\ /2\rho A^2) \qquad 9.30$$

$$\text{i.e.} \quad \frac{d\dot{m}_b}{dt} = \frac{A}{L}(P_o - P_i - \dot{m}_b\ \dot{m}_b\ /2\rho A^2) \qquad 9.31$$

The ratio A/L has the dimensions of length. For the short bore a 'Length parameter' of 2mm has been adopted, on the basis of a csa of 39mm^2 and a physical length of 20mm. For the stub at the back of the casting the length parameter is 1.6mm, based on a physical length of 20mm, and a csa of 32mm^2.

In order to see that the problem is closed and determinate, note that there are 9 unknown functions of time;- 3 mass flow rates, 3 pressures & 3 enclosed masses. Since the enclosed mass in a chamber is simply related to the gas density, one recognises that the relationship between density and pressure, i.e. the equation of state, furnishes 3 equations immediately. The time derivatives of the 3 enclosed masses are given by 3 simple equations involving only the mass flow rates, and lastly, one can write for the stub, bore and valve respectively, the 3 further equations;-

$$\frac{d\dot{m}_s}{dt} = l_s(P_{suc} - P_o - \dot{m}_s\left|\dot{m}_s\right| /2\rho A_s^2) \qquad 9.32$$

$$\frac{d\dot{m}_b}{dt} = l_b(P_o - P_i - \dot{m}_b\left|\dot{m}_b\right| /2\rho A_b^2) \qquad 9.33$$

$$\dot{m}_v = \frac{\left|P_i - P_c\right|}{P_i - P_c} A_v\sqrt{2\rho\ (P_i - P_c)} \qquad 9.34$$

For the purpose of this calculation, a simplified form of the equation of state is used, which relates pressure to density using a simple Taylor expansion

$$P = P_{suc} + (\rho - \rho_{suc}) \frac{\partial P}{\partial \rho_s} \qquad 9.35$$

Although the use of the isentropic modulus is inexact, since entropy is created in the suction system, the additional refinement of an exact treatment cannot justify the massive increase in complication that would result.

Needless to say, analytic solution of this coupled set of 4 algebraic equations and 5 differential equations is absolutely impossible, but it is straightforward to construct an algorithm that systematically calculates the evolution of the system with time, as listed in the procedure 'suction', page 336.

At the speed of sound in the suction gas it takes a little over 1ms to get from the valve back to the stub. Thus, starting from a quiescent state, flow through the stub is impossible until this time has elapsed after the start of the suction stroke. For the calculation to take proper account of the finite sound speed, the simplification of a uniform pressure throughout each plenum would have to give way to a much more complicated calculation for the time *and space* dependence of the pressure in each plenum. However, thanks to the inclusion of gas inertia in the short bores, the calculation emulates the effects of the non-infinite sound speed. This method which has been adopted here is analogous to the practice in A.C. theory of invoking equivalent circuits of lumped, ideal components, instead of solving Maxwell's equations for the circuit. In terms of this analogy, the plenums are modelled as pure capacitances, and the short bores are modelled as inductances in series with non-linear resistors.

9.7 Discharge stroke calculation

The purpose of the discharge stroke calculation is to estimate the excess indicated work caused by the excess of the cylinder pressure over the discharge pressure, to find the gas density in the cylinder when the discharge valve closes, & to estimate the losses associated with leakage past the piston. From figure 9.4 one can see that the discharge system is not complicated, consisting of a 29 cc plenum, into which the valve vents directly. This plenum, in turn, is vented by an internal discharge pipe 50 cms long and of 5mm i.d.

The discharge stroke algorithm is entered when the cylinder pressure first equals the pressure in the discharge plenum. The simplifying approximation is made that between the discharge valve's closing and its next re-opening, the gas in the discharge plenum & pipe returns to a quiescent state at the discharge pressure. Thus the cylinder volume at the end of the compression stroke is evaluated from the reference density ρ_{dvo} and the cylinder charge. The initial crank angle is then calculated from the cylinder volume.

At each time step the cylinder volume, gas density, pressure and excess PdV loss are all updated by 'IncrementPhi' as described for the suction stroke. Then the pressure difference acting on the valve is found, and the procedure 'ValvFlowArea' updates the area available for flow through the valve. From this pressure difference and valve flow area the mass flow rate from the cylinder to the plenum is computed.

It is from this point onwards that the discharge and suction stroke calculations differ.

The rate of leakage past the piston is calculated at each time step, using equation 9.25. From the resulting total mass flow rate out of the cylinder, the calculational cycle is completed by updating the cylinder charge in readiness for the next time step.

As for the suction valve, because of concerns about the reliability of calculations for the discharge valve's closure, it is artificially constrained to remain fully open after tdc until the cylinder volume has returned to 0.6cc. The re-expansion charge then follows from this volume, and the discharge plenum density.

The equations used for each step of the above outline are quite straightforward, well-known, and in no way novel. However, it is also necessary to update the plenum's charge, density & pressure at each time step. Otherwise, at the end of the discharge stroke the calculation would not include the additional increment in the re-expansion charge that results from the raised plenum pressure, nor would it include the associated increment in the indicated work. For the purpose of updating the plenum's charge, and hence deducing its enclosed gas density & pressure, an unconventional relationship has been adopted, which expresses the outward gas flow rate as a *linear* funcion of the enclosed pressure. There follows an explanation of the thinking behind this derivation.

Consider a model system. A gas bottle at a slight overpressure, δP, is vented by a long pipe as shown in figure 9.6. At time t=0 it is imagined that a seal between the bottle and the pipe is instantaneously removed. There follows a derivation of the equations governing the time dependence of the pressure distribution in the pipe.

By considering the rate of change of mass in a length element dx,

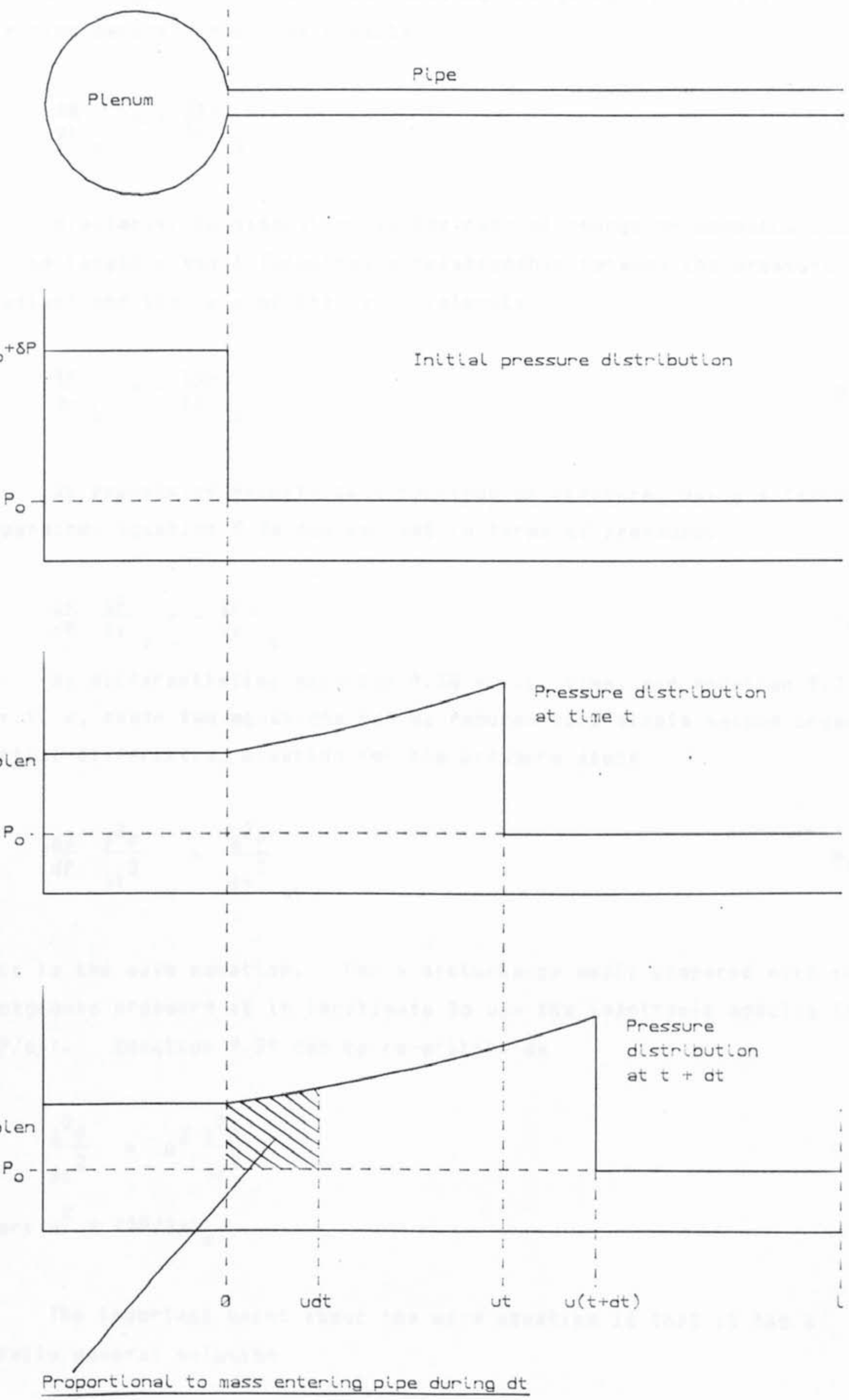

Figure 9.6. Illustrating proportionality of $\dot{m}$ to overpressure

an equation can be written down relating the gradient of the velocity to the time derivative of the density

$$\left.\frac{\partial \rho}{\partial t}\right|_x = -\left.\frac{\partial \rho v}{\partial x}\right|_t \qquad 9.36$$

Similarly, consideration of the rate of change of momentum stored in the length element furnishes a relationship between the pressure gradient and the rate of change of velocity

$$\left.\frac{\partial P}{\partial x}\right|_t = -\left.\frac{\partial \rho v}{\partial t}\right|_x \qquad 9.37$$

By expressing density as a function of pressure, using a Taylor expansion, equation 9.36 can be cast in terms of pressure.

$$\frac{d\rho}{dP}\left.\frac{\partial P}{\partial t}\right|_x = -\left.\frac{\partial \rho v}{\partial x}\right|_t \qquad 9.38$$

By differentiating equation 9.38 w.r.t. time, and equation 9.37 w.r.t. x, these two equations can be reduced to a single second order partial differential equation for the pressure alone

$$\frac{d\rho}{dP}\left.\frac{\partial^2 P}{\partial t^2}\right|_{xx} = \left.\frac{\partial^2 P}{\partial x^2}\right|_{tt} \qquad 9.39$$

This is the wave equation. For a disturbance small compared with the background pressure it is legitimate to use the isentropic modulus for $(dP/d\rho)$. Equation 9.39 can be re-written as

$$\frac{\partial^2 P}{\partial t^2} = u^2 \frac{\partial^2 P}{\partial x^2} \qquad 9.40$$

where $u^2 = (\partial P/\partial \rho)_s$

The important point about the wave equation is that it has a totally general solution

$$P(x,t) = f(x-ut) + g(x+ut) \qquad 9.41$$

where f & g are arbitrary functions. By virtue of the form of the argument of function f, this term describes an arbitrary pressure distribution which propagates to the right at speed u without change of shape. Similarly, the term in g describes a pressure distribution propagating to the left without change of shape.

For the finite plenum, volume V, vented by a pipe of c.s.a A and length l, the pressure in the plenum initially falls due to the flow of gas into the pipe. Consider 2 snapshots of the pressure distribution at t & at t+dt where t+dt<l/u, as illustrated in figure 9.6. Because the pressure distribution propagates to the right without change of shape, the increment in its integral above ambient pressure is simply given by $(P_{plen} - P_o)udt$. Therefore the mass which has entered the pipe during this interval is given by

$$dm = A(\partial\rho/\partial P)_s(P_{plen} - P_o)udt \qquad 9.42$$

Upon recalling that $(\partial\rho/\partial P)_s = 1/u^2$, one obtains

$$\frac{dm}{dt} = \frac{A}{u}(P_{plen} - P_o) \qquad 9.43$$

for the instantaneous mass flow rate out of the plenum. In other words, it is a consequence of the pressure distribution's propagating without change of shape that the instantaneous outward mass flow rate is directly proportional to the instantaneous overpressure.

By relating the plenum's pressure to its enclosed mass, m, this leads to a first order differential equation for the time dependence of the plenum pressure

$$P_{plen} = P_o + (\rho_{plen} - \rho_o)u^2 \quad \& \quad \rho_{plen} = m/V$$

$$\frac{dP}{dt}plen = u^2\frac{d\rho}{dt}plen = (u^2/V)\frac{dm}{dt} \qquad 9.44$$

Since the rate of change of enclosed mass, m, is the negative of the outward mass flow rate, equation 9.43 can be used to reduce this to a differential equation for the plenum pressure

$$\frac{dP_{plen}}{dt} = - \frac{uA}{V} (P_{plen} - P_o) \qquad 9.45$$

This has the solution

$$P_{plen} = P_o + \delta P \exp[(A/V)(0-ut)] \qquad 9.46$$

It follows that the pressure distribution is given by

$$P_{plen} = P_o + \delta P \exp[(A/V)(x-ut)] \qquad 9.47$$

At $t=l/u$ something interesting happens. This pressure pulse reaches the end of the pipe. In order to satisfy the boundary condition $P = P_o$ at the free end, it is necessary to make the function g describe a rarefaction of the same strength and shape as function f.

The point is that the original compressive wave propagating to the right is reflected as a rarefaction propagating to the left.

This simple idealised model has highlighted the two most important features of the discharge system. Firstly, equation 9.43 gives the requisite relationship between the flow rate out of the plenum and the instantaneous overpressure. The second important feature demonstrated by this model is the reflection of the initial compressive wave as a rarefaction. At the sound speed in the discharge gas it takes over 3ms to travel the length of the discharge pipe. Thus it takes over 6ms for the first rarefaction to return to the plenum. Since the discharge valve is never normally open for more than 5ms, it is thus not necessary to consider this effect explicitly, since the valve is already closed by the time the first rarefaction returns.

This matter of repeated reflections of compressions and rarefactions has been explained in some detail because it underlies the question of whether one should use equation 9.43 for flow into the pipe, or use the equation for the pressure drop needed to maintain a steady flow rate. For instance, if instead of a 50cm length of pipe one had a short narrow bore, then the use of equation 9.43 would be invalid on the grounds that during the discharge stroke there would be multiple reflections, giving an approach to steady state orifice flow in a time short compared with the time scale of the discharge stroke.

The specification-defining program

In order to keep the model uncluttered and maximise the memory available, all the constants are specified in this short programme, which writes all the specifications into a text file in the form of command lines. The model then starts with a single line to EXECute this text file, so obtaining the full problem definition, without having to carry all the associated code.

```
  10 MODE128:@%=&20308
 100 DIM Spec$(6),Pe$(6,14),Pc$(6,14),N(6)
 150 PROCexpSpecs: PROCrunData
 200
1000 OSCLI("*SPOOL IntrpModel.InfoText")
2000 PRINT"Suction system"
2010 PRINT"~~~~~~~~~~~~~~"
2020  Vo=7.0E-5 :PRINT"Outer plenum volume                   = ",Vo*1E6;" cc"
2030  Vi=5.5E-5 :PRINT"Inner plenum volume                   = ",Vi*1E6;" cc"
2040 PRINT
2050  bA=3.6E-5 :PRINT"c.s.a. of bores                       = ",bA*1E6;" mm^2"
2060  sA=2.9E-5 :PRINT"c.s.a. of outer stub                  = ",sA*1E6;" mm^2"
2070  sL=1.4E-3 :PRINT"Stub's length parameter               = ",sL*1E3;" mm"
2080  bL=1.8E-3 :PRINT"Bore's length parameter               = ",bL*1E3;" mm"
2090 PRINT
2100 SpA=1.7E-4: PRINT"Suction port area                     = ",SpA*1E4;" cm^2"
2110  Sk=4.5E+2: PRINT"Valve spring constant                 = ",Sk     ;" N/m"
2120  Sm=1.1E-3: PRINT"Mass of suction valve                 = ",Sm*1E3   ;" g"
2130 Sperm=6E-2: PRINT"Perimeter of suction ports            = ",Sperm*1E2;" cm"
2140 Slift=9E-4: PRINT"Maximum valve lift                    = ",Slift*1E3;" mm"
2150 PRINT
2160 PRINT"Discharge stroke model. The following specs are assumed."
2170 PRINT"~~~~~~~~~~~~~~~~~~~~~~~~~~~~~~~~~~~~~~~~~~~~~~~~~~~~~~~~"
2180DPvol=2.9E-5:PRINT"Discharge plenum volume               = ",DPvol*1E6;" cc"
2190 PRINT
2200  Adp=2.0E-5:PRINT"Internal discharge pipe c.s.a.        = ",Adp*1E6;" mm^2"
2210 PRINT
2220  DpA=0.8E-4:PRINT"Discharge port area                   = ",DpA*1E4;" cm^2"
2230   Dk=5.6E+2:PRINT"Valve + backing spring stiffness      = ",Dk;" N/m"
2240  Dpl=0.5   :PRINT"Pre-load on valve                     = ",Dpl ;" N"
2250   Dm=9.0E-4:PRINT"Mass of valve + backing spring        = ",Dm*1E3;" g"
2260Dperm=4.0E-2:PRINT"Perimeter of discharge port           = ",Dperm*1E2;" cm"
2270Dlift=9.0E-4:PRINT"Discharge valve tip lift              = ",Dlift*1E3;" mm"
2280 PRINT
2285  Uci=0.1    :PRINT"U value for condenser                = ",Uci;" W/mK"
2290  Udi=0.2    :PRINT"U value for discharge pipe ins'n = ",Udi;" W/K"
2296  UcT=0.12   :PRINT"Compressor to condenser conductance",UcT;" W/K"
2310 PRINT
2320 PRINT"Compressor model.   The following specifications are assumed."
2330 PRINT"~~~~~~~~~~~~~~~~~~~~~~~~~~~~~~~~~~~~~~~~~~~~~~~~~~~~~~~~~~~~~~~"
2332  crl=5.00E-2:PRINT"Con-rod length                       = ",crl *1E2;" cm"
2334  amp=6.35E-3:PRINT"Amplitude, i.e. half-stroke          = ",amp *1E3;" mm"
2336  off=2.50E-3:PRINT"Offset of bore from crank axis       = ",off *1E3;" mm"
2340 Vbdc=1.07E-5:PRINT"Total volume                         = ",Vbdc*1E6;" cc"
2350 Vtdc=0.50E-6:PRINT"Clearance volume                     = ",Vtdc*1E6;" cc"
2360  gap=1.00E-5:PRINT"Piston - bore clearance              = ",gap *1E6;" um"
2370  dep=2.00E-2:PRINT"Piston depth                         = ",dep *1E2;" cm"
2380  Pci=1.00E-1:PRINT"Piston circumference                 = ",Pci *1E2;" cm"
2383 PRINT
2386   dt=1.00E-5:PRINT"Time step for integrations           = ",dt  *1E6;" us"
```

```
2390 PRINT
2400 PROCderivedConstants
2410
2420      PRINT"Crank angle at top dead centre   = ",DEG(PhiTdc);" degrees"
2430      PRINT"Bottom dead centre crank angle   = ",DEG(PhiBdc);" degrees"
2440      PRINT"Bore cross sectional area        = ",Abore*1E4;" cm^2"
2570
2580 OSCLI("*Spool")
2592
2594 @%=&01070A
2595 OSCLI("*Spool IntrpModel.InfoEtc")
2602 PRINT"MODE128:@%=&01070A"
2604 PRINT"DIM F(41),Pe$(6,15),Pc$(6,15),N(6),Spec$(6)"
2970
2980 PRINT"Vo=";Vo
2982 PRINT"Vi=";Vi
2984 PRINT"bA=";bA
2986 PRINT"sA=";sA
2988 PRINT"sL=";sL
2990 PRINT"bL=";bL
2992
3000 PRINT"dt=";dt
3010 PRINT"SpA=";SpA
3014 PRINT"Sk =";Sk
3016 PRINT"Sm =";Sm
3018 PRINT"Sperm=";Sperm
3020 PRINT"Slift=";Slift
3022
3024 PRINT"Vbdc=";Vbdc
3026 PRINT"Vtdc=";Vtdc
3030 PRINT"crl=";crl
3032 PRINT"amp=";amp
3034 PRINT"off=";off
3036 PRINT"Ztdc=";Ztdc
3038 PRINT"Abore=";Abore
3040 PRINT"PhiTdc=";PhiTdc
3042 PRINT"PhiBdc=";PhiBdc
3045 PRINT"Uci=";Uci
3050 PRINT"Udi=";Udi
3051 PRINT"UcT=";UcT
3052 PRINT"LeakCof=";LeakCof
3054
3058 PRINT"DPvol=";DPvol
3062 PRINT"Adp=";Adp
3064 PRINT"Dpl=";Dpl
3072 PRINT"Dk=";Dk
3076 PRINT"Dm=";Dm
3078 PRINT"Dlift=";Dlift
3082 PRINT"Dperm=";Dperm
3084 PRINT"DpA=";DpA
3088 PRINT"CtoK=273.15"
3090
3100 FOR I=1 TO 6:PRINT"Spec$(";I;")=";CHR$(34);Spec$(I);CHR$(34):NEXT
3110
3120 FOR I=1 TO 6:PRINT"N(";I;")=";N(I)
3130 FOR J=1 TO N(I)
3140 PRINT"Pe$(";I;",";J;")=";CHR$(34);Pe$(I,J);CHR$(34)
3150 PRINT"Pc$(";I;",";J;")=";CHR$(34);Pc$(I,J);CHR$(34)
3160 NEXT
```

```
3170 NEXT
3200 PRINT"@%=&20308:VDU 26,12,28,0,31,79,28,24,0;150;1279;1023;"
3390 PRINT"GOTO20"
3400 OSCLI"*SPOOL"
3500 END
3600
4000 DEF PROCderivedConstants
4005
4010 LeakCof=Pci*gap^3/(12*dep)
4015
4020 Ztdc=SQR((crl+amp)^2-off^2)
4030 Zbdc=SQR((crl-amp)^2-off^2)
4035
4040 PhiBdc=2*PI-ASN(off/(crl-amp))
4050 PhiTdc=  PI-ASN(off/(crl+amp))
4055
4060 Abore=(Vbdc-Vtdc)/(Ztdc-Zbdc)
4070
4090 ENDPROC
5100
5170 DEF PROCexpSpecs
5180 Spec$(1)="Unmodified compressor.  Normal superheat"
5190 Spec$(2)="Unmodified compressor.  High superheat"
5200 Spec$(3)="Vital oil flows only.   Normal superheat"
5210 Spec$(4)="Vital oil flows only.   High superheat"
5220 Spec$(5)="Vital oil flows only.   Suction system bypassed"
5230 Spec$(6)="Trial of piston O-ring using new compressor"
5240 ENDPROC
8710 DEF PROCrunData
8720 DATA  9
8725 DATA 22,150, 21,89, 22,220, 78,220, 40,108, 40,150, 40,220, 64,220,
64,150
8730
8740 DATA 12
8745 DATA 21,90,   6,77,  6,90,   5,108,  6,150, 21,150, 21,220, 40,220,
40,150
8750 DATA 40,108, 63,151, 64,220
8754
8756 DATA  9
8760 DATA 21,90, 22,150, 22,220, 64,220, 63,150, 40,150, 40,108, 40,219,
78,220
8762
8765 DATA  4
8767 DATA  6,78,  5,150,  5,108,  0,79
8768
8770 DATA  4
8772 DATA 21,150, 40,150, 63,150, 6,150
8773
8775 DATA  2, 41,150, 40,220
8780
8785 FOR Rn=1 TO 6: READ N(Rn)    : REM No. of data sets in Run no. Rn.
8790 FOR  I=1 TO N(Rn)
8800 READ Pe$(Rn,I),Pc$(Rn,I)     : REM Bourdon gauge settings
8810 NEXT I
8850 NEXT Rn
8900 ENDPROC
```

Listing of the interpretive model

The main program

```
 10 OSCLI"*EXEC IntrpModel.InfoEtc" : END
 15 REM Constants assigned, arrays DIMed etc.
 12
 20 PROCloadCo_effs("R12")
100
115 FOR Rn%=1 TO 6
140 FOR J=1 TO N(Rn%)
143 VDU2:PRINT
150 PRINT"Run number ";STR$(Rn%);"    Data set number ";STR$(J)
160 PROCloadData
165 PROCmotor
170 RoomT=CtoK+(F(3)-174)/40
175 oilT=F(15)+CtoK
180 PROCOilVisc(oilT)
200
205 Tsuc=F(13)+CtoK
210 IF F(13)>F(7) THEN Tsuc=F(7)+CtoK   : REM Forcing Tsuc <= water T
215 Psuc=(F(22)+1.013)*1E5              : REM Suction state
220 PROCvsh(Psuc,Tsuc): vsuc=v: hsuc=h  : REM ~~~~~~~~~~~~~
222 RLawLoss=(FNPs(F(12)+CtoK)-Psuc)/1E5: REM Evaporating P loss
224 F(37)=F(26)*F(27)+F(25)             : REM Evap. IV + pump power
226 F(38)=4.186*F(16)*(F(6)-F(7))       : REM Evap. water C*mdot*DT
228
230 Tdis=F(8)+CtoK: Pdis=(F(23)+1.013)*1E5 : REM Discharge state
235 PROCvsh(Pdis,Tdis):vdis=v:sdis=s:hdis=h: REM ~~~~~~~~~~~~~~
237
260 Tsvc=Tsuc: Tdvo=Tdis
262 vsvc=vsuc: vdvo=vdis
265 DisSucX=0: DisPdV=0
340 PROCconHeatLoss: REM Finds condenser T distribution & heat loss
350 PROCmdot        : REM Find self consistent mdot & discharge state
360 PROCcylrEntropy: REM Obtains reference states, dvo & svc
385
390 md=mdot/RPS
400 V2=0.6E-6: PROChiPhi(V2): phi2=HiPhi
404
405   REM  Initial estimates for the unknowns
408   REM  ~~~~~~~~~~~~~~~~~~~~~~~~~~~~~~~~~
409
410 Vleak=0.1E-6: Vdse=V2:   REM 'dse' - discharge stroke ending
415 m4=md+(Vdse+Vleak)/vdvo
420 Vsvc=m4*vsvc
425 V4=Vsvc
430
435 It%=0
440 REPEAT   : REM  Kernel algorithm
442 It%=It%+1: REM  ~~~~~~~~~~~~~~~
454
460 OldV4=V4
475 PROCloPhi(Vsvc): Phisvc=LoPhi
480 PROCleaks(sdvo,m4,Phisvc,Psuc,Tsvc,hsvc,Pdis)   : REM Compression
485
490 CleakPdV=leakPdV*RPS: m1=mcyl: V1=m1*vdvo: PROCloPhi(V1):
phi1=LoPhi
505
```

```
 510 PROCdischarge
 512 DisPdV=(PdVx-LeakLoss)*RPS
 517 DleakPdV=(mleak*(hdvo-hsvc)+LeakLoss)*RPS
 525 Vleak=(mleak+(m4-m1))*vdvo
 538
 540 PROCleaks(sdvo,m2,phi2,Pdis,Tdvo,hsvc,Psuc)       : REM Re-expansion
 542
 545 RleakPdV=leakPdV*RPS: m3=mcyl: V3=m3*vsvc: PROChiPhi(V3):
phi3=HiPhi
 555
 560 PROCcylrEntropy
 565 m4=md+(Vdse+Vleak)/vdvo: Vsvc=m4*vsvc: m3=V3/vsvc
 570
 580 PROCsuction
 590 SucPdV=PdVx*RPS
 600
 610 PRINT STR$(It%);" V4 = ";V4*1E6;" cc. Vsvc = ";Vsvc*1E6;" cc. Phi4
= ";DEGphi4;" Phi3 = ";DEGphi3;" Vdvc = ";Vdvc*1E6;" cc."
 625 UNTIL ABS(1-OldV4/V4)<0.0001 AND It%>2
 627
 630 PHI1=DEGphi1: PHI2=DEGphi2: PHI3=DEGphi3: PHI4=DEGphi4
 963
 980 MinWk=mdot*(hdvo-hsvc)
1000 TleakPdV=CleakPdV+DleakPdV+RleakPdV
1150 PdVtot=MinWk+SucPdV+TleakPdV+DisPdV
1440
1450 VDU3
1500 PROCoutput
3400 NEXT J
3420 NEXT Rn%
3990 END
```

Estimating the condenser's heat loss

```
4200 DEF PROCconHeatLoss
4240 REM  Condenser T distribution
4241 REM  ~~~~~~~~~~~~~~~~~~~~~~~~
4242
4243 Psub=(F(21)+1.013)*1E5
4245 T1=F(9)+CtoK:PROCvsh(Pdis,T1):h1=h:v1=v: REM Condenser start state
4250 PROCsatT(Pdis): T2=T: PROCC_Cequn(T2): h2=Vh
4255 PROCsatT(Psub): T3=T: PROCC_Cequn(T3): h3=Lh
4260 T4=F(11)+CtoK: PROCC_Cequn(T4): h4=Lh  : REM Condenser end h
4261
4262 F(18)=F(18)/(Lv*1E3)          : REM Converting R12 cc/s to g/s
4265
4270 Ta=F(5)+CtoK: Td=F(4)+CtoK    : REM Water entry & exit Ts
4275 Tb=Ta+(Td-Ta)*(h3-h4)/(h1-h4)
4278 Tc=Ta+(Td-Ta)*(h2-h4)/(h1-h4) : REM Intermediate Ts
4280
4282 Wdot=4.186*F(29)              : REM Desuperheating length estimate
4284 ConPowr=Wdot*(Td-Ta)          : REM ~~~~~~~~~~~~~~~~~~~~~~~~~~~~~~
4288 mdot=ConPowr/(h1-h4)
4300 IF Tc>T2 THEN LMTD=LN(T1-Td) ELSE LMTD=LN((T1-Td)/(T2-Tc))
4305 PROChtc(mdot,T1,v1,2E-5)
4310 Ldes=Wdot*LMTD*(Td-Tc)/(htc*(T1-T2-Td+Tc))
4315
4320 desTdif=(Tc*T1-Td*T2)/(T1-T2-Td+Tc)+(T1-T2+Td-Tc)/(2*LMTD) - RoomT
4325 ConTdif=(T2+T3+Tb+Tc)/4 - RoomT
4330 SubTbar=(T3+T4+Ta+Tb)/4
4335
4340 HeatLoss=Ldes*desTdif + (13-Ldes)*ConTdif + 2*(SubTbar-RoomT)
4345 HeatLoss=Uci*HeatLoss
4350 ENDPROC
```

Calculation of R12 flow rate, discharge state, & compressor heat loss

This routine finds the discharge state by calculating the heat loss from the external discharge pipe, and the three sources of heat transfer to the can, as explained in section 9.4. For the calculation of the discharge state, it is not necessary to consider the transfer to the suction gas.

```
5300 DEF PROCmdot
5302 ExtDisCan=0: Itn%=0
5305 REPEAT
5307 Ttrial=Tdis: Itn%=Itn%+1
5310 CrossTok=UcT*(oilT-SubTbar): CompLoss=F(19)-mdot*(hdis-hsuc)
5330 IF CrossTok>CompLoss/8 THEN CrossTok=CompLoss/8
5340 mdot=(ConPowr + HeatLoss - CrossTok)/(h1-h4)
5350
5360 PROChtc(mdot,Tdis,vdis,2*Adp)
5370 DisAmbX=((T1+Tdis)/2-RoomT)/(2/htc+1/Udi)
5375 hdis=h1+(DisAmbX+ExtDisCan)/mdot
5377 PROChPsoln(hdis,Pdis,vdis,Tdis): Tdis=T: vdis=v
5380 cPdot=mdot*FNcP(Tdis)
5388
5390   REM  Forced convection estimate of heat transfer to can
5400   REM  ~~~~~~~~~~~~~~~~~~~~~~~~~~~~~~~~~~~~~~~~~~~~~~~~~~~~
5410   REM  Outer discharge pipe linear conduction calculation
5420   REM  k=398W/mK. csa of copper=20mm^2.  Therefore kA=7.96E-3 Wm/K
5440
5450 lp=htc/(2*cPdot): kA=7.96E-3
5460 alpha=SQR(lp^2+htc/kA)+lp
5470 U3eff=1/(1/(kA*alpha)-1/cPdot) : REM External pipe conductance to
can
5475
5480   REM  Linear heat conduction along inner pipe.
5490   REM  k=54W/mK. csa of steel=10mm^2.  Therefore kA=5.4E-4 Wm/K.
5502
5510 PROChtc(mdot,Tdis,vdis,Adp)
5540 lp=htc/(2*cPdot): kA=5.4E-4
5600 alpha=SQR(lp^2+htc/kA)-lp
5605 U1eff=1/(1/(kA*alpha)-1/cPdot) : REM Internal pipe conductance to
can
5606
5610 U2eff=htc*.05                    : REM Conductance to discharge stub
5725
5730   REM  Principal outputs evaluated below
5732   REM  Stub - sump resistance = 2K/W
5735
5750 Tstub    =oilT+2*(Tdis-oilT)/(2+1/(U1eff+U2eff+U3eff))
5780 ExtDisCan=(Tdis-Tstub)*U3eff         : REM Transfer to can from
outer pipe
5790 DisCanX  =(Tdis-Tstub)*(U1eff+U2eff): REM Internal pipe + stub
transfer
5800 UNTIL ABS(Tdis-Ttrial)<0.01 AND Itn%>2
5950 ENDPROC
```

Finding the reference states svc & dvo

Having found the discharge state and the forced convection terms in the discharge heat loss model, in order to find hdvo it only remains to find the loss to the suction gas, and to include the excess PdV work on the discharge stroke. This last term, 'DisPdV', constitutes the only coupling between the 'thermal' calculation and the 'dynamical' calculation.

```
6000 DEF PROCcylrEntropy
6005
6007   REM  Estimating reference states
6008   REM  ~~~~~~~~~~~~~~~~~~~~~~~~~~~
6010
6015 REPEAT
6020 Ttrial=Tsvc
6025 hdvo=hdis+(DisCanX + DisSucX - DisPdV)/mdot
6030 PROChPsoln(hdvo,Pdis,vdvo,Tdvo)
6035 Tdvo=T:vdvo=v:sdvo=FNs(T)
6037 DisMod=FNmod(T,v)                    :  REM Modulus needed for
discharge calc'n
6040 PROCsPsoln(sdvo,Psuc,vsvc,Tsvc)
6045 Tsvc=T: vsvc=v: hsvc=FNh(T,vsvc)
6047 SucMod=FNmod(T,v)                    :  REM Modulus needed for suction
calc'n
6050
6055   REM  Free convection transfer to can gas
6060   REM  ~~~~~~~~~~~~~~~~~~~~~~~~~~~~~~~~~~~~
6065
6070 Beta=(-1)*FNPT(T)/(v*FNPv(T))    :  REM Thermal expansion
co-efficient
6075 PROCConductivity(T,v)
6080 PROCviscosity(T,1/v)
6090 Pr=FNcP(T)*visc/Con                  :  REM Prandtl number
6100 PROCFreeConvn(Tdvo,T,0.07,Beta,KinVis,Pr,"vert")
6110
6120 DisSucX=(Tdvo-T)*Nu*Con*0.07     :  REM Plenum modelled as 7cm
square plate
6125
6130 PROCFreeConvn(Tdis,T,.006,Beta,KinVis,Pr,"cyl'r")
6150 DisSucX=DisSucX+((Tdis+Tdvo)/2-T)*PI*Con*Nu*0.5 : REM  Pipe is
0.5m long
6160
6170 UNTIL ABS(Tsvc-Ttrial)<0.05
6300 ENDPROC
6400
6500 DEF PROChtc(mdot,T,v,A)    : REM  Reynold's analogy used for Nu
6520 PROCviscosity(T,1/v)
6530 PROCConductivity(T,v)
6540 Re=2*(mdot/visc)/SQR(PI*A)
6550 PROCFf(Re,0.0001)
6560 htc=PI*Con*Re*Ff/8
6600 ENDPROC
```

Numerical integration of leakage past the piston

```
6800 DEF PROCleaks(s,Mstart,phiStart,Pstart,Tstart,href,endP)
6802 IF endP<Pstart THEN Pmult%=1 ELSE Pmult%=-1
6805
6810 mcyl=Mstart: phi=phiStart: Pcyl=Pstart: T=Tstart: eKT=EXP(-K*T)
6815 leakPdV=0: leakDm=0
6820
6825 dphi=w*dt
6830
6835 REPEAT
6840 OldP=Pcyl
6845 phi=phi+dphi
6850 vcyl=FNvCyl(phi)/mcyl
6855
6860 PROCYs(vcyl): PROCZs(vcyl): slope=1/FNsT(T)
6865 REPEAT:eKT=EXP(-K*T):dT=(s-FNs(T))*slope:T=T+dT:UNTIL ABS(dT)<.01
6870 Pcyl=FNP(T):hcyl=FNh(T,vcyl)
6875
6880 Tbar=(T+Tsvc)/2:Robar=(1/vcyl+1/vsvc)/2
6885 PROCviscosity(Tbar,Robar)
6887
6890 leakDm=dt*(Pcyl-Psuc)*LeakCof/KinVis
6895 mcyl=mcyl-leakDm
6900 leakPdV=leakPdV+leakDm*(hcyl-href)
6905 UNTIL(Pmult%*Pcyl<endP*Pmult%)
6910
6915 CorFactr=(Pcyl-endP)/(Pcyl-OldP)
6920 leakPdV=leakPdV-leakDm*(hcyl-href)*CorFactr
6930 mcyl=mcyl+leakDm*CorFactr
6940 ENDPROC
```

```
7000 DEF PROCsuction:   REM  Intake stroke.
7002                    REM  ~~~~~~~~~~~~~~
7005
7010 Ro0=1/vsvc:Mod=SucMod: Pref=Psuc
7020   Po=Psuc:  mo=Vo*Ro0: msdot=0
7030   Pi=Psuc:  mi=Vi*Ro0: mbdot=0: Roi=Ro0
7035 Pcyl=Psuc:mcyl=m3
7040 Vcyl=V3  : phi=phi3
7045 y=0:ydot=0
7060
7070 PdVx=0
7085 dphi=w*dt
7090
7095 REPEAT                              : REM keeps going till
Pcyl=Psuc recurs
7100 PROCincrementPhi
7103 IF (y<1E-4 AND OP<0 AND phi>=PhiBdc) THEN 7200:  REM Detects shut
valve
7105 OP=Pi-Pcyl
7110 PROCvalvFloArea(Sm,Sk,0,Sperm,SpA,Slift)
7115
7120 IF OP<0 THEN mvdot=-VFA*SQR(-2*OP*Roi) ELSE
mvdot=VFA*SQR(2*OP*RoCyl)
7125 mcyl=mcyl+mvdot*dt
7130 IF Rn%=5 THEN 7195
7135
7140 mi=mi+dt*(mbdot-mvdot):Roi=mi/Vi:Pi=Psuc+(Roi-Ro0)*Mod
7150 mo=mo+dt*(msdot-mbdot):Roo=mo/Vo:Po=Psuc+(Roo-Ro0)*Mod
7160 mb2dot=bL*((Po-Pi)-mbdot*ABS(mbdot)/(2*Roo*bA*bA))
7170 ms2dot=sL*((Psuc-Po)-msdot*ABS(msdot)/(2*Ro0*sA*sA))
7180 mbdot=mbdot+dt*mb2dot
7190 msdot=msdot+dt*ms2dot
7193
7195 IF (y>1E-4 AND mcyl<m4 AND OP<0 AND phi>=PhiBdc) THEN PROCcloseSV
7197
7200 IF y<1E-4 AND phi>PhiBdc AND (Pcyl-Psuc)*(Vcyl-Vsvc)>0 THEN
PRINT"Inconsistency suspected"
7202 UNTIL (Pcyl>=Psuc AND phi>=PhiBdc AND y<1E-4)
7203
7204   REM  Keeps going until the valve is closed AND the suction
          pressure has recurred.
7205
7207 PdVx=PdVx-(1/2)*(Pcyl-Psuc)*(Vsvc-Vcyl) :  REM Overshoot
correction
7210 ENDPROC
7214
7215 DEF PROCcloseSV
7217 V4=m4/Roi                        :REM charge adjusted to plenum
pressure
7220 PROCloPhi(V4)
7222 phi4=LoPhi
7225 y=0:VFA=0:mvdot=0
7235 mcyl=m4
7240 ENDPROC
7245
```

```
7305 DEF PROCdischarge
7310  Ro0=1/vdvo: Mod=DisMod: uson=SQR(Mod): Pref=Pdis
7315   Pp=Pdis  :  mp=DPvol*Ro0: mpdot=0: RoP=Ro0
7320 Pcyl=Pdis  :mcyl=m1
7325  phi=phi1  :Vcyl=V1
7330 ydot=0: y=0
7340 dphi=w*dt
7365 PdVx=0:LeakLoss=0:mleak=0
7370 Tbar=(Tdvo+Tsvc)/2:Robar=(1/vsvc+(mcyl+mp)/(DPvol+Vcyl/2))
7375 Robar=(Ro0+(mcyl+mp)/DPvol)/2: Robar=(Robar+1/vsvc)/2
7380 PROCviscosity(Tbar,Robar):LkMr=LeakCof*dt/KinVis
7390
7400 REPEAT                              : REM keeps going till
Pcyl=Pdis recurs
7405 OldP=Pcyl
7410 PROCincrementPhi
7420 leakDm=(Pcyl-Psuc)*LkMr: mleak=mleak+leakDm
7430 LeakLoss=LeakLoss+leakDm*Mod*LN(RoCyl/Ro0)
7432 mcyl=mcyl-leakDm
7435
7437 IF (y<1E-4 AND phi>=phi2) THEN
7720:           REM Detects shut valve
7440 DP=Pcyl-Pp
7450 PROCvalvFloArea(Dm,Dk,Dpl,Dperm,DpA,Dlift)
7470
7480 IF DP<0 THEN mvdot=-VFA*SQR(-2*DP*RoCyl) ELSE
mvdot=VFA*SQR(2*DP*RoP)
7520 mcyl=mcyl-mvdot*dt
7600
7620 mpdot=Adp*(Pp-Pdis)/uson
7640 mp=mp+(mvdot-mpdot)*dt
7700 RoP=mp/DPvol:Pp=Pdis+Mod*(RoP-Ro0)
7705
7710 IF (y>1E-4 AND phi>=phi2) THEN y=0: VFA=0: mcyl=V2*RoP:
Vdvc=V2*RoP/Ro0
7711
7712   REM  The ratio Vdvc/V2 indicates the increase in the
      re-expansion charge caused by the overpressure built up
      in the discharge plenum
7715
7720 UNTIL (phi>phi2 AND Pcyl<=Pdis)    : REM keeps going till
Pcyl=Pdis
7800
7804 CorFactr=(Pdis-Pcyl)/(OldP-Pcyl)   : REM Overshoot corrections
7806 mleak=mleak-leakDm*CorFactr
7808 m2=mcyl+leakDm*CorFactr            : REM cylinder charge at return
to Pdis
7809 Vdse=m2*vdvo                       : REM cylinder volume at return
to Pdis
7810 LeakLoss=LeakLoss-leakDm*Mod*LN(RoCyl/Ro0)*CorFactr
7820 PdVx=PdVx-(1/2)*(Pcyl-Pdis)*(OldVcyl-Vcyl)*CorFactr
7850  ENDPROC
7860
```

Utilities for valve & piston dynamics

```
8000 DEF PROCincrementPhi
8010 phi=phi+dphi
8020 OldVcyl=Vcyl
8030 Vcyl=FNvCyl(phi)
8040 RoCyl=mcyl/Vcyl
8050 Pcyl=Pref+(RoCyl-Ro0)*Mod
8060 PdVx=PdVx+(Pcyl-Pref)*(OldVcyl-Vcyl)
8100 ENDPROC


8200 DEF PROCvalvFloArea(m,k,pl,perm,pA,lift):  REM Hard wired for
opening only
8230 y2dot=(pA*OP-k*y-pl)/m
8240 IF y2dot<0 THEN y2dot=0
8250 Oldydot=ydot
8260 ydot=ydot+y2dot*dt
8270 y=y+(ydot+Oldydot)*dt/2
8275  IF y>lift THEN y=lift:ydot=0
8280  IF y<0 THEN y=0:ydot=0
8285 VFA=perm*y
8290 ENDPROC


8350 DEF
FNvCyl(phi)=Vtdc+Abore*(Ztdc-SQR(crl^2-(amp*SINphi-off)^2)+amp*COSphi)


8360 DEF FNphi(z)=ACS((crl^2-amp^2-off^2-z^2)/(2*amp*SQR(off^2+z^2)))


8370 DEF PROCloPhi(V)
8375 zp=Ztdc-(V-Vtdc)/Abore:LoPhi=FNphi(zp)-ATN(off/zp)
8380 ENDPROC


8390 DEF PROChiPhi(V)
8393 zp=Ztdc-(V-Vtdc)/Abore:HiPhi=2*PI-FNphi(zp)-ATN(off/zp)
8396 ENDPROC
```

Finding the motor speed & losses

```
9100 DEF PROCmotor
9110
9120   REM   Fits to motor spec furnished by Danfoss, including
9130   REM   current & temperature compensation
9140
9150 StatLoss=Rend*F(1)*F(1)/1E6
9160 RedInput=F(19)-StatLoss
9170 RedLoss=46+12.5*(1-COS((RedInput-130)*PI/340))
9180 ShaftWk=RedInput-RedLoss
9190 X=RedInput
9200 Slip=-9.24+X*(0.352+2.4E-7*X*X)
9210 RPS=50-Slip/60:w=2*PI*RPS
9220  ENDPROC
```

Loading the experimental raw data

```
9240 DEF PROCloadData
9250 Nam$=STR$(Rn%)+"E"+Pe$(Rn%,J)+"C"+Pc$(Rn%,J)
9260 F$="ExpData."+STR$(Rn%)+".E"+Pe$(Rn%,J)+"C"+Pc$(Rn%,J)
9270 ChanC=OPENIN(F$)
9280 FOR I=1 TO 32:INPUT£ChanC,F(I):NEXT
9290 INPUT£ChanC,Rstat,Rend,Oilfn,Indx1,Indx2
9300 CLOSE£ChanC
9310 ENDPROC
```

Loading the equation of state co-efficients

```
9400 DEF PROCloadCo_effs(R$)
9510 d%=OPENIN("RefCoeffs."+R$)
9520 INPUT£d%,A1,B1,C1,D1,E1,F1,G1
9530 INPUT£d%,A,B,C,D,E,F
9540 INPUT£d%,a,b,c,d,f
9550 INPUT£d%,R,bv
9560 INPUT£d%,A2,B2,C2,A3,B3,C3,A4,B4,C4,A5,B5,C5
9570 INPUT£d%,K,Tcrit,so,fo,Pc,vc
9580 CLOSE£d%
9590 K=K/Tcrit
9600
9610 xA5=A5*5:xA4=A4*4:xA3=A3*3:xA2=A2*2
9620 xB5=B5*5:xB4=B4*4:xB3=B3*3:xB2=B2*2
9630 xC5=C5*5:xC4=C4*4:xC3=C3*3:xC2=C2*2
9650
9660 zA5=A5/4:zA4=A4/3:zA3=A3/2
9670 zB5=B5/4:zB4=B4/3:zB3=B3/2
9680 zC5=C5/4:zC4=C4/3:zC3=C3/2
9700 ENDPROC
```

```
10000   REM     THERMODYNAMICS OF VAPOUR
10001   REM     ~~~~~~~~~~~~~~~~~~~~~~~~
10002
10010   REM  Volume dependent terms in dP/dv
10020   REM  ~~~~~~~~~~~~~~~~~~~~~~~~~~~~~~~
10025 DEF PROCXs(v)
10027 Ro=1/(v-bv):R2=Ro*Ro:R3=R2*Ro
10030 X1=-R3*(Ro*(Ro*(Ro*xA5+xA4)+xA3)+xA2)
10040 X2=-R2*(Ro*(Ro*(Ro*(Ro*xB5+xB4)+xB3)+xB2)+R)
10050 X3=-R3*(Ro*(Ro*(Ro*xC5+xC4)+xC3)+xC2)
10060 ENDPROC
10090
10100   REM  Volume dependent terms in P(v,T)
10110   REM  ~~~~~~~~~~~~~~~~~~~~~~~~~~~~~~~~
10115 DEF PROCYs(v)
10117 Ro=1/(v-bv):R2=Ro*Ro
10120 Y1=R2*(Ro*(Ro*(Ro*A5+A4)+A3)+A2)
10130 Y2=Ro*(Ro*(Ro*(Ro*(Ro*B5+B4)+B3)+B2)+R)
10140 Y3=R2*(Ro*(Ro*(Ro*C5+C4)+C3)+C2)
10160 ENDPROC
10190
10200   REM  Volume dependent terms in Integral(Pdv)
10210   REM  ~~~~~~~~~~~~~~~~~~~~~~~~~~~~~~~~~~~~~~~
10215 DEF PROCZs(v)
10217 Ro=1/(v-bv)
10220 Z1=-Ro*(Ro*(Ro*(Ro*zA5+zA4)+zA3)+A2)
10230 Z2=-Ro*(Ro*(Ro*(Ro*zB5+zB4)+zB3)+B2)-R*LN(Ro)
10240 Z3=-Ro*(Ro*(Ro*(Ro*zC5+zC4)+zC3)+C2)
10260 ENDPROC
10290
10500   REM  Functions of state P(T,v), h(T,v), s(T,v)
10510   REM  ~~~~~~~~~~~~~~~~~~~~~~~~~~~~~~~~~~~~~~~~~
10520   REM  Ensure that X1,X2,X3, Y1,Y2,Y3, Z1,Z2,Z3 are evaluated at
correct v
10530   REM  Ensure that eKT=EXP(-KT) is evaluated at correct T.
10540
10550 DEF FNP(T)=Y1+T*Y2+Y3*eKT
10560 DEF FNs(T)=a*LN(T)+b*T+c*T^2/2+d*T^3/3-f/(2*T^2)+Z2-K*Z3*eKT+so
10565 DEF FNu(T)=a*T+b*T^2/2+c*T^3/3+d*T^4/4-f/T-Z1-(1+K*T)*eKT*Z3+fo
10570 DEF
FNh(T,v)=a*T+b*T^2/2+c*T^3/3+d*T^4/4-f/T-Z1-(1+K*T)*eKT*Z3+v*(Y1+T*Y2+Y3
*eKT)+fo
10600
10700   REM  Differential co-efficients dP/dT, dP/dV, ds/dT
10710   REM  ~~~~~~~~~~~~~~~~~~~~~~~~~~~~~~~~~~~~~~~~~~~~~~
10720
10730 DEF FNPT(T)=Y2-K*eKT*Y3
10740 DEF FNPv(T)=X1+T*X2+eKT*X3
10750 DEF FNsT(T)=a/T+b+c*T+d*T^2+f/T^3+eKT*Z3*K^2
10755 DEF FNcP(T)=T*(FNsT(T)-(FNPT(T))^2/FNPv(T))
10760
10800   REM  Speed of sound
10805   REM  ~~~~~~~~~~~~~~
10900 DEF FNmod(T,v)=v*v*((FNPT(T))^2/FNsT(T)-FNPv(T))
10960
10990   REM  End of thermodynamics of vapour
10995   REM  ~~~~~~~~~~~~~~~~~~~~~~~~~~~~~~~
10997
```

```
11000   REM  THERMODYNAMICS OF LIQUID
11010   REM  ~~~~~~~~~~~~~~~~~~~~~~~~
11020
11030   REM  Liquid Density
11032   REM  ~~~~~~~~~~~~~~
11034
11040 DEF PROCliquid_rho(T)
11050 X1=1-T/Tcrit
11060
Lro=A1+B1*X1^(1/3)+C1*X1^(2/3)+D1*X1+E1*X1^(4/3)+F1*SQR(X1)+G1*X1^2
11065 ENDPROC
11100
11120   REM Saturated vapour pressure
11121   REM ~~~~~~~~~~~~~~~~~~~~~~~~~
11122
11130 DEF FNPs(T)=EXP(A+B/T+C*LN(T)+D*T+E*(F/T-1)*LN(F-T))
11150
11160 DEF FNdPdTs(T)=-B/T^2+C/T+D-(E/T)*(1+(F/T)*LN(F-T))
11170
11200   REM  Clausius-Clapeyron Equation
11210   REM  ~~~~~~~~~~~~~~~~~~~~~~~~~~~
11220
11230 DEF PROCC_Cequn(T)
11240 PROCliquid_rho(T):Lv=1/Lro
11250 P=FNPs(T)
11260 PROCvsh(P,T)
11270 DsCon=(v-Lv)*P*FNdPdTs(T)
11300 Vs=s: Vh=h               :REM  Vapour s & h
11310 Ls=Vs-DsCon:Lh=Vh-T*DsCon:REM  Liquid s & h
11390 ENDPROC
11400
11420 DEF PROCsatT(P)
11430 T=300
11440 REPEAT dT=(1-P/FNPs(T))/FNdPdTs(T): T=T-dT: UNTIL ABS(dT)<0.001
11450 ENDPROC
11460
```

```
11950   REM  Newton-Raphson routines for EoS inversions
11960   REM  ~~~~~~~~~~~~~~~~~~~~~~~~~~~~~~~~~~~~~~~~~~~~~
12000   REM   Solution for v given P & T
12010   REM   ~~~~~~~~~~~~~~~~~~~~~~~~~~~
12015 DEF PROCvsh(P,T)
12020 eKT=EXP(-K*T):v=R*T/P
12030 PROCXs(v):PROCYs(v)
12040 dv=0.8*(P-FNP(T))/FNPv(T)
12050 v=v+dv
12060 IF ABS(dv/v)>.00001 THEN 12030
12065 PROCZs(v): s=FNs(T): h=FNh(T,v)
12070 ENDPROC
12080
12100   REM   Solution for T given s & v
12105   REM   ~~~~~~~~~~~~~~~~~~~~~~~~~~~
12110 DEF PROCTsoln(s,v,Tt): T=Tt: PROCYs(v): PROCZs(v): slope=1/FNsT(T)
12130
12140 REPEAT:eKT=EXP(-K*T):dT=(s-FNs(T))*slope:T=T+dT:UNTIL ABS(dT)<.001
12180  ENDPROC
12200
12210   REM   Solution for v & T given s & P
12220   REM   ~~~~~~~~~~~~~~~~~~~~~~~~~~~~~~~
12230 DEF PROCsPsoln(s,P,vt,Tt)
12240 PROCXs(vt):PROCYs(vt):PROCZs(vt):eKT=EXP(-K*Tt)
12250 Pv=FNPv(Tt):sT=FNsT(Tt):PT=FNPT(Tt):Pt=FNP(Tt):st=FNs(Tt)
12260 Det=PT^2-Pv*sT
12270 dT= (PT*(P-Pt)-Pv*(s-st))/Det
12280 dv=(-sT*(P-Pt)+PT*(s-st))/Det
12290 vt=vt+dv:Tt=Tt+dT
12300 IF ABS(dv/vt)<.00001 AND ABS(dT/Tt)<.00001 THEN 12340
12310 GOTO 12240
12340 v=vt:T=Tt
12350 ENDPROC
12360
12400   REM   Solution for v & T given h & P
12410   REM   ~~~~~~~~~~~~~~~~~~~~~~~~~~~~~~~
12430 DEF PROChPsoln(h,P,vt,Tt)
12435 v=vt:T=Tt
12440 PROCXs(v):PROCYs(v):PROCZs(v):eKT=EXP(-K*T)
12450 Pv=FNPv(T):sT=FNsT(T):PT=FNPT(T):Pt=FNP(T):ht=FNh(T,v)
12460 dhdT=T*sT+v*PT
12470 dhdv=T*PT+v*Pv
12480 Det=T*(PT^2-Pv*sT)
12490 dT= (dhdv*(P-Pt)-Pv*(h-ht))/Det
12500 dv=(-dhdT*(P-Pt)-PT*(h-ht))/Det
12510 v=v+dv:T=T+dT
12520 IF ABS(dv/v)<.00001 AND ABS(dT/T)<.00001 THEN 12550
12530 GOTO 12440
12550 ENDPROC
```

```
13900   REM  Transport Properties & Phenomena  (JTR Watson, NEL 1975)
13910   REM  ~~~~~~~~~~~~~~~~~~~~~~~~~~~~~~~~~~~~~~~~~~~~~~~~~~~~~~~~~
13920
14000   REM  R12 Vapour kinematic viscosity & thermal conductivity
14005   REM  ~~~~~~~~~~~~~~~~~~~~~~~~~~~~~~~~~~~~~~~~~~~~~~~~~~~~~
14010 DEF PROCviscosity(T,Ro)
14020 roRed=vc*Ro
14035
visc=(1.2587*SQR(T)+roRed*(roRed*(roRed*(10.8028*roRed-14.1489)+12.8335)
+12.0594)-9.2006)/1E6
14040 KinVis=visc/Ro
14050  ENDPROC
14060
14100 DEF PROCConductivity(T,v)
14105 roRed=vc/v
14110
Con=(-4.474+.047796*T+10.8547*roRed-.06792*roRed^2+.92347*roRed^3+.76179
*roRed^4)/1E3
14120  ENDPROC
14130
14200   REM  R12 Liquid viscosity & conductivity
14210   REM  ~~~~~~~~~~~~~~~~~~~~~~~~~~~~~~~~~~
14230 DEF FNliqvis(T)=(173-1.7*(T-313.15)+.0075*(T-313.15)^2)/1E6
14240 DEF FNliqCon(T)=(64.4-.375*(T-313.15))/1E3
14300
14400 DEF PROCOilVisc(T):REM KELVIN
14405 LOCAL C,B
14410 C=8.10918092E10:B=-4.1587108
14420 X=T^B:X=X*C:X=EXP(X):V=X-.7:REM CENTISTOKES
14450 rho=0.872-0.00063*(T-288.7):REM g/cc
14460 Ov=V*rho:   REM  CENTIPOISE
14470 ENDPROC
14500
16000 DEF PROCFf(Re,Rp)
16050 LOCAL f,F
16100 F=.184/Re^.2
16150 f=F^.5
16200 Ff=1/(1.14-2*LOG(Rp+9.3/(Re*f)))^2
16300 IF ABS((Ff-F)/F)< .000001 THEN16500
16400 F=Ff:GOTO 16150
16500  ENDPROC
16600
17000 DEF PROCFreeConvn(Tw,To,L,Beta,vkin,Pr,Or$)
17005  LOCAL c
17010 Gr=9.81*Beta*(Tw-To)*L^3/(vkin^2)
17020 IF Or$="flat-"THEN c=.27
17040 IF Or$="flat+"THEN c=.54
17060 IF Or$="vert"THEN c=.401+0.035*LN(Pr)
17080 IF Or$="cyl'r"THEN c=.47
17100 REM ****** Handbook of Heat Transfer ch 6 (valid for gases only)
17120 Nu=c*(Pr*Gr)^.25
17130  ENDPROC
```

Printing the calculated results

```
21700 DEF PROCoutput
21800 @%=&20308
21810 OSCLI("*Spool Results."+Nam$)
22005 PRINTSpec$(Rn%):PRINT
22106 PRINT"Nominal Evaporating P ";Pe$(Rn%,J);"psig.  Nominal
Condensing P ";Pc$(Rn%,J);"psia."
22200 PRINT
22207 PRINT"Raw data                               Refrigerant states"
22309 PRINT"                                       Position        Temp   Press
Volume Enthalpy"
22420 PRINT"Current   mA    ",F(1)
22430 PRINT"Voltage  bits   ",F(2);"    dvo state
",Tdvo-CtoK,Pdis/1E5,vdvo*1E3,hdvo/1E3
22440 PRINT"Room temperature",RoomT-CtoK;"    Discharge
",Tdis-CtoK,Pdis/1E5,vdis*1E3,hdis/1E3
22450 PRINT"Cond. water out ",F(4);"    Cond.
start",T1-CtoK,Pdis/1E5,v1*1E3,h1/1E3
22515 PRINT"Cond. water in  ",F(5);"    Cond. end
",T4-CtoK,Psub/1E5,Lv*1E3,h4/1E3
22620 PRINT"Evap. water in  ",F(6);"    Evap. end
",Tsuc-CtoK,Psuc/1E5,vsuc*1E3,hsuc/1E3
22725 PRINT"Evap. water out ",F(7);"    svc state
",Tsvc-CtoK,Psuc/1E5,vsvc*1E3,hsvc/1E3
22800 PRINT
22827 PRINT"R12 Discharge   ",F(8);"    Condenser temperature
distribution"
22929 PRINT"R12 Cond. entry ",F(9)
23030 PRINT"R12 Condensing  ",F(10);"    R12 Ts
",T4-CtoK,T3-CtoK,T2-CtoK,T1-CtoK
23041 PRINT"R12 Cond. exit  ",F(11);"    Water
Ts",Ta-CtoK,Tb-CtoK,Tc-CtoK,Td-CtoK
23050 PRINT
23052 PRINT"R12 Evap. entry ",F(12);"    Discharge stub temperature
",Tstub-CtoK
23054 PRINT"R12 Evap. exit  ",F(13)
23056 PRINT"R12 Suction     ",F(14);"    Powers, Watts"
23060 PRINT"Sump oil Temp.  ",F(15);"                   measured   Xtalk
loss   R12 Dh"
23065 PRINT"Evap. flow rate ",F(16);"
Compressor",F(19),CrossTok,CompLoss-CrossTok,mdot*(hdis-hsuc)
23070 PRINT"Cond. flow rate ",F(17);"    Condenser
",ConPowr,CrossTok,HeatLoss,mdot*(h1-h4)
23075 PRINT"R12 flow meter  ",F(18);"    Evaporator",F(37),F(38);"
",mdot*(hsuc-h4)
23080 PRINT"Comp. power     ",F(19)
23090 PRINT"P at suction    ",F(20);"    Compressor performance"
23095 PRINT"P at cond. end  ",F(21);"        Vertex      phi    Volume
Vsvc etc mass,mg".
23100 PRINT"P at evap start ",F(22);"           1",PHI1,V1*1E6;"
",m1*1E6
23105 PRINT"P at discharge  ",F(23);"
2",PHI2,V2*1E6,Vdvc*1E6,m2*1E6
23110 PRINT "                                           3",PHI3,V3*1E6;"
",m3*1E6
23113 PRINT"PT supply volts ",F(24);"
4",PHI4,V4*1E6,Vsvc*1E6,m4*1E6
23116 PRINT"Water pump power",F(25)
```

```
23118 PRINT"Heater volts     ",F(26);"        Leakage loss on discharge,
mg",mleak*1E6
23123 PRINT"Heater Amps      ",F(27);"        Reference density ratio
 ",vsvc/vdvo
23126 PRINT"Room temperature",F(28);"        R12 mass flow rate
g/s",mdot*1E3
23128 PRINT"Manual cond mdot",F(29)
23130 PRINT"Bourdon Pe, psig",F(30);"    Indicator diagram breakdown,
Watts"
23133 PRINT"Bourdon Pc, psia",F(31)
23136 PRINT"Real time        ",F(32);"        Minimum work of
compression",MinWk
23150 PRINT"Oil fraction     ",Oilfn;"        Suction excess PdV
",SucPdV
23155 PRINT"Suction P loss   ",RLawLoss;"        Discharge excess PdV
  ",DisPdV
23160 PRINT"Stator res'tance",Rend ;"        Total leakage loss
",TleakPdV
23170 PRINT"Winding Temp     ",100+(Rend-10.2)*45;"        Total
indicated work       ",PdVtot
23180 PRINT
23190 PRINT"Motor performance          R12 Enthalpy gain summary,
Watts"
23195  PRINT
23200 PRINT"Estimated RPM    ",3000-Slip;"        Total suction gas
preheat",(hsvc-hsuc)*mdot
23205 PRINT"Winding loss     ",StatLoss;"        Calculated total PdV
work",PdVtot
23210 PRINT"Rotor Loss etc. ",RedLoss;"        Discharge - suction
exchange",DisSucX
23220 PRINT"Shaftwork        ",ShaftWk;"        Inner pipe, loss to the
can ",DisCanX
23230 PRINT"Bearing losses   ",ShaftWk-PdVtot;"        Outer pipe, loss
to the can ",ExtDisCan
23250 PRINT"Implied viscos'y",(ShaftWk-PdVtot)/4;"        Outer pipe,
loss to ambient ",DisAmbX
23260 PRINT"Sump viscosity   ",Ov
23265 PRINT
23300 PRINT"The discharge valve was open for ";1000*(phi2-phi1)/w;" ms."
23305 PRINT"The first rarefaction returns after ";1000/uson;" ms."
23310 OSCLI("*Spool")
23400 ENDPROC
```

Chapter 10. Results of the interpretive model

10.1 Introduction. Explanation of the model's output

The results of the interpretive model are presented at the back of this chapter. Before discussing the results, it is first necessary to explain the physical significance of all the output.

The measurements

The title is self explanatory. The following line indicates the nominal bourdon gauge readings. The raw data is shown at the left. It is listed in the same order as it was read from the A.D.Cs. The temperatures are quoted in centigrade, the pressures in gauge bar, and the flow rates in gramme/s, except for the refrigerant flowmeter, which got stuck, and recorded a flow rate only when the refrigerant flow rate was high enough to free it.

Early on, it was noticed that the pressure recorded by the evaporator start pressure transducer always reproduced the same reading if a given bourdon gauge setting was reproduced. However, the suction pressure transducer did not satisfy this test of consistency. This is in spite of the fact that the bourdon gauge measures the pressure in the can, i.e. the true suction pressure. On earlier tests it had already been observed that the evaporator's pressure drop is normally negligible. For these reasons the suction pressure reading was ignored, and the measured evaporator start pressure was used instead.

The ADC readings end with the discharge pressure. The subsequent measurements were performed manually. The "Suction P loss" indicates the shortfall of the evaporating pressure from the saturated vapour pressure at the R12 evaporator entry temperature. This deficit, expressed here in Bar, is probably due to oil accumulating in the evaporator.

The motor's performance and losses

The motor performance calculations have been based on fits to data supplied by Danfoss, as explained in more detail in Appendix 4. The measured stator resistance, current consumption & total power consumption are used to deduce the motor's speed, and to obtain the electrical losses. The shaftwork follows by subtracting the motor's losses from the measured power consumption. The "bearing" losses are then found by subtracting the total calculated indicated work from the shaftwork. The "Implied viscosity" refers to the viscosity of the oil in the bearings, and is simply (bearing loss)/4, using the rule of thumb mentioned in section 9.1. The "sump viscosity" is the viscosity of pure Alkylbenzene at the sump temperature. Because of the combined effects of refrigerant solution, and the presumed higher temperature of the bearings, the sump viscosity should be an upper limit, always exceeding the viscosity of the oil in the bearings. Thus, if the implied viscosity ever exceeds the sump viscosity, this is evidence for a mechanical loss other than viscous drag at the bearings. This is the purpose of quoting both these figures for viscosity.

The refrigerant's state

The main body of the calculated results is presented on the right hand side of the table. The first block of figures furnishes a comprehensive specification of the refrigerant's state at the cycle vertices, as well as specifying the reference states dvo & svc. The temperatures are quoted in centigrade, the pressures in absolute Bar, the specific volumes are in L/Kg, and the specific enthalpies are quoted in KJ/Kg.

Condenser temperature distribution

The temperatures quoted under "Condenser temperature distribution" have been layed out to correspond to figure 9.1.

The "Discharge stub temperature" indicates the temperature deduced for the discharge stub as part of the discharge system heat transfer calculation, which was explained in section 9.4. It was mentioned that the discharge thermocouple reads low because it is partially heatsinked by the discharge stub, and for this reason the discharge temperature was calculated from the condenser start temperature using a heat transfer model for the discharge gas pipework. With increasing R12 flow rate the discharge thermocouple error should get smaller. Figure 10.1 shows the estimated discharge thermocouple error plotted against the R12 flow rate. This plot shows the anticipated trend, so providing some re-assurance as to the validity of the interpretation of the discharge gas temperature measurements.

Powers and energy balances

As explained in section 9.2, the R12 flow rate is found from the condenser power measurement, after correcting for the two effects of direct transfer from the compressor, and loss to ambient. For the condenser, one can observe that the freon side power, recorded under the heading "R12 Dh", is reproduced by adding the "loss" and subtracting the "Xtalk" from the measured power. For the compressor, the product of the enthalpy increment, (hdis - hsuc), and R12 flow rate is recorded under "R12 Dh". This is always less than the compressor's measured power consumption due to the effects of heat loss to ambient, direct transfer to the condenser, and liquid return to the sump. The "loss" simply indicates this difference, and has been defined by

loss = [Power consumption - R12 enthalpy gain - Xtalk]

i.e. it specifically excludes the direct transfer to the condenser.

For the evaporator, there are two independent power measurements. The first figure follows from the electrical measurements. It is the IV product for the heater plus the water pump power. The second figure follows from the water temperature drop and flow rate. Lastly, the refrigerant side's power has been deduced from (hsuc - hsub)(R12 flow rate). Ideally, the R12 power would fall within the range of uncertainty indicated by the two measurements. In some cases, the measured powers are both lower than that implied by the refrigerant enthalpy change. While heat leakage in from ambient undoubtedly contributes to such a discrepancy, in some cases this discrepancy constitutes additional evidence to support the conclusion that there is liquid returning to the sump.

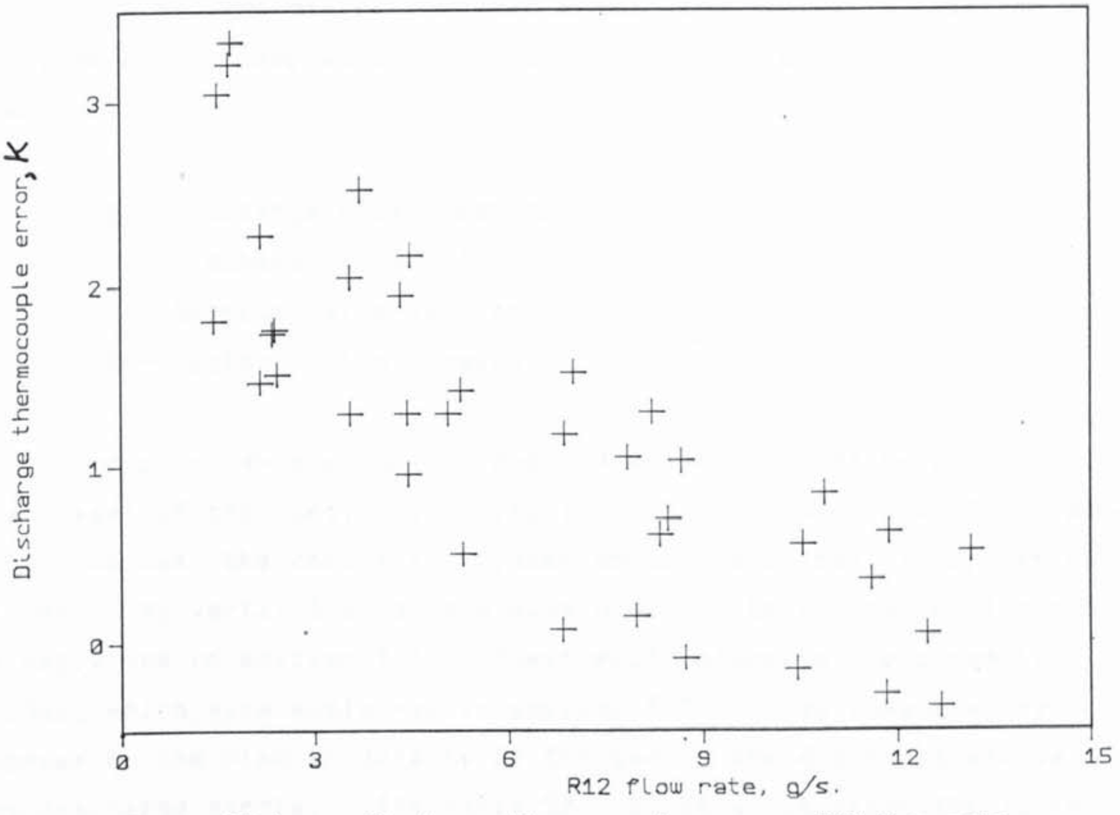

Figure 10.1 Discharge thermocouple error v R12 flow rate

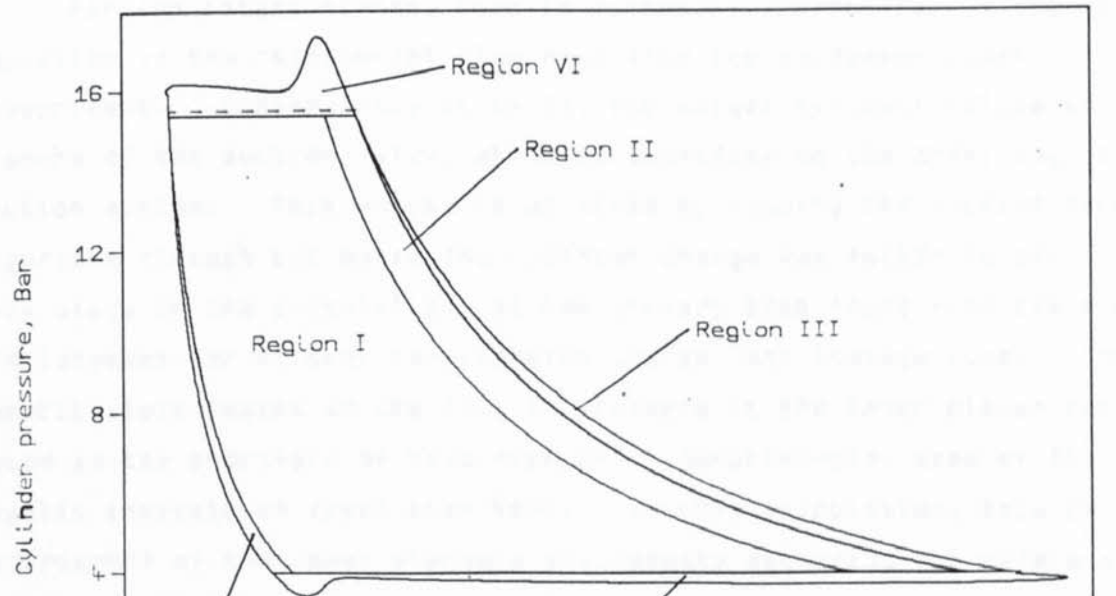

Figure 10.2 Indicator diagram. Leakage exaggerated

The compressor's performance

This section of the printout summarises the key parameters at the vertices of the compressor's cycle. The vertices are labelled numerically;-

1 - Discharge valve opening
2 - Discharge valve closing
3 - Suction valve opening
4 - Suction valve closing

The crank angles, under 'phi', are quoted in degrees. Because of the offset of the bore, bdc occurs at -3.3 degrees, not at 0 degrees. Under 'Volume' the enclosed cylinder volume is listed, in cc, at each vertex. At vertex 2 this is always 0.6cc in this version of the model, as explained in section 9.7. "Vsvc etc" refers to the parameters Vsvc & Vdvc, which were explained in section 9.3. Vdvc always exceeds 0.6cc because of the rise in density of the gas in the discharge plenum during the discharge stroke. The ratio Vdvc/V2 thus indicates the further capacity loss caused by the excess pressure at the end of the discharge stroke.

For the intake stroke, Vsvc is virtually pre-determined due to the deduction of the refrigerant flow rate from the condenser power measurement. Consequently it is V4, the actual cylinder volume at closure of the suction valve, which is dependent on the modelling of the suction system. This volume is obtained by running the suction stroke algorithm through bdc until the cylinder charge has fallen to m4. At this stage in the calculation, m4 has already been found from the known displacement per stroke, re-expansion charge, and leakage loss. The capacity loss caused by the fall in pressure in the inner plenum can be noted as the shortfall of Vsvc from V4. Surprisingly, some of the results indicate V4 *lower* than Vsvc. In this calculation, this is a consequence of the inner plenum's gas density exceeding the reference density at the time the suction valve is made to close. This calculated gas ramming is a result of the inductive treatment of the short bores. The results of the suction by-pass experiment suggest that this gas-ramming may be undercalculated by the model, and that the real system is much more inductive than the model.

Indicator diagram breakdown

The fate of the compressor's electrical power consumption is summarised below.

- Electrical input
  - Electrical losses
    - Stator Joule heating
    - Rotor, and other losses
  - Shaftwork
    - Mechanical losses
    - Indicated work
      - Gas flow losses
      - Theoretical minimum work.

As mentioned above, the electrical losses and shaftwork are obtained from an empirical motor model. It thus only remains to explain the exact significance of the quoted contributions to the total indicated work.

Figure 10.2 shows an indicator diagram, carved up to present its total area as the sum of 6 components, each of which has a distinct physical significance, explained below;-

Region i

This is the theoretical minimum required work. As explained in section 9.3, the associated power requirement is given rigorously by

$$\text{Minimum work of compression} = \dot{m}(h_{dvo} - h_{svc})$$

It may be conceptually helpful to think of this as the power requirement of a 'perfect' compressor producing the same flow rate when working between the same pressures and compressing along the same isentrope.

The importance of including this in the output cannot be overstated. Without this evaluation of the thermodynamic lower limit to the power requirement, the calculation of the losses would not be put into perspective.

Region ii

This is the nominal value of the work lost due to leakage past the piston on the discharge stroke. The associated power loss is given by

$$\text{Nominal discharge leakage} = f m_{leak}(h_{dvo} - h_{svc}) \qquad 10.1$$

where m_{leak} is the mass of gas that escapes.

Region iii

This is the work lost due to leakage past the piston on the compression stroke. It is numerically integrated in the procedure 'Leaks'.

Region iv

This is the work lost due to leakage on the re-expansion stroke, and is also numerically integrated by 'Leaks'.

Region v

This is the work expended due to the cylinder pressure reduction during the suction stroke. It is numerically integrated by the suction stroke calculation. It includes the loss due to the pressure drop through the valve, and due to the pressure reduction in the plenum system.

Region vi

This is the work expended during the discharge stroke due to the excess cylinder pressure. It is integrated numerically by the discharge stroke calculation, and includes the effects of the pressure drop through the valve, and of the overpressure in the discharge plenum. This excess work is included in the calculation of the discharge gas enthalpy change between its first reaching the discharge pressure, and its arrival at the condenser. However, some of this excess work has been done on the gas that leaks past the piston, and not on the discharge gas. Thus in order to avoid committing an internal inconsistency this loss is shared between the discharge gas and the leakage. This is the reason for the dotted line dividing region vi into two subregions. On the print of the calculation's results, the larger region, used in the discharge gas enthalpy change calculation, is identified as 'Discharge excess PdV', while the small region, associated with the leakage past the piston, has been added to the other three losses associated with leakage past the piston.

R12 enthalpy gain summary

The "Total suction gas preheat" is just the product of flow rate x the enthalpy increment (hsvc-hsuc). As mentioned in chapter 4, the basic principle of using the measured discharge gas state to obtain the cylinder gas enthalpy has by-passed the main uncertainties associated with any attempt to model the contributions to the suction gas preheat. The only calculational uncertainties in this figure are those associated with the discharge system heat transfer model.

The "Discharge - suction" exchange is the total of the two free convection terms introduced in equation 9.5, terms b & c. The "Inner pipe, loss to the can" is the sum of terms d & e. The "Outer pipe, loss to the can" is term f, and the "Outer pipe, loss to ambient" is term g. As mentioned in section 9.4 thesum of these last 2 terms is used to find the discharge gas enthalpy from the condenser start enthalpy.

10.2 Results of the interpretive model, and tests of consistency

As explained in chapter 8, the final set of experiments was designed to address 3 questions.

i) What is the effect of turning up the superheat?

ii) What is the effect of minimising the oil distribution system in the compressor?

iii) What penalties are caused by the suction plenum system?

For all the tests, the compressor's capacity can be systematically collated by plotting Vsvc against the reference density ratio.

An important advantage of plotting Vsvc is that the resulting conclusions are independent of the suction system model, since, as mentioned above, it is only V4 which is model dependent.

Figure 10.3 shows every test plotted in this way. One can see that there is a trend for Vsvc to fall with increasing density ratio, and that there is a large scatter about this trend. It will be shown that this scatter is not due to random errors, but is instead due to the fact that Vsvc is not a function of density ratio alone, and that there is also a non-monotonic component superposed on the trend.

Figure 10.4 shows the tests at 150 psi discharge pressure plotted in the same way. Suction pressures of 6, 20, 40 & 64 were tested for the unmodified compressor, minimised oil distribution, and with the suction system by-passed. This plot compares these three compressor configurations. One can see immediately that minimising the oil distribution has produced a small loss of capacity, compared to the unmodified compressor. This is a result which would be very difficult to pick out by inspection of the raw data, and would never be predicted by a conventional mathematical model. Thus the unorthodox modelling approach explained earlier is already justified.

A more dramatic difference is shown by the result of by-passing the suction system. Compared to the minimised oil distribution, which is the control for the suction by-pass test, by-passing the suction system gives a small advantage at 64psi, break even at 20psi, and a significant penalty at 6psi. In the original suction by-pass test, the interpretation of the result was uncertain, because a suction pressure lower than the break even point had not been obtained. With this observation of a definite capacity loss at 6psi, the effect of this modification is no longer in doubt. This result is also significant as experimental evidence of the need for the suction system model to be inductive.

If one looks up the tables on pages 402 & 408 one can see that for the intact suction system the model indicates a gas density enhancement of less than 1% (Vsvc/V4 = 9.532/9.469 = 1.007). For the by-passed suction system V4 is 9.138 cc. If V4 is, in reality, also 9.138 cc with the suction system retained, then this would imply that gas ramming is contributing an enhancement of 4%. This thus implies that the suction model used here is not inductive enough. However, one cannot rule out the possibility that the improvement furnished by the suction system results from a better timed valve closure, since it may be

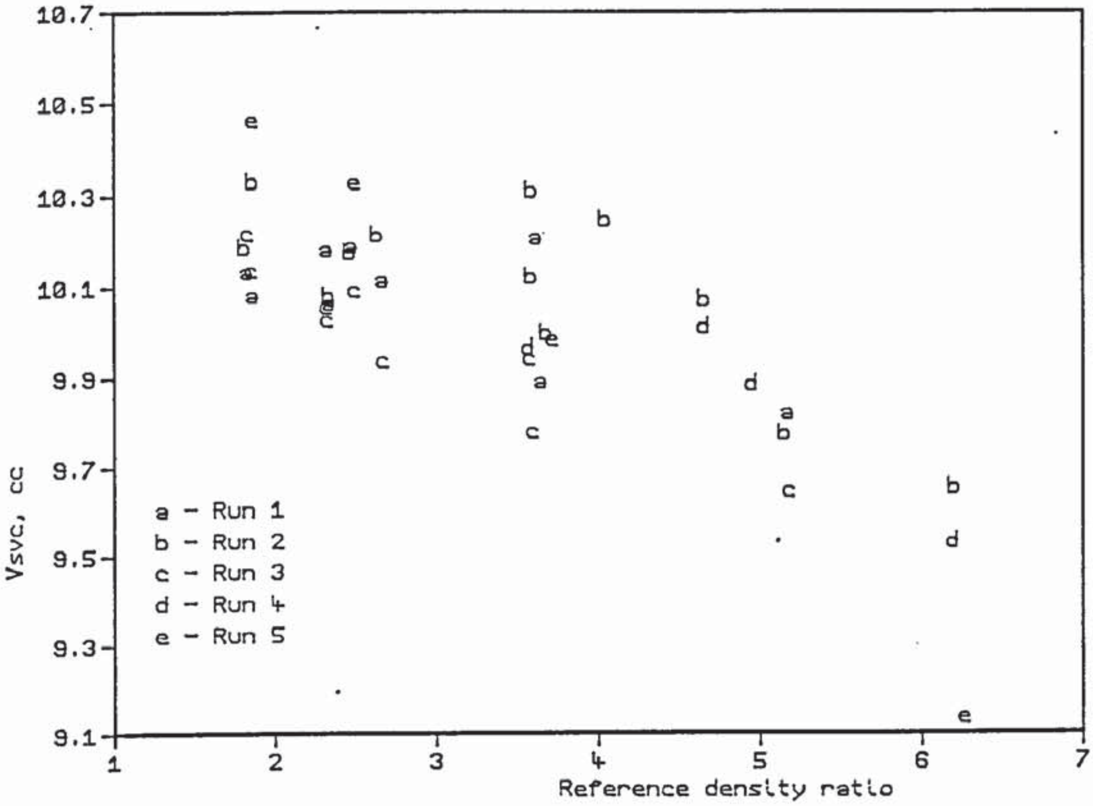

Figure 10.3 Compressor capacity v density ratio

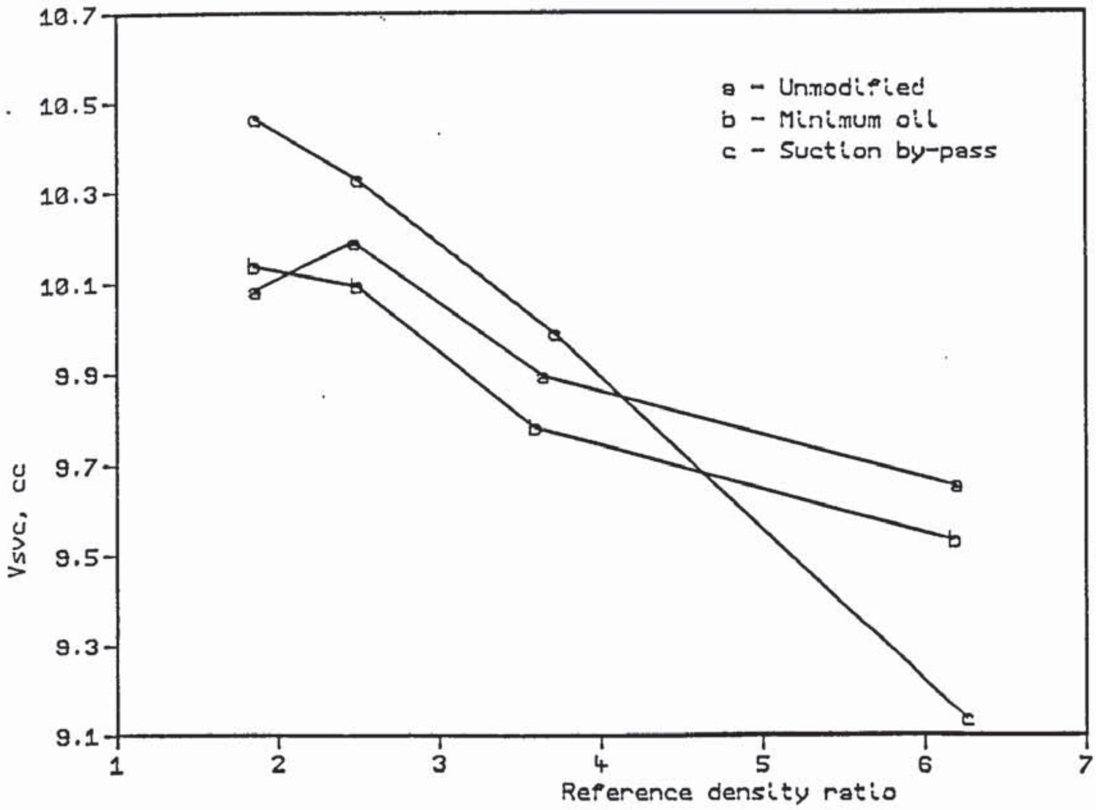

Figure 10.4 Compressor capacities for tests at 150psi discharge

the suction system, appendix 3, and (72).

It is possible to use this experiment to gauge the reliability of the calculation for the excess suction PdV work. For the suction system by-passed, the calculation of the mechanical losses is more reliable, because there is no modelling uncertainty introduced by the need to calculate the power loss associated with the gas flow through the suction system. The relevant figures are summarised in table 10.1, below.

Evaporating pressure	6psig	20psig	40psig	64psig
Status quo				
Minimum work	84.07	136.57	159.79	153.50
Suction excess PdV	3.34	6.76	10.37	14.42
Mechanical loss	34.72	40.94	40.02	26.42
By-passed plenums				
Minimum work	77.33	139.55	166.17	160.69
Suction excess PdV	1.85	2.85	3.91	4.97
Mechanical loss	32.98	40.16	35.89	25.31

Table 10.1

The figures for the lower limit to the power requirement have been quoted in order to put the losses into perspective. One can see that there is a consistency in the dependence of the implied mechanical loss on the operating conditions, in that both tests show a maximum of 40 Watts mechanical loss at 20 psi.

Consider the two tests at 6psi. With the suction system by-passed the mechanical loss is 33 Watts. With the suction system intact, the implied mechanical loss is 34.7 Watts, or, alternatively perhaps the suction model has undercalculated the suction stroke PdV loss by 1.7 Watts. Of course, this is too small a difference to attach much quantitative confidence to it, but it is additional evidence, however weak, to support the suspicion that the suction model is not however weak, to support the suspicion that the suction model is not inductive enough, since a bigger gas ram would also cause a bigger PdV loss.

In addition to collating all the tests at 150 psi discharge, it is also useful to examine all the results at 220psi discharge. This is shown on figure 10.5 Runs 1, 2 & 3 are shown here. By comparing run 3 with run 1, one can again see that the capacity is slightly reduced by eliminating all the non-essential oil sprays.

These three plots are showing another significant feature also shown by figure 10.4. Imagine fitting the best straight line to the result for each run. If a single run was considered in isolation, one might think that the straight line was "correct", and that the deviations from it were due to experimental error. However, the three runs shown here show that the pattern of deviation from the best straight line is reproduced from one run to the next, and this same property is also exhibited on figure 10.4 for the 2 tests of the unmodified suction system. Only for the by-passed suction system is the pattern altered. Co-incidentally, for the by-passed suction system, a straight line would fit the points quite well.

Experimentally, then, the implication is that there is a monotonic trend of capacity loss with increasing density ratio, perhaps due to late valve closure. The principle purpose of the suction system is to improve the capacity at low suction pressures, and because of gas oscillations in the suction system, there is a small non-monotonic dependence superposed on the trend. This point is also supported by MacLaren (73), who has observed that the inclusion of an explicit suction plenum model in a valve dynamic calculation results in a significantly reduced impact speed on the end stop. It is possible that, for the 6psi/150psi combination, it is this difference in behaviour which accounts for the 10% better capacity with the suction system retained.

The other experimental observation, of a 2% capacity loss caused by minimising all the non vital oil sprays, may be taken as tentative evidence for leakage past the valves other than that caused by late valve closure, the interpretation being that some oil entrainment is

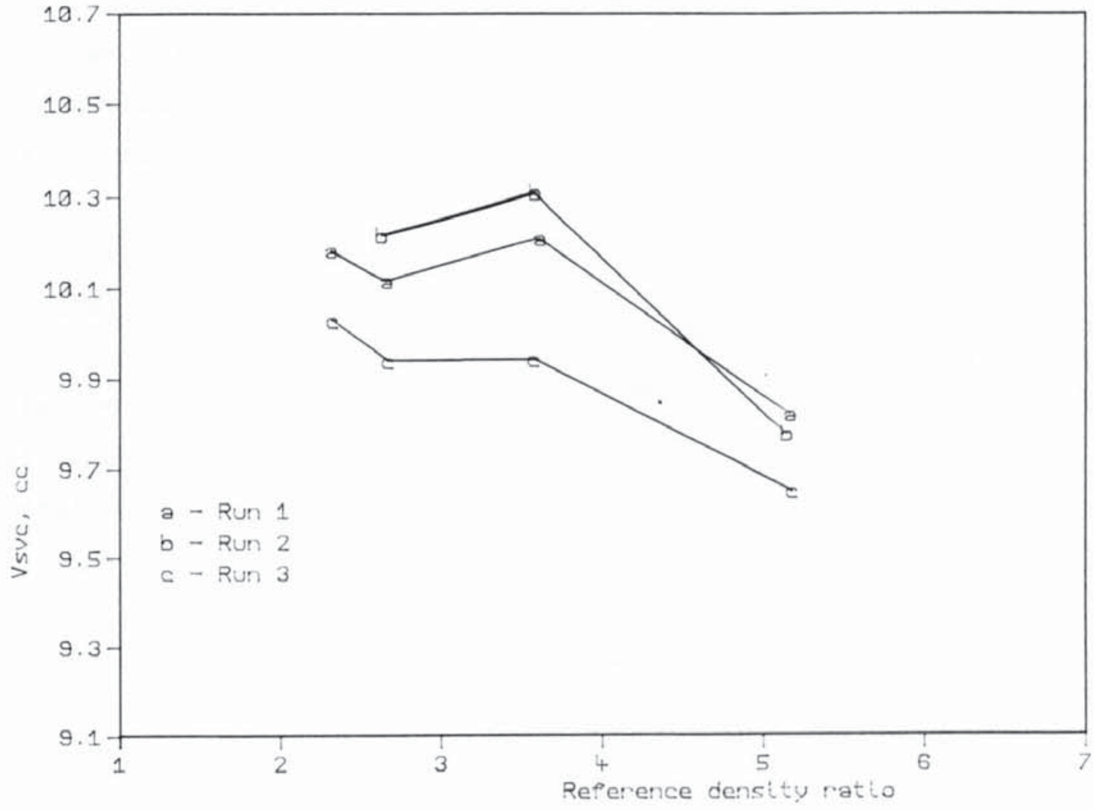

Figure 10.5 Compressor capacities for tests at 220psi discharge

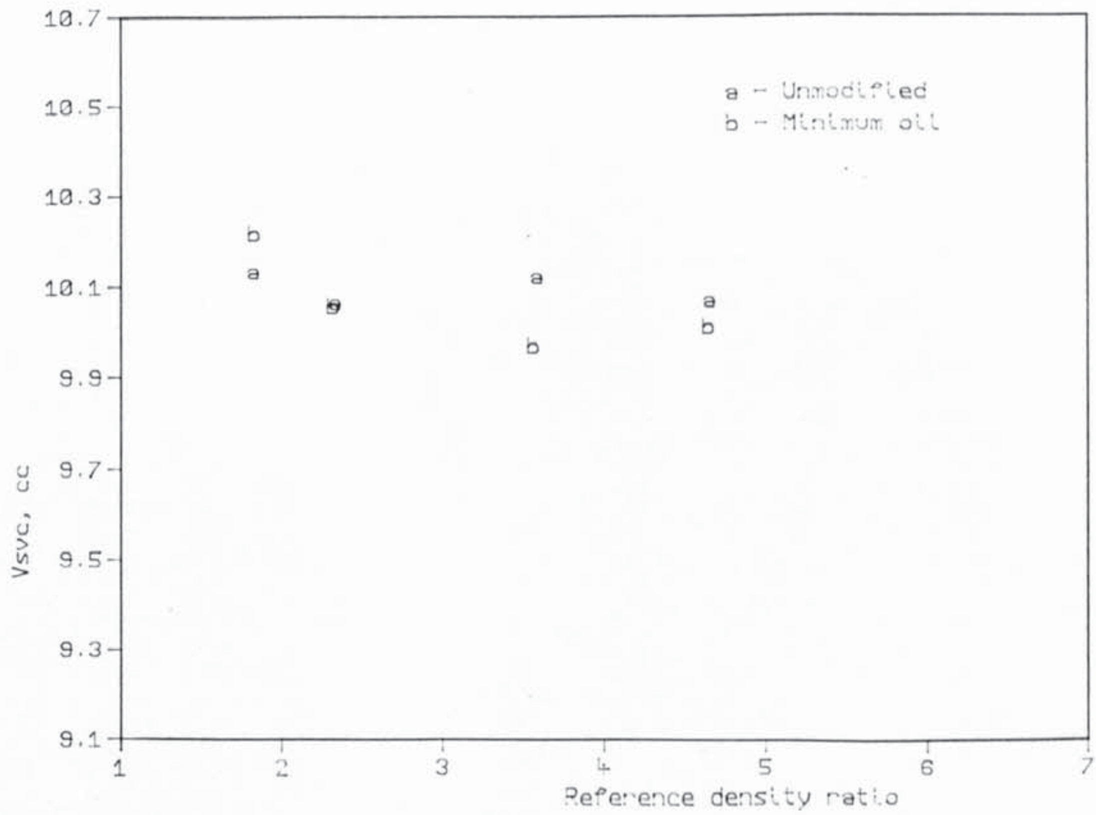

Figure 10.6 Compressor capacities. No mods v minimum oil

needed to seal the valves. Having demonstrated this for the discharge pressures of 150 psi & 220 psi, figure 10.6 shows the appropriate comparison for the other operating conditions tested. Altogether, only 2 counter examples have occurred, seen on figures 10.6 & 10.4. It may be significant that these counter examples have occurred only at the lowest density ratio.

The role of the model in interpreting the measurements and ultimately leading to the above picture cannot be overstated. It would be virtually impossible to get this far by inspection of the raw data, while the use of a purely predictive model would, at best, only lead to that cliched, sterile conclusion "The result of the model is not inconsistent with the measurements"

10.3 Using the compressor's heat loss as a diagnostic

Superficially, heat loss from the compressor might be considered a trivial consequence of its high temperature. By deducing this heat loss using the measurements, instead of making a crude attempt to model it, several interesting results have been found.

Figure 10.7 shows heat loss plotted against the compressor - room temperature difference. One can see that there is a monotonic trend with some scatter. The points from the 5 different runs are plotted as a, b, c, d, e respectively. The solid straight line marks the lower bound to all but 1 of the points from run 1, while simultaneously constituting the upper limit to the points from all the other runs, there being only 1 such point above the line. In other words, for the unmodified compressor, used with the normal superheat setting, the heat loss is consistently higher than for all the other runs. Since run 2 had the superheat set high, the oil returning from the evaporator is more effectively outgassed. Runs 3, 4 & 5 had the non-essential oil sprays eliminated, which appears to reduce oil entrainment into the suction stub. Consequently, the most likely interpretation consistent with the observed higher heat loss on run 1 is that liquid R12 returning to the sump was contributing a further cooling of order 10 Watts.

One of the problems in attempting to model this phenomenon is the need to assume thermodynamic equilibrium between the liquid and vapour phases in order to obtain the liquid composition from the superheat. This is a problem, because a supersaturated solution of R12 in oil can be very slow to equilibrate, so that an equilibrium model of the liquid return rate may underestimate the R12 fraction.

The oil circulation fraction was measured on three of the tests of run 1 which show a large excess compressor heat loss. From the excess of the heat loss over the boundary shown in figure 10.7, a lower estimate for the liquid R12 return rate can be deduced, using the known latent heat. By finding the oil circulation rate from the measured circulation fraction and known R12 flow rate, it is then possible to deduce a lower estimate for the molar R12 fraction in the liquid phase returning to the sump. Finally, the molar R12 fraction

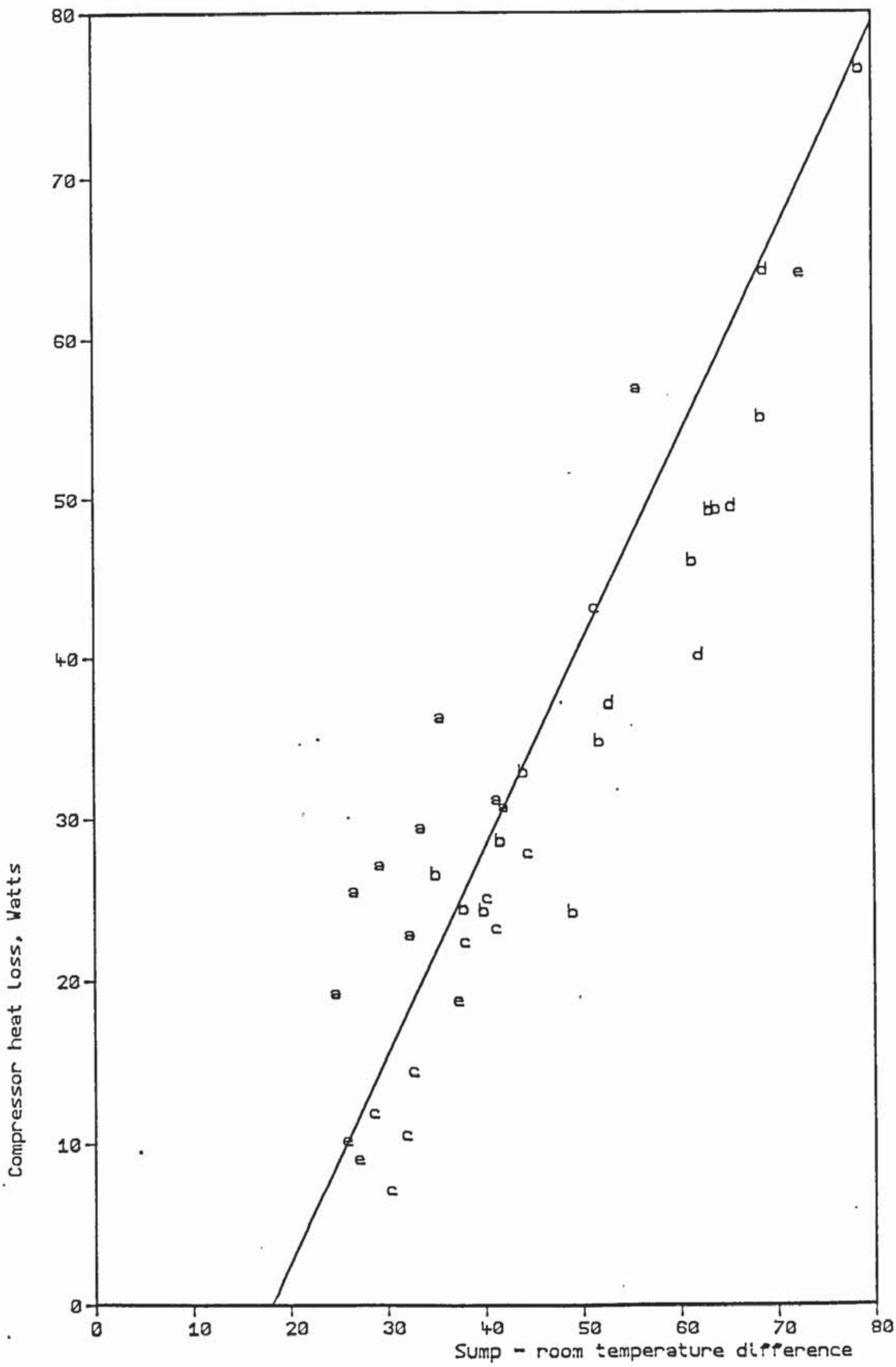

Figure 10.7 Compressor heat loss plot

expected from Raoult's law is found, and compared with the previous estimate.

Table 10.2 indicates these calculational steps. One can see that this data shows no evidence to support supersaturation of the returning liquid phase. However, it has to be pointed out that these estimates have been conservative, since the R12 liquid return rate has been calculated by finding the excess heat loss over the upper limit of all the other tests, and the equilibrium R12 fraction has been based on the refrigerant temperature at the evaporator exit, rather than the temperarature measured at the suction stub, so producing an upper estimate of the equilibrium R12 fraction.

If the estimated latent heat cooling were based instead on the lower envelope to the distribution on figure 10.7, then the implied R12 fraction in the liquid phase would indicate a significant supersaturation. While this question has a peripheral relevance to the performance of Danfoss' SC10H, there are other systems, especially those based on rotary sliding vane compressor's, whose performance is sensitive to the equilibration rate of an oil - refrigerant mixture.

Oil circulation fraction	0.005	0.018	0.019
refrigerant flow rate, g/s	5.265	3.719	13.15
oil circulation rate, g/s	0.026	0.067	0.25
Sump - room T difference, K	32.5	55.7	35.4
Bounding heat loss, Watts	16.9	47.0	21.0
Compressor heat loss	22.8	57.0	36.4
Latent heat cooling	5.9	10.0	16.4
Latent heat, J/g	152	152	138
R12 liquid return rate, g/s	0.039	0.066	0.118
Implied R12 molar fraction	0.80	0.73	0.56
Suction pressure, Bar	2.634	2.678	6.53
Vapour pressure at Tsuc	3.14	3.11	8.00
Equilibrium R12 fraction	0.84	0.86	0.81

Table 10.2

10.4 Further effects of minimising the oil distribution

Measurements of the oil circulation rate

Because of the practical difficulties attendant upon removing a liquid sample from the condenser's access point, only a few oil circulation measurements were made, the results of which are summarised below;-

Run number	Discharge P	Suction P	Oil circulation fraction
	150psi	22psi	0.020
1	89psi	21psi	0.005
	220psi	22psi	0.018
	220psi	78psi	0.019
	90psi	21psi	0.000
3	150psi	22psi	0.001
	220psi	78psi	0.000
4	108psi	5psi	0.010
	79psi	0psi	0.013

Table 10.3

These measurements indicate that eliminating all the non-essential oil sprays results in a reduced oil circulation rate. This suggests that for the unmodified compressor (run 1), entrainment of oil at the suction stub makes the main contribution to the oil circulation.

In addition to the reduced latent heat cooling of the compressor, discussed earlier, there is a further difference produced by this modification, which supports the directly measured change in the oil circulation rate.

Raoult law evaporating pressure loss

The non-essential oil flows within the compressor can be shown to have a deleterious effect on the cycle thermodynamics. At a low refrigerant flow rate it is possible for the boiling liquid in the evaporator to have an oil concentration very much higher than the flow rate ratio, as measured near the end of the condenser. The oil, being involatile, tends to accumulate in the evaporator, unless the refrigerant flow rate is high enough to keep the evaporator flushed out.

Consequently, the vapour pressure of this mixture is lower than would be anticipated on the basis of the vapour pressure of pure R12 at the measured evaporator entry temperature. Table 10.4 presents this 'Raoult Law Loss' for all the steady state conditions recorded. These figures result from subtracting the measured evaporating pressure from the vapour pressure of pure R12 at the measured evaporator entry temperature. The result is expressed in both KPa, and as a percentage of the evaporating pressure. For Raoult's Law, this percentage equals the molar fraction of oil in the mixture. As anticipated, the trend with increasing evaporating pressure (and hence increasing flow rate) is for this percentage to fall. The effect of the modification is most noticable at an evaporating pressure of 20psig, for which this Raoult Law loss has been halved. This is consistent with the direct measurements of the oil circulation fraction, and further supports the interpretation that entrainment makes a significant contribution to the oil circulation produced by the unmodified compressor.

The test at an evaporating pressure of 0psig was performed last in the fourth run. In preparation for the fifth run the compressor had to be removed. Before doing so, the charge in the system was pumped into the liquid accumulator, and valved off. After removing the compressor, it was realised that by opening the valve immediately downstream of the accumulator, the evaporator would be flushed out by the freon. Upon doing so, a deluge of oil came blasting out of the open end of the suction pipe, overwhelming the receptacle placed there for its capture. It is estimated that a volume of order 50cc was involved, which supports the above interpretation of the evaporating temperature and pressure measurements.

This Raoult law pressure loss shows that it was a mistake to have the evaporator mounted below the compressor. The lesson is that one has to design the layout to avoid depending on gas flow to carry the oil back.

Heat exchange with the motor

Table 10.5 collates the measured oil temperature and estimated motor winding temperature. Consider first evaporating pressures of 40psig and above. Inspection of table 10.5 shows that elimination of the non-essential oil flows has resulted in the temperatures of both the motor and the oil being higher than for the unmodified compressor. Recalling the result of section 10.3, this is consistent with the interpretation that, for the unmodified compressor at the normal superheat, liquid return to the sump contributes to its cooling. In this regime of high suction pressure, the lower oil temperature is undesirable, as it raises the equilibrium freon fraction. Since the winding temperature is consistently moderate, one would conclude that for this range of suction pressure, the non-essential oil flows produce no advantage.

For the tests at 6psig, it is observed that elimination of the non-essential oil flows consistently results in a lower oil temperature, by about 10C. In this regime of high temperature, and low pressure, the condition of the lubricant is better at the lower temperature. While there is consistent evidence at the higher evaporating pressures of the motor temperature being raised by the modification, at this low evaporating pressure, the effect is less marked. This is consistent with free running tests performed in air which showed a lower oil temperature, but no change in motor temperature, upon eliminating the oil spray from the top of the rotor. These observations are suggestive that the principle mechanism of cooling by the oil spray onto the stator winding is evaporation of the refrigerant dissolved in the oil, the cooling being least effective for conditions that would make the freon fraction in the lubricant very low.

Thus, since this method of motor cooling is effective only at moderate temperatures, when cooling is unnecessary, and ineffective at a high motor temperature, while the effect on the oil's condition is always deleterious, the conclusion may be drawn that for steady state operation of the compressor the non-essential oil flows are justified solely by the capacity improvement.

The possibility remains that the purpose of this design has been to speed the outgassing of the oil upon starting the compressor from cold. If this has been a significant consideration to the designer, then it may account for the endemic use by hermetic compressor manufacturers of very disappointing motors, because a more efficient motor makes less heat available to outgass the oil. An additional point relevant to Danfoss' motors is that by designing the rotors with oil ducts throgh the core, the magnetic field is constricted to a smaller available cross section of metal. This aggravates both the rotor's loss, and the stator's loss, due to the increased necessary stator current.

Effect on mechanical losses

The question of whether eliminating the non-essential oil flows produces a reduction in compressor power requirement can now be checked. Earlier tests had been suggestive that at a high suction pressure there is no difference, but at a low suction pressure there is a saving of a few Watts upon eliminating the non-essential oil flows. Table 10.6 presents the figures for the mechanical loss, and also indicates whether there is evidence for a loss other than viscous drag at the bearings. The most important point to note is that the mechanical loss ranges from 20 Watts to 50 Watts. This is in good agreement with the range observed for the free running tests, and so indirectly supports the validity of these deduced values for the bearing losses. One can see by inspection that comparison of the modified v unmodified compressor shows there to be no consistent difference at suction pressures of 40psig and above, while there is a reduction of about 10 watts for the modified compressor at 20psig and below.

For the lubricant in the sump, in equilibrium with a given pressure of R12, the viscosity passes through a maximum with increasing temperature. With increasing R12 pressure, the maximum in the viscosity moves to a higher temperature, so that the highest possible value of viscosity decreases monotonically with pressure. On taking account of this, one sees that the above results are consistent with there being a critical viscosity below which the oil is able to drain out of the gap, so causing no viscous drag there. While this suggestion fits all the observations, no claim is intended for its having been proven.

Table 10.6 also indicates tentative evidence for the failure of hydrodynamic lubrication, because at the most extreme operating conditions (6psi/150psi & 21psi/220psi), these tests on runs 3, 4 & 5 showed evidence of mechanical losses exceeding the highest credible viscous drag at the bearings. Since the last runs are thought to ensure an empty rotor-stator gap, the likelihood arises that full hydrodynamic lubrication did not occur on these particular tests.

Collating the Raoult law evaporating pressure loss

Discharge pressure	Run number	Evaporating pressure 0psig	6psig	21psig	40psig	64psig	78psig
78psi	2		0.192 13.4%	- - - - Pressure shortfall, Bar - - - - Percent of suction pressure			
	4	0.179 17.8%	0.164 11.5%				
90psi	1			0.279 10.6%			
	2		0.197 13.9%	0.281 10.7%			
	3			0.125 4.7%			
108psi	1				0.187 4.7%		
	2		0.181 12.6%		0.143 3.5%		
	3				0.135 3.4%		
	4		0.156 10.8%				
150psi	1			0.260 9.8%	0.127 3.1%	0.297 5.3%	
	2		0.169 11.7%	0.264 10.1%	0.113 2.8%	0.241 4.3%	
	3			0.118 4.4%	0.120 3.0%	0.003 0.1%	
	4		0.158 10.9%				
	5		0.157 10.9%	0.161 6.2%	0.146 3.6%	0.116 2.1%	
220psi	1			0.273 10.2%	0.210 5.3%	0.163 2.9%	0.061 0.9%
	2			0.208 7.8%	0.187 4.7%	0.139 2.5%	
	3			0.123 4.6%	0.111 2.7%	0.094 1.7%	0.009 0.1%

Table 10.4

Collation of sump temperatures & winding temperature estimates

Discharge pressure	Run number	Evaporating pressure 0psig	6psig	21psig	40psig	64psig	78psig
78psi	2		82.9 - - - - oil temperature 95.5 - - - - winding temperature				
	4	87.3 122.5	73.3 95.5				
90psi	1			53.8 46.0			
	2		85.5 95.5	63.2 59.5			
	3			50.6 55.0			
108psi	1				46.0 37.0		
	2		90.4 104.0		57.8 55.0		
	3				48.6 41.5		
	4		83.6 113.0				
150psi	1			64.9 59.5	50.8 46.0	51.0 41.5	
	2		100.7 127.0	73.9 82.0	64.1 64.0	61.6 55.0	
	3			61.0 73.0	54.0 50.5	53.9 46.0	
	4		90.2 127.0				
	5		94.2 136.0	58.3 73.0	47.0 55.0	48.4 46.0	
220psi	1			78.3 82.0	63.7 64.0	57.5 46.0	58.0 50.5
	2			87.7 100.0	74.0 82.0	68.0 68.5	
	3			73.7 95.5	65.0 73.0	60.9 59.5	61.7 59.5

Table 10.5

Collating the mechanical loss

Discharge pressure	Run number	Evaporating pressure 0psig	6psig	21psig	40psig	64psig	78psig
78psi	2		41.3 - - - - Loss, in Watts ****				
	4	20.5	31.6				
90psi	1			51.7			
	2		40.4 ****	47.4 ****			
	3			40.2			
108psi	1				39.4		
	2		41.3 ****		41.4		
	3				40.1		
	4		29.6 ****				
150psi	1			44.2 ****	36.6	25.7	
	2		43.9 ****	37.9 ****	37.4	29.0	
	3			40.9	40.0	26.4	
	4		34.7 ****				
	5		33.0 ****	40.2	35.9	25.3	
220psi	1			48.6 ****	34.5	28.2	33.6
	2			36.8 ****	26.9	34.1	
	3			38.8 ****	45.1 ****	36.8	36.9

Table 10.6

**** - Evidence exists for a loss other than viscous drag at the bearings.

Specifications used with the interpretive model

Suction system
~~~~~~~~~~~~~~

Outer plenum volume	=	70.000 cc
Inner plenum volume	=	55.000 cc
c.s.a. of bores	=	36.000 mm^2
c.s.a. of outer stub	=	29.000 mm^2
Stub's length parameter	=	1.400 mm
Bore's length parameter	=	1.800 mm
Suction port area	=	1.700 cm^2
Valve spring constant	=	450.000 N/m
Mass of suction valve	=	1.100 g
Perimeter of suction ports	=	6.000 cm
Maximum valve lift	=	0.900 mm

Discharge stroke model. The following specifications are assumed.
~~~~~~

Discharge plenum volume	=	29.000 cc
Internal discharge pipe c.s.a.	=	20.000 mm^2
Discharge port area	=	0.800 cm^2
Valve + backing spring stiffness	=	560.000 N/m
Pre-load on valve	=	0.500 N
Mass of valve + backing spring	=	0.900 g
Perimeter of discharge port	=	4.000 cm
Discharge valve tip lift	=	0.900 mm
U value for condenser	=	0.100 W/mK
U value for discharge pipe ins'n	=	0.200 W/K
Compressor to condenser conductance		0.120 W/K

Compressor model. The following specifications are assumed.
~~~~~~

Con-rod length	=	5.000 cm
Amplitude, i.e. half-stroke	=	6.350 mm
Offset of bore from crank axis	=	2.500 mm
Total volume	=	10.700 cc
Clearance volume	=	0.500 cc
Piston - bore clearance	=	10.000 um
Piston depth	=	2.000 cm
Piston circumference	=	10.000 cm
Time step for integrations	=	10.000 us
Crank angle at top dead centre	=	177.457 degrees
Bottom dead centre crank angle	=	356.717 degrees
Bore cross sectional area	=	8.021 cm^2
~~~~~~

Unmodified compressor. Normal superheat

Nominal Evaporating P 22psig. Nominal Condensing P 150psia.

Raw data	
Current mA	2004.384
Voltage bits	2795.637
Room temperature	22.992
Cond. water out	51.243
Cond. water in	19.594
Evap. water in	5.966
Evap. water out	1.484
R12 Discharge	96.558
R12 Cond. entry	93.576
R12 Condensing	41.968
R12 Cond. exit	21.444
R12 Evap. entry	-1.750
R12 Evap. exit	0.141
R12 Suction	5.604
Sump oil Temp.	64.902
Evap. flow rate	26.553
Cond. flow rate	6.238
R12 flow meter	0.090
Comp. power	293.877
P at suction	1.766
P at cond. end	9.114
P at evap start	1.638
P at discharge	9.627
PT supply volts	10.000
Water pump power	56.000
Heater volts	96.125
Heater Amps	4.100
Room temperature	24.000
Manual cond mdot	6.171
Bourdon Pe, psig	21.000
Bourdon Pc, psia	150.000
Real time	0.001
Oil fraction	0.020
Suction P loss	0.260
Stator res'tance	9.300
Winding Temp	59.500

Motor performance

Estimated RPM	2914.896
Winding loss	37.363
Rotor Loss etc.	53.611
Shaftwork	202.902
Bearing losses	44.151
Implied viscos'y	11.038
Sump viscosity	9.295

Refrigerant states

Position	Temp	Press	Volume	Enthalpy
dvo state	102.107	10.640	21.748	412.508
Discharge	98.720	10.640	21.467	410.009
Cond. start	93.576	10.640	21.034	406.208
Cond. end	21.444	10.127	0.755	220.209
Evap. end	0.141	2.651	65.482	352.497
svc state	45.641	2.651	79.137	381.720

Condenser temperature distribution

R12 Ts	21.444	42.178	44.226	93.576
Water Ts	19.594	23.090	44.838	51.243

Discharge stub temperature 84.551

Powers, Watts

	measured	Xtalk	loss	R12 Dh
Compressor	293.877	4.398	30.784	258.718
Condenser	817.502	4.398	23.620	836.724
Evaporator	450.112	498.159		595.105

Compressor performance

Vertex	phi	Volume	Vsvc etc	mass,mg
1	124.770	2.703		124.308
2	188.162	0.600	0.631	28.973
3	223.832	2.258		28.535
4	30.836	9.927	9.894	125.026

Leakage loss on discharge, mg	2.737
Reference density ratio	3.639
R12 mass flow rate g/s	4.499

Indicator diagram breakdown, Watts

Minimum work of compression	138.501
Suction excess PdV	6.702
Discharge excess PdV	8.011
Total leakage loss	5.538
Total indicated work	158.752

R12 Enthalpy gain summary, Watts

Total suction gas preheat	131.458
Calculated total PdV work	158.752
Discharge - suction exchange	12.826
Inner pipe, loss to the can	6.425
Outer pipe, loss to the can	3.399
Outer pipe, loss to ambient	13.701

The discharge valve was open for 3.625 ms.
The first rarefaction returns after 6.423 ms.

Unmodified compressor. Normal superheat

Nominal Evaporating P 21psig. Nominal Condensing P 89psia.

Raw data

Current mA	1955.322
Voltage bits	2806.325
Room temperature	21.624
Cond. water out	21.718
Cond. water in	16.862
Evap. water in	7.217
Evap. water out	1.907
R12 Discharge	74.062
R12 Cond. entry	72.242
R12 Condensing	20.761
R12 Cond. exit	17.204
R12 Evap. entry	-1.727
R12 Evap. exit	0.557
R12 Suction	4.494
Sump oil Temp.	53.836
Evap. flow rate	28.617
Cond. flow rate	47.485
R12 flow meter	0.091
Comp. power	260.802
P at suction	1.675
P at cond. end	4.809
P at evap start	1.621
P at discharge	5.564
PT supply volts	10.000
Water pump power	58.000
Heater volts	111.500
Heater Amps	4.840
Room temperature	21.000
Manual cond mdot	46.530
Bourdon Pe, psig	21.500
Bourdon Pc, psia	89.500
Real time	2336.080
Oil fraction	0.005
Suction P loss	0.279
Stator res'tance	9.000
Winding Temp	46.000

Motor performance

Estimated RPM	2926.765
Winding loss	34.410
Rotor Loss etc.	50.639
Shaftwork	175.754
Bearing losses	51.712
Implied viscos'y	12.928
Sump viscosity	13.773

Refrigerant states

Position	Temp	Press	Volume	Enthalpy
dvo state	75.350	6.577	33.499	397.287
Discharge	75.485	6.577	33.515	397.382
Cond. start	72.242	6.577	33.102	395.103
Cond. end	17.204	5.822	0.747	216.145
Evap. end	0.557	2.634	66.090	352.799
svc state	39.553	2.634	77.917	377.786

Condenser temperature distribution

R12 Ts	17.204	20.941	25.356	72.242
Water Ts	16.862	16.959	20.815	21.718

Discharge stub temperature 66.732

Powers, Watts

	measured	Xtalk	loss	R12 Dh
Compressor	260.802	3.260	22.821	234.733
Condenser	945.943	3.260	-0.457	942.226
Evaporator	597.660	636.067		719.492

Compressor performance

Vertex	phi	Volume	Vsvc etc	mass,mg
1	105.219	4.318		128.888
2	188.162	0.600	0.653	19.468
3	211.982	1.505		19.320
4	25.094	10.162	10.065	129.178

Leakage loss on discharge, mg		1.483
Reference density ratio		2.326
R12 mass flow rate	g/s	5.265

Indicator diagram breakdown, Watts

Minimum work of compression	102.675
Suction excess PdV	7.191
Discharge excess PdV	12.312
Total leakage loss	1.864
Total indicated work	124.042

R12 Enthalpy gain summary, Watts

Total suction gas preheat	131.558
Calculated total PdV work	124.042
Discharge - suction exchange	7.533
Inner pipe, loss to the can	4.279
Outer pipe, loss to the can	2.168
Outer pipe, loss to ambient	9.831

The discharge valve was open for 4.723 ms.
The first rarefaction returns after 6.521 ms.

Unmodified compressor. Normal superheat

Nominal Evaporating P 22psig. Nominal Condensing P 220psia.

Raw data

Current mA	2072.978
Voltage bits	2768.467
Room temperature	22.625
Cond. water out	75.305
Cond. water in	20.591
Evap. water in	4.743
Evap. water out	1.269
R12 Discharge	117.853
R12 Cond. entry	112.810
R12 Condensing	59.671
R12 Cond. exit	24.571
R12 Evap. entry	-1.338
R12 Evap. exit	0.203
R12 Suction	6.050
Sump oil Temp.	78.300
Evap. flow rate	27.497
Cond. flow rate	3.230
R12 flow meter	0.092
Comp. power	320.337
P at suction	1.893
P at cond. end	14.248
P at evap start	1.665
P at discharge	14.498
PT supply volts	10.000
Water pump power	58.000
Heater volts	83.200
Heater Amps	3.620
Room temperature	23.000
Manual cond mdot	2.950
Bourdon Pe, psig	22.000
Bourdon Pc, psia	220.000
Real time	159.540
Oil fraction	0.018
Suction P loss	0.273
Stator res'tance	9.800
Winding Temp	82.000

Motor performance

Estimated RPM	2906.136
Winding loss	42.113
Rotor Loss etc.	56.002
Shaftwork	222.222
Bearing losses	48.554
Implied viscos'y	12.139
Sump viscosity	6.191

Refrigerant states

Position	Temp	Press	Volume	Enthalpy
dvo state	127.293	15.511	15.586	427.202
Discharge	120.370	15.511	15.170	421.884
Cond. start	112.810	15.511	14.705	416.047
Cond. end	24.571	15.261	0.762	223.232
Evap. end	0.203	2.678	64.779	352.480
svc state	53.377	2.678	80.495	386.743

Condenser temperature distribution

R12 Ts	24.571	60.022	60.769	112.810
Water Ts	20.591	30.942	63.207	75.305

Discharge stub temperature 101.879

Powers, Watts

	measured	Xtalk	loss	R12 Dh
Compressor	320.337	5.312	56.952	258.096
Condenser	675.655	5.312	46.681	717.024
Evaporator	359.184	399.889		480.635

Compressor performance

Vertex	phi	Volume	Vsvc etc	mass,mg
1	136.518	1.881		120.702
2	188.162	0.600	0.619	39.663
3	235.149	3.118		38.738
4	33.193	9.819	9.822	122.016

Leakage loss on discharge, mg		4.264
Reference density ratio		5.165
R12 mass flow rate	g/s	3.719

Indicator diagram breakdown, Watts

Minimum work of compression	150.456
Suction excess PdV	5.983
Discharge excess PdV	5.419
Total leakage loss	11.809
Total indicated work	173.667

R12 Enthalpy gain summary, Watts

Total suction gas preheat	127.415
Calculated total PdV work	173.667
Discharge - suction exchange	17.646
Inner pipe, loss to the can	7.548
Outer pipe, loss to the can	4.241
Outer pipe, loss to ambient	17.467

The discharge valve was open for 2.962 ms.
The first rarefaction returns after 6.329 ms.

Unmodified compressor. Normal superheat

Nominal Evaporating P 78psig. Nominal Condensing P 220psia.

Raw data

Current mA	2413.197
Voltage bits	2773.638
Room temperature	22.580
Cond. water out	64.349
Cond. water in	19.417
Evap. water in	50.035
Evap. water out	34.214
R12 Discharge	88.059
R12 Cond. entry	87.110
R12 Condensing	52.324
R12 Cond. exit	25.130
R12 Evap. entry	25.433
R12 Evap. exit	32.747
R12 Suction	33.001
Sump oil Temp.	57.967
Evap. flow rate	28.360
Cond. flow rate	11.717
R12 flow meter	11.559
Comp. power	431.151
P at suction	5.564
P at cond. end	11.495
P at evap start	5.516
P at discharge	14.439
PT supply volts	10.000
Water pump power	58.000
Heater volts	212.875
Heater Amps	9.047
Room temperature	22.000
Manual cond mdot	11.837
Bourdon Pe, psig	79.250
Bourdon Pc, psia	220.000
Real time	407.370
Oil fraction	0.019
Suction P loss	0.061
Stator res'tance	9.100
Winding Temp	50.500

Motor performance

Estimated RPM	2863.150
Winding loss	52.994
Rotor Loss etc.	66.763
Shaftwork	311.394
Bearing losses	33.606
Implied viscos'y	8.401
Sump viscosity	11.811

Refrigerant states

Position	Temp	Press	Volume	Enthalpy
dvo state	88.452	15.452	13.161	396.930
Discharge	88.576	15.452	13.169	397.030
Cond. start	87.110	15.452	13.066	395.848
Cond. end	25.130	12.508	0.763	223.775
Evap. end	32.747	6.529	27.958	367.245
svc state	50.044	6.529	30.420	379.543

Condenser temperature distribution

R12 Ts	25.130	51.122	60.596	87.110
Water Ts	19.417	26.282	58.478	64.349

Discharge stub temperature 80.384

Powers, Watts

	measured	Xtalk	loss	R12 Dh
Compressor	431.151	3.297	36.351	391.554
Condenser	2226.456	3.297	38.959	2262.117
Evaporator	1983.987	1878.146		1886.094

Compressor performance

Vertex	phi	Volume	Vsvc etc	mass,mg
1	104.474	4.383		333.032
2	188.162	0.600	0.654	49.508
3	211.556	1.482		48.705
4	20.310	10.327	10.181	334.681

Leakage loss on discharge, mg		8.035
Reference density ratio		2.311
R12 mass flow rate	g/s	13.146

Indicator diagram breakdown, Watts

Minimum work of compression	228.575
Suction excess PdV	16.011
Discharge excess PdV	24.409
Total leakage loss	8.793
Total indicated work	277.788

R12 Enthalpy gain summary, Watts

Total suction gas preheat	161.672
Calculated total PdV work	277.788
Discharge - suction exchange	14.741
Inner pipe, loss to the can	8.361
Outer pipe, loss to the can	2.848
Outer pipe, loss to ambient	12.684

The discharge valve was open for 4.872 ms.
The first rarefaction returns after 7.029 ms.

Unmodified compressor. Normal superheat

Nominal Evaporating P 40psig. Nominal Condensing P 108psia.

Raw data

Current mA	1921.316
Voltage bits	2740.325
Room temperature	21.331
Cond. water out	24.393
Cond. water in	16.823
Evap. water in	26.794
Evap. water out	16.487
R12 Discharge	63.716
R12 Cond. entry	63.126
R12 Condensing	21.321
R12 Cond. exit	17.197
R12 Evap. entry	9.710
R12 Evap. exit	15.736
R12 Suction	16.379
Sump oil Temp.	45.978
Evap. flow rate	27.999
Cond. flow rate	47.736
R12 flow meter	6.541
Comp. power	269.570
P at suction	2.979
P at cond. end	4.746
P at evap start	2.994
P at discharge	6.582
PT supply volts	10.000
Water pump power	58.000
Heater volts	164.025
Heater Amps	7.085
Room temperature	22.000
Manual cond mdot	46.829
Bourdon Pe, psig	40.000
Bourdon Pc, psia	108.000
Real time	753.100
Oil fraction	-1.000
Suction P loss	0.187
Stator res'tance	8.800
Winding Temp	37.000

Motor performance

Estimated RPM	2922.588
Winding loss	32.485
Rotor Loss etc.	51.636
Shaftwork	185.450
Bearing losses	39.434
Implied viscos'y	9.858
Sump viscosity	18.934

Refrigerant states

Position	Temp	Press	Volume	Enthalpy
dvo state	63.124	7.595	27.162	387.435
Discharge	64.738	7.595	27.352	388.591
Cond. start	63.126	7.595	27.162	387.437
Cond. end	17.197	5.759	0.747	216.138
Evap. end	15.736	4.007	44.816	359.989
svc state	37.458	4.007	49.429	374.489

Condenser temperature distribution

R12 Ts	17.197	20.549	30.758	63.126
Water Ts	16.823	16.965	23.351	24.393

Discharge stub temperature 58.461

Powers, Watts

	measured	Xtalk	loss	R12 Dh
Compressor	269.570	2.747	19.229	247.692
Condenser	1483.937	2.747	2.256	1483.446
Evaporator	1220.117	1208.066		1245.753

Compressor performance

Vertex	phi	Volume	Vsvc etc	mass,mg
1	91.222	5.559		204.680
2	188.162	0.600	0.670	24.588
3	206.242	1.207		24.420
4	21.962	10.273	10.134	205.029

Leakage loss on discharge, mg		2.306
Reference density ratio		1.820
R12 mass flow rate	g/s	8.660

Indicator diagram breakdown, Watts

Minimum work of compression	112.117
Suction excess PdV	10.824
Discharge excess PdV	21.120
Total leakage loss	1.956
Total indicated work	146.016

R12 Enthalpy gain summary, Watts

Total suction gas preheat	125.562
Calculated total PdV work	146.016
Discharge - suction exchange	6.696
Inner pipe, loss to the can	4.410
Outer pipe, loss to the can	1.831
Outer pipe, loss to ambient	8.169

The discharge valve was open for 5.528 ms.
The first rarefaction returns after 6.787 ms.

Unmodified compressor. Normal superheat

Nominal Evaporating P 40psig. Nominal Condensing P 150psia.

Raw data

Current mA	2105.885
Voltage bits	2756.325
Room temperature	21.602
Cond. water out	45.629
Cond. water in	18.851
Evap. water in	25.134
Evap. water out	15.622
R12 Discharge	77.047
R12 Cond. entry	76.171
R12 Condensing	37.567
R12 Cond. exit	20.426
R12 Evap. entry	9.504
R12 Evap. exit	14.206
R12 Suction	14.903
Sump oil Temp.	50.786
Evap. flow rate	27.776
Cond. flow rate	12.546
R12 flow meter	5.807
Comp. power	326.561
P at suction	3.073
P at cond. end	7.893
P at evap start	3.027
P at discharge	9.521
PT supply volts	10.000
Water pump power	58.000
Heater volts	156.200
Heater Amps	6.730
Room temperature	22.000
Manual cond mdot	12.587
Bourdon Pe, psig	40.000
Bourdon Pc, psia	150.000
Real time	904.250
Oil fraction	-1.000
Suction P loss	0.127
Stator res'tance	9.000
Winding Temp	46.000

Motor performance

Estimated RPM	2902.687
Winding loss	39.913
Rotor Loss etc.	56.962
Shaftwork	229.686
Bearing losses	36.586
Implied viscos'y	9.146
Sump viscosity	15.519

Refrigerant states

Position	Temp	Press	Volume	Enthalpy
dvo state	78.536	10.534	19.957	395.150
Discharge	78.348	10.534	19.940	395.010
Cond. start	76.171	10.534	19.743	393.382
Cond. end	20.426	8.906	0.753	219.229
Evap. end	14.206	4.040	44.065	358.901
svc state	38.998	4.040	49.299	375.469

Condenser temperature distribution

R12 Ts	20.426	36.968	43.809	76.171
Water Ts	18.851	21.348	41.793	45.629

Discharge stub temperature 69.044

Powers, Watts

	measured	Xtalk	loss	R12 Dh
Compressor	326.561	3.167	27.130	296.269
Condenser	1410.842	3.167	21.204	1428.880
Evaporator	1109.226	1105.961		1145.973

Compressor performance

Vertex	phi	Volume	Vsvc etc	mass,mg
1	107.618	4.109		205.874
2	188.162	0.600	0.651	32.515
3	213.347	1.583		32.111
4	19.970	10.337	10.189	206.671

Leakage loss on discharge, mg		3.763
Reference density ratio		2.470
R12 mass flow rate	g/s	8.205

Indicator diagram breakdown, Watts

Minimum work of compression	161.482
Suction excess PdV	10.523
Discharge excess PdV	16.363
Total leakage loss	4.733
Total indicated work	193.101

R12 Enthalpy gain summary, Watts

Total suction gas preheat	135.937
Calculated total PdV work	193.101
Discharge - suction exchange	11.078
Inner pipe, loss to the can	6.435
Outer pipe, loss to the can	2.694
Outer pipe, loss to ambient	10.667

The discharge valve was open for 4.625 ms.
The first rarefaction returns after 6.786 ms.

Unmodified compressor. Normal superheat

Nominal Evaporating P 40psig. Nominal Condensing P 220psia.

Raw data

Current mA	2326.815
Voltage bits	2749.300
Room temperature	22.546
Cond. water out	70.343
Cond. water in	19.952
Evap. water in	22.473
Evap. water out	14.627
R12 Discharge	100.679
R12 Cond. entry	98.797
R12 Condensing	58.149
R12 Cond. exit	24.114
R12 Evap. entry	9.648
R12 Evap. exit	13.088
R12 Suction	14.536
Sump oil Temp.	63.737
Evap. flow rate	27.529
Cond. flow rate	5.891
R12 flow meter	2.610
Comp. power	382.249
P at suction	3.126
P at cond. end	13.557
P at evap start	2.962
P at discharge	14.348
PT supply volts	10.000
Water pump power	58.000
Heater volts	138.933
Heater Amps	6.000
Room temperature	23.000
Manual cond mdot	5.857
Bourdon Pe, psig	39.500
Bourdon Pc, psia	220.000
Real time	1050.550
Oil fraction	-1.000
Suction P loss	0.210
Stator res'tance	9.400
Winding Temp	64.000

Motor performance

Estimated RPM	2883.871
Winding loss	50.892
Rotor Loss etc.	62.071
Shaftwork	269.285
Bearing losses	34.507
Implied viscos'y	8.627
Sump viscosity	9.662

Refrigerant states

Position	Temp	Press	Volume	Enthalpy
dvo state	104.888	15.361	14.370	410.034
Discharge	102.198	15.361	14.194	407.932
Cond. start	98.797	15.361	13.969	405.262
Cond. end	24.114	14.570	0.761	222.789
Evap. end	13.088	3.975	44.622	358.278
svc state	47.133	3.975	51.834	380.996

Condenser temperature distribution

R12 Ts	24.114	57.906	60.322	98.797
Water Ts	19.952	29.504	61.516	70.343

Discharge stub temperature 88.616

Powers, Watts

	measured	Xtalk	loss	R12 Dh
Compressor	382.249	3.704	31.236	347.315
Condenser	1235.536	3.704	44.515	1276.347
Evaporator	891.600	904.148		947.705

Compressor performance

Vertex	phi	Volume	Vsvc etc	mass,mg
1	123.414	2.807		195.350
2	188.162	0.600	0.633	43.904
3	223.393	2.227		42.970
4	19.947	10.338	10.209	196.952

Leakage loss on discharge, mg		5.921
Reference density ratio		3.607
R12 mass flow rate	g/s	6.995

Indicator diagram breakdown, Watts

Minimum work of compression	203.112
Suction excess PdV	9.511
Discharge excess PdV	10.962
Total leakage loss	11.193
Total indicated work	234.778

R12 Enthalpy gain summary, Watts

Total suction gas preheat	158.911
Calculated total PdV work	234.778
Discharge - suction exchange	17.020
Inner pipe, loss to the can	8.651
Outer pipe, loss to the can	3.789
Outer pipe, loss to ambient	14.885

The discharge valve was open for 3.742 ms.
The first rarefaction returns after 6.681 ms.

Unmodified compressor. Normal superheat

Nominal Evaporating P 64psig. Nominal Condensing P 220psia.

Raw data

Current mA	2465.101
Voltage. bits	2791.367
Room temperature	24.085
Cond. water out	66.395
Cond. water in	18.964
Evap. water in	39.728
Evap. water out	27.010
R12 Discharge	89.725
R12 Cond. entry	88.751
R12 Condensing	55.161
R12 Cond. exit	23.778
R12 Evap. entry	20.605
R12 Evap. exit	25.191
R12 Suction	25.447
Sump oil Temp.	57.461
Evap. flow rate	28.314
Cond. flow rate	9.233
R12 flow meter	9.097
Comp. power	414.534
P at suction	4.688
P at cond. end	12.449
P at evap start	4.592
P at discharge	14.404
PT supply volts	10.000
Water pump power	58.000
Heater volts	186.000
Heater Amps	7.910
Room temperature	24.000
Manual cond mdot	9.381
Bourdon Pe, psig	64.000
Bourdon Pc, psia	220.000
Real time	1224.450
Oil fraction	-1.000
Suction P loss	0.163
Stator res'tance	9.000
Winding Temp	46.000

Motor performance

Estimated RPM	2871.392
Winding loss	54.690
Rotor Loss etc.	65.065
Shaftwork	294.779
Bearing losses	28.232
Implied viscos'y	7.058
Sump viscosity	12.029

Refrigerant states

Position	Temp	Press	Volume	Enthalpy
dvo state	91.201	15.417	13.391	399.178
Discharge	90.568	15.417	13.347	398.671
Cond. start	88.751	15.417	13.220	397.214
Cond. end	23.778	13.462	0.760	222.463
Evap. end	25.191	5.605	32.105	363.521
svc state	46.757	5.605	35.581	378.537

Condenser temperature distribution

R12 Ts	23.778	54.358	60.489	88.751
Water Ts	18.964	27.395	59.915	66.395

Discharge stub temperature 80.856

Powers, Watts

	measured	Xtalk	loss	R12 Dh
Compressor	414.534	3.160	29.463	381.981
Condenser	1862.560	3.160	39.660	1899.060
Evaporator	1529.260	1507.436		1532.910

Compressor performance

Vertex	phi	Volume	Vsvc etc	mass,mg
1	111.398	3.784		282.581
2	188.162	0.600	0.646	48.080
3	214.988	1.680		47.208
4	23.193	10.231	10.115	284.271

Leakage loss on discharge, mg		7.422
Reference density ratio		2.657
R12 mass flow rate	g/s	10.867

Indicator diagram breakdown, Watts

Minimum work of compression	224.308
Suction excess PdV	13.729
Discharge excess PdV	18.805
Total leakage loss	9.704
Total indicated work	266.546

R12 Enthalpy gain summary, Watts

Total suction gas preheat	163.181
Calculated total PdV work	266.546
Discharge - suction exchange	15.763
Inner pipe, loss to the can	8.550
Outer pipe, loss to the can	3.147
Outer pipe, loss to ambient	12.685

The discharge valve was open for 4.456 ms.
The first rarefaction returns after 6.963 ms.

Unmodified compressor. Normal superheat

Nominal Evaporating P 64psig. Nominal Condensing P 150psia.

Raw data

Current mA	2149.028
Voltage bits	2793.250
Room temperature	24.517
Cond. water out	41.149
Cond. water in	17.602
Evap. water in	44.597
Evap. water out	29.709
R12 Discharge	72.164
R12 Cond. entry	71.519
R12 Condensing	31.127
R12 Cond. exit	18.948
R12 Evap. entry	21.241
R12 Evap. exit	28.740
R12 Suction	28.947
Sump oil Temp.	51.040
Evap. flow rate	28.392
Cond. flow rate	21.022
R12 flow meter	10.430
Comp. power	321.592
P at suction	4.538
P at cond. end	6.384
P at evap start	4.562
P at discharge	9.621
PT supply volts	10.000
Water pump power	58.000
Heater volts	203.000
Heater Amps	8.600
Room temperature	25.000
Manual cond mdot	20.622
Bourdon Pe, psig	63.500
Bourdon Pc, psia	150.000
Real time	1331.500
Oil fraction	-1.000
Suction P loss	0.297
Stator res'tance	8.900
Winding Temp	41.500

Motor performance

Estimated RPM	2905.212
Winding loss	41.103
Rotor Loss etc.	56.259
Shaftwork	224.230
Bearing losses	25.713
Implied viscos'y	6.428
Sump viscosity	15.362

Refrigerant states

Position	Temp	Press	Volume	Enthalpy
dvo state	71.429	10.634	19.092	389.695
Discharge	72.781	10.634	19.217	390.714
Cond. start	71.519	10.634	19.101	389.764
Cond. end	18.948	7.397	0.750	217.812
Evap. end	28.740	5.575	32.902	366.061
svc state	44.109	5.575	35.381	376.747

Condenser temperature distribution

R12 Ts	18.948	29.749	44.201	71.519
Water Ts	17.602	19.037	38.246	41.149

Discharge stub temperature 66.553

Powers, Watts

	measured	Xtalk	loss	R12 Dh
Compressor	321.592	3.565	25.493	292.579
Condenser	2032.696	3.565	11.577	2040.709
Evaporator	1803.800	1769.389		1759.412

Compressor performance

Vertex	phi	Volume	Vsvc etc	mass,mg
1	92.700	5.428		284.283
2	188.162	0.600	0.668	34.866
3	206.556	1.222		34.543
4	23.946	10.204	10.082	284.961

Leakage loss on discharge, mg		4.316
Reference density ratio		1.853
R12 mass flow rate	g/s	11.868

Indicator diagram breakdown, Watts

Minimum work of compression	153.675
Suction excess PdV	14.508
Discharge excess PdV	26.716
Total leakage loss	3.619
Total indicated work	198.517

R12 Enthalpy gain summary, Watts

Total suction gas preheat	126.810
Calculated total PdV work	198.517
Discharge - suction exchange	8.922
Inner pipe, loss to the can	5.700
Outer pipe, loss to the can	2.057
Outer pipe, loss to ambient	9.226

The discharge valve was open for 5.476 ms.
The first rarefaction returns after 6.929 ms.

Unmodified compressor. High superheat

Nominal Evaporating P 21psig. Nominal Condensing P 90psia.

Raw data

Current mA	1936.881
Voltage bits	2810.643
Room temperature	21.600
Cond. water out	23.251
Cond. water in	16.103
Evap. water in	23.016
Evap. water out	12.503
R12 Discharge	84.383
R12 Cond. entry	81.755
R12 Condensing	20.984
R12 Cond. exit	16.677
R12 Evap. entry	-1.864
R12 Evap. exit	12.666
R12 Suction	17.544
Sump oil Temp.	63.153
Evap. flow rate	15.704
Cond. flow rate	32.363
R12 flow meter	0.094
Comp. power	256.210
P at suction	1.646
P at cond. end	4.741
P at evap start	1.606
P at discharge	5.537
PT supply volts	10.000
Water pump power	56.000
Heater volts	121.571
Heater Amps	5.283
Room temperature	22.000
Manual cond mdot	31.656
Bourdon Pe, psig	21.000
Bourdon Pc, psia	90.000
Real time	1919.300
Oil fraction	-1.000
Suction P loss	0.281
Stator res'tance	9.300
Winding Temp	59.500

Motor performance

Estimated RPM	2928.733
Winding loss	34.889
Rotor Loss etc.	50.192
Shaftwork	171.129
Bearing losses	47.395
Implied viscos'y	11.849
Sump viscosity	9.853

Refrigerant states

Position	Temp	Press	Volume	Enthalpy
dvo state	85.603	6.550	34.940	404.522
Discharge	85.670	6.550	34.948	404.569
Cond. start	81.755	6.550	34.458	401.816
Cond. end	16.677	5.754	0.746	215.642
Evap. end	12.503	2.619	70.238	360.429
svc state	49.460	2.619	81.261	384.251

Condenser temperature distribution

R12 Ts	16.677	20.521	25.206	81.755
Water Ts	16.103	16.244	21.713	23.251

Discharge stub temperature 76.519

Powers, Watts

	measured	Xtalk	loss	R12 Dh
Compressor	256.210	4.089	28.623	223.511
Condenser	947.169	4.089	-0.339	942.741
Evaporator	698.244	691.129		733.171

Compressor performance

Vertex	phi	Volume	Vsvc etc	mass,mg
1	105.133	4.325		123.785
2	188.162	0.600	0.653	18.659
3	211.976	1.505		18.521
4	24.839	10.172	10.081	124.056

Leakage loss on discharge, mg		1.386
Reference density ratio		2.326
R12 mass flow rate	g/s	5.064

Indicator diagram breakdown, Watts

Minimum work of compression	102.646
Suction excess PdV	7.053
Discharge excess PdV	12.226
Total leakage loss	1.810
Total indicated work	123.735

R12 Enthalpy gain summary, Watts

Total suction gas preheat	120.628
Calculated total PdV work	123.735
Discharge - suction exchange	7.566
Inner pipe, loss to the can	4.422
Outer pipe, loss to the can	2.261
Outer pipe, loss to ambient	11.680

The discharge valve was open for 4.725 ms.
The first rarefaction returns after 6.388 ms.

Unmodified compressor. High superheat

Nominal Evaporating P 6psig. Nominal Condensing P 77psia.

Raw data

Current mA	1872.944
Voltage bits	2826.937
Room temperature	21.510
Cond. water out	20.917
Cond. water in	16.491
Evap. water in	3.261
Evap. water out	-1.833
R12 Discharge	106.529
R12 Cond. entry	97.943
R12 Condensing	19.647
R12 Cond. exit	17.002
R12 Evap. entry	-18.108
R12 Evap. exit	-0.508
R12 Suction	17.013
Sump oil Temp.	82.883
Evap. flow rate	12.567
Cond. flow rate	27.070
R12 flow meter	0.088
Comp. power	216.177
P at suction	0.496
P at cond. end	4.564
P at evap start	0.418
P at discharge	4.777
PT supply volts	10.000
Water pump power	57.000
Heater volts	61.000
Heater Amps	2.680
Room temperature	22.000
Manual cond mdot	26.480
Bourdon Pe, psig	5.800
Bourdon Pc, psia	78.000
Real time	203.500
Oil fraction	-1.000
Suction P loss	0.192
Stator res'tance	10.100
Winding Temp	95.500

Motor performance

Estimated RPM	2944.200
Winding loss	35.430
Rotor Loss etc.	47.349
Shaftwork	133.398
Bearing losses	41.345
Implied viscos'y	10.336
Sump viscosity	5.466

Refrigerant states

Position	Temp	Press	Volume	Enthalpy
dvo state	111.988	5.790	43.477	423.756
Discharge	108.039	5.790	42.949	420.973
Cond. start	97.943	5.790	41.589	413.884
Cond. end	17.002	5.577	0.746	215.952
Evap. end	-1.833	1.431	125.068	353.771
svc state	57.055	1.431	155.496	390.562

Condenser temperature distribution

R12 Ts	17.002	19.414	20.742	97.943
Water Ts	16.491	16.542	19.713	20.917

Discharge stub temperature 95.396

Powers, Watts

	measured	Xtalk	loss	R12 Dh
Compressor	216.177	6.585	46.092	163.506
Condenser	490.598	6.585	-2.435	481.579
Evaporator	220.480	267.985		335.322

Compressor performance

Vertex	phi	Volume	Vsvc etc	mass,mg
1	123.225	2.822		64.899
2	188.162	0.600	0.633	14.544
3	223.618	2.243		14.425
4	23.906	10.206	10.122	65.095

Leakage loss on discharge, mg		0.771
Reference density ratio		3.577
R12 mass flow rate	g/s	2.433

Indicator diagram breakdown, Watts

Minimum work of compression	80.763
Suction excess PdV	3.951
Discharge excess PdV	5.644
Total leakage loss	1.695
Total indicated work	92.053

R12 Enthalpy gain summary, Watts

Total suction gas preheat	89.514
Calculated total PdV work	92.053
Discharge - suction exchange	8.705
Inner pipe, loss to the can	3.710
Outer pipe, loss to the can	2.547
Outer pipe, loss to ambient	14.703

The discharge valve was open for 3.676 ms.
The first rarefaction returns after 6.060 ms.

Unmodified compressor. High superheat

Nominal Evaporating P 6psig. Nominal Condensing P 90psia.

Raw data

Current mA	1888.672
Voltage bits	2838.240
Room temperature	21.601
Cond. water out	27.985
Cond. water in	17.795
Evap. water in	2.854
Evap. water out	-2.096
R12 Discharge	111.081
R12 Cond. entry	101.874
R12 Condensing	24.229
R12 Cond. exit	18.470
R12 Evap. entry	-18.229
R12 Evap. exit	-0.779
R12 Suction	17.893
Sump oil Temp.	85.454
Evap. flow rate	12.250
Cond. flow rate	10.932
R12 flow meter	0.088
Comp. power	221.176
P at suction	0.498
P at cond. end	5.339
P at evap start	0.405
P at discharge	5.537
PT supply volts	10.000
Water pump power	57.000
Heater volts	57.570
Heater Amps	2.514
Room temperature	22.000
Manual cond mdot	11.021
Bourdon Pe, psig	5.650
Bourdon Pc, psia	90.000
Real time	329.000
Oil fraction	-1.000
Suction P loss	0.197
Stator res'tance	10.100
Winding Temp	95.500

Motor performance

Estimated RPM	2942.544
Winding loss	36.028
Rotor Loss etc.	47.588
Shaftwork	137.561
Bearing losses	40.369
Implied viscos'y	10.092
Sump viscosity	5.112

Refrigerant states

Position	Temp	Press	Volume	Enthalpy
dvo state	117.928	6.550	38.870	427.377
Discharge	112.815	6.550	38.260	423.742
Cond. start	101.874	6.550	36.942	415.993
Cond. end	18.470	6.352	0.749	217.354
Evap. end	-2.096	1.418	126.052	353.637
svc state	57.397	1.418	157.038	390.796

Condenser temperature distribution

R12 Ts	18.470	24.083	25.205	101.874
Water Ts	17.795	18.072	25.203	27.985

Discharge stub temperature 98.981

Powers, Watts

	measured	Xtalk	loss	R12 Dh
Compressor	221.176	7.050	49.349	164.784
Condenser	470.091	7.050	3.863	466.905
Evaporator	201.731	253.838		320.337

Compressor performance

Vertex	phi	Volume	Vsvc etc	mass,mg
1	127.140	2.526		64.996
2	188.162	0.600	0.629	16.160
3	227.362	2.514		16.006
4	18.973	10.367	10.245	65.240

Leakage loss on discharge, mg		0.907
Reference density ratio		4.040
R12 mass flow rate	g/s	2.351

Indicator diagram breakdown, Watts

Minimum work of compression	85.983
Suction excess PdV	3.833
Discharge excess PdV	5.155
Total leakage loss	2.220
Total indicated work	97.192

R12 Enthalpy gain summary, Watts

Total suction gas preheat	87.344
Calculated total PdV work	97.192
Discharge - suction exchange	9.705
Inner pipe, loss to the can	3.993
Outer pipe, loss to the can	2.770
Outer pipe, loss to ambient	15.446

The discharge valve was open for 3.456 ms.
The first rarefaction returns after 6.036 ms.

Unmodified compressor. High superheat

Nominal Evaporating P 5psig. Nominal Condensing P 108psia.

Raw data

Current mA	1903.041
Voltage bits	2837.950
Room temperature	21.825
Cond. water out	37.808
Cond. water in	19.110
Evap. water in	1.373
Evap. water out	-2.868
R12 Discharge	117.974
R12 Cond. entry	107.737
R12 Condensing	30.496
R12 Cond. exit	20.086
R12 Evap. entry	-18.196
R12 Evap. exit	-1.443
R12 Suction	19.380
Sump oil Temp.	90.350
Evap. flow rate	12.418
Cond. flow rate	5.947
R12 flow meter	0.087
Comp. power	226.473
P at suction	0.540
P at cond. end	6.537
P at evap start	0.423
P at discharge	6.700
PT supply volts	10.000
Water pump power	57.000
Heater volts	49.400
Heater Amps	2.170
Room temperature	22.000
Manual cond mdot	5.537
Bourdon Pe, psig	5.300
Bourdon Pc, psia	108.000
Real time	520.100
Oil fraction	-1.000
Suction P loss	0.181
Stator res'tance	10.300
Winding Temp	104.500

Motor performance

Estimated RPM	2941.027
Winding loss	37.302
Rotor Loss etc.	47.822
Shaftwork	141.349
Bearing losses	41.282
Implied viscos'y	10.321
Sump viscosity	4.524

Refrigerant states

Position	Temp	Press	Volume	Enthalpy
dvo state	127.147	7.713	33.611	433.112
Discharge	120.243	7.713	32.903	428.145
Cond. start	107.737	7.713	31.603	419.177
Cond. end	20.086	7.550	0.753	218.903
Evap. end	-2.868	1.436	124.004	353.134
svc state	59.852	1.436	156.278	392.364

Condenser temperature distribution

R12 Ts	20.086	30.531	31.346	107.737
Water Ts	19.110	20.059	32.663	37.808

Discharge stub temperature 104.907

Powers, Watts

	measured	Xtalk	loss	R12 Dh
Compressor	226.473	7.864	55.049	163.568
Condenser	433.380	7.864	11.203	436.719
Evaporator	164.198	220.493		292.706

Compressor performance

Vertex	phi	Volume	Vsvc etc	mass,mg
1	132.367	2.155		64.120
2	188.162	0.600	0.623	18.530
3	231.938	2.863		18.317
4	26.077	10.125	10.070	64.434

Leakage loss on discharge, mg		1.102
Reference density ratio		4.650
R12 mass flow rate	g/s	2.181

Indicator diagram breakdown, Watts

Minimum work of compression	88.856
Suction excess PdV	3.708
Discharge excess PdV	4.449
Total leakage loss	3.053
Total indicated work	100.066

R12 Enthalpy gain summary, Watts

Total suction gas preheat	85.544
Calculated total PdV work	100.066
Discharge - suction exchange	11.030
Inner pipe, loss to the can	4.251
Outer pipe, loss to the can	3.027
Outer pipe, loss to ambient	16.529

The discharge valve was open for 3.162 ms.
The first rarefaction returns after 5.993 ms.

Unmodified compressor. High superheat

Nominal Evaporating P 6psig. Nominal Condensing P 150psia.

Raw data

Current mA	1929.333
Voltage bits	2896.733
Room temperature	21.925
Cond. water out	57.322
Cond. water in	20.240
Evap. water in	-0.673
Evap. water out	-4.276
R12 Discharge	129.703
R12 Cond. entry	116.233
R12 Condensing	43.337
R12 Cond. exit	22.371
R12 Evap. entry	-18.177
R12 Evap. exit	-2.509
R12 Suction	23.996
Sump oil Temp.	100.658
Evap. flow rate	10.313
Cond. flow rate	2.545
R12 flow meter	0.087
Comp. power	229.174
P at suction	0.614
P at cond. end	9.480
P at evap start	0.437
P at discharge	9.565
PT supply volts	10.000
Water pump power	57.000
Heater volts	30.000
Heater Amps	1.300
Room temperature	22.000
Manual cond mdot	2.132
Bourdon Pe, psig	5.800
Bourdon Pc, psia	150.000
Real time	659.100
Oil fraction	-1.000
Suction P loss	0.169
Stator res'tance	10.800
Winding Temp	127.000

Motor performance

Estimated RPM	2941.102
Winding loss	40.201
Rotor Loss etc.	47.810
Shaftwork	141.163
Bearing losses	43.875
Implied viscos'y	10.969
Sump viscosity	3.571

Refrigerant states

Position	Temp	Press	Volume	Enthalpy
dvo state	144.616	10.578	25.269	443.851
Discharge	133.026	10.578	24.374	435.310
Cond. start	116.233	10.578	23.046	422.959
Cond. end	22.371	10.493	0.757	221.103
Evap. end	-4.276	1.450	122.054	352.257
svc state	63.253	1.450	156.486	394.556

Condenser temperature distribution

R12 Ts	22.371	43.644	43.981	116.233
Water Ts	20.240	24.126	47.316	57.322

Discharge stub temperature 115.598

Powers, Watts

	measured	Xtalk	loss	R12 Dh
Compressor	229.174	8.767	76.644	143.775
Condenser	330.941	8.767	27.262	349.435
Evaporator	96.000	155.539		227.042

Compressor performance

Vertex	phi	Volume	Vsvc etc	mass,mg
1	142.088	1.546		61.191
2	188.162	0.600	0.614	24.295
3	242.605	3.740		23.901
4	37.415	9.609	9.654	61.695

Leakage loss on discharge, mg		1.580
Reference density ratio		6.193
R12 mass flow rate	g/s	1.731

Indicator diagram breakdown, Watts

Minimum work of compression	85.335
Suction excess PdV	3.310
Discharge excess PdV	3.117
Total leakage loss	5.526
Total indicated work	97.288

R12 Enthalpy gain summary, Watts

Total suction gas preheat	73.225
Calculated total PdV work	97.288
Discharge - suction exchange	13.704
Inner pipe, loss to the can	4.198
Outer pipe, loss to the can	3.272
Outer pipe, loss to ambient	18.110

The discharge valve was open for 2.611 ms.
The first rarefaction returns after 5.927 ms.

Unmodified compressor. High superheat

Nominal Evaporating P 21psig. Nominal Condensing P 150psia.

Raw data

Current mA	2056.637
Voltage bits	2821.720
Room temperature	22.171
Cond. water out	53.368
Cond. water in	19.274
Evap. water in	17.398
Evap. water out	10.700
R12 Discharge	106.681
R12 Cond. entry	102.652
R12 Condensing	42.379
R12 Cond. exit	21.279
R12 Evap. entry	-2.077
R12 Evap. exit	11.164
R12 Suction	18.487
Sump oil Temp.	73.931
Evap. flow rate	19.899
Cond. flow rate	5.908
R12 flow meter	0.088
Comp. power	292.107
P at suction	1.719
P at cond. end	9.135
P at evap start	1.602
P at discharge	9.605
PT supply volts	10.000
Water pump power	57.000
Heater volts	106.095
Heater Amps	4.625
Room temperature	22.000
Manual cond mdot	5.733
Bourdon Pe, psig	21.000
Bourdon Pc, psia	150.000
Real time	1020.300
Oil fraction	-1.000
Suction P loss	0.264
Stator res'tance	9.800
Winding Temp	82.000

Motor performance

Estimated RPM	2917.230
Winding loss	41.452
Rotor Loss etc.	52.996
Shaftwork	197.659
Bearing losses	37.890
Implied viscos'y	9.473
Sump viscosity	7.016

Refrigerant states

Position	Temp	Press	Volume	Enthalpy
dvo state	112.205	10.618	22.627	419.964
Discharge	108.622	10.618	22.336	417.327
Cond. start	102.652	10.618	21.846	412.930
Cond. end	21.279	10.148	0.755	220.050
Evap. end	10.700	2.615	69.783	359.287
svc state	54.898	2.615	82.950	387.814

Condenser temperature distribution

R12 Ts	21.279	42.261	44.137	102.652
Water Ts	19.274	22.948	45.522	53.368

Discharge stub temperature 94.029

Powers, Watts

	measured	Xtalk	loss	R12 Dh
Compressor	292.107	4.975	34.822	252.337
Condenser	818.168	4.975	25.382	838.575
Evaporator	547.742	557.907		605.355

Compressor performance

Vertex	phi	Volume	Vsvc etc	mass,mg
1	124.660	2.712		119.848
2	188.162	0.600	0.631	27.847
3	224.079	2.276		27.433
4	28.007	10.048	9.998	120.528

Leakage loss on discharge, mg		2.581
Reference density ratio		3.666
R12 mass flow rate	g/s	4.348

Indicator diagram breakdown, Watts

Minimum work of compression	139.775
Suction excess PdV	6.535
Discharge excess PdV	8.000
Total leakage loss	5.459
Total indicated work	159.769

R12 Enthalpy gain summary, Watts

Total suction gas preheat	124.025
Calculated total PdV work	159.769
Discharge - suction exchange	12.910
Inner pipe, loss to the can	6.553
Outer pipe, loss to the can	3.496
Outer pipe, loss to ambient	15.622

The discharge valve was open for 3.628 ms.
The first rarefaction returns after 6.288 ms.

Unmodified compressor. High superheat

Nominal Evaporating P 21psig. Nominal Condensing P 220psia.

Raw data

Current mA	2118.269
Voltage bits	2841.075
Room temperature	24.496
Cond. water out	77.737
Cond. water in	21.662
Evap. water in	15.426
Evap. water out	9.981
R12 Discharge	128.805
R12 Cond. entry	122.288
R12 Condensing	59.527
R12 Cond. exit	25.586
R12 Evap. entry	-2.240
R12 Evap. exit	10.569
R12 Suction	21.579
Sump oil Temp.	87.698
Evap. flow rate	19.594
Cond. flow rate	3.190
R12 flow meter	0.088
Comp. power	308.965
P at suction	1.865
P at cond. end	14.140
P at evap start	1.642
P at discharge	14.376
PT supply volts	10.000
Water pump power	57.000
Heater volts	91.630
Heater Amps	3.980
Room temperature	22.900
Manual cond mdot	2.855
Bourdon Pe, psig	21.425
Bourdon Pc, psia	220.000
Real time	1319.530
Oil fraction	-1.000
Suction P loss	0.208
Stator res'tance	10.200
Winding Temp	100.000

Motor performance

Estimated RPM	2912.219
Winding loss	45.768
Rotor Loss etc.	54.331
Shaftwork	208.866
Bearing losses	36.802
Implied viscos'y	9.200
Sump viscosity	4.830

Refrigerant states

Position	Temp	Press	Volume	Enthalpy
dvo state	138.181	15.389	16.368	435.617
Discharge	130.849	15.389	15.939	430.021
Cond. start	122.288	15.389	15.426	423.464
Cond. end	25.586	15.153	0.764	224.218
Evap. end	9.981	2.655	68.439	358.755
svc state	63.734	2.655	84.158	393.589

Condenser temperature distribution

R12 Ts	25.586	59.695	60.408	122.288
Water Ts	21.662	31.549	63.625	77.737

Discharge stub temperature 111.748

Powers, Watts

	measured	Xtalk	loss	R12 Dh
Compressor	308.965	6.369	49.261	253.361
Condenser	670.235	6.369	44.481	708.348
Evaporator	421.687	446.653		478.298

Compressor performance

Vertex	phi	Volume	Vsvc etc	mass,mg
1	136.512	1.882		114.955
2	188.162	0.600	0.619	37.762
3	235.001	3.106		36.909
4	34.451	9.759	9.776	116.163

Leakage loss on discharge, mg		3.947
Reference density ratio		5.141
R12 mass flow rate	g/s	3.555

Indicator diagram breakdown, Watts

Minimum work of compression	149.417
Suction excess PdV	5.897
Discharge excess PdV	5.388
Total leakage loss	11.363
Total indicated work	172.065

R12 Enthalpy gain summary, Watts

Total suction gas preheat	123.840
Calculated total PdV work	172.065
Discharge - suction exchange	17.622
Inner pipe, loss to the can	7.661
Outer pipe, loss to the can	4.364
Outer pipe, loss to ambient	18.950

The discharge valve was open for 2.956 ms.
The first rarefaction returns after 6.178 ms.

Unmodified compressor. High superheat

Nominal Evaporating P 40psig. Nominal Condensing P 220psia.

Raw data

Current mA	2333.221
Voltage bits	2808.600
Room temperature	24.980
Cond. water out	72.895
Cond. water in	19.435
Evap. water in	36.755
Evap. water out	22.909
R12 Discharge	111.938
R12 Cond. entry	109.287
R12 Condensing	58.279
R12 Cond. exit	23.720
R12 Evap. entry	9.601
R12 Evap. exit	22.942
R12 Suction	26.136
Sump oil Temp.	73.966
Evap. flow rate	15.959
Cond. flow rate	5.779
R12 flow meter	0.088
Comp. power	381.267
P at suction	3.155
P at cond. end	13.619
P at evap start	2.980
P at discharge	14.389
PT supply volts	10.000
Water pump power	57.000
Heater volts	147.320
Heater Amps	6.332
Room temperature	25.000
Manual cond mdot	5.683
Bourdon Pe, psig	39.700
Bourdon Pc, psia	220.000
Real time	1549.300
Oil fraction	-1.000
Suction P loss	0.187
Stator res'tance	9.800
Winding Temp	82.000

Motor performance

Estimated RPM	2885.351
Winding loss	53.350
Rotor Loss etc.	61.689
Shaftwork	266.228
Bearing losses	26.853
Implied viscos'y	6.713
Sump viscosity	7.009

Refrigerant states

Position	Temp	Press	Volume	Enthalpy
dvo state	115.850	15.402	15.017	418.497
Discharge	113.112	15.402	14.846	416.382
Cond. start	109.287	15.402	14.605	413.417
Cond. end	23.720	14.632	0.760	222.407
Evap. end	22.909	3.993	46.549	364.804
svc state	57.947	3.993	53.749	388.225

Condenser temperature distribution

R12 Ts	23.720	58.100	60.445	109.287
Water Ts	19.435	29.283	61.675	72.895

Discharge stub temperature 99.308

Powers, Watts

	measured	Xtalk	loss	R12 Dh
Compressor	381.267	3.451	24.157	353.674
Condenser	1271.849	3.451	41.378	1309.776
Evaporator	989.830	925.000		976.432

Compressor performance

Vertex	phi	Volume	Vsvc etc	mass,mg
1	122.765	2.857		190.261
2	188.162	0.600	0.633	42.036
3	223.180	2.212		41.162
4	15.268	10.468	10.308	191.777

Leakage loss on discharge, mg		5.635
Reference density ratio		3.579
R12 mass flow rate	g/s	6.857

Indicator diagram breakdown, Watts

Minimum work of compression	207.577
Suction excess PdV	9.438
Discharge excess PdV	11.272
Total leakage loss	11.087
Total indicated work	239.375

R12 Enthalpy gain summary, Watts

Total suction gas preheat	160.600
Calculated total PdV work	239.375
Discharge - suction exchange	16.969
Inner pipe, loss to the can	8.806
Outer pipe, loss to the can	3.865
Outer pipe, loss to ambient	16.465

The discharge valve was open for 3.777 ms.
The first rarefaction returns after 6.496 ms.

Unmodified compressor. High superheat

Nominal Evaporating P 40psig. Nominal Condensing P 150psia.

Raw data

Current mA	2184.108
Voltage bits	2857.960
Room temperature	24.275
Cond. water out	47.335
Cond. water in	18.986
Evap. water in	42.160
Evap. water out	25.024
R12 Discharge	90.969
R12 Cond. entry	89.345
R12 Condensing	38.205
R12 Cond. exit	20.707
R12 Evap. entry	9.594
R12 Evap. exit	24.947
R12 Suction	26.741
Sump oil Temp.	64.140
Evap. flow rate	15.510
Cond. flow rate	12.111
R12 flow meter	0.089
Comp. power	333.497
P at suction	3.107
P at cond. end	8.056
P at evap start	3.053
P at discharge	9.581
PT supply volts	10.000
Water pump power	57.000
Heater volts	163.580
Heater Amps	7.024
Room temperature	24.800
Manual cond mdot	11.990
Bourdon Pe, psig	40.500
Bourdon Pc, psia	150.000
Real time	1658.250
Oil fraction	-1.000
Suction P loss	0.113
Stator res'tance	9.400
Winding Temp	64.000

Motor performance

Estimated RPM	2901.861
Winding loss	44.841
Rotor Loss etc.	57.192
Shaftwork	231.463
Bearing losses	37.449
Implied viscos'y	9.362
Sump viscosity	9.533

Refrigerant states

Position	Temp	Press	Volume	Enthalpy
dvo state	92.206	10.594	21.022	405.241
Discharge	92.011	10.594	21.005	405.097
Cond. start	89.345	10.594	20.777	403.123
Cond. end	20.707	9.069	0.754	219.500
Evap. end	24.947	4.066	46.064	366.043
svc state	52.479	4.066	51.658	384.464

Condenser temperature distribution

R12 Ts	20.707	37.695	44.043	89.345
Water Ts	18.986	21.564	41.991	47.335

Discharge stub temperature 82.536

Powers, Watts

	measured	Xtalk	loss	R12 Dh
Compressor	333.497	3.472	24.302	305.731
Condenser	1422.827	3.472	18.110	1437.465
Evaporator	1205.986	1112.573		1147.188

Compressor performance

Vertex	phi	Volume	Vsvc etc	mass,mg
1	107.430	4.125		196.220
2	188.162	0.600	0.651	30.855
3	213.201	1.575		30.481
4	21.229	10.297	10.174	196.956

Leakage loss on discharge, mg		3.503
Reference density ratio		2.457
R12 mass flow rate	g/s	7.828

Indicator diagram breakdown, Watts

Minimum work of compression	162.652
Suction excess PdV	10.340
Discharge excess PdV	16.379
Total leakage loss	4.644
Total indicated work	194.015

R12 Enthalpy gain summary, Watts

Total suction gas preheat	144.208
Calculated total PdV work	194.015
Discharge - suction exchange	11.045
Inner pipe, loss to the can	6.464
Outer pipe, loss to the can	2.735
Outer pipe, loss to ambient	12.719

The discharge valve was open for 4.637 ms.
The first rarefaction returns after 6.564 ms.

Unmodified compressor. High superheat

Nominal Evaporating P 40psig. Nominal Condensing P 108psia.

Raw data

Current mA	2011.763
Voltage bits	2838.000
Room temperature	22.918
Cond. water out	25.736
Cond. water in	16.037
Evap. water in	50.233
Evap. water out	28.047
R12 Discharge	76.400
R12 Cond. entry	75.095
R12 Condensing	21.472
R12 Cond. exit	16.545
R12 Evap. entry	9.928
R12 Evap. exit	27.900
R12 Suction	28.943
Sump oil Temp.	57.850
Evap. flow rate	13.462
Cond. flow rate	38.462
R12 flow meter	0.089
Comp. power	278.442
P at suction	3.042
P at cond. end	4.770
P at evap start	3.066
P at discharge	6.655
PT supply volts	10.000
Water pump power	57.000
Heater volts	175.387
Heater Amps	7.500
Room temperature	24.000
Manual cond mdot	37.670
Bourdon Pe, psig	40.000
Bourdon Pc, psia	108.000
Real time	1915.350
Oil fraction	-1.000
Suction P loss	0.143
Stator res'tance	9.200
Winding Temp	55.000

Motor performance

Estimated RPM	2920.967
Winding loss	37.234
Rotor Loss etc.	52.039
Shaftwork	189.169
Bearing losses	41.383
Implied viscos'y	10.346
Sump viscosity	11.861

Refrigerant states

Position	Temp	Press	Volume	Enthalpy
dvo state	75.372	7.668	28.281	396.109
Discharge	77.095	7.668	28.475	397.339
Cond. start	75.095	7.668	28.249	395.911
Cond. end	16.545	5.783	0.746	215.516
Evap. end	27.900	4.079	46.515	367.994
svc state	49.863	4.079	50.962	382.691

Condenser temperature distribution

R12 Ts	16.545	20.700	31.121	75.095
Water Ts	16.037	16.251	24.019	25.736

Discharge stub temperature 70.672

Powers, Watts

	measured	Xtalk	loss	R12 Dh
Compressor	278.442	3.791	26.538	248.211
Condenser	1529.355	3.791	0.277	1525.840
Evaporator	1372.406	1250.248		1289.709

Compressor performance

Vertex	phi	Volume	Vsvc etc	mass,mg
1	90.275	5.644		199.559
2	188.162	0.600	0.670	23.626
3	206.011	1.196		23.470
4	20.277	10.328	10.187	199.887

Leakage loss on discharge, mg		2.189
Reference density ratio		1.802
R12 mass flow rate	g/s	8.458

Indicator diagram breakdown, Watts

Minimum work of compression	113.489
Suction excess PdV	10.777
Discharge excess PdV	21.595
Total leakage loss	1.925
Total indicated work	147.786

R12 Enthalpy gain summary, Watts

Total suction gas preheat	124.313
Calculated total PdV work	147.786
Discharge - suction exchange	6.658
Inner pipe, loss to the can	4.529
Outer pipe, loss to the can	1.882
Outer pipe, loss to ambient	10.199

The discharge valve was open for 5.585 ms.
The first rarefaction returns after 6.603 ms.

Unmodified compressor. High superheat

Nominal Evaporating P 63psig. Nominal Condensing P 151psia.

Raw data

Current mA	2143.138
Voltage bits	2809.180
Room temperature	23.824
Cond. water out	42.530
Cond. water in	18.069
Evap. water in	55.709
Evap. water out	38.846
R12 Discharge	83.673
R12 Cond. entry	82.454
R12 Condensing	31.604
R12 Cond. exit	20.275
R12 Evap. entry	20.786
R12 Evap. exit	38.464
R12 Suction	38.716
Sump oil Temp.	61.617
Evap. flow rate	24.580
Cond. flow rate	20.180
R12 flow meter	9.914
Comp. power	332.419
P at suction	4.522
P at cond. end	6.425
P at evap start	4.543
P at discharge	9.616
PT supply volts	10.000
Water pump power	57.000
Heater volts	205.800
Heater Amps	8.700
Room temperature	24.000
Manual cond mdot	20.152
Bourdon Pe, psig	62.900
Bourdon Pc, psia	150.800
Real time	2258.150
Oil fraction	-1.000
Suction P loss	0.241
Stator res'tance	9.200
Winding Temp	55.000

Motor performance

Estimated RPM	2901.239
Winding loss	42.256
Rotor Loss etc.	57.365
Shaftwork	232.798
Bearing losses	29.025
Implied viscos'y	7.256
Sump viscosity	10.383

Refrigerant states

Position	Temp	Press	Volume	Enthalpy
dvo state	82.540	10.629	20.104	398.028
Discharge	84.034	10.629	20.236	399.140
Cond. start	82.454	10.629	20.097	397.964
Cond. end	20.275	7.438	0.753	219.085
Evap. end	38.464	5.556	34.615	372.862
svc state	55.099	5.556	37.210	384.369

Condenser temperature distribution

R12 Ts	20.275	29.962	44.183	82.454
Water Ts	18.069	19.357	38.509	42.530

Discharge stub temperature 77.616

Powers, Watts

	measured	Xtalk	loss	R12 Dh
Compressor	332.419	3.489	24.424	304.591
Condenser	2063.423	3.489	13.408	2073.342
Evaporator	1847.460	1735.038		1782.384

Compressor performance

Vertex	phi	Volume	Vsvc etc	mass,mg
1	91.120	5.568		276.969
2	188.162	0.600	0.669	33.157
3	206.563	1.223		32.854
4	11.597	10.551	10.331	277.626

Leakage loss on discharge, mg		4.107
Reference density ratio		1.851
R12 mass flow rate	g/s	11.591

Indicator diagram breakdown, Watts

Minimum work of compression	158.310
Suction excess PdV	14.239
Discharge excess PdV	27.591
Total leakage loss	3.634
Total indicated work	203.773

R12 Enthalpy gain summary, Watts

Total suction gas preheat	133.384
Calculated total PdV work	203.773
Discharge - suction exchange	8.820
Inner pipe, loss to the can	5.875
Outer pipe, loss to the can	2.125
Outer pipe, loss to ambient	11.509

The discharge valve was open for 5.575 ms.
The first rarefaction returns after 6.723 ms.

Unmodified compressor. High superheat

Nominal Evaporating P 64psig. Nominal Condensing P 220psia.

Raw data

Current mA	2402.875
Voltage bits	2816.414
Room temperature	24.087
Cond. water out	68.238
Cond. water in	20.279
Evap. water in	49.277
Evap. water out	35.744
R12 Discharge	101.055
R12 Cond. entry	99.449
R12 Condensing	55.089
R12 Cond. exit	25.490
R12 Evap. entry	20.545
R12 Evap. exit	35.387
R12 Suction	36.092
Sump oil Temp.	68.046
Evap. flow rate	26.980
Cond. flow rate	9.302
R12 flow meter	8.912
Comp. power	425.099
P at suction	4.699
P at cond. end	12.465
P at evap start	4.606
P at discharge	14.391
PT supply volts	10.000
Water pump power	57.000
Heater volts	191.914
Heater Amps	8.150
Room temperature	24.000
Manual cond mdot	9.353
Bourdon Pe, psig	64.000
Bourdon Pc, psia	220.000
Real time	32.100
Oil fraction	-1.000
Suction P loss	0.139
Stator res'tance	9.500
Winding Temp	68.500

Motor performance

Estimated RPM	2866.731
Winding loss	54.851
Rotor Loss etc.	66.056
Shaftwork	304.192
Bearing losses	34.063
Implied viscos'y	8.516
Sump viscosity	8.397

Refrigerant states

Position	Temp	Press	Volume	Enthalpy
dvo state	102.201	15.404	14.147	407.890
Discharge	101.622	15.404	14.109	407.436
Cond. start	99.449	15.404	13.965	405.729
Cond. end	25.490	13.478	0.764	224.125
Evap. end	35.387	5.619	33.685	370.624
svc state	57.969	5.619	37.183	386.274

Condenser temperature distribution

R12 Ts	25.490	54.409	60.450	99.449
Water Ts	20.279	28.058	59.682	68.238

Discharge stub temperature 91.736

Powers, Watts

	measured	Xtalk	loss	R12 Dh
Compressor	425.099	4.318	32.962	387.893
Condenser	1877.733	4.318	40.175	1913.590
Evaporator	1621.101	1528.449		1543.682

Compressor performance

Vertex	phi	Volume	Vsvc etc	mass,mg
1	110.470	3.863		273.091
2	188.162	0.600	0.647	45.553
3	214.723	1.664		44.747
4	19.604	10.348	10.213	274.676

Leakage loss on discharge, mg		7.001
Reference density ratio		2.628
R12 mass flow rate	g/s	10.537

Indicator diagram breakdown, Watts

Minimum work of compression	227.769
Suction excess PdV	13.503
Discharge excess PdV	19.299
Total leakage loss	9.558
Total indicated work	270.129

R12 Enthalpy gain summary, Watts

Total suction gas preheat	164.908
Calculated total PdV work	270.129
Discharge - suction exchange	15.440
Inner pipe, loss to the can	8.643
Outer pipe, loss to the can	3.201
Outer pipe, loss to ambient	14.786

The discharge valve was open for 4.517 ms.
The first rarefaction returns after 6.734 ms.

Vital oil flows only. Normal superheat

Nominal Evaporating P 21psig. Nominal Condensing P 90psia.

Raw data

Current mA	1937.380
Voltage bits	2827.620
Room temperature	20.278
Cond. water out	22.600
Cond. water in	15.820
Evap. water in	7.354
Evap. water out	1.187
R12 Discharge	74.519
R12 Cond. entry	71.682
R12 Condensing	20.163
R12 Cond. exit	17.202
R12 Evap. entry	-3.241
R12 Evap. exit	-1.076
R12 Suction	3.888
Sump oil Temp.	50.597
Evap. flow rate	24.916
Cond. flow rate	34.026
R12 flow meter	0.095
Comp. power	248.327
P at suction	1.682
P at cond. end	4.627
P at evap start	1.631
P at discharge	5.551
PT supply volts	10.000
Water pump power	58.000
Heater volts	113.800
Heater Amps	5.000
Room temperature	21.000
Manual cond mdot	33.333
Bourdon Pe, psig	21.500
Bourdon Pc, psia	90.000
Real time	947.150
Oil fraction	0.000
Suction P loss	0.125
Stator res'tance	9.200
Winding Temp	55.000

Motor performance

Estimated RPM	2931.639
Winding loss	34.532
Rotor Loss etc.	49.563
Shaftwork	164.232
Bearing losses	40.174
Implied viscos'y	10.043
Sump viscosity	15.636

Refrigerant states

Position	Temp	Press	Volume	Enthalpy
dvo state	74.995	6.564	33.524	397.050
Discharge	75.024	6.564	33.527	397.071
Cond. start	71.682	6.564	33.100	394.723
Cond. end	17.202	5.640	0.747	216.143
Evap. end	-1.076	2.644	65.288	351.739
svc state	39.431	2.644	77.559	377.692

Condenser temperature distribution

R12 Ts	17.202	19.812	25.285	71.682
Water Ts	15.820	15.915	21.350	22.600

Discharge stub temperature 65.165

Powers, Watts

	measured	Xtalk	loss	R12 Dh
Compressor	248.327	1.026	7.184	240.130
Condenser	946.030	1.026	0.961	945.965
Evaporator	627.000	643.215		718.271

Compressor performance

Vertex	phi	Volume	Vsvc etc	mass,mg
1	105.003	4.337		129.356
2	188.162	0.600	0.654	19.463
3	211.852	1.498		19.315
4	25.412	10.150	10.055	129.644

Leakage loss on discharge, mg		1.480
Reference density ratio		2.314
R12 mass flow rate	g/s	5.297

Indicator diagram breakdown, Watts

Minimum work of compression	102.542
Suction excess PdV	7.245
Discharge excess PdV	12.422
Total leakage loss	1.850
Total indicated work	124.058

R12 Enthalpy gain summary, Watts

Total suction gas preheat	137.480
Calculated total PdV work	124.058
Discharge - suction exchange	7.476
Inner pipe, loss to the can	4.838
Outer pipe, loss to the can	2.446
Outer pipe, loss to ambient	9.990

The discharge valve was open for 4.728 ms.
The first rarefaction returns after 6.525 ms.

Vital oil flows only. Normal superheat

Nominal Evaporating P 22psig. Nominal Condensing P 150psia.

Raw data

Current mA	2063.613
Voltage bits	2824.244
Room temperature	20.828
Cond. water out	50.661
Cond. water in	18.334
Evap. water in	5.492
Evap. water out	0.769
R12 Discharge	98.534
R12 Cond. entry	93.990
R12 Condensing	41.965
R12 Cond. exit	31.697
R12 Evap. entry	-3.067
R12 Evap. exit	-1.062
R12 Suction	5.856
Sump oil Temp.	61.004
Evap. flow rate	24.602
Cond. flow rate	6.002
R12 flow meter	0.099
Comp. power	291.516
P at suction	1.798
P at cond. end	8.971
P at evap start	1.654
P at discharge	9.545
PT supply volts	10.000
Water pump power	58.000
Heater volts	96.944
Heater Amps	4.213
Room temperature	21.000
Manual cond mdot	5.646
Bourdon Pe, psig	22.000
Bourdon Pc, psia	150.000
Real time	1221.310
Oil fraction	0.001
Suction P loss	0.118
Stator res'tance	9.600
Winding Temp	73.000

Motor performance

Estimated RPM	2917.238
Winding loss	40.882
Rotor Loss etc.	52.994
Shaftwork	197.641
Bearing losses	40.940
Implied viscos'y	10.235
Sump viscosity	10.605

Refrigerant states

Position	Temp	Press	Volume	Enthalpy
dvo state	103.127	10.558	22.024	413.335
Discharge	99.484	10.558	21.720	410.651
Cond. start	93.990	10.558	21.255	406.596
Cond. end	31.697	9.984	0.778	230.213
Evap. end	-1.062	2.667	64.668	351.697
svc state	47.184	2.667	79.074	382.705

Condenser temperature distribution

R12 Ts	31.697	41.591	43.903	93.990
Water Ts	18.334	20.156	43.673	50.661

Discharge stub temperature 83.321

Powers, Watts

	measured	Xtalk	loss	R12 Dh
Compressor	291.516	3.587	25.107	262.851
Condenser	763.971	3.587	26.036	786.420
Evaporator	466.459	486.362		541.649

Compressor performance

Vertex	phi	Volume	Vsvc etc	mass,mg
1	124.702	2.709		122.989
2	188.162	0.600	0.631	28.615
3	223.417	2.229		28.189
4	33.839	9.788	9.780	123.684

Leakage loss on discharge, mg		2.673
Reference density ratio		3.590
R12 mass flow rate	g/s	4.459

Indicator diagram breakdown, Watts

Minimum work of compression	136.567
Suction excess PdV	6.756
Discharge excess PdV	7.999
Total leakage loss	5.378
Total indicated work	156.701

R12 Enthalpy gain summary, Watts

Total suction gas preheat	138.250
Calculated total PdV work	156.701
Discharge - suction exchange	12.676
Inner pipe, loss to the can	7.289
Outer pipe, loss to the can	3.869
Outer pipe, loss to ambient	14.211

The discharge valve was open for 3.626 ms.
The first rarefaction returns after 6.404 ms.

Vital oil flows only.   Normal superheat

Nominal Evaporating P 22psig. Nominal Condensing P 220psia.

Raw data

Current mA	2077.028
Voltage bits	2779.750
Room temperature	22.371
Cond. water out	73.535
Cond. water in	20.740
Evap. water in	4.004
Evap. water out	0.154
R12 Discharge	121.530
R12 Cond. entry	114.489
R12 Condensing	59.521
R12 Cond. exit	24.352
R12 Evap. entry	-3.168
R12 Evap. exit	-1.300
R12 Suction	8.748
Sump oil Temp.	73.657
Evap. flow rate	24.833
Cond. flow rate	3.384
R12 flow meter	0.102
Comp. power	304.981
P at suction	1.888
P at cond. end	14.215
P at evap start	1.640
P at discharge	14.404
PT supply volts	10.000
Water pump power	57.000
Heater volts	84.550
Heater Amps	3.690
Room temperature	22.250
Manual cond mdot	2.942
Bourdon Pe, psig	21.750
Bourdon Pc, psia	220.000
Real time	1457.150
Oil fraction	-1.000
Suction P loss	0.123
Stator res'tance	10.100
Winding Temp	95.500

Motor performance

Estimated RPM	2912.937
Winding loss	43.572
Rotor Loss etc.	54.137
Shaftwork	207.272
Bearing losses	38.751
Implied viscos'y	9.688
Sump viscosity	7.073

Refrigerant states

Position	Temp	Press	Volume	Enthalpy
dvo state	130.505	15.417	15.886	429.737
Discharge	122.822	15.417	15.426	423.850
Cond. start	114.489	15.417	14.915	417.433
Cond. end	24.352	15.228	0.761	223.020
Evap. end	-1.300	2.653	64.975	351.577
svc state	56.352	2.653	82.142	388.726

Condenser temperature distribution

R12 Ts	24.352	59.924	60.490	114.489
Water Ts	20.740	30.675	61.562	73.535

Discharge stub temperature   100.937

Powers, Watts

	measured	Xtalk	loss	R12 Dh
Compressor	304.981	4.768	43.190	257.025
Condenser	650.185	4.768	45.971	691.387
Evaporator	368.990	400.180		457.184

Compressor performance

Vertex	phi	Volume	Vsvc etc	mass,mg
1	137.073	1.846		116.211
2	188.162	0.600	0.619	38.882
3	235.177	3.120		37.989
4	37.335	9.614	9.649	117.465

Leakage loss on discharge, mg		4.078
Reference density ratio		5.171
R12 mass flow rate	g/s	3.556

Indicator diagram breakdown, Watts

Minimum work of compression	145.846
Suction excess PdV	5.951
Discharge excess PdV	5.239
Total leakage loss	11.485
Total indicated work	168.521

R12 Enthalpy gain summary, Watts

Total suction gas preheat	132.113
Calculated total PdV work	168.521
Discharge - suction exchange	17.495
Inner pipe, loss to the can	8.678
Outer pipe, loss to the can	4.962
Outer pipe, loss to ambient	17.860

The discharge valve was open for 2.923 ms.
The first rarefaction returns after 6.280 ms.

Vital oil flows only.   Normal superheat

Nominal Evaporating P 64psig. Nominal Condensing P 220psia.

Raw data

Current mA	2427.609
Voltage bits	2853.250
Room temperature	23.000
Cond. water out	64.659
Cond. water in	20.129
Evap. water in	40.872
Evap. water out	26.437
R12 Discharge	93.805
R12 Cond. entry	91.664
R12 Condensing	55.300
R12 Cond. exit	24.532
R12 Evap. entry	20.010
R12 Evap. exit	25.171
R12 Suction	26.096
Sump oil Temp.	60.914
Evap. flow rate	24.104
Cond. flow rate	9.912
R12 flow meter	9.010
Comp. power	417.864
P at suction	4.692
P at cond. end	12.680
P at evap start	4.565
P at discharge	14.400
PT supply volts	10.000
Water pump power	59.000
Heater volts	188.000
Heater Amps	8.000
Room temperature	22.500
Manual cond mdot	9.681
Bourdon Pe, psig	64.000
Bourdon Pc, psia	220.000
Real time	1708.250
Oil fraction	-1.000
Suction P loss	0.094
Stator res'tance	9.300
Winding Temp	59.500

Motor performance

Estimated RPM	2869.959
Winding loss	54.808
Rotor Loss etc.	65.378
Shaftwork	297.678
Bearing losses	36.799
Implied viscos'y	9.200
Sump viscosity	10.639

Refrigerant states

Position	Temp	Press	Volume	Enthalpy
dvo state	94.374	15.413	13.614	401.709
Discharge	93.659	15.413	13.565	401.141
Cond. start	91.664	15.413	13.428	399.552
Cond. end	24.532	13.693	0.762	223.194
Evap. end	25.171	5.578	32.278	363.555
svc state	49.787	5.578	36.238	380.670

Condenser temperature distribution

R12 Ts	24.532	55.115	60.477	91.664
Water Ts	20.129	27.994	58.040	64.659

Discharge stub temperature   83.899

Powers, Watts

	measured	Xtalk	loss	R12 Dh
Compressor	417.864	3.194	22.361	392.435
Condenser	1804.549	3.194	40.012	1841.367
Evaporator	1563.000	1456.538		1465.519

Compressor performance

Vertex	phi	Volume	Vsvc etc	mass,mg
1	112.248	3.712		272.672
2	188.162	0.600	0.645	47.218
3	214.996	1.680		46.366
4	29.160	10.000	9.940	274.296

Leakage loss on discharge, mg		7.174
Reference density ratio		2.662
R12 mass flow rate	g/s	10.441

Indicator diagram breakdown, Watts

Minimum work of compression	219.669
Suction excess PdV	13.549
Discharge excess PdV	18.115
Total leakage loss	9.546
Total indicated work	260.879

R12 Enthalpy gain summary, Watts

Total suction gas preheat	178.695
Calculated total PdV work	260.879
Discharge - suction exchange	15.677
Inner pipe, loss to the can	8.367
Outer pipe, loss to the can	3.125
Outer pipe, loss to ambient	13.464

The discharge valve was open for 4.409 ms.
The first rarefaction returns after 6.893 ms.

Vital oil flows only. Normal superheat

Nominal Evaporating P 63psig. Nominal Condensing P 150psia.

Raw data

Current mA	2104.294
Voltage bits	2793.911
Room temperature	22.049
Cond. water out	40.684
Cond. water in	17.293
Evap. water in	45.807
Evap. water out	28.902
R12 Discharge	74.379
R12 Cond. entry	72.754
R12 Condensing	30.926
R12 Cond. exit	19.959
R12 Evap. entry	19.260
R12 Evap. exit	28.078
R12 Suction	28.526
Sump oil Temp.	53.942
Evap. flow rate	23.709
Cond. flow rate	21.005
R12 flow meter	10.102
Comp. power	321.021
P at suction	4.542
P at cond. end	6.293
P at evap start	4.536
P at discharge	9.548
PT supply volts	10.000
Water pump power	57.000
Heater volts	202.100
Heater Amps	8.570
Room temperature	23.000
Manual cond mdot	20.625
Bourdon Pe, psig	63.000
Bourdon Pc, psia	150.000
Real time	1821.140
Oil fraction	-1.000
Suction P loss	0.003
Stator res'tance	9.000
Winding Temp	46.000

Motor performance

Estimated RPM	2904.934
Winding loss	39.852
Rotor Loss etc.	56.336
Shaftwork	224.833
Bearing losses	26.417
Implied viscos'y	6.604
Sump viscosity	13.718

Refrigerant states

Position	Temp	Press	Volume	Enthalpy
dvo state	72.649	10.561	19.362	390.706
Discharge	74.090	10.561	19.494	391.789
Cond. start	72.754	10.561	19.371	390.786
Cond. end	19.959	7.306	0.752	218.781
Evap. end	28.078	5.549	32.962	365.642
svc state	45.459	5.549	35.772	377.717

Condenser temperature distribution

R12 Ts	19.959	29.283	43.915	72.754
Water Ts	17.293	18.524	37.649	40.684

Discharge stub temperature 68.314

Powers, Watts

	measured	Xtalk	loss	R12 Dh
Compressor	321.021	1.512	10.587	308.994
Condenser	2019.534	1.512	14.685	2032.707
Evaporator	1788.997	1677.716		1735.570

Compressor performance

Vertex	phi	Volume	Vsvc etc	mass,mg
1	92.177	5.474		282.739
2	188.162	0.600	0.668	34.406
3	206.500	1.219		34.090
4	21.837	10.277	10.138	283.405

Leakage loss on discharge, mg		4.244
Reference density ratio		1.848
R12 mass flow rate	g/s	11.818

Indicator diagram breakdown, Watts

Minimum work of compression	153.505
Suction excess PdV	14.425
Discharge excess PdV	26.912
Total leakage loss	3.573
Total indicated work	198.416

R12 Enthalpy gain summary, Watts

Total suction gas preheat	142.693
Calculated total PdV work	198.416
Discharge - suction exchange	8.837
Inner pipe, loss to the can	5.280
Outer pipe, loss to the can	1.907
Outer pipe, loss to ambient	9.950

The discharge valve was open for 5.507 ms.
The first rarefaction returns after 6.898 ms.

Vital oil flows only.   Normal superheat

Nominal Evaporating P 40psig. Nominal Condensing P 150psia.

Raw data

Current mA	2145.775
Voltage bits	2852.650
Room temperature	21.385
Cond. water out	44.856
Cond. water in	18.492
Evap. water in	24.938
Evap. water out	14.413
R12 Discharge	81.032
R12 Cond. entry	78.841
R12 Condensing	38.046
R12 Cond. exit	20.080
R12 Evap. entry	9.214
R12 Evap. exit	12.391
R12 Suction	14.230
Sump oil Temp.	53.989
Evap. flow rate	23.858
Cond. flow rate	12.832
R12 flow meter	0.099
Comp. power	329.783
P at suction	3.071
P at cond. end	8.087
P at evap start	2.997
P at discharge	9.529
PT supply volts	10.000
Water pump power	60.000
Heater volts	155.020
Heater Amps	6.662
Room temperature	22.100
Manual cond mdot	12.547
Bourdon Pe, psig	40.000
Bourdon Pc, psia	150.000
Real time	1949.350
Oil fraction	-1.000
Suction P loss	0.120
Stator res'tance	9.100
Winding Temp	50.500

Motor performance

Estimated RPM	2902.179
Winding loss	41.900
Rotor Loss etc.	57.103
Shaftwork	230.780
Bearing losses	40.024
Implied viscos'y	10.006
Sump viscosity	13.693

Refrigerant states

Position	Temp	Press	Volume	Enthalpy
dvo state	81.436	10.542	20.200	397.304
Discharge	81.183	10.542	20.177	397.115
Cond. start	78.841	10.542	19.968	395.369
Cond. end	20.080	9.100	0.753	218.897
Evap. end	12.391	4.010	44.029	357.743
svc state	41.553	4.010	50.218	377.218

Condenser temperature distribution

R12 Ts	20.080	37.833	43.839	78.841
Water Ts	18.492	21.098	40.833	44.856

Discharge stub temperature   71.906

Powers, Watts

	measured	Xtalk	loss	R12 Dh
Compressor	329.783	2.072	14.502	313.217
Condenser	1384.702	2.072	21.238	1403.868
Evaporator	1092.743	1051.180		1104.542

Compressor performance

Vertex	phi	Volume	Vsvc etc	mass,mg
1	108.363	4.044		200.211
2	188.162	0.600	0.650	32.080
3	213.484	1.591		31.681
4	23.992	10.203	10.093	200.987

Leakage loss on discharge, mg		3.666
Reference density ratio		2.486
R12 mass flow rate	g/s	7.955

Indicator diagram breakdown, Watts

Minimum work of compression	159.786
Suction excess PdV	10.371
Discharge excess PdV	15.897
Total leakage loss	4.702
Total indicated work	190.756

R12 Enthalpy gain summary, Watts

Total suction gas preheat	154.933
Calculated total PdV work	190.756
Discharge - suction exchange	11.104
Inner pipe, loss to the can	6.294
Outer pipe, loss to the can	2.664
Outer pipe, loss to ambient	11.227

The discharge valve was open for 4.583 ms.
The first rarefaction returns after 6.735 ms.

Vital oil flows only. Normal superheat

Nominal Evaporating P 40psig. Nominal Condensing P 108psia.

Raw data

Current mA	1972.209
Voltage bits	2805.070
Room temperature	20.002
Cond. water out	24.716
Cond. water in	15.914
Evap. water in	28.179
Evap. water out	15.891
R12 Discharge	65.877
R12 Cond. entry	64.143
R12 Condensing	21.187
R12 Cond. exit	16.294
R12 Evap. entry	9.349
R12 Evap. exit	14.824
R12 Suction	16.148
Sump oil Temp.	48.575
Evap. flow rate	23.238
Cond. flow rate	41.911
R12 flow meter	0.099
Comp. power	274.560
P at suction	3.004
P at cond. end	4.786
P at evap start	3.000
P at discharge	6.614
PT supply volts	10.000
Water pump power	57.000
Heater volts	167.160
Heater Amps	7.200
Room temperature	21.500
Manual cond mdot	40.830
Bourdon Pe, psig	40.000
Bourdon Pc, psia	107.600
Real time	2132.360
Oil fraction	-1.000
Suction P loss	0.135
Stator res'tance	8.900
Winding Temp	41.500

Motor performance

Estimated RPM	2921.465
Winding loss	34.618
Rotor Loss etc.	51.914
Shaftwork	188.028
Bearing losses	40.127
Implied viscos'y	10.032
Sump viscosity	16.976

Refrigerant states

Position	Temp	Press	Volume	Enthalpy
dvo state	64.103	7.627	27.150	388.098
Discharge	65.794	7.627	27.348	389.309
Cond. start	64.143	7.627	27.155	388.126
Cond. end	16.294	5.799	0.745	215.278
Evap. end	14.824	4.013	44.540	359.367
svc state	38.315	4.013	49.525	375.052

Condenser temperature distribution

R12 Ts	16.294	20.797	30.915	64.143
Water Ts	15.914	16.134	23.483	24.716

Discharge stub temperature 60.055

Powers, Watts

	measured	Xtalk	loss	R12 Dh
Compressor	274.560	1.708	11.953	260.981
Condenser	1504.257	1.708	4.080	1506.630
Evaporator	1260.552	1195.297		1255.953

Compressor performance

Vertex	phi	Volume	Vsvc etc	mass,mg
1	90.861	5.592		205.950
2	188.162	0.600	0.670	24.608
3	206.311	1.210		24.440
4	18.236	10.389	10.217	206.305

Leakage loss on discharge, mg	2.326
Reference density ratio	1.824
R12 mass flow rate g/s	8.716

Indicator diagram breakdown, Watts

Minimum work of compression	113.713
Suction excess PdV	10.837
Discharge excess PdV	21.362
Total leakage loss	1.988
Total indicated work	147.901

R12 Enthalpy gain summary, Watts

Total suction gas preheat	136.712
Calculated total PdV work	147.901
Discharge - suction exchange	6.747
Inner pipe, loss to the can	4.060
Outer pipe, loss to the can	1.680
Outer pipe, loss to ambient	8.625

The discharge valve was open for 5.551 ms.
The first rarefaction returns after 6.774 ms.

Vital oil flows only. Normal superheat

Nominal Evaporating P 40psig. Nominal Condensing P 219psia.

Raw data

Current mA	2302.098
Voltage bits	2843.053
Room temperature	20.589
Cond. water out	68.197
Cond. water in	20.033
Evap. water in	23.212
Evap. water out	14.083
R12 Discharge	104.096
R12 Cond. entry	100.532
R12 Condensing	58.062
R12 Cond. exit	23.784
R12 Evap. entry	9.346
R12 Evap. exit	11.665
R12 Suction	14.903
Sump oil Temp.	64.983
Evap. flow rate	23.048
Cond. flow rate	6.247
R12 flow meter	0.098
Comp. power	388.048
P at suction	3.204
P at cond. end	13.705
P at evap start	3.024
P at discharge	14.408
PT supply volts	10.000
Water pump power	60.000
Heater volts	141.226
Heater Amps	6.108
Room temperature	1661.368
Manual cond mdot	6.020
Bourdon Pe, psig	40.368
Bourdon Pc, psia	219.737
Real time	52.590
Oil fraction	-1.000
Suction P loss	0.111
Stator res'tance	9.600
Winding Temp	73.000

Motor performance

Estimated RPM	2881.356
Winding loss	50.877
Rotor Loss etc.	62.709
Shaftwork	274.462
Bearing losses	45.067
Implied viscos'y	11.267
Sump viscosity	9.270

Refrigerant states

Position	Temp	Press	Volume	Enthalpy
dvo state	107.000	15.421	14.438	411.621
Discharge	104.173	15.421	14.256	409.415
Cond. start	100.532	15.421	14.018	406.563
Cond. end	23.784	14.718	0.760	222.469
Evap. end	11.665	4.037	43.546	357.204
svc state	49.625	4.037	51.486	382.586

Condenser temperature distribution

R12 Ts	23.784	58.365	60.500	100.532
Water Ts	20.033	29.298	59.506	68.197

Discharge stub temperature 90.217

Powers, Watts

	measured	Xtalk	loss	R12 Dh
Compressor	388.048	3.854	27.890	356.311
Condenser	1213.714	3.854	46.461	1256.322
Evaporator	922.595	880.733		919.479

Compressor performance

Vertex	phi	Volume	Vsvc etc	mass,mg
1	123.947	2.766		191.586
2	188.162	0.600	0.632	43.652
3	223.002	2.200		42.731
4	29.407	9.989	9.944	193.140

Leakage loss on discharge, mg		5.826
Reference density ratio		3.566
R12 mass flow rate	g/s	6.824

Indicator diagram breakdown, Watts

Minimum work of compression	198.144
Suction excess PdV	9.584
Discharge excess PdV	10.680
Total leakage loss	10.987
Total indicated work	229.394

R12 Enthalpy gain summary, Watts

Total suction gas preheat	173.216
Calculated total PdV work	229.394
Discharge - suction exchange	16.979
Inner pipe, loss to the can	8.750
Outer pipe, loss to the can	3.867
Outer pipe, loss to ambient	15.601

The discharge valve was open for 3.714 ms.
The first rarefaction returns after 6.647 ms.

Vital oil flows only. Normal superheat

Nominal Evaporating P 78psig. Nominal Condensing P 220psia.

Raw data

Current mA	2401.147
Voltage bits	2821.794
Room temperature	20.683
Cond. water out	63.119
Cond. water in	18.745
Evap. water in	49.320
Evap. water out	33.638
R12 Discharge	91.464
R12 Cond. entry	89.498
R12 Condensing	52.993
R12 Cond. exit	23.552
R12 Evap. entry	24.850
R12 Evap. exit	32.634
R12 Suction	33.060
Sump oil Temp.	61.746
Evap. flow rate	27.613
Cond. flow rate	11.994
R12 flow meter	0.094
Comp. power	429.622
P at suction	5.539
P at cond. end	11.911
P at evap start	5.465
P at discharge	14.407
PT supply volts	10.000
Water pump power	59.000
Heater volts	212.400
Heater Amps	9.000
Room temperature	21.000
Manual cond mdot	11.765
Bourdon Pe, psig	78.000
Bourdon Pc, psia	220.000
Real time	228.140
Oil fraction	0.000
Suction P loss	0.009
Stator res'tance	9.300
Winding Temp	59.500

Motor performance

Estimated RPM	2864.129
Winding loss	53.619
Rotor Loss etc.	66.574
Shaftwork	309.428
Bearing losses	36.935
Implied viscos'y	9.234
Sump viscosity	10.337

Refrigerant states

Position	Temp	Press	Volume	Enthalpy
dvo state	91.008	15.420	13.374	399.019
Discharge	91.102	15.420	13.381	399.094
Cond. start	89.498	15.420	13.269	397.810
Cond. end	23.552	12.924	0.760	222.245
Evap. end	32.634	6.478	28.203	367.254
svc state	52.421	6.478	31.021	381.290

Condenser temperature distribution

R12 Ts	23.552	52.554	60.499	89.498
Water Ts	18.745	26.162	56.935	63.119

Discharge stub temperature 83.117

Powers, Watts

	measured	Xtalk	loss	R12 Dh
Compressor	429.622	3.316	23.214	403.197
Condenser	2185.345	3.316	41.159	2223.188
Evaporator	1970.600	1812.694		1836.253

Compressor performance

Vertex	phi	Volume	Vsvc etc	mass,mg
1	105.396	4.302		321.671
2	188.162	0.600	0.653	48.632
3	211.604	1.484		47.847
4	26.283	10.117	10.028	323.255

Leakage loss on discharge, mg		7.767
Reference density ratio		2.319
R12 mass flow rate	g/s	12.663

Indicator diagram breakdown, Watts

Minimum work of compression	224.501
Suction excess PdV	15.778
Discharge excess PdV	23.555
Total leakage loss	8.659
Total indicated work	272.493

R12 Enthalpy gain summary, Watts

Total suction gas preheat	177.745
Calculated total PdV work	272.493
Discharge - suction exchange	14.662
Inner pipe, loss to the can	7.942
Outer pipe, loss to the can	2.744
Outer pipe, loss to ambient	13.520

The discharge valve was open for 4.816 ms.
The first rarefaction returns after 6.967 ms.

Vital oil flows only.   High superheat

Nominal Evaporating P 6psig. Nominal Condensing P 78psia.

Raw data

Current mA	1760.242
Voltage bits	2741.107
Room temperature	20.514
Cond. water out	20.872
Cond. water in	15.824
Evap. water in	2.709
Evap. water out	-1.450
R12 Discharge	104.279
R12 Cond. entry	95.478
R12 Condensing	19.270
R12 Cond. exit	16.378
R12 Evap. entry	-18.561
R12 Evap. exit	-0.275
R12 Suction	13.578
Sump oil Temp.	73.274
Evap. flow rate	15.310
Cond. flow rate	23.160
R12 flow meter	0.094
Comp. power	199.911
P at suction	0.503
P at cond. end	4.516
P at evap start	0.417
P at discharge	4.740
PT supply volts	10.000
Water pump power	56.000
Heater volts	60.333
Heater Amps	2.638
Room temperature	22.000
Manual cond mdot	22.681
Bourdon Pe, psig	5.800
Bourdon Pc, psia	78.000
Real time	316.000
Oil fraction	-1.000
Suction P loss	0.164
Stator res'tance	10.100
Winding Temp	95.500

Motor performance

Estimated RPM	2948.736
Winding loss	31.294
Rotor Loss etc.	46.787
Shaftwork	121.830
Bearing losses	31.603
Implied viscos'y	7.901
Sump viscosity	7.154

Refrigerant states

Position	Temp	Press	Volume	Enthalpy
dvo state	110.657	5.753	43.593	422.847
Discharge	106.038	5.753	42.970	419.596
Cond. start	95.478	5.753	41.537	412.191
Cond. end	16.378	5.529	0.745	215.358
Evap. end	-1.450	1.430	125.299	354.004
svc state	56.053	1.430	155.023	389.916

Condenser temperature distribution

R12 Ts	16.378	19.111	20.514	95.478
Water Ts	15.824	15.891	19.532	20.872

Discharge stub temperature   89.489

Powers, Watts

	measured	Xtalk	loss	R12 Dh
Compressor	199.911	5.310	37.171	157.437
Condenser	479.265	5.310	-1.505	472.449
Evaporator	215.159	266.574		332.786

Compressor performance

Vertex	phi	Volume	Vsvc etc	mass,mg
1	123.581	2.794		64.098
2	188.162	0.600	0.633	14.498
3	223.421	2.229		14.380
4	28.956	10.008	9.966	64.289

Leakage loss on discharge, mg		0.760
Reference density ratio		3.556
R12 mass flow rate	g/s	2.400

Indicator diagram breakdown, Watts

Minimum work of compression	79.042
Suction excess PdV	3.968
Discharge excess PdV	5.558
Total leakage loss	1.659
Total indicated work	90.226

R12 Enthalpy gain summary, Watts

Total suction gas preheat	86.198
Calculated total PdV work	90.226
Discharge - suction exchange	8.568
Inner pipe, loss to the can	4.794
Outer pipe, loss to the can	3.314
Outer pipe, loss to ambient	14.460

The discharge valve was open for 3.650 ms.
The first rarefaction returns after 6.072 ms.

Vital oil flows only. High superheat

Nominal Evaporating P 5psig. Nominal Condensing P 150psia.

Raw data

Current mA	1802.121
Voltage bits	2769.925
Room temperature	21.450
Cond. water out	57.114
Cond. water in	20.220
Evap. water in	-0.362
Evap. water out	-3.266
R12 Discharge	131.055
R12 Cond. entry	116.044
R12 Condensing	43.409
R12 Cond. exit	22.387
R12 Evap. entry	-18.244
R12 Evap. exit	-1.762
R12 Suction	20.291
Sump oil Temp.	90.197
Evap. flow rate	13.004
Cond. flow rate	2.343
R12 flow meter	0.092
Comp. power	212.958
P at suction	0.627
P at cond. end	9.505
P at evap start	0.443
P at discharge	9.593
PT supply volts	10.000
Water pump power	56.000
Heater volts	29.800
Heater Amps	1.300
Room temperature	21.000
Manual cond mdot	2.080
Bourdon Pe, psig	5.850
Bourdon Pc, psia	150.250
Real time	536.450
Oil fraction	-1.000
Suction P loss	0.158
Stator res'tance	10.800
Winding Temp	127.000

Motor performance

Estimated RPM	2945.274
Winding loss	35.075
Rotor Loss etc.	47.204
Shaftwork	130.680
Bearing losses	34.721
Implied viscos'y	8.680
Sump viscosity	4.541

Refrigerant states

Position	Temp	Press	Volume	Enthalpy
dvo state	147.253	10.606	25.397	445.778
Discharge	134.268	10.606	24.400	436.204
Cond. start	116.044	10.606	22.963	422.797
Cond. end	22.387	10.518	0.757	221.119
Evap. end	-3.266	1.456	122.004	352.853
svc state	65.721	1.456	156.977	396.156

Condenser temperature distribution

R12 Ts	22.387	43.744	44.092	116.044
Water Ts	20.220	24.106	47.186	57.114

Discharge stub temperature 110.438

Powers, Watts

	measured	Xtalk	loss	R12 Dh
Compressor	212.958	7.510	64.248	141.204
Condenser	321.231	7.510	27.942	341.663
Evaporator	94.740	158.062		223.171

Compressor performance

Vertex	phi	Volume	Vsvc etc	mass,mg
1	142.381	1.530		60.230
2	188.162	0.600	0.614	24.161
3	242.505	3.732		23.771
4	40.037	9.469	9.532	60.724

Leakage loss on discharge, mg		1.555
Reference density ratio		6.181
R12 mass flow rate	g/s	1.694

Indicator diagram breakdown, Watts

Minimum work of compression	84.066
Suction excess PdV	3.337
Discharge excess PdV	3.072
Total leakage loss	5.485
Total indicated work	95.960

R12 Enthalpy gain summary, Watts

Total suction gas preheat	73.358
Calculated total PdV work	95.960
Discharge - suction exchange	13.627
Inner pipe, loss to the can	5.665
Outer pipe, loss to the can	4.456
Outer pipe, loss to ambient	18.256

The discharge valve was open for 2.591 ms.
The first rarefaction returns after 5.902 ms.

Vital oil flows only. High superheat

Nominal Evaporating P 5psig. Nominal Condensing P 108psia.

Raw data

Current mA	1771.318
Voltage bits	2781.800
Room temperature	21.626
Cond. water out	37.424
Cond. water in	19.585
Evap. water in	1.673
Evap. water out	-2.535
R12 Discharge	119.951
R12 Cond. entry	108.185
R12 Condensing	30.546
R12 Cond. exit	20.554
R12 Evap. entry	-18.505
R12 Evap. exit	-1.159
R12 Suction	16.799
Sump oil Temp.	83.579
Evap. flow rate	12.111
Cond. flow rate	5.874
R12 flow meter	0.092
Comp. power	209.529
P at suction	0.554
P at cond. end	6.561
P at evap start	0.429
P at discharge	6.721
PT supply volts	10.000
Water pump power	57.000
Heater volts	48.500
Heater Amps	2.140
Room temperature	22.000
Manual cond mdot	5.721
Bourdon Pe, psig	5.800
Bourdon Pc, psia	109.000
Real time	744.300
Oil fraction	0.010
Suction P loss	0.156
Stator res'tance	10.500
Winding Temp	113.500

Motor performance

Estimated RPM	2945.761
Winding loss	32.944
Rotor Loss etc.	47.140
Shaftwork	129.445
Bearing losses	29.615
Implied viscos'y	7.404
Sump viscosity	5.367

Refrigerant states

Position	Temp	Press	Volume	Enthalpy
dvo state	129.067	7.734	33.709	434.480
Discharge	121.410	7.734	32.927	428.968
Cond. start	108.185	7.734	31.557	419.480
Cond. end	20.554	7.574	0.754	219.353
Evap. end	-2.535	1.442	123.659	353.324
svc state	61.667	1.442	156.542	393.534

Condenser temperature distribution

R12 Ts	20.554	30.649	31.451	108.185
Water Ts	19.585	20.460	32.488	37.424

Discharge stub temperature 101.978

Powers, Watts

	measured	Xtalk	loss	R12 Dh
Compressor	209.529	5.728	40.094	163.719
Condenser	427.211	5.728	11.661	433.145
Evaporator	160.790	213.306		289.961

Compressor performance

Vertex	phi	Volume	Vsvc etc	mass,mg
1	132.507	2.146		63.651
2	188.162	0.600	0.623	18.472
3	231.887	2.858		18.260
4	27.890	10.053	10.012	63.960

Leakage loss on discharge, mg		1.093
Reference density ratio		4.644
R12 mass flow rate	g/s	2.164

Indicator diagram breakdown, Watts

Minimum work of compression	88.622
Suction excess PdV	3.725
Discharge excess PdV	4.437
Total leakage loss	3.046
Total indicated work	99.830

R12 Enthalpy gain summary, Watts

Total suction gas preheat	87.028
Calculated total PdV work	99.830
Discharge - suction exchange	11.001
Inner pipe, loss to the can	5.367
Outer pipe, loss to the can	3.832
Outer pipe, loss to ambient	16.703

The discharge valve was open for 3.149 ms.
The first rarefaction returns after 5.975 ms.

Vital oil flows only. High superheat

Nominal Evaporating P 0psig. Nominal Condensing P 79psia.

Raw data

Current mA	1669.326
Voltage bits	2746.007
Room temperature	21.970
Cond. water out	23.468
Cond. water in	16.672
Evap. water in	-3.148
Evap. water out	-3.634
R12 Discharge	117.970
R12 Cond. entry	101.737
R12 Condensing	20.696
R12 Cond. exit	17.423
R12 Evap. entry	-26.008
R12 Evap. exit	-1.866
R12 Suction	23.626
Sump oil Temp.	87.326
Evap. flow rate	65.180
Cond. flow rate	10.418
R12 flow meter	0.093
Comp. power	167.373
P at suction	0.103
P at cond. end	4.728
P at evap start	-0.006
P at discharge	4.821
PT supply volts	10.000
Water pump power	56.000
Heater volts	0.000
Heater Amps	0.000
Room temperature	22.214
Manual cond mdot	10.614
Bourdon Pe, psig	0.000
Bourdon Pc, psia	79.214
Real time	1331.030
Oil fraction	0.013
Suction P loss	0.179
Stator res'tance	10.700
Winding Temp	122.500

Motor performance

Estimated RPM	2960.196
Winding loss	29.817
Rotor Loss etc.	46.030
Shaftwork	91.526
Bearing losses	20.489
Implied viscos'y	5.122
Sump viscosity	4.875

Refrigerant states

Position	Temp	Press	Volume	Enthalpy
dvo state	129.175	5.834	45.389	435.903
Discharge	119.785	5.834	44.161	429.234
Cond. start	101.737	5.834	41.768	416.507
Cond. end	17.423	5.741	0.747	216.354
Evap. end	-3.634	1.007	178.607	353.535
svc state	59.756	1.007	224.116	392.763

Condenser temperature distribution

R12 Ts	17.423	20.442	21.011	101.737
Water Ts	16.672	16.770	21.553	23.468

Discharge stub temperature 101.530

Powers, Watts

	measured	Xtalk	loss	R12 Dh
Compressor	167.373	7.071	49.498	110.808
Condenser	301.933	7.071	-1.879	292.983
Evaporator	56.000	132.492		200.805

Compressor performance

Vertex	phi	Volume	Vsvc etc	mass,mg
1	134.766	1.994		43.941
2	188.162	0.600	0.621	13.679
3	234.159	3.038		13.558
4	31.508	9.897	9.886	44.111

Leakage loss on discharge, mg		0.592
Reference density ratio		4.938
R12 mass flow rate	g/s	1.464

Indicator diagram breakdown, Watts

Minimum work of compression	63.148
Suction excess PdV	2.765
Discharge excess PdV	3.362
Total leakage loss	1.762
Total indicated work	71.036

R12 Enthalpy gain summary, Watts

Total suction gas preheat	57.422
Calculated total PdV work	71.036
Discharge - suction exchange	9.295
Inner pipe, loss to the can	3.829
Outer pipe, loss to the can	3.273
Outer pipe, loss to ambient	15.357

The discharge valve was open for 3.006 ms.
The first rarefaction returns after 5.904 ms.

Vital oil flows only. Suction system bypassed

Nominal Evaporating P 21psig. Nominal Condensing P 150psia.

Raw data

Current mA	1983.090
Voltage bits	2778.733
Room temperature	21.123
Cond. water out	49.792
Cond. water in	20.994
Evap. water in	6.046
Evap. water out	0.502
R12 Discharge	98.973
R12 Cond. entry	94.618
R12 Condensing	42.577
R12 Cond. exit	22.512
R12 Evap. entry	-3.215
R12 Evap. exit	-1.819
R12 Suction	4.894
Sump oil Temp.	58.336
Evap. flow rate	22.064
Cond. flow rate	7.016
R12 flow meter	0.131
Comp. power	286.693
P at suction	1.778
P at cond. end	9.249
P at evap start	1.597
P at discharge	9.680
PT supply volts	10.000
Water pump power	57.000
Heater volts	99.533
Heater Amps	4.333
Room temperature	23.000
Manual cond mdot	6.638
Bourdon Pe, psig	21.167
Bourdon Pc, psia	150.000
Real time	1813.000
Oil fraction	-1.000
Suction P loss	0.161
Stator res'tance	9.600
Winding Temp	73.000

Motor performance

Estimated RPM	2917.911
Winding loss	37.753
Rotor Loss etc.	52.819
Shaftwork	196.121
Bearing losses	40.160
Implied viscos'y	10.040
Sump viscosity	11.654

Refrigerant states

Position	Temp	Press	Volume	Enthalpy
dvo state	104.195	10.693	21.799	413.998
Discharge	100.258	10.693	21.474	411.093
Cond. start	94.618	10.693	21.003	406.926
Cond. end	22.512	10.262	0.758	221.239
Evap. end	-1.819	2.610	65.970	351.339
svc state	46.852	2.610	80.789	382.560

Condenser temperature distribution

R12 Ts	22.512	42.723	44.433	94.618
Water Ts	20.994	24.107	43.854	49.792

Discharge stub temperature 82.633

Powers, Watts

	measured	Xtalk	loss	R12 Dh
Compressor	286.693	2.686	18.802	265.238
Condenser	800.172	2.686	26.739	824.225
Evaporator	488.256	512.091		577.487

Compressor performance

Vertex	phi	Volume	Vsvc etc	mass,mg
1	125.097	2.679		122.885
2	188.162	0.600	0.631	28.890
3	224.400	2.298		28.449
4	29.484	9.986	9.986	123.606

Leakage loss on discharge, mg		2.721
Reference density ratio		3.706
R12 mass flow rate	g/s	4.439

Indicator diagram breakdown, Watts

Minimum work of compression	139.549
Suction excess PdV	2.854
Discharge excess PdV	7.920
Total leakage loss	5.638
Total indicated work	155.961

R12 Enthalpy gain summary, Watts

Total suction gas preheat	138.584
Calculated total PdV work	155.961
Discharge - suction exchange	12.882
Inner pipe, loss to the can	7.933
Outer pipe, loss to the can	4.216
Outer pipe, loss to ambient	14.285

The discharge valve was open for 3.602 ms.
The first rarefaction returns after 6.397 ms.

Vital oil flows only. Suction system bypassed

Nominal Evaporating P 40psig. Nominal Condensing P 150psia.

Raw data

Current mA	2094.493
Voltage bits	2779.015
Room temperature	21.153
Cond. water out	45.005
Cond. water in	18.781
Evap. water in	27.801
Evap. water out	15.202
R12 Discharge	79.469
R12 Cond. entry	77.784
R12 Condensing	38.145
R12 Cond. exit	20.315
R12 Evap. entry	9.836
R12 Evap. exit	13.756
R12 Suction	15.268
Sump oil Temp.	46.997
Evap. flow rate	21.306
Cond. flow rate	13.808
R12 flow meter	6.328
Comp. power	324.635
P at suction	3.126
P at cond. end	8.112
P at evap start	3.050
P at discharge	9.662
PT supply volts	10.000
Water pump power	57.000
Heater volts	160.940
Heater Amps	6.930
Room temperature	23.000
Manual cond mdot	13.109
Bourdon Pe, psig	40.200
Bourdon Pc, psia	150.000
Real time	2159.000
Oil fraction	-1.000
Suction P loss	0.146
Stator res'tance	9.200
Winding Temp	55.000

Motor performance

Estimated RPM	2903.662
Winding loss	40.359
Rotor Loss etc.	56.690
Shaftwork	227.585
Bearing losses	35.890
Implied viscos'y	8.973
Sump viscosity	18.131

Refrigerant states

Position	Temp	Press	Volume	Enthalpy
dvo state	80.446	10.675	19.819	396.413
Discharge	80.081	10.675	19.787	396.141
Cond. start	77.784	10.675	19.582	394.422
Cond. end	20.315	9.125	0.753	219.123
Evap. end	13.756	4.063	43.683	358.555
svc state	40.523	4.063	49.302	376.456

Condenser temperature distribution

R12 Ts	20.315	37.940	44.363	77.784
Water Ts	18.781	21.373	41.145	45.005

Discharge stub temperature 69.003

Powers, Watts

	measured	Xtalk	loss	R12 Dh
Compressor	324.635	1.463	10.242	312.938
Condenser	1439.025	1.463	21.969	1459.531
Evaporator	1172.314	1123.696		1160.904

Compressor performance

Vertex	phi	Volume	Vsvc etc	mass,mg
1	107.313	4.135		208.645
2	188.162	0.600	0.651	32.755
3	213.545	1.594		32.341
4	20.286	10.327	10.327	209.470

Leakage loss on discharge, mg		3.847
Reference density ratio		2.488
R12 mass flow rate	g/s	8.326

Indicator diagram breakdown, Watts

Minimum work of compression	166.167
Suction excess PdV	3.907
Discharge excess PdV	16.708
Total leakage loss	4.912
Total indicated work	191.695

R12 Enthalpy gain summary, Watts

Total suction gas preheat	149.042
Calculated total PdV work	191.695
Discharge - suction exchange	11.206
Inner pipe, loss to the can	7.773
Outer pipe, loss to the can	3.230
Outer pipe, loss to ambient	11.081

The discharge valve was open for 4.641 ms.
The first rarefaction returns after 6.764 ms.

Vital oil flows only.   Suction system bypassed

Nominal Evaporating P 63psig. Nominal Condensing P 150psia.

Raw data

Current mA	2055.990
Voltage bits	2753.380
Room temperature	21.378
Cond. water out	40.164
Cond. water in	17.131
Evap. water in	49.913
Evap. water out	29.311
R12 Discharge	72.479
R12 Cond. entry	71.243
R12 Condensing	30.766
R12 Cond. exit	18.383
R12 Evap. entry	20.279
R12 Evap. exit	28.450
R12 Suction	28.717
Sump oil Temp.	48.435
Evap. flow rate	21.228
Cond. flow rate	22.568
R12 flow meter	11.316
Comp. power	317.494
P at suction	4.589
P at cond. end	6.400
P at evap start	4.586
P at discharge	9.656
PT supply volts	10.000
Water pump power	57.000
Heater volts	212.000
Heater Amps	9.000
Room temperature	23.000
Manual cond mdot	22.101
Bourdon Pe, psig	63.125
Bourdon Pc, psia	150.000
Real time	2.260
Oil fraction	-1.000
Suction P loss	0.116
Stator res'tance	9.000
Winding Temp	46.000

Motor performance

Estimated RPM	2905.636
Winding loss	38.044
Rotor Loss etc.	56.141
Shaftwork	223.309
Bearing losses	25.307
Implied viscos'y	6.327
Sump viscosity	17.075

Refrigerant states

Position	Temp	Press	Volume	Enthalpy
dvo state	71.121	10.669	18.989	389.418
Discharge	72.526	10.669	19.118	390.478
Cond. start	71.243	10.669	19.000	389.510
Cond. end	18.383	7.413	0.749	217.271
Evap. end	28.450	5.599	32.686	365.816
svc state	43.830	5.599	35.162	376.517

Condenser temperature distribution

R12 Ts	18.383	29.831	44.339	71.243
Water Ts	17.131	18.615	37.369	40.164

Discharge stub temperature   65.786

Powers, Watts

	measured	Xtalk	loss	R12 Dh
Compressor	317.494	1.298	9.084	307.195
Condenser	2130.949	1.298	15.751	2145.402
Evaporator	1965.000	1830.709		1850.268

Compressor performance

Vertex	phi	Volume	Vsvc etc	mass,mg
1	90.342	5.638		296.887
2	188.162	0.600	0.670	35.186
3	206.628	1.226		34.857
4	15.403	10.465	10.465	297.617

Leakage loss on discharge, mg		4.493
Reference density ratio		1.852
R12 mass flow rate	g/s	12.456

Indicator diagram breakdown, Watts

Minimum work of compression	160.694
Suction excess PdV	4.973
Discharge excess PdV	28.564
Total leakage loss	3.771
Total indicated work	198.002

R12 Enthalpy gain summary, Watts

Total suction gas preheat	133.299
Calculated total PdV work	198.002
Discharge - suction exchange	8.954
Inner pipe, loss to the can	6.409
Outer pipe, loss to the can	2.267
Outer pipe, loss to ambient	9.795

The discharge valve was open for 5.611 ms.
The first rarefaction returns after 6.938 ms.

Vital oil flows only.   Suction system bypassed

Nominal Evaporating P 6psig. Nominal Condensing P 150psia.

Raw data

Current mA	1788.494
Voltage bits	2781.367
Room temperature	21.677
Cond. water out	55.159
Cond. water in	21.956
Evap. water in	0.367
Evap. water out	-1.840
R12 Discharge	135.355
R12 Cond. entry	117.852
R12 Condensing	43.852
R12 Cond. exit	23.563
R12 Evap. entry	-18.516
R12 Evap. exit	-0.273
R12 Suction	23.064
Sump oil Temp.	94.165
Evap. flow rate	15.695
Cond. flow rate	2.458
R12 flow meter	0.092
Comp. power	202.215
P at suction	0.618
P at cond. end	9.581
P at evap start	0.427
P at discharge	9.629
PT supply volts	10.000
Water pump power	57.000
Heater volts	29.000
Heater Amps	1.260
Room temperature	23.000
Manual cond mdot	2.070
Bourdon Pe, psig	6.000
Bourdon Pc, psia	150.000
Real time	557.100
Oil fraction	-1.000
Suction P loss	0.157
Stator res'tance	11.000
Winding Temp	136.000

Motor performance

Estimated RPM	2949.327
Winding loss	35.186
Rotor Loss etc.	46.725
Shaftwork	120.305
Bearing losses	32.978
Implied viscos'y	8.244
Sump viscosity	4.132

Refrigerant states

Position	Temp	Press	Volume	Enthalpy
dvo state	152.849	10.642	25.728	449.890
Discharge	138.396	10.642	24.628	439.220
Cond. start	117.852	10.642	23.021	424.097
Cond. end	23.563	10.594	0.760	222.256
Evap. end	-1.840	1.440	124.212	353.748
svc state	70.257	1.440	161.055	399.136

Condenser temperature distribution

R12 Ts	23.563	44.045	44.234	117.852
Water Ts	21.956	25.314	46.026	55.159

Discharge stub temperature   113.970

Powers, Watts

	measured	Xtalk	loss	R12 Dh
Compressor	202.215	7.853	64.139	130.227
Condenser	287.735	7.853	27.652	307.534
Evaporator	93.540	145.021		200.348

Compressor performance

Vertex	phi	Volume	Vsvc etc	mass,mg
1	143.865	1.448		56.272
2	188.162	0.600	0.613	23.804
3	242.981	3.772		23.423
4	45.725	9.138	9.138	56.741

Leakage loss on discharge, mg		1.468
Reference density ratio		6.260
R12 mass flow rate	g/s	1.524

Indicator diagram breakdown, Watts

Minimum work of compression	77.332
Suction excess PdV	1.853
Discharge excess PdV	2.805
Total leakage loss	5.338
Total indicated work	87.327

R12 Enthalpy gain summary, Watts

Total suction gas preheat	69.154
Calculated total PdV work	87.327
Discharge - suction exchange	13.633
Inner pipe, loss to the can	5.430
Outer pipe, loss to the can	4.473
Outer pipe, loss to ambient	18.569

The discharge valve was open for 2.503 ms.
The first rarefaction returns after 5.850 ms.

Chapter 11. Further work, including suggestions to improve performance

11.1 Introduction

The purpose of this chapter is to suggest ways of improving the heat pump's efficiency, starting with a very simple suggestion, progressing through modifications using off-the-shelf parts, and ending with suggestions for more experimental, speculative modifications. All the proposals suggested here have either followed directly from, or at least been influenced by the observations made in the previous 10 chapters.

11.2 Use of standard components

Before considering the compressor, there are a couple of modifications to the refrigerant circuit which are worth recommending.

Evaporator position

Firstly, as mentioned in chapter 10, the evaporator and associated pipework should be designed to avoid oil accumulating, as this results in an evaporating pressure reduction due to Raoult's law.

Using an intercooler

Figure 2.4 shows that, over the credible range of evaporating temperature, the COP of an R12 circuit with subcooling to around 25C is insensensitive to suction gas superheating. This theoretical result has been borne out experimentally, there being little difference in COP between the high & normal superheat tests (runs 1 & 2) of the final set of experiments. Table 11.1 summarises the COP figures.

Suction pressure	Discharge pressure	COPs Run 1	Run 2
21	90	3.61	3.68
21	150	2.85	2.87
21	220	2.24	2.29
40	108	5.50	5.48
40	150	4.37	4.31
40	220	3.34	3.44
64	150	6.35	6.24
64	220	4.58	4.50

Table 11.1

These COP figures are near-raw data. They come from the ratio of the refrigerant side condenser power and the measured compressor power, with no adjustment for variations in either subcooling or discharge pipe heat loss.

If an ambient source is used for both evaporation *and* superheating, then setting the superheat high has the effect of depressing the evaporating temperature. Alternatively, if an intercooler is used, then the superheat is furnished by transfer from the liquid line, so giving the freedom to set the superheat high without compromising the evaporating temperature.

In view of the desirability of minimising liquid refrigerant return to the sump, it thus seems beneficial always to use an intercooler, and to set the TXV for a high superheat. By attaching the vapour pressure bulb to the suction line, between the intercooler and the compressor, it becomes possible to satisfy the otherwise conflicting requirements of having a flooded evaporator *and* a high superheat.

Isolating the compressor

On the same theme, of minimising refrigerant in the sump, the migration of refrigerant to the sump may be avoided by using valves in the suction and discharge lines to isolate the compressor during periods of quiescence. This is equivalent to the more traditional practice of keeping the sump warm using a heater, but isolation is preferable for its avoiding any further waste of primary energy.

This simple suggestion has implications beyond its face value. By avoiding the need to boil out the sump at startup, the only objection to using a more efficient motor is eliminated. The other advantage of avoiding refrigerant migration to the sump is that, upon starting up, normal operation can become established quickly, without the long initial period of refrigerant starvation which results when starting with a saturated sump.

The proposed use of compressor isolating valves can thus eliminate one of the losses caused by start - stop operation, and so make developing a variable capacity compressor less important.

More efficient motor

Compressors are available, off the shelf, boasting more efficient motors than in the Danfoss SC10H. Danfoss themselves make the 'SC10HH' which has electrical losses lower by almost 30 Watts. Many contributors to the Compressor technology Conference at Purdue have been concerned with the development of more efficient compressors. In particular, two groups working independently managed to raise the refrigerating COP from 1 to 1.5 for the very testing operating condition of -10F evaporating and 130 F condensing. (74,75). In both cases the adoption of a more efficient motor made a major contribution to this improvement, and in particular, the avoidable loss that results from a low power factor was highlighted. As ilustration of this point, consider the Danfoss SC10H which takes 2 Amps at 300 Watts. At a unit power factor only 1.25 Amps would be necessary. With a 10 Ohm stator resistance, this would drop the stator Joule heating from 40 Watts to 16 Watts.

The only penalty associated with the more efficient motors is their reduced tolerance to a high starting torque. The resulting danger of stalling at startup can be avoided by opening a by-pass valve from discharge to suction.

Detailed comparison of high efficiency compressors with Danfoss' SC10H

The operating condition for the tests mentioned in (74) & (75) corresponds to a suction pressure of 1.35 Bar and a discharge pressure of 13.6 Bar. In the final set of experiments, the closest test was the combination of 1.45 Bar suction & 10.58 Bar discharge. For the unmodified compressor, the power consumption breakdown is listed below, and these figures are compared with estimates for one of the high efficiency compressors.

	SC10H	High efficiency
Minimum indicated work	85.3	120
Gas flow losses	12.0	16
Bearing losses	43.9	32
Electrical losses	88.0	56
Power consumption	229.2	224
Refrigerating capacity	227.0	284

The figures for the Danfoss SC10H come from page 384. The figures for the high efficiency compressor have been pieced together from the limited information available. The power consumption of 224 Watt was quoted, and the refrigerant flow rate was given as 2.168g/s. This is 25% higher than the 1.731 g/s estimated for the SC10H. This flow rate ratio was used to estimate evaporating capacity and minimum compression work, using the SC10H results. This minimum compression work was further raised by 12% to allow for the higher discharge pressure used in the test of the high efficiency compressor. To estimate motor losses, an efficiency of 75% was taken, on the basis of figures quoted in (75). The gas flow losses were guessed, again, on the basis of the flow ratio, and this just left the bearing losses to estimate from energy conservation.

The contrast between these sets of figures is quite dramatic. The high efficiency compressor does 40% more useful work for the same power consumption. This is essentially equivalent to the author's statement that the new compressor was 40% more efficient than the model it superseded. This shows that his original compressor had a performance similar to the Danfoss SC10H.

The suggestion that compressors can be made much more efficient is thus beyond debate, since this has already been demonstrated.

Summary of recommendations for an improved heat pump

Design the low pressure side to avoid oil accumulating in the evaporator and pipework.

Use an intercooler and set the TXV for a high superheat.

Use the most efficient compressor available, and worry not about starting torque.

Use valves in the suction and discharge lines to isolate the compressor when not in use.

Use a discharge - suction by-pass valve to minimise the starting torque.

Use an automatic control system to work the valve gear.

The above suggestions can all be implemented off the shelf, and probably have been already. The proposed system is obviously more expensive than the basic heat pump, but it has a better chance of having running costs which can compete with alternative heating systems. If a ground source is used, then the added cost of these proposed refinements would be small in comparison with the cost of installing the ground coil.

11.3 Less conservative modifications

An important feature of the high efficiency compressor in (74) was its use of a suction muffler to minimise the suction gas pre-heat. This feature necessitates using a high TXV superheat setting, because it results in the loss of the safety feature that any returning liquid runs into the sump. However, as explained above, this can be done with impunity if an intercooler is used. Although it has been shown that waste heat transfer to the suction gas causes no significant degradation of the performance as a heat pump, transfer from the discharge system is always detrimental, and for this reason thermal isolation of the suction gas is preferable.

Conventionally, suction mufflers make no attempt to seal off the suction system from the can gas, so that the can atmosphere is always at the suction pressure. However, if the idea of using a suction muffler is taken one step further, one recognises that by hermetically isolating the suction system from the can gas, the possibility arises of maintaining the can at an intermediate pressure between the suction and discharge pressures.

This suggestion introduces several possible advantages. Ordinarily, the compressor does virtually no work during the re-expansion stroke, intake stroke, and the start of the compression stroke. All the work of the cycle is crammed into a short, tight hump on the torque - time plot corresponding to the steep part of the compression stroke and the discharge stroke. The need for the motor to handle the peak torque rather than just the mean torque is one of the reasons why the SC10H, for instance, has been designed with an oversized motor. This statement, that the motor is oversized, is justified by observing that the motor coped easily with the combination of 78psig suction and 220psia discharge, for which the indicated work was 280 Watts. This is well in excess of the most demanding credible heat pump duty. Further justification is found in Danfoss' motor data, which shows that for peak efficiency the motor should be producing 320 Watts of shaftwork (Appendix 4).

By operating with an intermediate pressure in the can, both the peak torque and the torque's time dependence become much more favourable, so removing the need to oversize the motor. There is also a further advantage introduced by the less severe loading of the bearings.

Severe problems of gudgeon pin wear have been reported (76). One of the reasons for this is that, ordinarily, the gudgeon pin is always loaded in the same direction, which results in the lubricant tending to get squeezed out (60). Unlike a normal journal bearing, the gudgeon pin only rocks back and forward, it does not complete the oil-pumping full revolutions of a normal journal bearing. This problem goes away with a pressurised can, because at each revolution the direction of the gudgeon pin's loading reverses twice.

For a pressurised can, the gudgeon pin would have to be central in the length of the piston. This is in contrast to normal usage which dictates putting the gudgeon pin close to the piston crown. Also, it is normal practice to offset the bore in order to reduce the lateral component of the con-rod's thrust during compression and discharge. However, for a pressurised can it would be more appropriate to have the bore central. In order to avoid incurring any mechanical penalty through these two changes, their potentially detrimental effect could be avoided by making the con-rod longer.

In addition to the advantages noted above, an intermediate pressure in the can would result in a smaller total loss due to leakage past the piston. For the combination of 22psig suction, 220psia discharge, leakage accounted for a 5% capacity loss and an 11 Watt power loss, out of 173 Watts indicated work.

The implied mechanical loss of up to 50 Watts begs the question of whether a significant gain could be obtained by using either ball or roller bearings. This suggestion was pursued in (75). It appears that an attempt was made to use a needle bearing that retained the original cast-iron shaft as the central bearing surface for the rollers. This experiment was unsuccessful. However, this is no reason to rule out the use of proprietary pre-assembled bearings, which are extensively used in many other applications. Also, if the bearing load is reduced by using an intermediate can pressure, then this very much alleviates one of the worries about changing the bearings.

Rotor fabrication

One of the problems with induction motor rotors is that they usually have a steel shaft running through them. This is such a familiar sight that one forgets to question whether this is the best way to make them. From the structural point of view it is simple and obvious. But from an electromagnetic viewpoint it is detrimental.

In operation, the rotor becomes a magnetic dipole, with the magnetic flux running from one side to the other, ideally through the centre. With a large hole through the rotor's centre, partially filled by a hollow metal shaft, the magnetic flux has to squeeze round the remaining annulus of magnetic core. As the direction of magnetisation rotates relative to the rotor, the shaft also causes an eddy current loss. These losses can be avoided if the crankshaft's mechanical connection is made to the conductor, in order to keep the magnetic core continuous across the centre. Since compressor rotors are normally supported at one end only, there need be no fear of stray currents leaking into the rest of the compressor.

11.4 Other suggestions for further work

Activated PTFE

Activated PTFE has been widely advertised as an additive for engine oil, with the claim that it reduces sliding friction at partially lubricated interfaces. Obviously, it can make no difference to the viscous drag caused by full hydrodynamic lubrication. It might be worth trying this to see if it causes any reduction in the mechanical losses.

Novel flow rate measurement

The problems encountered in the automatic flow rate measurements eventually led to the recognition of a much simpler, cheaper, and potentially more reproducible method. The idea is to include a short section of pipe in the liquid line, equipped with a resistor in the middle of the flow. By wiring two thermocouples differentially, upstream and downstream from the resistor, it becomes possible to obtain a measured temperature increment resulting from a known power input to the resistor. The flow rate then follows from the specific heat. One of the major problems with the instrumentation was the lack of confidence in the Pelton wheel flowmeter used in the liquid refrigerant line. This problem ultimately led to the condenser capacity measurement being made manually, and deduction of the flow rate after calculating a heat loss correction for the condenser. If a reliable refrigerant flow rate measurement had been available, this would have provided a valuable check on the consistency of the flow rate estimate.

In-line motor diagnostic

Shortly after realising that it might be useful to find the stator's temperature, the practice was adopted of measuring its resistance at the end of a test in order to obtain a temperature estimate. In principle, an instrument could be devised to perform this stator resistance measurement during operation of the motor, and so obtain a continuous record of the winding temperature. The instrument would have to be based on the superposition of a DC current onto the AC consumption, and the measurement of the resulting DC component of the potential difference across the stator. Such an instrument might be useful as a diagnostic tool for all electrical machinery, not just heat pump motors.

Appendix 1. Converting Downing's imperial co-efficients to SI

```
30@%=&00010913
 40MODE3
 50DIM x(50),y(50)
 60
 70REM Temperature, density, pressure & entropy conversion factors
 80DATA 1.8,16.01891,6894.76,4186.8
 90READ Tc,Dc,Pc,Sc
100
110PRINT"                                P.PvTconv"
115PRINT
120PRINT"         This programme converts to S.I. units the imperial
equation of state   constants quoted in Downing's paper of '74, and
allows both the raw data and   the converted co-efficients to be stored
as disc data-files."
130PRINT
140INPUT"Which Refrigerant ";A$
150CLS:PRINT A$;" Liquid density co-efficients"
160INPUT"Enter Downing's 7 co-efficients A1,B1,C1,D1,E1,F1,G1
";x(1),x(2),x(3),x(4),x(5),x(6),x(7)
170CLS:PRINT A$;" Liquid density co-efficients"
180PRINT"~~~~~~~~~~~~~~~~~~~~~~~~~~~~~~~~~~~~~~"
190PRINT"       Imperial         S.I."
200FOR I=1 TO 7:y(I)=Dc*x(I):PRINTx(I),y(I):NEXTI
205A1=y(1):B1=y(2):C1=y(3):D1=y(4):E1=y(5):F1=y(6):G1=y(7)
210
250PRINT:PRINT"Saturated vapour co-efficients"
260INPUT"Enter Downing's 6 co-efficients A,B,C,D,E,F
";x(8),x(9),x(10),x(11),x(12),x(13)
265IF x(12)=0 THEN x(13)=900
270y(13)=x(13)/Tc
280y(8)=x(8)*LN(10)+LN(Pc)+(x(10)-x(12))*LN(Tc)
290y(9)=(x(9)/Tc)*LN10+x(12)*y(13)*LN(Tc)
300y(10)=x(10)
310y(11)=Tc*x(11)*LN(10)
320y(12)=x(12)
330CLS:PRINT A$;" Saturated vapour co-efficients"
340PRINT"~~~~~~~~~~~~~~~~~~~~~~~~~~~~~~~~~~~~~~~"
350PRINT"       Imperial         S.I."
360FOR I=8 TO 13:PRINTx(I),y(I):NEXTI
370A=y(8):B=y(9):C=y(10):D=y(11):E=y(12):F=y(13)
380
400PRINT"Specific heat co-efficients"
410INPUT"Enter Downing's 5 co-efficients
a,b,c,d,f";x(14),x(15),x(16),x(17),x(18)
420FOR I=14 TO 18:y(I)=Sc*x(I):NEXT
430y(15)=Tc*y(15):y(16)=y(16)*Tc^2:y(17)=y(17)*Tc^3:y(18)=y(18)/Tc^2
440CLS:PRINT A$;" Specific heat co-efficients"
450PRINT"~~~~~~~~~~~~~~~~~~~~~~~~~~~~~~~~~~~~~"
460PRINT"       Imperial         S.I."
470FOR I=14 TO 18:PRINTx(I),y(I):NEXTI
480a=y(14):b=y(15):c=y(16):d=y(17):f=y(18)
490
500PRINT"PvT equation of state"
510INPUT"Gas constant, R ";x(19)
520INPUT"Volume offset,b ";x(20)
530INPUT"A2, B2, C2       ";x(21),x(22),x(23)
```

```
540INPUT"A3, B3, C3          ";x(24),x(25),x(26)
550INPUT"A4, B4, C4          ";x(27),x(28),x(29)
560INPUT"A5, B5, C5          ";x(30),x(31),x(32)
570INPUT"Exponent, K         ";x(33)
580INPUT"Critical T          ";x(34)
590
600FOR I=21 TO 32:y(I)=x(I)*Pc:NEXT
610FOR I=22 TO 31 STEP 3:y(I)=y(I)*Tc:NEXT
620FOR J=2 TO 5:FOR I=15+3*J TO 17+3*J:y(I)=y(I)/(Dc^J):NEXTI:NEXTJ
630y(19)=x(19)*Pc*Tc/Dc
640y(20)=x(20)/Dc
645y(33)=x(33)
650y(34)=x(34)/Tc
660CLS:PRINT A$;" PvT equation of state"
670PRINT"~~~~~~~~~~~~~~~~~~~~~~~~~~~~"
680PRINT"        Imperial          S.I."
690FOR I=19 TO 34:PRINTx(I),y(I):NEXTI
700 R=y(19):bv=y(20):Tc=y(34):K=y(33)/Tc
710A2=y(21):B2=y(22):C2=y(23)
720A3=y(24):B3=y(25):C3=y(26)
730A4=y(27):B4=y(28):C4=y(29)
740A5=y(30):B5=y(31):C5=y(32)
750so=0:fo=0
755T=273.15
760PROCC_Cequn(T)
770PROCZs(v):sApp=FNs(T):hApp=FNh(T)
780sTrue=1000+DsCon:hTrue=200000+DhCon
790so=sTrue-sApp:fo=hTrue-hApp
795y(35)=so:y(36)=fo
800y(37)=FNPs(Tc):y(38)=1/y(1)
810Sf$="I."+A$:                       REM  Filename for original
co-efficients
820Cf$="C."+A$:                       REM  Filename for converted
co-efficients
830D=OPENOUT(Sf$)
840FOR I=1 TO 50
850PRINT£D,x(I)
860NEXT
870CLOSE£D
880D=OPENOUT(Cf$)
890FOR I=1 TO 50
900PRINT£D,y(I)
910NEXT
920CLOSE£D
1000
1500CHAIN"P.PvTwrit"
3000END
10000  REM     THERMODYNAMICS OF VAPOUR
10001  REM     ~~~~~~~~~~~~~~~~~~~~~~~~
10002
10010  REM  Volume dependent terms in dP/dv
10020  REM  ~~~~~~~~~~~~~~~~~~~~~~~~~~~~~~~
10025DEF PROCXs(v)
10030X1=-2*A2/(v-bv)^3-3*A3/(v-bv)^4-4*A4/(v-bv)^5-5*A5/(v-bv)^6
10040X2=-2*B2/(v-bv)^3-3*B3/(v-bv)^4-4*B4/(v-bv)^5-5*B5/(v-bv)^6-R/(v-b
v)^2
10050X3=-2*C2/(v-bv)^3-3*C3/(v-bv)^4-4*C4/(v-bv)^5-5*C5/(v-bv)^6
10060ENDPROC
10090
```

```
10100  REM  Volume dependent terms in P(v,T)
10110  REM  ~~~~~~~~~~~~~~~~~~~~~~~~~~~~~~~~
10115DEF PROCYs(v)
10120Y1=A2/(v-bv)^2+A3/(v-bv)^3+A4/(v-bv)^4+A5/(v-bv)^5
10130Y2=B2/(v-bv)^2+B3/(v-bv)^3+B4/(v-bv)^4+B5/(v-bv)^5+R/(v-bv)
10140Y3=C2/(v-bv)^2+C3/(v-bv)^3+C4/(v-bv)^4+C5/(v-bv)^5
10160ENDPROC
10190
10200  REM  Volume dependent terms in Integral(Pdv)
10210  REM  ~~~~~~~~~~~~~~~~~~~~~~~~~~~~~~~~~~~~~~~~
10215DEF PROCZs(v)
10220Z1=-A2/(v-bv)-A3/(2*(v-bv)^2)-A4/(3*(v-bv)^3)-A5/(4*(v-bv)^4)
10230Z2=-B2/(v-bv)-B3/(2*(v-bv)^2)-B4/(3*(v-bv)^3)-B5/(4*(v-bv)^4)+R*LN
(v-bv)
10240Z3=-C2/(v-bv)-C3/(2*(v-bv)^2)-C4/(3*(v-bv)^3)-C5/(4*(v-bv)^4)
10260ENDPROC
10290
10500  REM  Functions of state P(T,v), h(T,v), s(T,v)
10510  REM  ~~~~~~~~~~~~~~~~~~~~~~~~~~~~~~~~~~~~~~~~~
10520  REM  Ensure that X1,X2,X3, Y1,Y2,Y3, Z1,Z2,Z3 are evaluated at
correct v
10530  REM  Ensure that eKT=EXP(-KT) is evaluated at correct T.
10540
10550DEF FNP(T)=Y1+T*Y2+Y3*eKT
10560DEF FNs(T)=a*LN(T)+b*T+c*T^2/2+d*T^3/3-f/(2*T^2)+Z2-K*Z3*eKT+so

10570DEF
FNh(T)=a*T+b*T^2/2+c*T^3/3+d*T^4/4-f/T-Z1-(1+K*T)*eKT*Z3+v*(Y1+T*Y2+Y3*e
KT)+fo
10600
10700  REM  Differential co-efficients dP/dT, dP/dV, ds/dT
10710  REM  ~~~~~~~~~~~~~~~~~~~~~~~~~~~~~~~~~~~~~~~~~~~~~~
10720
10730DEF FNPT(T)=Y2-K*eKT*Y3
10740DEF FNPv(T)=X1+T*X2+eKT*X3
10750DEF FNsT(T)=a/T+b+c*T+d*T^2+f/T^3+eKT*Z3*K^2
10800
10900  REM  End of thermodynamics of vapour
10910  REM  ~~~~~~~~~~~~~~~~~~~~~~~~~~~~~~~
10950
10960
11000  REM  THERMODYNAMICS OF LIQUID
11010  REM  ~~~~~~~~~~~~~~~~~~~~~~~~
11020
11030  REM  Liquid Density
11032  REM  ~~~~~~~~~~~~~~
11034
11040DEF PROCliquid_rho(T)
11050X1=1-T/Tc
11060Lro=A1+B1*X1^(1/3)+C1*X1^(2/3)+D1*X1+E1*X1^(4/3)+F1*SQR(X1)+G1*X1^
2
11090ENDPROC
11100
11120  REM Saturated vapour pressure
11121  REM ~~~~~~~~~~~~~~~~~~~~~~~~~
11122
11130DEF FNPs(T)=EXP(A+B/T+C*LN(T)+D*T+E*(F/T-1)*LN(F-T))
11150
11200  REM  Clausius-Clapeyron Equation
```

```
11210  REM  ~~~~~~~~~~~~~~~~~~~~~~~~~~~
11220
11230DEF PROCC_Cequn(T)
11240PROCliquid_rho(T)
11250P=FNPs(T)
11260PROCv(P,T)
11270DsCon=(v-1/Lro)*P*(-B/T^2+C/T+D-(E/T)*(1+(F/T)*LN(F-T)))
11280DhCon=T*DsCon
11290ENDPROC
11300
12000  REM   Solution for v given P & T
12010  REM   ~~~~~~~~~~~~~~~~~~~~~~~~~~
12015DEF PROCv(P,T)
12020eKT=EXP(-K*T):v=R*T/P
12030PROCXs(v):PROCYs(v)
12040dv=(P-FNP(T))/FNPv(T)
12060IF ABS(dv/v)<.00001 THEN 12100 ELSE v=v+dv:GOTO 12030
12100ENDPROC
```

Conversion of Downing's Equation of state co-efficients for R12

Saturated liquid density		Imperial lb/ft^3	S.I. Kg/m^3
Critical density	A1	3.48400000 E1	5.58098825 E2
	B1	5.33411870 E1	8.54467674 E2
	C1	0.00000000 E0	0.00000000 E0
	D1	1.86913700 E1	2.99415374 E2
	E1	0.00000000 E0	0.00000000 E0
	F1	2.19839600 E1	3.52159077 E2
	G1	-3.15099400 E0	-5.04754893 E1

Saturated vapour pressure		Imperial	S.I.
	A	3.98838173 E1	9.33438056 E1
	B	-3.43663223 E3	-4.39618785 E3
	C.	-1.24715223 E1	-1.24715223 E1
	D	4.73044244 E-3	1.96060432 E-2
	E	0.00000000 E0	0.00000000 E0
	F	9.00000000 E2	5.00000000 E2

Vapour specific heat		Imperial	S.I.
	a	8.09450000 E-3	3.38900526 E1
	b	3.32662000 E-4	2.50702067 E0
	c	-2.41389600 E-7	-3.27450593 E-3
	d	6.72363000 E-11	1.64173681 E-6
	f	0.00000000 E0	0.00000000 E0

Vapour equation of state P(T,v)		Imperial	S.I.
Gas constant	R	8.87340000 E-2	6.87462094 E1
Volume offset	bv	6.50938860 E-3	4.06356525 E-4
	A2	-3.40972713 E0	-9.16163227 E1
	B2	1.59434848 E-3	7.71096954 E-2
	C2	-5.67627671 E1	-1.52516486 E3
	A3	6.02394465 E-2	1.01041839 E-1
	B3	-1.87961843 E-5	-5.67495562 E-5
	C3	1.31139908 E0	2.19965791 E0
	A4	-5.48737010 E-4	-5.74581396 E-5
	B4	0.00000000 E0	0.00000000 E0
	C4	0.00000000 E0	0.00000000 E0
	A5	0.00000000 E0	0.00000000 E0
	B5	3.46883400 E-9	4.08141136 E-11
	C5	-2.54390678 E-5	-1.66285944 E-7
Exponent	K	5.47500000 E0	5.47500000 E0
Critical Temp	Tc	6.93300000 E2	3.85166667 E2
Integ'n constant	so		9.99439817 E2
Integ'n constant	fo		2.55965649 E5
Critical Pressure	Pc		4.11548210 E6
Critical Volume	vc		1.79179736 E-3

Conversion of Downing's Equation of state co-efficients for R22

Saturated liquid density		Imperial lb/ft^3	S.I. Kg/m^3
Critical density	A1	3.27600000 E1	5.24779492 E2
	B1	5.46344090 E1	8.75183681 E2
	C1	3.67489200 E1	5.88677642 E2
	D1	-2.22925657 E1	-3.57102604 E2
	E1	2.04732886 E1	3.27959767 E2
	F1	0.00000000 E0	0.00000000 E0
	G1	0.00000000 E0	0.00000000 E0

Saturated vapour pressure		Imperial	S.I.
	A	2.93575445 E1	7.15541481 E1
	B	-3.84519315 E3	-4.81895751 E3
	C	-7.86103122 E0	-7.86103122 E0
	D	2.19093900 E-3	9.08068226 E-3
	E	4.45746703 E-1	4.45746703 E-1
	F	6.86100000 E2	3.81166667 E2

Vapour specific heat		Imperial	S.I.
	a	2.81283600 E-2	1.17767818 E2
	b	2.25540800 E-4	1.69972960 E0
	c	-6.50960700 E-8	-8.83043291 E-4
	d	0.00000000 E0	0.00000000 E0
	f	2.57341000 E2	3.32541759 E5

Vapour equation of state P(T,v)		Imperial	S.I.
Gas constant	R	1.24098000 E-1	9.61442862 E1
Volume offset	bv	2.00000000 E-3	1.24852440 E-4
	A2	-4.35354700 E0	-1.16975920 E2
	B2	2.40725200 E-3	1.16425280 E-1
	C2	-4.40668680 E1	-1.18403739 E3
	A3	-1.74640000 E-2	-2.92930095 E-2
	B3	7.62789000 E-5	2.30301728 E-4
	C3	1.48376300 E0	2.48877025 E0
	A4	2.31014200 E-3	2.41894494 E-4
	B4	-3.60572300 E-6	-6.79598127 E-7
	C4	0.00000000 E0	0.00000000 E0
	A5	-3.72404400 E-5	-2.43427226 E-7
	B5	5.35546500 E-8	6.30121121 E-10
	C5	-1.84505100 E-4	-1.20604280 E-6
Exponent	K	4.20000000 E0	4.20000000 E0
Critical Temp	Tc	6.64500000 E2	3.69166667 E2
Integ'n constant	so		9.71008053 E2
Integ'n constant	fo		3.00562764 E5
Critical Pressure	Pc		4.97691884 E6
Critical Volume	vc		1.90556227 E-3

Conversion of Downing's Equation of state co-efficients for R502

Saturated liquid density		Imperial lb/ft^3	S.I. Kg/m^3
Critical density	A1	3.50000000 E1	5.60661850 E2
	B1	5.34843700 E1	8.56761309 E2
	C1	6.38641700 E1	1.02303439 E3
	D1	-7.00806600 E1	-1.12261579 E3
	E1	4.84790100 E1	7.76580898 E2
	F1	0.00000000 E0	0.00000000 E0
	G1	0.00000000 E0	0.00000000 E0

Saturated vapour pressure		Imperial	S.I.
	A	1.06449550 E1	3.26523467 E1
	B	-3.67115381 E3	-4.52189982 E3
	C	-3.69835000 E-1	-3.69835000 E-1
	D	-1.74635200 E-3	-7.23802335 E-3
	E	8.16113900 E-1	8.16113900 E-1
	F	6.54000000 E2	3.63333333 E2

Vapour specific heat		Imperial	S.I.
	a	2.04190000 E-2	8.54902692 E1
	b	2.99680200 E-4	2.25846191 E0
	c	-1.40904300 E-7	-1.91139952 E-3
	d	2.21086100 E-11	5.39835163 E-7
	f	0.00000000 E0	0.00000000 E0

Vapour equation of state P(T,v)		Imperial	S.I.
Gas constant	R	9.61250000 E-2	7.44723486 E1
Volume offset	bv	1.67000000 E-3	1.04251787 E-4
	A2	-3.26133440 E0	-8.76291425 E1
	B2	2.05762870 E-3	9.95159617 E-2
	C2	-2.42487900 E1	-6.51543330 E2
	A3	3.48667480 E-2	5.84832787 E-2
	B3	-8.67913130 E-6	-2.62040870 E-5
	C3	3.32747790 E-1	5.58130106 E-1
	A4	-8.57656770 E-4	-8.98050643 E-5
	B4	7.02405490 E-7	1.32387722 E-7
	C4	2.24123680 E-2	2.34679445 E-3
	A5	8.83689670 E-6	5.77635831 E-8
	B5	-7.91680950 E-9	-9.31487533 E-11
	C5	-3.71672310 E-4	-2.42948686 E-6
Exponent	K	4.20000000 E0	4.20000000 E0
Critical Temp	Tc	6.39560000 E2	3.55311111 E2
Integ'n constant	so		7.80286821 E2
Integ'n constant	fo		2.39901533 E5
Critical Pressure	Pc		4.07480140 E6
Critical Volume	vc		1.78360629 E-3

Conversion of Downing's Equation of state co-efficients for R11

Saturated liquid density		Imperial lb/ft^3	S.I. Kg/m^3
Critical density	A1	3.45700000 E1	5.53773719 E2
	B1	5.76381100 E1	9.23299696 E2
	C1	4.36322000 E1	6.98940285 E2
	D1	-4.28235600 E1	-6.85986753 E2
	E1	3.67066300 E1	5.88000202 E2
	F1	0.00000000 E0	0.00000000 E0
	G1	0.00000000 E0	0.00000000 E0

Saturated vapour pressure		Imperial	S.I.
	A	4.21470287 E1	9.83165152 E1
	B	-4.34434381 E3	-5.54851694 E3
	C	-1.28459675 E1	-1.28459675 E1
	D	4.00837250 E-3	1.66133138 E-2
	E	3.13605356 E-2	3.13605356 E-2
	F	8.62070000 E2	4.78927778 E2

Vapour specific heat		Imperial	S.I.
	a	2.38150000 E-2	9.97086420 E1
	b	2.79882300 E-4	2.10926018 E0
	c	-2.12373400 E-7	-2.88089444 E-3
	d	5.99901800 E-11	1.46480528 E-6
	f	-3.36807030 E2	-4.35229529 E5

Vapour equation of state P(T,v)		Imperial	S.I.
Gas constant	R	7.81170000 E-2	6.05207433 E1
Volume offset	bv	1.90000000 E-3	1.18609818 E-4
	A2	-3.12675900 E0	-8.40132217 E1
	B2	1.31852300 E-3	6.37695637 E-2
	C2	-3.57699900 E1	-9.61107684 E2
	A3	-2.53410000 E-2	-4.25053913 E-2
	B3	4.87512100 E-5	1.47189955 E-4
	C3	1.22036700 E0	2.04696645 E0
	A4	1.68727700 E-3	1.76674428 E-4
	B4	-1.80506200 E-6	-3.40213808 E-7
	C4	0.00000000 E0	0.00000000 E0
	A5	-2.35893000 E-5	-1.54194684 E-7
	B5	2.44830300 E-8	2.88066009 E-10
	C5	-1.47837900 E-4	-9.66362640 E-7
Exponent	K	4.50000000 E0	4.50000000 E0
Critical Temp	Tc	8.48070000 E2	4.71150000 E2
Integ'n constant	so		7.07405630 E2
Integ'n constant	fo		2.83538148 E5
Critical Pressure	Pc		4.40919196 E6
Critical Volume	vc		1.80579173 E-3

Appendix 2. Incompleteness of the subcooled liquid specification

In section 2.2 the method of obtaining the saturated liquid's functions of state was indicated. For subcooled liquid, the enthalpy is approximately the same as for saturated liquid at the same temperature. To be more exact, a small pressure correction is needed;-

$$h(P,T) = h_s(T) + [P - P_s(T)] \frac{\partial h}{\partial P_T} \qquad \text{A1}$$

where the subscript "s" refers to the saturated liquid state. The only problem with this equation is that the equations of state quoted in chapter 2 are not quite sufficient to deduce a definite value for $\partial h/\partial P$. The relevant algebra is shown below;-

$$\frac{\partial h}{\partial P_T} = T \frac{\partial s}{\partial P_T} + v \qquad \text{A2}$$

$$\frac{\partial s}{\partial P_T} = - \frac{\partial v}{\partial T_P} = \frac{dv}{\delta T} - \frac{\partial v}{\partial P_T} \frac{dP}{dT} \qquad \text{A3}$$

The proper derivatives, above, refer to the saturation line.

There is no problem about finding either dv/dT or dP/dT, but this last equation still leaves $\partial v/\partial T$ indeterminate because of the unknown, $\partial v/\partial P$. The difficulty can be partially lifted by regarding $\partial v/\partial T$ as a multiple of dv/dT, and $\partial P/\partial T$, similarly, as a multiple of dP/dT. Dimensionless parameters A & B can thus be defined by;-

$$\frac{\partial v}{\partial T_P} = A \frac{dv}{dT} \quad \& \quad \frac{\partial P}{\partial T_v} = B \frac{dP}{dT} \qquad \text{A4}$$

If A3 is divided through by $\partial v/\partial T$, one obtains;-

$$-1 = 1/A - 1/B \qquad \text{A5}$$

which can be re-arranged into the form

$$(A - 1)(B - 1) = 1 \qquad \text{A6}$$

Of the 2 branches of this hyperbola, it is only the one having A & B both > 1 which is thermodynamically tenable. The other branch, which passes through the origin, would imply $\partial v/\partial P > 0$.

In principle, it is possible to get a handle on either A or B using quoted specific heat data. However, it is more reliable to use data for sound speed in the liquid (77).

Upon substituting equations A4, A3 & A2 into equation A1, one obtains

$$h(P,T) = h_s(T) + [P - P_s(T)][v - AT\frac{dv}{dT}] \qquad \text{A7}$$

The calculations presented in chapter 2 all included this pressure correction. Because of the availability analysis in chapter 2, it was necessary to obtain thermodynamically consistent enthalpy and entropy of the subcooled liquid, which necessitated paying attention to this detail. However, subsequent calculations did not involve finding the entropy of subcooled liquid, and since the enthalpy's pressure correction was always very small, (due to the term AT(dv/dT) being always close to v) it was considered unnecessary to include it in subsequent calculations.

While on the subject of refrigerant properties, it is pertinent to mention that the equations for refrigerant viscosity and thermal conductivity were obtained from (78).

Appendix 3. Attempts to model the valve Dynamics

1 Dimensional valve

If the valve was a perfectly rigid beam hinged at one end, and held shut by a spring acting on the free end, then this would conform to the 1D model. When, in the calculation, the valve has opened as far as permitted by the end stop, its velocity is set to zero. It then remains against the end stop until the pressure difference acting on it falls below the value needed to support it against its restoring spring. It then starts accelerating *from rest* back to its seat.

2 Dimensional valve model

In reality, when the tip of a reed valve hits the end stop, the valve is not instantly brought to rest. Instead, it bends into the approximate shape of a beam which is supported at both ends and loaded in the middle. This bend develops until the original incident kinetic energy has been converted to strain energy. From this strained state, the valve recovers elastically, and in so doing is accelerated back towards its seat. The valve's speed back towards its seat can be high enough for a large pressure difference to become re-established before its velocity is reversed. In this way, contrary to the 1 D model, the valve can oscillate throughout the stroke.

Valve Closure Timing

This difference in behaviour of the two models leads to an important difference in their calculation of the time of the valve's closure. For the 1 D model, if the suction gas density is low, then the valve begins its acceleration back to its seat early, and this results in a favourably timed valve closure close to b.d.c. With increasing suction gas density the valve is held against its end stop until later in the stroke. The resulting delay in the start of the valve's acceleration results in the timing of the valve's closure getting systematically less favourable with increasing suction gas density. This trend is an artificial feature of this model, because it is a direct consequence of the artificial treatment of the collision of the valve with its end stop. With a judicious choice of one's free parameters, the effect of this feature on one's calculated results may be masked, but this does not alter the fact that the 1 D model is deficient.

While the 2 D model produces a qualitatively correct valve motion, as a means of calculating the timing of the valve closure its main problem is sensitivity.

While attempting to fit a 2 D model to a set of measurements, the following observation was made. If the suction valve returned to its seat 7^0 before b.d.c. then it experienced a further impulse accelerating it open. This further impulse results from rarefaction of the cylinder gas as the piston continues towards bdc. The effect of accelerating the valve open just before bdc is to produce the situation that as the piston passes through bdc, the valve is half open, still coasting in the opening direction, and retarded only by its own stiffness. Because of the valve's being partly open, gas flows past it as the piston starts the compression stroke, which thus delays the build up of cylinder pressure needed to accelerate the valve back to its seat. In the worst case, the valve did not return until it had coasted to the end stop, deformed, and bounced back, giving a late closure of about 50^0.

If the penultimate valve closure is just 2^0 or 3^0 later, then the valve is not sufficiently open as the piston turns around to inhibit the development of the cylinder pressure, and so it is closed quickly by the cylinder gas pressure, with little loss of capacity. Similarly, if the penultimate closure is fractionally earlier than the worst case, then the valve receives a stronger impulse, so that its coasting across to the end stop, bounce and return all happen faster, with the result that the capacity loss is very much reduced.

The problem is that very tiny changes in the model's free parameters can influence the timing of this penultimate valve closure by 2^0or 3^0. The model thus suffers from a pathologically high sensitivity in that tiny changes of the free parameters can change the calculated capacity by over 10%. A similar difficulty has also been reported by Tramscheck (72).

The sensitivity illustrated here lies behind the problem that, upon tuning the free parameters to match the measurements made at one operating condition, the calculation fails to match the other operating conditions.

It is also pertinent to mention that the 2 D model involves numerical integration of a fourth order partial differential equation for the valve displacement. This incurs a massive penalty in computing time compared with a simpler, more expedient model.

Ultimately, a calculation was developed which included a full 2 D elastic - dynamic treatment not only of the suction valve, but also of the discharge valve and backing spring. After extensive testing of this calculation against the measurements, including tests of sensitivity to the free parameters, the conclusion was reached that this is an impractical and unreliable way to calculate the two key parameters V4 & V2.

Fortunately, in the course of inspecting the figures for some of the trial calculations, it was observed that if V4 & V2 were consistently adjusted to the same two values, then the calculated capacities could all be brought into line with the measurements. This was the genesis of an idea for a semi-empirical model.

In the semi-empirical model the opening of the valves was based on the 1 D valve model. However, instead of attempting to calculate the closure of the valves, they were constrained to remain fully open until a fixed time had elapsed after either top, or bottom dead centre, at which time they were shut instantly.

The parameters of the 1 D valve model were adjusted to make the calculated excess PdV work match the result of a 2 D valve calculation.

After adjusting the empirical valve delay to give the best fit to all the experimental data, the resulting calculation gave better, consistent agreement with all the measurements than any other predictive valve model that had been tried up to that point.

Because the disagreements between the calculated and measured capacity were nonetheless slightly in excess of the experimental uncertainty, the next step from this point was to use the measurements to answer the hypothetical question "If suction valve lateness is to account for the capacity shortfall, then how late would the valve have to shut ?". This led to the interpretive model explained in chapter 9.

Appendix 4. Fits to Danfoss motor data

Danfoss have supplied data for the motor's power consumption, current consumption, angular speed, shaftwork, and total electrical loss as functions of torque (34). This is reproduced in table A1 below.

Motor performance data supplied by Danfoss

Input Watts	Shaftwork Watts	Losses Watts	Current Amps	Speed RPM	Efficiency per-cent
101.00	31.00	71.00	1.55	2982.00	30.69
132.00	61.00	71.00	1.57	2971.00	46.21
163.00	91.00	71.00	1.60	2960.00	55.83
195.00	121.00	74.00	1.65	2949.00	62.05
229.00	151.00	78.00	1.72	2937.00	65.94
263.00	180.00	83.00	1.79	2925.00	68.44
299.00	210.00	90.00	1.88	2912.00	70.23
336.00	238.00	98.00	1.98	2898.00	70.83
373.00	267.00	106.00	2.09	2885.00	71.58
408.00	295.00	113.00	2.20	2872.00	72.30
445.00	323.00	122.00	2.33	2857.00	72.58
487.00	350.00	137.00	2.47	2841.00	71.87
531.00	377.00	154.00	2.63	2823.00	71.00
577.00	403.00	173.00	2.79	2803.00	69.84
623.00	429.00	195.00	2.97	2780.00	68.86
677.00	453.00	224.00	3.17	2754.00	66.91
735.00	475.00	259.00	3.40	2720.00	64.63
794.00	499.00	295.00	3.64	2699.00	62.85

Table A1

For the simple calculation introduced in chapter 4, an empirical relationship was used to find the motor's speed from the measured power consumption, P, using data supplied by Danfoss. This equation is;-

$$RPM = 2982-(P-101)(0.345 + 0.00005(P-101)) \quad A8$$

Table A2, below, summarises the Danfoss data for motor speed, and includes the result of using this fit.

Fitting the motor speed as a function of consumption

Input Watts	Speed RPM	Equation A8 RPM
101.00	2982.00	2982.00
132.00	2971.00	2971.26
163.00	2960.00	2960.42
195.00	2949.00	2949.13
229.00	2937.00	2937.02
263.00	2925.00	2924.80
299.00	2912.00	2911.73
336.00	2898.00	2898.16
373.00	2885.00	2884.46
408.00	2872.00	2871.37
445.00	2857.00	2857.40
487.00	2841.00	2841.38
531.00	2823.00	2824.40
577.00	2803.00	2806.45
623.00	2780.00	2788.29
677.00	2754.00	2766.69
735.00	2720.00	2743.17
794.00	2699.00	2718.90

Table A2

Empirical motor equations used in the Interpretive model

The data from Danfoss specifies a motor temperature of 80C. Because of the wide range in motor temperature encountered in the final set of tests, there was some concern about the best way to take account of this. Since the current consumption and stator resistance were both measured, it was considered best to find the stator's Joule heating from these measurements, and then to find the total of the other losses from the Danfoss data.

In order to use the Danfoss data in this way, it was necessary to subtract the stator Joule heating from the figures of total consumption and electrical loss. A nominal stator resistance of 10 ohms was assumed. Empirical relationships were then devised for the motor's speed, and non-stator losses as functions of the 'reduced' consumption.

Denoting the reduced consumption by X, the equation for the non-stator losses was;-

$$\text{Reduced loss} = 46+12.5*(1-\text{COS}(\pi(X-130)/340) \qquad \text{A9}$$

This unorthodox fit was borne of the need for a function that started off like a parabola, and then straightened up.

The equation for the motor speed was;-

$$RPM = 3000+9.24-X(0.352 + (2.4\ E-7)X^2) \qquad A10$$

Table A3, below, shows how well these equations match the Danfoss data.

Empirical fits for loss and speed after deducting stator Joule heating

Input Watts	Stator Loss	Reduced Input	Reduced Losses Data	Reduced Losses Fit	Speed, RPM Data	Speed, RPM Fit
101.00	24.02	76.97	46.98	47.47	2982.00	2982.04
132.00	24.65	107.35	46.35	46.27	2971.00	2971.16
163.00	25.60	137.40	45.40	46.03	2960.00	2960.25
195.00	27.23	167.77	46.77	46.75	2949.00	2949.05
229.00	29.58	199.42	48.42	48.48	2937.00	2937.14
263.00	32.04	230.96	50.96	51.06	2925.00	2924.99
299.00	35.34	263.66	54.66	54.38	2912.00	2912.03
336.00	39.20	296.80	58.80	58.13	2898.00	2898.49
373.00	43.68	329.32	62.32	61.85	2885.00	2884.75
408.00	48.40	359.60	64.60	65.04	2872.00	2871.50
445.00	54.29	390.71	67.71	67.79	2857.00	2857.40
487.00	61.01	425.99	75.99	69.98	2841.00	2840.74
531.00	69.17	461.83	84.83	70.96	2823.00	2823.03
577.00	77.84	499.16	95.16	70.55	2803.00	2803.69
623.00	88.21	534.79	106.79	68.83	2780.00	2784.29
677.00	100.49	576.51	123.51	65.42	2754.00	2760.32
735.00	115.60	619.40	143.40	60.86	2720.00	2734.18
794.00	132.50	661.50	162.50	56.03	2699.00	2706.92

Table A3

Appendix 5. Viscosity of Alkylbenzene

The kinematic viscosity of Alkylbenzene at 100F is given as 31.7 centistokes in (66). (66) quotes the following equation for the temperature dependence of oil viscosity;-

$$\text{Kinematic viscosity} = \exp(CT^{B}) - 0.7 \text{ centistokes} \qquad \text{A11}$$

where, for Alkylbenzene, C=8.10918092 E10, and B=-4.1587108

To convert from centistokes to centipoise, the following temperature dependent density was used, T in Kelvin;-

$$\rho = 0.872 - 0.00063*(T - 288.7) \text{ g/cc} \qquad \text{A12}$$

This followed from a stated density of 0.872 g/cc at 60F (42). The expansion co-efficient was obtained from a plot of density against temperature given in (66), which showed that refrigerating oils are all very similar in this respect.

The viscosity of Alkylbenzene at 210F is quoted as 4.5 centistokes in (41).

The two co-efficients were thus found after having obtained these two points on the curve, equation A11, from the literature. Figure A1 shows this curve. Using a Redwood viscometer, (79) viscosity measurements were made of the oil taken from the old compressor. These experimental points are shown superposed. The resulting supposition that the lubricant is Alkylbenzene was confirmed in private correspondence (42 & 48).

A diagram of the viscosity resulting from equilibration with various pressures of R12 is shown in (66), but the only indication of the origin of this diagram is a reference to a private communication from DuPont. Upon writing to DuPont in the hope of filling this gap in available information, the reply was received that there is a diagram in the ASHRAE handbook.

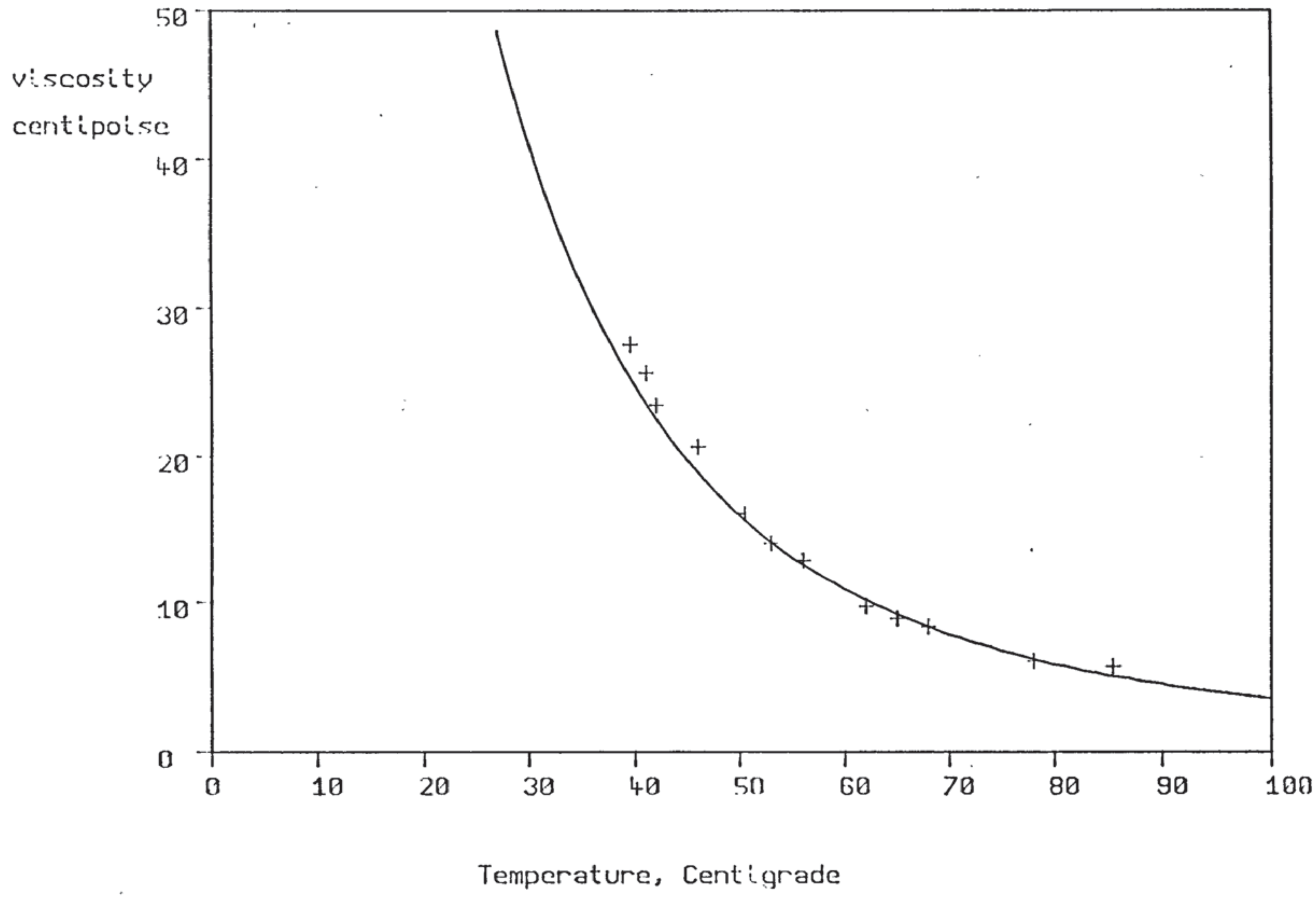

Figure A.1. Temperature dependence of Alkylbenzene viscosity

References

1 A B Pippard, "Classical Thermodynamics", C.U.P. 1979

2 K Mendelson, "The Quest for Absolute Zero", Mc Graw-Hill, New York, 1966.

3 McMullan & Morgan, "Heat Pumps", Adam Hilger, 1981

4 J. A. Sumner, "Domestic Heat Pumps", Prism Press, 1976

5 R C Downing & J B Gray: "R502 - a better heat pump refrigerant", Refrigeration and Air Conditioning, July 1972, pp 45, 46.

6 Reay & MacMichael: "Heat Pumps Design and Applications", Pergamon Press, 1979

7 W. Thomson: "On the economy of the heating and cooling of buildings by means of currents of air", Proc. Glasgow Phil. Soc., Vol.III, pp666-675, Dec. 1852.

8 J. Masters & J. Pearson: "Automotive Gas Engines Power Air Conditioning Systems, Heat Pump Installations and Heat and Power Units", Midlands Research Station, 1981

9 A. Bringmann, "Gas heat pumps for the heating of buildings", Sulzer Technical Review, 1982, no.2, pp47-50

10 Sarkes, Nicholls, Menzer, "Gas fired heat pumps: an emerging technology", ASHRAE Journal, March 1977 pp36-41

11 T. Finkelstein, "Analysis of a Heat-Activated Stirling Heat Pump", Proc. 15th International Energy Conversion Engineering Conference Paper no.809363, 1980

12 . E. H. Arctander, "Solar heat pump", Popular Science, V206 no.4, April 1975, pp106-107

13 W. E. J. Neal, "Cooling by solar energy: a review of current developments", Journal of the Institute of Energy, March 1980, pp25-30

14 McMullan & Morgan, "Development of domestic heat pumps", EEC Report, Contract no. 269-77-1 EEUK, 1981

15 P. D. Metz, "Design, Operation and Performance of a Ground Coupled Heat Pump System in a Cold Climate", Proc. 16th International Energy Conversion Engineering Conference Paper no. 819725, 1981

16 P. D. Metz, "The use of ground-coupled tanks in solar-assisted heat-pump systems", Trans. ASME, Journal of Solar Energy Engineering, V104, Nov.1982 pp366-372

17 J. R. Partin, "Closed Loop Earth Coupled Heat Pumps", 2nd International Symposium on The Large Scale Applications of Heatpumps, York, 1985

18 B. Capaldi, "Units to ventilate the home and to dry clothes", Electrical Review, Oct.1975, V197, no.14 p428.

19 T. Holland & S. Devotta, "Prospects for heatpumps in process applications", The Chemical Engineer, no.425, May 1986, pp61-67

20 R W Haywood: "A Simplified presentation of equations for the thermodynamic properties of dichlorodifluoromethane, CCl2F2 (Refrigerant-12)", Journal of Mechanical Engineering Science. 1969. Vol 11, No 4, pp 376-383.

21 J J Martin & Y C Hou: "Development of an equation of state for gases". A.I.Ch.E. Journal. 1955, Vol 1, No 2, pp 142-151.

22 R C McHarness, B J Eiseman, J J Martin: "Freon 12". Refrigerating engineering. September 1955. Vol 63. No 9, pp 32-44 R12 Equation of state (1956)

23 R C Downing: "Refrigerant equations". ASHRAE Transactions, 1974. Part 2. 158-169.

24 M Hussein et al, Cranfield: "Efficiencies of Exergy transductions", Applied Energy 1980.

25 E E Michaelides: "The second law of thermodynamics as applied to energy conversion processes", Energy Research, Vol 8 (1984) pp241-246.

26 "The economic implications of the exergy and thermal efficiencies of energy conversion systems" Proceedings of the International Energy Conversion Engineering Conference. A.S.M.E. 1981. pp3-8.

27 J W Gibbs' original papers were published in "The Transactions of the Connecticut Academy of Arts and Sciences" between 1875 and 1878.

28 Maneurop promotional literature on hermetic compressors from 2 to 10 Hp.

29 W Soedel, P N Pandeya: "On Suction gas heating in hermetic compressors (A technical note)", Proc. of the 1978 Purdue Compressor Technology conference. pp 144-147

30 F Perruzi, V Baci & G Scandurra: "EER improvement on a reciprocating hermetic compressor" Proc. of the 1980 Purdue Compressor Technology conference. pp 1-7

31 H Kawai, H Nishihara, K Hamada & S Nakaoka: "The development of high efficiency compressors by reducing suction gas temperature". Proc. of the 1982 Purdue Compressor Technology conference. pp 222-228

32 ASHRAE handbook 1985, Fundamentals, Chapter 1, "Thermodynamics and refrigeration cycles"

33 K A MaWhinney: "On the performance of vapour compression heat pumps" D. Phil thesis, new University of Ulster, 1981.

34 P.Vester, Danfoss. Private communication, November 1983, detailing motor performance figures, and including a double quadratic fit for COP and capacity.

35 C G Carrington: "Use of controlled water circulation in tap water heat pumps" Energy research, Vol 6, 1982, pp 233-240.

36 C G Carrington and T C Knopp: "Limiting performance of vapour compression heat pumps for heating water" Energy Research, Vol 7 1983 pp 255-264.

37 J A Anderson, R A Bradford, C G Carrington: "Assessment of a heat pump water heater" Energy Research, Vol 9, 1985, pp77-89

38 J H Hildebrand: "Regular & related solutions: The solubility of gases, liquids and solids", New York, Van Nostrand Reinhold, 1970

39 P W Atkins: "Physical chemistry", Oxford university press, 1978.

40 J S Rowlinson, F L Swinton: "Liquids & Liquid mixtures", (Butterworth's monographs in chemistry), Butterworths, London, 1982.

41 R C Downing, W D Cooper, J B Gray: "Alkylbenzene as compressor lubricants" Proc. of the 1974 Purdue Compressor Technology conference. pp 88-94.

42 P Vester, Danfoss, private communication, May 1985, confirming that 'Zerol 150' is Alkylbenzene, and including PTx plots.

43 B Mathiprakasam & T Sutikno: "Theoretical analysis of the use of binary refrigerant mixtures in the vapour compression cycle"; Heat Transfer - Niagara Falls 1984; AIChE Symposium series, No. 236, Vol 80 pp 122-127

44 R A Summers, W Flint, Dept. Mech. Eng. Aston University, & M R Williams, Hydrovane compressors: Private communication concerning effects of wet compression.

45 M Y H Othman. "Evaluation and modelling of a water-to-water heat pump system". PhD thesis. University of Aston in Birmingham. 1984.

46 Danfoss. Hermetic notes. Compressors for Heat Pump Systems. October 1978.

47 P Vester. Danfoss. Private comunication, March 1986, advising of change to 500 cc recommended oil charge.

48 D. Glova. DuPont. Private communication, August 1986, advising change of manufacturer of Zerol 150.

49 C G Carrington, during a stay at Aston University, 1981.

50 Danfoss technical notes on thermostatic expansion valves. Danfoss, 1978.

51 C.I.L. Electronics. PCI1001 Operating manual.

52 C.I.L. Electronics. PCI1002 Operating manual.

53 Litre Meter. Technical information on product range.

54 Maywood Instruments. Pressure transducer P102.

55) K W Cooper, A G Mount: "Oil circulation - Its effect on

compressor capacity, theory and experiment". Proc. of the 1972 Purdue Compressor Technology conference. pp 52-59

56) D W Hughes, J T McMullan, K A MaWhinney & R Morgan: "Experimental investigation of the influence of lubricating oil on heat pump performance". Energy research, Vol 8, 1984, pp 213-222

57) D W Hughes, J T McMullan, K A MaWhinney & R Morgan: "Lubricant related problems with heat pumps". Proc. of the 1980 Purdue Compressor Technology conference. pp 156-163

58) G Bambach: "The behaviour of mineral oil - F12 mixtures in refrigeration equipment". Abhandlungen des Deutschen Kaltetechnischen Vereins No. 9. Karlsruhe, Verlag C. F. Muller, 1955.

59) J Brown: "Cyclical heat interchanges between charge and cylinder in a refrigerating compressor operating on Freon 12". Proceedings of the general discussion on heat transfer. Inst. Mech. Eng. 1952

60) A. Cameron. "Principles of lubrication". Longmans. 1966.

61) T W B Kibble: "Classical Mechanics" second edition, McGraw-Hill, 1973.

62) F P Bowden, D Tabor: "Friction and lubrication of solids". Oxford, Clarendon press, (International series of monographs on physics) Part 1, 1950. Part 2, 1964.

63) J Young, A A Zu'bi, J F T MacLaren: "Piston leakage in hermetic refrigeration compressors". Proc. of the XVth International Congress of refrigeration (Venice 1979). pp 717-725.

64) R T S Ferreira & D E B Lilie. "Evaluation of the leakage through the clearance between piston and cylinder in hermetic compressors". Proc. of the 1984 Purdue Compressor Technology Conference. pp 1-6

65) D Chisholm: "Two phase flow in pipelines and heat exchangers", 1983, George Godwin (Part of Longman group Ltd." in association with the Institution of chemical engineers

66) ASHRAE 1984, Systems handbook. Ch29. "Lubricants in refrigerant systems"

67) P V Joshi: "Current pulsation calculations of an induction motor connected to a reciprocating compressor. Proc. of the 1984 Purdue Compressor Technology Conference. pp 181-191

68) A Cameron: "Heat transfer in Journal bearings: A Preliminary Investigation" Proceedings of the general discussion on heat transfer. Inst. Mech. Eng. 1952

69) W M Rohsenow, J P Hartnett: "Handbook of heat transfer", McGraw Hill, New York, 1973.

70) P Vester, Danfoss, private communication, February 1984, concerning clearance between the piston and the bore.

71) D Squarer, F J Sisk & S E Veyo: "Conceptual design of a better heat pump compressor for northern climates." Proc. of the 1976 Purdue

Compressor Technology Conference. pp 124-128

72) A B Tramschek & J F T McLaren "Simulation of a reciprocating compressor accounting for interaction between valve movement and plenum chamber pressure" Proc. of the 1980 Purdue Compressor Technology Conference. pp 354-364

73) J F T McLaren, A B Tramschek, I J Hussein and B A El-Geresy: " Can the impact velocities of suction valves be calculated". Proc. of the 1978 Purdue Compressor Technology conference. pp 177-186

74) D R Riffe: "High efficiency reciprocating compressors". Proc. of the 1976 Purdue Compressor Technology Conference. pp 129-133

75) R T Nelson & M G Middleton 'The Development of Energy Efficient Compressors for refrigerators and freezers' Proc. of the 1980 Purdue Compressor Technology Conference. pp 215-222

76) J D Mowery: "Rod loading of reciprocating compressors". Proc. of the 1978 Purdue Compressor Technology Conference. pp 73-89

77) Japanese Association of Refrigeration: "Thermophysical properties of refrigerants (R12 Dichlorodifluoromethane)" 1980

78) J T R Watson, National Engineering Laboratory: "Thermophysical properties of Refrigerant 12"

79) Boverton Redwood: "On Viscosimetry, or Viscometry". The Journal of the society of Chemical Industry. March 1886. p121-133